

People's Politics

www.oxfordjournals.org



Oxford

UNIVERSITY PRESS

ACS SYMPOSIUM SERIES **559**

Porphyric Pesticides

Chemistry, Toxicology, and Pharmaceutical Applications

Stephen O. Duke, EDITOR
*Agricultural Research Service,
U.S. Department of Agriculture*

Constantin A. Rebeiz, EDITOR
University of Illinois

Developed from a symposium sponsored
by the Division of Agrochemicals
at the 206th National Meeting
of the American Chemical Society,
Chicago, Illinois,
August 22–27, 1993



American Chemical Society, Washington, DC 1994



Library of Congress Cataloging-in-Publication Data

Porphyric pesticides: chemistry, toxicology, and pharmaceutical applications / Stephen O. Duke, editor; Constantin A. Rebeiz, editor.

p. cm.—(ACS symposium series, ISSN 0097-6156; 559)

“Developed from a symposium sponsored by the Division of Agrochemicals at the 206th National Meeting of the American Chemical Society, Chicago, Illinois, August 22–27, 1993.”

Includes bibliographical references and indexes.


ISBN 0-8412-2923-6

1. Pesticides—Congresses. 2. Porphyrins—Congresses.

I. Duke, Stephen O., 1944– . II. Rebeiz, Constantin A., 1936– .
III. American Chemical Society. Division of Agrochemicals.
IV. American Chemical Society. Meeting (206th: 1993: Chicago, Ill.)
V. Series.

SB952.P67P67 1994
668'.65—dc20

94-16418
CIP

The paper used in this publication meets the minimum requirements of American National Standard for Information Sciences—Permanence of Paper for Printed Library Materials, ANSI Z39.48-1984. 

Copyright © 1994

American Chemical Society

All Rights Reserved. The appearance of the code at the bottom of the first page of each chapter in this volume indicates the copyright owner's consent that reprographic copies of the chapter may be made for personal or internal use or for the personal or internal use of specific clients. This consent is given on the condition, however, that the copier pay the stated per-copy fee through the Copyright Clearance Center, Inc., 27 Congress Street, Salem, MA 01970, for copying beyond that permitted by Sections 107 or 108 of the U.S. Copyright Law. This consent does not extend to copying or transmission by any means—graphic or electronic—for any other purpose, such as for general distribution, for advertising or promotional purposes, for creating a new collective work, for resale, or for information storage and retrieval systems. The copying fee for each chapter is indicated in the code at the bottom of the first page of the chapter.

The citation of trade names and/or names of manufacturers in this publication is not to be construed as an endorsement or as approval by ACS of the commercial products or services referenced herein; nor should the mere reference herein to any drawing, specification, chemical process, or other data be regarded as a license or as a conveyance of any right or permission to the holder, reader, or any other person or corporation, to manufacture, reproduce, use, or sell any patented invention or copyrighted work that may in any way be related thereto. Registered names, trademarks, etc., used in this publication, even without specific indication thereof, are not to be considered unprotected by law.

PRINTED IN THE UNITED STATES OF AMERICA

1994 Advisory Board

ACS Symposium Series

M. Joan Comstock, *Series Editor*

Robert J. Alaimo
Procter & Gamble Pharmaceuticals

Douglas R. Lloyd
The University of Texas at Austin

Mark Arnold
University of Iowa

Cynthia A. Maryanoff
R. W. Johnson Pharmaceutical
Research Institute

David Baker
University of Tennessee

Julius J. Menn
Western Cotton Research Laboratory,
U.S. Department of Agriculture

Arindam Bose
Pfizer Central Research

Roger A. Minear
University of Illinois
at Urbana–Champaign

Robert F. Brady, Jr.
Naval Research Laboratory

Margaret A. Cavanaugh
National Science Foundation

Vincent Pecoraro
University of Michigan

Arthur B. Ellis
University of Wisconsin at Madison

Marshall Phillips
Delmont Laboratories

Dennis W. Hess
Lehigh University

George W. Roberts
North Carolina State University

Hiroshi Ito
IBM Almaden Research Center

A. Truman Schwartz
Macalaster College

Madeleine M. Joullie
University of Pennsylvania

John R. Shapley
University of Illinois
at Urbana–Champaign

Lawrence P. Klemann
Nabisco Foods Group

L. Somasundaram
DuPont

Gretchen S. Kohl
Dow-Corning Corporation

Michael D. Taylor
Parke-Davis Pharmaceutical Research

Bonnie Lawlor
Institute for Scientific Information

Peter Willett
University of Sheffield (England)

Foreword

THE ACS SYMPOSIUM SERIES was first published in 1974 to provide a mechanism for publishing symposia quickly in book form. The purpose of this series is to publish comprehensive books developed from symposia, which are usually "snapshots in time" of the current research being done on a topic, plus some review material on the topic. For this reason, it is necessary that the papers be published as quickly as possible.

Before a symposium-based book is put under contract, the proposed table of contents is reviewed for appropriateness to the topic and for comprehensiveness of the collection. Some papers are excluded at this point, and others are added to round out the scope of the volume. In addition, a draft of each paper is peer-reviewed prior to final acceptance or rejection. This anonymous review process is supervised by the organizer(s) of the symposium, who become the editor(s) of the book. The authors then revise their papers according to the recommendations of both the reviewers and the editors, prepare camera-ready copy, and submit the final papers to the editors, who check that all necessary revisions have been made.

As a rule, only original research papers and original review papers are included in the volumes. Verbatim reproductions of previously published papers are not accepted.

M. Joan Comstock
Series Editor

Preface

PESTICIDES THAT ACT THROUGH THE PHOTODYNAMIC ACTION of porphyrins are the focus of high and increasing research and interest. This is the first book devoted to the topic. Every major company involved in pesticide discovery has patents in this area and usually has a group of scientists devoted to the exploitation of the porphyrin pathway for pesticides. Furthermore, this work is providing valuable tools and information for public sector scientists to explore the workings of the porphyrin pathway in plants and animals. Many parallels exist between this area of pesticide research and the blossoming pharmaceutical and medical research on the use of porphyrins and porphyrin-generating chemicals in cancer therapy.

The idea for the American Chemical Society symposium upon which this book is based originated in discussions at a conference on pyrroles in photosynthetic organisms during the summer of 1991 at the University of California at Davis. We originally planned a more general symposium (and book) that would cover all photodynamic pesticides (such as an update of ACS Symposium Series 339, *Light-Activated Pesticides*). But during the planning stage, we decided that the area of porphyrinic pesticides had grown sufficiently to warrant a symposium and book devoted to this topic alone. Furthermore, there is relatively little interest at this time in nonporphyrinic, photodynamic pesticides.

About two-thirds of this book discusses the use of porphyrinic pesticides as herbicides. Various chapters deal with the synthesis, chemical structures, quantitative structure–activity relationships, and mode of action of porphyrinic herbicides. The rest of this book details the effects of porphyrins and porphyrinogenic compounds on animals. The use of porphyrins and porphyrinogenic compounds as insecticides and pharmaceuticals and their mammalian toxicology are covered. We feel that the latter aspect of the book is novel and very useful, because the works of these diverse scientists (toxicologists, medical scientists, pesticide chemists, and pesticide physiologists and biochemists) have never been brought together before, despite the high level of similarity of many aspects of their research.

This book should be a valuable resource for pesticide chemists, plant physiologists, porphyrin biochemists, toxicologists, and those interested in photodynamic medical therapy.

The American Chemical Society Division of Agrochemicals and the Agricultural Research Service of the U.S. Department of Agriculture financially supported the symposium from which this book resulted. We thank the authors for their outstanding contributions and efforts in synthesizing the latest information in their fields. We acknowledge the time and expertise of the many reviewers whose help improved the contributions. Finally we thank Anne Wilson of the Books Department of the American Chemical Society for her cheerful assistance.

STEPHEN O. DUKE
Southern Weed Science Laboratory
Agricultural Research Service
U.S. Department of Agriculture
Stoneville, MS 38766

CONSTANTIN A. REBEIZ
Laboratory of Pigment Biochemistry and Photobiology
240A Plant and Animal Biotechnology Laboratory
1201 West Gregory Avenue
University of Illinois
Urbana, IL 61801-4716

February 22, 1994

Chapter 1

Porphyrin Biosynthesis as a Tool in Pest Management

An Overview

Stephen O. Duke¹ and Constantin A. Rebeiz²

¹Southern Weed Science Laboratory, Agricultural Research Service, U.S. Department of Agriculture, P.O. Box 350, Stoneville, MS 38776

¹Laboratory of Plant Pigment Biochemistry and Photobiology, 240A Plant and Animal Biotechnology Laboratory, University of Illinois, 1201 West Gregory Avenue, Urbana, IL 61801-4716

Porphyrin biosynthesis can be manipulated chemically in pests to cause accumulation of sufficient photodynamic porphyrin intermediates for pesticidal activity. Chemicals used for this purpose are: δ -aminolevulinic acid (ALA, a porphyrin precursor); protoporphyrinogen oxidase (Protox) inhibitors; and modulators of the heme and chlorophyll biosynthetic pathways such as 2,2'-dipyridyl and 1,10-phenanthroline. A wide array of Protox inhibitors (herbicides) are commercially available, while ALA-based applications are still in the experimental stage. Protox inhibitors cause the accumulation of protoporphyrin IX and other porphyrins in plants via a complex mechanism. No weeds have thus far evolved resistance to herbicides with this mechanism of action. However, some plant species have natural tolerance to such herbicides by a variety of mechanisms. Protox inhibitors are apparently ineffective on insects; however, ALA and modulators of the heme pathway have insecticidal activity. Porphyrinogenic compounds such as ALA have been used or patented for use in photodynamic therapy, and as herbicides. The commercialization of ALA-based photodynamic herbicides will depend, however, on the success of efforts directed at translating successful greenhouse applications to field use. Protox inhibitors have been patented as pharmaceutical for treatment of disorders of the heme pathway. Protox inhibitor herbicides have been found to cause accumulation of certain porphyrins in non-target animals, although porphyria has not been reported.

Compounds that require direct interaction with light and molecular oxygen to produce highly reactive oxygen species (primarily singlet oxygen) are

0097-6156/94/0559-0001\$08.00/0

© 1994 American Chemical Society

known as photodynamic compounds. Such compounds are toxic to all living things because singlet oxygen reacts with many types of organic compounds necessary for life, especially membrane lipids. Photodynamic compounds, both natural and synthetic, have been tested as pesticides, and many of them are highly effective (1-6). However, the indiscriminating toxicity of photodynamic compounds toward all living things has reduced interest in using such compounds directly as pesticides. Pesticides that are not photodynamic, but which cause the accumulation of photodynamic compounds in target organisms offer a much greater potential.

This approach has only been successful with compounds that cause various cyclic tetrapyrroles (*i.e.*, porphyrins) to accumulate (7-11). Various intermediates and products of the heme and chlorophyll (Chl) biosynthetic pathways (Figure 1) are photodynamic. All animal, plant, and microbial pests produce cyclic tetrapyrroles and, thus, contain the potential machinery for their own destruction. There are three approaches to causing the accumulation of cyclic tetrapyrroles. First, pests can be treated with porphyrin precursors, thus increasing the amount of carbon flowing to porphyrins. This approach has been most successful with δ -aminolevulinic acid (ALA) (8, 10, 12-15). The second approach is to inhibit enzymes of the heme and Chl pathways in order to deregulate the pathways and cause accumulation of photodynamic tetrapyrroles. The only commercially available pesticides that act by this mechanism are the inhibitors of protoporphyrinogen oxidase (Protox) (7, 9, 11, 16-18). The last strategy is to use both ALA and compounds that modulate the heme and Chl biosynthetic pathways in order to maximize the accumulation of metabolic tetrapyrroles (8, 10, 12, 19-21).

Similarly, porphyrins and porphyrinogenesis are now being exploited in medicine as tools in photodynamic therapy (22). The knowledge gained in this research and from pesticide studies may result in the development of effective cancericides and environmentally safe and selective herbicides and insecticides

Herbicides

Three categories of porphyrin-generating photodynamic herbicides are presently known. We list them in the order of their sites in the porphyrin pathway (Figure 1). One consists of ALA alone. The second consists of inhibitors of Protox. Another is based on the use of ALA in concert with modulators of the heme and Chl biosynthetic pathways. The first and last categories are still experimental in nature. The second one comprises well established commercial herbicides. A brief preview of these porphyrin-dependent photodynamic herbicides follows.

ALA. ALA is a 5-carbon amino acid. It is the precursor of all natural porphyrins, hemes, Mg-porphyrins, and phorbins in nature. Hemes are the prosthetic groups of cytochromes. Mg-porphyrins and phorbins are tetrapyrrole intermediates of the Chl biosynthetic pathway. As a consequence, ALA is a natural metabolite present in both animal and plant mitochondria and in the plastids of plant cells. In mitochondria,

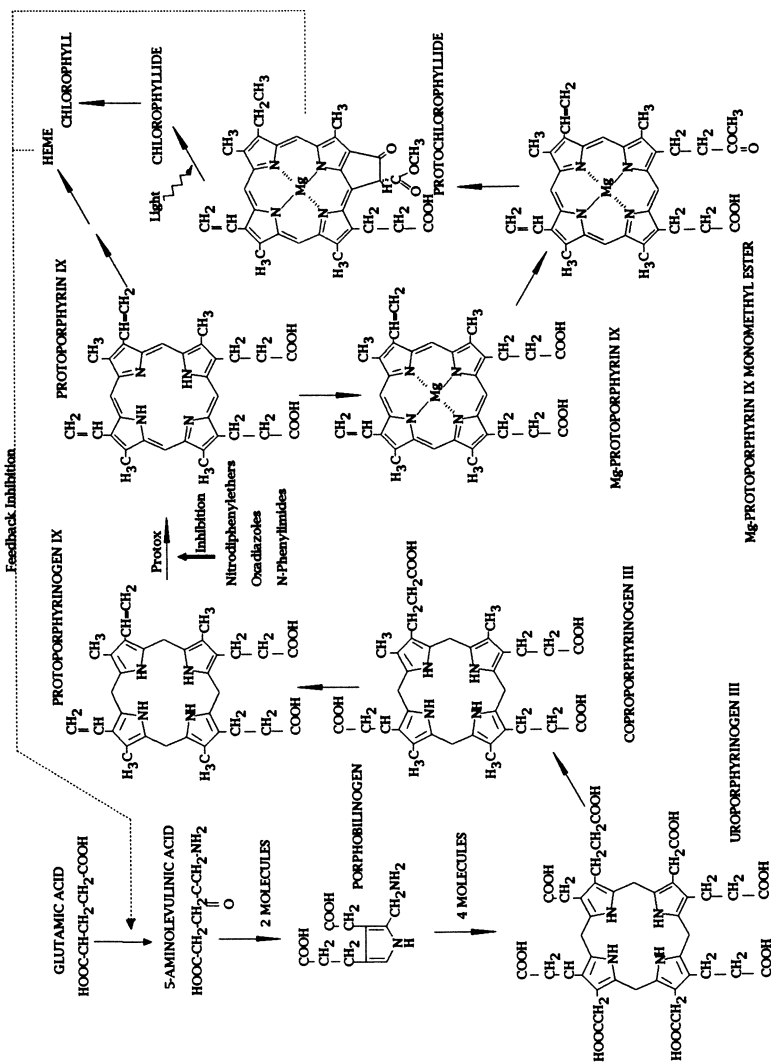


Figure 1. The heme and chlorophyll biosynthetic pathway.

cytochromes are involved in oxidative electron transport. In the chloroplasts, cytochromes are involved in photosynthetic electron transport, while Chls are involved in the conversion of solar energy to chemical energy via the process of photosynthesis.

Under natural conditions, ALA is present in very small amounts in plant tissues. This is because the biosynthesis of ALA is under very tight cellular control (23). The natural wisdom for this rigorous control of ALA biosynthesis and accumulation in living cells did not become obvious until the photodynamic herbicidal and insecticidal properties of ALA were discovered (12, 24). Etiolated plant tissues (plants grown in darkness, that lack Chl) are notorious for their propensity to accumulate protochlorophyllides (PChlides), (the immediate precursors of chlorophyllides, *i. e.*, Chls that lack the long chain fatty alcohol, phytol, at position 7 of the macrocycle), when treated with exogenous ALA in darkness (25). This was not surprising, since etiolated plant tissues lack Chl, but synthesize and accumulate Chl very rapidly in the light. In other words, since etiolated tissues contained the biosynthetic machinery for Chl biosynthesis they were perfectly capable of accumulating Chl precursors in darkness when the dark-dependent blockage of ALA formation was circumvented by supplying exogenous ALA.

For many years it was believed that fully mature green tissues had no need for an active Chl biosynthetic pathway, for obvious reasons of good cell management and economy (26, 27). This belief was reinforced by early experimentation with green plants treated with ALA. When the formation of tetrapyrroles was examined by spectrophotometry, none was found other than Chl (28). The adoption of extraction techniques that eliminated interference by Chl and the development of sensitive spectrofluorometric techniques for tetrapyrrole determinations (29, 30) led to a reevaluation of the aforementioned hypotheses. Many experiments, using newly developed analytical techniques (29, 30) demonstrated that green plants possessed a very active Chl biosynthetic pathway and accumulated massive amounts of tetrapyrroles after treatment with exogenous ALA in darkness (28). With the knowledge that green plants were capable of synthesizing massive amounts of tetrapyrroles in the presence of ALA in darkness and an awareness of the detrimental photodynamic properties of tetrapyrroles, the first herbicidal experiments with exogenous ALA were performed in 1982 and 1983. The first published account appeared in 1984 (12). Further research led to the discovery of other porphyrin-generating chemicals (see below).

Under laboratory conditions, ALA exhibits extremely potent photodynamic herbicidal properties. Treated plants placed in darkness accumulate massive amounts of tetrapyrroles, mainly monovinyl (MV) and divinyl (DV) PChlides. Upon exposure to light, treated tissues bleach, desiccate and die very rapidly within hours of exposure to light. It is believed that this destructive chain of events is caused by formation of singlet oxygen via photosensitized tetrapyrroles. The major site of tetrapyrrole biosynthesis in plants is in etioplasts and chloroplasts. Consequently it is expected that most of the photodynamic damage in

ALA-treated plants should start in these organelles. Indeed ALA treatment and subsequent exposure to light of cucumber seedlings resulted in photosystem II, photosystem I and whole chain reaction damage (31). Time course electron microscopic studies of degradative events in illuminated cucumber cotyledons treated with ALA and 2,2'-dipyridyl revealed, however, simultaneous degradative events in several subcellular organelles (10). Inherently there is no obvious reason for ALA treatments to exhibit herbicidal selectivity. Yet under greenhouse conditions we have observed a pronounced species-dependent photodynamic herbicidal selectivity. For example, treatments that result in the complete destruction of cucumber and pigweed seedlings leave corn unaffected. The molecular basis of this herbicidal selectivity of ALA in the absence of added modulators is not well understood.

The apparent simplicity of the photodynamic herbicidal action of ALA is deceiving, as it becomes more apparent that the development of commercial ALA-based herbicides requires a deeper understanding of ALA metabolism. For example the results of limited experimentation with ALA under field conditions has been less than adequate. Understanding the molecular basis responsible for the breakdown of ALA performance under field conditions promises to be an exciting and challenging field of research. Because of its environmental safety, ALA and ALA-based herbicides have the potential of becoming important field herbicides when this obstacle is finally overcome.

Protox Inhibitors. The only pesticides commercially available that act through porphyrinogenesis are the inhibitors of Protox, the last common enzyme to both heme and chlorophyll biosynthesis (7, 9, 11, 18). Most companies producing pesticides have such compounds on the market or under development, and this class of herbicides is represented by a large number of patents during recent years. Protox inhibitors are herbicides that cause accumulation of protoporphyrin IX (Proto IX), the product of Protox action (32-38). The effect is rapid and dramatic, requiring only a few minutes of cellular exposure for detectable increases of Proto IX (39, 40).

The mechanism of accumulation of the product of Protox is unique. Ultrastructural studies showed that the first cellular membrane to lose its integrity due to treatment by Protox inhibitors is the plasma membrane (16, 36, 41-43). Later, it was shown that Proto IX accumulates in the plasma membrane of treated cells (44). These findings led to the conjecture that when plastid Protox is inhibited, its substrate protoporphyrinogen IX, (Protogen IX) accumulates and is rapidly lost from the plastid envelope, the site of plastid Protox (45), to become oxidized by a herbicide-resistant Protox associated with the plasma membrane (46). More recent findings support this hypothesis by demonstrating (a) that intact plastids export almost all the formed Protogen IX when treated with a Protox inhibitor (47) and (b) that there is a distinctly separate plasma membrane-bound Protox that is herbicide resistant (48).

Since Matringe *et al.* (49) first discovered that *p*-nitrodiphenyl ether herbicides are potent Protox inhibitors, additional progress has been made (50-54). All plastid Protoxes tested have been found to be herbicide sensitive (11). Mitochondrial Protoxes from plants and animals are also herbicide sensitive with K_i values similar to those for plastid Protox (49, 52, 53). Bacterial Protoxes so far tested are herbicide-insensitive (47, 51). Protox activities associated with the plasma membrane of roots (46) and leaves (48) of barley are also insensitive to Protox inhibitors. All Protogen IX that is converted to Proto IX in herbicide-treated tissues is probably formed by plastids, as recent studies suggest that plant mitochondria do not produce Protogen IX (55).

In most intact plants, light greatly stimulates the herbicide-induced accumulation of Proto IX (37, 56-58). The light effect appears to be modulated through PChlide levels rather than through phytochrome or other photoreceptors (56). PChlide is a feedback inhibitor of the porphyrin pathway in plants, which inhibits glu^t -RNA-ligase, thereby blocking ALA biosynthesis (59-61). Light lowers PChlide levels by phototransforming it to Chlide, thereby enhancing carbon flow to Proto IX in herbicide-treated tissues through decreased feedback inhibition. For unknown reasons, this feedback inhibition does not appear to be as strong in some plant species as others or in excised tissues of any species.

Competition studies have demonstrated that Protox inhibitors compete for the Protogen IX binding site on the enzyme (53, 62, 63). Most data indicate that the binding of Protox inhibitors is reversible (62, 64). Furthermore, displacement of various Protox inhibitors by each other indicate that their binding sites overlap (63, 65). Comparative structural analyses of Protogen IX, diphenyl ether, and phenopylate Protox inhibitors support the view that Protox inhibitors mimic one half of the Protogen IX molecule (9, 66, 67). There is also a strong correlation between lipophilicity and Protox-inhibiting activity (62, 66, 67), indicating that the Protogen IX binding site is in a lipophilic environment. This is consistent with the plastid envelope location of herbicide-sensitive Protox (45).

The best Protox inhibitors are effective herbicides at concentrations approximately two orders of magnitude lower than other porphyrinogenic compounds (8). This may be the result of the unique compartmentation of plastid Protox in the plastid envelope. When Protox is inhibited, the substrate is rapidly lost to the cytoplasm (47), resulting in very little competition of the herbicide for the substrate-binding site. Furthermore, formation of Proto IX in the plasma membrane by a herbicide-insensitive Protox results in accumulation of this photodynamic compound in one of the least protected sites of the cell from photodynamic action (46, 48).

Other Modulators of Porphyrin Synthesis in Plants. In addition to unraveling the mode of action of Protox inhibitors, awareness of the potent photodynamic herbicidal properties of porphyrinogenesis, led to the discovery of a plethora of other chemicals that affected the normal chain of reactions during heme and Chl biosynthesis. These chemicals were collectively named modulators of the heme and Chl biosynthetic pathways

(8). The discovery of most of these modulators was made possible by advances in biological computation (10). A search of the literature for chemicals that affected the heme and Chl biosynthetic pathways, netted a dozen chemicals that affected tetrapyrrole biosynthesis in various ways (10). A closer examination of the structure of these chemicals revealed their similarity to a quadrant or half a tetrapyrrole. A search of chemical catalogues for similar commercially available compounds resulted in about three thousand, 5- and 6-membered N heterocyclic compounds. These were entered into a Chembase™ database for systematic substructure-herbicidal activity searches. The substructure searches led in turn to the selection of several hundred chemicals which were screened for primary photodynamic herbicidal activity on cucumber seedlings. The most promising, about 154 modulators, (13, 19) were then subjected to detailed biochemical and three-dimensional structure-function studies.

Depending on their site of action along the heme and Chl biosynthetic chains, various modulators have been classified into four categories: a) inducers of tetrapyrrole biosynthesis, b) enhancers of DV PChlide biosynthesis, c) enhancers of MV PChlide biosynthesis, and d) inhibitors of DV PChlide conversion to MV PChlide. Inducers of tetrapyrrole accumulation induce plant tissues to form large amounts of tetrapyrroles in the absence of exogenously added ALA. The tetrapyrroles consist of Proto IX, Mg-Proto IX monoester, PChlides, or mixtures of these tetrapyrroles. In the presence of exogenous ALA the accumulation of tetrapyrroles is enhanced further. Enhancers of ALA conversion to DV PChlide enhance the conversion of exogenous ALA to DV PChlide, while enhancers of ALA conversion to MV PChlide enhance the conversion of exogenous ALA to MV PChlide. Inhibitors of MV PChlide accumulation appear to block the detoxification of DV tetrapyrroles by inhibiting their conversion to MV tetrapyrroles. Of all the aforementioned modulators, only inducers of tetrapyrrole accumulation are capable of causing tetrapyrrole accumulation in the absence of added ALA. The three other classes of modulators do not lead to significant levels of tetrapyrrole accumulation in the absence of added ALA.

In nature, most of the Chl a is formed via two Chl biosynthetic routes, namely the DV and MV monocarboxylic routes (68-70). Accordingly green plants have been classified into three different greening groups, depending upon which Chl biosynthetic routes are used in forming MV and DV PChlides. On the basis of the photodynamic herbicide response of cucumber, a dark DV/light DV plant species, and soybeans a dark MV/light DV species, toward various ALA plus modulator treatments which caused the accumulation of various MV and DV tetrapyrroles, the following susceptibility hypothesis was proposed (8, 10): (a) that plants poised in the DV tetrapyrrole biosynthetic state are more photodynamically susceptible to the accumulation of MV tetrapyrroles than to the accumulation of DV tetrapyrroles, and (b) plants poised in the MV tetrapyrrole biosynthetic state are more susceptible to the accumulation of DV tetrapyrroles than to MV tetrapyrroles. This phenomenon was explained on the basis that MV plant species poised in the MV-greening pattern could not cope as well

with a massive influx of DV tetrapyrroles. Likewise, DV plants poised in the DV-greening pattern could not cope as effectively with a massive influx of MV tetrapyrroles. In the light, being unable to rapidly metabolize the wrong tetrapyrroles, the latter would linger and photosensitize the destruction of the host plant before being eventually degraded by light. This hypothesis was largely corroborated by investigations carried out under greenhouse conditions on corn, soybean, and ten common weed species (8, 10).

Preliminary field trials of ALA plus modulators sprays have been less satisfactory than greenhouse trials. While in the greenhouse results were outstanding for selective and non-selective ALA plus modulator formulations, performance was less satisfactory under field conditions. This discrepancy in photodynamic herbicidal activity is presently under investigation. It is hoped that its resolution will lead to the development a large number of selective and non selective commercial herbicides.

Insecticides

The discovery of porphyrin insecticides was built upon the discovery and development of photodynamic herbicides (24). Demonstration of the potential for tetrapyrrole accumulation in insects was initially achieved by spraying *Trichoplusia ni* (*T. ni*) larvae with 40 mM ALA plus 30 mM 2,2'-dipyridyl (Dpy). Treated larvae were placed overnight in darkness at 28°C in order to allow for putative tetrapyrrole accumulation. Extraction of treated, dark-incubated larvae with ammoniacal acetone, followed by spectrofluorometric examination of the larval extract, revealed the accumulation of massive amounts of a fluorescent compound which was not present in control larvae sprayed with solvent only. Following chemical derivatization coupled to spectrofluorometric analysis, the accumulated compound was identified as a tetrapyrrole, specifically Proto IX (24). A high positive correlation was observed between Proto IX accumulation in darkness and larval death in the light. A few hours after exposure to light, the larvae became sluggish and flaccid due to loss of body fluids. Death was accompanied by extensive desiccation.

Since control of insects by their ingesting insecticides is as viable an option as control by direct spraying, and offers certain advantages under household conditions, studies were conducted to determine whether combinations of ALA and porphyrin insecticide modulators would be effective if ingested with the food. Initially, the effect of 16 mM ALA and 12 mM 1,10-phenanthroline (Oph) were determined by incorporating them into the diet of *T. ni* larvae. Later on, 4 mM ALA and 3mM Oph were used. Upon exposure to light, following 17 h of dark incubation, larvae underwent violent convulsions and vomiting; followed by death within 20-40 s. Tetrapyrrole analysis of the treated larvae immediately after dark incubation revealed significant amounts of Proto IX and Zn-Proto IX accumulation. Correlation between tetrapyrrole accumulation and larval death was significant (20). Similar results were obtained when ALA plus Dpy were administered to the larvae with the diet. The above results

indicated that in addition to contact via spraying, porphyrin insecticides had the potential to be very potent when ingested.

For a more thorough understanding of the mode of action of porphyrin insecticides, the phenomenology of tissue, cellular, and subcellular sites of tetrapyrrole accumulation in representative insect species has been investigated. In *T. ni* larvae sprayed with ALA (40 mM) plus Dpy (30 mM), about 59% of the accumulated Proto IX was observed in the hemolymph, 35% in the gut, and 6% in the integument. Further understanding of the response of insect organs and tissues to porphyrin insecticide treatment was obtained by investigating the response of isolated organs and tissues to incubation with ALA plus Dpy or ALA plus Oph. In these experiments, the following insects were used: adult *Blattella germanica* (german cockroach), adult *Anthonomus grandis* (cotton boll weevil), fifth instar larvae of *Heliothis zea* (corn earworm), and fifth instar larvae of *T. ni* (cabbage looper). In *T. ni*, and *H. zea*, significant Proto IX accumulation was observed in incubated midgut, and fat bodies. Proto IX accumulation occurred when tissues were incubated with Dpy, ALA plus Dpy, Oph, and ALA plus Oph (71). No response to treatment with ALA alone was observed. In cockroaches, more of the Proto IX appeared to accumulate in the guts than in their abdomen. As in *T. ni* and *H. zea*, the response was elicited by each of the treatments that included Dpy or Oph. Cotton boll weevil abdomens appeared to be less responsive than the abdomens of the other three species.

To determine whether Proto IX accumulation resulted in photodynamic damage of incubated tissues, the effect of ALA, or ALA with Oph on oxygen consumption of isolated midguts was investigated. Decrease in oxygen consumption observed in treated *T. ni* midguts exposed to light suggested that toxicity of porphyrin insecticides may result from mitochondrial photodynamic damage. This hypothesis was further investigated by determining the site of Proto IX accumulation in various subcellular components of *T. ni* larvae treated with ALA plus Oph. Most of the Proto IX was found in the mitochondrial (37%) and microsomal (35%) fractions, while the balance (28%) was found in the cytosol. Upon exposure of the isolated mitochondria to 900 W·m⁻² of white fluorescent light for 30 min at 25°C, the activity of various mitochondrial marker enzymes, namely, succinate oxidase, NADH dehydrogenase, and NADH-cytochrome *c* reductase decreased markedly in comparison to dark mitochondrial controls. These results strongly indicated that Proto IX accumulation in mitochondria triggers mitochondrial damage in the light and may contribute significantly to photodynamic damage in treated insects.

As mentioned above, structure-function photodynamic herbicidal studies have led to the assembly of two databases of commercially available compounds with potential photodynamic herbicidal properties. The databases consisted of sets of 6-membered and 5-membered N-heterocyclics. A substructure computer search of these databases identified 322 putative photodynamic herbicide modulators. Extensive testing of these modulators on a variety of plant species led to the identification of about 154 modulators with excellent photodynamic

herbicidal properties (8, 19). A screening effort was undertaken to determine whether these 154 modulators exhibited porphyric insecticidal properties. Screening by food ingestion was performed on the german cockroach, cotton boll weevil, corn earworm, and cabbage looper as described in (71). Thirty-six compounds belonging to ten different chemical families were effective (> 70 % mortality) against at least one insect species. Of the 36 modulators, ten modulators exhibited potent activity toward cockroaches. One additional modulator, 1-phenyl pyrrole, exhibited considerable activity against cockroaches under closed, non aerated conditions (71). The porphyric insecticide technology is now poised for development of household and agricultural insecticide applications.

Other Pesticides

Early on, very limited experimentation was carried out on bread mold and powdery mildew (C. A. Rebeiz, unpublished data). Preliminary studies have indicated that ALA plus Dpy or Oph treatments followed by dark incubation and subsequent exposure to light exhibited effective antifungal properties. These initial observations were not pursued any further.

Mechanisms of Tolerance and Resistance

In this discussion, we will term naturally-occurring insensitivity to a herbicide "tolerance" and insensitivity imparted by selective forces "resistance." There are three basic strategies other than behavioral modifications to resist or tolerate a pesticide: (a) an altered site of action, so that the pesticide will no longer bind to the molecular site of action; (b) metabolic detoxification of the pesticide or toxic compounds caused to accumulate by the pesticides; and (c) restriction of movement of the pesticide to the molecular site of action. The first two have been invoked to explain tolerance to porphyric pesticides.

Little is known about the mechanisms of tolerance to any porphyric pesticides other than Protox inhibitors. There are apparently numerous mechanisms that can interact in a complex fashion.

There is no evidence of tolerance or resistance to Protox inhibitors at the site of action (54). However, an apparent herbicide-resistant Protox mutant of *Chlamydomonas reinhardtii*, a unicellular alga, has been selected in culture (72). This mutant has cross resistance to Protox inhibitors of various chemical classes, but is not cross-resistant to photodynamic herbicides with different mechanisms of action such as paraquat.

Clearly, in some plant species, the herbicide itself is rapidly degraded enzymatically reducing its cellular concentration below that which would be lethal. For example, the half life of acifluorfen and some related Protox inhibitors in soybeans is short enough for this herbicide to be used in soybeans (73, 74), even though soybeans can be made to produce Proto IX when treated with the herbicide (54). Rapid metabolism of herbicides by crops with which they are used is the most common mechanism of crop tolerance to herbicides. However, few herbicides act as

rapidly as porphyrinogenic herbicides, so other mechanisms may exist to give the plant time to detoxify the herbicide.

Mustard makes very little Proto IX in response to acifluorfen (54), and this effect cannot be explained entirely by reduced herbicide uptake or metabolism (unpublished data of M. V. Duke, S. O. Duke, J. M. Becerril, and H. J. Lee). Rice makes a high level of Proto IX in response to Protox inhibitors, yet is relatively unaffected (75). In such cases, the plant may be highly tolerant of singlet oxygen, as suggested by Finckh and Kunert (76) for a range of tolerant species. In some tolerant species, the oxidative stress caused by Protox inhibitors may induce high enough levels of protective enzymes, such as superoxide dismutase, ascorbate oxidase, and glutathione reductase, for induction of tolerance (*e. g.*, 77).

Although there are apparently many mechanisms of tolerance to Protox inhibitors among crops and weeds, there are no cases of resistance due to selection with a porphyrinogenic herbicide. Diphenyl ether herbicides have had wide-spread use for about 15 years, however, their use as fast-acting foliar sprays with little or no residual activity minimizes the duration of the selection pressure. A low level of cross resistance to Protox-inhibiting herbicides has been reported with some paraquat-resistant weed biotypes (79). The mechanism of such resistance is probably through enhanced resistance to oxidative stress, as paraquat exerts its phytotoxicity by catalytic formation of superoxide radical. Plants with higher superoxide dismutase levels have greater tolerance to herbicidal levels of ALA (80).

Relationship to Medicinal Chemistry

Porphyrins, both natural and synthetic, and porphyrinogenic compounds have been used in photodynamic therapy (22, 78, N. Rebeiz, K. W. Kelley, and C. A. Rebeiz, unpublished data). The objective of this type of therapy is to cause sufficient porphyrins to accumulate in unwanted tissues (*e.g.*, tumors) for treatment with high intensity light of the appropriate wavelengths to result in cancer cell death. Rapidly growing tissues as in certain tumors might be expected to have a relatively high rate of porphyrin synthesis and would, thus, be amenable to treatment with porphyrinogenic compounds. In this respect ALA with or without modulators has been the compound of choice (22, 78).

Protox inhibitors have been patented as pharmaceuticals for use in treatment of polycythemia vera and hyperbilirubinemia (81). The symptoms are alleviated by reducing heme levels. However, these compounds have thus far only been used in animal studies (B. P. Halling, *pers. commun.*). Further details are thus far unavailable. The potential use of Protox inhibitors in photodynamic therapy to preferentially induce Proto IX or other porphyrins in cancerous tissues for photodynamic therapy is being studied (82).

Toxicology

Since organellar Protoxes of all eukaryotes thus far studied appear to be sensitive to Protox inhibitors, the safety of these compounds has been questioned. One of the clues that led to the discovery of the molecular site of action of Protox inhibitors was that defects in human Protox leads to the genetic disorder of variegate porphyria (83, 84). Individuals with this defect accumulate high levels of Proto IX and have heme deficiencies. Thus far, there have been no reports of porphyria in animals exposed to these compounds, even though mammalian mitochondrial Protox is highly sensitive to commercially used Protox-inhibiting herbicides. However, there is evidence that, at sufficient concentrations, these compounds alter porphyrin metabolism in animals (85-88).

Proto IX, Proto IX monomethyl ester, and PChlide accumulate in treated plants (35, 40, 44, 58, 89). At high concentrations, Protox inhibitors cause the accumulation of Proto IX, coproporphyrin, uroporphyrin, and hepatocarbonylic porphyrin in livers of mice (88) and Proto IX, coproporphyrin, and uroporphyrin in cultured chick embryo hepatocytes (87). There is evidence that the mechanism of accumulation of porphyrins in animals may be similar to that of other cytochrome P450 monooxygenase-inducing aromatic compounds (87) rather than via inhibition of Protox.

Future Prospects

The commercial future of porphyric pesticides is unclear, despite some successes and the high level of interest. Only one group of porphyrinogenic pesticides is available at this time: Protox-inhibiting herbicides. Although there are a large number of patented Protox inhibitors, the market is limited by the similar selectivities of most of these compounds. That is, most of these herbicides control the same weed spectrum in the same crops. Another problem is that many of these compounds cause too much crop damage. Nevertheless, there are many excellent Protox-inhibiting herbicides that will never be marketed because companies are not willing to risk the approximately \$60 million required to register a new pesticide in the United States to replace an existing herbicide with an almost identical performance pattern. The use of ALA in concert with selective photodynamic herbicide modulators may overcome this problem, if efforts aimed at translating promising greenhouse results to field use prove successful.

Protox-inhibiting herbicides and potential ALA-based herbicides and insecticides may play an increasing role in combating pesticide resistance. Pesticide resistance has become an enormous problem with insecticides, and the incidence and spread of herbicide resistance is growing geometrically (90). There are no known cases of evolved resistance to Protox inhibitors. Thus, such herbicides are excellent choices to rotate or tank mix with herbicides to which resistance is known to evolve more readily (*e.g.*, PS II inhibitors, acetolactate synthase inhibitors, acetyl CoA carboxylase inhibitors, and paraquat). Acifluorfen, the most commonly

used Protox inhibitor, can now be bought pre-mixed with a PS II inhibitor (bentazon).

New market niches for Protox inhibitors might be opened by biotechnology. Insertion of a gene encoding a herbicide-resistant plastid Protox into susceptible crops would greatly expand field use. Even in crops with which these herbicides are currently used, such a gene would eliminate the phytotoxicity which sometimes arises. The technology for the creation of such a resistant crop already exists, as evidenced by successful efforts directed at the creation of crops resistant to other herbicides (91, 92). The *Chlamydomonas* mutant of Oshio *et al.* (72) may contain such a gene, however, efforts to clone it have so far been unsuccessful. Whether there would be undesirable pleiotrophic effects or even lethal effects of such a gene in a higher plant is unknown. However, the lack of any reports of evolution of resistant weeds with altered Protox would suggest that such a mutant would be at a competitive disadvantage, even in fields sprayed with the herbicide. Furthermore, a resistant plastid Protox has not been reported from any higher plant.

Recent additions to our knowledge of the mechanism of action of Protox inhibitors and other compounds that influence the porphyrin pathway provide those interested in the pharmaceutical and toxicological effects of these compounds a more useful information base. Research on the mechanism of action of Protox inhibitors has revealed new information about the porphyrin pathway and its manipulation. These findings should be useful in the design of safer pesticides and new pharmaceuticals or in the determination of the safety of existing and new commercial products.

Literature Cited

1. Towers, G. H. N.; Arnason, J. T. *Weed Technol.* 1988, 2, 545-9.
2. Knox, J. P.; Dodge, A. D. *Plant Cell Environ.* 1985, 8, 19-25.
3. Heitz, J. R. *Amer. Chem. Soc. Symp. Ser.* 1987, 339, 1-21.
4. Swain, L. A.; Downum, K. R. *Amer. Chem. Soc. Symp. Ser.* 1991, 449, 361-70.
5. Downum, K. R. *New Phytol.* 1992, 122, 401-20.
6. Mostowska, A. *Photosynthetica* 1992, 26, 19-31.
7. Duke, S. O.; Becerril, J. M.; Sherman, T. D.; Matsumoto, H. *Amer. Chem. Soc. Symp. Ser.* 1991, 449, 371-86.
8. Rebeiz, C. A.; Montzer-Zouhoor, A.; Mayasich, J. M.; Tripathy, B. C.; Wu, S. M.; Rebeiz, C. C. *Amer. Chem. Soc. Symp. Ser.* 1987, 339, 295-327.
9. Nandihalli, U. B.; Duke, S. O. *Amer. Chem. Soc. Symp. Ser.* 1992, 524, 62-78.
10. Rebeiz, C. A.; Montazer-Zouhoor, A.; Mayasich, J. M.; Tripathy, B. C.; Wu, S.-M.; Rebeiz, C. C. *Crit. Rev. Plant Sci.* 1988, 6, 385-436.
11. Scalla, R.; Matringe, M. *Rev. Weed Sci.* 1993, 6, In press.
12. Rebeiz, C. A.; Montazer-Zouhoor, A.; Hopen, H. J.; Wu, S.-M. *Enzyme Microb. Technol.* 1984, 5, 390-401.

13. Rebeiz, C. A.; Nandihalli, U. B.; Reddy, K. N. In *Topics in Photosynthesis - Volume 10, Herbicides*; Baker, N. R.; Percival, M. P., Eds.; Elsevier, Amsterdam, 1991; pp. 173-208.
14. Mayasich, J. M.; Mayasich, S. A.; Rebeiz, C. A. *Weed Sci.* **1990**, *38*, 10-5.
15. Chakraborty, N.; Tripathy, B. C. *J. Biosci.* **1990**, *15*, 199-204.
16. Duke, S. O.; Lydon, J.; Becerril, J. M.; Sherman, T. D.; Lehnen, L. P.; Matsumoto, H. *Weed Sci.* **1991**, *39*, 465-73.
17. Duke, S. O.; Becerril, J. M.; Sherman, T. D.; Lydon, J.; Matsumoto, H. *Pestic. Sci.* **1990**, *30*, 367-78.
18. Scalla, R.; Matringe, M. *Z. Naturforsch.* **1990**, *45c*, 503-11.
19. Rebeiz, C. A.; Reddy, K. N.; Nandihalli, U. B.; Velu, J. *Photochem. Photobiol.* **1990**, *52*, 1099-117.
20. Rebeiz, C. A.; Juvik, J. A.; Rebeiz, C. C.; Bouton, C. E.; Gut, L. J. *Pestic. Biochem. Physiol.* **1990**, *36*, 201-7.
21. Nandihalli, U. B.; Rebeiz, C. A. *Pestic. Biochem. Physiol.* **1991**, *40*, 201-7.
22. Kennedy, J. C.; Pottier, R. H. *J. Photochem. Photobiol. B. Biol.* **1992**, *14*, 275-92.
23. Beale, S.I., Weinstein, J. D. In *Chlorophylls*; Scheer, H., Ed, CRC Press, Boca Raton, FL. 1991; pp. 385-406.
24. Rebeiz, C. A.; Juvik, J. A.; Rebeiz, C. C. *Pestic. Biochem. Physiol.* **1988**, *30*, 11-27.
25. Sisler, E. C.; Klein, W. H. *Physiol. Plant.* **1963**, *16*, 315-22.
26. Wickliff, J. L.; Aronoff, S. *Plant Cell Physiol.* **1963**, *5*, 441-9.
27. Virgin, H. I. *Physiol. Plant.* **1961**, *14*, 384-92.
28. Rebeiz, C.A. In *Active Oxygen/Oxidative Stress and Plant Metabolism*, Pell, E.; Steffen, K., Eds.; Amer. Soc. Plant Physiol., MD, 1991, pp. 193-202.
29. Rebeiz, C. A.; Mattheis, J. R.; Smith, B. B.; Rebeiz, C. C.; Dayton, D. F. *Arch. Biochem. Biophys.* **1975**, *166*, 446-65.
30. Rebeiz, C. A.; Smith, B. B.; Mattheis, J. R.; Rebeiz, C. C.; Dayton, D. F. *Arch. Biochem. Biophys.* **1975**, *171*, 549-67.
31. Tripathy, B. C.; Chakraborty, N. *Plant Physiol.* **1991**, *96*, 761-767.
32. Matringe, M.; Scalla, R. *Plant Physiol.* **1988**, *86*, 619-22.
33. Lydon, J.; Duke, S. O. *Pestic. Biochem. Physiol.* **1988**, *31*, 74-83.
34. Witkowski, D. A.; Halling, B. P. *Plant Physiol.* **1988**, *87*, 632-7.
35. Becerril, J. M.; Duke, S. O. *Pestic. Biochem. Physiol.* **1989**, *35*, 119-26.
36. Duke, S. O.; Lydon, J.; Paul, R. N. *Weed Sci.* **1989**, *37*, 152-60.
37. Matringe, M.; Scalla, R. *Pestic. Biochem. Physiol.* **1988**, *32*, 164-72.
38. Sandmann, G.; Böger, P. *Z. Naturforsch.* **1988**, *43c*, 699-704.
39. Becerril, J. M.; Duke, S. O. *Plant Physiol.* **1989**, *90*, 1175-81.
40. Matsumoto, H.; Duke, S. O. *J. Agric. Food Chem.* **1990**, *38*, 2066-71.
41. Duke, S. O.; Kenyon, W. H. *Z. Naturforsch.* **1987**, *42c*, 813-8.
42. Kenyon, W. H.; Duke, S. O.; Vaughn, K. V. *Pestic. Biochem. Physiol.* **1985**, *24*, 240-50.
43. Kenyon, W. L.; Duke, S. O.; Paul, R. N. *Pestic. Biochem. Physiol.* **1988**, *30*, 57-66.
44. Lehnen, L. P.; Sherman, T. D.; Becerril, J. M.; Duke, S. O. *Pestic. Biochem. Physiol.* **1990**, *37*, 239-48.

45. Matringe, M.; Camadro, J.-M.; Block, M. A.; Joyard, J.; Scalla, R.; Labbe, P.; Douce, R. *J. Biol. Chem.* **1992**, *267*, 4646-51.
46. Jacobs, J. M.; Jacobs, N. J.; Sherman, T. D.; Duke, S. O. *Plant Physiol.* **1991**, *97*, 197-203.
47. Jacobs, J. M.; Jacobs, N. J. *Plant Physiol.* **1993**, *101*, 1181-7.
48. Lee, H. J.; Duke, M. V.; Duke, S. O. *Plant Physiol.* **1993**, *102*, 881-9.
49. Matringe, M.; Camadro, J.-M.; Labbe, P.; Scalla, R. *Biochem. J.* **1989**, *260*, 231-5.
50. Witkowski, D. A.; Halling, B. P. *Plant Physiol.* **1989**, *90*, 1239-42.
51. Jacobs, J. M.; Jacobs, N. J.; Borotz, S. E.; Guerinot, M. L. *Arch. Biochem. Biophys.* **1989**, *280*, 369-75.
52. Matringe, M.; Camadro, J.-M.; Labbe, P.; Scalla, R. , *FEBS Lett.* **1989**, *245*, 35-8.
53. Camadro, J.-M.; Matringe, M.; Scalla, R.; Labbe, P. *Biochem. J.* **1991**, *277*, 17-21.
54. Sherman, T. D.; Becerril, J. M.; Matsumoto, H.; Duke, M. V.; Jacobs, J. M.; Jacobs, N. J.; Duke, S. O. *Plant Physiol.* **1991**, *97*, 280-7.
55. Smith, A. G.; Marsch, O.; Elder, G. H. *Biochem. J.* **1993**, *292*, 503-8.
56. Becerril, J. M.; Duke, M. V.; Nandihalli, U. B.; Matsumoto, H.; Duke, S. O. *Physiol. Plant.* **1992**, *86*, 6-16.
57. Mayasich, J. M.; Nandihalli, U. B.; Leibl, R. A.; Rebeiz, C. A. *Pestic. Biochem. Physiol.* **1990**, *36*, 259-68.
58. Nandihalli, U. B.; Leibl, R. A.; Rebeiz, C. A. *Pestic. Sci.* **1991**, *31*, 9-23.
59. Gough, S. P.; Kannangara, G. *Carlsberg Res. Commun.* **1979**, *44*, 403-16.
60. Dörnemann, D.; Kotzabasis, K.; Richter, P.; Breu, V.; Senger, H. *Bot. Acta* **1989**, *102*, 112-5.
61. Dörnemann, D.; Breu, V.; Kotzabasis, K.; Richter, P.; Senger, H. In *Current Research in Photosynthesis, Vol. IV*; Baltscheffsky, Ed.; Kluwer Acad. Publ., Amsterdam, 1990; pp. 287-90.
62. Nicolaus, B.; Sandmann, G.; Böger, P. *Z. Naturforsch.* **1993**, *48c*, 326-33.
63. Matringe, M.; Mornet, R.; Scalla, R. *Eur. J. Biochem.* **1992**, *209*, 861-8.
64. Mito, N.; Sato, R.; Miyakado, M.; Oshio, H.; Tanaka, S. *Pestic. Biochem. Physiol.* **1991**, *40*, 128-35.
65. Varsano, R.; Matringe, M.; Magnin, N.; Mornet, R.; Scalla, R. *FEBS Lett.* **1990**, *272*, 106-8.
66. Nandihalli, U. B.; Duke, M. V.; Duke, S. O. *J. Agric. Food Chem.* **1992**, *44*, 1993-2000.
67. Nandihalli, U. B.; Duke, M. V.; Duke, S. O. *Pestic. Biochem. Physiol.* **1992**, *43*, 193-211.
68. Rebeiz, C. A.; Wu, S. M.; Kuhadja, M.; Daniell, H.; Perkins, E. J. *Plant Mol. Cell Biochem.* **1983**, *58*, 97-125.
69. Tripathy, B. C.; Rebeiz, C. A. *J. Biol. Chem.* **1986**, *261*, 13556-64.
70. Rebeiz, C. A. In *The Biosynthesis of the Tetrapyrrole Pigments*; The Ciba Foundation, London, 1993, In press.
71. Rebeiz, C. A.; Gut, L. J.; Lee, K.; Juvik, J. A.; Rebeiz, C. C.; Bouton, C. E. *Crit. Rev. Plant. Sci.* **1994**, In press.

72. Oshio, H.; Shibata, H.; Mito, N.; Yamamoto, M.; Harris, E. H.; Gillham, N. W.; Boynton, J. E.; Sato, R. *Z. Naturforsch.* **1993**, *48c*, 339-44.
73. Frear, D. S.; Swanson, H. R.; Mansager, E. R. *Pestic. Biochem. Physiol.* **1983**, *20*, 299-310.
74. Kouji, H.; Masuda, T.; Matsunaka, S. *Pestic. Biochem. Physiol.* **1990**, *37*, 219-26.
75. Lee, J. J.; Matsumoto, H.; Ishizuka, K. *Pestic. Biochem. Physiol.* **1992**, *44*, 119-25.
76. Finckh, B. F.; Kunert, K. J. *J. Agric. Food Chem.* **1985**, *33*, 574-7.
77. Kunert, K.; Dodge, A. D. In *Target Sites of Herbicide Action*; Böger, P.; Sandmann, G., Eds.; CRC Press, Boca Raton, FL, 1989; pp. 45-63.
78. Rebeiz, N.; Rebeiz, C. C.; Arkins, S.; Kelley, K. W.; Rebeiz, C. A. *Photochem. Photobiol.* **1992**, *55*, 431-5.
79. Shaaltiel, Y.; Glazer, A.; Bocion, P. F.; Gressel, J. *Pestic. Biochem. Physiol.* **1988**, *31*, 13-23.
80. Askira, Y.; Rubin, B.; Rabinowitch, H. D. *Free Rad. Res. Comms.* **1991**, *12-13*, 837-43.
81. Winkelman, J. R.; Halling, B. P.; Witkowski, D. A. *U.S. Patent Appl.* **535,794 Dec. 19, 1991.**
82. Halling, B. P.; Witkowski, D. A.; Fingar, V. F.; Winkelman, J. W. *Amer. Chem. Soc. Symp. Ser.* **1994**, this volume.
83. Deybach, J. C.; de Verneuil, H.; Nordmann, Y. *Hum. Genet.* **1981**, *58*, 425-8.
84. Brenner, D. A.; Bloomer, J. R. *New Eng. J. Med.* **1980**, *302*, 765-8.
85. Krijt, J.; Pleskot, R.; Sanitrák, J.; Janoušek, V. *Pestic. Biochem. Physiol.* **1992**, *42*, 180-7.
86. Krijt, J.; Sanitrák, J.; Vokura, M.; Janoušek, V. *Biomedical Chromatog.* **1991**, *5*, 229-30.
87. Jacobs, J. M.; Sinclair, P. R.; Gorman, N.; Jacobs, N. J.; Sinclair, J. F.; Bement, W. J.; Walton, H. *J. Biochem. Toxicol.* **1992**, *7*, 87-95.
88. Krijt, J.; van Holsteijn, I.; Hassing, I.; Vokurka, M.; Blaauboer, B. J. *Arch. Toxicol.* **1993**, *67*, 255-61.
89. Duke, S. O.; Duke, M. V.; Lee, H. J. *Z. Naturforsch.* **1993**, *48c*, 317-25.
90. LeBaron, H. M. In *Herbicide Resistance in Weeds and Crops*; Caseley, J. C.; Cussans, G. W.; Atkin, R. K., Eds.; Butterworth-Heinemann Ltd., Oxford, 1991; pp. 27-43.
91. Duke, S. O.; Hess, F. D.; Christy, A. L.; Holt, J. S. *Herbicide-Resistant Crops*; Comments from CAST, no. 1991-1, Council for Agricultural Science and Technology, Ames, IA, 1991; 24 pp.
92. Dyer, W.E.; Hess, F. D.; Holt, J. S.; Duke, S.O. *Hortic. Rev.* **1993**, *15*, 367-408.

RECEIVED February 1, 1994

Chapter 2

Synthetic Organic Chemicals That Act through the Porphyrin Pathway

R. J. Anderson, A. E. Norris, and F. D. Hess

Research Division, Sandoz Agro, Inc., 975 California Avenue, Palo Alto, CA 94304

A survey of the known inhibitors of protoporphyrinogen oxidase (Protox) has resulted in their classification into three main chemical classes: the diaryl ethers, the phenyl heterocycles, and the heterocyclic carboxamides. The first class, the diaryl ethers, is subdivided into the diphenyl ethers (e.g., oxyfluorfen, acifluorfen and lactofen) and the heterocyclyl phenyl ethers (e.g., AH 2.430, 6-aryloxy-1H-benzotriazoles). A second major class of protox inhibitors, the phenyl heterocycles, is characterized by the 2,4,5-substitution pattern of the phenyl ring and contains two major subclasses. Most prominent in the N-phenyl heterocycle subclass are the imides (e.g., S 23031, S 53482), the tetrazolones (F 5231), the triazolones (F 6285), the uracils (UBI C4243) and the pyrazoles (M&B 39279). The smaller C-phenyl heterocycle subclass also contains several heterocyclic systems. The O-phenylcarbamates (RH 1422) are included with the phenyl heterocycles based on their characteristic phenyl substitution pattern. A third, presently small class is the heterocyclic carboxamide class which can be subdivided into the pyridone carboxamides (DLH 1777) and the pyridine carboxamides (LS 82 556).

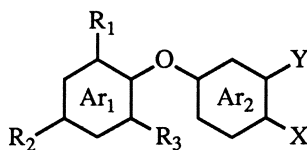
Diphenyl ether herbicides have been known for many years to cause rapid membrane disruption in plants in the presence of light (1). The bipyridyliums were the only other class of herbicides that showed this rapid membrane disruption; however, these two classes of herbicides differ in their biochemical site of action (2). The bipyridyliums undergo reversible redox reactions by diverting electron flow from photosystem I and producing superoxide from triplet oxygen. Lipid peroxidation by hydroxy radicals from the superoxide results in membrane disruption (2). The diphenyl ethers act more indirectly to destroy membrane integrity. They inhibit protoporphyrinogen oxidase (Protox) (3), the

0097-6156/94/0559-0018\$08.00/0
© 1994 American Chemical Society

last enzyme common to the heme and chlorophyll biosynthetic pathways, and cause protoporphyrin IX to accumulate *in vivo*. With light, protoporphyrin IX acts as a photosensitizer in the formation of singlet oxygen which causes lipid peroxidation and membrane disruption (4). More recently Duke, Lydon and Paul (5) showed that the herbicide oxadiazon has the same mechanism of action as the diphenyl ethers, even though its molecular structure is quite different. Currently there is significant patent and development activity on the N-phenyl imide herbicides, which are also known to act by inhibiting the Protox enzyme (6). Because several types of chemical structures have now been shown to inhibit Protox, a chemical classification system for Protox inhibitors would be useful and could help clarify the nomenclature used in literature reports. In this paper we propose the classification of the known Protox inhibitors into three major classes, with subclasses defined for each class. Specific compounds shown as examples of the various subclasses are primarily those that have been used in biological and biochemical studies reported in the literature. Patent citations for specific compounds or generic structures are listed in the text after the compound numbers or in columns within tables. Where available the patents cited are those claiming and/or disclosing the active compounds *per se*. US Patent citations have been given except where unavailable.

Diaryl Ethers

The diaryl ether class of protox inhibitors is characterized by two substituted aromatic rings (Ar_1 and Ar_2), usually six membered, linked by an oxygen atom. The pattern of aromatic substitution required for optimal herbicidal activity and protox inhibitory activity, is indicated below:



Of the several subclasses of diaryl ethers, the diphenyl ethers are most prominent. At least eleven diphenyl ethers are or have been commercial products (Table I). They are strikingly similar in structure, and typify the optimal substitution pattern for this class. Generally, phenyl ring Ar_1 is 2,4-disubstituted, R_1 is chloro, R_2 is trifluoromethyl or chloro, and R_3 is hydrogen. The second phenyl ring Ar_2 is usually 3,4-disubstituted and X is nitro or chloro.

The greatest variation of structure in the diphenyl ethers occurs in the substituent Y . Nitrofen, in which $Y = H$, was the first diphenyl ether to be commercialized. It is a relatively weak Protox inhibitor and is less herbicidally active than other commercialized diphenyl ethers (7). Other closely related analogs in which Y is also hydrogen are chloronitrofen, fluoronitrofen and fluorodifen. The latter is exceptional in structure with $R_1 = NO_2$ rather than chloro. Diphenyl ethers containing an alkoxy substituent ($Y = OMe, OEt$) or

Table I.

Commercialized Diphenyl Ethers

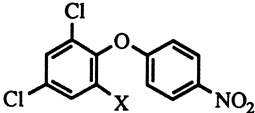
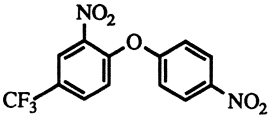
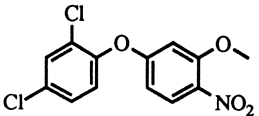
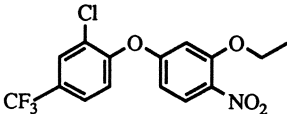
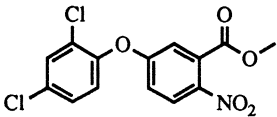
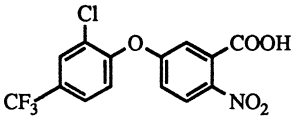
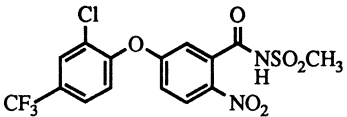
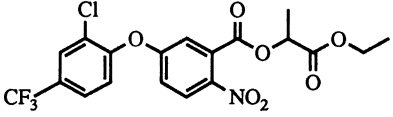
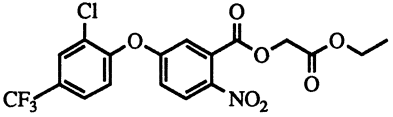
<i>Structure</i>	<i>Common Name</i>	<i>Patent References</i>
	X = H nitrofen (1, 7-9)	USP 3,080,225 (Rohm & Haas)
	X = Cl chloronitrofen (1, 8)	USP 3,316,080 (Mitsui)
	X = F fluoronitrofen (1)	USP 3,401,031 (Mitsui)
	fluorodifen (7, 9)	USP 3,420,892 (Ciba-Geigy)
	chlomethoxyfen chlomethoxynil (8)	USP 4,039,588 (Rohm & Haas)
	oxyfluorfen (8-10)	USP 3,798,276 (Rohm & Haas)

Table I. (continued)

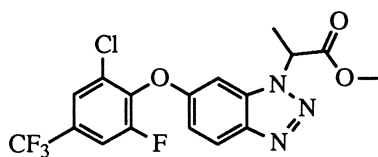
Commercialized Diphenyl Ethers

<i>Structure</i>	<i>Common Name</i>	<i>Patent References</i>
	bifenox (7, 8)	USP 3,652,645 (Mobil)
	acifluorfen (7, 8, 11-13)	USP 3,928,416 (Rohm & Haas)
	fomesafen (7, 14)	USP 4,285,723 (ICI)
	lactofen (7)	EP 20 052 (Rohm & Haas)
	fluoroglycofen ethyl (15)	EP 20 052 (Rohm & Haas)

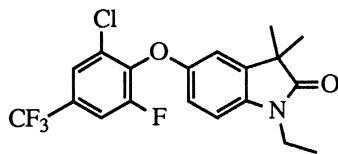
an acyl substituent ($Y = \text{COOH}$, COOR) predominate in the marketplace today due to their high herbicidal activity and crop selectivity. The most important of these are oxyfluorfen ($Y = \text{OEt}$) and acifluorfen ($Y = \text{COOH}$) and its derivatives; fomesafen, lactofen and fluoroglycofen ethyl (Table I).

Many other diphenyl ethers have been investigated for their biological and biochemical properties. Table II illustrates such compounds which display additional diversity in structure, especially in the Y substituent. Patent literature indicates that other Y ligands which have been explored include substituted alkyl, alkenyl, amino, amido, hydrazino, thio, imino; phosphoryl, phosphonyl, phosphoryloxy, and nitro. It is noteworthy that many of the diphenyl ethers contain a glycolate or a lactate moiety in the substituent Y, e.g. lactofen, fluoroglycofen ethyl.

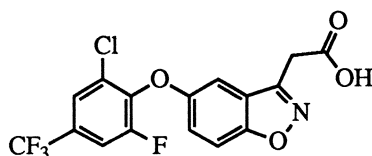
A second subclass of the diaryl ethers encompasses the heterocyclyl phenyl ethers. In this group of protox inhibitors, one of the aryl rings of the ether is an aromatic heterocycle. Some members of this subclass are listed in Table III. The pyrazolyl, pyridyl and furyl ring systems have been investigated as the heterocyclic component. As in the diphenyl ethers, the trifluoromethyl and chloro substituents are common to the Ar_1 aromatic ring, while the nitro and a variety of Y groups are substituents on the Ar_2 aromatic ring. A special group of heterocyclyl phenyl ethers results when X and Y of aryl ring Ar_2 are linked together to form a heterocyclic ring. In these cases, highest herbicidal activity is generally observed when R_3 of aryl ring Ar_1 is fluoro. A few recently reported examples include the 6-aryloxy-1H-benzotriazoles (16), the 5-aryloxyindolin-2(3H)-ones (17, 18), the 5-aryloxybenzisoxazoles (19), and the 6-aryloxyquinoxalin-2,3-diones. Specific examples of each of these systems are compounds 1 (EP 367 242; American Cyanamid), 2 (USP 4,911,754; American Cyanamid), 3 (USP 5,176,737; ICI), and 4 (GB 2,253,846; ICI), respectively. To date, none of the members of this subclass has been commercially developed.



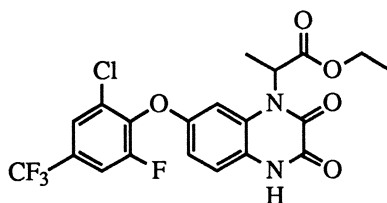
1



2



3



4

Table II.
Diphenyl Ethers

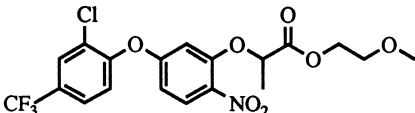
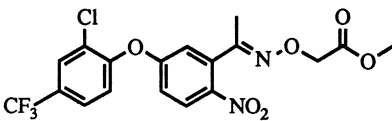
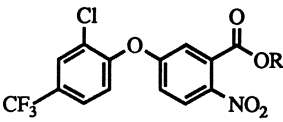
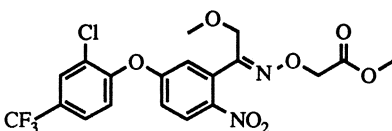
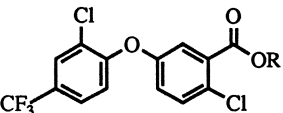
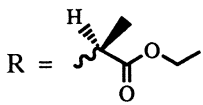
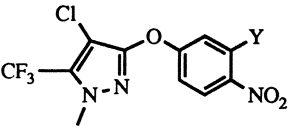
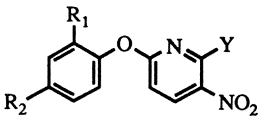
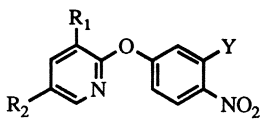
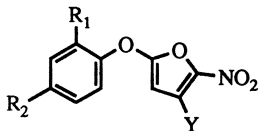
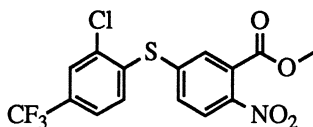
Structure	Code	Patent Reference
	CGA 84446 (20)	USP 4,221,581 (Ciba-Geigy)
	PPG 1013 (7, 10)	USP 4,344,789 (PPG)
	R = Me, RH 5782 (7, 8, 11, 12) R = Et, RH 8817 (21)	USP 3,928,416 (Rohm & Haas)
	AKH 7088 (8, 22)	USP 4,708,734 (Asahi)
	R = Me, LS 820 340 (11)	USP 3,957,852 (Ishihara)
	HC-252 (23)	USP 5,072,022 (Budapest Vegyimuvek)

Table III.
Heterocyclyl Phenyl Ethers

<i>Structure</i>	<i>Code</i>	<i>Patent Reference</i>
	Y = H, AH 2.430 (24) Y = COOH, AH 2.431 (24)	USP 4,964,895 (Monsanto)
	(25)	USP 4,493,730 (Ishihara) USP 4,547,218 (Dow)
	(25)	USP 4,539,039 (Dow) USP 4,326,880 USP 4,420,328 USP 4,626,275 (Ciba-Geigy)
		USP 4,382,814 (Rhône-Poulenc)

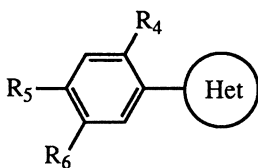
The bridging oxygen of the diaryl ethers can be replaced by sulfur. Although diaryl thioether **5** (RH 1460; USP 4,124,370; Rohm & Haas) is a potent Protox inhibitor comparable to methyl acifluorfen (RH 5782, Table II), it is nearly inactive *in vivo* (7).



5

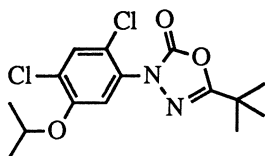
Phenyl Heterocycles

The second major class of Protox inhibitors is the phenyl heterocycle class, in which either a nitrogen (N-phenyl heterocycles) or a carbon atom (C-phenyl heterocycles) of the heterocyclic ring bears a usually 2,4,5-substituted phenyl moiety, as indicated below:



Generally, R_4 is fluoro or chloro, R_5 is chloro, and R_6 is variable; or R_5 and R_6 when linked together, form a heterocyclic ring. The N-phenyl heterocycles usually contain a carbonyl (or occasionally, thiocarbonyl) group adjacent to the nitrogen atom.

The first compound of this class to be commercially developed was oxadiazon **6** (USP 3,385,862; Rhone-Poulenc) (11, 26, 27). It is an oxadiazolone, and representative of the usual phenyl substitution pattern for this class.

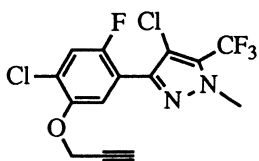


6

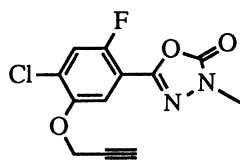
In recent years, the N-phenyl heterocycles have received considerable attention, due in large part to the discovery that a fluorine substituent in the 2-position ($R_4 = F$) of the phenyl ring markedly increased herbicidal activity. Over a dozen different heterocycles have appeared in published patent applications, and the number is steadily increasing. These heterocyclic systems are listed in Table IV along with the system name and patent references. Proforms and/or derivatives of especially the imides, hydantoin, and triazolodiones are also found in the patent literature. The last system in Table IV, the N-phenyl pyrazoles, is notable for its lack of carbonyl functionality in the heterocyclic ring.

Compounds from several of these subclasses have been or are presently being investigated as developmental herbicides. Some of these are shown in Table V. The imide, triazolone, tetrazolone, uracil, pyrazole, and oxazolodione systems are all represented.

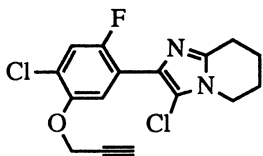
The C-phenyl heterocycle subclass is an emerging one based on very recent patent activity. Although presently smaller than the N-phenyl heterocycle subclass, the C-phenyl heterocycle subclass is likely to increase in size with additional research. Presently, this subclass includes the 3-phenylpyrazoles represented by **7** (WO 92/06962; Monsanto), the 5-phenyloxadiazolones such as **8** (JP 3066656A; Mitsubishi), the 2-phenyltetrahydroimidazopyridines such as **9** (DE 4120108; Schering) and the 3-phenylisoxazoles such as **10** (28).



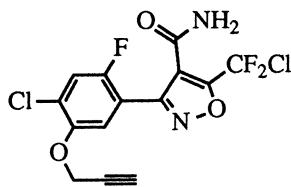
7



8

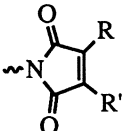
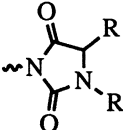
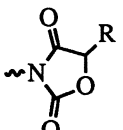
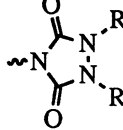
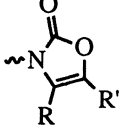
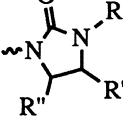
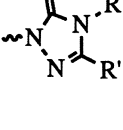


9



10

Table IV.
N-Phenyl Heterocycle Systems

<i>Heterocycle Structure</i>	<i>System Name</i>	<i>Patent Reference</i>
	Imides (29, 30)	USP 4,484,941 USP 4,640,707 USP 4,770,695 USP 4,938,795 (Sumitomo)
	Hydantoins	EP 311 135 (Schering) EP 493 323 (Sandoz)
	Oxazolodiones	USP 5,198,013 (Sagami)
	Triazolodiones	USP 4,619,687 (Sumitomo)
	Oxazolones	WO 92/12139 (Sankyo)
	Imidazolidinones	EP 484 776 (Bayer)
	Triazolones	USP 4,818,275 (FMC) JP 92079337 (Nihon)

Continued on next page

Table IV. (continued)

N-Phenyl Heterocycle Systems

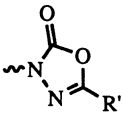
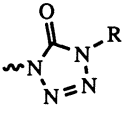
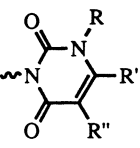
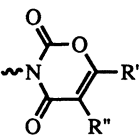
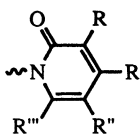
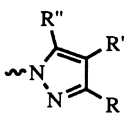
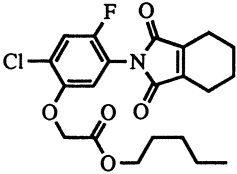
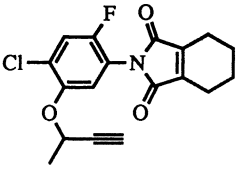
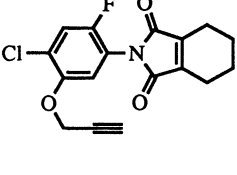
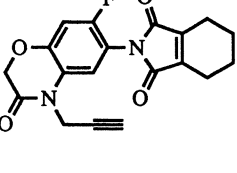
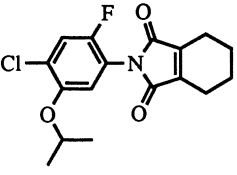
<i>Heterocycle Structure</i>	<i>Systems Name</i>	<i>Patent Reference</i>
	Oxadiazolones	USP 3,385,862 (Rhone-Poulenc)
	Tetrazolones	USP 5,136,868 (FMC)
	Uracils (10)	USP 5,169,430 (Uniroyal) EP 540 023 (Sumitomo) WO 92/11244 (Nissan)
	Oxazolinediones	EP 529 402 (Bayer)
	Pyridones	EP 488 220 (Sumitomo)
	Pyrazoles	USP 4,608,080 (Sumitomo) USP 4,804,675 USP 4,945,165 (Bayer) USP 4,666,507 (Nippon Kayaku) USP 4,752,326 (Hokko)

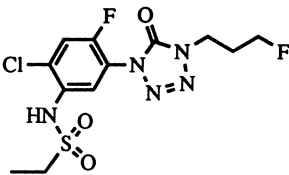
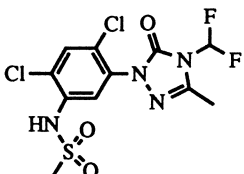
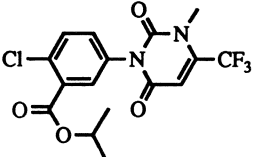
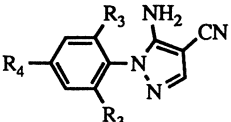
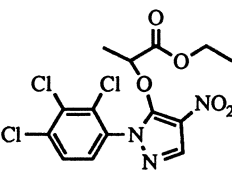
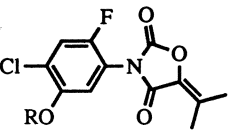

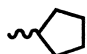
Table V.
N-Phenyl Heterocycles

<i>Structure</i>	<i>Code</i>	<i>Patent Reference</i>
	S 23031 V 23031 (flumiclorac pentyl)	USP 4,770,695 USP 4,938,795 (Sumitomo)
	S 23121 (flumipropyn) (6, 31)	USP 4,484,941 (Sumitomo)
	S 23142 (6, 21, 31-33)	USP 4,484,941 (Sumitomo)
	S 53482 (flumioxazin) (34)	USP 4,640,707 (Sumitomo)
	KS 307 829 (12)	USP 4,431,822 (Sumitomo)

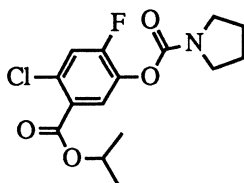
Continued on next page

Table V. (continued)

N-Phenyl Heterocycles

Structure	Code	Patent Reference
	F 5231 (35)	USP 5,136,868 (FMC)
	F 6285 (36)	USP 4,818,275 (FMC)
	UBI C4243 UCC C4243	USP 4,746,352 (Hoffmann-LaRoche) USP 4,943,309 USP 5,176,735 (Uniroyal)
	M & B 36701 R ₃ , R ₄ = H (12, 37) M & B 39279 R ₃ = Cl, R ₄ = CF ₃ (10, 12, 27, 37)	WO 92/10480 (BASF) USP 4,505,740 (May & Baker)
	TNPP ethyl (38)	EP 284 030 (Otsuka)
	BW - 3 R = 	USP 4,818,272 (Sagami)
	BW - 4 R = 	(39)

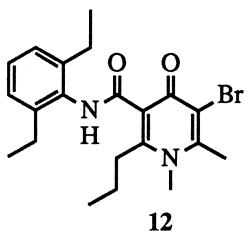
We have elected to include the O-phenylcarbamates (40, 41) represented by 11 (RH 1422; JP 2262573A; Mitsubishi) in the phenyl heterocycle class based on their 2,4,5-substituted phenyl ring.



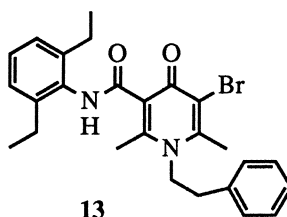
11

Heterocyclic Carboxamides

A third, presently smaller class of protox inhibitors is the heterocyclic carboxamide series. The pyridone carboxamide subclass is typified by 12

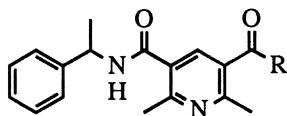


12



13

(DLH-1777; USP 4,844,732 and 4,943,314; Daicel) (42, 43) and 13 (USP 4,777,256; Daicel), whereas the pyridine carboxamide subclass is represented by 14 (LS 81 601) and 15 (LS 82 556; USP 4,566,899; Rhone-Poulenc) (12, 27, 44, 45).



14 R = OMe

15 R = Et

Biochemical investigations, demonstrating competitive binding of acifluorfen (a diaryl ether), oxadiazon and the imide KS 307 829 (N-phenyl heterocycles), and LS 82 556 (a heterocyclic carboxamide) to Protox (12, 13), suggest some structural relatedness between these three classes of protox inhibitors. The foregoing survey and classification should prove useful in the analysis of similarities between classes and may aid in the discovery of other novel inhibitors.

Acknowledgment. We gratefully acknowledge the valuable assistance of Martha Manion for conducting the patent searches.

Literature Cited

1. Matsunaka S. *J. Agric. Food Chem.* **1969**, *17*, 171-5.
2. Kunert, K. J.; Dodge, A. D. In *Target Sites of Herbicide Action*; Böger, P.; Sandmann, G., Eds.; CRC Press, Inc: Boca Raton, FL, 1989; pp 45-63.
3. Matringe, M.; Camadro, J.-M.; Labbe, P.; Scalla, R. *Biochem. J.* **1989**, *260*, 231-5.
4. Haworth, P.; Hess, F. D. *Plant Physiol.* **1988**, *86*, 672-6.
5. Duke, S. O.; Lydon, J.; Paul, R. N. *Weed Sci.* **1989**, *37*, 152-60.
6. Oshio, H.; Shibata, H.; Mito, N.; Yamamoto, M.; Harris, E. H.; Gillham, N. W.; Boynton, J. E.; Sato, R. *Z. Naturforsch.* **1993**, *48c*, 339-44.
7. Nandihalli, U. B.; Duke, M. V.; Duke, S. O. *Pestic. Biochem. Physiol.* **1992**, *43*, 193-211.
8. Osabe, H.; Morishima, Y.; Goto, Y.; Fujita, T. *Pestic. Sci.* **1992**, *35*, 187-200.
9. Yih, R. Y.; Swithenbank, C. *J. Agric. Food Chem.* **1975**, *23*, 592-3.
10. Akagi, T.; Sakashita, N. *Z. Naturforsch.* **1993**, *48c*, 345-9.
11. Camadro, J.-M.; Matringe, M.; Scalla, R.; Labbe, P. *Biochem. J.* **1991**, *277*, 17 21.
12. Matringe, M.; Mornet, R.; Scalla, R. *Eur. J. Biochem.* **1992**, *209*, 861-8.
13. Varsano, R.; Matringe, M.; Magnin, N.; Mornet, R.; Scalla, R. *FEBS Lett.* **1990**, *272*, 106-8.
14. Colby, S. R.; Barnes, J. W.; Sampson, T. A.; Shoham, J. L.; Osborn, D. J. *10th International Congress of Plant Protection 1983*; British Crop Protection Council: Croydon, England, 1983; Vol. 1, pp 295-302.
15. Maigrot, P. H.; Perrot, A.; Hede-Hauy, L.; Murray, A. *Brighton Crop Protection Conference, Weeds-1989*; British Crop Protection Council: Farnham, England, 1989; Vol. 1, pp 47-51.
16. Condon, M. E.; Arthen, F. J.; Birk, J. H.; Crews, A. D.; Lavanish, J. M.; Lies, T. A.; Nielsen, D. R. 205th ACS National Meeting, Denver, CO, March 1993, Agro 14.
17. Karp, G. M. *J. Org. Chem.* **1992**, *57*, 4765-72.
18. Karp, G. M.; Arthen, F. J.; Birk, J. H.; Condon, M. E.; Hunt, D. A.; Lavanish, J. M.; Marc, P. A.; Schwindeman, J. A. 205th ACS National Meeting, Denver, CO, March 1993, Agro 15.
19. Wepplo, P. J.; Birk, J. H.; Lavanish, J. M.; Manfredi, M. C.; Nielsen, D. R. 205th ACS National Meeting, Denver, CO, March 1993, Agro 16.
20. Gerber, H. R.; Maurer, W. *British Crop Protection Conference, Weeds-1982*, British Crop Protection Council: Croydon, England, 1982; Vol. 1, pp 39-45.
21. Sato, R.; Oshio, H.; Koike, H.; Inoue, Y.; Yoshida, S.; Takahashi, N. *Plant Physiol.* **1991**, *96*, 432-7.
22. Hayashi, Y.; Kouji, H.; Osada, H. *Brighton Crop Protection Conference, Weeds-1989*; British Crop Protection Council: Farnham, England, 1989; Vol. 1, pp 53-8.
23. Bakos, J.; Eifert, G.; Bihari, F.; Nagy, M. *Brighton Crop Protection Conference*,

- Weeds-1991*; British Crop Protection Council: Farnham, England, 1991; Vol. 1, pp 83-6.
24. Sherman, T. D.; Duke, M. V.; Clark, R. D.; Sanders, E. F.; Matsumoto, H.; Duke, S. O. *Pestic. Biochem. Physiol.* **1991**, *40*, 236-45.
 25. Fujikawa, K.; Kondo, K.; Yokomichi, I.; Kimura, F.; Haga, T.; Nishiyama, R. *Agr. Biol. Chem.* **1970**, *34*, 68-79.
 26. Burgaud, L.; Deloraine, J.; Desmoras, J.; Guillot, M.; Petrinko, P.; Riotto, M. *3rd Symposium on New Herbicides, Proceedings of the European Weed Research Council*; 1969; Vol. 1, pp 201-36 (*Weed Abstracts*, **1970**, *19*, 387).
 27. Matringe, M.; Camadro, J.-M.; Labbe, P.; Scalla, R. *FEBS Lett.* **1989**, *245*, 35-8.
 28. Hamper, B. C.; Leschinsky, K. L.; Massey, S. M.; Bell, C. L.; Prosch, S. D. 206th ACS National Meeting, Chicago, IL, August 1993, Agro 3.
 29. Watanabe, H.; Otori, Y.; Sandmann, G.; Wakabayashi, K.; Böger, P. *Pestic. Biochem. Physiol.*, **1992**, *42*, 99-109.
 30. Nicolaus, B.; Sandmann, G.; Böger, P. *Z. Naturforsch.* **1993**, *48c*, 326-33.
 31. Mito, N.; Sato, R.; Miyakado, M.; Oshio, H.; Tanaka, S. *Pestic. Biochem. Physiol.* **1991**, *40*, 128-35.
 32. Sato, R.; Nagano, E.; Oshio, H.; Kamoshita, K.; Furuya, M. *Plant Physiol.* **1987**, *85*, 1146-50.
 33. Sato, R.; Nagano, E.; Oshio, H.; Kamoshita, K. *Pestic. Biochem. Physiol.* **1987**, *28*, 194-200.
 34. Yoshida, R.; Sakaki, M.; Sato, R.; Haga, T.; Nagano, E.; Oshio, H.; Kamoshita, K. *Brighton Crop Protection Conference, Weeds-1991*; British Crop Protection Council: Farnham, England, 1991; Vol. 1, pp 69-75.
 35. Theodoridis, G.; Hotzman, F. W.; Scherer, L. W.; Smith, B. A.; Tymonko, J. M.; Wyle, M. J. *Pestic. Sci.* **1990**, *30*, 259-74.
 36. Van Saun, W. A.; Bahr, J. T.; Crosby, G. A.; Fore, Z. Q.; Guscar, H. L.; Harnish, W. N.; Hooten, R. S.; Marquez, M. S.; Parrish, D. S.; Theodoridis, G.; Tymonko, J. M.; Wilson, K. R.; Wyle, M. J. *Brighton Crop Protection Conference, Weeds-1991*; British Crop Protection Council: Farnham, England, 1991; Vol. 1, pp 77-82.
 37. Matringe, M.; Camadro, J.-M.; Block, M. A.; Joyard, J.; Scalla, R.; Labbe, P.; Douce, R. *J. Biol. Chem.* **1992**, *267*, 4646-51.
 38. Yanase, D.; Andoh, A. *Pestic. Biochem. Physiol.* **1989**, *35*, 70-80.
 39. Kohno, H.; Hirai, K.; Hori, M.; Sato, Y.; Böger, P.; Wakabayashi, K. *Z. Naturforsch.* **1993**, *48c*, 334-8.
 40. Nandihalli, U. B.; Sherman, T. D.; Duke, M. V.; Fisher, J. D.; Musco, V. A.; Becerril, J. M.; Duke, S. O. *Pestic. Sci.* **1992**, *35*, 227-35.
 41. Nandihalli, U. B.; Duke, M. V.; Duke, S. O. *J. Agric. Food Chem.* **1992**, *40*, 1993-2000.
 42. Morishima, Y.; Osabe, H.; Goto, Y. *J. Pestic. Sci.* **1990**, *15*, 553-9.
 43. Osabe, H.; Morishima, Y.; Goto, Y.; Masamoto, K.; Nakagawa, Y.; Fujita, T. *Pestic. Sci.* **1992**, *34*, 17-25.
 44. Matringe, M.; Dufour, J. L.; Lherminier, J.; Scalla, R. *Pestic. Biochem. Physiol.* **1986**, *26*, 150-9.
 45. Matringe, M.; Scalla, R. *Plant Physiol.* **1988**, *86*, 619-22.

RECEIVED December 14, 1993

Chapter 3

Synthesis of Protoporphyrinogen Oxidase Inhibitors

Robert D. Clark

Monsanto Company, 800 North Lindbergh Boulevard,
St. Louis, MO 63167

An overview of general synthetic approaches to inhibitors of protoporphyrinogen oxidase is presented. Categories covered include diphenyl and pyrazole nitrophenyl ethers; pyridone carboxanilides; phenyl uracils and carbamates; *C*- and *N*-phenyl pyrazoles; *N*-phenyl cyclic imides; oxadiazon; triazinediones; tetrazolones; and triazolidinone herbicides.

An exhaustive review of the enormous range of literature covered by the title is far beyond the scope of this paper. Instead, an effort is made to touch on general synthetic routes for herbicide classes discussed by other contributors to this symposium, while including those specific examples most often cited within each class as end-products. Acifluorfen and oxyfluorfen, for instance, were taken as archetypal diphenyl ethers. Such common names are used where possible to facilitate cross-reference with the biochemical and physiological literatures. To the same end, more arbitrary serial designations (*e.g.*, DLH-1777) are alluded to where they have been published.

Early preparative steps have been generalized as much as possible, in the hope of providing information useful for synthesis of analogs for studying quantitative structure/activity relationships (QSAR).

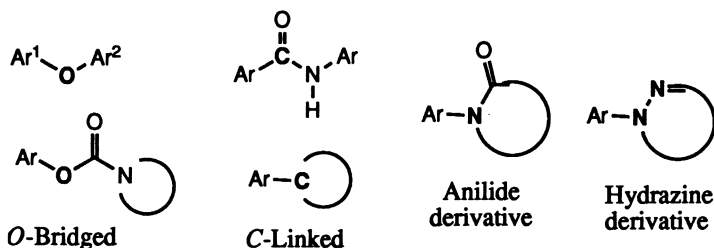
Because of space limitations, references are not necessarily to earliest publications. A conscious effort was made to preferentially cite literature which includes experimental details specific to archetypal examples of each class while at the same time maintaining generality. For ease of general access, reports from refereed journals and United States patents have been cited where available. In addition, more efficient synthetic methods are cited in most cases to the exclusion of less efficient methods published earlier.

0097-6156/94/0559-0034\$08.00/0
© 1994 American Chemical Society

Organization

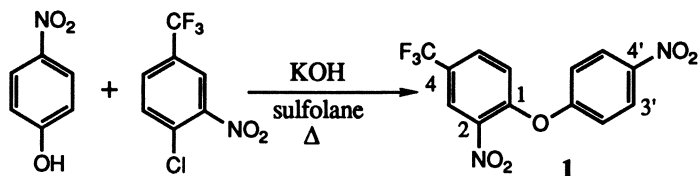
Most if not all protoporphyrinogen oxidase (Protox) inhibitors which have been identified to date are comprised of an aryl ring linked to some other cyclic functionality, which may or may not itself be aromatic. The different bridging groups involved provide a convenient way to organize a discussion of the synthetic methods used in preparation of the various classes. *O*-Bridged inhibitors include aryl nitrophenyl ethers such as acifluorfen, oxyfluorfen and pyrazole phenyl ethers, as well as phenyl carbamates such as phenopylate. For purposes of discussion, *C*-linked inhibitors are taken here to include all ketoaryl derivatives, encompassing pyridones such as DLH-1777 as well as *C*³-phenyl pyrazoles.

There are so many distinct classes of *N*-linked Protox inhibitors that it is useful to distinguish anilide derivatives from those prepared from phenyl hydrazines. The former group includes the *N*-phenyl uracils (*e.g.*, UCC-C4243) and *N*-phenyl cyclic imides such as chlorophthelim, S 23142 and KS 307829. Hydrazine derivatives include oxadiazon and *N*-aryl pyrazoles such as TNPP-Ethyl and M&K 39279, as well as triazinediones, tetrazolones and triazolidinones (*e.g.*, F6285).



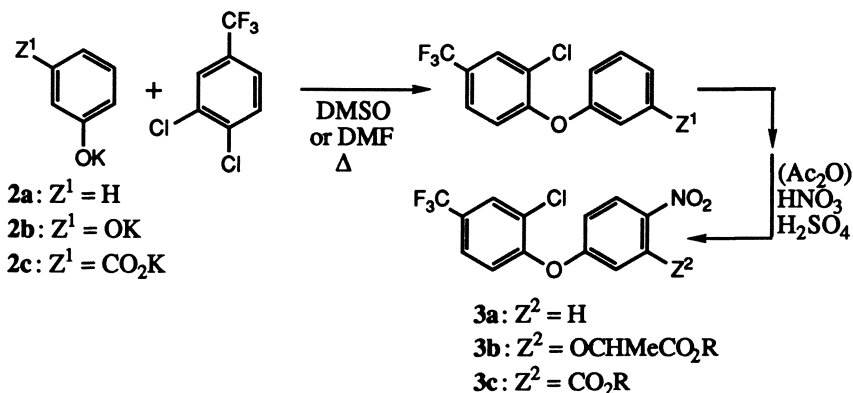
O-Bridged Inhibitors

Diphenyl ethers. The central reaction of nitrodiphenyl ether synthesis is generally coupling of a phenolate anion with a halophenyl ring activated toward aromatic nucleophilic substitution. Fluorodifen (**1**) and other 2,4'-dinitrophenylethers are readily prepared in this way (*1*).

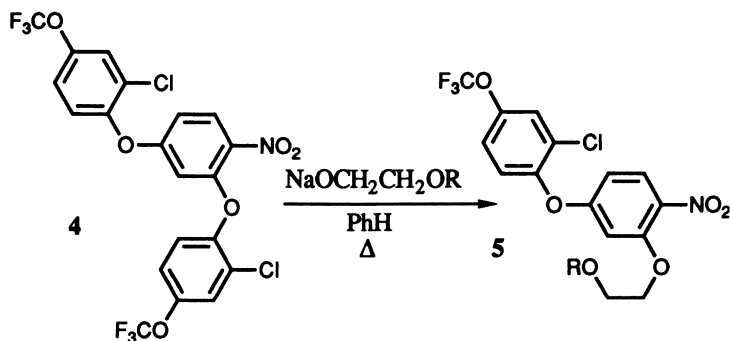


Such direct syntheses require rather harsh conditions and do not work well for less activated substrates such as 3,4-dichlorobenzotrifluorides, nor for more weakly nucleophilic phenols such as 5-hydroxy-2-nitrobenzoate. A more general approach is to condense a phenolate salt **2** with an aryl halide and nitrate afterwards in mixed acids, with acetic

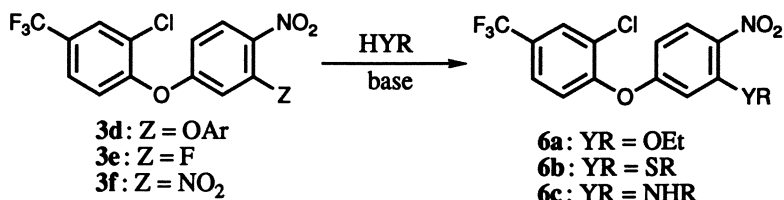
anhydride often being a useful co-solvent. Somewhat surprisingly, the latter reaction is usually quite regiospecific, giving the *para* nitrophenyl ether **3** as the major or exclusive product. Often an intermediate transformation of phenyl substituent Z (e.g., alkylation of a phenol or carboxylate) is involved. Chlorination and other electrophilic substitutions can also be carried out at the 4' position (2).



Adducts such as **3** may themselves be products of interest, as is the case for nitrofluorfen (**3a**) (3), acifluorfens (**3c**) (4,5), or lactate ethers (**3b**) (6). More often, they serve as substrates activated toward subsequent aromatic nucleophilic substitution. This tactic is general, and particularly useful for synthesis of 3'-polyethers such as **5** from sodium alkoxyethanolates (7) (an unusual example in which the 4-substituent is a trifluoromethoxy group). The simplest method entails exhaustive arylation of resorcinol, followed by nitration to an adduct such as **4**. Note that symmetry of substitution effectively increases the regioselectivity of nitration, and that subsequent phenolate displacement takes place almost exclusively *ortho* to the nitro group. This route is highly advantageous for large-scale syntheses where chromatographic separations may be impractical. Note, too, that **5** and analogous compounds cannot be obtained by direct alkylation of (nitro)phenolic intermediates.

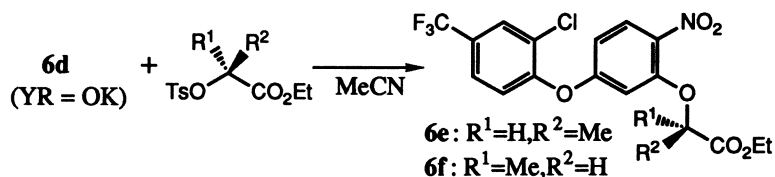


Triaryl diether **3d** has also been used in the preparation of oxyfluorfen (**6a**) (3,8,9), as has the 3'-fluoro **3e**. Unlike the diether, the fluoride can be converted to 3'-thioethers **6b** as well (10). The 3',4'-dinitrophenyl ether **3f**, prepared from *m*-nitrophenol, is even more versatile in that it can readily react with amines to form **6c** (11).



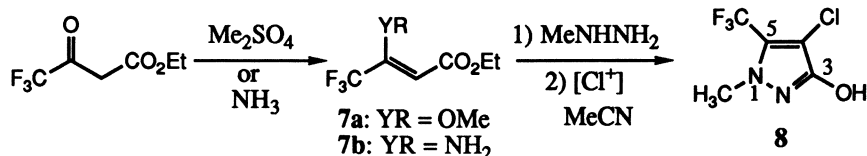
Introducing either an amino or a thioether functionality before nitration would likely lead to oxidation by-products. The broader applicability of 3'-fluoro **3e** may be offset, however, by reduced regioselectivity of nitration. The reported yield of 3'-nitro **3f**, on the other hand, is 91% (11).

Chiral lactate diphenyl ethers **6e** (RH-4638) and **6f** (RH-4639) can be prepared from the tosylates of ethyl (*S*)- and (*R*)-lactate, respectively, and potassium phenolate **6d** with clean inversion at the α -carbon (12).



5-Trifluoromethyl-2-pyridyl nitrophenyl ethers can also be prepared by displacement of chloride from precursors with phenolates (13).

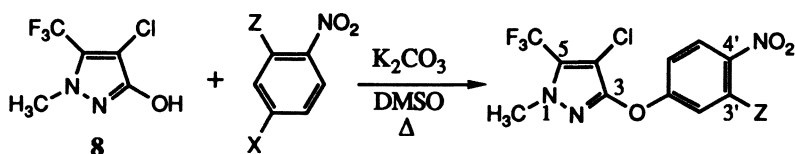
Pyrazole nitrophenyl ethers, in contrast to the usual case for diphenyl ethers, are synthesized from 4-halonitrobenzenes and 3-hydroxypyrazole **8**. The latter is prepared by reaction of the enamine **7a** or the enol ether **7b** of ethyl trifluoroacetoacetate with methyl hydrazine (14), followed by chlorination with 1,3-dichloro-5,5-dimethylhydantoin.



Direct condensation of trifluoroacetoacetate with methylhydrazine yields primarily (15) the 5-hydroxy pyrazole isomer, nitrophenyl ethers of which are much less potent herbicides (16). The 5-hydroxy isomer is a

minor component in preparations from enol ether **7a** or enamine **7b**, but is easily removed since its much higher acidity renders it soluble in bicarbonate. Hydroxypyrazole **8** can also be prepared from 4,4,4-trifluorobutyrate esters (**17**); methods for synthesizing other hydroxypyrazoles, including 5-methanesulfonyl analogs, are given in detail elsewhere (**18**).

2-Heterosubstituted nitrobenzenes **9b-c** may be prepared from 2,4-difluoronitrobenzene and subsequently coupled with hydroxypyrazole **8** to yield the respective 3'-amino, -alkoxy or -thioether products **10** (**18,19**); the 3'-unsubstituted **10a** is AH 2.430 (**16**).



9a: X = F, Z = H

9b: X = F, Z = OR

9c: X = F, Z = NR¹R²

9d: X = Cl, Z = CO₂R

10a: Z = H

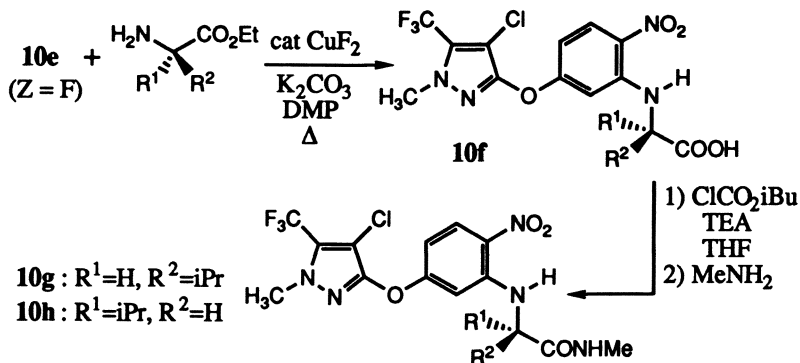
10b: Z = OR

10c: Z = NR¹R²

10d: Z = CO₂R

The nitrobenzoate **9d** is activated enough to undergo reaction as an aryl chloride to afford the acifluorfen analog AH 2.431 (**10d**, R = H), which is only very weakly herbicidal (**16**). In cases such as **10a** and **10d**, where the nitrophenyl ring in the product is not too activated towards electrophilic attack, it may be better to chlorinate the pyrazole ring after formation of the pyrazole phenyl ether rather than before coupling has been carried out.

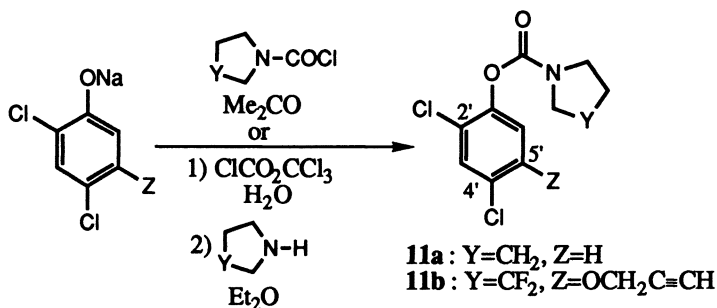
Chiral *N*-pyrazoloxypyphenyl amino acids **10f** are readily synthesized from the 3'-fluoro **10e** with excellent retention of configuration by using catalytic copper fluoride in *N*-methylpyrrolidinone (NMP) (**12**). Conversion to the corresponding amides **10g-h** (AH 4.441 and AH 4.442, respectively) is by way of the mixed anhydrides.



10g: R¹=H, R²=iPr

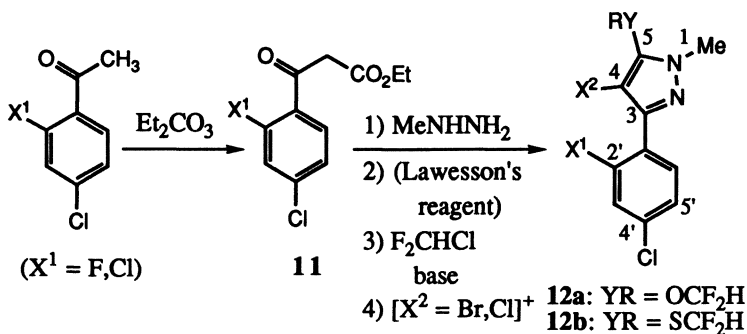
10h: R¹=iPr, R²=H

Phenyl carbamates, like 3'-alkoxy diphenyl ethers, are prepared from halophenols or haloresorcinols. Phenopylate (**11a**), for instance, is made by reaction of 2,4-dichlorophenol with a carbamoyl chloride (*20*); the latter is made using phosgene. Although 5'-substituted analogs such as RH 0978 (**11b**) can also be prepared this way (*21*), an alternative route (*22*) using trichloromethyl chloroformate (Diphosgene®) is to be preferred on a laboratory scale.



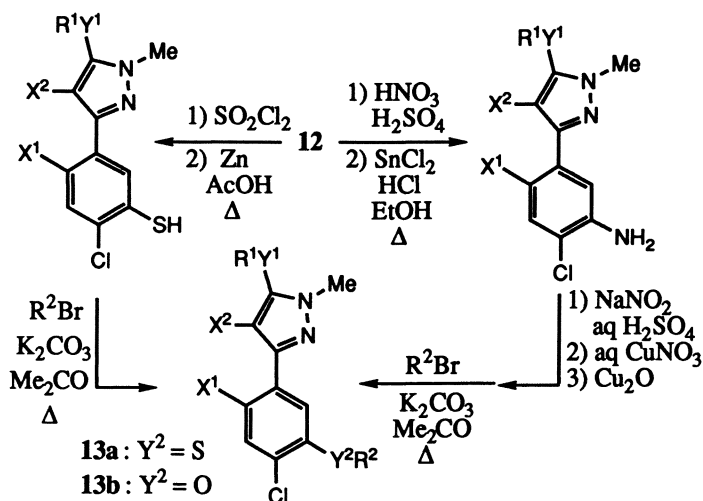
C-Bridged Inhibitors

C³-Aryl pyrazoles fall into two synthetic categories distinguished by the first steps in their respective syntheses. The 5-alkoxy compounds **13** are derived from benzoylacetates **11** formed by condensation of dihaloacetophenones with diethyl carbonate (*23*). Methylhydrazine reacts with **11** to afford hydroxyarylpiprazoles, which can then be alkylated and halogenated to give, for example, **12a**. Intervening reaction with Lawesson's reagent yields thioethers such as **12b**.

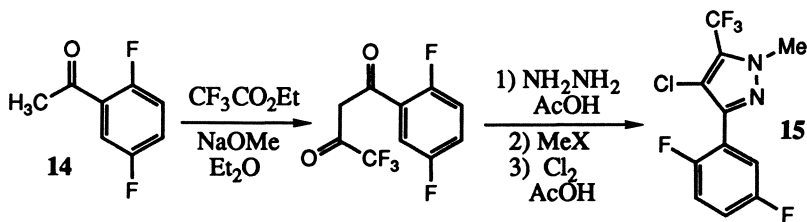


Further elaboration can be accomplished by electrophilic substitution

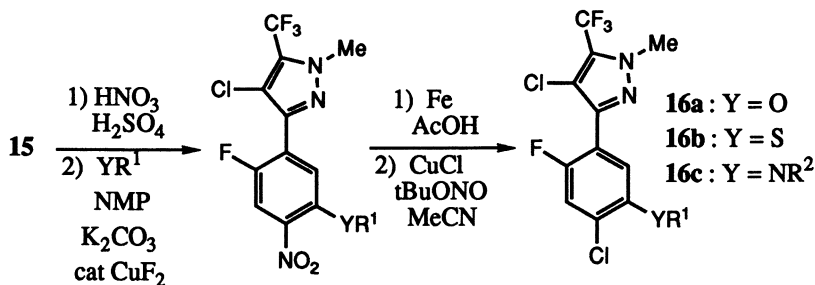
of the phenyl ring, followed by reduction and alkylation, typically with propargyl bromide or with a bromopropionate ester. Thus, chloro-sulfonylation leads to thioethers **13a**, whereas alkoxy analogs **13b** require a moderately efficient (46% yield) diazotization step following nitration and reduction.



3-Phenyl-5-fluoroalkyl analogs **16** are synthesized by a rather different route beginning with 2,5-difluoroacetophenone **14** (**24**). The product is condensed with trifluoroacetate, then with hydrazine. Alkylation and chlorination give the desired 3-phenylpyrazole isomer **15**.

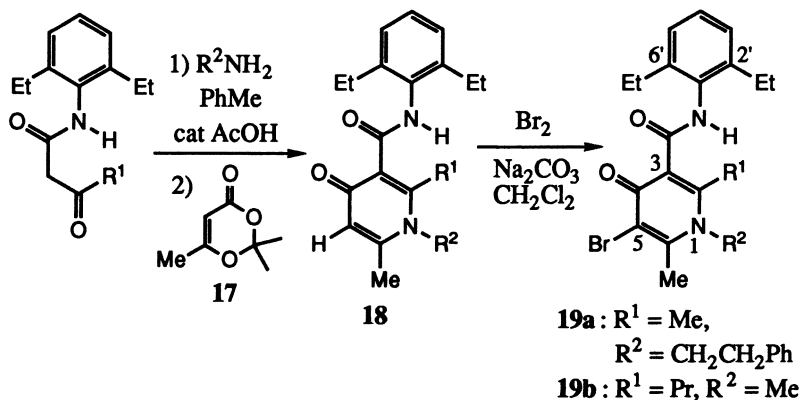


Nitration allows heterosubstituents to be introduced at the 5'-position by nucleophilic aromatic substitution utilizing catalytic copper fluoride in *N*-methylpyrrolidinone. Reduction with elemental iron followed by Sandmeyer diazonium chemistry yields the target compounds **16a-c**.



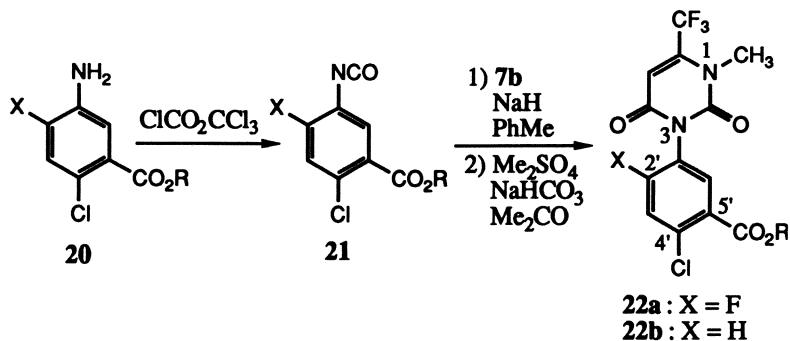
5'-Alkoxy analogs such as propargyl ethers are not directly accessible by this route. As an alternative, methoxy precursors (**16a**, $\text{YR}^1 = \text{OMe}$) can be cleaved with boron tribromide in methylene chloride, and the phenols obtained reacted with alkylbromide in dimethylformamide (**24**).

Pyridone carboxanilides are synthesized by condensation of a primary amine with an acylacetanilide and enol lactone **17** to give the parent pyridone carboxanilide **18**, which can be brominated regioselectively at C⁵ on the pyridone ring, even when the pendant N¹ substituent is an electron-rich aryl (**19a**) (**25**). Among the most active examples described to date is DLH-1777 (**19b**) (**26**).



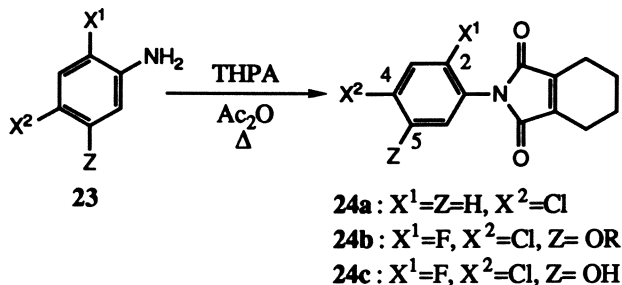
Anilide derivatives

Carbonylphenyl uracils. The published synthesis of these herbicides begins from isocyanate **21** (**27**), which can be prepared from aniline precursor **20**. This is condensed with trifluoromethyl enamine **7b** and alkylated to yield carboxyphenyl uracils **22**.

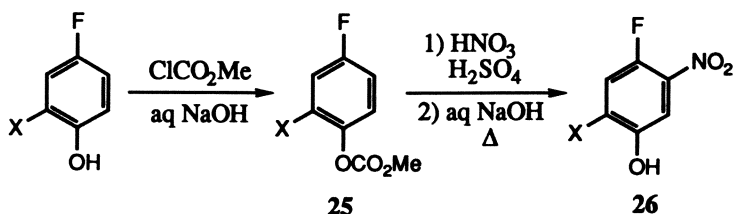


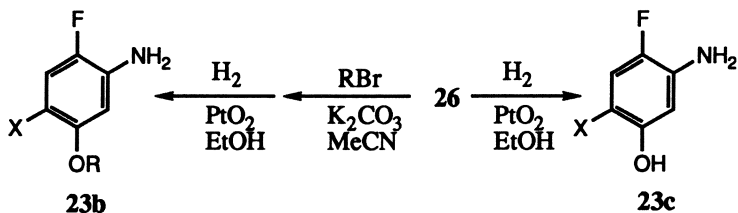
If an ester other than ethyl is desired in the final product, as is the case for UCC-C4243 (**22b** where R = *i*Pr), the ester may be introduced early in the synthesis by acid-catalyzed transesterification of **20**, or, later, by hydrolysis and re-esterification of **22**.

N-Phenyl imides are synthesized by reaction of substituted haloanilines **23** with tetrahydrophthalic anhydride (THPA). MK 616 (**24a**), for example, is prepared from the commercially available 4-chloroaniline (**28**).



More potent herbicidal analogs require more highly functionalized anilines, however. To obtain fluoroalkoxy derivatives such as KS 307829 (**24b**, R=*i*Pr), fluorohalophenol is protected by acylation to carbonate **25**, nitrated at *C*⁵ and then deprotected in base. Nitrophenol **26** so obtained can then be alkylated and reduced to give **23b**, a common intermediate key to synthesis of many *N*-phenylazole herbicides. Alkoxy anilines **23b** condense with THPA to yield imides **24b**.

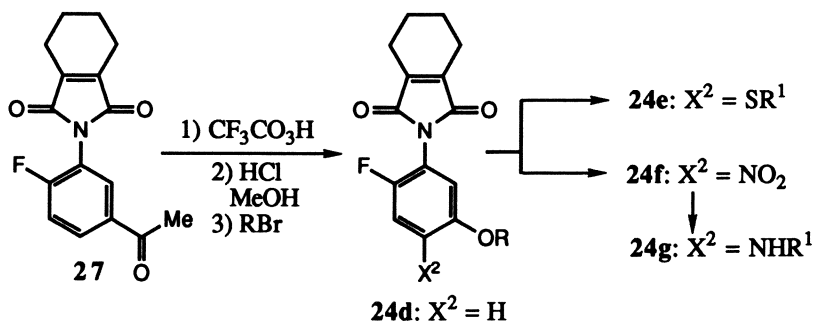




Nitrophenol **26** can also be reduced directly. The product aminophenol **23c** itself reacts cleanly with THPA to form the 5-hydroxyphenyl **24c**, which can then be alkylated. Published results suggest, however, that this alternative route gives a low overall yield (17% yield (**29**)). For those alkoxy substituents which may be sensitive to catalytic hydrogenation (*e.g.*, S 23142 (**24b**, R=propargyl)), the latter route may still be the preferred one.

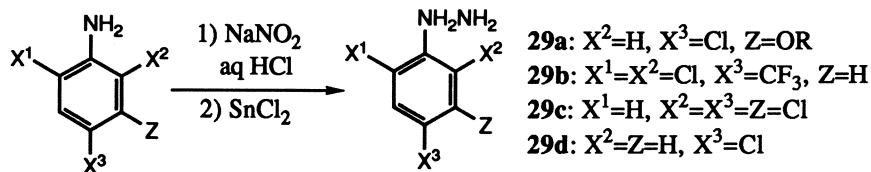
The strategy outlined above is restricted to those instances in which substituent X^2 is strongly *para*-directing: syntheses of analogs bearing *meta*-directing substituents require major departures from that route, as does preparation of 4'-unsubstituted imides (**24**, $X^2 = \text{H}$).

The imido acetophenone **27** can be prepared by reduction of the corresponding nitroacetophenone and reaction with THPA. Conversion to the alkoxy analog **24d** is accomplished by a Baeyer-Villiger oxidation, followed by hydrolysis and alkylation (**30**). Electrophilic substitutions and reduction then afford **24e-g**. 4'-Nitro **24f** is the most active of these analogs (**29**).



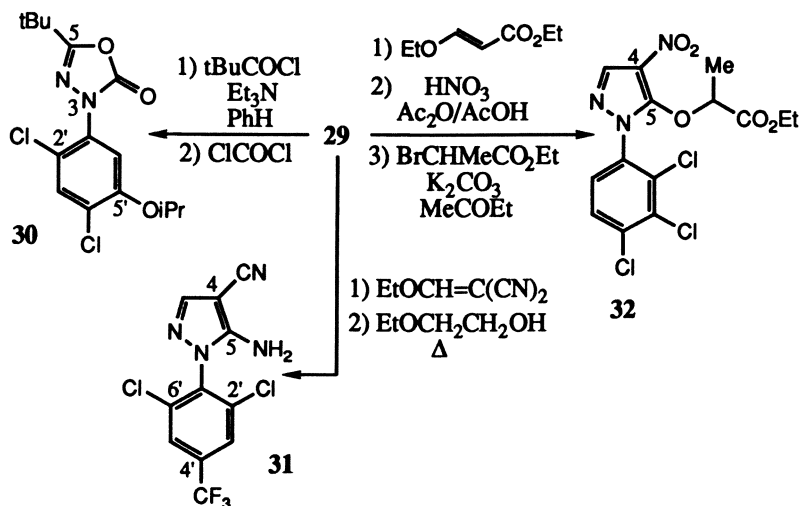
Phenyl Hydrazine Derivatives

There are several *N*-aryl heterocycle classes of Protox inhibitor which are derived from phenyl hydrazines. These are, in turn, prepared from various haloanilines by diazotization and reduction with stannous chloride.

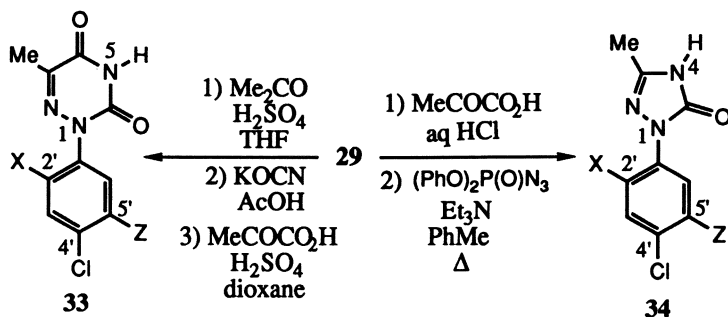


***N*-Aryl pyrazoles and oxadiazon.** Acylation of **29a** ($X^1=Cl$, $R=iPr$) with trimethylacetyl chloride and reaction of the resulting hydrazone with phosgene gives oxadiazon (**30**) (**31**). Condensation of phenylhydrazines with ethoxyacrylonitriles yields 5-aminopyrazoles, including the Protox inhibitor M&B 39279 (**31**) from hydrazine **29b** (**32**), whereas reaction with ethoxyacrylate esters affords 5-pyrazolones.

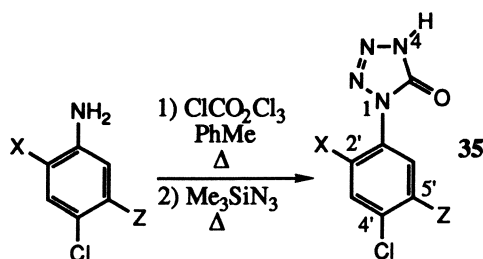
Nitration and alkylation of the pyrazolone derived from **29c** produces TNPP-ethyl (**32**) and analogous compounds (**33**). Note that although the particular herbicides cited are derived from specific hydrazines, the cyclization reactions are general. Subsequent transformations, however (such as regiospecific nitration of any *N*-(alkoxyphenyl)pyrazole prepared from **29a**), might well be difficult to achieve in particular cases.



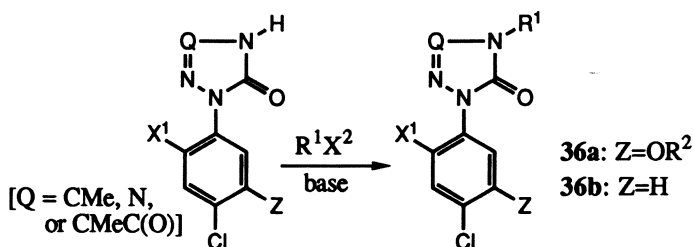
Triazinediones, tetrazolones and triazolidinones. Conversion of **29a** to a hydrazone and subsequent reaction with isocyanate and pyruvic acid gives triazinedione **33** (**34**), whereas reaction of **29** with pyruvic acid and phosphoryl azide gives triazolidinones **34** (**35,36**).



In a closely related reaction, tetrazolones **35** are formed from substituted anilines and trimethylsilyl azide (**37**).

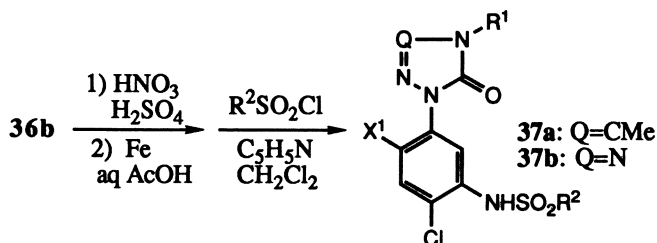


All three classes of chemistry must be *N*-alkylated to elicit full herbicidal activity. The most potent triazinediones (**36a**, Q=CMeC(O)) bear an *N*⁵-methyl group, whereas the most active tetrazolones (**36a**, Q=N) and triazolidinones (**36a**, Q=CMe) bear *N*⁴- fluoropropyl and difluoromethyl groups, respectively.



The first two alkylation reactions proceed in good yield, but the reaction of triazolidinone **34** with Freon-22 (CF₂HCl) is problematic. Potassium hydroxide as base in tetrahydrofuran, using phase transfer catalysis, gives a rather poor yield, and delaying that alkylation until later in the synthetic sequence does not improve the situation (**35**). A subsequent publication (**38**) describes running this reaction with potassium carbonate as base in dimethylformamide, but yields were not given.

O-Alkylation completes the synthesis for 5'-alkoxy herbicides (**36a**) (**35**). The more widely cited analogs, however, are 5'-sulfonamido analogs such as triazolidinone F6285 (**37a**, X¹=Cl, R¹=CHF₂, R²=Me) prepared from 5'-unsubstituted **36b** (**36,38**) by nitration, reduction and sulfonylation.



An alternative preparation of tetrazolone **37b** ($X^1=F$) by regioselective reduction of 2-fluoro-1,5-dinitrobenzene has also been reported (39); the chloro group is introduced subsequently by electrophilic substitution from sulfuryl chloride.

Acknowledgements

The Author wishes to thank Carl Hubenschmidt for indispensable bibliographic support. Kurt Moedritzer and Bruce C. Hamper provided access to key background literature. Along with James I. McLoughlin and Richard J. Anderson, they also provided helpful suggestions with regard to style and composition.

Literature Cited

1. Martin, H.; Aebi, H.; Ebner, L. U.S. Patent 3322525, 1967, Ciba Ltd.
2. Takahashi, R.; Fujikawa, K.; Yokomichi, I.; Toki, T.; Someya, S. U.S. Patent 3966453, 1976, Ishihara Sangyo Kaisha Ltd.
3. Yih, R.Y.; Swithenbank, C. *J. Agric. Food Chem.*, **1975**, *23*, 592.
4. Johnson, W.O. U.S. Patent 4031131, 1977, Rohm and Haas Co.
5. Johnson, W.O.; Kollman, G.E.; Swithenbank, C.; Yih, R.Y. *J. Agric. Food Chem.* **1976**, *26*, 705.
6. Rohr, O.; Pissiotas, G.; Bohner, B. U.S. Patent 4221581, 1980, Ciba-Geigy Corporation.
7. Hiraga, K.; Shibayama, S.; Yanai, I.; Harada, T. U.S. Patent 4226616, 1980, Nihon Nohyaku Company, Ltd.
8. Bayer, H.O.; Swithenbank, C.; Yih, R.P. U.S. Patent 4046798, 1977, Rohm and Haas Company.
9. Bayer, H.O.; Swithenbank, C.; Yih, R.Y. U.S. Patent 3798276, 1974.
10. Rohe, L.; Schramm, J.; Klauke, E.; Eue, L.; Schmidt, R.R. U.S. Patent 4104313, 1978, Bayer Aktiengesellschaft.
11. Yoshimoto, T.; Igarashi, K.; Oda, K.; Ura, M.; Sato, N. U.S. Patent 4277624, 1981, Mitsui Toatsu Chemicals, Inc.
12. Nandihalli, U.J.; Duke, M.V.; Ashmore, J.W.; Musco, V.A.; Clark, R.D.; Duke, S.O. *Pestic. Sci.*, **1994**, in press
13. Nishiyama, R.; Fujikawa, K.; Haga, T.; Toki, T.; Komyoji, T.; Saka-shita, N.; Maedea, K. U.S. Patent 4235621, 1980, Ishihara Sangyo Kaisha Ltd.
14. Gaede, B.J.; Torrence, L.L. U.S. Patent 4984902, 1990, Monsanto Company.
15. Lee, L.F.; Schleppe, F.M.; Schneider, R.W.; Campbell, J.W. *J. Heterocyclic Chem.*, **1990**, *27*, 243.
16. Sherman, T.D.; Duke, M.V.; Clark, R.D.; Sanders, E.F.; Matsumoto, H.; Duke, S.O. *Pestic. Biochem. Physiol.*, **1991**, *40*, 236.
17. Hamper, B.C.; Kurtzweil, M.L.; Beck, J.P. *J. Org. Chem.*, **1992**, *57*, 5680.
18. Moedritzer, K.; Allgood, S.G.; Charumilind, P.; Clark, R.D.; Gaede, B.J.; Kurtzweil, M.L.; Mischke, D.A.; Parlow, J.J.; Rogers, M.D.; Singh, R.K.; Stikes, G.L.; Webber, R.K. in *Synthesis and Chemistry of Agrochemicals III*; Baker, D.R., Fenyves, J.G., Steffens, J.J., Eds.; ACS Symposium Series No. 504; ACS Press: Washington, D.C., 1992; pp. 147-160.

19. Moedritzer, K.; Rogers, M.D. U.S. Patent 4964895, 1990, Monsanto Company.
20. Weiss, A.G. U.S. Patent 3142556, 1964, Monsanto Company.
21. Nandihalli, U.B.; Sherman, T.D.; Duke, M.V.; Fisher, J.D.; Musco, V.A.; Becerril, J.M.; Duke, S.O. *Pestic. Sci.*, **1992**, *35*, 227.
22. Takematsu, T.; Konnai, M.; Hosogai, T.; Nishida, T. U.S. Patent 4521242, 1985, Kuraray Co., Ltd.
23. Miura, Y.; Mabuchi, T.; Kajioka, M.; Yanai, I. U.S. Patent 5032165, 1991, Nihon Nohyaku Co., Ltd.
24. Dutra, G.A.; Hamper, B.C.; Mischke, D.A.; Moedritzer, K.; Rogers, M.D.; Woodard, S.S. PCT Int. Appln. WO 92/06962, 1992, Monsanto Co.; *Chem. Abstr.*, **1992**, *117*, 69859p.
25. Osabe, H.; Morishima, Y.; Goto, Y.; Masamoto, K.; Yagihara, H.; Fujita, T. *Pestic. Sci.* **1991**, *32*, 73.
26. Osabe, H.; Morishima, Y.; Goto, Y.; Fujita, T. *Pestic. Sci.* **1992**, *35*, 187.
27. Bell, A. U.S. Patent 5176735, 1993, Uniroyal Chemical Co., Ltd.
28. Matsui, K.; Kasugai, H.; Matsuya, K.; Aizawa, H. U.S. Patent 3878224, 1975, Mitsubishi Chemical Industries, Ltd.
29. Nagano, E.; Hashimoto, S.; Yoshida, R.; Matsumoto, H.; Kamoshita, K. U.S. Patent 4484940, 1984, Sumitomo Chemical Co.
30. Lyga, J.W.; Patera, R.M.; Theodoridis, G.; Halling, B.P.; Hotzman, F.W.; Plummer, M.J. *J. Agric. Food Chem.*, **1991**, *39*, 1667.
31. Metivier, J.; Boesch, R. U.S. Patent 3385862, 1968, Rhone-Poulenc SA.
32. Hatton, L.R.; Parnell, E.W.; Roberts, D.A. Eur. Patent Appl. EP 34945, 1980, May and Baker, Ltd.; *Chem. Abstr.*, **1980**, *96*, 6721q.
33. Yoshinori, E. Eur. Patent EP 284030, 1988, Otsuka Chemical Co., Ltd.; *Chem. Abstr.*, **1989**, *110*, 38992c.
34. Lyga, J.W. PCT Int. Patent Appl. WO 86/00072, 1986, FMC Corp.; *Chem. Abstr.*, **1986**, *105*, 110512n.
35. Maravetz, L.L.; Theodoridis, G. U.S. Patent 4818276, 1989, FMC Corporation.
36. Theodoridis, G. U.S. Patent 4818275, 1989, FMC Corp.
37. Theodoridis, G.; Hotzman, F.W.; Scherer, L.W.; Smith, B.A.; Tymonko, J.M.; Wyle, J.M. *Pestic. Sci.*, **1990**, *30*, 259.
38. Theodoridis, G.; Baum, J.S.; Hotzman, F.W.; Manfredi, M.C.; Maravetz, L.L.; Lyga, J.W.; Tymonko, J.M.; Wilson, K.R.; Poss, K.M.; Wyle, M.J., in *Synthesis and Chemistry of Agrochemicals III*; Baker, D.R., Fenyés, J.G., Steffens, J.J., Eds.; ACS Symposium Series No. 504; ACS Press: Washington, D.C., 1992; pp. 134-146.
39. Theodoridis, G.; Hotzman, F.W.; Scherer, L.W.; Smith, B.A.; Tymonko, J.M.; Wyle, M.J., in *Synthesis and Chemistry of Agrochemicals III*; Baker, D.R., Fenyés, J.G., Steffens, J.J., Eds.; ACS Symposium Series No. 504; ACS Press: Washington, D.C., 1992; pp. 122-133.

RECEIVED December 14, 1993

Chapter 4

δ -Aminolevulinic Acid Based Herbicides and Tetrapyrrole Biosynthesis Modulators

Constantin A. Rebeiz, S. Amindari, Krishna N. Reddy,
Ujjana B. Nandihalli, M. B. Moubarak, and J. A. Velu

Laboratory of Plant Pigment Biochemistry and Photobiology, 240A Plant
and Animal Biotechnology Laboratory, University of Illinois, 1201 West
Gregory Avenue, Urbana, IL 61801-4716

Tetrapyrrole-dependent photodynamic herbicides (TDPH) are compounds which force green plants to accumulate undesirable amounts of metabolic intermediates of the chlorophyll and heme biosynthetic pathways, namely tetrapyrroles. In the light the accumulated tetrapyrroles photosensitize the formation of singlet oxygen which kills the treated plants by oxidation of their cellular membranes. Tetrapyrrole-dependent photodynamic herbicides usually consist of a 5-carbon amino acid, δ -aminolevulinic acid, the precursor of all tetrapyrroles in plant and animal cells, and one of several chemicals referred to as modulators. δ -Aminolevulinic acid and the modulators act in concert. The amino acid serves as a building block of tetrapyrrole accumulation, while the modulator alters quantitatively and qualitatively the pattern of tetrapyrrole accumulation. The tetrapyrrole-dependent connotation is meant to differentiate between this class of photodynamic herbicides and other light activated herbicides such as paraquat which are not dependent on tetrapyrrole metabolism for herbicidal activity. During the past nine years, the scope of TDPH research has expanded considerably, as some established herbicides and a plethora of new compounds which act via the TDPH phenomenon have been discovered.

Since the discovery in 1984 of the porphyrinogenic photodynamic herbicide phenomenology (1,2), there has been considerable expansion in its scope and in the understanding of its mode of action. One significant development has been the discovery of important families of established herbicides that act via this phenomenology (3). Several authors will cover this topic in this volume. Another important development centers on the discovery of many chemicals that modulate and

0097-6156/94/0559-0048\$08.00/0
© 1994 American Chemical Society

magnify the photodynamic herbicidal properties of δ -aminolevulinic acid (ALA). ALA is a natural 5-carbon amino acid which is the precursor of all tetrapyrroles in living cells, and is at the core of the ALA-based photodynamic herbicide technology (see Chapter 1). Essentially this technology is based on the conversion of ALA to tetrapyrroles in treated plant tissues. In the light the accumulated tetrapyrroles photosensitize the formation of singlet oxygen which in turn oxidizes membranes lipoprotein constituents and other important biomolecules which results in rapid plant death. In what follows, the present status of the ALA-based photodynamic herbicide technology will be described.

Photodynamic Effects of Several Metabolic Tetrapyrroles on Isolated Chloroplasts

The effect of several tetrapyrrole intermediates of the Chl biosynthetic pathway on isolated chloroplasts has been investigated by Amindari (4). Incubation of isolated cucumber chloroplasts with various exogenous tetrapyrroles, in the light, exhibited different effects on the pigments and pigment-protein complexes of the plastids. Only one of five exogenous tetrapyrroles failed to trigger chloroplast destruction in the light, namely divinyl (DV) Mg-protoporphyrin IX (Mg-Proto). Esterification of DV Mg-Proto to yield DV Mg-Proto monomethyl ester (Mpe) rendered this tetrapyrrole extremely destructive. While overall degradative effects were manifested by Chl *a* and *b* disappearance and the appearance of Chl degradation products, such as chlorophyllide (Chlide) *a*, Chlide *b* and pheophytin and pheophorbide *a*, more specific effects on the pigment-protein complexes became evident from *in organello* 77°K fluorescence emission spectroscopy. DV protoporphyrin IX (Proto), an early intermediate in Chl *a* biosynthesis, affected the photosystem (PS) II antenna Chl *a* pigment-protein complex, but had no effect on the PS I antenna complex. On the other hand DV-Mpe and monovinyl (MV) protochlorophyllide (Pchlide), destroyed completely the PS I antenna complex and caused disorganization of the light harvesting chlorophyll-protein (LHCP) complex. As for DV-Pchlide, it caused the disorganization of the PS I and II antenna complexes. Altogether these results indicated that individual tetrapyrroles have distinct and different disruptive effects on the structure of thylakoid membranes in the light. Specific effects appear to be related to the position of particular tetrapyrrole in the Chl *a* biosynthetic chain.

δ -Aminolevulinic Acid as a Herbicide

If an ideal field herbicide is a safe biorational compound which acts very rapidly on target plants and disappears very rapidly from the environment without leaving any residues, then ALA has the potential to be such a herbicide. Actually under laboratory conditions, ALA does behave like an ideal herbicide. Under these conditions treatment consists of (a) spraying potted growth chamber-grown plants with a solution of ALA, at a pH of 3-4, (b) wrapping the treated plants with aluminum foil, (c) placing the plants in darkness for several hours, then (d) exposing the plants to light. Plants subjected to such a treatment desiccate and die within a few hours (1,2). The acid pH keeps ALA in the protonated form for better penetration through the

cuticle. Wrapping treated plants in aluminum foil prevents rapid evaporation of the spray solution which leads in turn to better ALA translocation. Placing the plants in darkness, leads to the biosynthesis and accumulation of tetrapyrroles, in particular DV and MV Pchlides, which accumulate in the plastids. DV and MV Pchlides are the immediate precursors of DV and MV Chlide *a* respectively. Finally, exposing treated plants to light triggers tetrapyrrole-sensitized formation of singlet oxygen which oxidizes membrane lipoproteins and other constitutive biomolecules and results in rapid tissue desiccation and death.

Of course in practice, it is neither practical nor feasible to wrap a field in aluminum foil for better ALA penetration. To solve this problem, a formulation was developed for use under field conditions that insured better ALA translocation through plant surfaces. (5). The formulation consisted of: polyethylene glycol 600 (PEG):methanol:Tween 80:water (7:2:1:90 v/v/v/v/), at a pH of 3.5. None of these additives by themselves exhibited photodynamic herbicidal effects. PEG slowed down solvent evaporation and prolonged the contact of ALA with leaf surfaces, thus improving ALA penetration through the cuticle, while methanol improved the conversion of exogenous ALA to tetrapyrroles. Tween 80 was added as an agent to reduce the water surface tension.

The first porphyrinogenic field application of ALA in the absence of added modulators of the chlorophyll (Chl) biosynthetic pathway was in apple defoliation (6). Controlled defoliation of nursery stock is essential for the effective management of rootstocks and grafted trees. Presently defoliation is done by hand. This expensive operation sometimes causes damage to shoots, bark and buds and adds significantly to the cost of nursery operation. In an effort to develop an effective and safe chemical apple defoliant, mature, field-grown Golden Delicious apple trees were sprayed with ALA at a rate of 3 kg ALA per hectare. ALA was dissolved in the PEG/methanol/Tween 80/solvent system which was just described. Average droplet size was about 150 μm . Thirteen days after spraying, 100% defoliation was achieved.

The successful field defoliation of mature apple tree by ALA alone, indicated that it may be possible to develop specific ALA photodynamic herbicidal applications for special purposes. Because of the role of ALA as a precursor of all tetrapyrroles in living cells, it is doubtful, however, that ALA will exhibit high species selectivity. Photodynamic herbicidal selectivity will require the use of additional chemicals, which act in concert with ALA. These chemicals have been named tetrapyrrole-dependent photodynamic herbicide (TDPH) modulators. They act by modulating the Chl biosynthetic pathway and by amplifying the conversion of ALA to tetrapyrroles (see Chapter 1).

Discovery of TDPH Modulators

Because of the central importance of modulators to the performance of TDPH, considerable time and efforts have been devoted during the past six years to the discovery of novel TDPH modulators. The experimental strategy used in that successful undertaking as well as the first results of that research effort have been described (7,8).

The use of modulators of the heme and Chl biosynthetic pathways in photodynamic herbicide formulations was triggered by the successful use of 2,2'-dipyridyl (Dpy) as a TDPH modulator (1,2). The successful synergistic use of ALA + DPY for TDPH purposes prompted in turn a search for additional compounds that may affect the Chl biosynthetic pathway. A search of the literature was undertaken, for chemicals and biochemicals which have been known to affect, in a general way, Chl and Pchlide biosynthesis. That search netted a certain number of compounds which had been implicated in one way or another in Chl, Pchlide, and Mpe formation. One compound, 8-hydroxyquinoline, had been described by Jones (9) for its effects on bacteriochlorophyll biosynthesis in *Rhodospseudomonas spheroides*. Four compounds, namely: 1,10-phenanthroline, 2-pyridyl aldoxime, 2-pyridyl aldehyde, and picolinic acid had been described by Duggan and Gassman (10) for their effects on the Chl biosynthetic pathway in etiolated seedlings of Red Kidney bean, corn and cucumber. Two other compounds namely: 1,7-phenanthroline and phenanthridine (11) were selected because of their effect on the chlorophyll biosynthetic pathway in *Chlamydomonas reinhardtii*. A close examination of these chemicals revealed that they were all derivatives of pyridine. Detailed mode of action studies of these compounds performed on cucumber seedlings revealed significant TDPH modulating activity (5).

Encouraged by these initial results, a search was initiated for pyridine derivatives that may have TDPH modulating potential. The following compounds were selected: Nicotinic acid, because it is a geometrical isomer of picolinic acid; nicotinamide, because of its structural similarity to nicotinic acid; 2-oxypyridine and 4-oxypyridine, because of their structural similarity to pyridine; 2,3-dipyridyl, 2,4-dipyridyl and 4,4'-dipyridyl because they are structural isomers of Dpy; 2,2'-dipyridylamine and 2,2'-dipyridyl disulfide because of their structural similarity to Dpy; quinoline because of its structural similarity to 8-OH-quinoline; and 4,7-phenanthroline because it is a structural isomer of 1,10-phenanthroline. Pyridinium was also selected because of its structural similarity to pyridine, and because a data base of herbicidal compounds available from ISI, Philadelphia, PA, listed several pyridiniums with general herbicidal properties. Finally 1,2-diazine and 1,4-benzodiazine were also chosen from the ISI data base for the same reason as choosing pyridinium.

Rapid testing for TDPH activity of representative members of the aforementioned chemical categories, which will be referred to hereafter as TDPH templates or templates for short, unraveled interesting TDPH properties. A closer examination of the chemical structure of the various templates revealed that they fell into two separate categories: (a) those that were structurally related to half a tetrapyrrole molecule such as the dipyridyls and the phenanthrolines, and (b) those that were structurally related to one quadrant of a tetrapyrrole molecule i.e. to an individual pyrrole such as picolinic acid, nicotinic acid, substituted pyridyls, porphobilinogen, etc. This in turn suggested that this similarity between the chemical structures of the templates and between tetrapyrrole halves or quadrants may be essential for TDPH activity as it may facilitate the binding of the templates, to, or close to the receptor site of specific enzymes of the Chl biosynthetic pathway. It is indeed feasible to visualize how such enzymes may be tricked by structural similarities between

modulators and those parts of the tetrapyrrole substrates that bind to Chl biosynthetic enzymes. A brief description of some of the TDPH modulators will follow.

Classifications of TDPH Modulators

Depending on their site of action along the heme and Chl biosynthetic chains, various modulators have been classified into four categories (5): (a) inducers of tetrapyrrole accumulation, which induce plant tissues to form large amounts of Proto IX, Mpe, Pchlides or mixtures of these tetrapyrroles (in the presence of exogenous ALA the accumulation of these tetrapyrroles is accelerated); (b) enhancers of ALA conversion to DV Pchlide, which enhance the conversion of exogenous ALA to DV Pchlide; (c) enhancers of ALA conversion to MV Pchlide, which enhance the conversion of exogenous ALA to MV Pchlide, and (d) inhibitors of MV Pchlide accumulation, which block the detoxification of DV tetrapyrroles by inhibiting their conversion to MV tetrapyrroles. Of all the aforementioned modulators, only inducers of tetrapyrrole accumulation cause tetrapyrrole accumulation in the absence of added ALA. The three other classes of modulators do not.

In nature, most of the Chl *a* is formed via two Chl biosynthetic routes, namely the DV and MV monocarboxylic routes (Figure1) (12, 13). Accordingly green plants have been classified into three different greening groups, depending upon which Chl biosynthetic routes are used in forming MV and DV Pchlides under light and dark conditions (Figure 2) (14, 16). The following susceptibility hypothesis was proposed on the basis of the photodynamic herbicide response of cucumber, a dark divinyl/light divinyl plant species and soybean, a dark monovinyl/ light divinyl species, toward various ALA + modulator treatments which caused the accumulation of various MV and DV tetrapyrroles (8, 10): (a) that plants poised in the DV tetrapyrrole biosynthetic state are more photodynamically susceptible to the accumulation of MV tetrapyrroles than to the accumulation of DV tetrapyrroles, and (b) plants poised in the MV tetrapyrrole biosynthetic state are more susceptible to the accumulation of DV tetrapyrroles than to MV tetrapyrroles. This phenomenon was explained on the basis that MV plant species poised in the MV-greening pattern could not cope as well with a massive influx of DV tetrapyrroles. Likewise, DV plants poised in the DV-greening pattern could not cope as effectively with a massive influx of MV tetrapyrroles. In the light, being unable to rapidly metabolize the wrong tetrapyrroles, the latter would linger around and photosensitize the destruction of the host plant before being eventually degraded by light. This hypothesis was largely corroborated by investigations on corn, soybean and ten common weed species under greenhouse conditions (5, 15).

Six-Membered N-Heterocyclic Modulators that Mimic Half a Tetrapyrrole

These include phenanthrolines and their geometrical isomers, dipyrindyls and their geometrical isomers, quinolines, and related compounds.

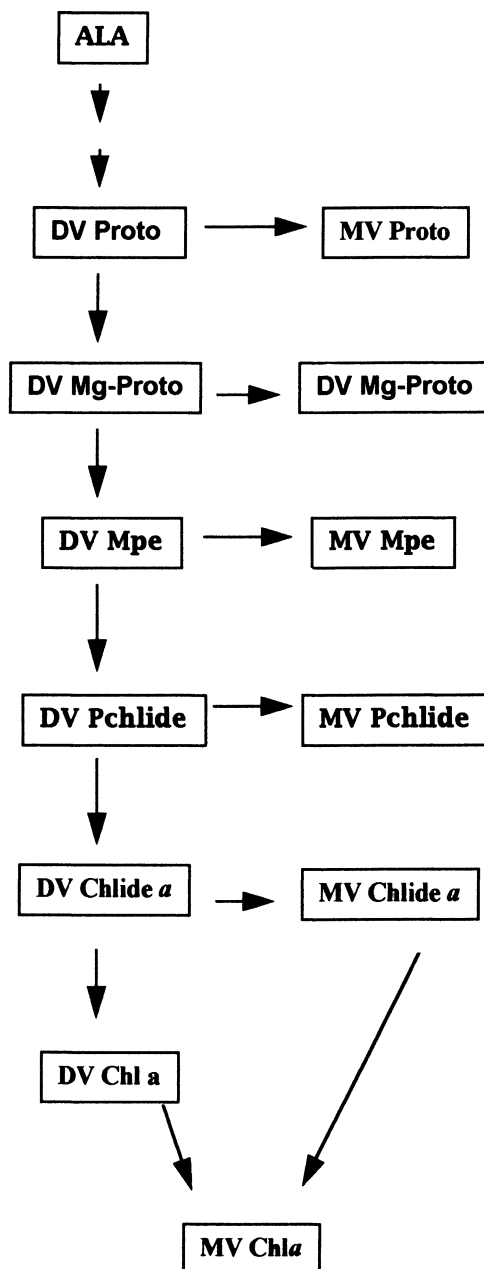


Figure 1. The MV and DV monocarboxylic routes of Chl *a* biosynthesis in green plants. DV = divinyl, MV = monovinyl, ALA = δ -aminolevulinic acid, Proto = protoporphyrin IX, Mpe = Mg-Proto monoester, Pchlido = protochlorophyllido, Chlido = Chlorophyllido, Chl = chlorophyll. Arrows joining the DV and MV branches refer to reactions catalyzed by 4-vinyl reductases. Adapted from ref. 12.

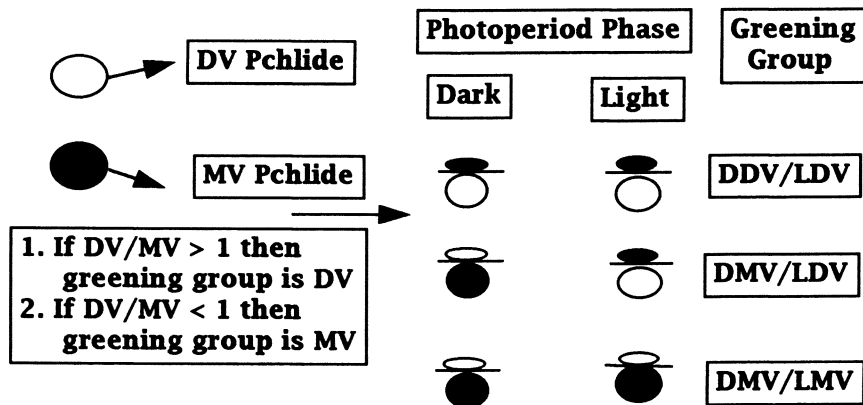
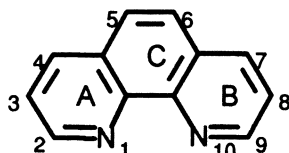
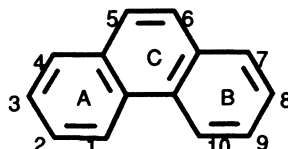


Figure 2. Greening group affiliation of plants. If the DV/MV ratio for a plant species is larger than 1, for a particular phase of the photoperiod, then the plant is considered to be DV for that phase of the photoperiod. If the ratio is less than one, the plant is considered to be MV. Plants that are DV during the dark phase of the photoperiod, are referred to as DDV. Plants that are MV during the dark phase of the photoperiod, are referred to as DMV. Likewise Plants that are DV during the light phase of the photoperiod, are referred to as LDV. Plants that are MV during the light phase of the photoperiod, are referred to as LMV. For the whole photoperiod, plants can be DDV/LDV, DMV/LDV or DMV/LMV. The DDV/LMV group has not been observed under natural conditions. Adapted from ref. 16.

Phenanthrolines. 1,10-phenanthroline (Oph) (I) is an analog of phenanthrene (II)

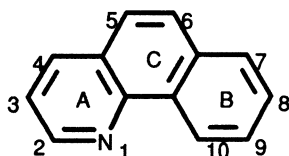


I. 1,10-Phenanthroline

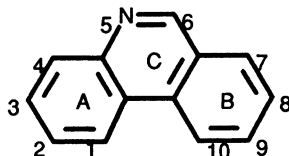


II. Phenanthrene

in which carbons 1 and 10 have been replaced by nitrogen atoms. A phenanthrene infrastructure is not sufficient however, for expression of photodynamic herbicidal activity. Likewise, 7,8-benzoquinoline (III) is another analog of phenanthrene in which one of the two carbons at position 1 or 10 has been replaced by a nitrogen atom. Substitution of both carbons 1 and 10 with N atoms, as in Oph, or one carbon atom in ring C with a N atom as in phenanthridine (IV) was mandatory for activity (4, 15).



III. 7,8-Benzoquinoline

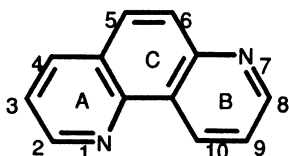


IV. Phenanthridine

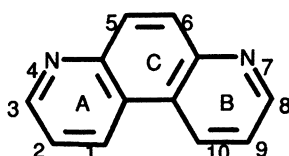
1,10-Phenanthrolines. 1,10-Phenanthroline (Oph) (I) is a potent modulator of the heme (19, 20) and Chl biosynthetic pathways (4, 5, 7, 8, 17, 18, 21). It is also a very potent non selective TDPH modulator, in the absence and presence of ALA. Its TDPH potency in the absence of added ALA is due to its tetrapyrrole inducing properties. Indeed in the absence of added ALA, Oph induces the biosynthesis and accumulation of Proto, and DV and MV Mpe. In the presence of added ALA, the inducing properties of Oph are reinforced by the enhanced conversion of added ALA to Proto, Mpe, and Pchlides (4, 17, 18). In addition to the induction and enhanced biosynthesis of the aforementioned anabolic tetrapyrroles, Oph also causes the accumulation of photodynamic catabolic tetrapyrroles such as Chlide *a*, (i.e. Chl *a* without phytol) and pheophorbide *a* (i.e. Chlide *a* without Mg) (4, 16). These catabolic tetrapyrroles also exhibit potent TDPH properties (4, 17).

The TDPH properties of Oph are profoundly altered by various peripheral substitutions. Various methyl substitutions around the Oph periphery do not significantly alter the pattern of tetrapyrrole biosynthesis and accumulation. However, phenyl substitution at position 4 and 7 of the Oph macrocycle results in loss of Proto induction, and a shift in the enhancement of ALA conversion from DV to MV Pchlides (17). Further substitution with methyl groups at position 2 and 9 results in a loss of Proto and DV MPE induction and restoration of DV Pchlides enhancement. Nucleophilic substitution with chloro or nitro groups at position 5 of the Oph macrocycle results in maintenance of the enhanced conversion of exogenous ALA to DV Pchlides. However, induction of Proto accumulation is lost and enhancement of exogenous ALA conversion to DV Mpe is activated (18).

Geometrical Isomers of 1,10-Phenanthrolines. It has been proposed that the tetrapyrrole biosynthetic modulating properties of 1,10-phenanthrolines are due exclusively to the bidentate metal (Fe^{++} , Mg^{++}) chelating properties of these compounds (10). This hypothesis is not compatible with the observation that geometrical isomers of Oph such as 1,7-phenanthroline (V), 4,7-phenanthroline (VI), and phenanthridine (IV),



V. 1,7-Phenanthroline



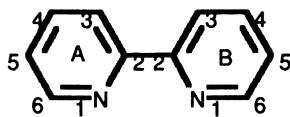
VI. 4,7-Phenanthroline

which are not bidentate metal chelators, exhibit tetrapyrrole biosynthetic and TDPH properties (4, 17). The TDPH properties of these modulators are less potent, however, than those of Oph. In cucumber, a dark (D) DV/light (L) MV plant species, the most prominent effect was enhancement of ALA conversion to DV Pchlide. In soybean, a DMV/LDV dicotyledonous plant species, 1,7-phenanthroline (V) and 4,7-phenanthroline (VI) acted mainly as inhibitors of DV Pchlide conversion to MV Pchlide, while phenanthridine (IV) acted as an enhancer of ALA conversion to MV Pchlide. In johnsongrass, a DMV/LMV plant species, the three Oph geometrical isomers had different effects on the Chl biosynthetic pathway. 1,7-Phenanthroline (V), acted mainly as an inducer of DV and MV Mpe biosynthesis and resulted in the accumulation of Chlide α . 4,7-Phenanthroline (VI) mainly inhibited the conversion of DV Pchlide to MV Pchlide. Phenanthridine (IV), which is not a geometrical isomer but an analog of Oph, caused induction of Proto biosynthesis, enhancement of DV and MV Mpe formation and inhibition of DV to MV Pchlide formation. Its major effect was the accumulation of Chlide α and pheophorbide α .

Quantitative Structure-Function Studies of Various Phenanthrolines.

Quantitative structure-activity studies between the molecular properties of 1,10-phenanthroline, its substituted analogs and various phenanthroline geometrical isomers and herbicidal and tetrapyrrole biosynthesis modulating activities have been extensively investigated (4, 18). A detailed discussion of these studies is beyond the scope of this paper. In summary, these studies suggested that most of the variance in *in vivo* herbicidal photodynamic activity could be explained by the pattern of electronic density over specific regions of the molecules and specific alterations in molecular electrostatic potentials (4, 18).

Dipyridyls. Dipyridyls such as 2,2'-dipyridyl (VII) differ from Oph (I) by the absence of the etheno-bridge which is fused with rings A and B in Oph (I). Obviously the



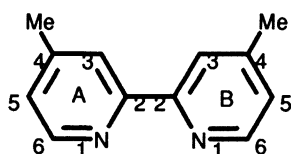
VII. 2,2'-Dipyridyl

etheno-bridge has minor effects on the tetrapyrrole modulating activities and TDPH properties of tetrapyrroles as evidenced by the similarity in the mode of action of Oph and Dpy (see below).

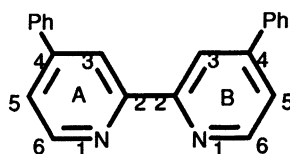
2,2'-Dipyridyls. Dpy (VII) like Oph (I) is mainly a non-selective TDPH modulator and an inducer of tetrapyrrole accumulation. In cucumber, a DDV/LDV plant, it induces the formation of Proto, and DV and MV Mpe, in the absence of added ALA. In the presence of exogenous ALA, it further enhances the biosynthesis of these tetrapyrroles. It also results in the formation of pheophorbide α . In soybean, a DMV/LDV plant species, it also induces the formation of MV Pchlide and enhances the formation of DV Pchlide. In johnsongrass, a DMV/LMV plant species, it induces

the formation of Proto and MV Mpe, and in the presence of added ALA, it enhances the formation of DV Pchlde.

The effects of various peripheral substitutions on the TDPH properties of Dpy have been investigated in cucumber, a DDV/LDV plant species, by Reddy and Rebeiz (in preparation). The TDPH properties of Dpy are profoundly altered by such substitutions. Methyl (Me) substitutions at the 4,4'-position as in 4,4'-dimethyl-2,2'-dipyridyl (VIII) lowers the inducing and enhancing properties in comparison to Dpy, and result in the onset of MV Pchlde inhibition. Phenyl (Ph) substitution at the 4,4'-positions, as in 4,4'-diphenyl-2,2'-dipyridyl (IX), eliminates tetrapyrrole induction and

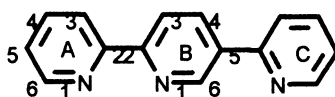


VIII. 4,4'-Dimethyl-2,2'-dipyridyl



IX. 4,4'-Diphenyl-2,2'-dipyridyl

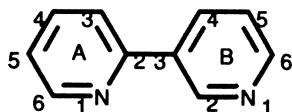
inhibits MV Pchlde biosynthesis. As a consequence, this modulator exhibited very poor photodynamic herbicidal properties. Covalent linkage of Dpy to a third pyridine ring (ring C), at the 5' position of the Dpy macrocycle yields 2,2':5',2''-terpyridine (X) (Tpy). Tpy is a potent TDPH modulator which induces DV Mpe as well as MV and



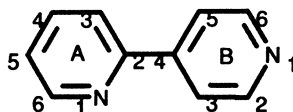
X. 2,2':5',2''-terpyridine

DV Pchlde formation in the absence of added ALA. In the presence of added ALA, it enhances the formation of DV Pchlde.

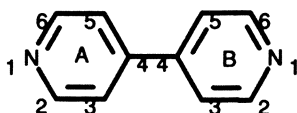
Geometrical Isomers of 2,2'-dipyridyl. It has also been proposed that the tetrapyrrole biosynthetic modulating properties of dipyridyls are due exclusively to their bidentate metal (Fe^{++} , Mg^{++}) chelating properties (10). In this case too, this hypothesis is not compatible with the observation that geometrical isomers of Dpy such as 2,3-dipyridyl (XI), 2,4-dipyridyl (XII), and 4,4'-dipyridyl (XIII), which are not bidentate chelators, exhibit tetrapyrrole biosynthesis modulation and selective TDPH properties. These modulators inhibit tetrapyrrole accumulation in cucumber, and as a consequence exhibit very poor herbicidal properties in this plant species (16). In soybean, a DMV/LDV plant species, they enhance DV Pchlde accumulation and exhibit more evident herbicidal properties (17). In johnsongrass, a DMV/LMV plant



XI. 2,3-Dipyridyl



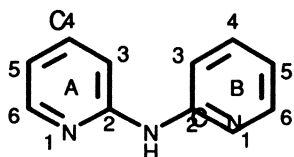
XII. 2,4-Dipyridyl



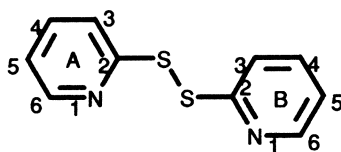
XIII. 4,4'-Dipyridyl

species, they act as enhancers of DV Mpe and Pchlide formation and inhibit the conversion of ALA to MV Pchlide. 2,3-Dipyridyl and 4,4'-dipyridyl also lead to the formation of Chlide α , and pheophorbide α . As a consequence, in johnsongrass these three modulators exhibit potent herbicidal activity (4).

Dipyridyl Analogs. The TDPH properties of two dipyridyl analogs, in which the distance between rings A and B was stretched by the insertion of either an amine as in 2,2'-dipyridyl amine (XIV), or a disulfide as in 2,2'-dipyridyl disulfide (XV) has been investigated in the three greening groups of plants. Both modulators exhibit mild



XIV. 2,2'-Dipyridyl amine



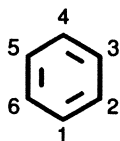
XV. 2,2'-Dipyridyl disulfide

tetrapyrrole modulating activities and poor photodynamic herbicidal properties. 2,2'-Dipyridyl amine (XIV) acts as an enhancer of DV Pchlide formation in cucumber, and an enhancer of MV Pchlide formation in soybean and johnsongrass. 2,2'-dipyridyl disulfide (XV) acts as a mild enhancer of MV Pchlide in cucumber and soybean and as an inhibitor of tetrapyrrole formation in johnsongrass.

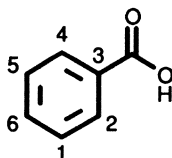
Quantitative Structure-Activity Studies of Various Dipyridyls. In cucumber, significant correlations were observed between van der Waals volumes, specific electronic densities over certain regions of the dipyridyl molecules, and photodynamic damage. For example, in all cases modulation of photodynamic damage and tetrapyrrole biosynthetic activities were related to van der Waals volumes and superdelocalisability (*i.e.* electron density) over the lowest unoccupied molecular orbitals (Reddy and Rebeiz, in preparation). In johnsongrass, activity appeared to be related to superdelocalisability in molecular orbitals located one step above the lowest unoccupied molecular orbital (4).

Six-Membered N-Heterocyclic Modulators that Mimic a Tetrapyrrole Quadrant

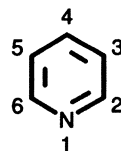
Benzene (XVI), which is the simplest chemical to somehow mimic a tetrapyrrole quadrant is completely inactive as a TDPH modulator. Addition of a carboxylic group to yield benzoic acid (XVII), or an endocyclic N to yield pyridine (XVIII), does not impart any TDPH activity.



XVI. Benzene



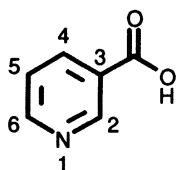
XVII. Benzoic acid



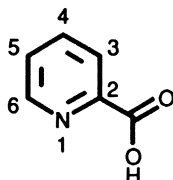
XVIII. Pyridine

TDPH activity appears, however, when the benzene ring contains both a N atom at position 1 and a carboxylic group at position 3, as in nicotinic acid (XIX).

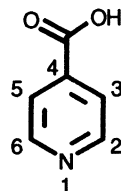
Nicotinic Acid and Substituted Analogs. The TDPH and pyrrole modulating activities of nicotinic acid and several of its analogs were investigated in cucumber. Nicotinic acid (XIX) exhibits moderate TDPH activity and acts as an enhancer of MV Pchl_{id} and to a lesser extent as an enhancer of DV Pchl_{id}. The position of the carboxylic group is critical. Activity is preserved in picolinic acid (XX) with a carboxylic group at position 2, but is lost in isonicotinic acid (XXI), with a carboxylic group at position 4. Reintroduction of a carboxylic group at position 3 of isonicotinic acid as in diethyl-3,4-pyridine carboxylic acid (XXII) restores TDPH activity.



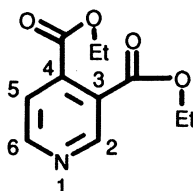
XIX. Nicotinic acid



XX. Picolinic acid

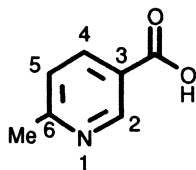


XXI. Isonicotinic acid

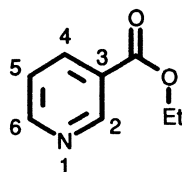


XXII. Diethyl-3,4-pyridine carboxylic acid

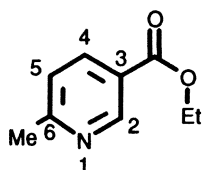
Peripheral methyl substitution of nicotinic acid as in 6-methyl nicotinic acid (**XXIII**) has little effect on TDPH activity in comparison to nicotinic acid. Esterification of the carboxylic function as in ethyl nicotinate (**XXIV**)



XXIII. 6-Methyl nicotinic



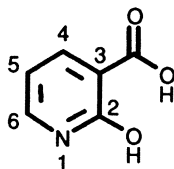
XXIV. Ethyl nicotinate



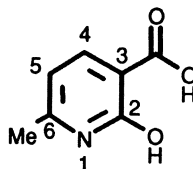
XXV. Ethyl-2-methyl nicotinate

significantly improves the TDPH activity and the conversion of ALA to DV and MV Pchlde. High ethyl nicotinate concentrations inhibit the conversion of ALA to MV Pchlde and enhances the formation of DV Pchlde. Insertion of a methyl group at position 2 of ethyl nicotinate as in ethyl-2-methyl nicotinate (**XXV**) does not alter the TDPH activity.

Insertion of a hydroxyl group at position 2 of nicotinic acid as in 2-OH-nicotinic acid (**XXVI**) does not affect the TDPH and Pchlde enhancing activities. Likewise insertion of a methyl group at position 6 of 2-OH nicotinic acid to yield 2-OH-6-methyl nicotinic acid (**XXVII**) has no effects on either activities.

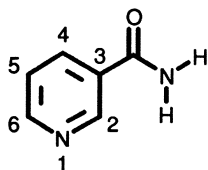


XXVI. 2-OH-Nicotinic acid

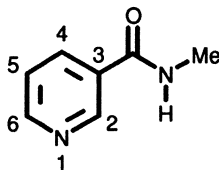


XXVII. 2-OH-6-Methyl nicotinic acid

Replacement of the carboxylic function of nicotinic acid by an amide as in nicotinamide (**XXVIII**) mimics the esterification effect observed in ethyl nicotinate (**XXIV**). In other words, nicotinamide acts as an enhancer of DV and MV Pchlde formation at low ALA concentrations (2.5 mM), and at higher ALA concentrations (5 mM) it inhibits the conversion of ALA to MV Pchlde and enhances DV Pchlde formation. Replacing one of the amide hydrogens with a methyl group, as in

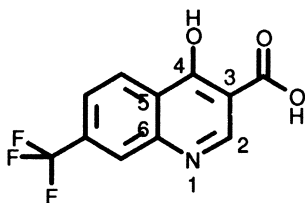


XXVIII. Nicotinamide

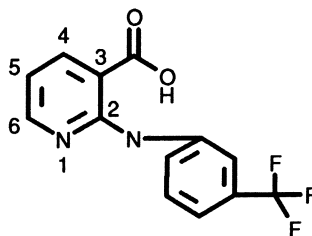


XXIX. N-methyl nicotinamide

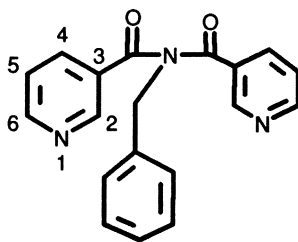
N-methyl nicotinamide (XXIX) has no effect on activity. More bulky and extensive peripheral substitutions, as in 4-hydroxy-7-trifluoromethyl-3-quinoline carboxylic acid (XXX), niflumic acid (XXXI), and N-benzyl-dinicotinamide (XXXII) eliminate Pchlide enhancement and result in MV and DV Pchlide inhibition. This was accompanied by the formation of catabolic



XXX. 4-Hydroxy-7-trifluoromethyl-3-quinoline carboxylic acid



XXXI. Niflumic acid

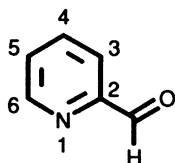


XXXII. N-Benzyl dinicotinamide

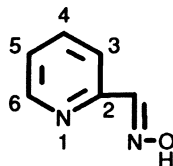
photodynamic tetrapyrroles such as Chlides, and pheophorbides. Quantitative structure-activity studies of nicotinic acid and substituted analogs will be reported elsewhere.

Picolinic Acid and Substituted Analogs. As with other TDPH modulators the moderate herbicidal effects of picolinic acid (XX) depend upon the greening group affiliation of the target plant. For example in cucumber, picolinic acid acts as an enhancer of MV and DV Pchlide. Its TDPH activity in cucumber a DDV/LDV plant species is more pronounced than in soybean, a DMV/LDV plant species. In johnsongrass it induces the formation of MV and DV Mpe and in the presence of ALA acts as an enhancer of DV Mpe, and MV and DV Pchlide formation. It also

results in the accumulation of some Chlide *a* and pheophorbide *a*. Replacement of the carboxylic group at position 2 with an aldehyde as in 2-pyridine aldehyde (XXXIII) results in an enhancement of MV Pchlide formation. As a consequence, 2-pyridyl aldehyde exhibits more potent TDPH effects on cucumber than on soybean or johnsongrass. Replacement of the aldehyde group by an aldoxime at position 2, as in 2-pyridine aldoxime (XXXIV) changes the activity profile. Although enhancement of



XXXIII. 2-Pyridine aldehyde



XXXIV. 2-Pyridine aldoxime

MV Pchlide formation is retained in cucumber and soybean, in soybean it also causes enhancement of DV Mpe formation. In johnsongrass, it becomes an inhibitor of MV Pchlide formation, and enhances the formation of Proto and MV and DV Mpe. Quantitative structure-activity investigations in johnsongrass revealed that Proto enhancement and DV-Pchlide inhibition corresponded to modulators with larger negative electrostatic volumes. On the other hand the accumulation of Chl degradation products was observed with picolinic acid, a molecule with the largest negative electrostatic volume and dipole moment in the group. As the negative electrostatic volume and the net charges at position 2 of the molecules increased the photodynamic damage caused by the modulators alone and in the presence of added ALA increased.

Pyridiniums That Mimic a Quadrant or Half a Tetrapyrrole.

These modulators are discussed by Reddy and Rebeiz in Chapter 12.

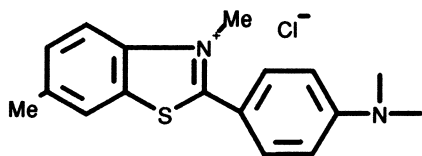
Five-Membered N-Heterocyclic Modulators that Mimic a Tetrapyrrole Quadrant

Recently, considerable emphasis has been placed on 5-membered N-heterocyclic modulators that mimic a pyrrole. These modulators belong to ten different chemical families which have been described in (8). A brief discussion of ongoing work is presented below.

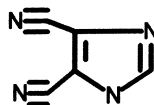
Pyrroles. Several pyrrolic modulators are discussed by Reddy and Rebeiz in chapter 12.

Other Five Membered N Heterocyclic Modulators that Mimic a Tetrapyrrole Quadrant. Of the 75 modulators that exhibited 88-100% kill on cucumber, pigweed, and johnsongrass, and minimal phytotoxicity on corn, twenty modulators proved promising enough to warrant further in-depth investigations. These investigations are

in progress and include TDPH effects on cucumber, pigweed, corn, johnsongrass, velvetleaf and morningglory, as well as detailed tetrapyrrole biosynthetic effects and quantitative 3-dimensional structure-activity studies. Only two particularly promising modulators, namely thioflavin T (XXXV) and 4,5-dicyanoimidazole (XXXVI) will be briefly described.



XXXV. Thioflavin T



XXXVI. 4-5-Dicynaoimidazole

Preliminary investigations indicate that Thioflavin T (XXXV) is a very potent non selective TDPH modulator and a potent household insecticide. A solvent system has been developed for its efficient delivery under greenhouse conditions. The solvent system consists of PEG:Tween 80:acetone:sylgard:soybean oil:water (9:1:2.25:0.25:6:81.5, v/v/v/v/v/v). Concentrations of 1.125 kg ALA and 250 g thioflavin T per ha resulted in 100 % kill of cucumber, pigweed, johnsongrass, velvetleaf, and morningglory. Furthermore it completely defoliated greenhouse-grown cotton seedlings.

In contrast to thioflavin T, 4,4-dicyanoimidazole (XXXVI) is a selective TDPH modulator. Under greenhouse conditions, it does not affect corn, but results in 100 % kill on cucumber, pigweed, johnsongrass, velvetleaf and morningglory.

Future Prospects

So far the most promising TDPH modulators appear to be 5-membered N-heterocyclics. These modulators are presently under intensive investigations. Hopefully, in concert with ALA they will be developed to achieve a field performance as good as their greenhouse performance.

Abbreviations. Abbreviations: ALA, δ -aminolevulinic acid; Chl, chlorophyll; Chlide, chlorophyllide; D, dark; DV, divinyl; Dpy, 2,2'-dipyridyl; Et, ethyl; L, light; LHCP, light harvesting chlorophyll-protein complex; Me, methyl; Mpe, Mg-protoporphyrin IX monomethyl ester; MV, monovinyl; Oph, 1,10-phenanthroline; Pchlide, protochlorophyllide; Proto, protoporphyrin IX; PS, photosystem.

Acknowledgments. Supported by funds from the Illinois Agricultural Experimental Station and by the John P. Trebellas Photobiotechnology Research Endowment to C.A.R.

Literature Cited

1. Rebeiz, C. A.; Montazer-Zouhoor, A.; Hopen, H. J.; Wu, S.-M. *Enzyme Microb. Technol.* **1984**, *5*, 390-401.
2. Rebeiz, C. A. Photodynamic Herbicides. *U. S. Patent* No. 5,127,938, **1992**, pp 37.
3. Duke, S. O.; Becerril, J. M.; Sherman, T. D.; Matsumoto, H. *Amer. Chem. Soc. Symp. Ser.* **1991**, *449*, 371-86.
4. Amindari, S. *PhD thesis*, University of Illinois, Urbana, **1992**, pp 242-287.
5. Rebeiz, C. A.; Montazer-Zouhoor, A.; Mayasich, J. M.; Tripathy, B. C.; Wu, S.-M.; Rebeiz, C. C. *Crit. Rev. Plant Sci.* **1988**, *6*, 385-436.
6. Rebeiz, C. A. Photodynamic defoliants. *U. S. Patent* No. 5,163,990, **1992**, pp 25.
7. Rebeiz, C. A.; Nandihalli, U. B.; Reddy, K. N. In *Topics in Photosynthesis - Volume 10, Herbicides*; Baker, N. R.; Percival, M. P., Eds.; Elsevier, Amsterdam, 1991; pp. 173-208.
8. Rebeiz, C. A.; Reddy, K. N.; Nandihalli, U. B. Velu, J. *Photochem. Photobiol.* **1990**, *52*, 1099-227.
9. Jones, O. T. G. *Biochem. J.* **1963**, *88*, 335-343.
10. Duggan, J. Gassman, M. *Plant Physiol.* **1974**, *53*, 206-215.
11. Bednarick, D. P.; Hooper, J. K. *Biochem. Biophys. Acta.* **1985**, *240*, 269-275
12. Rebeiz, C. A.; Wu, S. M.; Kuhadja, M.; Daniell, H.; Perkins, E. J. *Mol. Cel. Biochem.* **1983**, *58*, 97-125.
13. Rebeiz, C. A., Parham, R., Ioannides, Y.; Fasoula, D. *Ciba Foundation Symposium*, **1994**, In press.
14. Rebeiz, C. A. Ever Green. *The Sciences.* **1987**, *27*, 40-45.
15. Mayasich, J. M., Mayasich S. A., Rebeiz, C. A. Response of corn (*Zea mays*), soybean (*Glycine max.*), and several weed species to dark-applied photodynamic herbicide modulators. *Weed Sci.* **1990**, *38*, 10-15.
16. Ioannides, I. M., Fasoula, D. A., Robertson K. R., Rebeiz, C. A. *Biochem. System. Ecol.* **1993**, in press.
17. Montazer-Zouhhor, A. *PhD thesis*, University of Illinois, Urbana, **1988**, pp 409.
18. Nandihalli, U. B.; Rebeiz, C. A. *Pestic. Biochem. Physiol.* **1991**, *40*, 27-46.
19. Rebeiz, C. A.; Juvik, J. A.; Rebeiz, C. C.; Bouton, C. E.; Gut, L. J.; *Pestic. Biochem. Physiol.* **1990**, *36*, 201-207.
20. Rebeiz, N.; Rebeiz, C. C.; Arkins, S.; Kelley, K. W.; Rebeiz, C. A. *Photochem. Photobiol.* **1992**, *55*, 431-435..
21. Rebeiz, C. A.; Montazer-Zouhoor, A.; Mayasich, J. M.; Tripathy, B. C.; Wu, S. M.; Rebeiz, C. C. *Amer. Chem. Soc. Symp. Ser.* **1987**, *339*, 295-327.

RECEIVED April 7, 1994

Chapter 5

δ -Aminolevulinic Acid Induced Photodynamic Damage to Cucumber (*Cucumis sativus* L.) Plants Mediated by Singlet Oxygen

Baishnab Charan Tripathy

School of Life Sciences, Jawaharlal Nehru University, New Delhi 110067, India

Cucumber (*Cucumis sativus* L. cv Poinsette) plants were sprayed with 20 mM solution of 5-aminolevulinic acid (ALA), the precursor of tetrapyrroles, and then incubated in darkness for 14 h. Upon transfer to sunlight (800 W m^{-2}), the plants died after 6 h of exposure due to photodynamic damage. The photosystem II (PSII) and photosystem I (PSI) photochemical reactions were impaired. Intact chloroplasts, isolated from the control and ALA-treated plants in the dark were exposed to weak light ($250 \mu\text{moles m}^{-2} \text{ s}^{-1}$). Within 30 min, PSII activity was reduced by 50%, and the variable fluorescence was significantly reduced. Thylakoid membranes prepared in darkness from control and 20 mM ALA-treated plants were illuminated ($250 \mu\text{moles m}^{-2} \text{ s}^{-1}$) in the presence of scavengers of active oxygen species. The singlet oxygen scavengers histidine and sodium azide protected the thylakoid membrane linked function of PSII from photodynamic damage. However, the hydroxyl radical scavenger formate and the superoxide radical scavengers superoxide dismutase and 1,2-dihydroxybenzene-3,5-disulfonic acid failed to protect the PSII reaction. Non-phototransformable protochlorophyllide was the most abundant pigment in the thylakoid membranes isolated from ALA-treated plants and acted as a type II photosensitizer.

The control of weeds by herbicides is an important modern agricultural practice. Photodynamic herbicides are compounds capable of inducing green plants to accumulate excess amounts of tetrapyrroles which act as photosensitizers and cause lethal damage to plants (1-12). Mg-tetrapyrroles are type II photosensitizers. They have a tendency to absorb radiant energy and to photosensitize the formation of singlet oxygen (13-14), a very powerful oxidant that can trigger a free radical chain reaction and destroy biological membranes, nucleic acids, enzymes, and many other proteins (15). Mg-tetrapyrroles are extremely biodegradable and their environmental impact is negligible (1).

5-Aminolevulinic acid (ALA) is a precursor of heme and chlorophyll (Chl) and its synthesis is highly regulated by plants (16). Protochlorophyllide (Pchl) is the feed-back inhibitor of ALA biosynthesis from its 5-carbon precursor glutamate (17). Exogenous application of ALA to green plants bypasses the feed-back inhibition of the regulatory ALA biosynthesis site and induces excess accumulation of Mg-tetrapyrroles. Therefore, ALA could be used as a commercial herbicide, if it were

0097-6156/94/0559-0065\$08.00/0
© 1994 American Chemical Society

economical. In the present investigation it is demonstrated that the radiant energy absorbed by over-accumulated tetrapyrroles is not utilized in photosynthetic reactions, rather it reacts with molecular oxygen and photosensitizes the formation of singlet oxygen which ultimately causes lethal damage to plants.

MATERIALS AND METHODS

Plant Material. Cucumber (*Cucumis sativus* L., cv Poinsette) plants were grown in Petri plates (14.5 cm diameter) on moist filter paper at 25° C (18).

ALA Treatment. A volume of 5 ml of aqueous ALA solution (20 mM, pH adjusted to 4.8) was sprayed on each Petri plate containing fifteen 6-day-old cucumber plants (2). A glass sprayer (atomizer) attached to a rubber bulb was used for spraying ALA. After the ALA spray, the plants were kept in darkness for 14 h. Control plants were sprayed with water (pH 4.8) and kept for 14 h in darkness.

Light Treatment. After a 14 h dark period, the control and ALA-treated plants were exposed to light (800 W m⁻²). The cotyledons were then harvested after the desired time period for chloroplast isolation.

Chloroplast Isolation. Chloroplasts were isolated from cucumber cotyledons at 4° C by hand-homogenizing the cotyledons in a grinding medium consisting of 0.4 M sucrose, 10 mM NaCl, and 20 mM Hepes/NaOH buffer (pH 7.6) (2). The same grinding medium was used for the chloroplast suspension. When required, intact chloroplasts were obtained by centrifugation through a 40% percoll gradient and were washed and suspended in the grinding medium (3). Chlorophyll (Chl) was extracted in 80% acetone and was determined as described in (2).

Preparation of Thylakoid membranes. Thylakoid membranes were prepared from intact chloroplasts. The latter were osmotically shocked by diluting 10-fold with 20 mM Hepes/NaOH buffer. The thylakoid membranes were sedimented by centrifugation at 3,000 g for 5 min and the pellet was suspended in the isolation buffer (5)

PSII Reactions. Electron transport activity through PSII supported by K₃Fe(CN)₆ and phenylenediamine (PD) was monitored polarographically with a YS I model 53 Clark type O₂ electrode (2).

Whole Chain Electron Transport. Electron transport through both photosystems was measured from H₂O to methylviologen (MV) as O₂ uptake in the above O₂ electrode (2).

PSI Reaction. Partial electron transport through PSI was measured polarographically as O₂ uptake (2). Electron flow from PSII was blocked by 3-(3,4-dichlorophenyl) 1,1-dimethylurea (DCMU). Ascorbate/2,6-dichlorophenol indophenol (DCIP) was used as electron donor to PSI, and MV was used as the electron acceptor.

Measurement of Chl *a* Fluorescence Transients. Chl *a* fluorescence transients of isolated chloroplasts were measured in a Waltz pulse amplitude modulated (PAM) fluorometer (2). Thylakoid membranes were suspended at a concentration of 15 µg chl ml⁻¹ and were dark adapted for 10 min before the fluorescence measurements.

Measurement of Electrolyte Leakage. Electrolyte leakage was measured with a conductivity meter. Ten cotyledon discs (8 mm diameter) were punched with a cork borer, washed in deionized water and were kept in 50 ml of deionized water for 4 h. The extent of solute leakage was monitored by measuring the conductivity of the bathing medium (19).

Extraction of Tetrapyrroles. Chloroplasts or thylakoid membranes from control and treated plants were illuminated at a concentration of 1 mg chl ml⁻¹ at a light intensity of 100 W m⁻², and aliquots were taken after various durations of light treatment. The pigments were then extracted in 80% acetone. Fully esterified tetrapyrroles were extracted with an equal volume of hexane. While the mono- and dicarboxylic tetrapyrroles remained in the hexane-extracted acetone residue (HEAR) phase, the fully esterified ones entered the hexane fraction.

Spectrofluorometric Determination of Tetrapyrroles. Quantitative estimation of protoporphyrin IX (Proto IX), Mg-protoporphyrin IX monoester (MPE), and protochlorophyllide (Pchl_{id}) was carried out spectrofluorometrically (20-21). Fluorescence spectra of the HEAR and hexane fractions were recorded with a computer driven spectrofluorometer having photon counting device (SLM Aminco 8000 C) and were corrected for photomultiplier tube sensitivity. Fluorescence spectra were recorded in the ratio mode. Rhodamine B was used in the reference channel as a quantum counter. The photomultiplier tube was cooled to -20^o C by a thermoelectric device to reduce the noise level. A tetraphenylbutadiene block was used to adjust the voltage in both sample as well as reference channels to 20,000 counts s⁻¹ at excitation and emission wavelengths of 348 nm and 422 nm, respectively. The emission spectra were recorded from 580-700 nm, at excitation and emission band widths of 4 nm.

Determination of O₂⁻ Content. Intact chloroplasts were isolated by centrifugation through a 40% percoll gradient and thylakoid membranes were prepared as described before. This procedure of thylakoid membrane isolation from the intact chloroplasts eliminated mitochondrial contamination and consequent presence of cytochrome c oxidase. To remove stromal superoxide dismutase (SOD), the thylakoid membranes were suspended in 50 mM phosphate buffer (pH 7.8) containing 1 mM EDTA, kept for 1 h at 4^o C, and then centrifuged at 3000 g for 8 min. This washing procedure was repeated twice. The production of O₂⁻ was determined spectrophotometrically by monitoring cytochrome c reduction at 550 nm using an extinction coefficient of 19 mM⁻¹ cm⁻¹ (22). The 3 ml reaction mixture consisted of 50 mM phosphate buffer (pH 7.8), 10 mM NaCl, and 20 mM ferricytochrome c. The thylakoid membranes containing 50 μg Chl were added to the above reaction mixture. The reaction rate was determined from the initial absorbance increase 1 min after illumination. Under the above experimental conditions an increase in 0.01 A at 550 nm equals the production of 1.05 nmoles of O₂⁻.

RESULTS

There was no damage to the ALA-treated cucumber plants kept in the dark up to 48 h. However, ALA-treated plants incubated in the dark for 14 h that were transferred to light (800 W m⁻²) became wilted and prominent necrotic patches appeared later. The plants looked dead within 6 h of light exposure.

Pigment Content

Due to dessication, the moisture content of the ALA-treated plants was reduced by 4-

12% after 1-4 h of light treatment. The moisture content of the control plants remained constant throughout the light exposure. While calculating the pigment contents in the photodynamically damaged plants, the values were corrected for the decrease in fresh weight due to desiccation. The Chl content of both control and ALA-treated plants were almost the same after 14 h of dark incubation. After 30 min light treatment, the Chl and carotenoid content decreased slightly in ALA-treated plants. Upon further light treatment, there was a rapid decrease in pigment content (Figure 1). The total Chl content was reduced by 60% after 4 h of light exposure. The loss of Chl *a* was higher than that of Chl *b*. The Chl *a* content was reduced by 61% while Chl *b* was reduced by 42%. Therefore, the Chl *a/b* ratio decreased from 2.8 at 0 h to 2.0 after 4 h of light treatment. The carotenoid content was reduced by 40 and 60% after 1 and 4 h of light treatment respectively. In the control plants the Chl and carotenoid contents remained the same under identical conditions.

Electrolyte Leakage

Conductivity changes in the bathing medium were measured to assess the extent of destruction of plasma membranes in ALA treated plants. The leaf discs were prepared from control and 20 mM ALA-treated plants exposed to light (800 W m⁻²) for 2 h exposed. These leaf discs were immediately kept in bathing medium for 4 h in order to measure electrolyte leakage. The bathing medium of the leaf discs prepared from treated sample had an increase in the conductivity within 1 h of light exposure and continued up to 4 h. There was almost no change in the conductivity of the bathing medium of control leaf discs under identical conditions (Figure 2).

Effect of Photodynamic Damage on Thylakoid Membrane Linked Functions

Most plant tetrapyrroles are localized in chloroplasts. As photodynamic damage is induced by over-accumulated tetrapyrroles, it is likely that the chloroplast membranes would be affected by photodynamic reactions. Therefore, the effect of photodynamic damage on PSI and PSII, the two major functional units of thylakoid membranes, was investigated. The effect of photodynamic damage on the electron transport activities in chloroplasts isolated from control and photodynamically damaged plants was measured polarographically.

Figure 3 shows the electron transport rates of chloroplasts isolated from control and ALA-treated plants exposed to sunlight for 1/2, 1, and 2 h. PSII is most susceptible to membrane perturbation (2). Photodynamic damage is no exception. PD-supported, PSII-dependent O₂ evolution was inhibited around 60% within 30 min of exposure to sunlight. After 1 and 2 h of exposure, the PSII activity was reduced by 75% and 80%, respectively. PSI catalyzed electron transport from DCIPH₂ to MV was relatively resistant to photodynamic damage. PSI activity was reduced by 38%, 49% and 54% after 1/2, 1, and 2 h of exposure to light respectively.

The loss of PSII reaction prompted us to investigate the turnover rate of the 32kd D1 protein to which the reaction center P₆₈₀ is bound. The D1 protein has a high turnover rate, especially under stress conditions. The Pulse-chase experiments using ³⁵S-methionine reveal that due to photodynamic damage the D1 protein is rapidly degraded to a 29 KD protein and it is not replenished by the newly synthesized proteins (data not shown). These data suggest that the degradation of the above protein is highly accelerated and its synthesis is inhibited due to photodynamic damage.

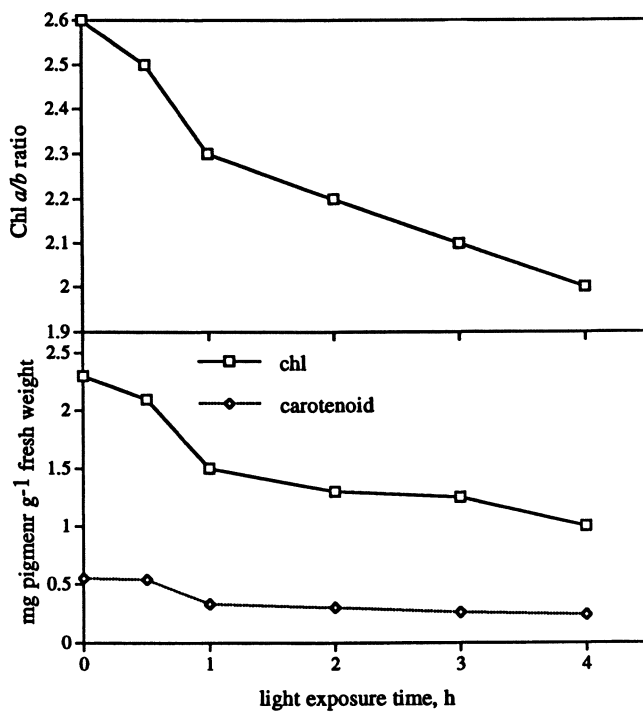


Figure 1. Pigment contents of 20 mM ALA-treated plants exposed to light (800 W m⁻²) for 4 h.

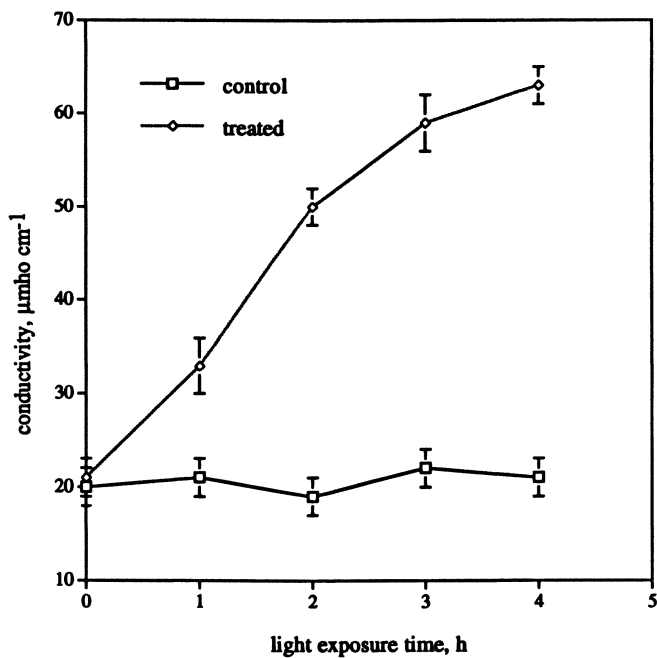


Figure 2. Changes in the conductivity of the bathing medium of cotyledon discs from control and 20 mM ALA-treated and 2h light-exposed cucumber seedlings.

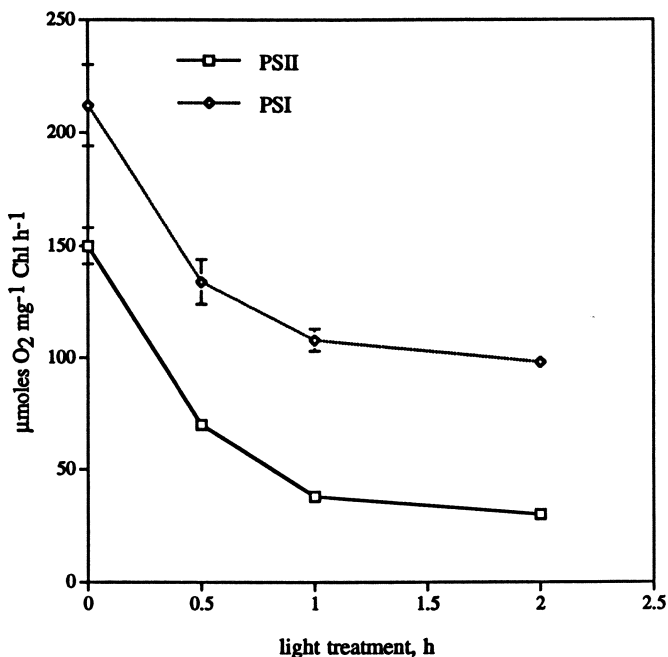


Figure 3. Effect of photodynamic damage on photochemical reactions of the thylakoid membranes. Cucumber seedlings sprayed with 20 mM ALA were incubated for 14 h in dark and were exposed to sunlight (800 W m^{-2}) for 1/2, 1, and 2 h. The chloroplasts were isolated from the cotyledons immediately after light treatment and electron transport reactions were measured as described in Materials and Methods.

Photodynamic Damage at Low Light Intensity

ALA-treated plants that were exposed to relatively low light intensity (250 W m^{-2}) had reduced photodynamic damage. PD-supported PSII dependent O_2 evolution was inhibited by 35% and 70% after 6 and 12 h of light exposure, respectively (Table I). PSI was less susceptible to photodynamic damage and was reduced by 27% and 39% after 6 and 12 h. The whole chain electron transport was reduced by 38% and 65% due to light treatment for 6 and 12 h, respectively. These results demonstrate that the photodynamic damage is light intensity dependent.

Table I: Effect of photodynamic damage under low light intensity on the photochemical reactions of thylakoid membranes. ALA-treated plants were exposed to light (250 W m^{-2}) for 6 and 12 h. Polarographic measurements of electron transport were carried out as described in Materials and Methods. Percent inhibitions are given in parentheses.

Photochemical reaction	control	6 h light treatment	12 h light treatment
	$\mu\text{moles O}_2 \text{ mg}^{-1} \text{ Chl h}^{-1}$		
PSII assay $\text{H}_2\text{O} \rightarrow \text{PD}$	45	29 (35)	14 (70)
PSI assay $\text{DCIPH}_2 \rightarrow \text{MV}$	327	239 (27)	199 (39)
Whole chain assay $\text{H}_2\text{O} \rightarrow \text{MV}$	34	21 (38)	11 (65)

ALA-Induced Photodynamic Damage in Isolated Chloroplasts

Cucumber plants treated with ALA accumulate Mg-tetrapyrroles in the dark. Upon exposure of ALA-treated plants to light, the excess tetrapyrroles are photo-sensitized and the consequent photodynamic reactions kill the plants within a few hours (2). Active oxygen species are involved in photodynamic damage of plants. However, it is difficult to demonstrate the production of $^1\text{O}_2$ or any other oxy-radicals in an intact plant. Since ALA-induced accumulation of Mg-tetrapyrroles occurs in chloroplasts (3), it is likely that chloroplasts may be the primary site of photodynamic reactions. In order to investigate if the photodynamic damage to the photosynthetic functions observed in chloroplasts isolated from photodynamically damaged plants was primary in nature, intact chloroplasts were isolated in dark from control and 20 mM ALA-treated cucumber plants and their PSII activity was monitored during light exposure. Chloroplasts were suspended at a concentration of 1 mg chl ml^{-1} and were illuminated at 100 W m^{-2} for 30 min. Chl concentration, light intensity and duration of light exposure were chosen that caused substantial damage (50%) to PSII reaction in the treated chloroplasts and only a marginal damage (8%) in control chloroplasts. Exposure of chloroplasts to high light intensities (400 W m^{-2}), highly impaired PSII function in the treated chloroplasts and also caused 60% damage in control chloroplasts (Figure 4). These results demonstrate that the pigments present in chloroplasts of ALA-treated plants cause photodynamic reactions.

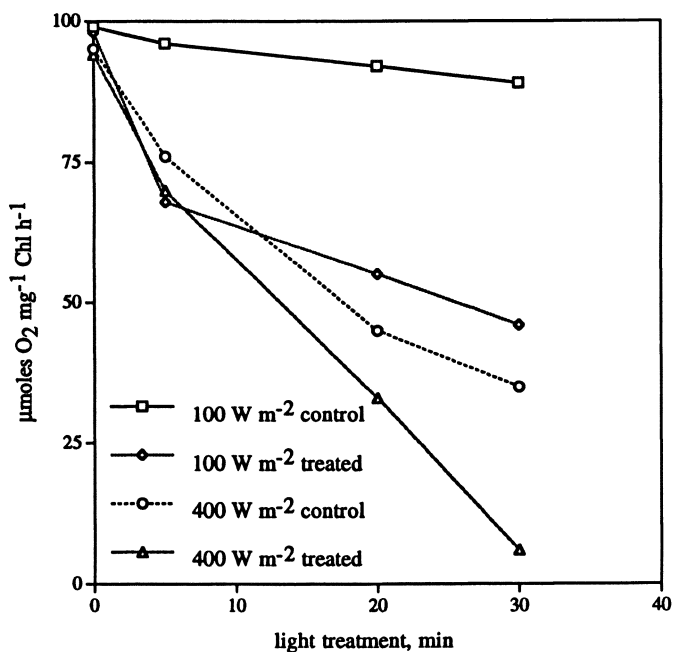


Figure 4. ALA-induced photodynamic damage in isolated chloroplasts. The chloroplasts were isolated from control or 20 mM ALA-treated plants in dark and were exposed to light intensity of 100 or 400 W m⁻². PD supported PSII activity of above chloroplasts was measured as a function of duration of light exposure.

Effect of Exogenous PSII Electron Donors

As discussed above, ALA-induced photodynamic reactions caused impairment of PSII-dependent O_2 evolution. In order to localize the site of damage to PSII, the effect of exogenous electron donors; Mn^{2+} , diphenylcarbazine (DPC) and NH_2OH on PSII-supported DCIP photoreduction was measured in the treated chloroplasts illuminated (100 W m^{-2}) for 30 min. None of the above electron donors could restore PSII-mediated DCIP photoreduction in photodynamically damaged chloroplasts (Table II). NH_2OH at high concentrations (10 mM) donates electrons very close to the reaction center (23). The failure of NH_2OH to restore the photochemical function of PSII suggests that damage had occurred very close to the reaction center. The nature of photodynamic damage to PSII in isolated chloroplasts is identical to the same observed *in vivo* (2).

Table II: Effect of exogenous electron donors on PSII reaction of photodynamically damaged chloroplasts. ALA-treated cucumber seedlings were incubated in the dark for 14 h. Chloroplasts isolated from these plants were exposed to white light (100 W m^{-2}) for 30 min and the PSII-dependent DCIP photoreduction was measured as described in Materials and Methods. The dark DCIP reduction rates for DPC and NH_2OH were subtracted from the observed rates under illumination.

Exogenous electron donor	Donor concentration	Rate of DCIP reduction		
		control	treated	inhibition
	mM	$\mu\text{moles } O_2 \text{ mg}^{-1} \text{ Chl h}^{-1}$		%
None	0	77	32	55
$MnCl_2$	1.0	74	36	50
DPC	2.0	80	44	45
NH_2OH	10.0	60	30	50

Variable Fluorescence

Chloroplasts dark-adapted for 15 min show minimal fluorescence (F_0) when PSII reaction centers are open and maximum fluorescence (F_m), when all PSII reaction centers are closed. The amount of variable fluorescence (F_v) which is equal to $F_m - F_0$, is an index of the functional status of PSII-mediated photochemical reactions.

Table III: Effect of exogenous electron donors on variable fluorescence of illuminated (100 W m^{-2}) chloroplasts isolated from ALA-treated plants. Chloroplasts were isolated from ALA-treated plants and were exposed to light for 0 or 30 min and the Chl *a* fluorescence transients were measured.

Electron donor	concentration	treated 0 h		treated 0.5 h	
		F_0	F_v	F_0	F_v
	mM	arbitrary units			
None	0	4.0	11.0	4.0	6.0
$MnCl_2$	1.0	4.0	10.5	4.0	6.5
DPC	1.0	4.0	11.0	4.0	6.0
NH_2OH	10.0	4.0	11.0	4.0	6.0

As shown in table III, the apparent F_v was reduced by 45% in the treated chloroplasts exposed to light (100 W m^{-2}) for 30 min. The apparent F_0 , however, was not affected by photodynamic reactions. The loss of F_v suggests damage to PSII photochemical function. The exogenous electron donors, Mn^{2+} , DPC, and NH_2OH failed to restore the F_v in treated chloroplasts (Table III). These results confirm that in isolated chloroplasts the photodynamic damage occurs at the oxidizing side of PSII, at a location close to the reaction center.

Protection of PSII by Scavengers of Active Oxygen Species

Activated forms of O_2 are implicated in the damage to the thylakoid membranes (24). The possible toxic oxygen species generated are OH^\bullet , O_2^\bullet , H_2O_2 , and $^1\text{O}_2$ (25). A variety of scavengers and quenchers of specific reactive oxygen species were employed to trace their relative contributions to photodynamic damage in isolated intact chloroplasts (3). It was shown previously that in treated chloroplasts, the $^1\text{O}_2$ scavenger histidine (10 mM) (26) protected PSII-mediated O_2 evolution by 85%, the singlet oxygen quencher NaN_3 (2 mM) (27) protected PSII reaction by 65% and OH^\bullet scavenger formate (28) did not have any effect.

Scavengers of O_2^\bullet , SOD (29-31) and 1,2-dihydroxybenzene-3,5-disulphonic acid (tiron) (32), are impermeable to intact chloroplasts. It was thus difficult to determine whether the O_2^\bullet -scavengers could protect PSII photochemical function. Thylakoid membranes were prepared from the intact chloroplasts isolated from ALA-treated and dark-incubated plants. Most of the Pchl ide is bound to the thylakoid membranes. Therefore, the permeability problem of SOD and tiron was overcome by using the isolated thylakoid membranes prepared from control and treated plants. The isolated thylakoid membranes were suspended at a concentration of 1 mg chl ml^{-1} and were illuminated at an intensity of 100 W m^{-2} . Like intact chloroplasts, illumination of naked thylakoid membranes for 30 min inactivated PSII reaction of PD-supported O_2 evolution of treated samples to the extent of 50% and did not cause any substantial damage to the control samples (figure 5). Illumination of the thylakoid membranes in the presence of O_2^\bullet scavengers, superoxide dismutase and tiron, did not protect PSII. However, as observed for intact chloroplasts, illumination of thylakoid membranes in the presence of the $^1\text{O}_2$ scavengers histidine and NaN_3 protected the PSII reaction to the extent of 85% and 65%, respectively. The OH^\bullet scavenger formate also failed to protect PSII. These results suggest that the $^1\text{O}_2$ is the active oxygen species involved in ALA-induced photodynamic damage of plants.

Involvement of Tetrapyrroles in Photodynamic Damage

In order to determine the nature of pigments involved in photodynamic damage, the thylakoid membranes isolated from control and ALA-treated plants were exposed to light (100 W m^{-2}) for various lengths of time and the concentrations of tetrapyrrole intermediates of the chl biosynthetic pathway present in the membranes were measured spectrofluorometrically (20-21). The pigments present in the membrane were extracted in 80% acetone. Hexane extracted acetone residue (HEAR) were prepared from the acetone extract as described in materials and methods. The HEAR fraction contains the non-esterified tetrapyrroles of Proto IX, Mg-proto IX, Mg-protoporphyrin monoester, Pchl ide and Chl ide . The fluorescence emission spectra of HEAR excited at 400 nm (E_{400}), 420 nm (E_{420}), and 440 nm (E_{440}) elicit the peaks of Proto IX at 632 nm ($E_{400} F_{632}$), Mg-Proto and MPE at 592 nm ($E_{420} F_{592}$), Pchl ide at 638 nm ($E_{440} F_{638}$) and Chl ide at 675 nm ($E_{440} F_{675}$). However, these components, especially Proto IX, Pchl ide , and Chl ide , have overlapping

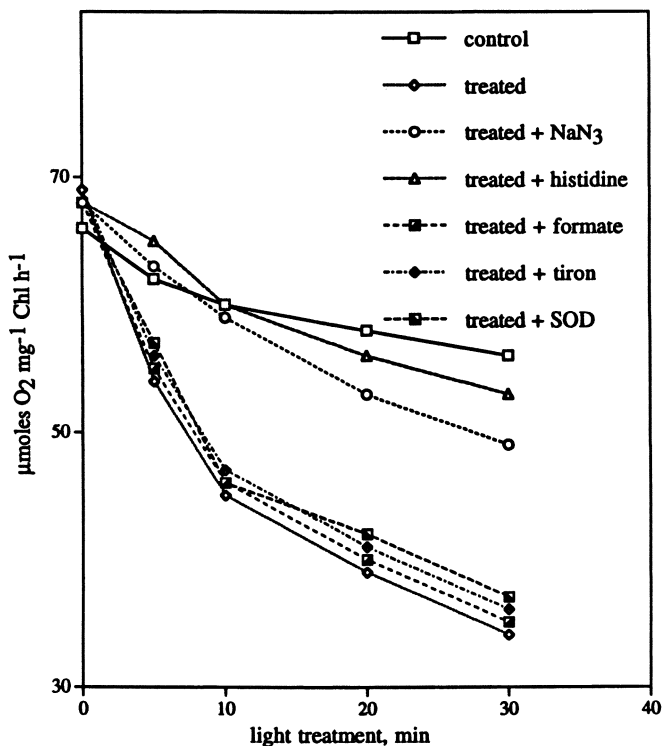


Figure 5. Effect of scavengers on light (100 W m^{-2}) induced photodynamic damage of PS II photochemical reaction in isolated thylakoid membranes isolated from control and ALA-treated plants. The concentrations of the scavengers of active O_2 species were: histidine, 10 mM; NaN_3 , 2mM; formate, 10 mM; tiron, 30 mM; SOD, 100 units ml^{-1} .

fluorescence spectra and need to be corrected at their respective peak positions for the contributions due to other interfering components. The corrected and deconvoluted emission amplitudes were calculated and quantified using appropriate equations and calibration curves (20).

As shown in figure 6, the concentrations of Proto IX, and MPE in the thylakoid membranes isolated from ALA-treated cucumber plants were very low and remained almost constant throughout the illumination. As Pchl_a remains attached to the thylakoid membranes its content was very high (1075 nmoles 100 mg⁻¹ thylakoid protein). Upon illumination Pchl_a concentration decreased to an extent of 20% within 15 min probably due to its photo-transformation to Chl_a and may be partially due to photodegradation. The remaining Pchl_a was non-phototransformable and slightly declined after 1 h, probably due to its partial photo-destruction. The protein content of the thylakoid membrane remained constant throughout the light treatment. It is possible that the Chl_a formed by phototransformation of Pchl_a was phytylated by the chl synthetase reaction and was integrated into the thylakoid membranes where it participated in light-driven photosynthetic reactions. However, the light energy absorbed by the nonphoto-transformable Pchl_a population would not transfer energy to the photosynthetic reaction centers. Consequently, the absorbed energy in a type II photo-sensitization reaction would be transferred to molecular O₂, leading to the formation of highly reactive ¹O₂. Therefore, the non-transformable Pchl_a appears to be the most likely candidate responsible for the photodynamic damage.

Production of Superoxide Radical (O₂⁻)

In a type I photosensitization reaction, the triplet sensitizer directly reacts with the substrate to generate O₂⁻ (15). To investigate if O₂⁻ is formed in tetrapyrrole-induced photodynamic reactions due to type I photosensitization reactions, its production was monitored in the thylakoid membranes isolated from dark-incubated plants. The production of O₂⁻ by the thylakoid membranes exposed to light (400 W m⁻²) was monitored by cytochrome c reduction, as described in Materials and Methods. As shown in table IV, the amount of O₂⁻ produced by the control and the treated thylakoid was almost the same. The O₂⁻ produced by the control and treated thylakoid membranes in light was abolished by DCMU, an inhibitor acting at the reducing side of PSII of the photosynthetic electron transport chain. This suggests that the production of O₂⁻ in the control and treated thylakoids had its origin from the photosynthetic electron transport chain due to the Mehler (33) reaction at the acceptor side of PSI and therefore, type I photosensitization reaction was not involved.

Table IV: Production of O₂⁻ in thylakoid membranes isolated from control and ALA-treated plants. Thylakoid membranes were suspended at a concentration of 1 mg Chl ml⁻¹ and illuminated at a light intensity of 400 W m⁻².

Sample	-DCMU	+DCMU	Inhibition
	nmoles O ₂ ⁻ mg ⁻¹ protein h ⁻¹		%
Control	20	4	80
ALA-treated	25	5	80

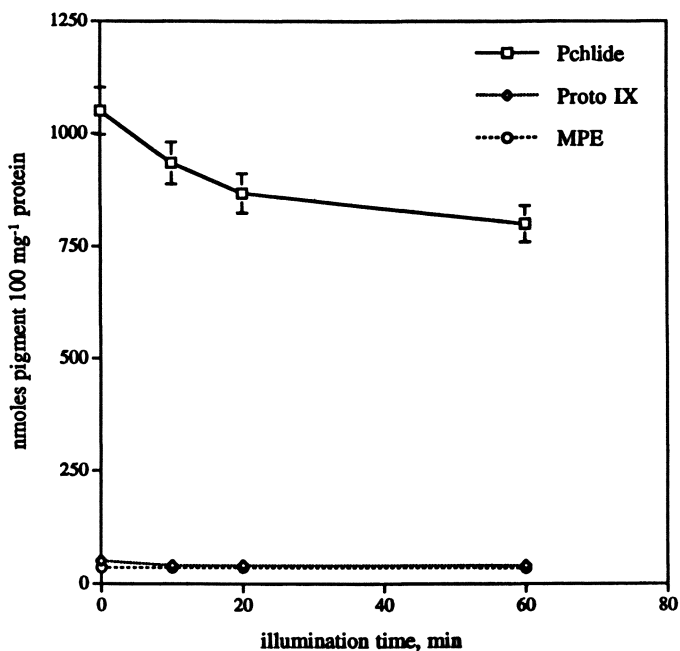


Figure 6. ProtoIX, MPE, and Pchl a contents of light exposed (100 W m^{-2}) thylakoid membranes isolated from ALA-treated plants. The above pigment contents of the thylakoid membranes isolated from control plants were 20-30 nmol 100 mg^{-1} protein.

DISCUSSION

Due to photodynamic damage, the Chl content was reduced by 60 % within 4 h of light exposure (Figure 1). However, the rate of loss of Chl *a* was higher than that of Chl *b*. The progressive decrease in the Chl *a/b* ratio suggests preferential loss of Chl *a* enriched light harvesting chlorophyll protein complex I over that of Chl *b* enriched light harvesting chlorophyll protein complex II. The increase in conductivity (Figure 2) of the bathing medium of photodynamically damaged leaves suggests that the plasma membrane is damaged, causing solute leakage. Therefore, the death of the plants could be due to ultimate destruction of plasma membrane and cellular integrity.

ALA-induced photodynamic damage of plants could also be due to the impairment of various vital functions. Mg-porphyrins which accumulate due to ALA treatment are localized in the chloroplasts. Therefore, the photodynamic damage should affect the chloroplasts. The inhibition of PSII and PSI electron transport suggests that the photodynamic reactions damage thylakoid membranes. The damage to PSII was higher than to PSI (Figure 3). The former is usually more sensitive to stress than the latter (2). The 32 KD D1 protein has a high turnover rate which rapidly increases during stress such as photoinhibition (19). Pulse chase experiments demonstrated a rapid degradation of D1 protein due to photodynamic damage.

Photodynamic damage is dependent on light intensity. Reduction of light intensity from 800 W m⁻² to 250 W m⁻² reduced the extent of damage of ALA-treated plants (Table I). The electron transport chain of chloroplasts isolated from ALA-treated plants exposed to low light intensity of 250 W m⁻² was only partially impaired. This suggests that the production of toxic O₂ species mediated by photodynamic reaction in ALA-treated plants is limited by light intensity.

The loss of photochemical function due to photodynamic reaction is primary in nature. In illuminated chloroplasts isolated from ALA-treated plants the failure of exogenous PSII electron donors, Mn²⁺, DPC, and NH₂OH to restore the P₆₈₀-mediated photochemical reactions (Tables II, III) suggests that the damage to PSII is very close to the reaction center. The nature of photodynamic damage to PSII in isolated chloroplasts is identical to the same observed in vivo (2). Identical nature of damage to PSII in intact plants and isolated chloroplasts suggest that the photodynamic damage to photosynthetic apparatus is primary and not due to any indirect effect.

The ¹O₂ scavengers, histidine, and NaN₃, could protect the thylakoid membrane linked function of PSII (Figure 5). However, formate, the scavenger of OH⁰, failed to protect PSII activity against photodynamic damage. Neither SOD nor tiron protected the PSII reaction. These results confirm that ¹O₂ is the active oxygen species involved in the photodynamic damage. The involvement of ¹O₂ has also been demonstrated in photodynamic therapy of cancerous cells of animal tissues (31).

In thylakoid membranes, isolated from ALA-treated plants the abundant Chl precursor is Pchl_{ide} (Figure 6). Photodynamic damage to PSII in thylakoids prepared from ALA-treated tissues confirm that Pchl_{ide} is the photosensitizer responsible for the damage. However, this remains to be ascertained by studying the action spectrum of photodynamic damage. If the action spectrum of photodynamic reaction matches the absorption spectrum of Pchl_{ide}, it could be then concluded that Pchl_{ide} is responsible for photodynamic reaction.

In addition to type II photosensitization of tetrapyrroles that generate ¹O₂, type I photosensitization could lead to the production of O₂⁻. However, abolition of O₂⁻ production by DCMU in both control and treated thylakoid membranes (Table IV) indicates that O₂⁻ was formed at the reducing side of PSI and not from the type I photosensitization reaction of Pchl_{ide}.

ACKNOWLEDGEMENTS

This work was supported by a grant from the Council of Scientific and Industrial Research, New Delhi, India. The author wishes to thank Dr. David Obenland for editing the manuscript.

LITERATURE CITED

1. Rebeiz, C. A.; Montazer-Zouhoor, A.; Hopen, H.; Wu, S- M. *Enzyme Microb. Technol.* 1984, 6, 390-401.
2. Tripathy, B. C.; Chakraborty, N. *Plant Physiol.* 1991, 96, 761-767.
3. Chakraborty, N.; Tripathy, B. C. *Plant Physiol.* 1992, 98, 7-11.
4. Chakraborty, N.; Tripathy, B. C. *J. Biosc.* 15, 199-204.
5. Chakraborty, N.; Tripathy, B. C. *J. Plant Biochem. Biotech.* 1992, 65-68.
6. Rebeiz, C. A.; Montazer-zouhoor, A.; Mayasich, J. M.; Tripathy, B. C.; Wu, S-M; Rebeiz, C. C. *CRC Crit. Rev. Plant Sci.* 1988, 6,385-436.
7. Rebeiz, C. A.; Reddy, K. N.; Nandihalli, U. B.; Velu, J. *Photochem. Photobiol.* 1990, 52, 1099-1117.
8. Duke, S. O.; Becerril, J. M.; Sherman, T. D.; Lydon, J.; Matsumoto, H. *Pestic. Sci.* 1990, 30, 367-378.
9. Lydon, J.; Duke, S. O. *Pestic. Biochem. Physiol.* 1988, 31, 74-83.
10. Martinge, M.; Scalla, R. *Plant Physiol.* 1988, 31, 74-83.
11. Witkowski, D. A.; Halling, B. P. *Plant Physiol.* 1988, 86, 619-22
12. Jacobs, J. M.; Jacobs, N. J.; Sherman, T. D.; Duke, S. O. *Plant Physiol.* 1991, 97, 197-203.
13. Heath, R. L.; Packer, L. *Arch. Biochem. Biophys.* 1968, 125, 189-98.
14. Hopf, F. R.; Whitten, D. G. in *The Porphyrins*, Dolphin, D. Eds. Academic Press, New York, 1978 vol. 2; pp 191-195.
15. Foote, C. S.; Shook, F. C.; Abakerli, R. B. *Methods Enzymol.* 1984, 105, 36-47.
16. Granick, S. in *Biochemistry of Chloroplasts*; Goodwin, T. W. Eds. Academic Press, New York, 1967, Vol 2, pp 373-406.
17. Stobart, A. K.; Ameen-Bukhari, I. *Biochem. J.* 1984, 222, 419-426.
18. Tripathy, B. C.; Mohanty, P. *Plant Physiol.* 1980, 66, 1174-1178.
19. Chakraborty, N. *Ph. D. Thesis*, Jawaharlal Nehru University, New Delhi, India, 1992.
20. Hukmani, P., Tripathy, B. C. *Anal. Biochem.* 1992, 206, 125-130.
21. Rebeiz, C. A.; Matheis, J. R.; Smith, B. B.; Rebeiz, C. C. *Arch. Biochem. Biophys.* 1975, 166, 446-465.
22. Asada, K. *Methods Enzymol.* 1984, 105, 422-429.
23. Sharp, R. R.; Yocum, C. F. *Biochim. Biophys. Acta* 1981, 635, 90-104.
24. Knox, J. P.; Dodge, A. D. *Planta* 1985, 164, 30-34
25. Elstner, E. F. *Ann. Rev. Plant Physiol.* 1982, 33, 73-96.
26. Matheson, B. C.; Etheridge, R. D.; Kratowich, N. R.; Lee, J. *Photochem. Photobiol.* 1975, 21, 165-171.
27. Anderson, S. M.; Krinsky, N. L.; Stone, M. J.; Clagett, D. C. *Photochem. Photobiol.* 1974, 20, 65-69.
28. Kar, M.; Feierabend, J. *Planta* 1984, 160, 385-391.
29. Fridovich, I. *Science* 1978, 201, 875-880.
30. McCord, J. M.; Fridovich, I. *J. Biol. Chem.* 1969, 244, 6049-6054.
31. Dougherty, T. J. *Photochem. Photobiol.* 1987, 45, 875-889.
32. Miller, R. W.; Macdowall, F. D. H. *Biochim. Biophys. Acta* 1975, 387, 176-187.
33. Mehler, A. H. *Arch. Biochem. Biophys.* 1951, 33, 65-77.

RECEIVED December 14, 1993

Chapter 6

Characterization of Plant and Yeast Protoporphyrinogen Oxidase

Molecular Target of Diphenyl Ether Type Herbicides

Jean-Michel Camadro¹, Michel Matringe², Nicole Brouillet¹,
Françoise Thomé¹, and Pierre Labbe¹

¹Laboratoire de Biochimie des Porphyrines, Institut Jacques Monod,
Centre National Recherche Scientifique, Université Paris 7, 2 Place
Jussieu, F-75251 Paris Cedex 05, France

²Laboratoire de Physiologie Végétale, Centre d'Etudes Nucléaires de
Grenoble—Université Joseph Fourier, 85X, F-38041 Grenoble Cedex,
France

Protoporphyrinogen oxidase is the molecular target of diphenylether (DPEs) type herbicides. In order to better understand the mechanism of action of DPEs, we purified to homogeneity protoporphyrinogen oxidase from lettuce etiochloroplasts and from yeast mitochondria. Both enzymes are 55 KDa flavo-proteins, the lettuce enzyme contains FMN while the yeast enzyme contains FAD. The kinetic properties of the purified enzymes are very comparable to those reported for the membrane-bound enzymes in terms of affinity toward protoporphyrinogen IX and inhibition by DPEs. We further characterized a yeast strain deficient in protoporphyrinogen oxidase activity as containing normal amounts of immunodetectable protoporphyrinogen oxidase. However, the mutant protein was unable to bind a tritiated DPE.

Diphenylether-type herbicides (DPEs) induce characteristic light-dependent phytotoxic damages through induction of protoporphyrin IX accumulation in treated plants (for a review, see 1). This abnormal accumulation of protoporphyrin IX is the consequence of the strong inhibitory effect of DPEs on protoporphyrinogen oxidase, an enzyme of the common branch of the heme and chlorophyll biosynthesis pathways (2, 3). Protoporphyrinogen oxidase catalyzes the oxidative aromatization of protoporphyrinogen IX [1] to protoporphyrin IX [2] (Figure 1). The massive accumulation of protoporphyrin IX within DPE-treated plant cells is somewhat puzzling since the inhibition of protoporphyrinogen oxidase should yield protoporphyrinogen accumulation. The general assumption is that protoporphyrinogen IX is non-enzymatically oxidized out of its site of synthesis and is thus no more available for further metabolism by the magnesium- or iron-chelatase systems. Recent data indicate that some DPE-insensitive extraplastidic protoporphyrinogen IX oxidizing activity (4) may be involved in the rapid accumulation of protoporphyrin IX in DPE-treated cells. Protoporphyrinogen oxidase has a complex pattern of localization within plants that involves the presence of the enzyme in mitochondria and on both the envelope and the thylakoid membranes of chloroplasts (5, 6). This supports the idea of a tight physiological control of protoporphyrin IX and metalloprophyrin synthesis through intracellular metabolite compartmentation.

0097-6156/94/0559-0081\$08.00/0

© 1994 American Chemical Society

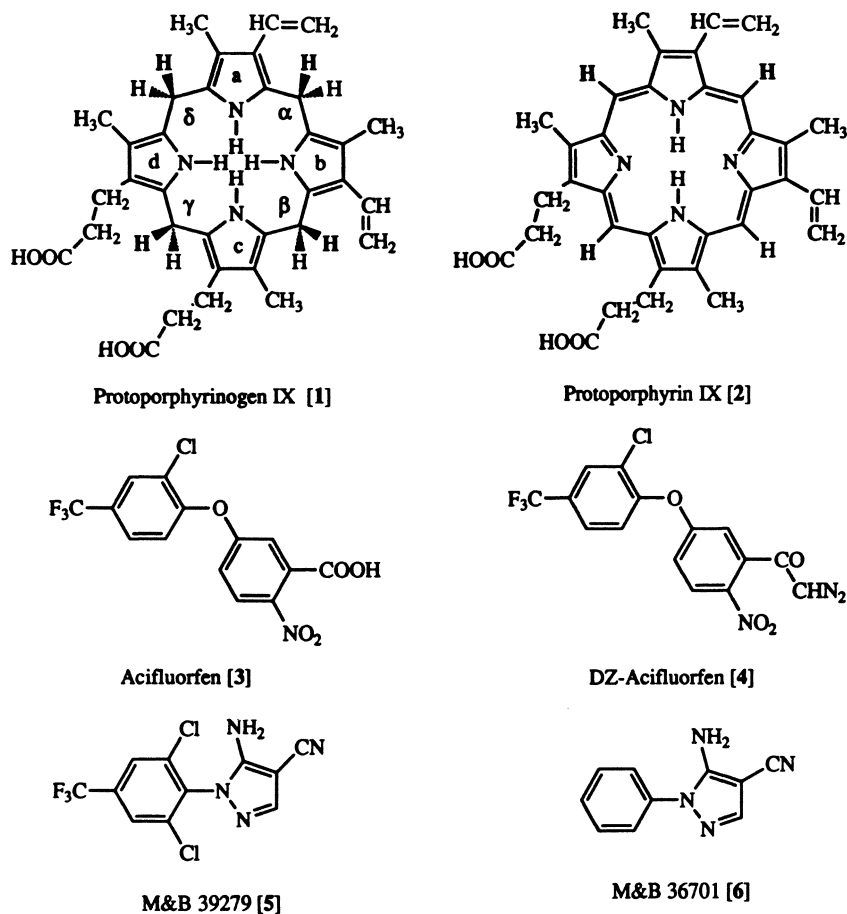


Figure 1. Structures of protoporphyrinogen oxidase substrate [1], product [2] and protoporphyrinogen oxidase-inhibiting herbicides from different chemical classes

The availability of radiolabeled acifluorfen (Figure 1) [3] (7) allowed demonstration that the different inhibitors of protoporphyrinogen oxidase share the same binding site on the plant enzyme (8). Furthermore, tritiated acifluorfen specific binding to pea etioplast membranes was competitively displaced by protoporphyrinogen IX, the substrate of protoporphyrinogen oxidase (9). These results were thus in full agreement with the kinetic studies that showed that DPEs are competitive inhibitors (with respect to the tetrapyrrole substrate) of plant and mouse protoporphyrinogen oxidase (10).

In order to get more insight into the mechanism of inhibition of protoporphyrinogen oxidase by diphenyl ethers, we undertook the purification of the enzyme from yeast cells, by taking advantage of the powerful molecular genetic techniques available for this organism, and from lettuce etiolated leaves (hearts of lettuce heads) where the activity was higher than in green leaves. Lettuce was chosen as starting material for the purification since it is available fresh almost throughout the year. Furthermore, we used DZ-[³H]AF [4], a diazocetone derivative of [³H]acifluorfen (7) as a potential photoaffinity label for yeast protoporphyrinogen oxidase. This compound was used for further characterization of a yeast strain previously described as heme-deficient (11) due to lack of protoporphyrinogen oxidase activity (12).

Biochemical Characterization of Protoporphyrinogen oxidase.

Chemicals : Acifluorfen (sodium salt) {5-[2-chloro-4-(trifluoromethyl)phenoxy]-2-nitrobenzoic acid} was from ChemService, West Chester, PA, USA; M&B 39279 {5-amino-4-cyano-1-(2,6-dichloro-4-trifluoromethylphenyl)pyrazol} [5] and M&B 36701 {5-amino-4-cyano-1-phenylpyrazol} [6] were kindly provided by Rhône-Poulenc Agrochimie, France. [³H]acifluorfen was radiolabeled at position 3 of the nitrobenzene ring with a specific activity of 9.5 Ci/mmol (7); the diazocetone derivative of [³H]acifluorfen was synthesized in two steps from [³H]acifluorfen (Mornet *et al.*, manuscript in preparation). Protoporphyrin IX hydrochloride was from Porphyrin Products, Logan, UT, USA. Protoporphyrinogen IX was prepared by chemical reduction of protoporphyrin IX with 3% sodium amalgam, and protoporphyrinogen oxidase activity was assayed as already described (13).

Preparation of Membrane Fractions for Protoporphyrinogen Oxidase Studies. Yeast (*Saccharomyces cerevisiae*) mitochondrial membranes were prepared from the haploid wild-type strain GRF18 (a, his3, leu2) and from the protoporphyrinogen oxidase-deficient strain CG122-6C (a, his3, leu2, hem14-1). The cells were grown on a complete medium, harvested during the late exponential phase of growth and broken with glass beads in a 25 mM Tris-HCl buffer pH 7.6 containing 0.65 M sorbitol. Fractions enriched in mitochondrial membranes were obtained by differential centrifugations. The strain CG122-6C was obtained after tetrad analysis from the cross between the original mutant strain G122 (12) and the wild-type strain GRF18.

Fractions enriched in etioplastic membranes were prepared as follows: the etiolated leaves (1 kg) were washed with deionized water, grinded with a Waring blender for 6 seconds in a 25 mM Tris-HCl buffer (pH 7.6) containing 0.5 M sucrose, 1 mM MgCl₂, 1 mM DTT, 1 mM EDTA, and 60 µg/ml PMSF (1.6 l of buffer/kg leaves) and filtered through one layer of nylon mesh (50 µm) and four layers of gauze. The resulting cell-free suspension was centrifuged for 5 min at 1000 g. The pellet was suspended in the grinding buffer without sucrose and magnesium, Potter homogenized and centrifuged for 60 min at 150,000 g.

Membrane fractions (yeast and lettuce) were resuspended in 0.1 M potassium phosphate buffer (pH 7.6) to a protein concentration of about 20 mg/ml. Wild-type yeast protoporphyrinogen oxidase activity was 7.5 nmol protoporphyrinogen IX oxidized/h/mg total membrane-bound proteins. Lettuce etioplast protoporphyrinogen

oxidase activity was 5.1 nmol protoporphyrinogen IX oxidized/h/mg total membrane-bound proteins. Yeast protoporphyrinogen oxidase was purified 5600 fold with a 25 % yield. The purification process involved solubilization of the membrane-bound proteins with the ionic detergent CHAPS, ammonium sulfate fractionation of the solubilized proteins, hydrophobic interactions chromatography on Phenyl-Sepharose followed by ionic interaction chromatography on Mono-P and DEAE-Sepharose. Lettuce protoporphyrinogen oxidase was purified 1800 fold with a 33 % yield. The purification process involved solubilization of the membrane-bound proteins with the non-ionic detergent Tween 80, pseudo-affinity chromatography on Blue-Sepharose, ionic interaction chromatography on DEAE-Sepharose followed by hydrophobic interactions chromatography on Phenyl-Sepharose. Details on yeast and lettuce protoporphyrinogen oxidase purifications will be published elsewhere (Camadro *et al*, manuscripts in preparation).

Radioligand Binding Assay. Equilibrium binding of [³H]AF and DZ-[³H]AF to yeast mitochondrial membranes was determined as previously described for pea etioplast membranes (9). Basically, the incubation mixture (1 ml) contained 0.1 M potassium phosphate buffer (pH 7.2) 1 mg of proteins and from 1.45 to 30 nM radioligand. The assay medium was incubated for 30 min at 30°C and filtered through GF/B glass filters (Whatman). The filters were washed 3 times with 3 ml ice cold phosphate buffer and further processed for liquid scintillation counting with HiSafe-3. Non-specific binding was determined in the presence of 15 μM (final concentration) of cold competitive ligand. Control experiments were run with the inactive analog of M&B 39279, M&B 36701 (Figure 1).

Photolabeling of DZ-[³H]AF Binding Sites on Yeast Mitochondrial Membranes. Membranes (50 μg protein/ml) were preincubated in 0.1 M potassium phosphate buffer pH 7.2 at 30°C for 15 min with DZ-[³H]AF (25 nM of final concentration) in the dark. They were further irradiated for 10 min to dissociate DZ-AF into N₂ and a highly reactive carbene derivative of acifluorfen. A Wilmer Lourmat fluorescence table 302 was used to irradiate the membranes; the lamps emit a broad spectrum ultraviolet radiation, with a maximum at 366 nm. Aliquots (0.5 ml) of the membrane suspensions were transferred into UV-transparent spectrophotometric plastic cuvettes and placed on the fluorescence table. After irradiation, mitochondrial membranes were harvested by centrifugation, the pellet was solubilized in SDS-PAGE sample buffer (14) and the proteins were separated by standard SDS-PAGE (14). After electrophoretic migration, the gels were processed for fluorography (30 min fixation in isopropanol/acetic acid/water (40/10/50)) followed by treatment with the fluorographic reagent Amplify™ (Amersham) for 20 min, and drying under vacuum. The radioactivity was monitored on a Molecular Dynamics PhosphorImager with a disposable tritium-sensitive screen.

Determination of Protoporphyrinogen Oxidase Relative Abundance and Specific Activity.

Protoporphyrinogen oxidase relative abundance was determined through Scatchard analysis of [³H]AF binding to yeast mitochondrial and lettuce etioplast membranes. As shown in Figure 2, both membranes contained a single class of high affinity specific binding sites. The specific binding of [³H]AF could be displaced by M&B 39279, a compound active as an inhibitor of protoporphyrinogen oxidase activity *in vitro*. By contrast, M&B 36701 which is not an inhibitor of protoporphyrinogen oxidase, is not able to displace [³H]AF binding (Figure 3). The Scatchard plots allowed calculation of then dissociation constant (K_d) and maximum number of

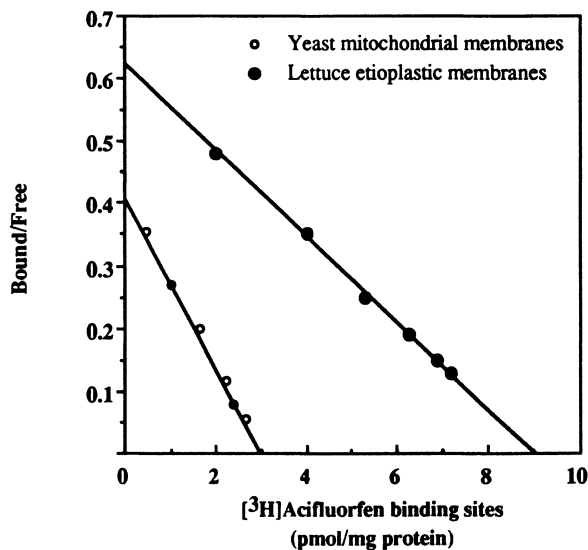


Figure 2. Scatchard plot of acifluorfen binding to yeast mitochondrial membranes and lettuce etioplastic membranes.

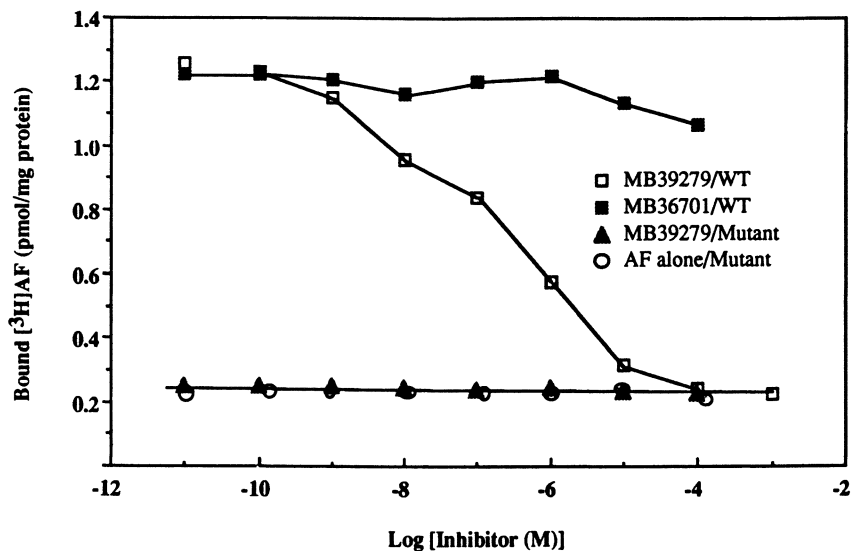


Figure 3. Displacement curves of acifluorfen binding on wild-type and protoporphyrinogen oxidase-deficient yeast mitochondrial membranes by M&B 39279 and M&B 36701

specific binding sites (B_{\max}) values as 7 nM and 3 pmol/mg protein respectively for yeast protoporphyrinogen oxidase. The amount of protoporphyrinogen oxidase activity and protein was found to be higher in etiolated tissues than in mature chloroplasts by means of direct activity measurement and Scatchard analysis of binding of [^3H]AF (B_{\max} = 9 pmol/mg protein vs 2.3 pmol/mg protein). However, the catalytic properties of the enzyme were identical and the dissociation constant of [^3H]AF was 14.5 nM in both cases. Taking into account the protoporphyrinogen oxidase activity of the crude membrane preparations (7.5 nmol protoporphyrinogen IX oxidized/h/mg total protein in yeast and 5.1 nmol/h/mg protein in etioplasts), the maximum number of specific binding sites (B_{\max} = 3 pmol/mg protein in yeast and 9 pmol/mg protein in lettuce) allowed us to calculate the specific activities of protoporphyrinogen oxidase as 2500 mol protoporphyrinogen IX oxidized/h/mol for the yeast enzyme and 570 mol protoporphyrinogen IX oxidized/h/mol for the lettuce enzyme.

Molecular Properties of Purified Yeast and Lettuce Protoporphyrinogen Oxidases

Lettuce protoporphyrinogen oxidase was found to be a 55 KDa polypeptide with a pI at 6.5 and a specific activity of 9300 nmol protoporphyrinogen IX oxidized/h/mg protein at 30°C. The K_m for protoporphyrinogen was 0.3 μM . Fluorescence spectra of the purified enzyme revealed the presence of a flavin. The intensity of fluorescence was identical at neutral and acidic pH, suggesting the presence of FMN. The purified enzyme activity was inhibited by diphenylether-type herbicides. The IC_{50} were found to be of the same order of magnitude as those measured on the membrane-bound enzyme as shown in Table I.

Yeast protoporphyrinogen oxidase was found to be a 55 KDa polypeptide with a pI at 8.5 and a specific activity of 40,000 nmol protoporphyrinogen IX oxidized/h/mg protein at 30°C. The K_m for protoporphyrinogen was 0.07 μM . Fluorescence spectra of the purified enzyme revealed the presence of a flavin. The intensity of fluorescence was 10 times higher at acidic pH than at neutral pH, suggesting the presence of FAD as a cofactor. Diphenylether-type herbicides competitively inhibited purified yeast protoporphyrinogen oxidase while the inhibition of the membrane-bound enzyme was previously found to be mixed-competitive. Antibodies raised in rabbits against yeast protoporphyrinogen oxidase were used to study protoporphyrinogen oxidase biogenesis. Protoporphyrinogen oxidase is synthesized as a higher molecular weight precursor (58 KDa) which is very rapidly converted *in vivo* to the mature (55 KDa) membrane-bound form. This precursor form of protoporphyrinogen oxidase was immunoprecipitated from proteins synthesized *in vitro* by translation of total yeast RNAs in a rabbit reticulocyte lysate system or from *in vivo* metabolically labelled proteins in pulse-chase experiments (data not shown).

Photoaffinity Labeling of Yeast Mitochondrial Membranes by DZ-[^3H]AF.

DZ-[^3H]AF bound to a single saturable binding sites on mitochondrial membranes from a wild-type yeast strain. Saturation curves yielded K_d and B_{\max} values of 12.5 nM and 3 pmol/mg protein for DZ-[^3H]AF. DZ-[^3H]AF did not bind specifically to the mitochondrial membranes of the protoporphyrinogen oxidase deficient strain CG122-6C. The photolabeled sites were analysed by solubilization of the membrane-bound proteins in sodium dodecyl sulfate and electrophoretic separation of the proteins on polyacrylamide gel. A single polypeptide appeared to be specifically labeled by DZ-

[³H]AF. By reference to [¹⁴C]molecular mass marker proteins, the apparent molecular mass of the labeled protein was estimated to be 55,000 (Figure 4). The labeling of this protein could be prevented completely by the presence 10 μM of M&B39279 (an efficient inhibitor of protoporphyrinogen oxidase) during the incubation of the membranes with DZ-[³H]AF. The inactive analog of M&B39279, M&B36701 (10 μM final concentration) was not able to inhibit [³H]AF binding and to prevent the covalent photoreaction of DZ-[³H]AF with protoporphyrinogen oxidase. Furthermore, in the absence of excess of cold competitor, this protein failed to be labeled in mitochondrial membranes prepared from the protoporphyrinogen oxidase-deficient mutant strain CG122-6C.

Conclusions and Prospects.

The availability of a radiolabeled ligand of protoporphyrinogen oxidase allowed us to demonstrate that the protein is of low abundance but is very active in yeast mitochondria as well as in plant etioplasts. The specific activity of the yeast enzyme (40,000 nmol protoporphyrinogen IX oxidized/h/mg enzyme) is much higher than that previously described for other protoporphyrinogen oxidases (15, 16) but is of the same order of magnitude as that reported for yeast ferrochelatase (17). Both yeast and lettuce protoporphyrinogen oxidases were purified as 55 KDa polypeptides. This molecular mass is in good agreement with those reported for the mouse and beef enzymes (15, 16). Purified lettuce protoporphyrinogen oxidase is more active than the previously described barley enzyme (5). Another major difference lies in the molecular mass of the enzyme (55 KDa vs 35 KDa). During the purification process we consistently observed the proteolytic degradation of lettuce (as well as yeast) protoporphyrinogen oxidase into active fragments of molecular mass ranging from 30 KDa to 45 KDa. This may explain the discrepancies between our results and those previously described (5). Both purified protoporphyrinogen oxidases are inhibited by diphenylether-type herbicides. This confirms that a direct inhibition of protoporphyrinogen oxidase is actually the primary effect of diphenylether-type herbicides in treated plants.

Yeast and lettuce protoporphyrinogen oxidases appear as flavoproteins differing by the nature of the flavin associated with the protein. Such difference in the flavin moiety was previously observed in mammals where the beef enzyme contains FAD (15) while the mouse enzyme contains FMN (18). The occurrence of a flavin at the active site of protoporphyrinogen oxidase may explain some catalytic properties of the enzyme. Jones *et al.* (19) studied the oxidation of protoporphyrinogen stereospecifically tritiated at the methylene bridges. These authors determined that three hydrogen atoms from the methylene bridges are removed from one side of the protoporphyrinogen nucleus while the fourth one is removed from the other side of the cyclic tetrapyrrole. Furthermore, the protons from bridges α and β [1] appeared to be removed through two distinct mechanisms. A model was proposed for protoporphyrinogen oxidation involving the removal of three hydrides and one proton. Thus, it is reasonable to suggest that while the flavin may be involved in hydrides removal, another functional group on the protein, possibly a basic amino-acid residue may be involved in the fourth proton removal. Such a model is supported by molecular dynamics calculations based on the protoporphyrinogen oxidase inhibitors QSAR (20, 21) which pointed out in turn the potential role of charge transfer and electrostatic interactions in protoporphyrinogen oxidase functioning.

DZ-[³H]AF is a powerful photoaffinity ligand for protoporphyrinogen oxidase. The labeled enzyme appears to be a 55 KDa polypeptide. This value is identical to that obtained with purified yeast protoporphyrinogen oxidase. The specificity of the interaction between DZ-[³H]AF and the protein is ascertained by the

Table I . Inhibition of lettuce protoporphyrinogen oxidase by diphenylether-type herbicides (IC₅₀)

<i>Chemical family</i>	<i>Inhibitor</i>	<i>IC₅₀ (nM) Membrane bound enzyme</i>	<i>IC₅₀ (nM) Purified enzyme</i>
Diphenylether	AFM	3	1.5
	AF	450	500
	LS 820340	11	6.3
	RH 5348	690	1500
Pyridine	LS 82556	19000	17000
Phtalimide	KS 307829		1.8
	MK 616		8
Oxadiazole	Oxadiazon	12.5	17.7
Pyrazole	M&B 39279	70	20
	M&B 36701	> 100000	> 100000

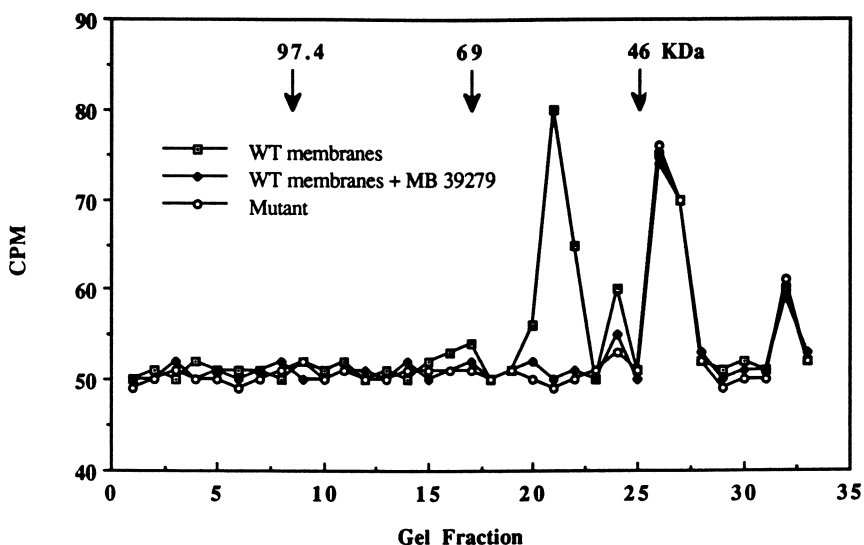


Figure 4. Radioactivity profile analysis of wild-type and protoporphyrinogen oxidase deficient yeast mitochondrial proteins photolabeled with DZ-[³H]AF in the presence or in the absence of M&B39279

competition experiments and the lack of specific binding and labeling of mitochondrial membranes from the protoporphyrinogen oxidase-deficient yeast strain. However, under our experimental conditions, some membrane-bound proteins are non specifically photolabeled by DZ-[³H]AF (labeling not displaced by excess cold competitor or present in the membranes from the mutant). A major difference in [³H]AF and DZ-[³H]AF binding to yeast mitochondrial membranes lies in the high non-specific binding observed with the diazocetone derivative of acifluorfen (even in incubations without light) compared to that measured with acifluorfen. This must be mainly due to the different bulk hydrophobicity of the two compounds. Acifluorfen, bearing a free carboxylic acid group, must be more hydrosoluble than the photoreactive compound where this carboxylic group is derivatized to yield the diazocetone function. It appears from immunological studies that the mutant strain contains an inactive protein of the same size and abundance as the wild type strain. This suggests that the mutation is either a mis-sense point mutation or a small deletion. This mutation not only abolished the catalytic activity of the enzyme but also prevented any binding of radiolabeled inhibitors. This may be due to modifications in the active site of the protein either directly through a mutation modifying an amino-acid essential in the catalysis or through a drastic modification of the accessibility of the active site of the enzyme to substrates and inhibitors which is induced by an improper folding of the mutated protein. It is generally recognized that grossly mis-folded proteins are rapidly degraded by specialized proteases. The fact that in the CG122-6C mutant, the abundance of the protein is normal suggests that the overall folding of the protein must be correct. Although not demonstrated, it seems more likely that the mutation may rather directly affect the topology of the active site of protoporphyrinogen oxidase.

DZ-[³H]AF together with the availability of purified protoporphyrinogen oxidases will thus provide powerful tools to probe the active site of the enzyme through peptide mapping of the purified radiolabeled protein and structure determination of the labeled peptides. This approach will complement the characterization of the mutation in the protoporphyrinogen oxidase-deficient yeast strain and may provide the molecular basis for further site-directed mutagenesis of the yeast protoporphyrinogen oxidase gene.

Acknowledgments. This work was supported by grants from the Centre National de la Recherche Scientifique, University Paris 7 and the Institut National pour la Recherche Agronomique. We are particularly indebted to Dr R. Scalla and Dr R. Mornet for their involvement in some aspects of this work.

Literature Cited

1. Scalla, R.; Matringe, M.; Camadro, J. M.; Labbe, P. *Z. Naturforsch* **1990**, *45c*, 503-11.
2. Matringe, M.; Camadro, J. M.; Labbe, P.; Scalla, R. *Biochem. J.* **1989**, *260*, 231-5.
3. Witkowski, D. A.; Halling, B. P. *Plant Physiol.* **1989**, *90*, 1239-42.
4. Jacobs, J.M.; Jacobs, N.J.; Sherman, T.D.; Duke, S. O. *Plant Physiol.* **1991**, *97*, 197-203.
5. Jacobs, J. M.; Jacobs, N. J. *Biochem J.* **1987**, *244*, 219-24.
6. Matringe, M.; Camadro, J. M.; Block, M. A.; Joyard, J.; Scalla, R.; Labbe, P.; Douce, R. *J. Biol. Chem.* **1992**, *267*, 4646-51.
7. Mornet, R.; Gouin, L.; Matringe, M.; Scalla, R.; Swithenbank, C. *J. Labelled Compd Radiopharm* **1992**, *31*, 175-82.
8. Varsano, R.; Matringe, M.; Magnin, N.; Mornet, R.; Scalla, R. *Febs Lett.* **1990**, *272*, 106-8.
9. Matringe, M.; Mornet, R.; Scalla, R. *Eur. J. Biochem.* **1992**, *209*, 861-8.

10. Camadro, J. M.; Matringe, M.; Scalla, R.; Labbe, P. *Biochem. J.* **1991**, *277*, 17-21.
11. Urban-Grimal, D.; Labbe-Bois, R. *Mol. Gen. Genet.* **1981**, *183*, 85-92.
12. Camadro, J. M.; Urban-Grimal, D.; Labbe, P. *Biochem. Biophys. Res. Commun.* **1982**, *106*, 724-30.
13. Camadro, J.M.; Matringe, M.; Scalla, R.; Labbe, P. in *Target assays for modern herbicides and related phytotoxic compounds* (Böger, P.; Sandmann, G., eds), 1993 pp. 29-34, CRC Press/Lewis Publishers,
14. Laemmli, U. K. *Nature* **1970**, *227*, 680-5.
15. Siepker, L. J.; Ford, M.; de, K. R.; Kramer, S. *Biochim. Biophys. Acta* **1987**, *913*, 349-58.
16. Dailey, H. A.; Karr, S. W. *Biochemistry* **1987**, *26*, 2697-701.
17. Camadro, J. M.; Labbe, P. *J Biol Chem* **1988**, *263*, 11675-82.
18. Proulx, K.; Dailey, H. *Prot. Sci.* **1992**, *1*, 801-9.
19. Jones, C.; Jordan, P. M.; Akhtar, M. J. *Chem. Soc. Perkin Trans. I* **1984**, 2625-33.
20. Nandihalli, U. B.; Duke, M.V.; Duke, S.O. *Pest. Biochem. Biophys.* **1992**, *43*, 193-211.
21. Akagi, T.; Sakashita, N. Z. *Naturforsch.* **1993**, *48c*, 345-49.

RECEIVED April 15, 1994

Chapter 7

Characterization of a Mutant of *Chlamydomonas reinhardtii* Resistant to Protoporphyrinogen Oxidase Inhibitors

Ryo Sato^{1,2}, Masako Yamamoto², Hideyuki Shibata², Hiromichi Oshio², Elizabeth H. Harris¹, Nicholas W. Gillham¹, and John E. Boynton¹

¹Department of Botany and Zoology, Duke University, Box 90338, Durham, NC 27708-0338

²Takarazuka Research Center, Sumitomo Chemical Company Ltd., 4-2-1 Takatsukasa, Takarazuka, Hyogo 665, Japan

A nuclear mutant of *Chlamydomonas reinhardtii* (*rs-3*) is resistant to several herbicides which inhibit the enzyme protoporphyrinogen oxidase (Protox) in plants, including S-23142 [N-(4-chloro-2-fluoro-5-propargyloxy)-phenyl-3,4,5,6-tetrahydrophthalimide], acifluorfen-ethyl, oxyfluorfen, and oxadiazon. Protox enzyme activity in Percoll-purified chloroplast thylakoids from *rs-3* is less sensitive to S-23142 than that from wild type, indicating that the *rs-3* mutation either directly or indirectly confers resistance on the enzyme. Genetic analysis of *rs-3* showed that resistance results from a single dominant nuclear mutation that maps to linkage group IX, 13.7 and 12.3 map units from *sr-1* and *pf-16* respectively. Efforts to identify the resistance gene from a cosmid library of *rs-3* nuclear DNA by transformation have yielded one S-23142 resistant isolate from the cell wall-less arginine-requiring strain CC-425 (*arg-2*, *cw-15*). Since no isolates resistant to S-23142 were seen in control experiments, this suggests that the resistant isolate is a transformant and that the *rs-3* gene can be isolated by screening individual cosmid clones by transformation.

While herbicide resistant weeds pose problems in weed management (1), they can also be useful experimental materials to study the mode of action of herbicides. This in turn may lead to better weed management technology, including the control of resistant weeds. For this reason, resistant mutants, both spontaneous and artificially induced, are being isolated in different laboratories, using genetically well characterized plant species. If the resistance results from a mutation at the site of action of the herbicide, this is particularly useful for elucidating the mechanism of action of the herbicide at the molecular level. Such a mutant can be used for cloning of the gene encoding the target site of the herbicide.

As discussed elsewhere in this volume, significant progress has been made in the study of the mode of action of photobleaching herbicides in the past decade. Identification of protoporphyrinogen oxidase (Protox) as the target site of action of the photobleaching (or Protox inhibiting) herbicides is an especially important finding (2-4), since this enzyme provides the starting point of future studies on the molecular mechanism of action of these herbicides. However, a number of points remain to be

0097-6156/94/0559-0091\$08.00/0

© 1994 American Chemical Society

clarified. First, little is known about the Protox enzyme and the gene encoding it (5). Thus, the number of Protox genes and Protox isozyme species present in a cell (6), the differential sensitivity of isozymes to Protox inhibitors (6), the cellular and subcellular localization of various isozymes (7), and the regulation of expression of Protox genes remain to be investigated in detail. A complete understanding of the foregoing subjects will be necessary to explain how Protox inhibitors target the Protox enzyme and induce porphyrin accumulation leading to subsequent phytotoxicity (8). Cloning the Protox gene(s) and purification of the Protox enzyme(s) will be very useful for elucidating the mechanism of action of the photobleaching herbicides.

Unlike other herbicides with different sites of action, such as sulfonylureas and triazines, no naturally occurring mutants or biotypes of weeds resistant to Protox inhibiting herbicides have been found so far. Nonetheless, resistant weeds are considered to be a potential agricultural concern, for several Protox inhibiting herbicides which have been widely used (see ref 1). Several resistant mutants of *Chlamydomonas* and cell lines of higher plants have been isolated in the laboratory to examine the molecular mechanism of action of the herbicides (9-11). In this chapter, we characterize a mutant of the green alga *Chlamydomonas reinhardtii* resistant to the experimental *N*-phenylphthalimide herbicide S-23142 (Figure 1) which is a potent inhibitor of the plant Protox enzyme (12, 13) and shares a common mechanism of action with other photobleaching herbicides (14-17).

Advantages in using *Chlamydomonas reinhardtii* to study the mechanism of action of Protox inhibitors

We initially tested a variety of prokaryotes and lower eukaryotes to determine if any showed the same sensitivity to S-23142 as higher plants. Among microorganisms often used for molecular biology, *E. coli*, yeast (*Saccharomyces cerevisiae*), *Neurospora crassa*, photosynthetic bacteria (*Rhodospseudomonas sphaeroides*), and cyanobacteria (*Anacystis nidulans*) were not sensitive to S-23142 added to their culture media (Sato, R.; Shibata, H., unpublished data). A xanthophycean alga *Bumilleriopsis* has been reported to produce a high level of porphyrins including protoporphyrin IX (Proto) in response to a diphenylether herbicide, but to survive by excreting Proto into the media (18). In contrast, green algae including *Chlamydomonas* and *Scenedesmus* are very sensitive to Protox inhibiting herbicides. S-23142 inhibits growth of wild type *Chlamydomonas reinhardtii* (strain CC-407) by 90% at 6 nM in liquid culture (12). All characteristic biochemical responses to this herbicide, including inhibition of Protox activity in isolated chloroplast fragments (12, 13), blockage of porphyrin synthesis from 5-aminolevulinic acid (ALA) in isolated chloroplast fragments (13), porphyrin accumulation *in vivo* (9, 12, 18, 19), deterioration of photosystem II function (20), and enhanced ethane production (lipid peroxidation) (19, 21) are seen in these algae. Moreover, the wavelengths of light effective in inducing the phytotoxicity of a Protox inhibiting herbicide are virtually the same in *Chlamydomonas eugametos* (22) as in green cucumber cotyledons (15). Therefore, Protox inhibiting herbicides appear to exert their phytotoxicity in these green algae via the same mechanism as in higher plants.

Chlamydomonas reinhardtii also has several other useful characteristics for the study of mechanism of action of Protox inhibitors. First, the alga is haploid (23) and spontaneous or induced nuclear mutations are expressed directly whether recessive or dominant. Second, *C. reinhardtii* has a much shorter life cycle than higher plants, which enables genetic and physiological experiments to be carried out more rapidly. Third, classical genetic analysis is routinely used (see following section) to see whether a given mutation is encoded in the nuclear, chloroplast, or mitochondrial

genome. The map position of a given nuclear mutation is easily determined by genetic crosses to defined tester strains (23). Fourth, a wide variety of mutant strains are publicly available from the *Chlamydomonas Genetics Center* at Duke University. Finally, most common methods in molecular biology are applicable to *C. reinhardtii* (24). Recent advances in both chloroplast (25, 26) and nuclear (27-30) transformation in *C. reinhardtii* have made this alga a favored model system for investigations in plant molecular biology (23, 24).

Isolation of the S-23142 resistant mutant *rs-3*

Three RS-mutants (Resistant to S-23142), named RS-1, RS-2, and RS-3, were independently isolated from wild type strain CC-407 treated with the mutagen *N*-methyl-*N'*-nitro-*N*-nitrosoguanidine as described (9). More than 10⁹ cells were screened to obtain these three mutants. RS-3 shows the highest resistance level to S-23142 of the three isolates and tolerates up to 3 μM S-23142 in agar plates (I₉₀ value, see Table 1 in ref. 9). Unlike the other resistant isolates, RS-3 shows resistance only to herbicides known to be Prottox inhibitors, including S-23142 (12, 13), oxadiazon (3), and diphenyl ethers (2). RS-3 has the same sensitivity as CC-407 to herbicides with different modes of action including paraquat, diuron, fluridone, and butachlor (9). These data suggested that RS-3 may have a mutation which confers resistance to Prottox inhibitors by affecting the common site of action of these herbicides. RS-1 and RS-2 are less resistant to S-23142 than RS-3 and show a different cross-resistance pattern from RS-3 to various herbicides. RS-1 is slightly resistant to fluridone and diuron as well as to S-23142, oxadiazon, and acifluorfen-ethyl (AFE). RS-2 shows a high resistance level to oxadiazon and a moderate resistance level to S-23142, AFE, diuron, fluridone and paraquat. We chose RS-3 for further characterization and designated the resistance mutation in RS-3 as *rs-3*.

Physiological characterization of *rs-3*.

As in higher plants treated with S-23142 *in vivo* (31), wild type *C. reinhardtii* accumulates porphyrins in response to the herbicide treatment. Porphyrin accumulation can be detected within less than one hour, when early log phase cells of CC-407 (1 x 10⁶ cells/ml) are treated with 0.3 μM S-23142 in the light (200 μE/m²/sec). The dose response for growth inhibition by S-23142 correlates well with that for enhancement of porphyrin accumulation in wild type *C. reinhardtii* (9). When treated with 100 times higher concentration of S-23142, the *rs-3* mutant shows essentially the same profiles of porphyrin accumulation and growth inhibition as CC-407. RS-3 cells treated with 0.3 μM S-23142 first exhibit a transient increase in porphyrin accumulation (Figure 2) and then begin to grow just after the cessation of porphyrin accumulation (Figure 3). A similar transient increase in porphyrin accumulation is observed in CC-407 cells treated with sublethal concentration of S-23142 (3 nM, data not shown). Since this transient porphyrin accumulation is not seen in RS-3 cells treated with AFE at a wide range of concentrations (100 - 0.01 μM, data not shown), the transient porphyrin accumulation in S-23142-treated cells is probably due to gradual decomposition of S-23142 in the media, which allows cells to recover from the porphyrin accumulation at sublethal concentrations. Since porphyrin accumulation closely relates to the primary action of Prottox inhibitors (2, 3, 8), these physiological characteristics of *rs-3* suggest that the mutation confers resistance to Prottox inhibitors at or near the site of action of the herbicides. Other than resistance to Prottox inhibitors, no phenotypic changes are seen in the *rs-3* mutant; it grows as normally as wild type in all culture conditions in the absence of Prottox inhibitors.

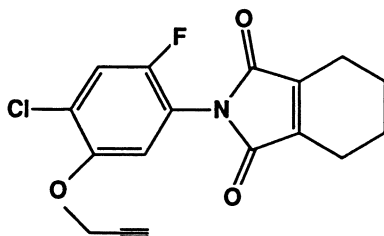


Figure 1. The experimental *N*-phthalimide herbicide S-23142.

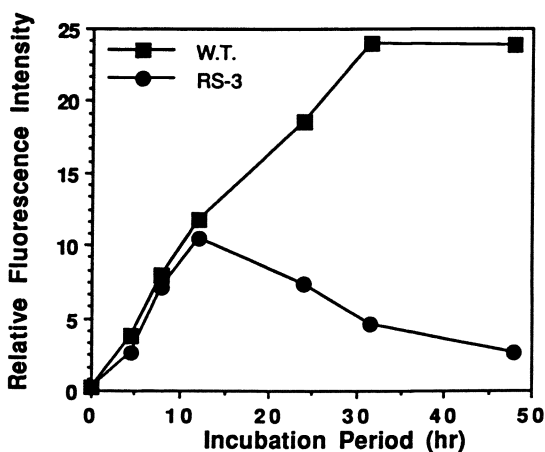


Figure 2. Time course of porphyrin accumulation in *Chlamydomonas reinhardtii* cells. Wild type CC-407 and RS-3 cells were grown autotrophically in a liquid medium containing $0.3 \mu\text{M}$ S-23142 and fluorescence at 620 nm (excitation wavelength at 400 nm) of the cell suspension was measured. No porphyrin accumulation was observed in control cultures. Reproduced with permission from ref. 9. Copyright 1990 Pesticide Science Society of Japan.

Genetic characterization of *rs-3*

Tetrad analysis of *rs-3*. *C. reinhardtii* has a sexual life cycle, induced by nitrogen starvation, in which gametes of opposite mating type fuse pairwise to yield diploid zygotes that germinate on nitrogen-containing media (see 23). The four meiotic products form colonies which are readily analyzed genetically. In *C. reinhardtii*, nuclear genes are inherited biparentally, but organelle (chloroplast and mitochondria) genomes are inherited uniparentally from opposite mating types (23). Thus, tetrads from a cross of a nuclear mutant and wild type segregate two mutant and two wild type progeny. Tetrads from a cross of a chloroplast mutant in the plus mating type (mt^+) and a wild type stock (mating type minus, mt^-) yield all mutant progeny (23), while the converse situation applies to mitochondrial mutants.

The original RS-3 isolate (mt^+) was crossed to a wild type stock (CC-124, mt^-). Four tetrads were dissected and the resulting progeny tested for their sensitivity to 0.3 μ M S-23142 in agar plates. All tetrads segregated to two S-23142 sensitive and two S-23142 resistant isolates, indicating that the *rs-3* mutation is nuclear in origin. A mt^- S-23142-resistant progeny clone was isolated from this cross (RS-322) and used for further genetic analysis. This clone mated more efficiently than the original RS-3 isolate.

Mapping of *rs-3*. *C. reinhardtii* has 18 linkage groups in its nuclear genome with many genes mapped on each group (32). The map position of new mutations can be determined by recombination frequencies with known marker genes on each linkage group. Recombination (map distance) between two genes is usually calculated from the following equation: Map distance = $(NPD + 0.5 T) / (PD + NPD + T) \times 100$ where PD (parental ditype), NPD (non-parental ditype), and T (tetatype) represent different tetrad types based on their segregation patterns (see 23).

Table I. Summary of segregation data of the cross of RS-322 (*rs-3*, mt^-) x CC-28 (*ac-17*, *can-1*, *nic-13*, *pf-2*, *y-1*, *pyr-1*, *msr-1*, *act-2*, *sr-1*, mt^+)

Marker (linkage group)	Ratio	% Recombination
	(PD : NPD : T)	
<i>rs-3</i> , + X +, <i>act-2</i> (II)	11 : 7 : 34	46.2
<i>rs-3</i> , + X +, <i>ac-17</i> (III)	12 : 9 : 27	46.9
<i>rs-3</i> , + X +, <i>pyr-1</i> (IV)	16 : 14 : 36	42.1
<i>rs-3</i> , + X +, <i>sr-1</i> (IX)	44 : 0 : 16	13.3
<i>rs-3</i> , + X +, <i>nic-13</i> (X)	13 : 16 : 38	52.2
<i>rs-3</i> , mt^- X +, mt^+ (VI)	10 : 12 : 35	51.8

PD, parental ditype; NPD, nonparental ditype; T, tetatype

To find out which linkage group *rs-3* belongs to, RS-322 (*rs-3*, mt^-) was crossed to CC-28 (mt^+) which has multiple marker genes for several different linkage groups (Table I). *y-1* (yellow in dark) and *can-1* (canavanine resistance) were not scored, since RS-322 also carries a *y-1* mutation and tolerates 500 μ g/ml canavanine. Since no NPD tetrads were observed out of 60 tetrads scored in this cross between

rs-3 and *sr-1*, *rs-3* seemed to map in linkage group IX. To verify this, three *rs-3* isolates were crossed to stocks carrying linkage group IX markers (Table II). The results showed that *rs-3* maps 13.7 and 12.3 map units from *sr-1* and *pf-16* respectively, on the left arm of linkage group IX (Figure 4).

Table II. Summary of segregation data for *rs-3* and *sr-1*, *nit-1* and *pf-16* markers in linkage group IX

Cross		Interval	Ratio	% Recombination
(PD : NPD : T)				
RS-373 X (<i>rs-3</i> , <i>sr-1</i>)	CC-1373 (+, +)	<i>rs-3</i> - <i>sr-1</i>	48 : 0 : 16	12.5
RS-322 X (<i>rs-3</i> , +, +)	CC-1329 (+, <i>sr-1</i> , <i>nit-1</i>)	<i>rs-3</i> - <i>sr-1</i>	46 : 0 : 16	12.9
		<i>rs-3</i> - <i>nit-1</i>	9 : 3 : 50	45.2
		<i>sr-1</i> - <i>nit-1</i>	14 : 2 : 46	40.3
RS-379 X (<i>rs-3</i> , +, <i>sr-1</i>)	CC-1034 (+, <i>pf-16</i> , +)	<i>rs-3</i> - <i>sr-1</i>	50 : 0 : 19	13.7
		<i>rs-3</i> - <i>pf-16</i>	52 : 0 : 17	12.7
		<i>pf-16</i> - <i>sr-1</i>	67 : 0 : 2	1.4

PD, parental ditype; NPD, nonparental ditype; T, tetratype

Dominance test of *rs-3*. In *C. reinhardtii*, about 5% of mated gametes spontaneously form mitotic diploids that are stable under vegetative growth conditions and behave like *mt⁻* cells with respect to mating (23). Heterozygous diploids were used to determine whether *rs-3* is dominant or recessive to wild type (12). For this purpose, RS-352 (*rs-3*, *arg-2*, *mt⁺*) was isolated from a cross of RS-322 x CC-48 (*arg-2*, *mt⁺*). RS-352 was then crossed to CC-1861 (*arg-7*, *mt⁻*) to select vegetative diploids. Since *arg-2* and *arg-7* are tightly linked complementing arginine auxotrophic mutations (33), only diploid cells (*arg-2/arg-7*, *rs-3/+*) or very rare recombinants arising from meiotic zygotes can grow on arginine free media. Thirteen isolates from this cross were randomly selected from TAP (Tris-Acetate-Phosphate media, see 23) plates and their mating type and resistance to S-23142 were tested. All isolates had the minus mating type, confirming that they were diploid, and grew normally on TAP plates containing 0.3 μ M S-23142. Diploids #5, #8, #13 were further examined for cell growth and porphyrin accumulation at various concentrations of S-23142. The wild type diploid CC-127 (*arg-2/arg-7*, +/+) was as sensitive as the wild type haploid CC-125 in both cell growth and porphyrin accumulation, while the three diploid isolates showed the same level of S-23142 resistance as RS-352 in these two physiological parameters (12). These results indicate that *rs-3* is a dominant mutation.

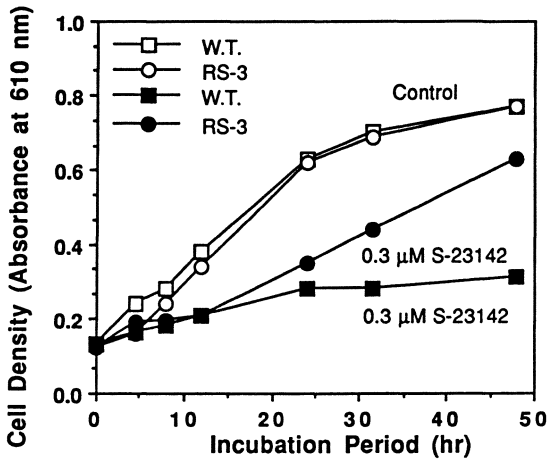


Figure 3. Effect of S-23142 on growth of *Chlamydomonas reinhardtii*. Cells were grown as in Figure 2 and absorbance at 610 nm of cell suspension was measured. Reproduced with permission from ref. 9. Copyright 1990 Pesticide Science Society of Japan.

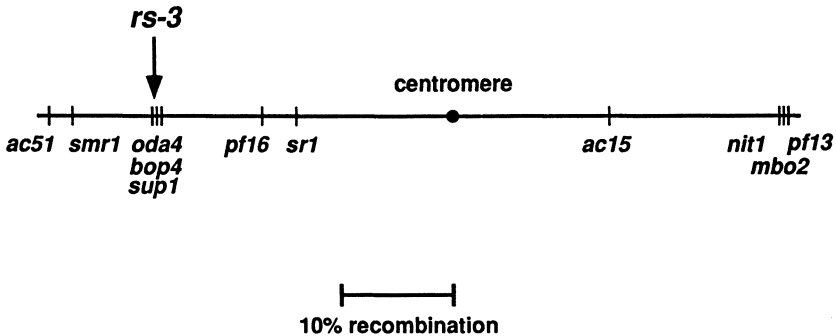


Figure 4. Map of *Chlamydomonas* linkage group IX showing the position of *rs-3* mutation. The linkage map was adapted from ref. 32. *sr-1*, streptomycin resistant; *pf-16*, paralyzed flagella; *oda-4*, outer dynein arms deficient; *bop-4*, "bypass of paralysis" suppressor of *pf-10*; *sup-1*, suppressor of central pair and radial spoke mutations; *smr-1*, sulfometuron methyl resistant; *ac-51*, acetate requiring.

Biochemical characterization of *rs-3*

Resistance in porphyrin synthesis activity *in vitro*. In order to see if the *rs-3* mutant shows resistance to Protox inhibitors at the enzyme level, effects of S-23142 and AFE on porphyrin synthesis in isolated chloroplast fragments were examined (13). Chloroplast fragments, prepared from log phase cells of RS-3 and wild type CC-407 by sonication and centrifugation, were incubated with 5-aminolevulinic acid (ALA) as a substrate (12, 13). No significant difference was found in the amounts of Mg-protoporphyrin IX (Mg-Proto) synthesized per chlorophyll by RS-3 and CC-407 chloroplast fragments. S-23142 and AFE inhibited Mg-Proto synthesis in CC-407 chloroplast fragments by 50% at 0.016 μM and 0.39 μM , respectively. The Mg-Proto synthesizing activity of RS-3 chloroplast fragments was significantly less sensitive to both compounds, with 50% inhibition being achieved at 0.21 μM S-23142 and 4.8 μM AFE, respectively.

Protox resistance in chloroplast fragments prepared from *rs-3*. Since Protox has been shown to be the enzyme in the ALA to Mg-Proto pathway sensitive to Protox inhibitors *in vitro* (2-4), we examined whether the Protox activity of the *rs-3* mutant was resistant to S-23142 *in vitro*. However, autooxidation of protoporphyrinogen IX (Protox) was too high to measure Protox activity in the preparations described, necessitating purification of the chloroplast fragments on Percoll density gradients (12). Protox activity in RS-3 and CC-407 chloroplast fragments without inhibitors was found to be the same, 0.22 and 0.23 pmol/ μg protein/min, respectively (12). This result suggests that the *rs-3* mutation does not affect efficiency of the catalytic site of the Protox enzyme. However, Protox activity in RS-3 chloroplast fragments was significantly less sensitive to S-23142 and AFE than the activity from CC-407. S-23142 (1 nM) and AFE (10 nM) inhibited Protox activity in CC-407 and RS-3 chloroplasts by 70% and 45%, respectively (12). The Protox activity of the wild type diploid CC-127 was as sensitive as CC-407 to S-23142 and AFE, while Protox activity of diploid #13 was less sensitive to these inhibitors than that of CC-127 (12). No significant difference in Protox resistance between RS-3 and diploid #13 was found. Thus, the *rs-3* mutation confers resistance to S-23142 and AFE either directly or indirectly on Protox activity. Considering the specific resistance of *rs-3* to Protox inhibitors (9), the mutation most likely affects a possible herbicide binding site in either Protox itself or co-factor of the enzyme.

Lack of induction of resistant Protox. As discussed in the physiological characterization section, the *rs-3* mutant accumulates porphyrins for about 12 hr after treatment with 0.3 μM S-23142 before showing resistance (9). This phenomenon may be explained either by a gradual reduction in the level of S-23142 in the media due to decomposition or by induction of resistant enzyme molecules in the *rs-3* mutant by the herbicide. To see if resistant Protox is induced by S-23142, Protox activity was extracted from RS-3 at 14 and 70 hr after the addition of 10 nM S-23142 to the media and was compared to Protox activity prepared from a S-23142-free culture at early log-growth phase (12). No significant difference was found in the sensitivity of the three preparations to S-23142, indicating that higher Protox resistance to S-23142 in the *rs-3* mutant is not induced *in vivo* by addition of S-23142 (12).

Strategies for cloning the *rs-3* gene

Although *rs-3* may be a mutation in a gene encoding Protox, a cloned Protox gene has not yet been obtained from any organism. A plant Protox enzyme has been

purified from greening barley seedlings (34), however, its molecular weight (36,000 kDa) is different from purified Protox of mouse liver (65,000 kDa, ref. 35) and yeast (56,000 kDa, ref. 36). Neither the amino acid sequence of Protox nor Protox antibody cross-reacting to the enzymes from different sources have been reported. Hence, no useful probes for attempting to isolate the Protox gene from a nuclear DNA library are available currently. However, based on our physiological, biochemical, and genetic characterization of *rs-3*, several strategies for cloning the putative Protox gene may be feasible.

RFLP mapping and chromosome walking. Since the *rs-3* gene maps to linkage group IX and RFLP maps of the *Chlamydomonas* linkage groups are being constructed by other laboratories (37), the *rs-3* gene might be identified by chromosome walking from the nearest RFLP marker. However, this has not been done successfully in *Chlamydomonas* as yet and might prove to be very time consuming, depending on the physical distance between the nearest RFLP marker and *rs-3*.

Tagging of *rs-3* by gene disruption. Alternatively, the *rs-3* gene could be tagged by disruption with a foreign piece of DNA introduced into *rs-3/+* diploid cells either by particle gun- or glass bead-mediated transformation. By disrupting the mutant *rs-3* allele in diploid cells, the S-23142 resistant phenotype of these cells would be expected to be changed to a sensitive phenotype. In the presence of an appropriate concentration of S-23142, the porphyrin non-accumulating phenotype of *rs-3* would be converted to a porphyrin accumulating wild type phenotype. However, the frequency of gene disruption should be much less than 10^{-5} , a reported optimum transformation frequency for non-homologous insertions (29). The rare cells in which the *rs-3*-gene is disrupted might be detected among the *rs-3/+* cells with the aid of a fluorescence activated cell sorter (38). Preliminary experiments show that at least some of the porphyrin accumulating wild type cells survive in the presence of S-23142 for up to at least three days in liquid TAP medium in the light ($200 \mu\text{E}/\text{m}^2/\text{sec}$) and form green colonies when transferred to S-23142 free TAP plates. However, our preliminary efforts to sort out a minority of wild type diploid (CC-127) cells from a majority of diploid #13 (heterozygous for *rs-3*) cells, when the mixture was grown on S-23142, were not successful, based on difference in the fluorescence emission peaks of protoporphyrin IX (633 nm) and chlorophyll (680 nm). A large number of #13 cells as well as CC-127 cells were found to be present in the porphyrin accumulating cell population upon plating. This is probably due to the short term accumulation of porphyrins in #13 cells treated with S-23142 and the slow recovery of some cells from this treatment. Another possible explanation for this unexpected result is that wild type *Chlamydomonas* treated with S-23142 excretes porphyrin(s) into the media. The excreted porphyrin(s) possibly stick to the surface of both CC-127 and #13 cells, making them indistinguishable to the cell sorter. Culture medium containing excreted porphyrin(s) shows a fluorescence emission peak at 620 nm, while porphyrin accumulating cells resuspended in fresh media show a fluorescence emission peak at 633 nm. Therefore, by determining appropriate herbicide concentration, sampling time and flow cytometry conditions, one may be able to sort out the few cells with a disrupted *rs-3* gene from the remainder of the cell population, based on the difference in the amount of porphyrins accumulated in the cell.

Isolation of the *rs-3* gene by transformation. Another strategy for cloning the *rs-3* gene is to identify genomic clones which rescue sensitive wild type cells in the presence of S-23142 by transformation with a nuclear DNA library made from the *rs-3* mutation. Since *rs-3* is a single dominant nuclear gene, clones carrying the *rs-3*

gene would be expected to transform sensitive wild type cells to resistance. This cloning method has been often employed in *E. coli* and yeast, but no successful reports of its use have been published in green plants, probably because their large genome size would make screening a nuclear genomic library very laborious. A nuclear transformation system has been developed for *Chlamydomonas* only recently (27-30) and has involved non-homologous integration of only a limited number of genes.

Attempts to clone the *rs-3* gene by transformation

Construction of a cosmid genomic library of *rs-3* nuclear DNA. Nuclear DNA was extracted from RS-3 cells grown to late log phase (7.6×10^6 cells/ml) in TAP media containing $0.03 \mu\text{M}$ S-23142 in the light ($200 \mu\text{E}/\text{m}^2/\text{sec}$) and purified by NaI density gradients as described (23). Nuclear DNA partially digested with *Sau* 3A I to an average size of about 50 kb, was ligated to the Stratagene cosmid vector SuperCos-1 (39), packaged into lambda phage *in vitro* using GigaPack II XL packaging extract (Stratagene), and then transduced into an *E. coli* NM544 strain following the Stratagene protocol. Transformants were selected on LB plates containing $50 \mu\text{g}/\text{ml}$ ampicillin. The transformation frequency was 1.7×10^5 transformants per μg non-size selected DNA. 10,080 individual colonies were transferred to 420 microtiter plates (24 well) containing 0.5 ml LB in each well and cultured for 20 hr at 37°C . Aliquots of $187 \mu\text{l}$ culture from each well of the 24 well plate were combined and plasmid DNA was extracted from the 420 separate pools by the alkaline lysis method (40). DNA was treated with the RNase, phenol/chloroform extracted and then chloroform extracted. An ordered library was prepared from the remaining cells of the 10,080 individual cultures which were frozen at -20°C after adding an equal volume of LB plus 30% glycerol. We also pooled more than 10,000 bacterial clones in 60 ml of LB. Half of the mixture of 10,000 clones was used for plasmid DNA preparation and the other half was frozen as described above. Thus, our genomic cosmid library of the *rs-3* mutant consists of an ordered library of 10,080 individual clones, a mixture of ca. 10,000 clones, 420 pools of plasmid DNA each extracted from 24 clones, and total DNA extracted from ca. 10,000 pooled clones. Assuming a nuclear genome size of 75,000 kb, the 10,080 clones with an average insert size of 40 kb would cover the entire nuclear genome of *C. reinhardtii* with 99.5% probability.

Selection of rare *rs-3* cells in a population of wild type cells. To examine whether a few *rs-3* cells in large number of S-23142-sensitive wild type cells can be selected on S-23142 containing plates, *rs-3* and wild type CC-125 cells were mixed at the concentration of 0.8×10^3 and 1.6×10^9 or 1.6×10^{10} cells/ml respectively and spread on TAP plates containing 0.3 or $0.03 \mu\text{M}$ S-23142 ($100 \mu\text{l}$ of the mixture for each plate, Table III). At $0.03 \mu\text{M}$ S-23142, wild type cells formed a green lawn which hid the *rs-3* colonies. At $0.3 \mu\text{M}$ S-23142, *rs-3* cells formed colonies normally and growth of the lawn of wild type cells was inhibited. The number of *rs-3* colonies formed was not affected by the presence of wild type cells on the S-23142 containing plates, suggesting that porphyrins formed by wild type cells were not inhibitory for *rs-3* growth. This preliminary experiment showed that one should be able to select S-23142 resistant transformants by spreading wild type cells transformed with the *rs-3* gene on herbicide containing plates.

Transformation of strain CC-425 with total *rs-3* library DNA. To see if a clone carrying a given gene could be identified in the cosmid library by transformation, an arginine requiring cell wall less strain CC-425 (*arg-2*, *cw-15*, *mr⁺*) was transformed with either pARG7.8 (27) or total *rs-3* library DNA by the

glass bead method (29). Cells grown in TAP media in the light ($200 \mu\text{E}/\text{m}^2/\text{sec}$) were harvested at $1.5 - 3 \times 10^6$ cells/ml and $400 \mu\text{l}$ of cell suspension in TAP media containing 2×10^8 cells/ml, 1.25% PEG, $0.5-1.5 \mu\text{g}$ DNA was added to 0.3 gram glass beads (0.5 mm, baked at 250°C for 3 hr). The tubes were vortexed twice for 15 sec with a 2 min interval between. Arginine prototroph transformants and S-23142 resistant transformants were selected respectively on TAP and TAP plus arginine ($50 \mu\text{g}/\text{ml}$) plus $0.3 \mu\text{M}$ S-23142 plates.

Table III. Reconstruction experiment for selection of *rs-3* cells

Ratio	Number of Colonies per TAP + S-23142 Plate	
	0.3 μM	0.03 μM
<i>rs-3</i> : wild type		
1 : 0	87	70
1 : 2×10^6	76	79
1 : 2×10^7	82	green lawn
0 : 2×10^6	0	green lawn
0 : 2×10^7	0	green lawn

rs-3, 0.8×10^3 cells/ml; wild type (CC-125), 1.6×10^9 or 1.6×10^{10} cells/ml

Table IV. Summary of transformation experiments

Recipient	DNA	Number of Cells Transformed	Arginine Prototrophs (Frequency)	S-23142 Resistant Isolates
CC-425 (<i>arg-2</i> , <i>cw-15</i>)	pARG7.8	7×10^8	3469 (0.5×10^{-5})	-
CC-425	pARG7.8	7×10^8	-	0
CC-425	<i>rs-3</i> Cosmid Library (ca. 10,000 clones)	3×10^9	3 (1×10^{-9})	-
CC-425	<i>rs-3</i> Cosmid Library (ca. 10,000 clones)	3×10^9	-	1

7×10^8 cells were transformed with pARG7.8, and 3469 arginine prototroph isolates were obtained (Table IV). Assuming that all isolates are bona fide transformants, the frequency was 0.5×10^{-5} or 550 transformants per μg DNA. The frequency is comparable to reported transformation frequency for *nit-1* gene by the glass bead method in the *cw-15* mutant (29). No S-23142 resistant isolates were

obtained out of 7×10^8 cells transformed with pARG7.8, suggesting that the spontaneous mutation rate to S-23142 resistance is less than 10^{-9} .

In the same experiment, 3×10^9 cells were transformed with total library DNA (Table IV). Assuming that a cosmid having 40-50 kb insert has a similar transformation frequency to the pARG7.8 (7.8 kb insert), ca. 15,000 potential transformants should be obtained from 3×10^9 cells. Since total library DNA was prepared from ca. 10,000 clones, at least one transformant should have been obtained if the library DNA contained equal amounts of DNA for each clone. Actually, three arginine prototroph isolates were obtained from 3×10^9 cells transformed with total library DNA. The SuperCos-1 vector sequence was found in one of the three isolates by genomic southern analysis (data not shown), suggesting that at least one bona fide transformant was obtained from the library. These results suggested that the wild type cosmid clone which complements the arginine auxotroph has a similar transformation frequency to pARG7.8 plasmid, even when present at low concentration in a DNA mixture, and can be screened from the library by transformation.

Table V. Sensitivity of CC-425 and T-002 to photobleaching herbicides and DCMU

Compound	I_{50} (μM)	
	CC-425	T-002
S-23142	0.006	0.18
AFE	0.015	0.15
DCMU	0.86	0.86

Similarly, one S-23142 resistant isolate has been obtained from 3×10^9 cells transformed with total library DNA. Our evidence is still not conclusive as to whether this isolate (numbered T-002) is a bona fide transformant or a new resistant mutant, since no cosmid vector sequence was detected by genomic southern analysis. However, vector sequences are not always integrated into the genome in nuclear transformants of *Chlamydomonas* (27, 30). Foreign pieces of DNA integrate randomly into nuclear genome of this alga during transformation and homologous gene replacement has not yet been reported (27-30). Therefore, S-23142 resistant transformants are likely to have the resistance gene at a locus different from the wild type *rs-3* allele, but to show the same level of resistance to Prottox inhibitors such as *rs-3*, since the mutant gene is dominant. T-002 shows very similar resistance to S-23142 and AFE as the *rs-3* mutant, but shows same sensitivity to DCMU as recipient strain CC-425 (Table V). To see whether T-002 is a bona fide transformant, it was analyzed genetically. In a cross to wild type (CC-124, *mr*⁻) four tetrads were isolated and segregated two S-23142 sensitive and two resistant progeny. This indicates that T-002 behaved as if it carried a single nuclear resistance gene. One of the S-23142 resistant isolates obtained from this cross (*mr*⁻) was crossed to an *rs-3*, *mr*⁺ mutant strain. Four out of eight tetrads segregated S-23142 sensitive isolates, indicating that the S-23142 resistance allele in T-002 is at a different locus from the wild type *rs-3* allele. Thus, unless a second gene exists that can be mutated to impart S-23142 resistance, T-002 is more likely to be a

transformant than to be a new mutant. Since no S-23142 isolates were obtained from cells (7×10^8) transformed with pARG7.8, identification of individual clones possessing the *rs-3* gene from the cosmid library may be possible using transformation.

Concluding remarks

In this study, we demonstrate that *rs-3* is highly likely to be a mutant in the nuclear gene encoding the Protox enzyme. Furthermore we present preliminary data suggesting that the *rs-3* gene can be isolated from the genomic cosmid library made from *rs-3* nuclear DNA by screening individual clones by transformation. Once the mutant *rs-3* gene is cloned, the wild type *rs-3* allele can be easily identified in *Chlamydomonas* and it may be very useful for finding the corresponding wild type gene in other organisms. Characterization of these genes will help us to understand (1) the molecular mechanism of action of Protox inhibiting herbicides, (2) the mechanism of resistance to Protox inhibiting herbicides, and (3) the distinct differences in sensitivity to Protox inhibiting herbicides between green plants, microorganisms, and animals. This should lead to the design of safer herbicides with improved efficacy and of crops resistant to Protox inhibiting herbicides.

Acknowledgment

We would like to thank Dr. Mike Cook for his help in conducting fluorescence activated cell sorting experiments. We are grateful to Yoshihisa Nagano for his technical assistance and to the *Chlamydomonas* Genetics Center, Duke University, for providing us many *Chlamydomonas* strains.

Literature Cited

1. LeBaron, H. M.; McFarland, J. In *Managing resistance to agrochemicals: from fundamental research to practical strategies*; Green M. B.; LeBaron, H. M.; Moberg, W. K., Eds.; ACS Symposium series 421; American Chemical Society: Washington, DC, **1990**, 336-352.
2. Matringe, M.; Camadro, J. M.; Labbe, P.; Scalla, R. *Biochem. J.* **1989**, *260*, 231.
3. Matringe, M.; Camadro, J. M.; Labbe, P.; Scalla, R. *FEBS Lett.* **1989**, *245*, 35.
4. Witkowsky, D. A.; Halling, B. P. *Plant Physiol.* **1989**, *90*, 1239.
5. Dailey, H. A. In *Biosynthesis of Heme and Chlorophyll*; Dailey, H. A., Ed.; McGraw Hill: New York, NY, **1990**, 123-161.
6. Jacobs, J. M.; Jacobs, J. N.; Sherman, T. D.; Duke, S. O. *Plant Physiol.* **1991**, *97*, 197.
7. Matringe, M.; Camadro, J. M.; Block, M. A.; Joyard, J.; Scalla, R.; Labbe, P.; Douce, R. *J. Biol. Chem.* **1992**, *267*, 4646.
8. Jacobs, J. M.; Jacobs, J. N. *Plant Physiol.* **1993**, *101*, 1181.
9. Kataoka, M.; Sato, R.; Oshio, H. *J. Pestic. Sci.* **1990**, *15*, 449.
10. Che, F. S.; Takemura, Y.; Suzuki, N.; Ichinose, K.; Wang, J. M.; Yoshida, S. *Z. Naturforsch.* **1993**, *48c*, 350.
11. Shioda, N.; Torii, K.; Matsunaka, S. *Weed Res. (Japan)* **1991**, *36*, Suppl. 1, 176.
12. Shibata, H.; Yamamoto, M.; Sato, R.; Harris, E. H.; Gillham, N. W.; Boynton, J. E. In *Research in Photosynthesis*; Murata, N., Ed.; Kluwer Academic Publishers: Dordrecht, Netherland, **1992**, Vol. III; 567-570.

13. Oshio, H.; Shibata, H.; Mito, N.; Yamamoto, M.; Harris, E. H.; Gillham, N. W.; Boynton, J. E.; Sato, R. *Z. Naturforsch.* **1993**, *48c*, 339.
14. Sato, R.; Nagano, E.; Oshio, H.; Kamoshita, K. *Pestic. Biochem. Physiol.* **1987**, *28*, 194.
15. Sato, R.; Nagano, E.; Oshio, H.; Kamoshita, K.; Furuya, M. *Plant Physiol.* **1987**, *85*, 1146.
16. Sato, R.; Nagano, E.; Oshio, H.; Kamoshita, K. *Pestic. Biochem. Physiol.* **1988**, *31*, 213.
17. Mito, N.; Sato, R.; Miyakado, M.; Oshio, H.; Tanaka, S. *Pestic. Biochem. Physiol.* **1991**, *40*, 128.
18. Sandmann, G.; Böger, P. *Z. Naturforsch.* **1988**, *43c*, 699.
19. Nicolaus, B.; Sandmann, G.; Watanabe, H.; Wakabayashi, K.; Böger, P. *Pestic. Biochem. Physiol.* **1989**, *35*, 192.
20. Karapetyan, N. V.; Strasser, R.; Böger, P. *Z. Naturforsch.* **1983**, *38c*, 556.
21. Kunert, K. J.; Böger, P. *Weed Sci.* **1981**, *29*, 169.
22. Ensminger, M. P.; Hess, F. D. *Plant Physiol.* **1985**, *77*, 503.
23. Harris, E. H. *The Chlamydomonas Sourcebook*; Academic Press: San Diego, CA, **1989**.
24. Boynton, J. E.; Gillham, N. W.; Newman, S. M.; Harris, E. H. In *Plant Gene Research: Cell Organelles*; Herrmann, R. Ed.; Springer Verlag: Wien, **1992**, 3-64.
25. Boynton, J. E.; Gillham, N. W.; Harris, E. H.; Hosler, J. P.; Johnson, A. M.; Jones, A. R.; Randolph-Anderson, B. L.; Robertson, D.; Klein, T. M.; Shark, K. B.; Sanford, J. C. *Science*, **1989**, *240*, 1534.
26. Boynton, J. E.; Gillham, N. W. In *Methods in Enzymol.: Recombinant DNA, Part H*; Wu, R. Ed.; Academic Press: San Diego, CA, **1993**, Vol. 217; 510-536.
27. Debuchy, R.; Purton, S.; Rochaix, J. D. *EMBO J.* **1989**, *8*, 2803.
28. Kindle, K. L.; Schnell, R. A.; Fernandez, E.; Lefebvre, P. A. *J. Cell Biol.* **1989**, *109*, 2589.
29. Kindle, K. L. *Proc. Natl. Acad. Sci. USA.* **1990**, *87*, 1228.
30. Mayfield, S. P.; Kindle, K. L. *Proc. Natl. Acad. Sci. USA.* **1990**, *87*, 2087.
31. Sato, R. *Chem. Regul. Plants (Tokyo)* **1990**, *25*, 68.
32. Harris, E. H. In *Genetic Maps. Locus maps of complex genomes*; O'Brien, S.J. Ed.; 6th ed; Cold Spring Harbor Laboratory: Cold Spring Harbor, NY, **1990**, 2.157 - 2.164.
33. Matagne, R. F. *Mol. Gen. Genet.* **1978**, *160*, 95.
34. Jacobs, J. H.; Jacobs, N. J. *Biochem. J.* **1987**, *244*, 219.
35. Dailey, H. A.; Karr, S. W. *Biochemistry* **1987**, *26*, 2697.
36. Labbe-Bois, R.; Labbe, P. In *Biosynthesis of Heme and Chlorophyll*; Dailey, E. H. Ed.; McGraw Hill: New York, NY, **1990**, 235-285.
37. Ranum, L. P. W.; Thompson, M. D.; Schloss, J. A.; Lefebvre, P. A.; Silflow, C. D. *Genetics* **1988**, *120*, 109.
38. Shapiro, H. M. *Practical Flow Cytometry*; 2nd ed.; Alan R. Liss, Inc.: New York, NY, **1988**.
39. Evans, G. A.; Lewis, K.; Rothenberg, B. E. *Gene* **1989**, *79*, 9.
40. Sambrook, J.; Fritsch, E. F.; Maniatis, T. *Molecular Cloning: a Laboratory Manual*; 2nd ed.; Cold Spring Harbor Laboratory Press: Cold Spring Harbor, NY, **1989**, Vol I, 1.38-1.39.

RECEIVED December 14, 1993

Chapter 8

Factors Affecting Protoporphyrin Accumulation in Plants Treated with Diphenyl Ether Herbicides

Judith M. Jacobs and Nicholas J. Jacobs

Department of Microbiology, Dartmouth Medical School,
Hanover, NH 03755-3842

The toxic action of photobleaching diphenylether herbicides is dependent upon their ability to cause accumulation of the phototoxic tetrapyrrole intermediate, protoporphyrin. Although these herbicides inhibit the plastid enzyme which converts protoporphyrinogen to protoporphyrin, the mechanism by which accumulated protoporphyrinogen is converted to protoporphyrin remains unknown. It has recently been demonstrated that this conversion can be mediated by herbicide-resistant mechanisms associated with extraorganellar membranes such as the plasma membrane. In addition, we have reported that protoporphyrinogen is preferentially exported from isolated intact plastids incubated in the presence of porphyrin precursors and herbicide. In this report, we summarize our findings that protoporphyrinogen can also be decomposed to non-porphyrin compounds by cytosolic factors under conditions where protoporphyrin is quite stable. We also summarize our recent findings on the distribution of the terminal enzymes of heme biosynthesis in mitochondria and plastids. All these results are discussed in terms of their role in explaining the accumulation of protoporphyrin in herbicide treated plants. It is concluded that this is best explained by the export of protoporphyrinogen from the plastid, followed by its oxidation to protoporphyrin through the mediation of herbicide-resistant mechanisms associated with extraorganellar membranes.

The purpose of this chapter is to discuss factors affecting the accumulation of the porphyrin intermediate, protoporphyrin, which occurs when plants are treated with diphenylether (DPE) herbicides. The toxic action of photobleaching DPE herbicides is dependent upon their ability to cause the accumulation of excessive levels of protoporphyrin. In the presence of light, protoporphyrin catalyzes photooxidative destruction of plant cell membranes (1-13). Thus, a complete understanding of the mechanism of herbicide action requires elucidation of the factors which govern the levels of protoporphyrin which accumulate upon treatment with herbicide.

0097-6156/94/0559-0105\$08.00/0

© 1994 American Chemical Society

The primary mechanism by which these herbicides cause protoporphyrin accumulation is their ability to strongly inhibit the porphyrin biosynthetic enzyme protoporphyrinogen oxidase (15-20). This enzyme converts protoporphyrinogen to protoporphyrin and is present in the plastid which contains all of the enzymes necessary for heme and chlorophyll synthesis from early precursors (see Figure 1 for this biosynthetic pathway).

Herbicide inhibition of protoporphyrinogen oxidase would be expected to cause accumulation of protoporphyrinogen, the substrate of the inhibited enzyme. The question remains unanswered as to how this accumulated protoporphyrinogen is converted to protoporphyrin in herbicide-treated plants. The assumption had been made that this accumulated protoporphyrinogen was oxidized spontaneously to protoporphyrin by chemical autooxidation. However, we will discuss data which suggest that the oxidation of protoporphyrinogen to protoporphyrin occurs through the mediation of herbicide-resistant oxidizing factors present in the plasma membrane or other membranes located outside of plastids or mitochondria. We will also discuss some recent data concerning the nature of this extraplastidic oxidizing mechanism and how it differs from the biosynthetic protoporphyrinogen oxidase present in the plastid. Our recent findings that protoporphyrinogen can be preferentially exported from isolated intact plastids incubated with early porphyrin precursors in the presence of herbicide lends support to the importance of this extraplastidic protoporphyrinogen oxidation.

Protoporphyrin accumulation would also be influenced by reactions which utilize accumulated protoporphyrinogen without giving rise to protoporphyrin. For instance, we will mention recent findings from our laboratory that protoporphyrinogen can be decomposed to non-porphyrin products in the presence of plant cytoplasm. We will also present and discuss recent evidence that protoporphyrin itself can be converted to later intermediates in the biosynthetic pathway even in the presence of herbicide.

Our recent findings on the interorganellar localization of the three terminal enzymes of heme synthesis in plants will also be summarized. These findings have implications for protoporphyrin and protoporphyrinogen accumulation in the plant cytoplasm, since a recent hypothesis has proposed that the plastid synthesizes protoporphyrinogen for export and use by the plant mitochondria for mitochondrial heme synthesis (to be discussed in a later section).

Formation of Protoporphyrin from Accumulated Protoporphyrinogen

Demonstration of Extraplastidic, Herbicide-Resistant Protoporphyrinogen Oxidation. The question of why protoporphyrin accumulates when protoporphyrinogen oxidase is inhibited first arose when it was discovered that the human hereditary disease *variagata porphyria* was a result of a partial deficiency of the mitochondrial protoporphyrinogen oxidase enzyme (21, 22). Protoporphyrin accumulates in the tissue of these patients and causes photosensitivity. The assumption was that protoporphyrinogen is spontaneously oxidized to protoporphyrin. Chemical studies indicate that most porphyrinogens are spontaneously oxidized to the porphyrin form, a process which is accelerated by low pH, light, and aeration. In fact, in other porphyria diseases involving deficiencies in the enzymes utilizing other porphyrinogens, such as uroporphyrinogen or coproporphyrinogen, uroporphyrin and coproporphyrin are found in urine and feces.

However, the spontaneous oxidation of protoporphyrinogen has been less well studied, and there were early indications that it was difficult to chemically

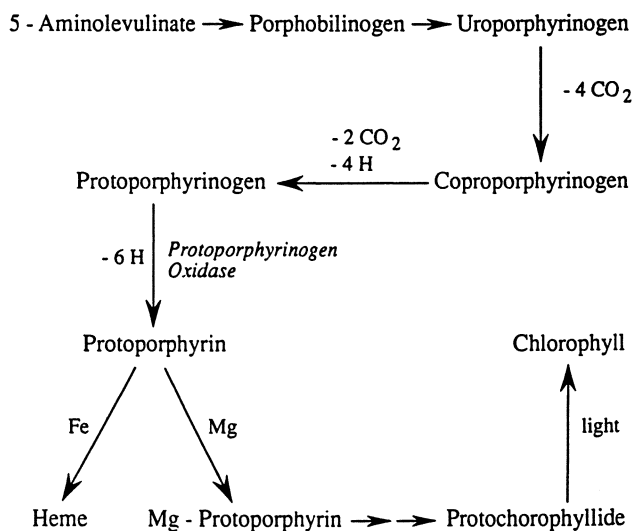


Figure 1. Biosynthetic pathway to heme and chlorophyll

oxidize protoporphyrinogen with a good yield of protoporphyrin (23). In our own laboratory, we have repeatedly observed that the chemical conversion of protoporphyrinogen to protoporphyrin is much more difficult to achieve than is the chemical oxidation of uroporphyrinogen and coproporphyrinogen to their respective porphyrins. This is especially true in the presence of biological reducing agents (unpublished observations). From these observations, we have tentatively concluded that the spontaneous slow oxidation of protoporphyrinogen to protoporphyrin is unlikely to explain the rapid accumulation of protoporphyrin which occurs in plant tissues when plants are treated with herbicide in the dark (7). Other observations were also more difficult to explain by spontaneous oxidation. For instance, intact plants accumulated protoporphyrin rapidly upon herbicide treatment, but suspensions of isolated chloroplasts were actually inhibited in protoporphyrin formation when herbicide was added to the assay mixture (24, 25). Thus it seemed reasonable to examine other plant cell membranes for their capacity to rapidly oxidize protoporphyrinogen to protoporphyrin by herbicide-resistant mechanisms.

Jacobs and co-workers obtained evidence for a herbicide-resistant mechanism for oxidizing protoporphyrinogen to protoporphyrin in a fraction from barley roots enriched for plasma membranes by means of sucrose gradient purification. Protoporphyrinogen oxidation by different preparations of plasma membrane showed 12 to 38% inhibition by herbicide (26), whereas mitochondrial protoporphyrinogen oxidase from these roots was 90% inhibited by herbicide. The plasma membrane enriched fragments showed minimal contamination with a mitochondrial marker enzyme, and less than 10% contamination with carotenoids, which were used as a marker for plastid contamination. An important unresolved question is why the plasma membrane fraction showed a partial inhibition by the herbicide if it represented a different activity from the plastid enzyme. Although it was desirable to repeat these studies with more highly purified plasma-membrane fractions from leaves, we concluded that these data represent evidence for an extraplastidic and extramitochondrial mechanism for oxidizing protoporphyrinogen to protoporphyrin in the presence of herbicide, which is different from the biosynthetic protoporphyrinogen oxidase in the plastid.

Lee and co-workers have very recently extended these findings and conclusively demonstrated the presence of protoporphyrinogen oxidizing activity in highly purified preparations of plasma membrane from etiolated barley leaves. This activity was much more resistant to herbicide inhibition than was the activity in purified etioplasts from these leaves (27). The plasma membrane activity also differed from the plastid enzyme in substrate specificity, with the former oxidizing coproporphyrinogen I at a rate almost as fast as protoporphyrinogen (27). In addition, this study found that microsomal preparations from these leaves also exhibited protoporphyrinogen oxidizing activity which was less sensitive to herbicide inhibition than was the plastid enzyme (27). In this study all membrane fractions were assayed for purity with the use of marker enzymes.

Several observations suggest the hypothesis that this herbicide-resistant protoporphyrinogen oxidation catalyzed by extraplastidic membranes offers the best explanation for the protoporphyrin accumulation which occurs when plants are treated with herbicide. Six lines of evidence which support this hypothesis are listed below:

1. A rapid oxidation of protoporphyrinogen catalyzed by extraplastidic membranes best explains the rapid accumulation of protoporphyrin seen within 15 minutes of exposure of cucumber cotyledon discs to herbicide in the dark (1).

2. Since this hypothesis suggests that protoporphyrin formation occurs at a site far removed from the plastid, it also explains why protoporphyrin accumulates rather than being further metabolized by plastid enzymes to later chlorophyll intermediates.

3. This hypothesis offers an explanation for the anomalous observation that protoporphyrin accumulates when intact plants are treated with herbicide, but protoporphyrin formation is actually decreased by herbicide in suspensions of isolated plastids (24, 25). Only in intact plants is the extraplastidic mechanism available for oxidizing accumulated protoporphyrinogen in the presence of herbicide.

4. This hypothesis also explains the localization of protoporphyrin accumulation in intact plants treated with herbicide. These localization studies were *in vivo* observations made by exposing intact plant tissue to herbicide and observing the appearance of typical porphyrin fluorescence in the intact cell by fluorescence microscopy. In these studies, the plasma membrane or the cytoplasm were the first to exhibit fluorescence following a brief exposure to herbicide, and it was concluded that protoporphyrin accumulated outside the plastid (7).

5. This hypothesis also offers an explanation for why these herbicides cause damage first at the plasma membrane and at other extraplastidic membranes before damage to the plastid membrane occurs (see reference 7 and references therein).

6. In addition, we will present below some new observations from our laboratory indicating that protoporphyrinogen is relatively unstable in the plant cytoplasm and will decompose to non-porphyrin products if not rapidly converted to protoporphyrin.

Effect of Reductants on Protoporphyrinogen Oxidation. In our initial investigation (26), we reported an unusual observation concerning the effect of reducing agents on *in vitro* protoporphyrinogen oxidation. When studying the biosynthetic enzyme present in crude preparations of plastids, we noted that the extent of inhibition by herbicide of the enzyme activity was much greater when a reducing agent such as dithiothreitol (DTT) was present in the enzyme assay mixture. The rate of oxidation in the absence of inhibitor was also markedly suppressed by the presence of reducing agent in the assay.

These effects of reductant were puzzling. One possible explanation could be that our crude mitochondrial and plastid preparations were contaminated with membrane fragments exhibiting the non-biosynthetic type of protoporphyrinogen oxidizing activity, which is less sensitive to herbicide inhibition and more sensitive to inhibition by strong reductants. Therefore, when measuring protoporphyrinogen oxidase of crude plant organellar preparations in the absence of a strong reductant like DTT, much of the observed protoporphyrinogen oxidizing activity may be due to the herbicide-resistant, non-biosynthetic activity rather than the herbicide-sensitive biosynthetic enzyme.

This phenomenon probably explains our previous observation that a crude soybean root mitochondrial preparation exhibited herbicide-resistant protoporphyrinogen oxidizing activity (16). This activity was markedly inhibited by DTT and probably represented only non-biosynthetic protoporphyrinogen oxidation associated with contaminating non-mitochondrial membranes. Most other studies on plant and animal systems have reported that all plastid and mitochondrial preparations exhibit herbicide sensitive protoporphyrinogen oxidase activity (17, 28). Most studies on plant protoporphyrinogen oxidase have routinely added DTT as reductant in the enzyme assay, and have therefore not noticed this effect of reductant.

The recent study by Lee et al. (27) clarified these effects of reductant using highly purified plasma membrane and plastid preparations. Protoporphyrinogen oxidation by the plasma membrane preparation was much more suppressed by the presence of reductant in the assay than was protoporphyrinogen oxidation by the plastid enzyme. These findings establish that an important difference between the biosynthetic enzyme and the extraplastidic, herbicide-resistant activity is the greater ability of the former to oxidize protoporphyrinogen rapidly in a highly reducing environment.

Although the biochemical basis for these effects of reductant on the *in vitro* assay is unknown, these observations may have implications for the *in vivo* effect of herbicides in causing protoporphyrin accumulation in intact plants. For instance, we suggest that protoporphyrinogen oxidation by the biosynthetic enzyme would function in a highly reducing environment within the plastid. If herbicide was present, the enzyme would be inhibited and protoporphyrinogen would accumulate and be released into the cytoplasm. If the level of endogenous reductant were depleted in the cytoplasm, then the extraplastidic, herbicide-resistant activity would function optimally and protoporphyrinogen would be rapidly oxidized to protoporphyrin even in the presence of herbicide. This would be compatible with a model whereby protoporphyrinogen could be rapidly oxidized to protoporphyrin only in the cytoplasm in the presence of herbicide.

Role of Light in Conversion of Accumulated Protoporphyrinogen to Protoporphyrin in Herbicide-Treated Plants. Light has a stimulatory effect on *in vivo* protoporphyrin accumulation in herbicide-treated plants (25, 29, 30), although the biochemical basis for this has not been addressed. One explanation could be a role for light in stimulating the early enzymes of chlorophyll biosynthesis, which would increase the synthesis of porphyrin precursors (14). An additional factor in explaining the stimulatory effect of light could be an increased availability of the early precursor ALA resulting from the reduction of feedback inhibition by protochlorophyllide (31).

There is another possible explanation for this effect of light which has not been previously mentioned. Light could exert its effect by oxidizing the protoporphyrinogen which accumulated in the herbicide-inhibited plant cell. Chemical studies have shown that porphyrinogens such as uroporphyrinogen and coproporphyrinogen can be chemically oxidized to porphyrins by exposure to sunlight under strongly acidic conditions. However, if this effect of light in oxidizing protoporphyrinogen to protoporphyrin is an important factor in protoporphyrin accumulation, it must occur specifically in the cytoplasm and not within the plastid. As an explanation for why light causes oxidation of protoporphyrinogen mainly in the cytoplasm, we suggest that the reducing environment in the plastid prevents light catalyzed protoporphyrinogen oxidation. In our laboratory, we have noted that the light catalyzed chemical oxidation of protoporphyrinogen to protoporphyrin in acidic solution occurs rapidly and quantitatively, but the presence of reducing agents such as DTT or glutathione inhibits this conversion (unpublished observations). Thus, we propose that in the plant cell, light can catalyze spontaneous protoporphyrinogen oxidation in the cytoplasm under conditions where the concentration of reducing agents is depleted. However, this effect of light does not occur in the plastid when the reducing potential is high. It is possible that extraplastidic membranes such as the plasma membrane may play an important role in facilitating light catalyzed, herbicide-resistant oxidation of protoporphyrinogen in the cytoplasm.

Demonstration of Protoporphyrinogen Export from Intact Plastids

The demonstration of extraplastidic protoporphyrinogen oxidation made it important to determine the extent to which protoporphyrinogen was exported from the intact plastid. This had not been previously studied.

In our recent publication (32), we investigated the formation of porphyrin intermediates by isolated barley plastids incubated for 40 minutes in darkness with an excess of the porphyrin precursor 5-aminolevulinic acid (ALA), and in the presence and absence of a DPE herbicide. In the absence of herbicide, about 50% of the protoporphyrin formed was found in the extraplastidic medium, which was separated from intact plastids by centrifugation at the end of the incubation period. In contrast, uroporphyrinogen, an earlier porphyrin intermediate, and magnesium protoporphyrin, a later intermediate, were located mainly within the plastid. When the incubation was carried out in the presence of herbicide, protoporphyrin formation by the plastids was completely abolished, but large amounts of protoporphyrinogen accumulated in the extraplastidic medium. To detect extraplastidic protoporphyrinogen, it was necessary to first oxidize it to protoporphyrin with the use of the herbicide-resistant protoporphyrinogen oxidase enzyme present in *E. coli* membranes. Protoporphyrin and protoporphyrinogen found outside the plastid did not arise from plastid lysis, since the percentage of plastid lysis, measured with a stromal marker enzyme, was far less than the percentage of these porphyrins in the extraplastidic fraction. These findings suggest that of the tetrapyrrolic intermediates synthesized by the plastids, protoporphyrinogen and protoporphyrin are the most likely to be exported from the plastid to the cytoplasm.

These findings indicated that protoporphyrinogen was exported from plastids in the presence of herbicide. However, in the absence of herbicide, protoporphyrin was also exported in similar quantities. It will be important to determine whether both of these are exported with equal facility from plastids, as these results suggested. In this study, protoporphyrin(ogen) export took place under conditions of a massive excess of porphyrin production within the plastid caused by furnishing high levels of ALA, which bypasses the rate limiting step in tetrapyrrole synthesis. At this time, we do not know if protoporphyrinogen (and also protoporphyrin) are exported from intact plastids during a more physiological rate of porphyrin synthesis. Of particular interest would be the demonstration of protoporphyrinogen export when the ALA precursor, glutamate, is given to intact plastid suspensions.

Several questions arise from these findings: How is protoporphyrin or protoporphyrinogen released from the plastid? Is there an active export mechanism or a simple diffusion through the outer membrane? The location of the early enzymes of chlorophyll synthesis within the chloroplast may provide some insight. Protoporphyrinogen oxidase has recently been shown to be present on the envelope of the chloroplast (33). Since protoporphyrinogen is converted to protoporphyrin at the envelope, both intermediates may be exported when physiological conditions are such that they become present in excess. In their recent study, Lee and co-workers (27) demonstrated that protoporphyrinogen was more hydrophilic than protoporphyrin, which is the most lipophilic of the early porphyrin intermediates. These workers suggest that protoporphyrinogen may therefore have a greater tendency to escape from the plastid envelope. Alternatively, there may be an active transport mechanism for protoporphyrinogen. These transport mechanisms may have evolved for the purpose of carrying protoporphyrinogen from the plastid into the cytoplasm and

then into the mitochondrion for the synthesis of mitochondrial heme (to be discussed in a later section).

Evidence that Protoporphyrinogen Can Be Readily Destroyed and Converted to Non-Porphyrin Products by Factors in the Plant Cytosolic Fraction

Another important factor governing the levels of herbicide-induced protoporphyrin accumulation would be any reactions which would utilize protoporphyrinogen without giving rise to protoporphyrin. Of most importance, we have recently observed that protoporphyrinogen disappeared and was converted to non-porphyrin products by a cytosolic fraction from green barley leaves prepared by differential centrifugation which removed organelles and other membranes. In contrast, protoporphyrin was stable in these cytosolic fractions. The rate of protoporphyrinogen disappearance was dependent upon the amount of cytosolic fraction present and the time of exposure. For instance, a cytosolic preparation from green barley shoots containing 0.25 mg of protein decomposed 0.5 nmole of protoporphyrinogen in a 60 minute period. The reducing agent DTT (5 mM) markedly inhibited protoporphyrinogen disappearance, suggesting an oxidative process. Boiling of the cytoplasmic extract only partially prevented protoporphyrinogen disappearance, but trypsin treatment had no effect, suggesting that protoporphyrinogen disappearance was not enzymatically mediated (manuscript-in-preparation).

These findings have implications for the action of DPE herbicides since they suggest that the protoporphyrinogen which accumulates in the cytosol of herbicide-treated plants will degrade to non-porphyrin (and therefore non-toxic) products if it is not rapidly converted to protoporphyrin in the cytosol. These findings are strong evidence in favor of our suggestion that the conversion of accumulated protoporphyrinogen to protoporphyrin in the cytoplasm of herbicide-treated plants must occur rapidly, through the mechanism of herbicide-resistant oxidation associated with the extraplastidic membranes. If the conversion of protoporphyrinogen to protoporphyrin occurred solely by slow auto-oxidation, the protoporphyrinogen would more likely be destroyed than converted to protoporphyrin.

These findings also may have implications for herbicide tolerance in some plants. If a plant had elevated levels of cytosolic factors which destroy accumulated protoporphyrinogen before it is converted to protoporphyrin, this plant would not accumulate sufficient protoporphyrin for phytotoxicity on herbicide treatment and would therefore be herbicide tolerant. We are currently examining the cytosolic fraction from a variety of plants to determine whether tolerant plants may have elevated levels of cytosolic factors which destroy protoporphyrinogen. Preliminary results indicate high levels of these factors in the cytosol of broadleaf mustard, a tolerant weed. We also find higher levels in older (7 weeks) as compared to younger (4 weeks) mustard leaves. Previous studies on two weed species demonstrated that older plants are more tolerant to these herbicides than are younger plants (28). In addition, we very recently demonstrated protoporphyrinogen destruction in the cytosolic fraction of radish cotyledons. Radishes are relatively herbicide tolerant (Matsumoto, H., University of Tsukuba, Japan, personal communication).

These observations suggest that factors destroying protoporphyrinogen may be present in the cytoplasmic fraction of a variety of plant cells. To assess the role of protoporphyrinogen destruction in human porphyrin metabolism, it will be important to determine whether the cytoplasmic fraction of animal cells also

contains factors capable of destroying protoporphyrinogen. In a preliminary experiment, we failed to detect any protoporphyrinogen destroying capacity in a cytoplasmic fraction prepared from a homogenate of rat liver. In addition, recent observations using cultured rat hepatocytes treated with DPE herbicides have indicated that protoporphyrinogen can accumulate to relatively high levels and remain stable for many hours in these cells (Sinclair, P. R., Gorman, N., Walton, H. S., Sinclair, J. F., Jacobs, J. M., and Jacobs, N. J.; manuscript in preparation). Thus, it seems likely that the capacity of cytoplasmic fractions to destroy protoporphyrinogen is not present in animal cells and is an exclusive property of plant cells.

Evidence that Protoporphyrin Can Be Converted to Later Porphyrin Intermediates in the Presence of Herbicide.

In cucumber cotyledon discs, protoporphyrin accumulates rapidly upon herbicide exposure in the dark, but the rate of accumulation decreases after one hour. Subsequently, protochlorophyllide accumulation occurs after a 10 hour lag period. The accumulation of this late chlorophyll intermediate in the dark is eventually enhanced by the presence of herbicide (7). The best explanation for this phenomenon is that the protoporphyrin formed outside of the plastid by the oxidation of exported protoporphyrinogen can re-enter the plastid and be converted to later chlorophyll intermediates.

Our preliminary *in vitro* experiments offer support for this explanation of this *in vivo* phenomenon. When given ALA, isolated plastids synthesized both protoporphyrin and magnesium protoporphyrin. The latter is present only within the plastid. In the presence of herbicide however, the synthesis of both compounds was blocked (32). However, as shown in Table I, when *E. coli* membranes were included in the assay mixture along with the herbicide, the synthesis of both protoporphyrin and a small but significant amount of magnesium protoporphyrin was restored. Evidently in this *in vitro* system, when there was an extraplastidic source of herbicide-resistant protoporphyrinogen oxidase, the protoporphyrin formed external to the plastid could re-enter the plastid and be converted to magnesium protoporphyrin. Under these conditions, the magnesium protoporphyrin was present within the plastid, but most of the protoporphyrin was extraplastidic. In this *in vitro* experiment, the herbicide-resistant extraplastidic protoporphyrinogen oxidase was furnished by the *E. Coli* membranes, but *in vivo*, this would be furnished by the herbicide-resistant activity associated with extraplastidic membranes.

Factors Affecting the Rate of Protoporphyrinogen Synthesis

Obviously, another factor of critical importance in determining the level of protoporphyrin which accumulates in the presence of herbicide is the rate at which a plant synthesizes protoporphyrinogen from early precursors. Plants with a more rapid rate of chlorophyll synthesis might be expected to synthesize protoporphyrinogen more rapidly, and therefore eventually accumulate more protoporphyrin in the presence of herbicide. Of particular interest is the possibility that herbicide treatment may actually enhance protoporphyrinogen synthesis by inhibiting the synthesis of heme. Heme has been shown to repress the porphyrin synthesis pathway in plants by inhibiting the enzymes responsible for the synthesis of ALA from glutamate, the first step in the porphyrin pathway (14). Herbicide treatment caused a decrease in heme content and induced the ALA synthesis enzymes in tobacco cells. The addition of hemin to these cells

reversed this induction by herbicide (34). In *Lemna pausicostata* plants, herbicide treatment reduced total extractable heme levels. Exogenously supplied heme reduced herbicide-caused protoporphyrin accumulation and herbicidal damage in the light, and also reduced protoporphyrin accumulation caused by herbicide in darkness (29,31).

TABLE I Effect of Acifluorfen methyl on the synthesis and export of protoporphyrin and Mg-protoporphyrin in isolated barley plastids

Plastids were isolated from six-days old barley shoots, purified on Percoll gradients, tested for intactness and incubated with ALA as described (32). Where indicated, AFM and *E. coli* membranes were added (32). After an incubation period of 40 minutes the assay mixture was separated by centrifugation into plastids and supernatant fractions (32). Protoporphyrin (Proto) was determined by extraction with PCA/ methanol and Mg-protoporphyrin was determined by extraction with acetone/NH₄OH (32). Plastid intactness was 90% as determined by latency of 6-phosphogluconate dehydrogenase (32). The plastid protein concentration was 0.32 mg/assay.

Treatment	<u>pmoles porphyrin/mg protein</u>			
	<u>inside plastid</u>		<u>outside plastid</u>	
	<u>Proto</u>	<u>Mg proto</u>	<u>Proto</u>	<u>Mg proto</u>
None	497±91	116±3	562±62	12±0
AFM	<5	0	12±5	0
AFM + <i>E. coli</i> membranes	56±6	16±0	209±28	0

Interorganellar Localization of the Terminal Enzymes of Heme Synthesis and Its Importance for Understanding Protoporphyrin Accumulation Upon Herbicide Treatment

There has been much current interest in the question of whether the plant mitochondrion is dependent upon the plastid for the synthesis of heme compounds. To evaluate this question, Smith et al. (35) compared the levels of coproporphyrinogen oxidase and protoporphyrinogen oxidase in plant mitochondria and plastids, and reported that coproporphyrinogen oxidase was essentially absent from plant mitochondria. Earlier studies had indicated that both protoporphyrinogen oxidase and ferrochelatase are present in gradient purified plant mitochondria (36, 37). These findings led to a proposal which has important implications for herbicide action.

We have also recently completed a study to determine whether the three terminal enzymes of heme synthesis are located in both the plastid and the plant mitochondria. Our goal was to confirm and extend the findings of Smith et al. (35), using alternate methodologies and tissues from other plants. We compared

the activities of coproporphyrinogen oxidase, protoporphyrinogen oxidase, and ferrochelatase in plant organelles carefully isolated to prevent cross contamination. Carotenoids were used as the marker to evaluate contamination of mitochondria with plastid membrane fragments. Mitochondria isolated on Percoll gradients from greening barley shoots had 4-5% of the activity of coproporphyrinogen oxidase compared to that found in Percoll-isolated plastids (Table II). The protoporphyrinogen oxidase activity of purified mitochondria was 60-70% that of the plastids, while the activity of mitochondrial ferrochelatase was 35% that of the plastids (Table II). We conclude that the plant mitochondrion, unlike the animal mitochondrion, is lacking in coproporphyrinogen oxidase, but contains sufficient protoporphyrinogen oxidase and ferrochelatase to support some heme synthesis from protoporphyrinogen.

TABLE II Comparison of the specific activities of the terminal enzymes of heme synthesis in mitochondria and plastids from barley shoots

Mitochondria and plastids were isolated from barley on Percoll gradients (32, 38). Intactness of these isolated organelles as measured by latency of succinate cytochrome c oxidoreductase or 6-phosphogluconate dehydrogenase was 90% or greater. Succinate-cytochrome c oxidoreductase and carotenoid content were used as mitochondrial and plastid markers respectively (38). Coproporphyrinogen (copro'gen) oxidase and protoporphyrinogen (proto'gen) oxidase were assayed fluorometrically (26, 16). Ferrochelatase was assayed by the method of Daily (39). The results from 2 separate batches of barley are shown.

	<u>Homogenate</u>	<u>Plastids</u>	<u>Mitochondria</u>
Cytochrome c reductase (nmol/min/mg protein)	9.0 ± 0 21.9 ± 1.5	3.0 ± 0 5.8 ± 0.2	151.0 ± 3.0 236.0 ± 2.0
Carotenoids (ugrams/mg protein)	0.38 ± 0 1.06 ± 0.12	2.85 ± 0.08 6.49 ± 1.34	0.03 ± 0.02 0.18 ± 0.01
Copro'gen Oxidase (nmol/h/mg protein)	0.46 ± 0.2 0.80 ± 0.04	2.60 ± 0.60 4.80 ± 0.1	0.14 ± 0.02 0.18 ± 0.01
Proto'gen Oxidase (nmol/h/mg protein)	0.68 ± 0 0.06 ± 0.02	1.3 ± 0 3.2 ± 0	0.94 ± 0 2.1 ± 0
Ferrochelatase (nmol/h/mg protein)	0.46 ± 0.4 0.87 ± 0	2.83 ± 0 9.25 ± 0.45	0.96 ± 0.05 3.25 ± 0.05

Our results confirmed those of Smith et al. (35). To explain the absence of coproporphyrinogen oxidase in the mitochondrion, these workers have postulated that protoporphyrinogen is exported from the plastid to the mitochondrion for synthesis of mitochondrial heme. This hypothesis suggests that protoporphyrinogen may be the only porphyrin precursor which is exported into the cytoplasm under normal physiological conditions. Thus, in the presence of herbicide, this natural process may be greatly accelerated by inhibition of protoporphyrinogen oxidase, causing even more protoporphyrinogen to be exported to the cytoplasm.

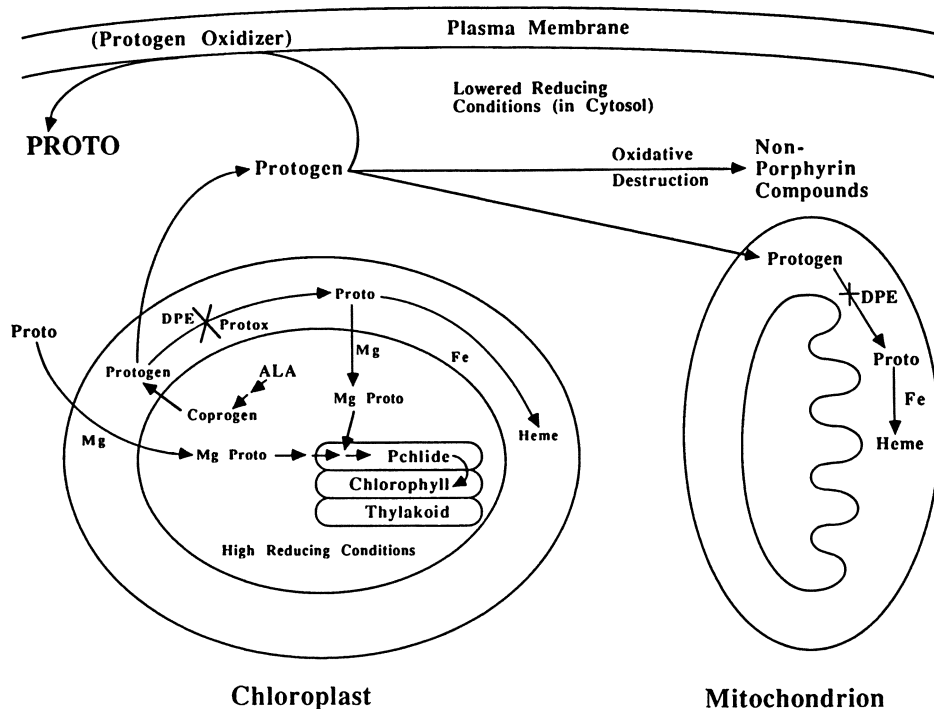


Figure 2. Model depicting factors affecting protoporphyrin accumulation in the herbicide-treated plant cell. See text for a detailed explanation of the steps depicted. The abbreviations used are: ALA (5-aminolevulinic acid); Coprogen (coproporphyrinogen); Protogen (protoporphyrinogen); Prottox (protoporphyrinogen oxidase, the biosynthetic, herbicide-sensitive enzyme); DPE (inhibition by diphenyl ether herbicide); Proto (protoporphyrin); Mg Proto (magnesium protoporphyrin); Pchlase (protoporphyrin synthase); Pchlide (protoporphyrinide); Heme synthase (the non-biosynthetic, herbicide resistant activity for oxidizing protoporphyrinogen to protoporphyrin which is associated with extra organellar membranes such as the plasma membrane).

A Model Describing Factors Affecting Protoporphyrin Accumulation in Herbicide-Treated Plants.

Figure 2 depicts our model for porphyrin metabolism in the plant cell. The model shows ALA conversion to coproporphyrinogen in the chloroplast stroma, and the formation of protoporphyrinogen from coproporphyrinogen at the outer chloroplast membrane. In the absence of herbicide, protoporphyrinogen is then converted to protoporphyrin by the membrane-associated, herbicide-sensitive, biosynthetic protoporphyrinogen oxidase. The protoporphyrin formed by this enzyme is made either into heme, or into magnesium protoporphyrin within the plastid. The latter is eventually converted to protochlorophyllide in the dark, and then chlorophyll in the light.

In the presence of herbicide, protoporphyrinogen accumulates at the protoporphyrinogen oxidase site in the chloroplast outer membrane, and is then exported into the cytoplasm. If this protoporphyrinogen first contacts extraplastidic membranes such as the plasma membrane, it will be rapidly oxidized to protoporphyrin by the herbicide-resistant protoporphyrinogen oxidizing activity (the "protogen oxidizer") in these membranes. This activity would be stimulated by any decrease in the concentration of reducing agents in the cytoplasm. The protoporphyrin formed by this extraplastidic activity would be the main source of protoporphyrin accumulation in the herbicide-treated cell. This protoporphyrin could accumulate to high levels, and a portion of it could slowly re-enter the plastid and be converted to magnesium protoporphyrin and chlorophyll.

However, if the exported protoporphyrinogen is not rapidly oxidized by this extraplastidic mechanism, the protoporphyrinogen which accumulates in the presence of herbicide could then be decomposed to non-porphyrin compounds by factors we have demonstrated in the cytoplasm. Protoporphyrinogen decomposition would be enhanced by a decrease in the concentration of reducing agents in the cytoplasm. Protoporphyrin is not decomposed by these cytoplasmic factors.

This model also has implications for mitochondrial heme synthesis. In the absence of herbicide, small amounts of protoporphyrinogen are also exported from the plastid to the cytoplasm and into the mitochondrion for synthesis into heme by mitochondrial enzymes. The question arises as to how this exported protoporphyrinogen can avoid being degraded to non-porphyrin products by the cytoplasmic factors mentioned above. We suggest that this degradation is prevented by high concentrations of reducing agents present in the cytoplasm. We have shown that reducing agents can prevent *in vitro* protoporphyrinogen destruction. Furthermore, it seems likely that heme synthesis may be most active in young, healthy plants, which probably contain high levels of reducing agents.

This model suggests that the fate of protoporphyrinogen is dependent not only on its localization within the cell, but also the reducing equivalents in the environment. In their discussion of this question, Lee and co-workers have pointed out that treatment of intact plants with herbicide can decrease the concentration of reductants in the cytoplasm both in the light and after prolonged incubation in the dark (27). These effects of herbicide on cytoplasmic reductants may be important for explaining factors governing protoporphyrin accumulation in herbicide-treated plants.

Acknowledgments

Studies in the authors' laboratory were supported by U.S. Department of Agriculture Competitive Grant 92 37303-7660, with additional support from

National Science Foundation Grant IBN-9205174 to J. M. Jacobs. We also thank Dr. Stephen O. Duke for helpful discussions.

Literature Cited

1. Becerril, M.; Duke, S. O. *Plant Physiol* **1989**, *90*, 1175-81.
2. Becerril, M.; Duke, S. O. *Pestic Biochem Physiol* **1989**, *35*, 119-26.
3. Bowyer, J. R.; Hallahan, B. J.; Camilleri, P.; Howard, J. *Plant Physiol* **1989**, *89*, 674-80.
4. Duke, S. O.; Lydon, J.; Paul, R. N. *Weed Sci* **1989**, *37*, 152-60.
5. Kouji, H.; Masuda, T.; Matsunaka, S. *Pestic Biochem Physiol* **1989**, *33*, 230-8.
6. Kouji, H.; Masuda, T.; Matsunaka, S. *J Pestic Sci* **1988**, *13*, 495-9.
7. Lehnen, L. P.; Sherman, T. D.; Becerril, J. M.; Duke, S. O. *Pestic Biochem Physiol* **1990**, *37*, 239-48.
8. Lydon, J.; Duke, S. O. *Pestic Biochem Physiol* **1988**, *31*, 74-83.
9. Matringe, M.; Scalla, R. *Proc Brit Crop Prot Conf B* **1987**, *9*, 981-8.
10. Matringe, M.; Scalla, R. *Plant Physiol* **1988**, *86*, 619-22.
11. Matringe, M.; Scalla, R. *Pestic Biochem Physiol* **1988**, *32*, 164-72...
12. Sandmann, G.; Boger, P. *Z Naturforsch C* **1988**, *43*, 699-704.
13. Witkowski, D. A.; Halling, B. P. *Plant Physiol* **1988**, *87*, 632-7.
14. Beale, S. I.; Weinstein, J. D. In *Biosynthesis of Heme and Chlorophyll*; Dailey, H. A., Ed.; McGraw-Hill: New York, **1990**, pp 286-331.
15. Camadro, J-M; Matringe, M.; Scalla, R.; Labbe, P. *Biochem J* **1991**, *277*, 17-21.
16. Jacobs, J. M.; Jacobs, N. J.; Borotz, S. E.; Guerinot, M. L. *Arch Biochem Biophys* **1990**, *280*, 369-75.
17. Matringe, M.; Camadro, J-M; Labbe, P.; Scalla, R. *Biochem J* **1989**, *260*, 231-5.
18. Matringe, M.; Camadro, J-M; Labbe, P.; Scalla, R. *FEBS Lett* **1989**, *245*, 35-48.
19. Varsano, R.; Matringe, M.; Magnin, N.; Mornet, R.; Scalla, R. *FEBS Lett* **1990**, *272*, 106-8.
20. Witkowski, D. A.; Halling, B. P. *Plant Physiol* **1989**, *90*, 1239-42.
21. Brenner, D. A.; Bloomer, J. R. *N Engl J Med* **1980**, *302*, 765-9.
22. Deybach, J. C.; de Verneuil, H.; Nordmann, Y. *Hum Genet* **1981**, *58*, 425-8.
23. Sano, S.; Granick, S. *J Biol Chem* **1961**, *236*, 1173-80.
24. Mito, N.; Sato, R.; Miyakado, M.; Oshio, H.; Tanaka, S. *Pestic Biochem Physiol* **1991**, *40*, 128-35.
25. Nandihalli, U. B.; Liebl, R. A.; Rebeiz, C. A. *Pestic Sci* **1991**, *31*, 9-23.
26. Jacobs, J. M.; Jacobs, N. J.; Sherman, T. D.; Duke, S. O. *Plant Physiol* **1991**, *97*, 197-203.
27. Lee, H. J.; Duke, M. V.; Duke, S. O. *Plant Physiol* **1993**, *102*, 881-9.
28. Sherman, T. D.; Becerril, J. M.; Matsumoto, H.; Duke, M. V.; Jacobs, J. M.; Jacobs, N. J.; Duke, S. O. *Plant Physiol* **1991**, *97*, 280-7.
29. Matsumoto, H.; Duke, S. O. *J. Agric. Food Chem.* **1990**, *38*, 2066-71.
30. Lee, J. J.; Matsumoto, H.; Ishizuka, K. *Pestic. Biochem. Physiol* **1992**, *44*, 119-25.
31. Becerril, J. M.; Duke, M. V.; Nandihalli, U. B.; Matsumoto, H.; Duke, S. O. *Physiologia Plantarum* **1992**, *86*, 6-16.
32. Jacobs, J. M.; Jacobs, N. J. *Plant Physiol* **1993**, *101*, 1181-7.
33. Matringe, M.; Camadro, J-M; Block, M. A.; Joyard J.; Scalla, R.; Labbe, P.; Douce, R. *J Biol Chem* **1992**, *267*, 4646-51.

34. Masuda, T.; Kouji, H.; Matsunaka, S. *Pesticide Biochem Physiol* **1990**, *36*, 106-14.
35. Smith, A. G.; Marsh, O.; Elder, G. H. *Biochem J* **1993**, *292*, 503-8.
36. Little, H. N.; Jones, O. T. G. *Biochem J* **1976**, *156*, 309-14.
37. Jacobs, J. M.; Jacobs, N. J.; DeMaggio, A. E. *Arch Biochem Biophys* **1982**, *218*, 233-9.
38. Neuberger, M; In *Encyclopedia of Plant Physiol* (R. Douce, D. A. Day, Eds). **1985** Vol 18, Springer-Verlag, New York, USA pp 7-24.
39. Dailey, H. A. *Methods Enzymol* **1986**, *123*, 408-15.

RECEIVED December 28, 1993

Chapter 9

Variation in Crop Response to Protoporphyrinogen Oxidase Inhibitors

H. Matsumoto, J. J. Lee¹, and K. Ishizuka

Institute of Applied Biochemistry, University of Tsukuba, Tsukuba, Ibaraki 305, Japan

Tolerance of nine plant species to diphenyl ether (DPE) herbicides oxyfluorfen and chlomethoxyfen were tested *in vivo*. There was considerable variation in tolerance to the herbicides between the species. Although both herbicides cause photodynamic damage as a result of protoporphyrinogen oxidase (Protox) inhibition, resulting in abnormally high levels of protoporphyrin IX (Proto IX) accumulation, there is little information on the reasons for differential interspecific tolerance to the herbicides. We compare uptake, movement and metabolism, Proto IX accumulation *in vivo*, Protox inhibition *in vitro*, and activities of antioxidative systems between the species to investigate the physiological basis of differential tolerance to two diphenyl ethers. Our findings suggest that differential tolerance of the species examined in this study is mainly due to differences in rates of herbicides absorption, Proto IX accumulation, and intrinsic antioxidative activity.

Several classes of herbicides, including diphenyl ethers, cyclic imides and oxadiazoles cause light-dependent bleaching in sensitive plants by causing the accumulation of the photodynamic tetrapyrrole, protoporphyrin IX (Proto IX) (1-14). They are also known to inhibit protoporphyrinogen oxidase (Protox), which is the last enzyme of the common branch of the heme- and chlorophyll-synthetic pathways in plants (15-22). It has been suggested that accumulated protoporphyrinogen (Protogen), a substrate of Protox, leaks from the porphyrin-synthesizing plastid and is oxidized to Proto IX spontaneously and/or by an oxidizing activity located in the plasma membrane (20, 23-25). Proto IX is a potent photosensitizer and can generate singlet oxygen in the light (26-29). This active oxygen species is highly toxic to plants because it effectively peroxidizes membrane lipids.

Among the Protox inhibitors, the mechanism of action of diphenyl ether (DPE) herbicides have been investigated most intensively. Although DPE herbicides inhibit a

¹Current address: National Institute for Environmental Studies, Tsukuba, Ibaraki 305, Japan

vitaly important metabolic process, namely chlorophyll biosynthesis, considerable variation in susceptibility to the herbicides exists between plant species. Tolerance of peanut to fluorodifen (30), rice to chlomethoxyfen (31, 32), and soybean to acifluorfen (33) is due to metabolic detoxification of these chemicals. Therefore, interspecific differential metabolism can account for selectivity in some crop species. However, other factors must be involved in the mechanism of DPE tolerance in some species since they are highly tolerant but poorly metabolize the herbicides (34). In this paper, we confirm variation in plant species in response to DPE herbicides and describe the possible factors involved in their differential tolerance.

Response of Crop and Weed Seedlings to Oxyfluorfen and Chlomethoxyfen

Growth Response. Tolerance of nine plant species including crops and weeds to the DPE herbicides oxyfluorfen [2-chloro-1-(3-ethoxy-4-nitrophenoxy)-4-(trifluoromethyl)benzene] and chlomethoxyfen [2,4-dichloro-1-(3-methoxy-4-nitrophenoxy)benzene] was evaluated. The gramineous and dicotyledonous species were grown to the 2-leaf stage and fully expanded cotyledonous stage, respectively, by hydroponic culture in an environmental chamber maintained at 25/20 °C day/night and with a 12-h photoperiod of 450 $\mu\text{E}\cdot\text{m}^{-2}\cdot\text{s}^{-1}$ photosynthetic photon density. For the herbicide treatment, whole shoots excluding the roots of the plants were soaked for 2 h in 1 μM herbicide solution (containing 1% (v/v) ethanol as a solvent) in darkness. Plants were kept in darkness for 24 h and then transferred to the growth chamber and grown for 6 days. Fresh weight determination (Figure 1) clearly demonstrated differential response of these plant species to oxyfluorfen and chlomethoxyfen. The shoot fresh weight of corn, the most tolerant species tested, was reduced only 31% compared with non-treated control, and that of tomato, the most susceptible one, was reduced 90% at 6 days after treatment with oxyfluorfen. Chlomethoxyfen was less phytotoxic than oxyfluorfen. Rice was completely tolerant to the chlomethoxyfen treatment. This herbicide has been used for barnyardgrass and broadleaf weeds control in paddy rice. The order of the tolerance of the plant species was very similar between the herbicides; corn and rice were tolerant, while dicotyledonous plants such as tomato, cabbage, and buckwheat were very susceptible.

Ethane Evolution. Ethane evolution has been determined as an index of oxidative damage caused by the photobleaching herbicides (35-38). The hydrocarbon gas is a decomposition product of peroxidized fatty acids in membrane lipids (39, 40). A time course of ethane production from oxyfluorfen-treated shoots was determined by gas chromatography. When the plants were treated with oxyfluorfen, as in the study of growth response, ethane evolution from the shoots of susceptible species occurred immediately after exposure to the light (Figure 2). Furthermore, susceptible species tended to evolve large amounts of the gas. A small amount of ethane was detected from non-treated plants. This suggested that membrane disruption in the susceptible species was initiated immediately after light irradiation. Because ethane evolution was observed faster than loss of fresh weight, it was assumed that membrane disruption led to water loss from the susceptible species.

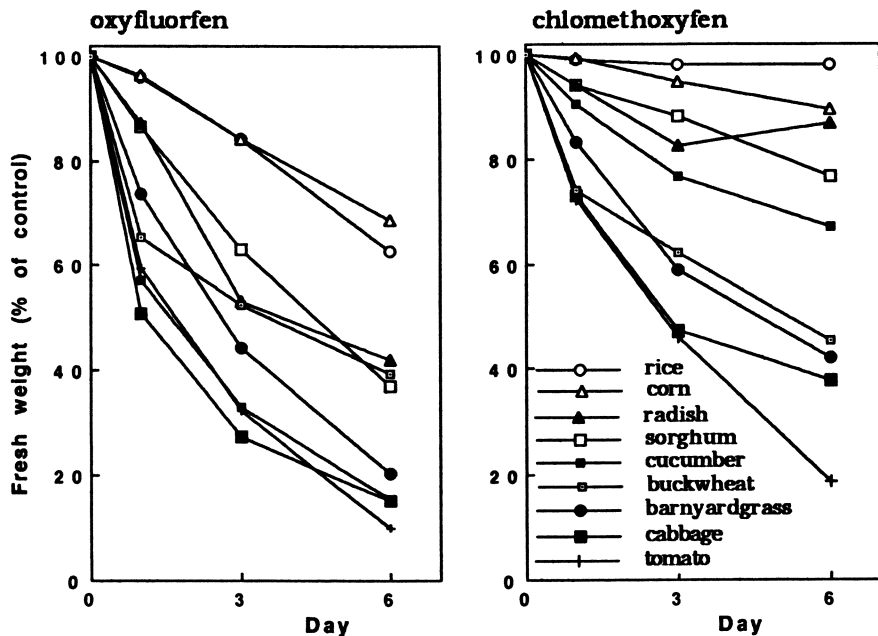


Figure 1. Effect of oxyfluorfen and chlomethoxyfen on plant growth. (Reproduced with permission from ref. 34. Copyright 1991 Weed Sci. Soc. Japan.)

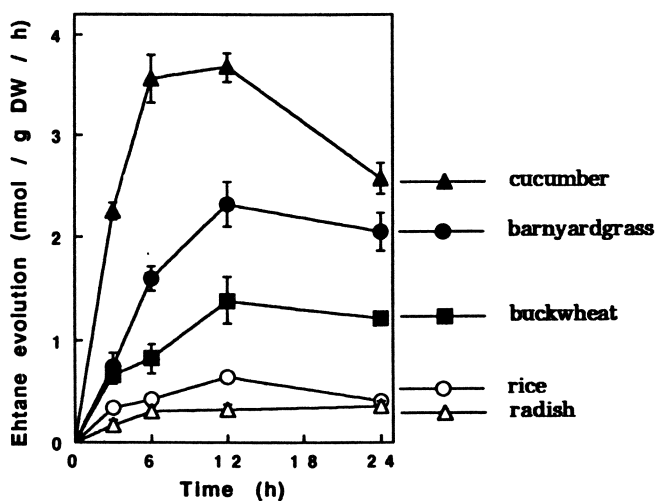


Figure 2. Ethane evolution from shoots of different plant species treated with oxyfluorfen.

Mechanism of Differential Tolerance between Plant Species

The plants tested in these soaking experiments showed clear differential tolerance to the DPE herbicides. To identify the basis of differential tolerance, uptake and metabolism of the herbicides, Proto IX accumulation, inhibition of Protox, and activities of antioxidative systems were compared.

Uptake and Metabolism. Uptake of oxyfluorfen and chlomethoxyfen by shoots was measured by placing shoots in $1 \mu\text{M}$ ^{14}C -oxyfluorfen or ^{14}C -chlomethoxyfen solution containing 1% ethanol, and periodically sampling. Shoots were rinsed with distilled water, dried, and combusted with a tissue oxidizer. The radioactivities in shoots were determined by a liquid scintillation spectrometry (Figure 3). Uptake of both herbicides increased throughout 2-h soaking periods in all plant species; however, it was more rapid in the dicotyledonous species, especially in tomato, than the gramineae. The order of the amounts of absorbed ^{14}C in plant shoots during 2 h were similar between the two herbicide treatments and it was negatively correlated with the order of the tolerance determined by the fresh weight. This indicates that differential uptake may account for some of the tolerance seen in some plant species. Autoradiography of the plants following ^{14}C -labeled herbicide treatment indicated that little translocation from treated parts occurred both in shoots and roots (data not shown).

We previously investigated metabolism of absorbed ^{14}C -oxyfluorfen and ^{14}C -chlomethoxyfen in shoots of five plant species by a thin-layer chromatography (34). None of the plants metabolized oxyfluorfen, and over 90% of radioactivity remained as the parent compound after 24 h incubation. Metabolism of chlomethoxyfen in the plants was also very limited except in rice and cucumber in which only 20 and 51% of the absorbed activity, respectively, remained as the parent compound. The main metabolites in rice were desmethyl chlomethoxyfen and unidentified water-soluble compounds. It seems that metabolism has little importance in differential tolerance of these species to oxyfluorfen. However, the greater metabolic degradation of chlomethoxyfen in rice and cucumber possibly contribute to their tolerance to the chemical. It should be noted that radish was the most tolerant to the herbicides among the dicotyledonous species tested in spite of its greater uptake and less metabolism. Other factors must be responsible for the tolerance of this plant.

Proto IX Accumulation. Proto IX content in shoots of oxyfluorfen-treated plants was determined. The shoots of the plants were soaked in $1 \mu\text{M}$ solution for 2 h in darkness. They were then either exposed to light ($450 \mu\text{E}\cdot\text{m}^{-2}\cdot\text{sec}^{-1}$) or kept in darkness. Among five species tested, only cucumber and buckwheat showed phytotoxic symptom during 8 h incubation in the light. Porphyrins were extracted from their shoots and analyzed as previously described (11). In the light (Figure 4A), Proto IX content rose rapidly during the 1 h in all plants; however, profiles of Proto IX during the following light exposure varied greatly among the species (41). Buckwheat, one of the most sensitive species, accumulated the greatest amount of Proto IX until 2 h and then it decreased rapidly. Cucumber, also susceptible, showed higher Proto IX accumulation until 1 h. Amounts of Proto IX in untreated control plants were less than the limit of detection ($1 \text{ nmol} / \text{g}$ dry weight) throughout the time course. Therefore, it seems that the amounts of oxyfluorfen-induced Proto IX within a short period (1-2 h) correlate with tolerance to the herbicide in some plant species. Watanabe *et al.* (42) also reported that the intensities of cyclic imide-

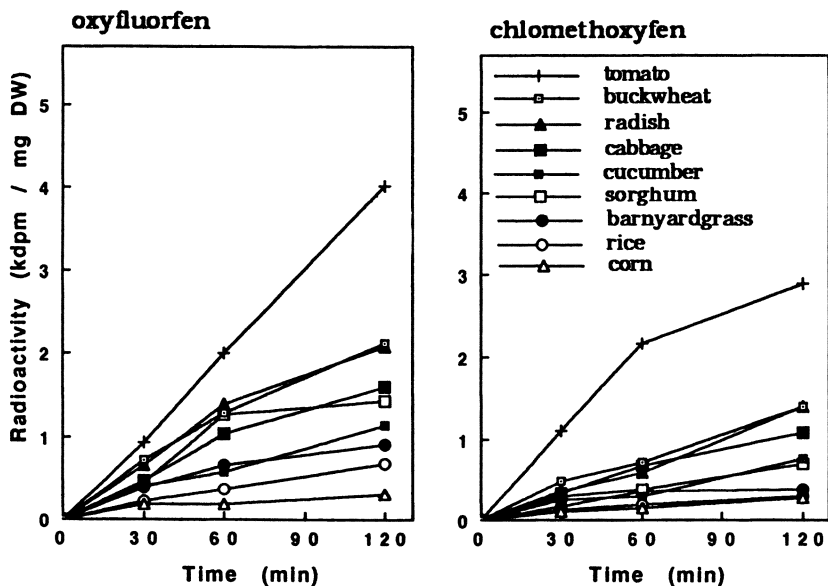


Figure 3. Uptake of ^{14}C -oxyfluorfen and ^{14}C -chlormethoxyfen from shoots of different plant species. (Reproduced with permission from ref. 34. Copyright 1991 Weed Sci. Soc. Japan.)

induced bleaching and amount of ethane evolution from *Scenedesmus acutus* correlated well with Proto IX level after 1 h incubation. The faster accumulation of Proto IX in buckwheat may be due in part to greater absorption of oxyfluorfen from its shoots. Interestingly, Proto IX content in rice and barnyardgrass increased constantly throughout 8-h light irradiation. Proto IX level in rice at 8 h was much higher than that in the susceptible species, however, no phytotoxic symptoms were observed. Therefore, it is hypothesized that rice has some mechanism to protect it from Proto IX-induced lipid peroxidation. In contrast, radish accumulated less Proto IX and this may relate to the herbicide tolerance, although the mechanism which suppresses Proto IX accumulation is still unclear. Varying rates of porphyrin synthesis (43) and Protogen oxidizing activity in the plasma membrane (20) have been suggested as mechanisms for the differential Proto IX accumulation. At 8 h, no correlation between amounts of Proto IX in the plants and their tolerance to the herbicide was observed.

Interestingly, the decrease of accumulated Proto IX in the light was initiated earlier in oxyfluorfen-susceptible species. Since Proto IX is known to be photolabile (8), photodegradation of Proto IX in oxyfluorfen-sensitive plants may explain rapid dissipation seen in these plants. In the susceptible species, the porphyrin synthesis pathway located in the plastid membrane was apparently disrupted within a shorter period, and this interrupted further accumulation of Proto IX. The susceptible plants may have less capacity to protect the membranes from the active oxygen-induced peroxidation. Little is known about the nature of the photodegradation products of Proto IX and their possible involvement in the photodynamic action of DPE herbicides.

In darkness (Figure 4B), no Proto IX accumulation occurred in rice, radish, and cucumber. In contrast, buckwheat and barnyardgrass accumulated significantly large amounts of Proto IX although the accumulation rates were slower than in the light. This indicated that, in some species, light is not necessary for oxyfluorfen-induced Proto IX accumulation. This result is different with that reported by others (44, 45) who found that light is mandatory for Proto IX accumulation. Our data also indicated that light acts as an enhancer of oxyfluorfen-induced Proto IX accumulation in the plants. Again, no Proto IX was detected in non-treated plants.

δ -Aminolevulinic acid (ALA) synthesis from glutamate has been reported as a rate-limiting step in the porphyrin synthesis and the step is regulated by light (46, 47). Therefore, there is a possibility that the rate of ALA synthesis and/or its regulation by light differed among the species and could account for some of the tolerances seen in certain plant species. To examine this possibility, the contents of ALA in light and dark and the effects of oxyfluorfen on the contents were compared between three plant species (Figure 5). As in the above mentioned experiments, whole shoots of intact plants were exposed to 1 μ M oxyfluorfen solution in darkness and then exposed to the light or kept in darkness. ALA was extracted with 4% TCA and determined spectrophotometrically (48). The data indicated that the rates of ALA synthesis in the plants were somewhat greater in the light; however, the amounts of ALA differed considerably between the species. ALA in buckwheat was significantly higher than the other species and the plant generated a considerable amount of ALA even in darkness. In *Euglena gracilis*, which has the same pathway of ALA synthesis as higher plants, ALA synthesis enzymes, especially GSA aminotransferase were reported to be light dependent (47). Because buckwheat shows a rather high rate of ALA formation in darkness, it would be a interesting to investigate the light regulation of ALA-forming enzymes. The data also showed that ALA formation was not inhibited or stimulated by oxyfluorfen. Thus, the greater accumulation of Proto IX in

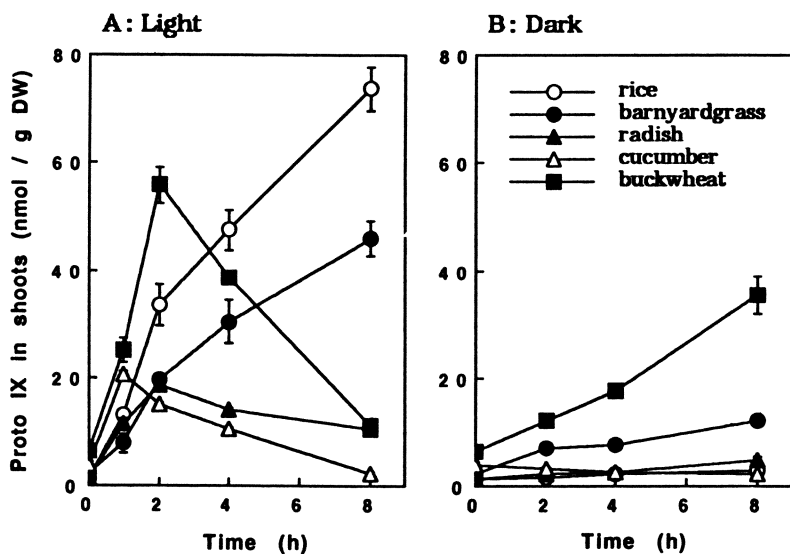


Figure 4. Time course of protoporphyrin IX accumulation in shoots of differential species in the light (A) and dark (B). (Figure 4A: Reproduced with permission from ref. 41. Copyright Academic Press.)

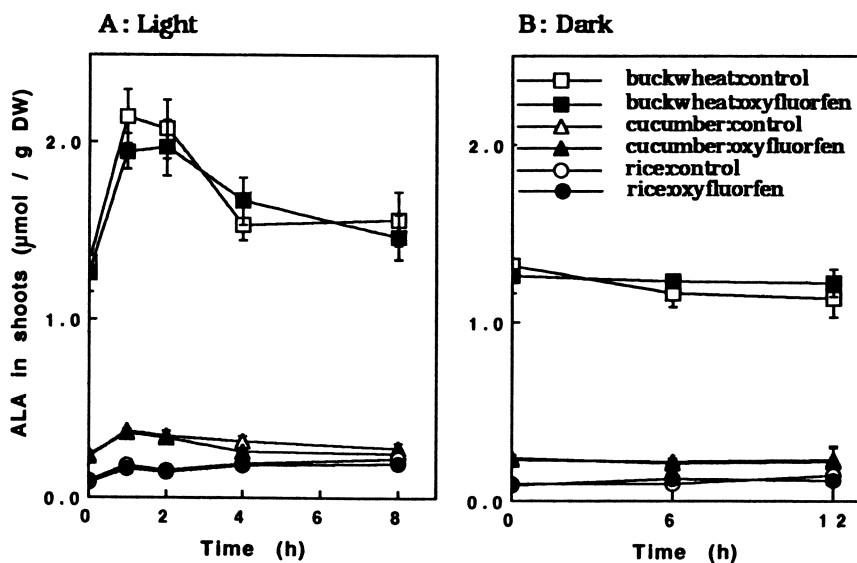


Figure 5. Rates δ -aminolevulinic acid synthesis in shoots in the light (A) and dark (B).

buckwheat in darkness could be explained by this greater ALA formation or a greater pool of ALA.

Inhibition of Protox. Proto IX accumulation in DPE-treated plants is caused by inhibition of the enzyme Protox. Protox preparations from various plant species were isolated and their inhibition by oxyfluorfen was compared by the methods of Sherman *et al.* (21). The enzyme substrate, Protogen, was prepared in the dim light according to Jacobs and Jacobs (49). In the assay, oxyfluorfen in the nanomolar range inhibited Protox. The *in vitro* study indicated that I_{50} concentrations of Protox activities from rice, barnyardgrass, radish, cucumber, and buckwheat were 1.4, 3.4, 7.0, 25, and 30 nM, respectively (Table I). These values are very similar to those of acifluorfen-methyl on cucumber and corn Protox (4, 5). The data indicate that Protox in these plants is very sensitive to the herbicide. Our result also indicated that the sensitivity of the enzyme preparations differed about 20 times between the most sensitive (rice) and insensitive (buckwheat) species. Protox activities from dicotyledonous species were less sensitive than those from monocotyledons. This is an opposite tendency to the growth response in which monocots showed greater tolerance.

Table I. I_{50} Concentrations of Oxyfluorfen for Protoporphyrinogen Oxidase from Different Plant Species

Plant Species	Rice	Barnyardgrass	Radish	Cucumber	Buckwheat
I_{50} (nM)	1.4	3.4	7.0	25	30

The enzyme activities of non-treated preparations were 28.9, 43.3, 26.7, 25.9, and 10.3 nmol protoporphyrin IX /h /mg protein for rice, barnyardgrass, radish, cucumber, and buckwheat, respectively.

Antioxidative Systems. Plant cell death by DPE herbicides is a consequence of peroxidation of membrane lipids. Since Proto IX is known to be a strong photosensitizing pigment generating singlet oxygen (26-29), it is believed that this active oxygen species induces the oxidative reaction. Plants have an antioxidative system consisting of antioxidants, which can inactivate a variety of oxygen radicals. They also have many enzymes responsible for quenching the radicals and maintaining a protective redox state of the antioxidants. Exogenously applied antioxidants and oxygen radical scavengers are also reported to slow lipid peroxidation by DPE herbicides (50-54). Therefore, different levels of antioxidants or protective enzyme activities in the species, as well as sensitivity of the antioxidative systems to DPE treatment, could possibly be factors determining their tolerance to the herbicides.

Finckh and Kunert (55) reported that susceptibility of plant species to oxyfluorfen was directly related to the ratio of vitamin C (ascorbate) to vitamin E (α -tocopherol). They found ratios of approximately 10 to 15 associated with species that were highly tolerant. Using five plant species, we determined the content of these vitamins before and after

oxyfluorfen treatment (Table II). The content of both vitamins differed significantly between species. Especially, vitamin C contents differed more than 8-fold between radish (the highest) and rice (the lowest). However, among the tested plants, there was no relationship between the C/E ratio and their tolerance to oxyfluorfen. The ratio in buckwheat, highly susceptible species, was 16.7, and the value was almost same with the oxyfluorfen-tolerant species reported by others (55). Because radish has extremely high vitamin C content, it is possible that this contributes to the relatively higher tolerance to the herbicide. The vitamin contents in other species and their ratios were apparently not a factor in determining their tolerance. After 6 h light irradiation, significant depletion of the vitamins was detected in some plant species (Table II). This was more obvious in susceptible species such as cucumber and buckwheat. The decrease of the vitamins may be caused by oxidative damage in plant cells as mentioned before (56).

Table II. Antioxidant Contents in Different Plant Species and Effect of Oxyfluorfen on the Content

Plant Species	Antioxidant	Antioxidant Contents ^a (mg/ g dry weight)		
		Oxyfluorfen-Treated	Non-Treated	Ratio ^b
Rice	Vitamin C	3.11 (±0.12)	3.83 (±0.26) ^c	0.81
	Vitamin E	0.39 (±0.02)	0.39 (±0.01)	1.00
	C/E ratio		9.8	
Barnyardgrass	Vitamin C	4.29 (±0.10)	6.03 (±0.33)	0.71
	Vitamin E	0.23 (±0.01)	0.23 (±0.01)	1.00
	C/E ratio		26.2	
Radish	Vitamin C	29.61(±2.25)	30.37(±1.37)	0.98
	Vitamin E	0.70 (±0.02)	0.71 (±0.02)	0.99
	C/E ratio		42.8	
Cucumber	Vitamin C	6.91 (±0.24)	11.70 (±0.83)	0.59
	Vitamin E	0.45(±0.02)	0.63(±0.03)	0.71
	C/E ratio		18.6	
Buckwheat	Vitamin C	10.71 (±0.96)	15.91 (±0.84)	0.67
	Vitamin E	0.61 (±0.07)	0.95 (±0.12)	0.67
	C/E ratio		16.7	

^a The plant shoots were soaked to oxyfluorfen (1 μM) or herbicide-free solution for 2 h, kept in darkness for 24 h and then exposed to light (450 $\mu\text{Em}^{-2}\text{s}^{-1}$). Analysis was conducted after 6 h light irradiation.

^b Ratio of oxyfluorfen-treated shoots to non-treated shoots.

^c Values in parenthesis indicate standard error.

Superoxide dismutase (SOD) (57), catalase (58), ascorbate peroxidase (59), ascorbate free radical reductase (60), and glutathione reductase (61) which act as protectant from peroxidative damage by capturing oxygen radicals or by inhibiting free radical formation, were extracted from the five plant species and their activities and effect of oxyfluorfen on

them were investigated. These enzyme activities differed much between the species (Table III). It should be noted that rice has very high enzyme activities compared with other species. Activities of SOD, catalase, and ascorbate peroxidase were especially significantly higher than others. These enzymes protect from free radical formation by quenching superoxide radical and peroxide. However, the role of the enzymes in the protective reaction from oxyfluorfen-induced lipid peroxidation is not understood. Proto IX is a potent inducer of singlet oxygen and this reacts with the membrane lipids by a type II reaction to form lipid peroxide. In the presence of metal ions, decomposition of lipid peroxides and formation of lipid free radicals have been suggested (62). This radical species is highly reactive and may induce the chain reaction in lipid peroxidation. Since rice is very tolerant to oxyfluorfen in spite of its higher Proto IX accumulation, these antioxidative enzymes may be involved in protection from lipid peroxidation. Further investigation of the process of singlet oxygen-induced rapid peroxidation is necessary to demonstrate involvement of the enzymes in herbicide tolerance.

Table III. Activity of Protective Enzymes in Different Plant Species

Plant Species	Rice	Barnyardgrass	Radish	Cucumber	Buckwheat
SOD	>3500	67(±19)	86 (±8)	205(±11)	52(±11)
Catalase	529(±57)	261(±30)	321(±22)	380(±21)	28(±2)
Ascorbate Peroxidase	7.0(±0.7)	5.9(±0.6)	2.0(±0.2)	3.5(±0.3)	<0.6
AFR Reductase	2.6(±0.2)	2.6(±0.1)	2.6(±0.1)	3.4(±0.2)	0.8(±0.2)
Glutathione Reductase	0.83(±0.05)	0.92(±0.02)	0.49(±0.05)	0.74(±0.04)	<0.1

Units of enzyme activities were as follows ; SOD, units / g FW ; catalase, $\mu\text{mol} / \text{H}_2\text{O}_2$ oxidized / g FW / min ; ascorbate peroxidase, μmol ascorbic acid oxidized / g FW / min ; ascorbate free radical (AFR) reductase, μmol NADH oxidized / g FW / min ; glutathione reductase, μmol NADPH oxidized / g FW / min.

Values in parenthesis indicate standard error.

The effects of oxyfluorfen on the enzymes were investigated with a time course. Shoots of five plant species were treated by oxyfluorfen as above, and extracted enzyme activities were compared with that from non-treated plants. None of enzymes was inhibited until 4-h light exposure. At 8 h, only catalase activity extracted from buckwheat and that of ascorbate peroxidase from cucumber were diminished (unpublished data of Matsumoto *et al.*). Since ethane evolution from oxyfluorfen-treated shoots was initiated quickly after light exposure, it is considered that this reduction observed in the susceptible plants was also caused by oxidative damage in the cell.

Mechanism of Differential Activity of Oxyfluorfen and Chlomethoxyfen

As indicated above, the two DPE herbicides used had differential activity, with oxyfluorfen more phytotoxic to all plant species than chlomethoxyfen. Oxyfluorfen inhibited Protox *in vitro* with a lower concentrations than chlomethoxyfen (unpublished data of Matsumoto *et al.*) and this may be attributed as a major factor of the greater phytotoxicity. Furthermore, uptake of oxyfluorfen from shoots of intact plants was faster than that of chlomethoxyfen (Figure 3). Metabolism experiments revealed that tested plant species degraded neither herbicide except for rice and cucumber degradation of chlomethoxyfen. Interestingly, rice degraded chlomethoxyfen effectively but it could not degrade oxyfluorfen. Differential inhibitory activity of Protox as well as uptake rate from shoots are considered to be the primary contributors to differential activity of the two herbicides.

Summary

Laboratory studies were conducted to determine the basis of differential response of crop species to the Protox inhibitors oxyfluorfen and chlomethoxyfen. Possible mechanisms involved in determining tolerance of each species to oxyfluorfen are summarized in Table IV. The herbicide-sensitive species, in general, absorbed the herbicides faster than tolerant

Table IV. Possible Factors in Determining Tolerance of Each Plant Species to Oxyfluorfen

Plant Species		Possible Factors
Rice	Tolerant	Higher antioxidative activity Less absorption
Radish	Intermediately tolerant	Less Proto IX accumulation Higher antioxidant (vitamin C) content
Buckwheat	Susceptible	Faster Proto IX accumulation Lower antioxidative activity
Cucumber	Susceptible	Faster Proto IX accumulation Lower antioxidative activity
Barnyardgrass	Susceptible	Greater Proto IX accumulation Lower antioxidative activity

ones from their shoots. It is hypothesized that rapid uptake resulted in faster Protox inhibition and greater Proto IX accumulation within a shorter period. In the tested plants, buckwheat and cucumber showed such characteristics. These species also had less activity

of antioxidative systems, and this may relate with their higher sensitivity to lipid peroxidation. In contrast, the herbicide tolerance of some species examined in this study may be due to two differential mechanisms. The first type was observed in rice. Rice absorbed less herbicide but had sensitive Protox and accumulated Proto IX continuously. However, no detrimental effect of the herbicide appeared. Higher activity of antioxidative enzymes may possibly be involved in the tolerance. The second type was observed in radish. The plant absorbed greater amounts but showed less Proto IX accumulation. Tolerance of this species may be mainly due to suppression of Proto IX accumulation. Further investigation is required for elucidation of the mechanism of this suppression.

Literature Cited

1. Matringe, M.; Scalla, R. *Proc. Br. Crop Prot. Conf.* **1987**, *B9*, 981-88.
2. Matringe, M.; Scalla, R. *Plant Physiol.* **1988**, *86*, 619-22.
3. Lydon, J.; Duke, S. O. *Pestic. Biochem. Physiol.* **1988**, *31*, 74-83.
4. Matringe, M.; Scalla, R. *Pestic. Biochem. Physiol.* **1988**, *32*, 164-72.
5. Witkowski, D. A.; Halling, B. P. *Plant Physiol.* **1988**, *87*, 632-37.
6. Sandmann, G.; Böger, P. *Z. Naturforsch.* **1988**, *43c*, 699-704.
7. Duke, S. O.; Lydon, J.; Paul, R. N. *Weed Sci.* **1989**, *37*, 152-60.
8. Becerril, J. M.; Duke, S. O. *Plant Physiol.* **1989**, *90*, 1175-81.
9. Becerril, J. M.; Duke, S. O. *Pestic. Biochem. Physiol.* **1989**, *35*, 119-26.
10. Yanase, D.; Andoh, A. *Pestic. Biochem. Physiol.* **1989**, *35*, 70-80.
11. Matsumoto, H.; Duke, S. O. *J. Agr. Food Chem.* **1990**, *38*, 2066-71.
12. Sandmann, G.; Böger, P. *Z. Naturforsch.* **1990**, *45c*, 512-517.
13. Kojima, S.; Matsumoto, H.; Ishizuka, K. *Weed Res. (Tokyo)* **1991**, *36*, 318-23.
14. Mito, N.; Sato, R.; Miyakado, M.; Oshio, H.; Tanaka, S. *Pestic. Biochem. Physiol.* **1991**, *40*, 128-35.
15. Matringe, M.; Camadro, J-M.; Labbe P.; Scalla, R. *FEBS Lett.* **1989**, *245*, 35-8.
16. Matringe, M.; Camadro, J-M.; Labbe P.; Scalla, R. *Biochem. J.* **1989**, *260*, 231-35.
17. Witkowski, D. A.; Halling B. P. *Plant Physiol.* **1989**, *90*, 1239-42.
18. Jacobs, J. M.; Jacobs, N. J.; Borotz, S. E.; Guerinot, M. L. *Arch. Biochem. Biophys.* **1990**, *280*, 369-75.
19. Versano, R.; Matringe, M.; Magnin, N.; Mornet, R.; Scalla, R. *FEBS Lett.* **1990**, *272*, 106-8.
20. Jacobs, J. M.; Jacobs, N. J.; Sherman, T. D.; Duke, S. O. *Plant Physiol.* **1991**, *97*, 197-203.
21. Sherman, T. D.; Duke, M. V.; Clark, R. D.; Sanders, E. F.; Matsumoto, H.; Duke, S. O. *Pestic. Biochem. Physiol.* **1991**, *40*, 236-45.
22. Camadro, J-M.; Matringe, M.; Scalla, R.; Labbe, P. *Biochem. J.* **1991**, *277*, 17-21.
23. Lehnen, L. P.; Sherman, T. D.; Becerril, J. M.; Duke, S. O. *Pestic. Biochem. Physiol.* **1990**, *37*, 239-48.
24. Jacobs, J. M.; Jacobs, N. J. *Plant Physiol.* **1993**, *101*, 1181-8.
25. Lee, H. J.; Duke, M. V.; Duke, S. O. *Plant Physiol.* **1993**, *102*, 881-9.
26. Hopf, F. R.; Whitten, D. G. In *The Porphyrins*; Dolphin, D., Ed.; Academic Press: New York, 1980; Vol. 2; pp 161-95.

27. Cox, G. C.; Whitten, D. G. In *Porphyrin Photosensitization*; Kassel, D.; Dougherty, T. J., Eds.; Plenum: New York, 1983; pp 279-92.
28. Haworth, P.; Hess, F. D. *Plant Physiol.* **1988**, *86*, 672-6.
29. Duke, S. O.; Becerril, J. M.; Sherman, T. D.; Matsumoto, H. *Am. Chem. Soc. Symp. Ser.*, **1990**, *449*, 371-86.
30. Eastin, E. F. *Weed Sci.* **1971**, *19*, 261-65.
31. Niki, Y.; Kuwatsuka, S.; Yokomichi, I. *Agr. Biol. Chem.* **1976**, *40*, 683-90.
32. Ishizuka, K.; Matsumoto, H.; Hyakutake, H. *Weed Res. (Tokyo)* **1988**, *33*, 41-8.
33. Frear, D. S.; Swanson, H. R.; Mansager, E. R. *Pestic. Biochem. Physiol.* **1983**, *20*, 299-310.
34. Lee, J. J.; Matsumoto, H.; Ishizuka, K. *Weed Res. (Tokyo)* **1991**, *36*, 162-70.
35. Kunert, K. J.; Böger, P. *Weed Sci.* **1981**, *29*, 169-73.
36. Kunert, K. J.; Böger, P. *J. Agric. Food Chem.* **1984**, *32*, 725-28.
37. Schmidt, A.; Kunert, K. J. *Plant Physiol.* **1986**, *82*, 700-2.
38. Matringe, M.; Scalla, R. *Pestic. Biochem. Physiol.* **1987**, *27*, 267-74.
39. Tappel, A. L. In *Free Radicals in Biology*; Pryor, W. A., Ed.; Academic Press: New York, 1980; pp 1-44.
40. Dumelin, E. E.; Tappel, E. L. *Lipids* **1977**, *12*, 894-900.
41. Lee, J. J.; Matsumoto, H.; Ishizuka, K. *Pestic. Biochem. Physiol.* **1992**, *44*, 119-25.
42. Watanabe, H.; Ohori, Y.; Sandmann, G.; Wakabayashi, K.; Böger, P. *Pestic. Biochem. Physiol.* **1992**, *42*, 99-109.
43. Sherman, T. D.; Becerril, J. M.; Matsumoto, H.; Duke, M. V.; Jacobs, J. M.; Jacobs, N. J.; Duke, S. O. *Plant Physiol.* **1991**, *97*, 280-287.
44. Mayasich, J. M.; Nandihalli, U. B.; Liebl, R. A.; Rebeiz, C. A. *Pestic. Biochem. Physiol.* **1990**, *36*, 259-68.
45. Nandihalli, U. B.; Liebl, R. A.; Rebeiz, C. A. *Pestic. Sci.* **1991**, *31*, 9-23.
46. Beale, S. I.; Casterflanco, P. A. *Plant Physiol.* **1974**, *53*, 291-96.
47. Mayer, S. M.; Beale, S. I. *Plant Physiol.* **1990**, *94*, 1365-75.
48. Lew, R.; Tsui, H. *Plant Physiol.* **1982**, *69*, 663-7.
49. Jacobs, N. J.; Jacobs, J. M. *Enzyme* **1982**, *28*, 206-16.
50. Orr, G. L.; Hess, F. D. *Plant Physiol.* **1982**, *69*, 502-7.
51. Kunert, K. J.; Böger, P. *J. Agric. Food Chem.* **1984**, *32*, 725-28.
52. Ensminger, M. P.; Hess, F. D.; Bahr, J. T. *Pest. Biochem. Physiol.* **1985**, *23*, 163-70.
53. Kunert, K. J.; Homrighausen, G.; and Böger, P. *Weed Sci.* **1985**, *33*, 766-70.
54. Matsumoto, H.; Kojima, S.; Ishizuka, K. *Weed Res. (Tokyo)* **1990**, *35*, 36-43.
55. Finckh, B. F.; Kunert, K. J. *J. Agric. Food Chem.* **1985**, *33*, 574-77.
56. Kenyon, W. H.; Duke, S. O. *Plant Physiol.* **1985**, *79*, 862-6.
57. McCord, J. M.; Fridovich, I. *J. Biol. Chem.* **1969**, *244*, 6049-55.
58. Blume, E.; McClure, J. W. *Plant Physiol.* **1980**, *65*, 238-44.
59. Nakano, Y.; Asada, K. *Plant Cell Physiol.* **1981**, *22*, 867-80.
60. Arrigoni, O.; Dipierro, S.; Borraccino, G. *FEBS Lett.* **1981**, *125*, 242-44.
61. Schaedle, M.; Bassham, J. A. *Plant Physiol.* **1977**, *59*, 1011-12.
62. O'Brien, P. J. *Can. J. Biochem.* **1969**, *47*, 485-92.

RECEIVED December 21, 1993

Chapter 10

Structure–Activity Relationships of Protoporphyrinogen Oxidase Inhibiting Herbicides

Ujjana B. Nandihalli¹ and Stephen O. Duke²

¹Hazleton Laboratories, P.O. Box 7545, Madison, WI 53707

²Southern Weed Science Laboratory, Agricultural Research Service, U.S.
Department of Agriculture, P.O. Box 350, Stoneville, MS 38776

Herbicidal protoporphyrinogen oxidase (Protox) inhibitors are competitive with respect to protoporphyrinogen IX (Protox). The most potent Protox inhibitors more closely mimic one half of the Protox molecule. These compounds are all bicyclic, non-planar molecules, similar to one half of the Protox tetrapyrrole macrocycle. Among diphenyl ether Protox inhibitors, molecular bulk and overall electrostatic potentials were most responsible for variations in herbicidal effects, although other factors such as lipophilicity were also important. From QSAR analyses of various classes of peroxidizing herbicides, it appears that Protox-inhibiting activity responds primarily to the substitutional modifications on the phenyl ring (*p*-nitrophenyl in diphenyl ethers). Furthermore, a substitution at the meta position on the *p*-chloro (phenopylate) or *p*-nitro (diphenyl ether) ring is essential for greatest herbicidal activity.

Even though several photobleaching herbicides such as diphenyl ethers (DPE) have been in commercial use since the early 1970s, their target site in the porphyrin pathway was not identified until recently (1-3). The DPE and certain other classes of herbicides cause rapid peroxidative bleaching and/or desiccation of plant tissues (4-12). The primary site of action of these herbicides is protoporphyrinogen oxidase (Protox) (11-15), the last common enzyme in the synthesis of both heme and chlorophylls. A question arises as to how the inhibition of Protox leads to the accumulation of the product of the enzyme protoporphyrin IX (Proto IX) and why Proto IX is not converted to later intermediates. Recently, a detailed scheme that describes the mechanism of the accumulation of Proto IX in the presence of the photobleaching herbicide, acifluorfen-methyl has been proposed (16, 17). By inhibiting plastid Protox, these

0097-6156/94/0559-0133\$08.00/0

© 1994 American Chemical Society

herbicides induce protoporphyrinogen (ProtoGen) accumulation which is exported out of the plastid envelope into the cytoplasm. The exported ProtoGen is oxidized by acifluorfen-methyl-resistant extraorganellar oxidases associated with the plasma membrane and microsomes. High levels of Proto IX build up in extraplastidic sites. Some of this may re-enter the porphyrin pathway, but most accumulates and appears to participate in a type II photoperoxidation process which damages plants.

The discovery that a large number of peroxidizing herbicides are potent Protox inhibitors has important implications for those interested in QSAR studies. Similarly, the discovery of the D-1 protein binding site of photosystem II inhibitors spurred a better understanding of the QSAR of photosystem II-inhibiting compounds (18). The finding that Protox inhibitors are analogues of one half of the ProtoGen molecule has helped in understanding the QSAR of Protox inhibitors.

Competitive inhibition

Herbicidal Protox inhibitors apparently inhibit the Protox enzyme by competitive inhibition (19). In enzyme kinetics studies, acifluorfen and three analogues were found to competitively inhibit (with respect to ProtoGen) the Protox activity from mouse liver mitochondria, corn mitochondria, and corn etioplast membranes. In binding studies, both ProtoGen and Protox-inhibiting herbicides displaced bound ^3H -acifluorfen from corn etioplast preparations (20). Similarly, five phenopylate Protox-inhibiting analogues competed with ^{14}C -acifluorfen for binding sites on Protox (21). The specific binding constants and Protox inhibitory activities (I_{50}) of these analogues were highly correlated. The binding of the ^{14}C -labeled *N*-phenylimide herbicide S-23121 to a plastid preparation from greening corn seedlings was inhibited by acifluorfen-methyl (22). Similarly, KS 307829, a *N*-phenylimide derivative, prevented the binding of acifluorfen to pea etioplasts (23), and this compound exerted a mixed competitive type of inhibition on the binding of acifluorfen. In a mixed type of competitive inhibition the binding is not mutually exclusive and therefore KS 307829 and acifluorfen do not bind to the same binding site, rather they bind to two overlapping sites.

Molecular Similarities Between the ProtoGen and Protox Inhibitors

For an inhibitor to compete with the substrate for the same active site on the enzyme it must have structural complementarity with some part of the substrate molecule. From enzyme kinetic and radiolabeled herbicide binding experiments it was apparent that Protox inhibitors are competitive inhibitors of Protox. In an attempt to draw molecular similarities between ProtoGen and Protox-inhibiting herbicides, we proposed that the Protox inhibitors must be two aromatic ring structures, representing approximately one half fractions of the ProtoGen molecule for proper geometrical fit into the active site (Figure 1).

This hypothesis was developed from the observations that (a) all the known Protox inhibiting herbicides belonging to different chemical classes contain two aromatic rings and (b) the monocyclic compounds such as

picolinic acid and pyrrole-2-carboxaldehyde which are found to interfere with the porphyrin pathway do not effectively inhibit Protox. Furthermore, the Protopen macrocycle is non-planar (therefore two adjacent pyrrole rings are non-coplanar). It appears that because of this non-planarity, the substrate binding site on Protox may accommodate only two adjacent pyrrole rings of the Protopen molecule at a time. This hypothesis is supported by the existence of one (tetrahydroprotoporphyrin IX, P-503) (25) or most probably two reaction intermediates in the enzymic oxidation of Protopen to Proto IX (Figure 2). Tetrahydroprotoporphyrin IX may accumulate *in vivo* in acifluorfen-treated plant tissues (26).

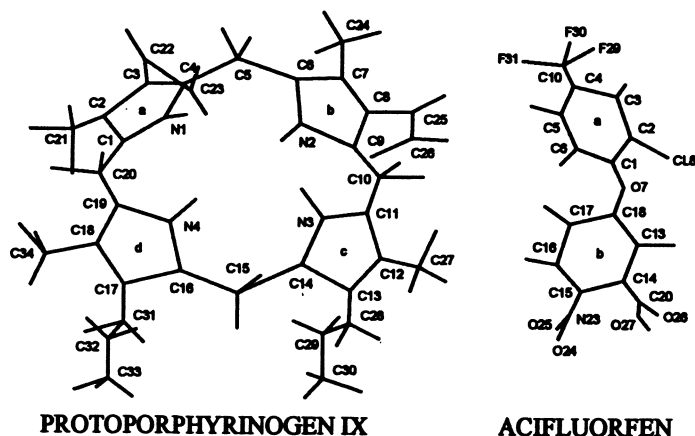


Figure 1. Three dimensional structures of Protopen and acifluorfen optimized by quantum mechanics (Reproduced with permission from reference 24. Copyright 1992 Academic Press).

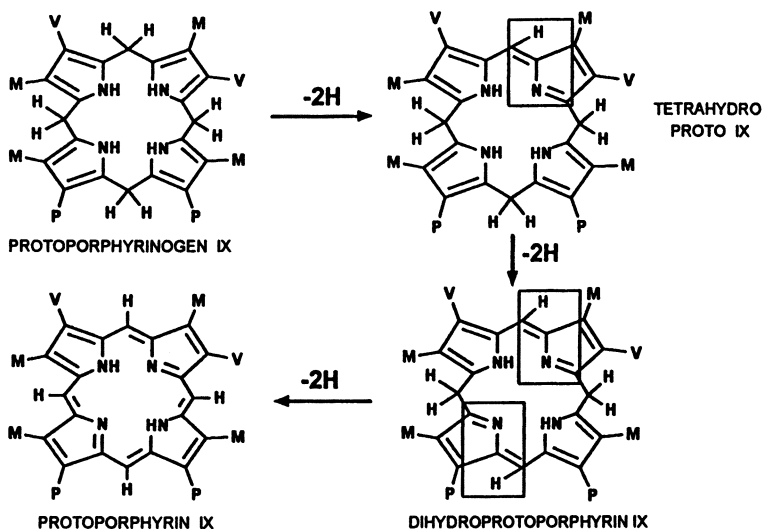


Figure 2. Proposed reaction pathway of oxidation of Protopen to Proto IX.

In other words, the enzymatic reaction appears to be a stepwise process in which various sections of the Protogen molecule are oxidized at different times, either by the same or different enzyme molecule(s). All known Protox-inhibiting herbicides contain two aromatic rings, and all of those examined for competitive inhibition of Protox activity are competitive inhibitors. All of these herbicides contain non-coplanar rings, facilitating their ability to bind to the same site on Protox as Protogen.

The hypothesis that Protox-inhibiting herbicides compete with Protogen by mimicking its one half fraction was tested by comparing the molecular properties of Protogen and several analogues of diphenyl ether and phenopylate herbicide classes (27). It was found that the three dimensional (lengths of x, y, and z coordinates) geometry and van der Waals volume (bulk parameter) of the most active compounds from both herbicide groups matched more closely with the one half structure of the Protogen molecule than the least active analogues, except for the y coordinate and van der Waals volume for diphenyl ethers (Table I).

Table I. Mean Three-Dimensional Geometries and van der Waals Volumes of One Half Fraction of Protogen and Five Most Active and Five Least Active Analogues from Diphenyl Ether and Phenopylate Classes of Protox-Inhibiting Herbicides

Substrate/Inhibitor	Length (y-axis)	Width (x-axis)	Height (z-axis)	van der Waals volume \AA^3
	----- \AA -----			
Protogen (Half fraction)	11.1	8.2	6.5	218
Diphenyl ether (Most active)	13.4	8.3	6.2	263
Phenopylate (Most active)	10.8	9.3	4.9	241
Diphenyl ether (Least active)	10.4	5.3	5.3	201
Phenopylate (Least active)	8.6	6.8	4.5	181

Recently, Kohno *et al.* (28) determined the X-ray crystal structures of two oxazolidinedione derivatives, chlorophthalim, and oxyfluorfen. These peroxidizing herbicides had about the same size and matched closely with the full length of the Protogen, suggesting that these lengths (*ca.* 11-13 Å) may represent the size of the active site on Protox.

Detailed structural comparisons between Protogen and acifluorfen revealed that both the bond and torsion angles of acifluorfen at the ether oxygen matched closely with the angles at the methylene bridge between rings B and C of Protogen structure (Figure 1) (24). These results supported the hypothesis that the bicyclic Protox-inhibiting herbicides compete with the Protogen molecule by mimicking one half of its structure (Figure 1).

Quantitative Structure-Activity Relationships (QSAR)

Our knowledge of the molecular site of most peroxidizing herbicides simplifies QSAR studies by allowing us to correlate molecular structure

with activity at the molecular site. Previous studies were done without this capability (e.g., 29-32). In these previous QSAR studies, herbicidal activity was determined at the whole plant level or by measuring effects on such general physiological parameters as photosynthetic pigment content. Whole plant QSAR studies can be confounded by different QSAR requirements for movement to the site of action than for activity at the molecular site and by differential metabolic degradation. Furthermore, the DPE herbicides are known to have several molecular sites of action (32, 33), each probably with its own QSAR.

Diphenyl Ether Analogues. In a QSAR analysis of DPE herbicides, the electronic properties (partial charge, superdelocalisability of the lowest unoccupied molecular orbital (S_{LUMO}), and dipole moment) and lipophilicity ($\log P$) properties accounted for the variation in the Protox-inhibiting activity (24). The multiple regression equation for Protox I_{50} was as shown below:

$$\log I_{50} = 11.95 - 2.84 (\log P) - 12.04 (C5) - 1.82 (S_{LUMO}) - 0.61 (\mu) \quad [1]$$
$$n = 23, F(4,18) = 28.7, s = 0.65 \quad R^2 = 0.86$$

where C5 is the charge on the C5 atom (Figure 1), μ = the dipole moment, n = the number of analogues used to generate the equation, F = ratio between regression and residual variances, s = standard deviation, and R^2 = the coefficient of determination. Figure 3 shows the plot of the observed I_{50} values versus the calculated I_{50} values using the regression equation 1.

The molecular bulk and overall electrostatic potentials were most responsible for the observed variation in the herbicidal effects. In general, the analogues with substitutions on the 3'-position (*m*-carbon) of the *p*-nitrophenyl ring were highly active as both enzyme-inhibitors and herbicides. The activity increased with an increase in surface area and electrostatic potentials of the substituent group. It appears that the active site might display considerable flexibility with respect to the length of the substituents at the 3'-position of the *p*-nitrophenyl ring. Neither the enzyme-inhibitory activity nor the initial herbicidal activity were changed by substituting a *p*-chloro for a *p*-nitro group. In the acifluorfen-methyl structure, the herbicidal activity was completely lost when the CF_3 group was moved from the *para* to the *meta* position (Figure 1). Compounds with either sulfide, sulfoxide, or sulfone bridges between the phenyl rings were herbicidally inactive.

Protox-inhibiting pyrazole phenyl ethers (phenoxyypyrazoles) are structurally similar to diphenyl ethers (34, 35). Too few analogues have been tested at the molecular level to draw significant conclusions regarding QSAR at the site of action. At the whole plant level, structure/activity studies with two isomeric sets (3- and 5-phenoxyypyrazoles) showed that the 3-phenoxyypyrazoles are orders of magnitude more active than the 5-phenoxyypyrazoles (35). Best herbicidal activity was obtained with substitutions on the phenyl ring similar to those of the *p*-nitro phenyl ring of diphenyl ether Protox inhibitors.

Substitutions of the pyrazole ring that gave best activity were chemically and geometrically similar to those that provide the best activity in the non-*p*-nitro phenyl ring of diphenyl ethers, except for substituents of the pyrazole 1-position. A methyl group at this site gave maximal activity. The single crystal X-ray bond angle of the C-O-C bond of an active 3-phenoxy pyrazole was 119°; a value between the 117° and 122° corresponding bond angles for optimized Protogen IX and acifluorfen that we obtained from conformational analysis for locating the lowest free energy conformers (24).

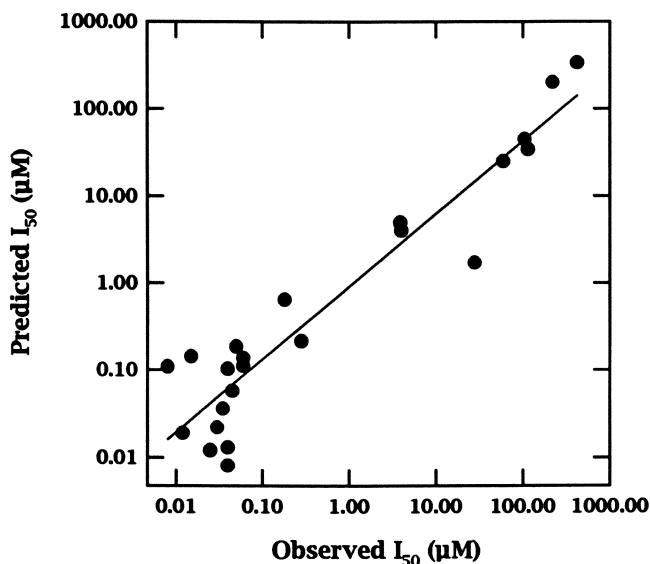


Figure 3. A plot of observed versus calculated I_{50} values of 23 diphenyl ether analogues using equation 1 (24).

Phenopylate analogues. The molecular properties of phenopylate (2,4-dichlorophenyl-1-pyrrolidinecarboxylate) and 13 of its *O*-phenyl pyrrolidino- and piperidino-carbamate analogues were correlated with their capacity to inhibit Protox, to cause Proto IX accumulation, and to inflict herbicidal injury (HI) measured by cellular leakage (10, 21). All three biological properties correlated well with the van der Waals volume (VDW_{volume}) and electrophilic superdelocalisability (S_E). Protox inhibition and Protox IX accumulation were related to $\log P$ in a non-linear fashion. The regression equations are presented below:

$$\log I_{50} = 26.29 + 1.67 (S_E) - 10.10 (\log P) + 1.33 (\log P)^2 \quad [2]$$

$$n = 13 \quad R^2 = 0.93$$

$$\log I_{50} = 28.92 - 0.037 (\text{VDW}_{\text{volume}}) - 11.56 (\log P) + 1.55 (\log P)^2 \quad [3]$$

$$n = 13 \quad R^2 = 0.94$$

$$\log \text{Proto IX} = -11.54 - 1.01 (S_F) + 3.92 (\log P) - 0.50 (\log P)^2 \quad [4]$$

$$n = 13 \quad R^2 = 0.96$$

$$\log \text{Proto IX} = -13.13 + 0.02 (\text{VDW}_{\text{volume}}) + 4.74 (\log P) - 0.63 (\log P)^2 \quad [5]$$

$$n = 13 \quad R^2 = 0.97$$

$$\text{HI} = 1331.3 - 386.9 (S_F) \quad n = 14 \quad R^2 = 0.71 \quad [6]$$

$$\text{HI} = 1302.1 + 7.7 (\text{VDW}_{\text{volume}}) \quad n = 14 \quad R^2 = 0.66 \quad [7]$$

A comparative analysis of molecular electrostatic potentials of phenopylate analogues showed a relationship between molecular electrostatic potential (MEP) distribution pattern and Protox-inhibiting potency (21). The most active analogues had negative MEP present around the molecule as two distinct fields and these regions appear to participate in the interaction with the enzyme, possibly by hydrogen bonding. The least active analogues contained negative MEP as a single field.

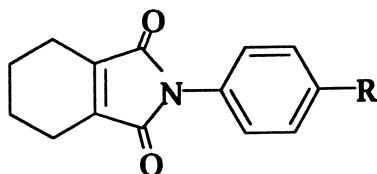
Phenyl Tetrahydrophthalimides and Related Compounds. The QSAR of phenyl tetrahydrophthalimides has been studied in both *in vitro* and *in vivo* systems (6, 7, 36, 37). Lyga *et al.* (6) examined the QSAR of phenyl tetrahydrophthalimides using tissue growth inhibition as determined by dry weight reduction (pI_{50}) and greenhouse postemergence visual injury (ED_{50}) data as biological parameters. Selected analogues with their biological activities are presented in Table II.

Table II. Biological Activities of Selected Phenyl Tetrahydrophthalimide Analogues (6)

X	Laboratory pI_{50} ($-\log (M/L)$)	Greenhouse ED_{50} (M/ha)
NO ₂	6.7	0.05
Br	6.7	0.017
Cl	6.4	0.013
I	6.3	0.05
CH ₃	5.6	0.11
OCH ₃	4.8	0.41
NH ₂	2.7	13.8
OH	3.7	>4 kg/ha
OAc	3.2	>4 kg/ha

The molecular properties such as Hansch hydrophobicity constants, para-inductive and resonance parameters, and molar refractivity effectively predicted the pI_{50} and ED_{50} . For optimal activity, the *para* position of the phenyl ring (same as *p*-nitro position in DPE) required a small, hydrophobic, electronegative group. Furthermore, a proper balance of $\log P$ and molecular size appeared necessary for good activity. The best herbicides had calculated $\log P$ values of 2.3 to 3.6 and calculated molar refractivity values of 7.3 to 8.4 (6). Nicolaus *et al.* (37) found a strong positive correlation between Protox-inhibiting potency of 11 phenyl tetrahydrophthalimides and their Hansch-Fujita lipophilicity constants (Table III).

Table III. The Inhibition of Protox (pI_{50} , $-\log$ Molar Concentration) from Corn Etioplasts by Phenyl Tetrahydrophthalimide Herbicides and Their Lipophilicity Constants (35)



Ligand R	Lipophilicity	pI_{50}
Br	0.86	7.8
Cl	0.71	7.6
OCH ₃	-0.02	7.0
SCH ₃	0.61	6.7
CF ₃	0.88	6.6
F	0.14	6.4
NO ₂	-0.28	6.4
H	0	5.8
CH ₃	0.56	5.7
NH ₂	-1.23	4.8
CONH ₂	-1.49	4.2

There are no published data directly comparing molecular similarities of phenyl tetrahydrophthalimides to Protogen IX. The molecular similarities between phenyl tetrahydrophthalimides or other Protox inhibitors without an atomic bridge between the two ring structures (*e.g.*, oxadiazon, M&B 39279) and Protogen IX are not as intuitively obvious as with those with ether and other ring linkages. The molecular lengths of a phenyl tetrahydrophthalimide (chlorophthalim) and related Protox inhibitors were measured and calculated to be about 12 Å (28), very close to the length of pyrrole ring pairs of Protogen IX (24). However, the angles between the planes of the two rings for a diphenyl ether (oxyfluorfen), chlorophthalim, and related compound varied from 68 to 137° (28). McFadden *et al.* (38) described the conformation of a 5-amino phenylpyrazol-4-yl alkyl ketone Protox inhibitor with X-ray

crystallography. The rings were found to be almost exactly perpendicular to each other. The best activity of a series of these compounds was obtained with those analogues with 2,4,6-halogenated phenyl substituents, a substitution pattern that one might expect to generate perpendicular rings. This result seems inconsistent with mimicry of Protogen IX; however, these compounds appear to bind the same site as acifluorfen.

Considerable structure activity relationship research has been done on Protox-inhibiting 1-aryl-4-substituted-1,4-dihydro-5H-tetrazol-5-ones (39) and aryltriazaolinones (40). The results are summarized in Figure 4.

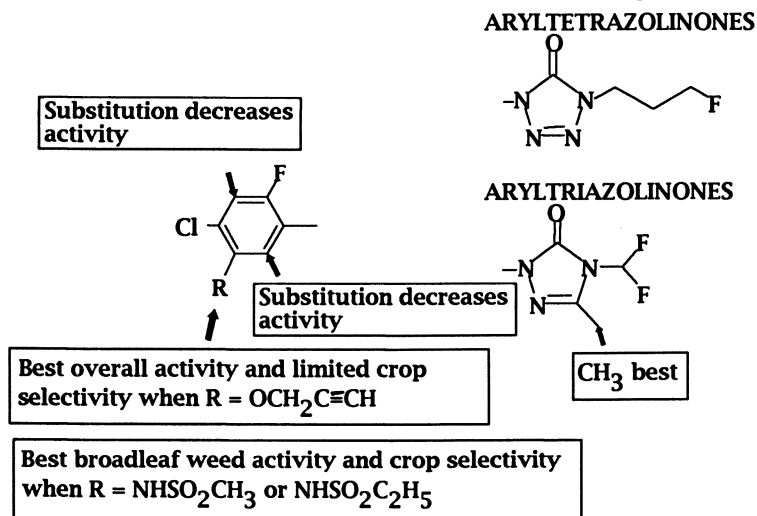


Figure 4. SAR summary of aryltetrazolinones and aryltriazaolinones (39, 40).

The substitution pattern of the phenyl ring of the analogues of these compounds is somewhat like that of the ring without the nitro group of diphenyl ethers. and the substitution pattern of the tetrazolinone and triazaolinone rings should provide a strong negative electrostatic potential at the terminus of the molecules' longitudinal axis, as the *p*-nitro group provides in diphenyl ethers.

Comparison of Protox Inhibitors from Different Chemical Classes.

We have compared various highly active Protox inhibitors belonging to 10 different chemical classes (Figure 5) for their ability to inhibit Protox, induce Proto IX accumulation, and cause herbicidal injury. Their capacity to compete with the binding of radiolabeled acifluorfen to Protox was also investigated. Preliminary results indicate that a DPE analogue (PPG-1013) was most active on Protox inhibition, followed by an analogue of pyrimidinedione (UCC-C4243) (Table IV). LS 82-556 was least active as a Protox inhibitor. Oxadiazon and AH-2.430, a pyrazole-phenyl ether, were intermediate. A somewhat similar pattern was observed with respect to accumulation of Proto IX and induction herbicidal damage. All of the

analogues reduced the binding of acifluorfen to Protox, suggesting that they share common binding sites on Protox.

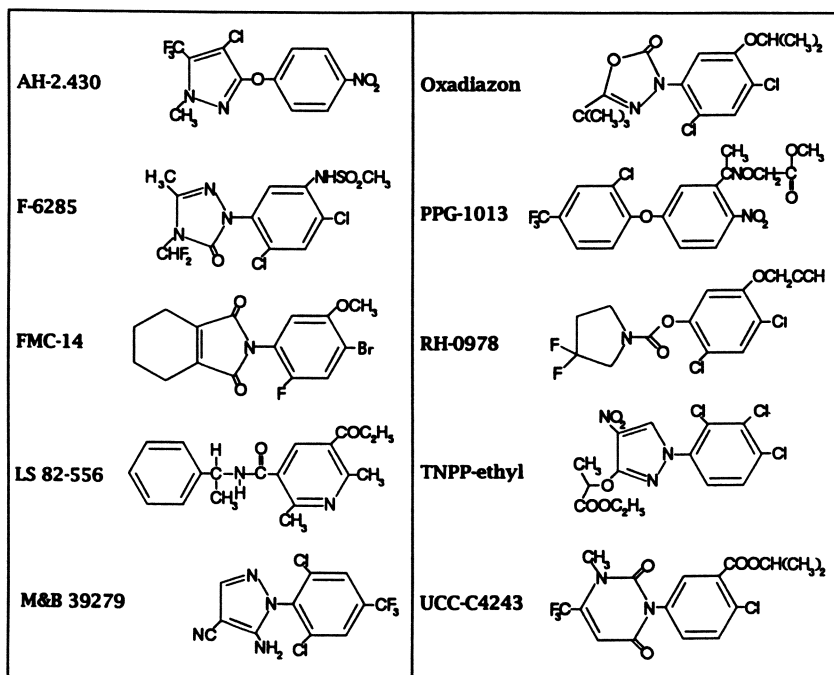


Figure 5. Structures of members of ten classes of Protox inhibitors.

Table IV. Protox inhibition and porphyrin accumulation in barley by the herbicides belonging to different chemical classes

Herbicides	Protox I_{50}^a (μM)	Proto IX ^b -(nmoles/g fresh weight)-	Protochlorophyllide ^b
Control		0.27	5.04
PPG-1013	0.021	10.08	10.66
UCC-C4243	0.030	13.36	15.89
RH-0978	0.042	9.32	7.83
FMC-14	0.11	7.56	5.54
AH-2.430	0.20	9.37	10.23
Oxadiazon	0.40	11.61	10.64
F-6285	1.1	15.95	17.88
TNPP-ethyl	3.8	7.01	10.53
M&B 39279	4.2	5.01	6.85
LS 82-556	33.2	5.44	8.02

^aDetermined with barley etioplast preparations as before (24).

^bDetermined from green barley leaf sections as before (24).

Akagi and Sakashita (41) have shown that the four compounds, oxyfluorfen, chlorophthalim, M&B-39279, and pyrimidinedione, which belong to different classes exhibited some common electronic features. All showed a low value of energy of the lowest unoccupied molecular orbital (LUMO). The phenyl rings on which the LUMO was located had non-planar groups at the *para* position and functional groups containing lone electron pair at the *ortho* position. From QSAR analyses of various classes of peroxidizing herbicides, it appears that Protox activity responds primarily to the substitutional modifications on the phenyl ring (*p*-nitrophenyl in DPEs). Furthermore, a substitution at the *meta* position on the *p*-chloro (phenopylate) or *p*-nitro (DPE) ring is essential for greater herbicidal activity. Hayashi (42) made similar conclusions regarding the *meta* position of the *p*-nitro ring in a QSAR study of 22 analogues of a DPE herbicide.

Chirality Effects. Chirality can be an important structural determinant in herbicidal activity, and this information has the potential for elucidating the nature of herbicide binding sites. Chirality in the *meta*-substitution of the *para*-nitrophenyl ring of Protox-inhibiting herbicides has been reported previously to affect activity at the molecular and whole plant levels (24, 43-45).

Protox was inhibited stereoselectively by three pairs of enantiomers belonging to the DPE and pyrazole phenyl ether herbicide classes (Figure 6) (45). The (R) enantiomers were 10- to 44-fold more active than the (S) enantiomers as Protox inhibitors. Activity at the molecular level was reflected in herbicidal activity at the tissue and whole plant levels, as well as on binding to Protox. The only molecular property found to account for differences in activity between members of chiral pairs were steric parameters.

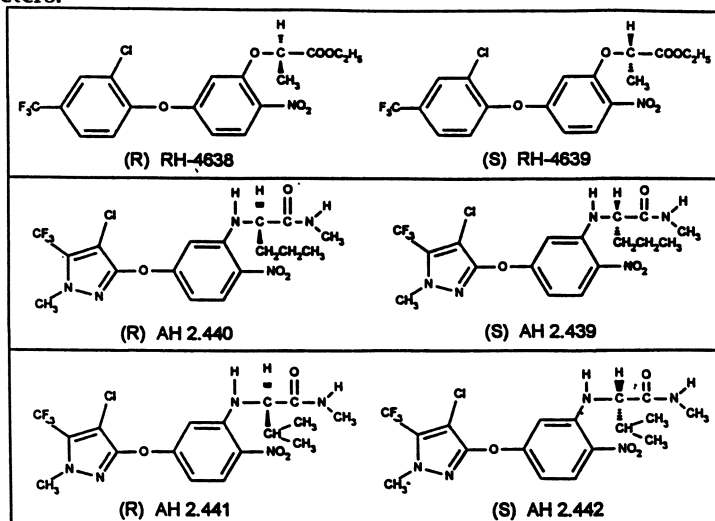


Figure 6. Structures of stereoisomers of three chiral pairs of Protox inhibitors.

Future Research

Sufficient information is now available to plan a quite sophisticated approach to the study of the QSAR of Protox-inhibiting herbicides. We know that these compounds compete with the Protogen-binding niche on the Protox molecule, suggesting that designing mimics of portions of the Protogen molecule, or of one or more of its transition states during conversion to Proto IX, could be a successful strategy for herbicide design.

Determination of the primary and tertiary structure of Protox and the elucidation of the Protogen-binding niche will facilitate QSAR approaches to herbicide design. Cloning of the Protox-encoding gene is the most likely means of determining the primary structure of Protox. Protox mutants that are resistant to Protox-inhibiting herbicides have the potential for revealing the amino acids contributing to the Protogen binding site. Two chapters in this book suggest that this information will be available in the near future (46, 47).

Literature Cited

1. Lydon, J.; Duke, S. O. *Pestic. Biochem. Physiol.* **1988**, *31*, 74-83.
2. Matringe, M.; Scalla, R. *Plant Physiol.* **1988**, *86*, 619-22.
3. Witkowski, D. A.; Halling, B. P. *Plant Physiol.* **1988**, *87*, 632-7.
4. Nandihalli, U. B.; Liebl, R. A.; Rebeiz, C. A. *Pestic. Sci.* **1991**, *31*, 9-23.
5. Matringe, M.; Scalla, R. *Pestic. Biochem. Physiol.* **1988**, *32*, 164-72.
6. Lyga, J. W.; Patera, R. M.; Theodoridis, G.; Halling, B. P.; Hotzman, F. W.; Plummer, M. J. *J. Agric. Food Chem.* **1991**, *39*, 1667-73.
7. Lyga, J. W.; Halling, B. P.; Witkowski, D. A.; Patera, R. M.; Seeley, J. A.; Plummer, M. J.; Hotzman, F. W.; *Amer. Chem. Soc. Symp. Ser.*, **1991**, *443*, 170-81.
8. Mito, N.; Sato, R.; Miyakado, M.; Oshio, H.; Tanada, S. *Pestic. Biochem. Physiol.* **1991**, *40*, 128-35.
9. Morishima, Y.; Osabe, H.; Goto, Y. *J. Pestic. Sci.* **1990**, *15*, 553-9.
10. Nandihalli, U. B.; Sherman, T. D.; Duke, M. V.; Fischer, J. D.; Musco, V. A.; Becerril, J. M.; Duke, S. O. *Pestic. Sci.* **1992**, 227-35.
11. Matringe, M.; Camadro, J. M.; Labbe, P.; Scalla, R. *FEBS Lett.* **1989**, *245*, 35-8.
12. Witkowski, D. A.; Halling, B. P. *Plant Physiol.* **1989**, *90*, 1239-42.
13. Duke, S. O.; Becerril, J. M.; Sherman, T. D.; Lydon, J.; Matsumoto, H. *Pestic. Sci.* **1990**, *30*, 367-78.
14. Duke, S. O.; Becerril, J. M.; Lydon, J.; Matsumoto, H.; Sherman, T. D. *Weed Sci.* **1991**, *39*, 465-73.
15. Scalla, R.; Matringe, M.; Camadro, J.-M.; Labbe, P. *Z. Naturforsch.* **1990**, *45c*, 503-11.
16. Jacobs, J. M.; Jacobs, N. J.; Sherman, T. D.; Duke, S. O. *Plant Physiol.* **1991**, *97*, 197-203.
17. Lee, H. J.; Duke, M. V.; Duke, S. O. *Plant Physiol.* **1993**, *102*, 881-89.
18. Draber, W. In *Rational Approaches to Structure, Activity, and Ecotoxicology of Agrochemicals*; Draber, W.; Fujita, T., Eds.; CRC Press, Boca Raton, FL, 1992, pp. 277-313.

19. Camadro, J. M.; Matringe, M.; Scalla, R.; Labbe, P. *Biochem. J.* 1991, 227, 17-21.
20. Varsano, R.; Matringe, M.; Magnin, N.; Mornet, R.; Scalla, R. *FEBS Lett.* 1990, 272, 106-8.
21. Nandihalli, U. B.; Duke, M. V.; Duke, S. O. *J. Agric. Food Chem.* 1992, 40, 1993-2000.
22. Oshio, H.; Shibata, H.; Mito, N.; Yamamoto, M.; Harris, E. H.; Gillham, N. W.; Boynton, J. E.; Sato, R. *Z. Naturforsch.*, 1991, 43c, 339-44.
23. Matringe, M.; Mornet, R.; Scalla, R. *Eur. J. Biochem.* 1992, 209, 861-68.
24. Nandihalli, U. B.; Duke, M. V.; Duke, S. O. *Pestic. Biochem. Physiol.* 1992, 43, 193-211.
25. Poulson, R.; Polglase, W. J. *Biochem. Biophys. Acta* 1973, 329, 256-63.
26. Duke, S. O.; Duke, M. V.; Lee, H. J. *Z. Naturforsch.* 1993, 48c, 317-25.
27. Nandihalli, U. B.; Duke, S. O. *Amer. Chem. Soc. Symp. Ser.* 1993, 524, 62-78.
28. Kohno, H.; Hirai, K.; Hori, M.; Sato, Y.; Böger, P.; Wakabayashi, K. *Z. Naturforsch.* 1993, 48c, 334-38.
29. Lambert, L.; Sandmann, G.; Böger, P. *Pestic. Biochem. Physiol.* 1983, 19, 309-20.
30. Ohta, H.; Suzuki, S.; Watanabe, H.; Jikihara, T.; Matsuya, K.; Wakabayashi, K. *Agric. Biol. Chem.* 1976, 40, 745-51.
31. Sato, Y.; Yokawa, H.; Katsuyama, N.; Oomikawa, R.; Wakabayashi, K. *Bull. Fac. Agric., Tamagawa Univ.* 1991, 31, 45-57.
32. Ohnishi, J.; Yukitake, K.; Eto, M. *J. Fac. Agric., Kyushu Univ.* 1993, 37, 239-46.
33. Kunert, K.-J.; Sandmann, G.; Böger, P. *Rev. Weed Sci.* 1987, 3, 35-55.
34. Sherman, T. D.; Duke, M. V.; Clark, R. D.; Sanders, E. F.; Matsumoto, H.; Duke, S. O. *Pestic. Biochem. Physiol.* 1991, 40, 236-45.
35. Moedritzer, K.; Allgood, S. G.; Charumilind, P.; Clark, R. D.; Gaede, B. J.; Kurtzweil, M. L.; Mischke, D. A.; Parlow, J. J.; Roger, M. D.; Singh, R. K.; Stikes, G. L.; Webber, R. K. *Amer. Chem. Soc. Symp. Ser.* 1992, 504, 147-60.
36. Watanabe, H.; Ohori, Y.; Sandmann, G.; Wakabayashi, K.; Boger, P. *Pestic. Biochem. Physiol.* 1992, 42, 99-109.
37. Nicolaus, B.; Sandmann, G.; Böger, P. *Z. Naturforsch.* 1993, 48c, 326-33.
38. McFadden, H. G.; Huppatz, J. L.; Couzens, M.; Kennard, C. H. L.; Lynch, D. E. *Pestic. Sci.* 1992, 36, 247-53.
39. Theodoridis, G.; Hotzman, F. W.; Scherer, L. W.; Smith, B. A.; Tymonko, J. M.; Wyle, M. J. *Amer. Chem. Soc. Symp. Ser.* 1992, 504, 122-33.
40. Theodoridis, G.; Baum, J. S.; Hotzman, F. W.; Manfredi, M. C.; Maravetz, L. L.; Lyga, J. W.; Tymonko, J. M.; Wilson, K. R.; Poss, K. M.; Wyle, M. J. *Amer. Chem. Soc. Symp. Ser.* 1992, 504, 134-46.
41. Akagi, T.; Sakashita, N. *Z. Naturforsch.* 1993, 48c, 345-49.
42. Hayashi, Y. *J. Agric. Food Chem.* 1990, 38, 839-44.
43. Camilleri, P.; Gray, A.; Weaver, K.; Bowyer, J. R. *J. Agric. Food Chem.* 1988, 37, 519-23.

44. Hallahan, B. J.; Camilleri, P.; Smith, A.; Bowyer, J. R. *Plant Physiol.* 1992, 100, 1211-6.
45. Nandihalli, U. B.; Duke, M. V.; Clark, R. D.; Ashmore, J. W.; Musco, V. A.; Duke, S. O. *Pestic. Sci.* 1994 (in press).
46. Camadro, J.-M.; Matringe, M.; Brouillet, N.; Thome, F.; Labbe, P. *Amer. Chem. Soc. Symp. Ser.* 1994 (this volume).
47. Sato, R.; Yamamoto, M.; Shibata, H.; Oshio, H.; Harris, E. H.; Gillham, N. W.; Boynton, J. E. *Amer. Chem. Soc. Symp. Ser.* 1994 (this volume).

RECEIVED April 6, 1994

Chapter 11

Porphyrin Synthesis in Liverwort Cells Induced by Peroxidizing Herbicides

Shuji Iwata¹, Motoo Sumida¹, Naoko Nakayama¹, Takaharu Tanaka¹,
Ko Wakabayashi², and Peter Böger^{3,4}

¹Institute for Biomedical Research, Research Center, Suntory Ltd., 1-1-1
Wakayamadai, Shimamoto-cho, Mishima-gun, Osaka 618, Japan

²Department of Agricultural Chemistry, Faculty of Agriculture,
Tamagawa University, Machida-shi, Tokyo 194, Japan

³Lehrstuhl für Physiologie und Biochemie der Pflanzen, Universität
Konstanz, D-78434 Konstanz, Germany

The kinetics of protoporphyrin IX (PPIX) accumulation and of a pigment fluorescing at 590 nm (590FP) in *Marchantia polymorpha* L. cells were investigated after treatment with acifluorfen methyl (AFM) at various stages of cell growth in the light or dark. A correlation between accumulation of 590FP and herbicidal damage of cultured cells was observed, but not with accumulation of PPIX. - Using cells of the exponential growth phase in the light and treated with AFM, start of 590FP accumulation coincided with the decrease of PPIX after a 15-h treatment. Loss of chlorophyll in the culture correlated with the decrease of 590FP. After pre-incubation of cells with AFM for 48 h in the dark a high level of 590FP was attained, leading rapidly to peroxidizing activity in the light with a concurrent fast decrease of 590FP. Dark pre-incubation with AFM for 12 h only yielded a high level of PPIX but little peroxidation occurred as long as 590FP had not markedly accumulated. - In cells of the stationary phase, substantial PPIX levels were found when grown with AFM present in the light for two days, and then cultivated without AFM for additional 28 days. However, 590FP did not accumulate, and neither cell disruption nor inhibition of growth occurred. - The findings indicate that PPIX may be transformed to 590FP at least under the oxidative condition induced by AFM and that 590FP causes phytotoxicity in the light.

Liverwort cells, *Marchantia polymorpha* L., can be maintained for long time under photoheterotrophic culture conditions and in a chemically defined simple medium. (1). Using this experimental system, we have confirmed that peroxidizing herbicides exert their light-dependent phytotoxic effects by inducing an accumulation of proto-

⁴Corresponding author

0097-6156/94/0559-0147\$08.00/0
© 1994 American Chemical Society

porphyrin IX (PPIX) (2). A number of laboratories have reported that accumulation of PPIX can be explained by the capacity of peroxidizing herbicides to inhibit of protoporphyrinogen oxidase, which normally catalyzes the enzymatic oxidative aromatization of protoporphyrinogen to yield PPIX (3-7). PPIX is also recognized as a potent photo-sensitizer (8, 9). Therefore, these observations have led to the hypothesis that PPIX produces activated oxygen in the light that results in a light-dependent peroxidation of membrane lipids and the following membrane disruptions are responsible for the major herbicidal effects. At the moment it is not clear whether singlet oxygen or the superoxide anion are formed (10). It may further be speculated that the accumulation of PPIX in the treated plant is caused by inhibition of the Mg-chelatase. It was found, however, that peroxidizing herbicides are 2,000 to 10,000 times more inhibitory to protoporphyrinogen oxidase than to Mg-chelatase (5). These authors explained accumulated PPIX molecules as being due to diffusion of protoporphyrinogen out of its site of synthesis which is subjected to non-enzymic oxidation. That could explain why in whole plants inhibition of protoporphyrinogen oxidase results in accumulation of PPIX since the displaced PPIX cannot be processed to heme or chlorophylls.

To get some insight into the mode of PPIX formation, we analyzed in some detail and quantitatively the change of PPIX and another fluorescent pigment in herbicide-treated cells under light and dark conditions. Previously, it was shown that accumulation of PPIX in the cultured cells is induced by herbicide treatment under the light and dark conditions, and that a new fluorescent pigment different from PPIX shows up (2). The findings presented demonstrate that apparently PPIX is converted to a derivative (590FP) under the oxidative stress induced by peroxidizing herbicides. The 590FP pigment has a fluorescence emission peak at 590 nm when excited at 410 nm. It appears, that 590FP but not PPIX shows phytotoxicity in the light resulting in peroxidative degradation of cellular constituents.

Materials and Methods

Chemicals. Acifluorfen methyl (AFM), methyl 5-[2-chloro-4-(trifluoromethyl)-phenoxy]-2-nitrobenzoate; oxyfluorfen; 2-chloro-1-(3-ethoxy-4-nitrophenoxy)-4-(trifluoromethyl)benzene, and chlorophthalim, N-(4-chlorophenyl)-3,4,5,6-tetrahydrophthalimide were produced in our laboratory. AFM was synthesized according to (11). Oxyfluorfen and chlorophthalim were prepared by the method of Wakabayashi et al. (12). PPIX was purchased from Sigma Chemical Co. (St. Louis, USA). Other chemicals were purchased from Nacalai Tesque Inc. (Kyoto, Japan).

Cell Culture and Herbicide Treatments. A cell suspension culture of *Marchantia polymorpha* L., has been routinely subcultured every two weeks using a modified medium of Murashige and Skoog (see our previous paper [2]) for more than ten years. The suspension cultures were grown in 100 ml flasks containing 40 ml of medium on a rotary shaker (Model LR-3, Iwashiyama K. Sawada Co., Tokyo) at 110 rpm/min at 25°C. The cultures were continuously illuminated from the bottom by fluorescent lamps (Matsushita FL40W, "natural white", Matsushita Electric Works,

Osaka) with an average light intensity of about 8.7 W/m^2 at the bottom of the flasks. Dark suspension cultures were grown by placing the flasks in black bags.

For experimental purposes, 6-day old cells of the exponential growth phase, called "immature cells", or 20-day old cells (of the stationary growth phase, called "mature cells") were adjusted to a cell density of $1 \text{ mg dry weight/ml}$ culture medium. Aliquots were treated with herbicides at the concentrations indicated and incubated either in dark or light at 25°C .

Extraction and Determination of Chlorophyll. Cells of 1-ml culture aliquots were collected by centrifugation (5 min at $3,000 \times g$) and the pellet was extracted 3 times with boiling 90% methanol. Absorbances at 653 nm (A_{653}) and 666 nm (A_{666}) were measured (model-210A spectrophotometer, Shimadzu, Kyoto) and the total chlorophyll concentration c ($\mu\text{g/ml}$) was calculated using the equation, $c = 23.6 \times A_{653} + 2.57 \times A_{666}$ (13). The cell dry weight was determined as reported (2).

Fluorescent Pigment Extraction and Spectrofluorometry. Extraction and estimation of the fluorescent pigments PPIX, 590FP, and Mg-PPIX were carried out according to (14). Cells of 1-ml culture aliquots collected by centrifugation were suspended in 1 ml of water and extracted with 5 ml of a mixture of cold acetone : $0.1 \text{ N NH}_4\text{OH}$ (9:1, v/v) overnight. After centrifugation at 3,000 rpm for 5 min at 5°C , the clear supernatant was collected and washed twice with same volume of hexane. The acetone fraction contained the fluorescent pigments and protochlorophyllide; their fluorescence was measured with a Hitachi F3000 fluorometer, using an excitation wavelength of 410 and emission wavelengths of 633, 590, 595 and 673 nm, respectively.

For further purification the acetone was evaporated, the sample freeze-dried and subjected to a Sephadex LH-20 column ($23 \times 350 \text{ mm}$, 50% methanol). The fractions containing PPIX and 590FP were separated by HPLC (reversed phase, Cosmocil C18, $4.6 \times 150 \text{ mm}$) with a water/acetonitrile linear gradient (40-95%) containing 0.05% trifluoroacetic acid. Details will be published elsewhere. Of course, Mg-PPIX could only be separated from PPIX under neutral to alkaline HPLC conditions.

Results

Effects of Acifluorfen methyl on Immature Cells of *Marchantia polymorpha*. In the experiment of Figure 1A cell cultures of the exponential growth phase (immature cells) were treated with the peroxidizing herbicide AFM, at 10, 1, 0.1, and $0.01 \mu\text{M}$, respectively, to determine the inhibitory effect of AFM on cell growth in the light as indicated by the chlorophyll content of the culture. Growth in the light was completely inhibited by $10 \mu\text{M}$ within 4 days and chlorophyll decreased to zero after 6 to 7 cultivation days. With this AFM concentration and treatment for 4 days, cellular disruption was complete in most cells as seen by plasmalemma and chloroplast membrane disruption, visualized by light microscopy. The impaired increase of chlorophyll per ml culture medium was positively correlated with the AFM concentrations applied. After incubation with $0.01 \mu\text{M}$ AFM chlorophyll content and membrane components of most cells appeared normal as compared to the control cells.

Figure 1B shows that AFM induced a high PPIX accumulation in the immature cells during a 1-day light incubation. The level of accumulation of PPIX was positively correlated with the light-dependent phytotoxic activity on cultured cells. A detailed analysis showed that 1 and 10 μM AFM induced a high PPIX accumulation in the immature cells during 24 h, reaching a peak and decreasing rapidly during the following 24 h. It is noteworthy that with these concentrations of AFM no significant light-dependent chlorophyll decrease was observed in cells during 24 hours after the decline of PPIX (Fig. 1A).

A New Tetrapyrrole in Herbicide-treated Immature Cells and its Physiological Effect. Figure 2A demonstrates the appearance of a new fluorescent compound in the cells (called 590FP herein) besides PPIX. This pigment could be visualized by its typical 590-nm fluorescence peak after cultivation with AFM in the light or darkness. (In Figure 4 of our previous paper (2) this 590-nm peak was assigned to 580 nm. In crude samples the fluorescence peak is between 580 and 590 nm). PPIX and 590FP are obtained by HPLC chromatography under both neutral and acidic conditions with prominent Soret absorption bands at 377 and 415 nm, respectively (Fig. 2B). The 590FP peak can be observed after the 27-min retention time in acidic medium indicating that 590FP is not a Zn- or Mg-chelate of PPIX.

The 590FP accumulation by AFM-treatment can be clearly observed in the cells before light-induced disruption of cell membrane components started (Fig. 3). Other peroxidizing herbicides like oxyfluorfen and chlorophthalim also induced formation of 590FP. As shown further in Figure 3 with 10 μM AFM present the 590FP level rose rapidly after decline of PPIX reaching a peak with subsequent bleaching effects. In the dark, 590FP increased slowly with the decline of PPIX attaining a stationary level of PPIX as demonstrated by Figure 4; cell and membrane structures appeared normal as compared to the control cell (data not shown).

When liverwort cells were pre-incubated for 12 h in the dark with AFM present a high level of PPIX was attained accompanied with little 590FP (Fig. 5A), while an extended dark incubation for 48 h led to a strong accumulation of 590FP together with a high content of PPIX (Fig. 5B). These differently pretreated cells were subsequently exposed to light or kept in the dark in order to check for both the levels of the two fluorescent pigments under these conditions (Fig. 5A, B) as well as for the peroxidative effect determined by decrease of chlorophyll per ml culture volume (Fig. 5C).

Using cells pretreated with herbicide for 12 h in the dark - having a low 590FP and high content of PPIX - the latter decreased in light and dark, while 590FP increased steadily in the dark and in the light (Fig. 5A). In the light, however, it was destroyed after having reached a peak after one day. Comparing Figure 5B with 5C (see "12-h pre-incubation") it is evident that substantial peroxidation (photo-bleaching of chlorophyll) started together with the decrease of 590FP (\circ , \bullet) and only after about a 1-day light exposure. A certain level of 590FP seems to be required before peroxidation can be initiated in these liverwort cells.

Assaying the cell culture pretreated with AFM for 48 h in the dark (Fig. 5B) which contained a high level of 590FP, an immediate rapid peroxidation was

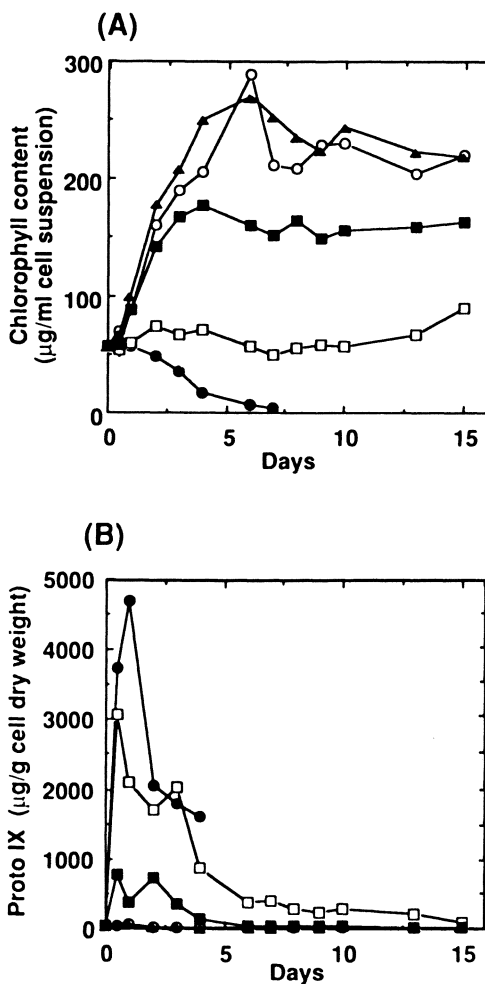


Figure 1. Effect of acifluorfen methyl (AFM) on chlorophyll and protoporphyrin-IX (PPIX) content of immature liverwort cells (*Marchantia polymorpha*). (A) Chlorophyll per ml culture suspension and (B) PPIX content in light-grown cells. Immature cells (6-day old culture) were cultured with 10 μM (●), 1 μM (□), 0.1 μM (■), 0.01 μM (▲) of AFM present and without AFM (○).

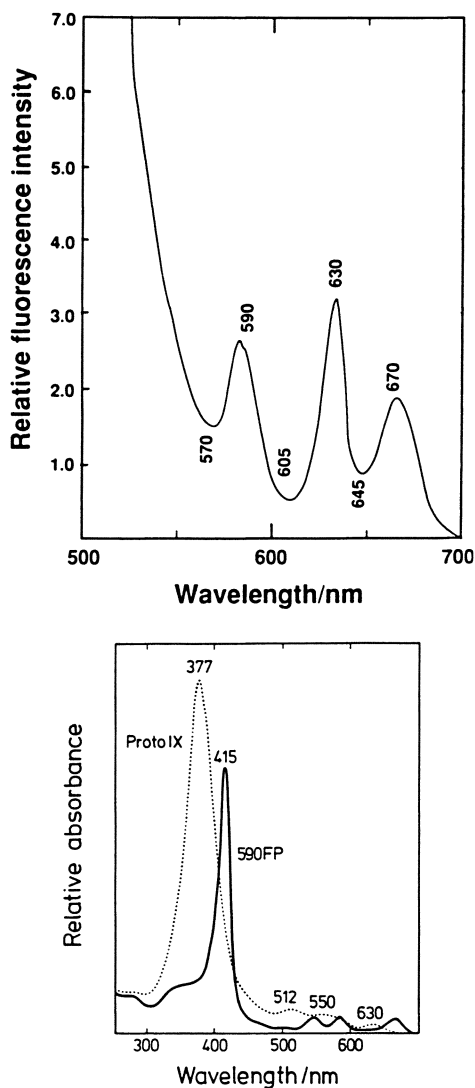


Figure 2. (A) Fluorescence emission spectrum (excited at 410 nm) of cell extracts after incubation of liverwort cells with peroxidizing herbicides. (B) Absorption spectra of purified protoporphyrin IX (PPIX, dashed line) and pigment 590FP (solid line).

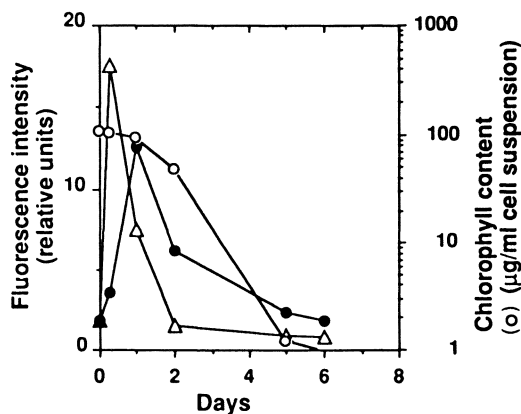


Figure 3. Effect of acifluorfen methyl on chlorophyll content, PPIX and the fluorescent pigment 590FP of an immature liverwort cell culture. Immature cells were cultured for 6 days with fresh medium including $10 \mu\text{M}$ AFM in the light. Chlorophyll (○), PPIX (△) and 590FP (●).

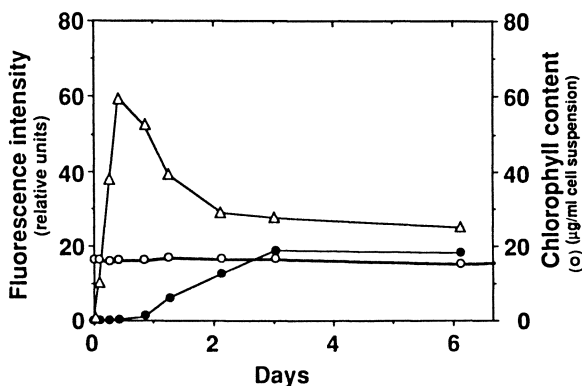


Figure 4. Effect of AFM on chlorophyll content, PPIX and 590FP of immature liverwort cells cultured in the dark. Immature cells were cultured with fresh medium including $10 \mu\text{M}$ AFM in the dark, and then the levels of chlorophyll (○), PPIX (△) and 590FP (●) were determined.

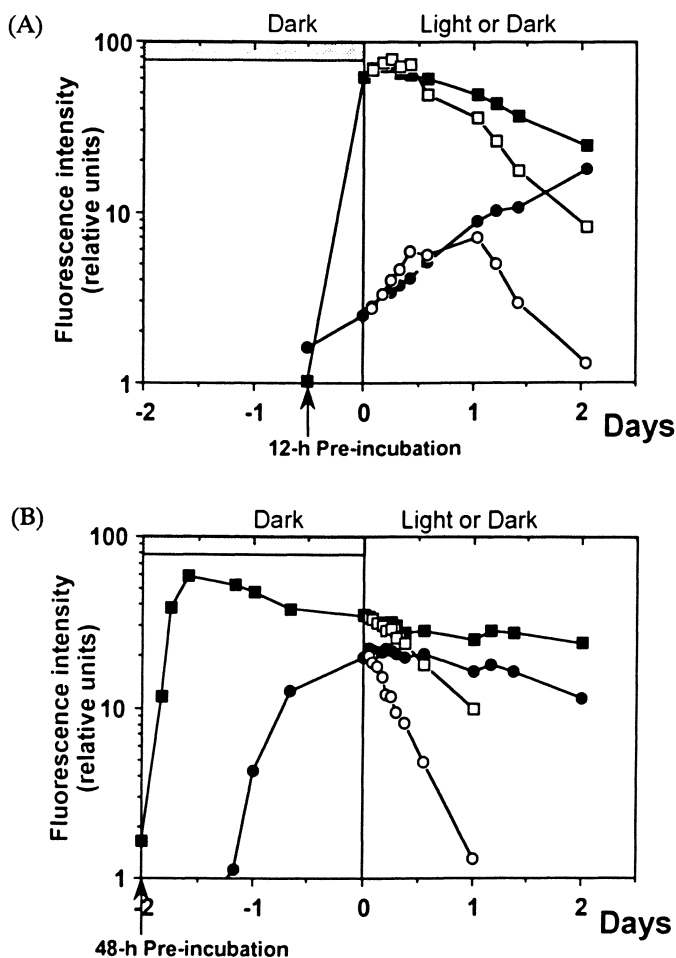


Figure 5. Effect of light on immature liverwort cells with high levels of either PPIX (\square, \blacksquare) or 590FP (\circ, \bullet). (A) Immature cells were pre-incubated with $10 \mu\text{M}$ AFM for 12 h in the dark, thereafter cultured either in the light or dark, and the levels of PPIX and 590FP content in the light (open symbols) or dark (closed symbols) were determined, respectively. (B) Immature cells were pre-incubated with $10 \mu\text{M}$ AFM for 48 h in the dark, then cultured either in the light or dark and the level of PPIX (\square, \blacksquare) and 590FP (\circ, \bullet) in the light (open symbols) or dark (closed symbols) were determined, respectively. (C) Chlorophyll decrease: immature cells were pre-incubated with $10 \mu\text{M}$ AFM for either 12 h or 48 h in the dark (according to part A and B, respectively). Then the cells were cultured in the light (open symbols) or dark (closed symbols). Proto IX and 590FP indicate the major tetrapyrrole form instrumental in the cells of these two chlorophyll-degrading expts.

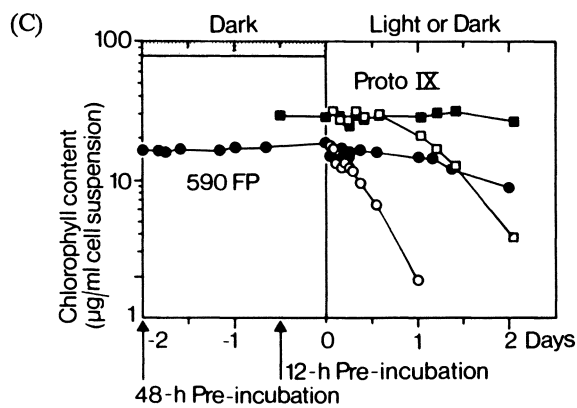


Figure 5. Continued.

observed in the light (Fig. 5C) accompanied with a fast decrease of 590FP and smaller decay of PPIX (Fig. 5B). Little change of the levels of the two fluorescent pigments was observed when the pretreated culture was kept in darkness.

Accumulation of PPIX in Mature Cells. The effect of the peroxidizing herbicides, AFM, oxyfluorfen, and chlorophthalim, on accumulation of PPIX and 590FP was measured by fully green-pigmented *mature* cells obtained by subcultivation of 20-day old cells of the stationary phase. Either 15 μM AFM, 15 μM oxyfluorfen, or 20 μM chlorophthalim, respectively, was added to the 20-day old cells and subsequently cultivated for two days in the light. After cultivation with these herbicides present, the cells were washed with 0.9% NaCl solution, and then cultivated in fresh medium without herbicide. A significant chlorophyll decrease was observed after a three-day cultivation in fresh medium (Fig. 6A). The decrease, however, reached its fullest extent after six days of cultivation, followed by a normal cell growth. The PPIX content referred to cell dry weight was found constant once a normal growth phase was established after 16 to 17 culture days. A significant accumulation and rapid decline of PPIX occurred after 18 to 23 culture days. An accumulation and decline of a 595 nm fluorescence pigment (Mg-protoporphyrin IX) was observed during this period but 590FP did not appear. Some 590FP and its decay in connection with a decrease of the chlorophyll content of the culture is seen during the first five days only. Again this experiment indicates that PPIX is not instrumental in causing chlorophyll degradation in these cells.

Discussion

To explain the mode of action of peroxidizing herbicides, a number of reports point to accumulation of protoporphyrin IX in treated plants and correlate herbicide-induced PPIX formation with typical peroxidative cell parameters like chlorophyll degradation, ethane formation or membrane leakage (12, 15, 16). We have also investigated the kinetics of accumulation of PPIX in liverwort cells treated with several peroxidizing herbicides at various stages of cell growth, and observed a correlation between accumulation of PPIX and herbicidal damage. However, this finding leaves open the question as to why PPIX accumulates in herbicide-treated cells rather than being converted to Mg-protoporphyrin and further chlorophyll precursors since these herbicides appear to have no effect on Mg-chelatase. Witkowski and Halling, and Matringe and coworkers (4, 17, 5, 18) presented an explanation. The primary effect is inhibition of protoporphyrinogen oxidase by peroxidizing herbicides resulting in build-up of protoporphyrinogen IX which oxidizes to form PPIX in the stroma and/or cytosol. The PPIX formed in this manner is either inaccessible to Mg-chelatase, or the rate of PPIX reentry into the membrane-bound pathway is significantly less than the rate of accumulation so that the concentration of the photosensitized PPIX increases until irreversible membrane damage occurs through lipid peroxidation. Jacobs et al. (19) favor the hypothesis that excess protoporphyrinogen is easily exported and enzymatically oxidized by protoporphyrinogen oxidase(s) located outside the chloroplast. They found that the plasma membrane enzyme (of barley) is

much less sensitive to inhibition by diphenyl ethers than the plastidic or mitochondrial protoporphyrinogen oxidase. More experimental proof is needed to understand the mode of action mechanisms of peroxidizing herbicides. The liverwort cell culture system can contribute to understand the mode of action of peroxidizing herbicides, because controlled growth conditions can be maintained and determination of uptake of the compounds, accumulation and excretion of metabolites can be followed easily and quantitatively. Green liverwort cells of the exponential growth phase exposed to AFM accumulate tetrapyrroles, obviously PPIX, in the light which declines after having reached a peak. It is followed by another 590 nm fluorescent pigment (590FP) clearly observed in the cells before light-induced disruption of cell membrane components started. Assuming the same fluorescence intensity of 590FP as PPIX it is evident from Figures 3 and 5 A, B that 590FP can be formed in amounts comparable to PPIX in the herbicide-treated cells. After preincubation of cells with AFM for 48 h in the dark a high level of 590FP was attained leading rapidly to peroxidizing activity in the light with a concurrent fast decrease of 590FP. Dark pre-incubation with AFM for 12 h only yielded a high level of PPIX accumulation but little peroxidation occurred as long as the amount of 590FP had not markedly increased (Fig. 5 A-C). Furthermore, substantial PPIX accumulated in mature liverwort cells of the stationary phase, after grown with AFM present in the light for two days, and then cultivated without AFM for a prolonged light incubation (Fig. 6). 590FP did not accumulate in these cells, and the PPIX present neither resulted in cell disruption nor inhibition of cell growth. The findings indicate that 590FP causes the toxicity by cell disruption in the light.

The observations led us to propose a mode of action pathway for AFM and other peroxidizing herbicides activity as shown in Figure 7. The primary action is inhibition of protoporphyrinogen oxidase with light activation of PPIX which induces an "oxidative condition" in liverwort cells. On the other hand, biosynthesis of glutathione and ascorbate in the cells is important. We have previously shown (2) that both formation of PPIX and of reduced glutathione (GSH) is induced by AFM. Presence of substantial amounts of GSH may explain why only comparatively high concentrations of peroxidizing herbicides were effective in liverwort cells. The GSH level decreases after PPIX has attained its peak. When the antioxidative system cannot cope any longer with the amount of herbicide-induced radicals, possibly oxidative processes produce a species of porphyrin not identical with PPIX. Apparently, accumulated and delocalized PPIX does not cause toxicity by cell disruption in the light, but PPIX is transformed to 590FP at least under the oxidative condition of our liverwort experiment, so that radicals or activated oxygen formed by accumulated light-activated 590FP become toxic leading to irreversible degradation of cell constituents.

Little is known about metabolic alterations by oxidative stress in plants. In chick hepatocytes AFM induces cytochrome P450 oxidase activity leading to accumulation of uroporphyrin (20). Formation of the latter can be excluded in our case (fluorescence peak at 581 nm), as well as presence of the fluorescent Zn-chelate of coproporphyrin (fluorescence peak at 580 nm (21)). Furthermore, uroporphyrin was not

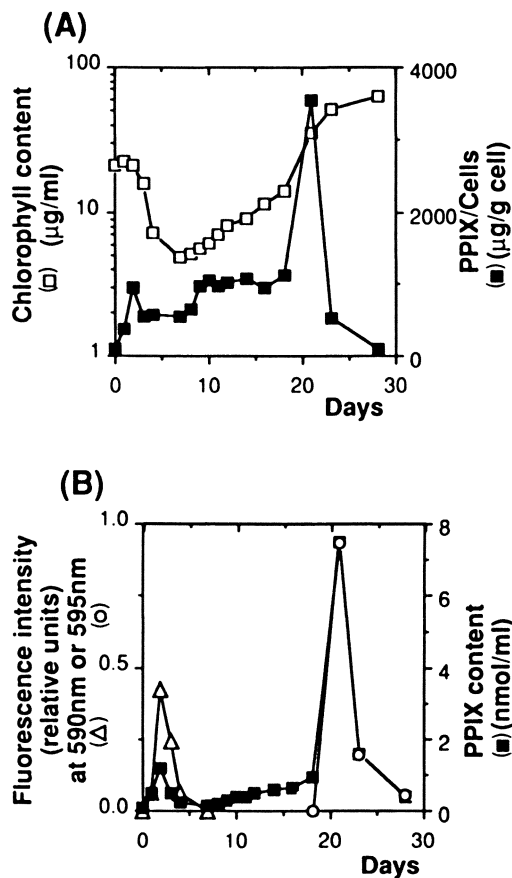


Figure 6. Effect of acifluorfen methyl on protoporphyrin-IX accumulation and growth using *mature* liverwort cells. Cells were cultured with 10 μ M AFM for two days in the light. Cells were then washed twice with sterile 0.9% NaCl solution and grown in fresh medium without AFM for 28 days. (A) Levels of chlorophyll in the culture (□) and PPIX per cell (■), after precultivation with AFM. (B) Levels of 590FP (Δ), PPIX (■), and Mg-protoporphyrin (595FP, ○) in the culture after precultivation with AFM.

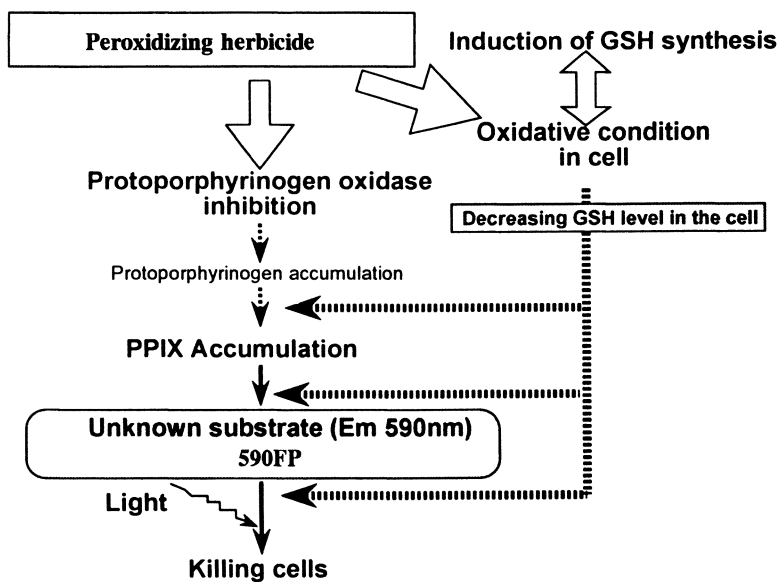


Figure 7. Mode of action of a peroxidizing herbicide.

found to accumulate in AFM-treated duckweed (6). We are working on the chemical structure of 590FP which should lead to further insight as to how it is formed.

Literature Cited

1. Ohta, Y.; Katoh, K.; Miyake, K. *Planta* **1977**, *136*, 229-232.
2. Iwata, S.; Nakayama, N.; Nakagawara, S.; Ohta, Y.; Tanaka, T.; Wakabayashi, K.; Böger, P. *Z Naturforsch.* **1992**, *47c*, 394-399.
3. Sandmann, G.; Böger, P. *Z Naturforsch.* **1988**, *43c*, 699-704.
4. Witkowski, D. A.; Halling, B. P. *Plant Physiol.* **1989**, *90*, 1239-1242.
5. Matringe, M.; Camadro, J. M.; Labbe, P., Scalla, R. *Biochem. J.* **1989**, *260*, 231-235.
6. Matsumoto, H.; Duke, S. O. *J. Agric. Food Chem.* **1990**, *38*, 2066-2071.
7. Watanabe, H.; Otori, Y.; Sandmann, G.; Wakabayashi, K.; Böger, P. *Pestic. Biochem. Physiol.* **1992**, *42*, 99-109.
8. Carlson, R. E.; Sivasothy, R.; Dolplin, D.; Bernstein, M.; Shivji, A. *Anal. Biochem.* **1984**, *140*, 360-365.
9. Rebeiz, C. A.; Montazer-Zouhoor, A.; Mayashich, J. M.; Tripathy, B. C.; Wu, S. M.; Rebeiz, C. C. in *Light Activated Pesticides*, Heitz, J. R.; Downum, K. R. Eds.; ACS Symp. Series No. 339, American Chemical Society: Washington D.C., **1987**; pp. 295-328.
10. Böger, P.; Sandmann, G. in *Chemistry of Plant Protection*, Bowers, W. S.; Ebing, W.; Martin, D.; Wegler, R., Eds.; Vol. 6, Springer Publ.: Berlin-Heidelberg, **1990**; pp. 173-216.
11. Johnson, W. O. *US Patent* **1977**, 4031, 131.
12. Wakabayashi, K.; Sandmann, G.; Ohta, H.; Böger, P. *J. Pestic. Sci.* **1988**, *13*, 461-471.
13. Iwamura, T.; Nagai, H.; Ichimura, S. *Int. Rev. ges. Hydrobiol.* **1970**, *55*, 131-147.
14. Lee, H. J.; Ball, M. D.; Rebeiz, C. A. *Plant Physiol.* **1991**, *96*, 910-915.
15. Lydon, J.; Duke, S. O. *Pestic. Biochem. Physiol.* **1988**, *31*, 74-83.
16. Becerril, J.; Duke, S. O. *Plant Physiol.* **1989**, *90*, 1175-1181.
17. Witkowski, D. A.; Halling, B. P. *Plant Physiol.* **1988**, *87*, 632-637.
18. Matringe, M.; Scalla, R. *Plant Physiol.* **1988**, *86*, 619-622.
19. Jacobs, J. M.; Jacobs, N. J.; Sherman, T. D.; Duke, S. O. *Plant Physiol.* **1991**, *97*, 197-203.
20. Jacobs, J. M.; Sinclair, P. R.; Gorman, N.; Jacobs, N. J.; Sinclair, J. F.; Bement, W. J.; Walton, H. *J. Biochem. Toxicol.* **1992**, *7*, 87-95.
21. Horiuchi, K.; Adachi, K.; Fujise, Y.; Naruse, H.; Sumimoto, K.; Kanayama, N.; Terao, T. *Clin. Chem.* **1991**, *37*, 1173-1177.

RECEIVED February 23, 1994

Chapter 12

Modulators of the Porphyrin Pathway beyond Protoporphyrinogen Oxidase

Krishna N. Reddy¹ and Constantin A. Rebeiz²

¹Southern Weed Science Laboratory, Agricultural Research Service, U.S.
Department of Agriculture, P.O. Box 350, Stoneville, MS 38776

²Laboratory of Plant Pigment Biochemistry and Photobiology, 240A Plant
and Animal Biotechnology Laboratory, University of Illinois, 1201 West
Gregory Drive, Urbana, IL 61801-4716

Pyrroles and pyridiniums (structurally related to a tetrapyrrole quadrant), and dipyridyls (structurally related to a tetrapyrrole half) were evaluated for their photodynamic herbicidal effects in cucumber (*Cucumis sativus* L.). The ability of these modulators to induce the accumulation of large amounts of porphyrins *viz.*, protoporphyrin IX (Proto), magnesium-Proto and magnesium-Proto monomethylester (MPE), and protochlorophyllide (Pchlde) in the presence or absence of exogenous δ -aminolevulinic acid (ALA) was also investigated. Substituted pyrroles exhibited moderate photodynamic herbicidal effects and caused the accumulation of Pchlde only. Pyridinium analogues induced significant amounts of MPE or Pchlde accumulation and caused photodynamic injury. Dipyridyls caused greater photodynamic herbicidal injury than either pyrroles or pyridiniums, and induced the accumulation of Proto as well.

The concept and phenomenology of photodynamic herbicides were first described by Rebeiz *et al.* (1). Since then, the scope of photodynamic herbicides also referred to as porphyric herbicides has been expanded considerably (2-5). Plants treated with porphyric herbicides accumulate large amounts of one or more porphyrin species. Porphyrins are relatively high molecular weight metabolic intermediates of the chlorophyll (Chl) and heme biosynthetic pathways. Porphyrins are photosensitizers. In the light, they photosensitize the formation of singlet oxygen ($^1\text{O}_2$). Singlet oxygen triggers the oxidative photodestruction of cellular membranes and ultimately result in tissue death. ALA-based porphyric herbicides usually consist of a 5-carbon amino acid, ALA, and one of several chemicals referred to as modulators.

0097-6156/94/0559-0161\$08.00/0

© 1994 American Chemical Society

ALA and modulators act in concert. ALA serves as a building block of porphyrins, while modulators alter quantitatively and qualitatively the pattern of porphyrin accumulation. Chemicals which act in concert with ALA and which are capable of modulating the porphyrin pathway were designated collectively as modulators by Rebeiz *et al.* (2). ALA is a natural compound present in both plants and animals. Rapid degradability of ALA and its metabolic products (porphyrins) has generated considerable interest for the development of environmentally safe ALA-based porphyric herbicides.

DPY (2,2'-dipyridyl) was the first modulator used in concert with ALA (1). ALA plus DPY treated cucumber plants kept in darkness for about 17 h accumulated large amounts of Proto, MPE, and Pchlide (1). The synergism of ALA plus DPY in forcing plants to accumulate porphyrins prompted the search and testing for additional compounds which may modulate porphyrin biosynthesis. Over one hundred and twenty modulators belonging to several chemical families in the presence of ALA have exhibited photodynamic herbicidal effects in cucumber seedlings treated with ALA (2-4). A closer examination of the chemical structures of the various modulators revealed that they were structurally related to either one half or one quadrant of a tetrapyrrole molecule. It is believed that this similarity between the chemical structures of active modulators and tetrapyrrole halves or quadrants may facilitate the binding of modulators, to, or close to the target sites of specific enzymes of the Chl and heme biosynthetic pathways. Since chemical structure plays an important role in producing biological activity, a relatively minor variation in structure can significantly alter biological activity. Detailed mode of action studies on o-phenanthroline, nicotinic acid, and nicotinamide analogues have recently been reported (5, 6). Preliminary investigations of several pyrrole, pyridinium, and dipyridyl analogues which exhibited herbicidal effects during rapid screening are described in this report.

Materials and Methods

Chemicals. Pyrrole, pyridinium, and dipyridyl analogues (Table I, Figure 1) were purchased from Aldrich Chemical Company, Milwaukee, WI. ALA was obtained from Biosynth AG International, Chicago, IL.

Plant Material. Cucumber (*Cucumis sativus* L. cv. Muncher) seeds were planted in vermiculite in cylindrical glass containers, 9-cm-diameter and 9-cm-height. Seedlings were grown in the growth chamber at 27/21 °C day/night temperatures with a 14 h photoperiod (21.1 mW cm⁻²). The plants were watered regularly with Hoagland's nutrient solution. Five-day-old seedlings (6 per container) were used in the studies.

Plant Treatment. Plant treatment consisted of a solvent control, 5 mM ALA, and 20 mM modulator with or without 5 mM ALA. The solvent system consisted either of water: methanol: Polyethylene glycol 600: Tween 80

Table I. Pyrroles, Pyridiniums, and Dipyriddyls Used in the Study

Abbreviation	Chemical name
Pyrroles:	
BAMPC	tert-butyl 4-acetyl-3,5-dimethyl-2-pyrrolicarboxylate
EDMPC	Ethyl 3,5-dimethyl-2-pyrrolicarboxylate
EMTET	3-Ethyl-2-methyl-4,5,6,7-tetrahydroindol-4-one
MBMPP	Methyl 5-(benzyloxycarbonyl)-2,4-dimethyl-3-pyrrolicpropionate
MPYCO	1-Methyl-2-pyrrolicarboxylic acid
PLACD	Pyrrole-2-carboxyaldehyde
PQUIN	Pyrrolo[1,2-a]quinoxaline
DEMPC	Diethyl 2,4-dimethylpyrrole-3,5-dicarboxylate
Pyridiniums:	
CAPCL	1-(Carboxymethyl)pyridinium chloride
DOPCL	1-Dodecylpyridinium chloride monohydrate
EHYPB	1-Ethyl-3-hydroxypyridinium bromide
246CO	2,4,6-Collidine <i>p</i> -toluenesulfonate
MVDH	Methyl viologen dichloride hydrate
D22CI	1,1'-Diethyl-2,2'-cyanine iodide
D24CI	1,1'-Diethyl-2,4'-cyanine iodide
D44CI	1,1'-Diethyl-4,4'-cyanine iodide
DMPYI	2-[4-(Dimethylamino)styryl]-1-methylpyridinium iodide
DEPYI	2-[4-(Dimethylamino)styryl]-1-ethylpyridinium iodide
BBHCL	Berberine hydrochloride hydrate
BMACR	Bis- <i>N</i> -methylacridinium nitrate
CYDPF	1-Cyano-4-(dimethylamino)pyridinium tetrafluoroborate
PPOXA	5-Phenyl-2-(4-pyridyl)oxazole
Dipyriddyls:	
DPY	2,2'-Dipyridyl
BCLCR	2,2'-Bipyridinium chlorochromate
TPY	2,2':6',2"-Terpyridine
DMDPY	4,4'-Dimethyl-2,2'-dipyridyl
DPDPY	4,4'-diphenyl-2,2'-dipyridyl

Modulator	Chemical Structure
BAMPC	
EDMPC	
EMTET	
MBMPP	
MPYCO	
PCALD	
PQUIN	
DEMPC	

Figure 1. Chemical structures of the modulators listed in Table I.

Modulator	Chemical Structure
CAPCL	
DOPCL	
EHYPB	
246CO	
MVDH	
D22CI	
D24CI	
D44CI	

Figure 1. Continued. *Continued on next page.*

Modulator	Chemical Structure
DMPYI	
DEPYI	
BBHCL	
BMACR	
CYDPF	
PPOXA	
DPY	

Figure 1. Continued.

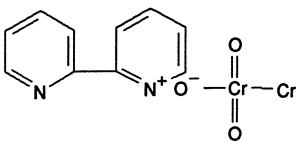
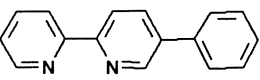
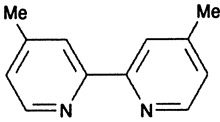
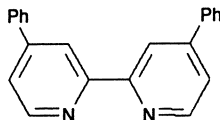
Modulator	Chemical Structure
BCLCR	
TPY	
DMDPY	
DPDPY	

Figure 1. Continued.

(90:2:7:1; v/v/v/v) or water: methanol: ethanol: Polyethylene glycol 600: Tween 80 (2:45:45:7:1; v/v/v/v/v) depending on the modulator solubility. The pH of the various solutions was adjusted to 3.5 with HCl/KOH. Seedlings were sprayed at a rate of 0.35 mL solution per container with a modified Pierce quixpray aerosol spray kit (2). Sprayed plants were wrapped in aluminum foil and placed in darkness overnight. After 15 to 16 h dark incubation, the plants were unwrapped for porphyrin determination and exposure to light.

Evaluation of Herbicidal Injury. Following postspray dark incubation, one cotyledon from each plant was excised under a dim green light and used for porphyrin determination. The plants with the remaining cotyledon were exposed to light in the growth chamber for induction of photodynamic injury. Herbicidal injury was monitored visually on a scale of 0 (no injury) to 100 (death) over a period of 10 days.

Determination of Porphyrin Content. One gram of plant tissue was homogenized in 7 mL acetone: 0.1 N NH₄OH (9:1, v/v) at 0 to 4 °C under a green safelight. The homogenate was cleared of cell debris by centrifugation at 39,000 g for 10 min at 1 °C. The pellet was resuspended in 10 mL water and protein was determined on a 0.5 mL aliquot (7) after delipidation (8). Supernatant containing the pigments was extracted first with an equal volume of hexane followed by one-third volume of hexane. An aliquot of the hexane extracted acetonetic hypophase was used for the determination of Proto, MPE, and Pchlide by spectrofluorometry at room temperature with a precision of 3 to 6% (9, 10). Recovery ranged from 86% for Proto to 94% for MPE. The amounts of monovinyl (MV) and divinyl (DV) Pchlide were determined as described by Tripathy and Rebeiz (11). Porphyrin content was expressed as nmol per 100 mg protein.

Spectrofluorometry. Fluorescence spectra were recorded on a fully corrected photon counting spectrofluorometer model SLM 8000 C, equipped with two red-sensitive, extended S₂₀ photomultipliers (EMI 9658), and interfaced with an IBM computer model 30. Porphyrins were monitored at room temperature in 3 mm cylindrical microcells at emission and excitation bandwidths of 4 nm. Low temperature spectra were recorded as described elsewhere at emission and excitation bandwidths that varied from 0.5 to 4 nm depending on signal intensity (11, 12). The photon count was integrated for 0.5 second at each 1 nm increment.

Statistical Analysis. Modulators were tested one at a time in a randomized complete block design with 3 replications. The data were subjected to analysis of variance and means were separated by Fisher's LSD at the 5% level of significance.

Results and Discussion

Treated plants were kept in darkness for 15 to 16 h before exposure to light in order to allow for porphyrin accumulation. Upon exposure to light, the photodynamic response to accumulated porphyrins was very rapid. Symptoms of photodynamic herbicidal injury became apparent within the first hour of illumination and were essentially irreversible. Initial symptoms appeared on green foliage as isolated bleaching spots which rapidly became contiguous. Bleaching was accompanied by severe loss of turgidity followed by desiccation. Within 24 h the green plant tissue turned into a brownish desiccated mass of dead tissue. When photodynamic injury was initially moderate, the plants either recovered or died, depending upon the modulator.

The relationship between photodynamic injury in various plant species treated with ALA-based or synthetic porphyrin herbicides and porphyrin accumulation is well documented (13-20). Pchlde was the only porphyrin that accumulated when plants were treated with ALA alone. However, plants treated with ALA plus modulator, accumulated several other types of porphyrins, depending upon the chemical nature of the modulator. The effect of several tetrapyrrole intermediates of the Chl biosynthetic pathway on isolated chloroplasts has been investigated by Amindari (21). Overall degradative effects were manifested by Chl *a* and *b* disappearance and the appearance of Chl degradation products such as chlorophyllides, pheophytins and pheophorbides. More specific effects on the pigment protein complexes became evident from *in organello* 77 °K fluorescence emission spectroscopy (21). DV Proto affected the photosystem (PS) II antenna Chl *a* pigment-protein complex, but had no effects on the PS I antenna pigment-protein complex. On the other hand divinyl MPE and monovinyl Pchlde, destroyed completely the PS I antenna complex and caused disorganization of the light harvesting Chl-protein *a/b* complex. Divinyl Pchlde caused the disorganization of the PS I and II antenna complexes (21).

Based on the ALA plus modulator interaction and the types of accumulated porphyrins, modulators have been classified into four groups by Rebeiz *et al.* (2, 3): a) enhancers of ALA conversion to DV Pchlde, which enhance the conversion of exogenous ALA to DV Pchlde; b) enhancers of ALA conversion to MV Pchlde, which enhance the conversion of exogenous ALA to MV Pchlde; c) inducers of porphyrin accumulation, which induce accumulation of porphyrins in the absence of exogenous ALA, and d) inhibitors of MV Pchlde accumulation, which inhibit the conversion of DV to MV Pchlde. Modulators in (a), (b), and (d), do not lead to significant levels of porphyrin accumulation in the absence of added ALA. When used with ALA they result in enhanced porphyrin accumulation and photodynamic herbicidal injury over and beyond the levels caused by ALA alone.

Pyrrrole analogues in combination with ALA exhibited moderate photodynamic herbicidal activity one day after exposure to light (Table II). After 10 days, five of the pyrrole analogues induced over 94% injury. None of

Table II. Porphyrin Production and Herbicide Injury in Cucumber Caused by Pyrrole Related Modulators^a

MOD ^b	Treatment	MV	DV	Herbicide injury	
		Pchlide	Pchlide	1 day	10 day
		-(nmol/100 mg protein)-		-----(%)-----	
BAMPC	Control	8 c	18 c	0 c	0 c
	ALA	128 a	124 b	35 b	75 b
	MOD	1 c	18 c	0 c	100 a
	ALA + MOD	25 b	175 a	48 a	100 a
EDMPC	Control	3 b	6 b	0 b	0 c
	ALA	71 a	85 a	21 a	71 b
	MOD	2 b	8 b	0 b	0 c
	ALA + MOD	64 a	96 a	35 a	94 a
EMTET	Control	2 c	7 c	0 b	0 b
	ALA	59 a	65 a	42 a	66 a
	MOD	1 c	12 c	0 b	0 b
	ALA + MOD	7 b	47 b	0 b	12 b
MBMPP	Control	3 c	6 c	0 b	0 b
	ALA	101 a	100 a	42 a	71 a
	MOD	4 c	6 c	0 b	0 b
	ALA + MOD	38 b	60 b	4 b	8 b
MPYCO	Control	4 c	8 c	0 b	0 c
	ALA	82 b	125 a	46 a	67 b
	MOD	7 c	16 c	0 b	0 c
	ALA + MOD	124 a	89 b	46 a	79 a
PCALD	Control	6 b	19 b	0 b	0 c
	ALA	94 a	94 a	35 a	58 b
	MOD	9 b	21 b	41 a	50 b
	ALA + MOD	91 a	120 a	62 a	100 a
PQUIN	Control	6 b	12 b	0 c	0 c
	ALA	65 a	89 a	44 b	62 b
	MOD	1 b	13 b	0 c	17 c
	ALA + MOD	0 b	111 a	96 a	100 a
DEMPC	Control	4 b	18 b	0 c	0 c
	ALA	96 a	87 b	17 b	62 b
	MOD	2 b	13 b	0 c	67 b
	ALA + MOD	111 a	192 a	54 a	100 a

^aMeans within a column and modulator followed by the same letter are not significantly different at the 5% level as determined by Fisher's LSD test.

^bMOD = modulator, other abbreviations are as in Table I.

the pyrroles induced porphyrin accumulation when applied alone, and Pchlide were the only porphyrins that accumulated when the pyrroles were applied with ALA (Table II). Two of the pyrroles, EMTET and MBMPP, were antagonistic toward ALA. When applied jointly with ALA, reduced MV and DV Pchlide formation was observed in comparison to ALA alone (Table II).

Pyridinium analogues, in concert with ALA exhibited moderate to severe photodynamic herbicidal injury after one day in the light (Table III). Two pyridinium analogues caused over 92% injury after one day and 10 analogues caused over 90% injury after 10 days. Various pyridiniums caused different effects. DOPCL, D22CI, D24CI, D44CI, BBHCL, and BMACR, acted as inducers of tetrapyrrole accumulation (2, 3). In the absence of added ALA, they induced the formation of Pchlide and caused significant photodynamic damage. MVDH (*i.e.* methyl viologen dichloride hydrate) is known to act via conversion to a potent free radical. It acts in the absence of tetrapyrrole accumulation (Table III). EHYPB, DMPYI, DEPYI, and PPOXA, acted as enhancers of exogenous ALA conversion to Pchlide (2, 3) and exhibited significant photodynamic herbicidal activity. On the other hand, CYDPF inhibited the conversion of exogenous ALA to tetrapyrroles and resulted in complete loss of photodynamic injury. None of the pyridiniums, caused the formation of Proto, either in the presence or absence of added ALA.

In the presence of ALA, four of the five dipyridyl analogues, exhibited over 96% injury after one day in the light, and one had no effect (Table IV). The four active dipyridyl analogues acted as both inducers and enhancers of tetrapyrrole accumulation (2, 3). Furthermore in addition to Pchlide, the accumulation of Proto and MPE was observed (Table IV).

Pyrroles, consisting of 5-membered N-heterocyclic rings and pyridiniums, consisting of 6-membered N-heterocyclic rings are structurally related to a tetrapyrrole quadrant. On the other hand, dipyridyls derived from two 6-membered N-heterocyclic rings relate structurally to a tetrapyrrole half. Several analogues of nicotinic acid, nicotinamide, picolinic acid (like pyridinium structurally related to tetrapyrrole quadrant), and o-phenanthroline (like DPY structurally related to tetrapyrrole half) groups have been reported to cause the accumulation of one or more porphyrins (5, 6). It is believed that this similarity between the chemical structures of active modulators and tetrapyrrole halves or quadrants may facilitate the binding of modulators, to, or close to the target sites of specific enzymes of the tetrapyrrole biosynthetic pathways.

Based on the pattern of porphyrin accumulation, the potential target sites for the modulators described in this report are assigned as shown below. Arrows pointing upward indicate a stimulatory effect and those pointing downward indicate an inhibitory effect at the indicated sites.

The exact mode of action of various modulators in affecting porphyrin biosynthesis is not well understood. Nandihalli and Duke (5) have conjectured that modulators may stimulate enzyme activity by acting as cofactor analogues. A fuller understanding of the mode of action of various modulators will have to await the purification of involved enzymes, the determination of their three dimensional structure, and their specific interaction with particular modulators.

Table III. Porphyrin Production and Herbicide Injury in Cucumber Caused by Pyridinium Related Modulators^a

MOD ^b	Treatment	MV		DV	Herbicide Injury	
		MPE	Pchlde	Pchlde	1 day	10 day
		---(nmol/100 mg protein)---			-----(%)-----	
CAPCL	Control	1 b	11 b	20 b	0 c	0 b
	ALA	2 a	128 a	119 a	46 a	62 a
	MOD	1 b	12 b	22 b	0 c	0 b
	ALA + MOD	2 a	141 a	116 a	33 b	69 a
DOPCL	Control	1 b	10 b	19 c	0 c	0 c
	ALA	2 b	98 a	95 a	30 b	53 b
	MOD	2 b	19 b	15 c	38 a	100 a
	ALA + MOD	4 a	78 a	38 b	45 a	100 a
EHYPB	Control	1 b	12 b	20 b	0 c	0 c
	ALA	3 a	90 a	109 a	40 b	58 b
	MOD	1 b	10 b	17 b	0 c	0 c
	ALA + MOD	2 a	100 a	126 a	54 a	85 a
246CO	Control	1 b	11 c	20 b	0 b	0 b
	ALA	2 a	98 a	101 a	40 a	57 a
	MOD	1 b	11 c	22 b	0 b	0 b
	ALA + MOD	2 a	68 b	93 a	43 a	65 a
MVDH	Control	1 b	10 c	20 b	0 c	0 c
	ALA	2 b	81 a	107 a	30 b	53 b
	MOD	1 b	2 c	14 b	100 a	100 a
	ALA + MOD	32 a	36 b	112 a	100 a	100 a
D22CI	Control	1 b	9 c	19 b	0 d	0 c
	ALA	3 a	146 a	187 a	47 b	64 b
	MOD	2 a	4 c	79 b	10 c	95 a
	ALA + MOD	3 a	44 b	245 a	92 a	100 a
D24CI	Control	1 c	7 c	14 d	0 c	0 c
	ALA	2 b	130 a	165 b	45 b	61 b
	MOD	2 b	4 c	63 c	0 c	89 a
	ALA + MOD	3 a	36 b	242 a	53 a	90 a

Table III. Continued.

MOD ^b	Treatment	MPE	MV Pchlide	DV Pchlide	Herbicide Injury	
					1 day	10 day
D44CI	Control	1 c	7 b	23 b	0 c	0 c
	ALA	2 b	133 a	121 a	45 b	62 b
	MOD	2 b	27 b	53 b	35 b	95 a
	ALA + MOD	4 a	49 b	88 a	67 a	97 a
DMPYI	Control	1 c	5 b	14 c	0 c	0 c
	ALA	2 c	83 a	110 b	39 b	70 b
	MOD	24 b	15 b	53 c	3 c	82 b
	ALA + MOD	37 a	25 b	170 a	71 a	98 a
DEPYI	Control	1 c	8 c	18 c	0 c	0 c
	ALA	2 c	104 a	109 b	43 b	63 b
	MOD	12 b	10 c	104 b	15 c	56 b
	ALA + MOD	24 a	43 b	192 a	70 a	96 a
BBHCL	Control	1 c	9 c	17 c	0 d	0 c
	ALA	2 c	106 a	108 b	42 b	64 b
	MOD	4 b	3 c	68 b	16 c	95 a
	ALA + MOD	6 a	17 b	322 a	82 a	95 a
BMACR	Control	1 c	10 b	20 c	0 c	0 c
	ALA	3 c	158 a	179 a	46 b	63 b
	MOD	37 b	22 b	31 c	68 a	100 a
	ALA + MOD	57 a	125 a	109 b	47 b	100 a
CYDPF	Control	1 b	8 c	15 c	0 b	0 b
	ALA	2 a	131 a	161 a	44 a	61 a
	MOD	1 b	5 c	22 c	0 b	0 b
	ALA + MOD	1 b	46 b	62 b	0 b	0 b
PPOXA	Control	1 c	5 b	14 c	0 c	0 d
	ALA	2 b	88 a	112 b	39 b	71 b
	MOD	2 b	0 b	56 c	4 c	33 a
	ALA + MOD	3 a	0 b	330 a	89 a	100 a

^aMeans within a column and modulator followed by the same letter are not significantly different at the 5% level as determined by Fisher's LSD test.

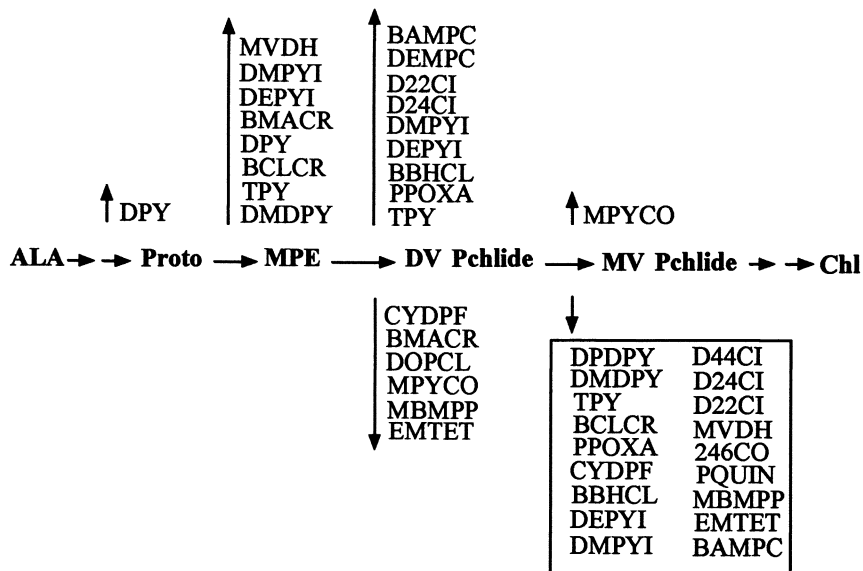
^bMOD = modulator, other abbreviations are as in Table I.

Table IV. Porphyrin Production and Herbicide Injury in Cucumber Caused by Dipyridyl Related Modulators^a

MOD ^b	Treatment	Proto	MPE ----- (nmol/100 mg protein)	MV Pchlide	DV Pchlide	Herbicide injury	
						1 day	10 day
DPY	Control	0 b	0 c	7 b	15 b	0 c	0 c
	ALA	0 b	2 c	124 a	130 a	26 b	61 b
	MOD	25 b	17 b	24 b	30 b	31 b	70 b
	ALA + MOD	96 a	56 a	107 a	145 a	100 a	100 a
BCLCR	Control	0 a	1 b	9 d	16 b	0 c	0 c
	ALA	0 a	2 b	126 a	132 a	38 b	62 b
	MOD	3 a	30 a	48 c	42 b	31 b	64 b
	ALA + MOD	0 a	41 a	84 b	134 a	96 a	97 a
TPY	Control	0 a	1 c	9 c	14 c	0 c	0 c
	ALA	0 a	2 c	127 a	132 b	37 b	62 b
	MOD	0 a	44 a	31 c	161 b	97 a	100 a
	ALA + MOD	0 a	29 b	60 b	349 a	100 a	100 a
DMDPY	Control	0 b	0 c	7 c	15 b	0 c	0 c
	ALA	0 b	1 c	102 a	140 a	36 b	45 b
	MOD	6 b	34 b	24 c	35 b	39 b	96 a
	ALA + MOD	14 a	72 a	63 b	123 a	100 a	100 a
DPDPY	Control	0 a	1 a	7 c	14 b	0 b	0 c
	ALA	0 a	1 a	102 a	130 a	36 a	44 b
	MOD	0 a	1 a	9 c	18 b	0 b	0 c
	ALA + MOD	0 a	1 a	73 b	118 a	36 a	53 a

^aMeans within a column and modulator followed by the same letter are not significantly different at the 5% level as determined by Fisher's LSD test.

^bMOD = modulator, other abbreviations are as in Table I.



Acknowledgments

K. N. Reddy thanks Drs. Stephen O. Duke and Martin A. Locke, USDA-ARS, SWSL, Stoneville, Mississippi, for their encouragement, advice, and help while preparing the manuscript.

Literature Cited

1. Rebeiz, C. A.; Montazer-Zouhoor, A.; Hopen, H. J.; Wu, S. M. *Enzyme Microbiol. Technol.* **1984**, 6, 390-403.
2. Rebeiz, C. A.; Montazer-Zouhoor, A.; Mayasich, J. M.; Tripathy, B. C.; Wu, S. M.; Rebeiz, C. C. *CRC Crit. Rev. Plant Sci.* **1988**, 6, 385-436.
3. Rebeiz, C. A.; Reddy, K. N.; Nandihalli, U. B.; Velu, J. *Photochem. Photobiol.* **1990**, 52, 1099-1117.
4. Rebeiz, C. A.; Nandihalli, U. B.; Reddy, K. N. In *Herbicides*, Baker, N. R.; Percival, M. P., Eds.; Elsevier Science Publishers, New York, **1991**, pp 173-208.
5. Nandihalli, U. B.; Duke, S. O. *Amer. Chem. Soc. Symp. Ser.* **1993**, 524, 62-78.
6. Nandihalli, U. B.; Rebeiz, C. A. *Pestic. Biochem. Physiol.* **1991**, 40, 27-46.
7. Smith, P. K.; Krohn, R. I.; Hermanson, G. T.; Mallia, A. K.; Gartner, F. H.; Rovenzano, M. D.; Fujimoto, E. K.; Goeke, N. M.; Olson, B. J.; Klenk, D. C. *Anal. Biochem.* **1985**, 150, 76-85.
8. Rebeiz, C. A.; Castlefranco, P.; Engelbrecht, A. H. *Plant Physiol.* **1965**, 40, 281-286.
9. Rebeiz, C. A.; Mattheis, J. R.; Smith, B. B.; Rebeiz, C. C.; Dayton, D. F. *Arch. Biochem. Biophys.* **1975**, 171, 549-567.

10. Belanger, F. C.; Rebeiz, C. A. *J. Biol. Chem.* **1982**, *257*, 1360-1371.
11. Tripathy, B. C.; Rebeiz, C. A. *Anal. Biochem.* **1985**, *149*, 43-61.
12. Cohen, C. E.; Rebeiz, C. A. *Plant Physiol.* **1978**, *61*, 824-829.
13. Lydon, J.; Duke, S. O. *Pestic. Biochem. Physiol.* **1988**, *31*, 74-83.
14. Becerril, J. M.; Duke, S. O. *Plant Physiol.* **1989**, *90*, 1175-1181.
15. Mayasich, J. M.; Mayasich, S. A.; Rebeiz, C. A. *Weed Sci.* **1990**, *38*, 10-15.
16. Nandihalli, U. B.; Liebl, R. A.; Rebeiz, C. A. *Pestic. Sci.* **1991**, *31*, 9-23.
17. Nandihalli, U. B.; Sherman, T. D.; Duke, M. V.; Fisher, J. D.; Musco, V. A.; Becerril, J. M.; Duke, S. O. *Pestic. Sci.* **1992**, *35*, 227-235.
18. Nandihalli, U. B.; Duke, M. V.; Duke, S. O. *Pestic Biochem. Physiol.* **1992**, *43*, 193-211.
19. Nandihalli, U. B.; Duke, M. V.; Duke, S. O. *J. Agric. Food Chem.* **1992**, *40*, 1993-2000.
20. Witkowski, D. A.; Halling, B. P. *Plant Physiol.* **1988**, *87*, 632-637.
21. Amindari, S. *Ph.D thesis*, University of Illinois, Urbana, **1992**, pp 242-247.

RECEIVED April 8, 1994

Chapter 13

Mechanisms of Plant Tolerance to Photodynamic Herbicides

T. Komives and G. Gullner

Plant Protection Institute, Hungarian Academy of Science, H-1525
Budapest, P.O.B. 102, Hungary

Phytotoxicity of photodynamic herbicides is the result of a highly complicated set of biochemical and biophysical reactions, elements of which may play significant roles in promoting or antagonizing tissue damage. Plant tolerance is primarily influenced by the ability of the plant to escape deleterious concentrations of the herbicide and the active oxygen species that are generated in treated tissues. The key role of the glutathione-conjugation system in the metabolic detoxication of nitrodiphenyl ether herbicides and the importance of the antioxidant systems to counteract photodynamic damage in several tolerant plants have been clearly established. Levels of accumulated protoporphyrin IX following protoporphyrinogen IX oxidase inhibition are as important in determining selective photodynamic toxicity as the ability of the herbicide to inhibit the enzyme.

It is now well established that photodynamic herbicides (PDHs), such as acifluorfen and related diphenyl ethers (DPEs), oxadiazon, phenylimides, phenoxy-pyrazoles, carbamoylphenols, *etc.* affect the enzymatic oxidation of protoporphyrinogen IX to protoporphyrin IX (PPIX) by protoporphyrinogen oxidase (Protox, E.C. 1.3.3. 4.). In the presence of light and molecular oxygen the accumulated PPIX generates toxic oxygen species, including singlet oxygen, superoxide, peroxide, and hydroxyl radical. These toxic oxygen species trigger peroxidation of polyunsaturated fatty acid moieties of membrane lipids resulting in plant cell death (Figure 1). (1,2).

Evaluation of the selective action of PDHs is complicated by the complexity of their phytotoxic mode of action. In addition to the "usual" physiological and biochemical mechanisms that may influence plant tolerance or susceptibility to

0097-6156/94/0559-0177\$08.00/0
© 1994 American Chemical Society

an exogenously applied toxicant, such as 1) herbicide uptake into the tissue, 2) translocation within the plant, 3) compartmentation of the herbicide or its bioactive transformation products, 4) chemical transformation of the herbicide in the plant, and 5) herbicide target site characteristics, selectivity of PDHs is also affected by factors determining a) the level(s) of photodynamic agent(s) as well as b) the activities of active oxygen detoxication systems in the plant (Figure 1).

An investigation of research findings on a) weed spectra, b) weed resistance, c) metabolism, d) target site, including molecular modelling and quantitative structure-activity relationship (QSAR) data for herbicide active ingredients as enzyme inhibitors, e) factors determining basic and maximum PPIX contents in cells, f) factors that determine the levels of active oxygen species in a given tissue, h) indications of compartmentation or an active exclusion of the herbicide from the site of action, or of its bioactive metabolite(s) and PPIX from the cell help us in explaining PDH selectivity. In this paper we shall attempt to evaluate the possible role of these factors in determining plant tolerance to PDHs. Some of the areas that are closely related to our topic, such as herbicide QSAR results, variations in crop response to Protox inhibitors, and characterization of mutants resistant to PDHs, will be discussed in detail elsewhere in this volume and will only be briefly addressed here.

PDH Phytotoxicity

Herbicide Selectivity, Weed Spectrum. Considerable variation in tolerance to PDHs exists between plant species. Traditionally, these herbicides (mostly nitrodiphenyl ethers) have been regarded as inexpensive and efficient agents to control broadleaves in a relatively small number of crops. Recently developed compounds, however, expanded the PDH chemistry to imides, pyrazoles, phenyl carbamates, *etc.*, and significantly broadened the crop and weed spectra of PDHs as well.

In mode of action studies, peas (*Pisum sativum* L.) were used as tolerant plants to fluorodifen (2-nitro-4-trifluoromethyl-4'-nitrodiphenyl ether, Figure 2) (3), soybean (*Glycine max* L.) to acifluorfen (2-chloro-4-trifluoromethyl-phenoxy-2'-nitrobenzoic acid, Figure 2) (4), mustard (*Brassica juncea* L.) and spinach (*Spinacia oleracea* L.) to acifluorfen methyl (2-chloro-4-trifluoromethyl-phenoxy-2'-nitrobenzoic acid methyl ester) (5), and rice (*Oryza sativa* L.) to oxyfluorfen (2-chloro-4-trifluoromethyl-3'-ethoxy-4'-nitrodiphenylether)(6). *Lemnospira* proved to be tolerant against acifluorfen as a sodium salt, but it was sensitive to acifluorfen as the methyl ester (7). The microalga *Bumilleriopsis* was found to be tolerant to oxyfluorfen (8). The herbicidal activity of acifluorfen (measured by cellular leakage after light exposure) varied considerably between species (5).

Differential sensitivity of barley (*Hordeum vulgare* L.) and cucumber (*Cucumis sativus* L.) to 24 DPEs led to a low correlation coefficient for the herbicidal effects and effects at the molecular level (9).

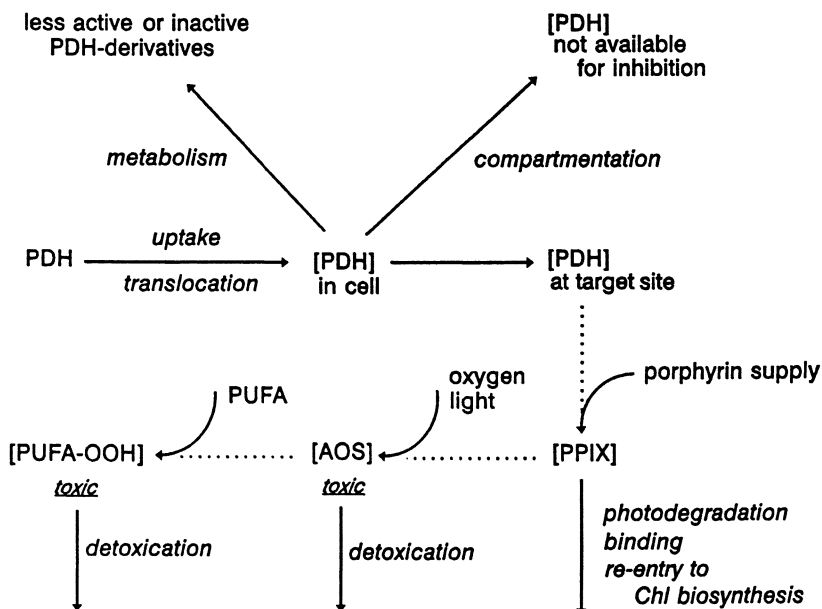
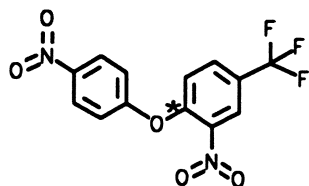
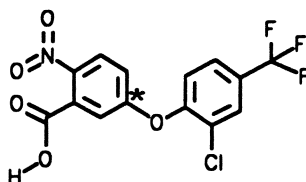


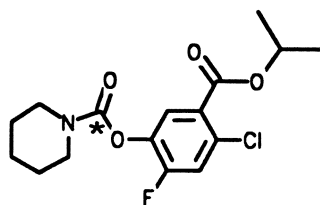
Figure 1. Phytotoxicity scheme of PDHs. Abbreviations: PDH: photo-dynamic herbicide; PPIX: protoporphyrin IX; AOS: active oxygen species; PUFA: polyunsaturated fatty acids; PUFA-OOH: polyunsaturated fatty acid hydroperoxides



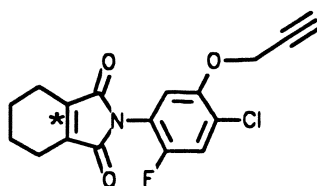
Fluorodifen



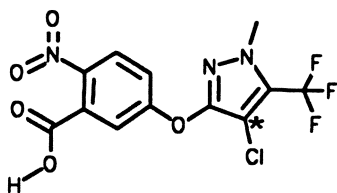
Acifluorfen



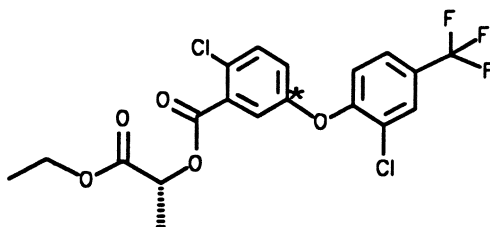
RH-1422



S-23142



AH 2.430



Etoxifen

Figure 2. Chemical structures of selected PDH herbicides that may react with glutathione in plants (the asterisk denotes the chemical bond in the herbicide molecule which is split by glutathione during the conjugation reaction).

Structure-optimization studies in the laboratory and in the field leading to the development of etoxifen (ethyl-*O*-[2-chloro-5-(2-chloro-4-trifluoromethyl)-benzoyl-*L*-lactate *S*-isomer, Figure 2) (10) showed that this compound was less toxic to peas (*Pisum sativum* L.), wheat (*Triticum aestivum* L.), and alfalfa (*Medicago sativa* L.) and better controlled mono- and dicotyledonous weeds than the racemic mixture. Interestingly, opposite results were found when the chlorine atom of the benzoyl ring was replaced with a nitro group: the racemic mixture showed higher selectivity and more efficient weed control. In case of the bromo-analogue no significant differences were observed between the biological activities of the optically pure *S*-isomer and the racemic mixture (Timar, J., Budapest Chemical Works, personal communication, 1993).

Tissue Sensitivity. Acifluorfen herbicidal efficacy is highest on very young seedlings and older established plants are only partially controlled (5,11). The buildup of PPIX in acifluorfen-treated cucumber cotyledons appears to be primarily in the palisade cells and vascular bundles with only an occasional mesophyll cell being affected. The action is tissue specific and the first membranes being disrupted are the plasmalemma and the tonoplast (12).

Herbicide Resistance. In spite of the rapid increase in occurrence of resistance of weeds to triazine and other classes of herbicides in the field, a recent review (13) reports no such case for PDHs. The possibility, however, of appearance of PDH-resistant weeds is likely, as indicated by a paper on acifluorfen-resistant eastern black nightshade (EBN, *Solanum ptycanthum* Dun.) somaclones selected *in vitro* (14).

PDH Uptake and Translocation

Uptake. Since PDHs are mostly applied as postemergent treatments, their uptake into the plant tissue may contribute to selective phytotoxic action. Susceptible common ragweed (*Ambrosia artemisiifolia* L.) and common cocklebur (*Xanthium strumarium* L.) absorbed more ¹⁴C-acifluorfen than tolerant soybean (15). Susceptible pitted morningglory (*Ipomea lacunosa* L.) absorbed 35 to 37% more acifluorfen than tolerant ivyleaf morningglory (*I. hederacea* L.) (16). Circumstances, such as low humidity and cool temperatures which reduce acifluorfen penetration enhance tolerance of velvetleaf (*Abutilon theophrasti* Medik.) (17). Tolerance of *Lemna paucicostata* against acifluorfen as a sodium salt, but not to acifluorfen as the methyl ester, is apparently due to lack of absorbance of the ionized form of the herbicide by the plant (7).

There are several examples, however, when herbicide absorbance does not play a role in determining PDH selective action. Equal amounts of acifluorfen were absorbed into the treated leaves of susceptible control and tolerant somaclones of EBN. Less than 6% of the acifluorfen was absorbed by either the susceptible control or tolerant EBN somaclones: the majority of the herbicide

remained on the leaf surface (14). The amounts of acifluorfen absorbed did not correlate with tolerance or susceptibility of *Solanum* or *Lycopersicon* genotypes (18). No clear correlation between phytotoxicity measured as herbicide-induced desiccation and ethane formation in five plant species and oxyfluorfen absorption was observed (6).

Little is known on the dependence of PDH absorption on leaf surface characteristics. Tolerant, more pubescent *Ipomea* species took up less acifluorfen than glabrous, susceptible *Ipomea* species (16). Similarly, more pubescent tomato cultivars were more tolerant to acifluorfen than tomato cultivars with fewer trichomes, but there was no relationship between their acifluorfen sensitivity and cuticle density (19). Tolerance of a cabbage (*Brassica oleracea* L.) cultivar to nitrofen (2,4-dichlorophenoxy-4'-nitrobenzene) was attributed to a thicker cuticle that decreased herbicide penetration (20).

Translocation. Differential translocation has been implicated as a PDH selectivity mechanism. Both acropetal and basipetal translocation of acifluorfen were found in the susceptible control and tolerant EBN somaclones (14). More herbicide moved from the treated leaf to the upper leaves in the susceptible plants than in tolerant ones. Lack of general injury to the leaves of tolerant somaclones by acifluorfen was also attributed to the limited translocation of the herbicide in this plant. The amount of basipetal translocation was similar between the somaclones (14). More translocation in addition to more absorption, coupled with limited metabolism of acifluorfen by susceptible common ragweed and common cocklebur may account for their susceptibility to this herbicide (15). Differential translocation of acifluorfen, however, does not explain its selectivity between tomato genotypes: translocation out of treated leaves of this plant species is minimal (15,16,18,21).

PDH Detoxication in the Plant

Metabolism. Herbicide metabolism is involved in determining selectivity between plant species and has been found to play an important role in development of herbicide-resistant weeds (13). Biotransformation reactions of xenobiotics are generally referred to as phases I and II, where phase I includes oxidation of xenobiotics and phase II deals with the conjugation of phase I products (22). In plants, the oxidative metabolism in the phase I system is usually mediated by cytochrome P-450 mixed function oxidase (23). In the phase II systems activated hydrophobic xenobiotics are converted to more hydrophilic forms *via* conjugation with sugars or the sulfhydryl group-containing tripeptide glutathione (GSH, γ -L-glutamyl-L-cysteinyl-glycine) (23).

Differences in rates of chemical transformations leading to herbicide detoxication alone are occasionally sufficiently large to explain differential PDH selectivity between crop and weed species. For example, tolerance of pea to fluorodifen (3) and of soybean to acifluorfen (4,15) is due to metabolic

detoxication of the herbicides. Two tolerant somaclones of EBN metabolized 52.6% and 28.3% of the acifluorfen within 24 h after treatment, respectively. In comparison, less than 2% of acifluorfen was metabolized in the susceptible control 1 week after treatment (14). Metabolism of acifluorfen is slower in susceptible common ragweed and common cocklebur than in tolerant soybean (15).

In other plant-PDH systems the differences in the rates of herbicide inactivation between resistant and susceptible biotypes are not large enough to account for the observed differences in tolerance. Rice plants, for example, that are tolerant to oxyfluorfen did not degrade the herbicide faster than the susceptible plant species (6). No metabolism of acifluorfen took place in one of the tolerant EBN somaclones (14) and any absorbed acifluorfen remained unmetabolized within 11 *Lycopersicon* genotypes of different sensitivity to this herbicide. In comparison, after 48 h, acifluorfen metabolites were detected in soybean control (18,24).

Different major metabolites of acifluorfen were detected in two EBN somaclones (14). Four metabolites of acifluorfen were found in ivyleaf morningglory 24 h after treatment (16), and four metabolites of acifluorfen in soybean and five in common cocklebur (15). Rapid metabolism of acifluorfen by common cocklebur and by some EBN somaclones may partially explain their tolerance to the herbicide (14,15).

Transformation Products. Although several papers have indicated that differential metabolism may be a factor in the selective action of PDHs (3,4,15,18), detailed information on the nature of herbicide metabolites and metabolic pathways in susceptible and tolerant plants are scarcely available. Results of the limited number of metabolic studies characterizing the transformation products of PDHs in plants reveal no evidence of phase I type oxidative transformations. The only indication of the possible oxygenation of a PDH molecule is related to dramatic differences in the *in vitro* and *in vivo* biological activities of a structural analog of acifluorfen methyl, in which the diphenyl ether oxygen has been replaced by a sulfur atom. This chemical was non-herbicidal, while its Prottox inhibitory activity *in vitro* was identical to that of the parent compound. This finding has been explained by rapid oxidation of the sulfide bridge, leading to inactive product(s) (9). Of the different phase II reactions that are most commonly involved in herbicide metabolism in plants, conjugation with GSH or homoglutathione (hGSH, γ -L-glutamyl-L-cysteinyl- β -alanine) in some plants is one of the most important reactions and often the rate limiting step in the detoxication of a compound.

Early studies indicated that in the tolerant pea fluorodifen reacts readily with GSH to form a conjugate (3). This conjugate was detected in excised roots, hypocotyls, leaves, and callus tissues from several plant species.

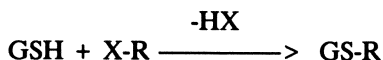
Acifluorfen was rapidly metabolized by leaf tissues of the tolerant soybean (4). Within 24 h after treatment, 90-95 % of the absorbed ^{14}C -acifluorfen was converted to soluble products. Insoluble residues were negligible. A proposed scheme for acifluorfen metabolism in tolerant soybean involves a rapid initial

attack by hGSH (in anionic hGS⁻ form) at the C1 carbon followed cleavage of the DPE bond leading to the formation of a phenolic intermediate (2-chloro-4-trifluoromethylphenol) and *S*-3-carboxy-4-nitrophenyl-hGSH. The phenolic cleavage product is rapidly conjugated as an *O*-glucoside intermediate and quantitatively acylated to form a malonyl-beta-*D*-glucoside. Further metabolism of the hGSH-derivative results in the rapid formation of *S*-3-carboxy-4-nitrophenyl-cysteine. Intermediate dipeptide metabolites were not detected and further metabolism of the cysteine-conjugate to a possible malonylcysteine conjugate was not observed (4).

In peanut (*Arachis hypogaea* L.) the GSH-conjugate of acifluorfen was identified (4). Spruce (*Picea abies* L. Karst) cell cultures metabolized fluorodifen to a GSH conjugate, further metabolism of which resulted in the formation of two novel terminal metabolites, both containing a glucose moiety and the sulfur atom of GSH (25,26).

An investigation of the chemical structures of several PDHs reveals that not only fluorodifen and acifluorfen contain sites that are susceptible to nucleophilic substitution or addition reactions by GSH or hGSH (Figure 2). Further research will clarify, if such reactions of other PDHs take place in plants, as well as their possible role in herbicide selectivity.

Catalytic Conjugation with Endogenous Thiols. It has long been shown that GSH transferases (GT, EC. 2.5. 1.18) mediate the GSH-conjugation of many herbicides according to the reaction:



X-R = herbicide, in which X⁻ is a leaving group

GS-R = GSH-herbicide conjugate

GTs represent a family of enzymes with usually broad and overlapping substrate specificities, which facilitate the above reactions of hydrophobic, electrophilic substrates (23). With the exception of two early and three recent studies using fluorodifen as substrate, evidence for the involvement of GTs in PDH conjugation is indirect and based primarily on metabolite identification. Our knowledge on plant GTs has expanded greatly in recent years. Evidence is accumulating that there are multiple forms of these enzymes. The majority of the information on plant GTs concerns enzymes which are involved in the detoxication of chlorotriazine, chloroacetanilide, and thiolcarbamate sulfoxide herbicides (23), but evidence is gathering that plant GTs have a much wider role, and may be involved in general plant stress phenomena (27,28).

The microsomal fraction of corn shoot extracts contains measurable levels of GT. It has been suggested that microsomal GTs may be effective in the detoxication of lipophilic herbicides (23). However, their possible role in determining selectivity of lipophilic PDHs remains to be determined.

The conjugation reaction between fluorodifen and GSH is catalyzed by GT.

Enzyme activity varied from one tissue to another and tissues from fluorodifen-tolerant plants (cotton [*Gossypium hirsutum* L.], corn [*Zea mays* L.], pea, soybean, and okra [*Hibiscus esculentus* L.]) generally contained higher enzyme levels than similar tissues from susceptible species (tomatoes, cucumber, and squash [*Cucurbita maxima* Duchesne]) (3). Other DPEs, such as nitrofen, bifenoxy (methyl-5-[2,4-dichlorophenoxy]-2-nitrobenzoate), and 2-amino-4'-nitro-4-trifluoromethyl diphenylether were not effective substrates for the pea epicotyl GT enzyme, but were strong inhibitors. Based on these observations the necessity of ring substitutions that cause large decrease in electron density at the nucleophilic site of the molecule for significant GT activity were emphasized (3). A recent, comparative, semiempirical quantum mechanical calculation of the electron densities at these sites of nine known substrates (23) of plant GTs and ten commercial DPEs (Komives, T. and Bordas, B., unpublished results, 1993) supported this hypothesis. The differences, however, in the electron densities at the site of nucleophilic attack of the compounds were not large enough to explain the superiority of fluorodifen as a substrate of GT as compared to other structural analogs. The necessity of an excellent leaving group, such as the chloride in chloroacetanilide herbicides underlines the importance of the ability of the phenoxy leaving group of DPEs to depart during the formation of the GSH conjugate.

The phase II conjugation system is regarded as a detoxication process of herbicides. GSH conjugates of herbicides, however, are not devoid of biological activity (23). Thus, accumulation of the resulting metabolites in cells can lead to a reduction in the detoxification activity of the phase II system. Several GSH conjugates have been found to inhibit both GTs and GSH reductase (GR, EC 1.6.4.2). The binding of the GSH conjugate of 1-chloro-2,4-dinitrobenzene to the active site of GR was demonstrated by X-ray crystallography (29). Accordingly, rates of biochemical transformations of GSH conjugates of herbicides reducing their concentration in the cytosol are of importance. In addition, an active intracellular process, mediating the transmembrane export of these GSH conjugates may also play a role. Mammalian studies showed the existence of a phase III system that is involved in the elimination of GSH conjugates from the cells (22). Since plants lack the active excretion system of mammals, it is interesting to speculate, whether a phase III type transport of GSH conjugates into the plant cell vacuole exists, and if so, whether its activity plays a role in determining herbicide selectivity.

Target Site Sensitivity to Herbicide

Recent studies provided strong evidence that Protox is the site of action of PDHs. The evidence for this comes from a number of sources (2,30-35), including inhibition studies with purified enzyme. Inhibition of Protox by DPEs, *N*-phenylimides, and other PDHs is due to reversible binding of these herbicides (31,33,34).

Structure-activity relationship studies using pyrazole phenyl ethers (36) and *O*-phenyl pyrrolidino and piperidino carbamates (37) have clearly established correlations between Protox-inhibiting and herbicidal activities of the compounds thereby explaining selective toxicity of chemicals binding to the same site of action. Further research will clarify, if differential target site sensitivity in different plants may lead to PDH species selectivity. A comparative study of the effects of acifluorfen on Protox of plastid preparations of three species with large differences in their susceptibility to this herbicide at the tissue level revealed only small differences between *in vitro* herbicide inhibition (5). The I_{50} values of some PDHs for Protox from barley (9) were higher than those from corn (30). The *ca.* tenfold difference in the I_{50} values of acifluorfen methyl in these plants was not attributed to variations between species, rather to differences in assay conditions and tissues investigated (9).

Modifications at the herbicide target site are responsible for most cases of herbicide resistance found in weed biotypes (13). To date, there are no examples for resistance to PDHs due to the presence of a tolerant form of Protox.

Concentration of PPIX in the Plant Cell

In spite of the clearly identified site of action of PDHs in plants, their ultimate herbicidal efficacy may be determined by factors other than their ability to inhibit Protox. According to time-course, dose-response, structure-activity relationship, and species-sensitivity studies, a major factor in determining phytotoxicity is the amount of PPIX accumulated in PDH-treated plant tissues (5,36,38). An increase of about 20- to 600-fold over the very low but detectable control levels of PPIX in tissues of different plants treated with the same acifluorfen concentration was found (5).

The relationship between herbicidal damage and tissue levels of PPIX is closer than that with Protox inhibition values, because PPIX accumulation reflects both the herbicide concentration at the target site and its ability to inhibit the Protox enzyme. Accordingly, there are highly efficient inhibitors of Protox that are not phytotoxic *in vivo* (9,37). On the other hand, structural analogs unable to inhibit Protox are also invariably without PDH activity (9,37). It was proposed that differential accumulation of PPIX due to porphyrin substrate limitations is the mechanism for species selectivity of acifluorfen (5). Other studies, however, found poor correlations between herbicidal effects of PDHs (acifluorfen, oxyfluorfen, and *N*-phenylimides) and PPIX synthesis (tomato genotypes, based on Chl levels), and accumulation in algae, tomato genotypes and five plant species (6,18,39).

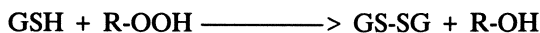
Conflicting conclusions were reached also when the importance of dark-accumulated PPIX in PDH selective phytotoxicity was investigated. While its determining role as the origin of PDH action has been shown in several species

(6,40), the involvement of light in inducing the porphyrin pathway in some other plants has also been emphasized (41,42).

In addition to its rate of formation, levels of PPIX in PDH-treated plants are determined by rates of its consumption by a) channeling back to chlorophyll biosynthesis, b) binding, and/or c) decomposition (Figure 1). Although there is little possibility for the accumulated PPIX to re-enter into the chlorophyll biosynthesis pathway, the high tolerance of rice to oxyfluorfen (6) and barley to Protox-inhibiting pyrazole phenyl ethers (36) has been attributed to re-entry of PPIX formed as a result of herbicide action into the porphyrin pathway. The presence of a protein in the thylakoid membrane that binds PPIX specifically (43) further complicates the phytotoxicity scheme. Depending on the peroxidative activity of the PPIX-protein complex, even the factors determining the concentration of this protein in the cell will influence PDH selectivity (39). PPIX is also light labile. For example, a short-term incubation of herbicide-treated algae under a moderate light intensity resulted in PPIX accumulation (39). Longer illumination, however, decreased the tetrapyrrole almost to control levels. Light has multiple roles in PDH phytotoxicity: a) it induces PPIX formation in autotrophic herbicide-treated cells, b) it sensitizes PPIX, thereby producing starter radicals for peroxidative reactions; c) it causes photooxidation of PPIX; and d) it provides precursors and energy for tetrapyrrole buildup by photosynthesis (39).

Detoxication of the Active Oxygen Species Generated by the Herbicide

Antioxidant Defense Mechanisms. Plants contain a variety of defenses to protect against the damaging effects of oxygen radicals that are produced at various electron transfer sites or *via* autooxidation reactions. It has been shown that a critical balance exists between oxyradical-generating factors and the activity of the systems that protect the cell from their harmful effects. Antioxidant defenses belong to three general classes including: 1) water-soluble reductants, *e.g.* compounds that contain thiol-groups (cysteine, GSH, *etc.*), ascorbate and catechols; 2) lipid-soluble compounds, *e.g.* α -tocopherol and β -carotene; and 3) enzymatic antioxidants, *e.g.* GSH peroxidase (GP, E.C. 6.4.11.6), ascorbate peroxidase (E.C. 1.11.1.11), catalase (E.C. 1.11. 1.6), and superoxide dismutase (E.C. 1.15. 1.1) (44). Microsomal and cytosolic GT enzymes in mammals may act as GP by catalyzing the reaction between GSH and lipophilic hydroperoxides:



thereby protecting cell membrane polyunsaturated fatty acid moieties against lipid peroxidation (23). Though not reported in plants, such an activity of plant GT enzymes may contribute to PDH selectivity.

Thus, plant tolerance to PDHs could be related to the level of protection

against photodynamic damage. Fifteen-fold higher levels of ascorbate were measured in oxyfluorfen-tolerant microalgae of *Bumilleriopsis* than in the susceptible *Scenedesmus* (8). Adding ascorbate to the reaction media increased the tolerance to paraquat in spinach and acifluorfen in alfalfa (*Medicago sativa* L.) (45). Differential tolerance among plant species to oxyfluorfen was associated with the ratio of ascorbate to tocopherol (46). Acifluorfen was shown to cause increases in GSH, ascorbate and GR levels in tolerant bean (*Vicia faba* L.) leaf tissues (47), and elevate the levels of phenolics in several plant species (48,49). Differential susceptibility of tobacco biotypes to acifluorfen and the cyclic imide herbicide S-23142 (*N*-[4-chloro-2-fluoro-5-propargyloxyphenyl]-3,4,5,6-tetrahydrophthalimide, Figure 2) was attributed to enhanced inducibility of the antioxidant system in the tolerant biotype (50,51). In contrast, reduced levels of antioxidants were found in highly sensitive cucumber cotyledon tissues during exposure to acifluorfen (52).

Paraquat-resistant tobacco (50) and *Coryza bonariensis* (L.) Cronq. biotypes (53) were also resistant to acifluorfen. However, another paraquat-resistant *C. bonariensis* biotype was susceptible to toxic oxygen species generators (54), and acifluorfen-tolerant *Lycopersicon* to paraquat (18). Levels of ascorbate in tomato biotypes, quackgrass (*Agropyron repens* L.), soybeans, and sorghum (*Sorghum bicolor* L.) were inversely related to plant DPE tolerance, indicating that high levels of ascorbate could cause increased sensitivity instead of protecting against DPEs (55). This may be due to the peroxidative action of ascorbate under certain conditions (56).

Conclusions

Our knowledge of the factors that determine selective action of PDHs has expanded greatly in recent years. It became evident that PDH phytotoxicity may be influenced by a number of factors, promoting or antagonizing tissue damage, depending on the plant-herbicide system. Tolerance seems to be strongly influenced by the plant's capacity to reduce tissue levels of PDHs and active oxygen species. In addition to herbicide uptake and translocation, important roles of phase II metabolism in the detoxication of nitrodiphenyl ether herbicides in some tolerant plants, and the antioxidant systems to counteract photodynamic damage have been confirmed. However, much is yet to be learned about these systems in plants, especially, with respect to their specificity and their mechanism of induction. Recent studies demonstrated that levels of accumulated PPIX as a result of Protox inhibition are as important in determining PDH selective phytotoxicity as the ability of the PDH to inhibit Protox. Thus, a major question needing further clarification is the nature and the relative weight of the factors that are involved regulating PPIX levels in PDH-treated plants. *In vivo* and *in vitro* studies to follow PDH-induced changes in plant biochemistry and biophysics provide us with intriguing challenges for further research.

Literature Cited

1. Matringe, M.; Scalla, R. *Plant Physiol.* **1988**, *86*, 619-622.

2. Duke, S.O.; Becerril, J.M.; Sherman, T.D.; Matsumoto, H. In *Naturally Occurring Pest Bioregulators*; Hedin, P.A., Ed.; ACS Symposium Series No. 449; American Chemical Society: Washington D.C., 1991, pp. 371-386.
3. Frear, D.S.; Swanson, H.R. *Pestic. Biochem. Physiol.* **1973**, *3*, 473-482.
4. Frear, D.S.; Swanson, H.R.; Mansager, E.R. *Pestic. Biochem. Physiol.* **1983**, *20*, 299-316.
5. Sherman, T.D.; Becerril, J.M.; Matsumoto, H.; Duke, M.V.; Jacobs, J.M.; Jacobs, N.J.; Duke, S.O. *Plant Physiol.* **1991**, *97*, 280-287.
6. Lee, J.J.; Matsumoto, H.; Ishizuka, K. *Pestic. Biochem. Physiol.* **1992**, *44*, 119-125.
7. Matsumoto, H.; Duke, S.O. *J. Agric. Food Chem.* **1990**, *38*, 2066-2071.
8. Sandmann, G.; Böger, P. In *Managing Resistance to Agrochemicals*; Green, M.B.; LeBaron, H.M.; Moberg, W.K., Eds.; ACS Symposium Series No. 421; American Chemical Society: Washington D.C., 1990, pp. 407-418.
9. Nandihalli, U.B.; Duke, M.V.; Duke, S.O. *Pestic. Biochem. Physiol.* **1992**, *43*, 193-211.
10. Bakos, J.; Eifert, G.; Bihari, F.; Nagy, M. In *Proc. British Crop Prot. Conf., Vol. 3.*, Lavenham Press: Lavenham, UK, 1991, pp. 83-86.
11. Abdallah, M.M.F.; Bayer, D.E.; Elmore, C.E. *Pestic. Biochem. Physiol.* **1992**, *42*, 271-278.
12. Lehnen, L.P., Jr.; Sherman, T.D.; Becerril, J.M.; Duke, S.O. *Pestic. Biochem. Physiol.* **1990**, *37*, 239.
13. Holt, J.S. *Weed Technol.* **1992**, *6*, 615-620.
14. Yu, C.Y.; Masiunas, J.B. *Weed Sci.* **1992**, *40*, 408-412.
15. Ritter, R.L.; Coble, H.D. *Weed Sci.* **1981**, *29*, 474-480.
16. Higgins, J.M.; Whitwell, T.; Corbin, F.T.; Carter, G.E.; Hill, H.S. *Weed Sci.* **1988**, *36*, 141-145.
17. Willingham, G.L.; Graham, L.L. *Weed Sci.* **1988**, *36*, 824-829.
18. Ricotta, J.A.; Masiunas, J.B. *Weed Sci.* **1992**, *40*, 413-417.
19. Ricotta, J.A.; Masiunas, J.B. *Weed Sci.* **1992**, *40*, 402-407.
20. Pereira, J.F.; Splittstoesser, W.E.; Hopen, H.J. *Weed Sci.* **1971**, *19*, 647-651.
21. Hook, B.J.; Glenn, S. *Weed Sci.* **1984**, *32*, 691-694.
22. Ishikawa, T. *Trends Biochem. Sci.* **1992**, *17*, 463-468.
23. Komives, T.; Dutka, F. In *Herbicide Safeners: Development, Uses and Modes of Action*; Hatzios, K.K.; Hoagland, R.E., Eds.; Academic Press: New York, 1989, pp. 129-145.
24. Stokes, J.D.; Archer, T.E.; Winterlin, W.L. *J. Environ. Sci. Health* **1990**, *B25*, 55-65.
25. Schroder, P.; Lamoureux, G.L.; Rusness, D.G.; Rennenberg, H. *Pestic. Biochem. Physiol.* **1990**, *37*, 211-218.
26. Schroder, P.; Rusness, D.G.; Lamoureux, G.L. In *Sulfur Nutrition and Sulfur Assimilation in Higher Plants*; Rennenberg, H.; Brunold, C.; De Kok, L.J.; Stulen, I., Eds.; SPB Academic Publishing bv: The Hague, 1990, pp. 245-248.
27. Dudler, R.; Hertig, C.; Rebmann, G.; Bull, J.; Mauch, F. *Mol. Plant-Microbe Interact.* **1991**, *4*, 14-18.
28. Meyer, R.C., Jr.; Goldsbrough, P.B.; Woodson, W.R. *Plant Mol. Biol.* **1991**, *17*, 277-281.

29. Bilzer, M. *Eur. J. Biochem.* **1984**, *138*, 373-378.
30. Matringe, M.; Camadro, J.-M.; Labbe, P.; Scalla, P. *Biochem. J.* **1989**, *260*, 231-235.
31. Nandihalli, U.B.; Duke, M.V.; Duke, S.O. *J. Agric. Food Chem.* **1992**, *40*, 1993-2000.
32. Jacobs, J.M.; Jacobs, N.J.; Borotz, S.E.; Guerinot, M.L. *Arch. Biochem. Biophys.* **1990**, *280*, 369-375.
33. Matringe, M.; Mornet, R.; Scalla, R. *Eur. J. Biochem.* **1992**, *209*, 861-868.
34. Varsano, R.; Matringe, M.; Magnin, N.; Mornet, R.; Scalla, R. *FEBS Lett.* **1990**, *272*, 106-108.
35. Mito, N.; Sato, R.; Miyakado, M.; Oshio, H.; Tanaka, S. *Pestic. Biochem. Physiol.* **1991**, *40*, 128-135.
36. Sherman, T.D.; Duke, M.V.; Clark, R.D.; Sanders, E.F.; Matsumoto, H.; Duke, S.O. *Pestic. Biochem. Physiol.* **1991**, *40*, 236-245.
37. Nandihalli, U.B.; Sherman, T.D.; Duke, M.V.; Fisher, J.D.; Musco, V.A.; Becerril, J.M.; Duke, S.O. *Pestic. Sci.* **1992**, *35*, 227-235.
38. Becerril, J.M.; Duke, S.O. *Plant Physiol.* **1989**, *90*, 1175-1181.
39. Watanabe, H.; Ohori, Y.; Sandmann, G.; Wakabayashi, K.; Böger, P. *Pestic. Biochem. Physiol.* **1992**, *42*, 99-109.
40. Matringe, M.; Clair, D.; Scalla, R. *Pestic. Biochem. Physiol.* **1990**, *36*, 300-307.
41. Nandihalli, U.B.; Leibl, R.A.; Rebeiz, C.A. *Pestic. Sci.* **1991**, *31*, 9-23.
42. Becerril, J.M.; Duke, M.V.; Nandihalli, U.B.; Matsumoto, H.; Duke, S.O. *Plant Physiol.* **1992**, *86*, 6-16.
43. Sato, R.; Oshio, H.; Koike, H.; Inoue, Y.; Yoshida, S.; Takahashi, N. *Plant Physiol.* **1991**, *96*, 432-437.
44. Winston, G.W. In *Stress Responses in Plants: Adaptation and Acclimation Mechanisms*; Alscher, R.G.; Cumming, J.R., Eds.; Wiley-Liss, Inc.: New York, 1990, pp. 57-86.
45. Kunert, K.J.; Dodge, A.D. In *Target Sites of Herbicide Action*; Böger, P.; Sandmann, G., Eds.; CRC Press: Boca Raton, FL, 1989, pp. 45-63.
46. Finckh, B.F.; Kunert, K.J. *J. Agric. Food Chem.* **1985**, *33*, 574-577.
47. Schmidt, A.; Kunert, K.J. *Plant Physiol.* **1986**, *82*, 700-702.
48. Komives, T.; Casida, J.E. *Pestic. Biochem. Physiol.* **1982**, *18*, 191-196.
49. Komives, T.; Casida, J.E. *J. Agric. Food Chem.* **1983**, *31*, 751-755.
50. Gullner, G.; Komives, T.; Király, L. *Z. Naturforsch.* **1991**, *46c*, 875-881.
51. Gullner, G.; Király, L.; Komives, T. In *Proceedings of the Brighton Crop Protection Conference. Weeds-1991*; Lavenham Press Ltd.: Suffolk, 1991, pp. 1111-1118.
52. Kenyon, W.H.; Duke, S.O. *Plant Physiol.* **1985**, *79*, 862-866.
53. Jansen, M.A.K.; Malan, C.; Shaaltiel, Y.; Gressel, J. *Z. Naturforsch.* **1989**, *45c*, 463-469.
54. Vaughn, K.C.; Vaughan, M.A.; Camilleri, P. *Weed Sci.* **1989**, *37*, 5-11.
55. Böger, P. *Z. Naturforsch.* **1984**, *39c*, 468-475.
56. Kunert, K.J.; Böger, P. *J. Agric. Food Chem.* **1984**, *32*, 725-728.

RECEIVED December 21, 1993

Chapter 14

Protoporphyrinogen Oxidase as the Optimal Herbicide Site in the Porphyrin Pathway

Stephen O. Duke¹, Ujjana B. Nandihalli², Hee Jae Lee¹, and
Mary V. Duke¹

¹Southern Weed Science Laboratory, Agricultural Research Service, U.S.
Department of Agriculture, P.O. Box 350, Stoneville, MS 38776

²Hazleton Laboratories, Madison, WI 53707

Herbicide discovery efforts have yielded a large number of excellent herbicides that target the porphyrin pathway. Protoporphyrinogen oxidase (Protox) is the only molecular site inhibited by the commercially available members of this herbicide class. We hypothesize that this site of action is much better for herbicidal activity than other sites of the porphyrin pathway because of the location of herbicide-susceptible Protox within the cell (the plastid envelope and the mitochondrion), the existence of a herbicide-resistant form of the enzyme in the plasma membrane (which rapidly causes accumulation of protoporphyrin IX when plastid Protox is inhibited), and two chemical features of the substrate (its relatively low lipophilicity and its non-planar macrocycle). Although enzymes of the porphyrin pathway beyond Protox can be inhibited to cause the accumulation of phytotoxic levels of porphyrins, these sites do not share the unique properties of Protox. As a result, the number of active analogues that effectively inhibit these enzymes *in vivo* is much smaller than for Protox, and the amount of herbicide needed for effective herbicidal action is relatively higher.

Thousands of herbicides have been patented that apparently exert their phytotoxicity through induced accumulation of phototoxic porphyrins (1, 2). All of those for which the molecular site of action is known are inhibitors of protoporphyrinogen oxidase (Protox), the last enzyme common to the synthesis of both chlorophyll and heme in green plants (1, 3-8). Theoretically, inhibition of any enzyme of the porphyrin pathway (Figure 1; see Figure 1 of Chapter 1 for structures of intermediates) past porphobilinogen deaminase (uroporphyrinogen III cosynthase) would result in the accumulation of a photodynamic porphyrin. Sites in the

0097-6156/94/0559-0191\$08.00/0
© 1994 American Chemical Society

chlorophyll synthesis pathway beyond Protox should be especially sensitive because each of these enzymes utilizes a photodynamic porphyrin as a substrate, whereas the two enzymes before Protox use non-photodynamic porphyrinogens as substrates. Their substrates would probably have to autooxidize to their respective porphyrins in order for their inhibition to result in accumulation of a photodynamic compound. Thus, enzymic targets between Protox and the chlorophyllase that produces chlorophyll from chlorophyllide should be potential sites for herbicide action. Why only Protox inhibitors have been successful as herbicides is the theme of this chapter.

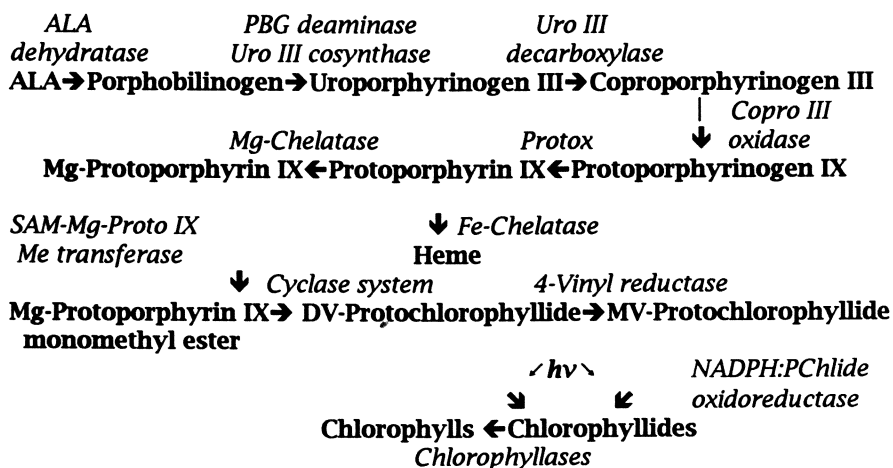


Figure 1. The porphyrin pathway in plants. Products are in bold fonts and enzymes are in italics.

Porphyrins that Accumulate

Since Matringe and Scalla (9) first reported that certain photobleaching or peroxidizing herbicides cause the accumulation of protoporphyrin IX (Proto IX), many others have confirmed their findings (Table I). The preponderance of results supports the conclusion that Proto IX is the porphyrin of primary importance accumulating in plants with inhibited Protox. Identical conclusions have been arrived at with humans (19, 20) and yeast (21) with defective Protox. In the case of humans, defective Protox results in the human genetic disease *variegate porphyria*.

There have been reports that Proto IX is not accumulated in some organisms under some circumstances when treated with herbicidal doses of Protox inhibitors (*e.g.*, 22, 23). However, these results were obtained after lengthy treatment durations, during which accumulated Proto IX could have been destroyed or re-entered the chlorophyll pathway. Kinetic evidence suggests that under non-photooxidizing conditions, Proto IX accumulates rapidly, sometimes followed by elevated levels of protochlorophyllide (PChlide), presumably due to spillover of accumulated

Proto IX into the chlorophyll pathway (24). This may not occur in all species or in all tissues of a particular species. For example, we have found elevated PChlide levels in response to Protox inhibitors (diphenyl ethers and pyrazole-phenyl ethers) only in non-green cucumber cotyledons (18, 24).

Table I. Effects of Various Peroxidizing Herbicides on Proto IX Accumulation in Various Plant Tissues

Herbicide Conc.(μ M)	Plant species	Tissue	Treatment Duration (h)	Increase X-fold	Ref.
Acifluorfen					
10	cucumber	cotyledon	2	>100	(10)
10	pigweed	leaf	20	80	(11)
10	velvetleaf	leaf	20	>100	(11)
100	morningglory	leaf	20	45	(12)
100	lambsquarters	leaf	20	>100	(12)
Acifluorfen-methyl					
1	duckweed	frond	2	>100	(13)
Chlorophthalim					
5	mung bean	leaf	20	9	(14)
Fluorodifen					
10	cucumber	cotyledon	20	>100	(11)
Oxadiazon					
10	cucumber	cotyledon	20	>100	(15)
Oxyfluorfen					
10	cucumber	cotyledon	20	>100	(12)
1	duckweed	frond	12	>100	(16)
Phenopylate					
100	barley	leaf	20	>100	(17)
Pyrazole phenyl-ethers (AH 2.430)					
100	barley	leaf	20	50	(18)

PChlide is phototransformed to chlorophyllide, which is subsequently converted to chlorophyll (Figure 1). PChlide is a feedback inhibitor of the porphyrin pathway in some, if not all, plants (25-27). Thus, elevated PChlide levels could reduce the effect of a Protox inhibitor on porphyrin accumulation. This has been shown to be the case in acifluorfen-methyl-treated duckweed (28) (Figure 2). Others have shown that light stimulates the accumulation of Proto IX in Protox-inhibited tissues (29, 30). Our results have indicated that PChlide is the photoreceptor for this effect (28).

Proto IX monomethyl ester is also elevated in tissues with inhibited Protox (31, 32). Considering the proposed intracellular distribution of Proto IX in Protox-inhibited cells (see next section), it is likely that Proto IX is methylated in the cytoplasm. Proto IX monomethyl ester is not found in untreated cells and is not a normal plant metabolite (Figure 1).

No elevation of porphyrin pathway intermediates earlier in the pathway than Proto IX has been reported. We found neither uroporphyrin nor

coproporphyrin to accumulate above control levels in either duckweed (13) or cucumber (4) treated with Protox inhibitors. Figure 3 summarizes the effects of acifluorfen-methyl on most porphyrinogen and porphyrin intermediates from uroporphyrinogen III (converted to uroporphyrin III) to PChlide (see Figure 1).

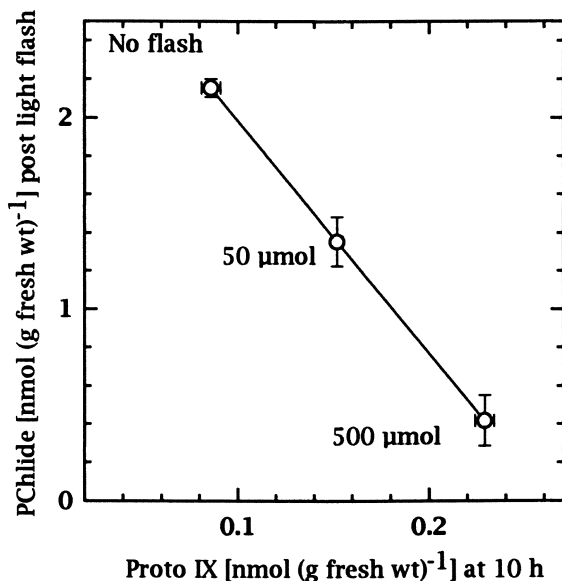


Figure 2. Relationship between PChlide present in *Lemna paucicostata* colonies after incubation in darkness for 5 h and then 5 min of exposure to 0, 50, or 500 $\mu\text{mol m}^{-2} \text{s}^{-1}$ white light and Proto IX present at the end of a 5-h subsequent period of darkness in the presence of 1 μM acifluorfen-methyl. From reference 28.

Like PChlide, heme levels are generally reduced by Protox inhibitors (28, 33). Heme is also a feedback inhibitor of porphyrin synthesis (25, 34), and exogenous heme can decrease the effects of Protox inhibitors on Proto IX accumulation and herbicidal damage (13, 28, 33). However, heme can have effects on oxidative damage through means other than modulating porphyrin levels. Our studies with duckweed indicated that the influence of PChlide levels is much more important in regulation of Proto IX accumulation in Protox-inhibited plant cells than are heme levels (28, Figure 2).

A strong positive relationship generally exists between Proto IX accumulated and later herbicidal activity of Protox inhibitors (11, 12, 16, 17, 35, 36), indicating that Proto IX is responsible for the herbicidal

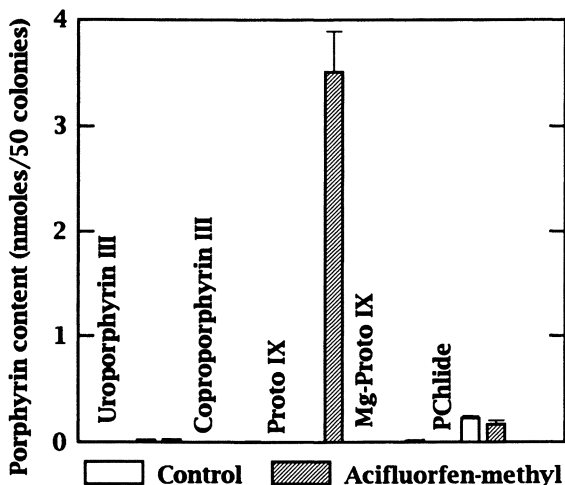


Figure 3. Effects of 1 μM acifluorfen-methyl on porphyrin content of *Lemna paucicostata* colonies after incubation in darkness for 20 h with or without herbicide in the media. Data are from reference (13).

activity. Not all studies have found positive correlations between Proto IX accumulation and herbicidal damage (*e.g.*, 22, 23). However, to find such a correlation, the measurements of Proto IX and herbicidal damage must be made at the proper times during the development of effects (*e.g.*, Figure 4). Another reason why the correlation between Proto IX accumulated and herbicidal activity may be weak is that a herbicide may have more than one mechanism of action. Diphenyl ethers and other Protox inhibitors can have a number of molecular sites of action (37, 38). A correlation between levels of porphyrins other than Proto IX and herbicidal activity of these herbicides has not been found. Thus, Proto IX clearly appears to be the primary porphyrin responsible for photodynamic damage to plant cells exposed to Protox-inhibiting herbicides.

The observation that Proto IX accumulates in plant tissues treated with these herbicides led to the speculation that Proto IX magnesium chelatase and/or ferrochelatase was inhibited by peroxidizing herbicides because these enzymes use Proto IX as a substrate (15, 39, 40). However, the ferro- and magnesium and chelatases were discovered to be only weakly inhibited by these herbicides compared to their effect on Protox (8). Although the accumulation of Proto IX in Protox-limited organisms (19-21) provided the clue that Protox could be the target site of the these herbicides, the mechanism by which these Protox inhibitors cause the accumulation of the enzyme product in plants appears to be unique.

Those Protox inhibitors that are commercially available appear to exert most or all of their effects through inhibition of Protox. Within some chemical classes of Protox inhibitors, such as phenopylate analogues and pyrazole phenyl ethers, good correlations have been found between *in vitro* Protox inhibition, Proto IX accumulation *in vivo*, and herbicidal damage (17, 18) (*e.g.*, Figure 5).

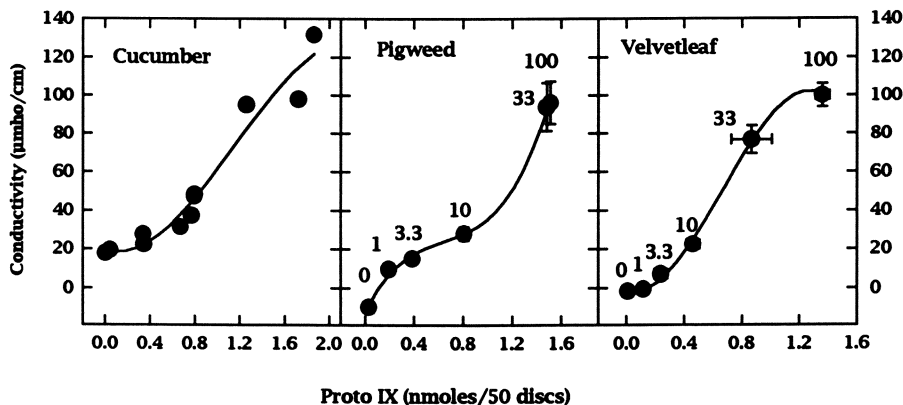


Figure 4. Relationships between cellular damage in green cucumber cotyledon discs and green leaf discs of redroot pigweed (*Amaranthus retroflexus* L.) and velvetleaf (*Abutilon theophrasti* Medic.) and Proto IX accumulation caused by acifluorfen treatment. Discs were incubated for 20 h in darkness, Proto IX sampled, and then tissues were exposed to 1 h white light and electrolyte leakage measured. Numbers beside each data point in the pigweed and velvetleaf graphs represent the concentrations (μM) of acifluorfen used. (Reproduced with permission from reference 5. Copyright 1991, Weed Science Society of America.)

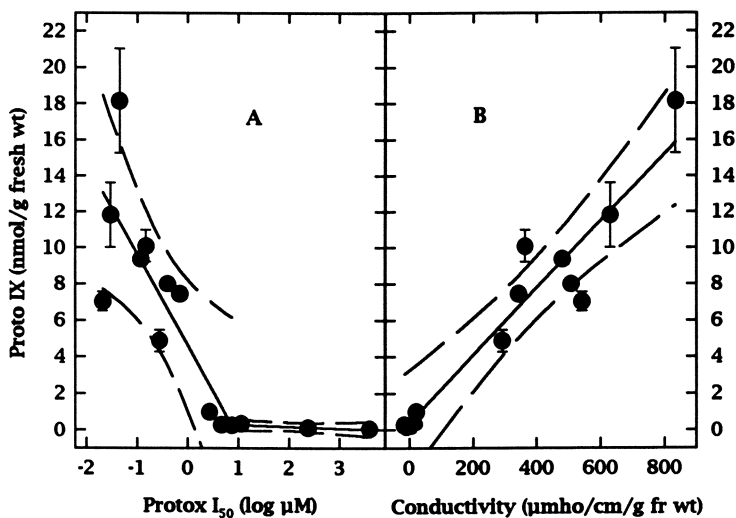


Figure 5. Relationships between effects of 14 phenopylate analogues on Proto IX accumulation in barley (after incubation for 20 h in darkness in $100 \mu\text{M}$ of each compound) and (A) Protox I_{50} values for each compound and (B) herbicidal damage, as measured by electrolyte leakage, at 4 h after exposure of the tissues to light. Dashed lines are 99% confidence limits. (Reproduced with permission from reference 17. Copyright 1992, Society of Chemical Industry).

Plant Protox Forms

Protox converts protoporphyrinogen IX (Proto IX) to Proto IX in a multistep process involving the oxidation of the secondary amines of two pyrrole rings to tertiary amines. The process requires the removal of six hydrogens from Proto IX, probably two at a time, with two reaction intermediates (see Chapter 10).

Plant cells clearly contain two Protox forms that are involved in the normal synthesis of porphyrins; the plastid and the mitochondrial forms of Protox. Both of these forms are highly sensitive to herbicidal Protox inhibitors (Table II). Recently, a plasma membrane-bound enzyme has been found that will act as a herbicide-resistant oxidizer of Proto IX to Proto IX (45, 46). The role of this enzyme is apparently important in the mode of action of Protox inhibitors, although its role in porphyrin metabolism in healthy cells is questionable. There is evidence that Proto IX for extraplastidic, cytoplasmic synthesis of Proto IX may be synthesized by the plastid (47, 48).

Table II. Effects of Various Protox Inhibitors on Protox from Different Sources

Protox source	Protox inhibitor	I_{50} (μM)	Ref.
Barley etioplast	acifluorfen	2.5-4	(12, 41)
	acifluorfen-methyl	0.04	(41)
	AH 2.430	0.2	(18)
	bifenox	0.03	(41)
	fomesafen	0.28	(41)
	oxyfluorfen	0.025	(41)
	phenopylate	2.7	(17)
Cucumber etioplast	acifluorfen	4.0	(12)
	AH 2.420	0.3	(18)
Maize etioplast	acifluorfen	0.5	(42)
	acifluorfen-methyl	0.005	(8, 42)
	oxadiazon	0.012	(43)
Maize mitochondria	acifluorfen	0.5	(42)
	acifluorfen-methyl	0.006	(8)
	S-23121	0.001	(44)
Morningglory etioplast	acifluorfen	1.0	(12)
Mustard etioplast	acifluorfen	1.0	(12)
Potato mitochondria	acifluorfen	0.05	(42)
	acifluorfen-methyl	0.0004	(8)
Mouse mitochondria	acifluorfen-methyl	0.002	(8)
	oxadiazon	0.3	(43)

Plastid Protox Properties. Plastids can be non-green (etioplasts, proplastids, leucoplasts, or amyloplasts) or highly pigmented (chloroplasts or chromoplasts), depending on the tissues from which they are isolated (49). The plastid envelope is highly enriched in Protox (50). With crude organelle preparations, Protox can only be measured directly by

spectrofluorometric detection of Proto IX product with non-pigmented plastids. Etioplasts are the most easily obtained non-pigmented plastids and, thus, have been the most common source of the enzyme in herbicide studies. Although there is an apparent anomaly in the accumulation of Proto IX in plant cells treated with Protox inhibitors (accumulation of the product of an inhibited enzyme), in cell-free assays Protox inhibitors prevent the production of Proto IX from Protogen IX, as expected. The *in vivo* anomaly will be explained below.

In good etioplast preparations with relatively little contamination with plasma membrane, inhibition of Protox by herbicidal inhibitors in the presence of dithiothreitol (*e.g.*, 46, 51) is almost complete. The presence of this reductant in the reaction mixture enhances the effects of the herbicides. This may be due in part to inhibition of the herbicide-resistant plasma membrane-bound Protox that may contaminate the etioplast preparation (see below).

Inhibition of plastid Protox is competitive with respect to Protogen IX (42, 52). Furthermore, Protox inhibitors of all chemical structures tested so far compete other radiolabeled Protox inhibitors off of the binding site (44, 53-55). Thus, these inhibitors appear to all be binding the same molecular site. There appears to be a positive correlation between this competitive ability and I_{50} values for inhibition of Protox (Figure 6).

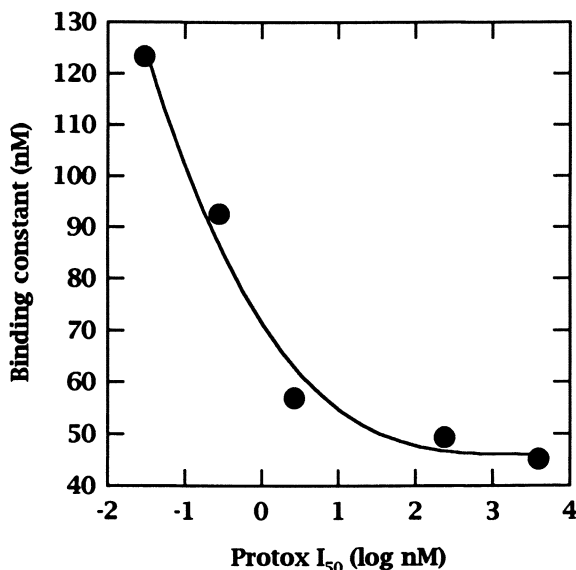


Figure 6. Relationship between the Protox I_{50} values and binding constants in competing radiolabeled acifluorfen off of Protox (data from ref. 53).

Plastid Protox is not inhibited by relatively specific cytochrome P-450 monooxygenase inhibitors nor by copper chelators (46). Furthermore,

quinones such as juglone and duroquinone have little effect on its activity. It will oxidize uroporphyrinogen and coproporphyrinogen to their porphyrins at 10 and 27%, respectively, of its efficiency as an oxidizer of Protogen IX to Proto IX (46).

Mitochondrial Protox. Mitochondrial Protox of both plants and animals is highly sensitive to herbicidal Protox inhibitors (8, 43) (Table II). A comparative study of plant mitochondrial and chloroplast Protox has not been done. However, judging from its similarity to plastid Protox in susceptibility to herbicidal inhibitors, it is reasonable to speculate that mitochondrial Protox is similar in other respects to plastid Protox. Thus, in plant cells treated with Protox inhibitors, both plastid and mitochondrial Protox can be expected to be inhibited.

Plasma Membrane-Bound Protogen IX Oxidizer. Plasma membrane-bound Protox activity of etiolated barley roots or leaves is insensitive to herbicidal inhibitors of plastid Protox (45, 46). In this respect it is similar to bacterial Protox (56). It is strongly inhibited by the copper chelator diethyldithiocarbamate (DETC) and by strong reductants (46). However, it is not inhibited by NADPH. It has less substrate specificity than plastid Protox, oxidizing uroporphyrinogen and coproporphyrinogen to their respective porphyrins at 31 and 77%, respectively, the efficiency of Protogen IX. Plasma membrane-bound Protogen oxidizing activity is strongly enhanced by duroquinone and the plant quinone juglone (46).

The physiological function of this Protogen oxidizer is unknown. However, it is unlikely that it is involved in porphyrin synthesis, as no other enzymes of the porphyrin pathway are known to be associated with the plasma membrane. Functionally, Protox is a polyamine oxidase, as it oxidizes the secondary amines of two of the pyrrole rings of the Protogen IX macrocycle to tertiary amines. Plant polyamine oxidases are copper-containing quinoproteins (57) sometimes associated with cell walls (58). The plasma membrane-bound Protogen oxidizer also has characteristics similar to those of the plant duroquinone reductase localized in the plasma membrane (59). Further study will be required to determine the identity of this enzyme.

Table III summarizes the differences between plastid and plasma membrane-bound Protogen oxidizer characteristics. The lack of dramatic differences in some features may be due, in part, to low level cross contamination.

Table III. Characteristics of Plant Plastid and Plasma Membrane-Bound Protogen Oxidizer Activities

Characteristic	Plastid	Plasma membrane
Herbicide susceptibility	high	low
Quinone effect	low stimulation	strong stimulation
Substrate specificity	high	low
Effects of reductants	low inhibition	high inhibition
Effects of NADPH	moderate inhibition	low
Effects of DETC	none	strong inhibition

Protox Substrate, Product, and Inhibitor Properties

Protogen IX and Proto IX differ in two major properties of relevance to this discussion. First, the lipophilicity of Proto IX is significantly greater than for Protogen IX (46). Thus, Protogen IX is more likely to escape membranes than Proto IX, and, conversely, Proto IX is more likely to remain in membranes within which it is formed. Second, the macrocycle of Protogen IX is a non-planar, flexible structure, whereas that of Proto IX is planar and rigid. The first of these properties has implications for the intracellular distribution of porphyrins in Protox-inhibited plant cells (see below), and the second appears to be important in the explanation of why there are so many good inhibitors of this enzyme.

We have found that the two cycles of diphenyl ether and phenopylate-type Protox inhibitors approximate the structure of two of the pyrroles of the Protogen IX macrocycle (1, 41, 53, 60, see Chapter 10). All other known herbicidal Protox inhibitors are bicyclic compounds. It is likely that they are all competitive inhibitors of Protox, with respect to Protogen IX. The large, flexible Protogen IX macrocycle apparently binds a niche that can also be bound by a large number of non-planar bicyclic compounds.

The Unique Mechanism of Protox Inhibitors

The reasons why herbicidal Protox inhibitors cause the rapid accumulation of the enzyme product is now reasonably clear (45, 46, 48). Plastid Protox in the strong reducing environment of the plastid (61) is inhibited by the herbicidal Protogen IX mimic. Protogen IX accumulates rapidly and leaves the plastid envelope because it is only weakly lipophilic. Leaving the membranous site of plastid Protox, little Protogen IX is left in the membrane to compete with the inhibitor, increasing the effectiveness of the herbicide. Inhibition of porphyrin synthesis leads to lower PChlide and heme levels, resulting in increased carbon flow into the porphyrin pathway because of reduced feedback inhibition. This cytoplasmic Protogen IX cannot be converted to Proto IX by the mitochondria because the mitochondrial Protox is also inhibited by the herbicide.

Upon contact with plasma membrane-bound Protogen IX oxidizer, Protogen IX is rapidly converted to Proto IX because this form of Protox is not inhibited by the herbicide. Proto IX largely remains in the plasma membrane because it is relatively lipophilic. In the presence of light and molecular oxygen, singlet oxygen is generated and membrane lipids undergo lipid peroxidation chain reactions, resulting in rapid cellular disruption. This scheme is entirely consistent with all available data, including the rapid appearance of Proto IX (11, 13), the apparent appearance of porphyrins in the plasma membrane (5, 24), and the rapid loss of plasma membrane integrity (15, 62, 63) in treated cells.

This process by which a herbicidal inhibitor causes the rapid and dramatic buildup of its product is unique. The product is lethal to the plant in the light. Light synergizes the herbicidal process through reducing feedback inhibition of the porphyrin pathway by PChlide and by being a requirement for the photodynamic action of Proto IX. No other

enzymes of the porphyrin pathway have such a convergence of fortuitous factors for herbicidal action.

Enzymes Beyond Protox

The enzymes beyond Protox in the porphyrin pathway have porphyrin substrates. Porphyrins have rigid, planar macrocycles. Thus, competitive inhibitors of these enzymes are likely to be rigid, planar bicyclic compounds. From the variety of porphyrins that accumulate in plants treated with such compounds, there appear to be several enzymes beyond Protox that are inhibited by rigid, planar bicyclic compounds (64, 65). Direct enzymological data to support this are scarce. There are many fewer planar bicyclic compounds than non-planar bicyclic compounds. Thus, the probability of finding a good inhibitor of these enzymes may be significantly lower than that of discovering an effective Protox inhibitor.

These enzymes are found within the plastid and their substrates are relatively lipophilic. Thus, accumulated substrates are unlikely to leave the plastid. If the inhibitor is reversible and competitive, accumulated substrate will reduce its effectiveness. This may partially explain the relative effectiveness of Protox-inhibiting herbicides and those inhibiting later steps of the porphyrin pathway. Furthermore, the plastid is relatively well buffered against singlet oxygen and other toxic oxygen species (61), compared to the plasma membrane. Thus, accumulation of photodynamic porphyrins in the chloroplasts should be less damaging to the plant than the localization of similar compounds in the plasma membranes.

In summary, enzymes of the porphyrin pathway beyond Protox are unlikely to be as good for herbicide target sites as is Protox because they do not share the unique mechanism of porphyrin accumulation that occurs upon inhibition of Protox.

Conclusions

Enough information has accumulated during the past few years to suggest an answer to the question: Why have only Protox inhibitors, but no other inhibitors of the porphyrin pathway emerged from herbicide discovery programs? We suggest that this is due to the unique mechanism of action of Protox inhibitors and to the characteristics of the substrate and product of Protox. The structure of the substrate, Protogen IX, lends itself to a relatively large number of molecules that can mimic one half of the porphyrinogen macrocycle, thereby competitively inhibiting Protox. The relative lipophilicity of Protogen IX and Proto IX lends itself to the proper compartmentation of each for maximal herbicidal activity. The occurrence of an inhibitor-sensitive Protox the plastid envelope and an insensitive Protogen IX-oxidizing activity in the plasma membrane are also requisites for this mechanism of action. No other enzymic sites of the porphyrin pathway share all of the features of Protox that make it a particularly good herbicide target in this pathway. The mechanism of action of Protox inhibitors is a case in which simplicity does not prevail; however, this complex mechanism appears to be universal among higher plants.

Acknowledgments

We thank Nick and Judy Jacobs for their helpful comments and discussions. Krishna Reddy provided helpful editorial comments. This work was supported in part by United States Department of Agriculture Competitive Grant No. 9000705.

Literature Cited

1. Nandihalli, U. B.; Duke, S. O. *Amer. Chem. Soc. Symp. Ser.* **1993**, *524*, 62-78.
2. Anderson, R. J.; Norris, A. E.; Hess, F. D. *Amer. Chem. Soc. Symp. Ser.* **1994**, *this volume*.
3. Scalla, R.; Matringe, M. *Rev. Weed Sci.* **1994**, *6*, 103-132.
4. Duke, S. O.; Becerril, J. M.; Sherman, T. D.; Matsumoto, H. *Amer. Chem. Soc. Symp. Ser.* **1991**, *449*, 371-86.
5. Duke, S. O.; Lydon, J.; Becerril, J. M.; Sherman, T. D.; Lehnen, L. P.; Matsumoto, H. *Weed Sci.* **1991**, *39*, 465-73.
6. Scalla, R.; Matringe, M. *Z. Naturforsch.* **1990**, *45c*, 503-11.
7. Duke, S. O.; Becerril, J. M.; Sherman, T. D.; Lydon, J.; Matsumoto, H. *Pestic. Sci.* **1990**, *30*, 367-78.
8. Matringe, M.; Camadro, J.-M.; Labbe, P.; Scalla, R. *Biochem. J.* **1989**, *260*, 231-5.
9. Matringe, M.; Scalla, R. *Proc. Brit. Crop Prot. Conf. -Weeds* **1987**, *3*, 981-8.
10. Becerril, J. M.; Duke, S. O. *Pestic. Biochem. Physiol.* **1989**, *35*, 119-26.
11. Becerril, J. M.; Duke, S. O. *Plant Physiol.* **1989**, *90*, 1175-81.
12. Sherman, T. D.; Becerril, J. M.; Matsumoto, H.; Duke, M. V.; Jacobs, J. M.; Jacobs, N. J.; Duke, S. O. *Plant Physiol.* **1991**, *97*, 280-7.
13. Matsumoto, H.; Duke, S. O. *J. Agric. Food Chem.* **1990**, *38*, 2066-71.
14. Sandmann, G.; Nicolaus, B.; Böger, P. *Z. Naturforsch.* **1990**, *45c*, 512-7.
15. Duke, S. O.; Lydon, J.; Paul, R. N. *Weed Sci.* **1989**, *37*, 152-60.
16. Kojima, S.; Matsumoto, H.; Ishizuka, K. *Weed Res., Japan* **1991**, *36*, 318-23.
17. Nandihalli, U. B.; Sherman, T. D.; Duke, M. V.; Fischer, J. D.; Musco, V. A.; Becerril, J. M.; Duke, S. O. *Pestic. Sci.* **1992**, *35*, 227-35.
18. Sherman, T. D.; Duke, M. V.; Clark, R. D.; Sanders, E. F.; Matsumoto, H.; Duke, S. O. *Pestic. Biochem. Physiol.* **1991**, *40*, 236-45.
19. Deybach, J. C.; de Verneuil, H.; Nordmann, Y. *Hum. Genet.* **1981**, *58*, 425-8.
20. Brenner, D. A.; Bloomer, J. R. *New Eng. J. Med.* **1980**, *302*, 765-8.
21. Camadro, J. M.; Urban-Grimal, D.; Labbe, P. *Biochem. Biophys. Res. Commun.* **1982**, *106*, 724-30.
22. Mayasich, J. M.; Nandihalli, U. B.; Leibl, R. A.; Rebeiz, C. A. *Pestic. Biochem. Physiol.* **1990**, *36*, 259-68.
23. Sandmann, G.; Böger, P. *Z. Naturforsch.* **1988**, *43c*, 699-704.
24. Lehnen, L. P.; Sherman, T. D.; Becerril, J. M.; Duke, S. O. *Pestic. Biochem. Physiol.* **1990**, *37*, 239-48.
25. Gough, S. P.; Kannangara, G. *Carlsberg Res. Commun.* **1979**, *44*, 403-6.

26. Dörnemann, D.; Breu, V.; Kotzabasis, K.; Richter, P.; Senger, H. *Bot. Acta* **1989**, *102*, 112-5.
27. Dörnemann, D.; Breu, V.; Kotzabasis, K.; Richter, P.; Senger, H. In *Current Research in Photosynthesis, Vol. IV*; Baltscheffsky, M., Ed.; Kluwer Acad. Publ., Amsterdam, 1990; pp. 287-90.
28. Becerril, J. M.; Duke, M. V.; Nandihalli, U. B.; Matsumoto, H.; Duke, S. O. *Physiol. Plant.* **1992**, *86*, 6-16.
29. Nandihalli, U. B.; Leibl, R. A.; Rebeiz, C. A. *Pestic. Sci.* **1991**, *31*, 9-23.
30. Witkowski, D. A.; Halling, B. P. *Plant Physiol.* **1988**, *87*, 632-7.
31. Duke, S. O.; Duke, M. V.; Sherman, T. D.; Nandihalli, U. B. *Weed Sci.* **1991**, *39*, 505-13.
32. Duke, S. O.; Duke, M. V.; Lee, H. J. *Z. Naturforsch.* **1993**, *48c*, 317-25.
33. Masuda, T.; Kouji, H.; Matsunaka, S. *Pestic. Biochem. Physiol.* **1990**, *36*, 106-14.
34. Padmanaban, G.; Ventkateswar, V.; Rangarajan, P. N. *Trends Biochem.* **1990**, *14*, 492-6.
35. Matringe, M.; Clair, D.; Scalla, R. *Pestic. Biochem. Physiol.* **1990**, *36*, 300-7.
36. Watanabe, H.; Otori, Y.; Sandmann, G.; Wakabayashi, K.; Böger, P. *Pestic. Biochem. Physiol.* **1992**, *42*, 99-109.
37. Kunert, K.-J.; Sandmann, G.; Böger, P. *Rev. Weed Sci.* **1987**, *3*, 35-55.
38. Ohnishi, J.; Yukitake, K.; Eto, M. *J. Fac. Agric. Kyushu Univ.* **1993**, *37*, 239-46.
39. Witkowski, D. A.; Halling, B. P. *Plant Physiol.* **1989**, *90*, 1239-42.
40. Lydon, J.; Duke, S. O. *Pestic. Biochem. Physiol.* **1988**, *31*, 74-83.
41. Nandihalli, U. B.; Duke, M. V.; Duke, S. O. *Pestic. Biochem. Physiol.* **1992**, *43*, 193-211.
42. Camadro, J.-M.; Matringe, M.; Scalla, R.; Labbe, P. *Biochem. J.* **1991**, *277*, 17-21.
43. Matringe, M.; Camadro, J.-M.; Labbe, P.; Scalla, R. *FEBS Lett.* **1989**, *245*, 35-8.
44. Mito, N.; Sato, R.; Miyakado, M.; Oshio, H.; Tanaka, S. *Pestic. Biochem. Physiol.* **1991**, *40*, 128-35.
45. Jacobs, J. M.; Jacobs, N. J.; Sherman, T. D.; Duke, S. O. *Plant Physiol.* **1991**, *97*, 197-203.
46. Lee, H. J.; Duke, M. V.; Duke, S. O. *Plant Physiol.* **1993**, *102*, 881-9.
47. Smith, A. G.; Marsch, O.; Elder, G. H. *Biochem. J.* **1993**, *292*, 503-8.
48. Jacobs, J. M.; Jacobs, N. J. *Plant Physiol.* **1993**, *101*, 1181-7.
49. Kirk, J. T. O.; Tilney-Bassett, R. A. E. *The Plastids, Their Chemistry, Structure, Growth and Inheritance*; Elsevier/North-Holland: Amsterdam, 1979, 960 pp.
50. Matringe, M.; Camadro, J.-M.; Block, M. A.; Joyard, J.; Scalla, R.; Labbe, P.; Douce, R. *J. Biol. Chem.* **1991**, *97*, 197-203.
51. Nicolaus, B.; Sandmann, G.; Böger, P. *Z. Naturforsch.* **1993**, *48c*, 326-33.
52. Varsano, R.; Matringe, M.; Magnin, N.; Mornet, R.; Scalla, R. *FEBS Lett.* **1990**, *272*, 106-8.
53. Nandihalli, U. B.; Duke, M. V.; Duke, S. O. *J. Agric. Food Chem.* **1992**, *40*, 1993-2000.

54. Oshio, H.; Shibata, H.; Mito, N.; Yamamoto, M.; Harris, E. H.; Gillham, N. W.; Boynton, J. E.; Sato, R. *Z. Naturforsch.* **1993**, *48c*, 339-44.
55. Matringe, M.; Mornet, R.; Scalla, R. *Eur. J. Biochem.* **1992**, *209*, 861-8.
56. Jacobs, J. M.; Jacobs, N. J.; Borotz, S. E.; Guerinot, M. L. *Arch. Biochem. Biophys.* **1990**, *280*, 369-75.
57. Duine, J. A. *Eur. J. Biochem.* **1991**, *200*, 271-84.
58. Federico, R.; Angelini, R.; Cona, A.; Niglio, A. *Phytochemistry* **1992**, *31*, 2955-7.
59. Buckhout, T. J.; Luster, D. G. In *Oxidoreduction at the Plasma Membrane: Relation to Growth and Transport, Volume V. Plants*; Crane, F. L.; Morré, D. J.; Löw, H. E., Eds.; CRC Press, Boca Raton, FL, 1991, pp. 61-84.
60. Nandihalli, U. B.; Duke S. O. *Amer. Chem. Soc. Symp. Ser.* **1994**, this volume.
61. Halliwell, B. In *Topics in Photosynthesis, Vol. 10: Herbicides*; Barber, J., Ed.; Elsevier, Amsterdam, 1991, pp. 87-127.
62. Kenyon, W. H.; Duke, S. O.; Paul, R. N. *Pestic. Biochem. Physiol.* **1988**, *30*, 57-66.
63. Duke, S. O.; Kenyon, W. H. *Z. Naturforsch.* **1987**, *42c*, 813-8.
64. Nandihalli, U. B.; Rebeiz, C. A. *Pestic. Biochem. Physiol.* **1991**, *40*, 27-46.
65. Bednarik, D. P.; Hooper, J. K. *Arch. Biochem. Physiol.* **1985**, *240*, 369-79.

RECEIVED April 6, 1994

Chapter 15

Porphyric Insecticides

Larry J. Gut¹, John A. Juvik, and Constantin A. Rebeiz

Laboratory of Plant Pigment Biochemistry and Photobiology, 240A Plant and Animal Biotechnology Laboratory, University of Illinois, 1201 West Gregory Avenue, Urbana, IL 61801-4716

Porphyric insecticides are comprised of a group of chemicals, referred to as modulators, which in concert with δ -aminolevulinic acid act via the induction of protoporphyrin IX (Proto) and Zn-Proto accumulation in treated insects. In the light, treated insects are destroyed by the photodynamic action of the accumulated tetrapyrroles. It is believed that this is achieved by tetrapyrrole dependent sensitized formation of singlet oxygen. In a series of experiments, ALA and various substituted phenanthrolines, pyridyls, pyridiniums, quinolines, oxypyridines and pyrroles exhibited potent porphyric insecticidal activity against larvae of *Trichoplusia ni*. The relationship between photodynamic damage in *T. ni* and physical chemical properties of these modulators was rather complex and involved specific alterations in van der Waals energy and volumes, in molecular electrostatic potentials, and in the 1,2,2'1' torsion angles. Several modulators also showed porphyric insecticidal activity against *Helicoverpa zea*, *Anthonomus grandis*, and *Blatella germanica*.

The development of porphyric insecticides was based on the development of tetrapyrrole-dependent photodynamic herbicides (TDPH) (*1-4*). This novel class of herbicides acts by forcing green plants to produce undesirable amounts of metabolic intermediates of the chlorophyll biosynthetic pathway, namely tetrapyrroles. In the light, the accumulated tetrapyrroles photosensitize the formation of singlet oxygen which kills treated plants by oxidation of their cellular membranes. TDPH generally consist of the natural precursor of tetrapyrroles, δ -aminolevulinic acid (ALA), and one of several chemicals, termed modulators. ALA serves as a building block, while the modulator alters quantitatively and qualitatively the pattern of tetrapyrrole accumulation. Since plant and animal cells have similar porphyrin-heme biosynthetic pathways we conjectured that tetrapyrrole-dependent photodynamic insecticidal activity may be possible as well. The discovery and development of a tetrapyrrole-dependent, alternatively termed porphyric, insecticidal system constitutes the subject of this chapter.

¹Current address: Tree Fruit Research and Extension Center, Washington State University, 1100 North Western Avenue, Wenatchee, WA 98801

Discovery of the Porphyric Insecticidal System

The potential for tetrapyrrole accumulation in insects was initially demonstrated by spraying *Trichoplusia ni* (Hübner) larvae with a mixture of ALA (40mM) and 2,2'-dipyridyl (30 mM) (5). This combination was known to have potent TPDH activity (4). *T. ni* larvae treated with 2,2'-dipyridyl (DPY) plus ALA were placed in darkness for 17 h to allow for putative tetrapyrrole accumulation. Extraction of treated larvae with ammoniacal acetone, followed by spectrofluorometric analysis, revealed the presence of massive amounts of a fluorescent compound in the acetone. Following chemical derivatization coupled to spectrofluorometric analysis, the compound was identified as a tetrapyrrole, specifically Protoporphyrin IX (Proto) (5).

Porphyric Insecticidal Activity of 2,2'-Dipyridyl. Further experiments with *T. ni* indicated potent, tetrapyrrole-dependent, insecticidal activity of DPY plus ALA treatments (5). Third instar larvae sprayed with these chemicals and placed in darkness for 17 h consistently accumulated toxic amounts of Proto (Table I). Treated larvae that were exposed to metal halide lights ($21.1 \text{ mW}\cdot\text{cm}^{-2}$) after the initial period of dark incubation, immediately became sluggish and flaccid due to loss of body fluid. Photodynamic death was accompanied by extensive desiccation. Larval mortality after 3 d in the growth chamber (28°C, 14:10 LD) ranged from 47 to 89% (Table I).

Table I. Proto Accumulation and Mortality in Third Instar *Trichoplusia ni* Sprayed with a Solution of ALA (40 mM) plus DPY (30 mM)

<i>Experiment</i>	<i>Treatment</i>	<i>Proto content (nmoles/100 mg protein)</i>	<i>Larval mortality after 3 days (%)</i>
A	Control (solvent only)	0.1	3
	ALA + DPY	85.0	80
B	Control (solvent only)	0	1
	ALA + DPY	96.7	75
C	Control (solvent only)	0.1	13
	ALA + DPY	12.8	47
D	Control (solvent only)	0.1	6
	ALA + DPY	89.7	89

SOURCE: Adapted from ref. 5.

To determine the relative, and possibly synergistic, effects of the two components of this insecticidal system, treatments of ALA only, DPY only, and ALA plus DPY were compared. Proto accumulation after 17 h dark incubation and mortality after 3 d illumination was determined as previously described. Mortality of third instars following various treatments was highly correlated with the degree of Proto accumulation (Table II). Spraying with ALA (40mM) alone caused little Proto production and, thus, was the least effective photodynamic insecticide (experiments A & D). In contrast, treatment with DPY (40mM) alone induced the accumulation of up to 15 nmoles (per 100 mg of insect protein) of Proto and caused levels of larval mortality as high as 61% (experiments A & B). Dramatically higher levels of Proto accumulation (up to 89 nmoles) and larval mortality (up to 90%) were recorded when ALA and DPY were used in combination (experiments A-D). In summary, DPY acted

as both an inducer and enhancer of Proto accumulation in *T. ni*. This porphyrin biosynthesis modulator induced the production of higher levels of Proto than occur naturally, as indicated by treatment with solvent only, and greatly enhanced the conversion of exogenous ALA to Proto. In addition, ALA and DPy appeared to act synergistically, with Proto accumulation and larval death caused by treatment with both chemicals exceeding the sum of Proto accumulation and larval death caused by separate ALA and DPy treatments.

Table II. Synergistic Effects of ALA and DPy on Proto Accumulation and Mortality in Third Instar *Trichoplusia ni*

<i>Experiment</i>	<i>Treatment</i>	<i>Proto content</i> (nmoles/100 mg protein)	<i>Larval mortality</i> after 6 days (%)
A	Control (solvent only)	0	3
	40 mM ALA	2	26
	30 mM DPy	15	41
	40 mM ALA + 30 mM DPy	80	90
B	Control (solvent only)	0	2
	30 mM DPy	11	61
	30 mM DPy + 10 mM ALA	75	86
	30 mM DPy + 20 mM ALA	89	76
	30 mM DPy + 40 mM ALA	73	92
C	Control (solvent only)	0	7
	15 mM DPy	1	22
	15 mM DPy + 10 mM ALA	8	42
	15 mM DPy + 20 mM ALA	34	40
	15 mM DPy + 40 mM ALA	27	43
D	Control (solvent only)	0	5
	40 mM ALA	1	7
	40 mM ALA + 5 mM DPy	3	4
	40 mM ALA + 10 mM DPy	7	18
	40 mM ALA + 20 mM DPy	12	34
	40 mM ALA + 40 mM DPy	15	71
Correlation between Proto content and larval death		0.857	
Level of significance		0.1%	

SOURCE: Adapted from ref. 5.

Effect of Various Light-Dark Regimes. During the course of experimentation, we observed that the ALA + DPy treatment consistently caused larval death in darkness. To investigate the extent of this non-photodynamic mortality, third instar *T. ni* larvae were initially treated as described above, but subsequent to the 17 h dark incubation period were exposed to various light-dark regimes. Evaluation of larval mortality after 17 h darkness revealed that about 20 % of the insects died before exposure to light (Table III). While some of the surviving larvae died when held in darkness for an additional 48 h, higher mortality occurred if they were exposed to light. During illumination the accumulated Proto disappeared probably as a result of photodestruction, a well known tetrapyrrole phenomenon.

To determine if a post-spray dark incubation period was required for expression of porphyric insecticidal activity, the mortality of second instar *T. ni* larvae treated in the dark or light was compared. The dark treatment entailed the standard protocol, including a 17 h dark incubation period, as described above. In the light treatment, larvae were sprayed at the beginning of the 14:10 LD photoperiod. Both treatments were equally effective (Table IV). Thus, although in the light Proto is destroyed as rapidly as it is formed (Table III), the steady-state formation of Proto in the light appears to be sufficient to cause extensive photodynamic damage.

Table III. Proto Accumulation and Mortality in Third Instar *Trichoplusia ni* Sprayed with a Solution of ALA (40 mM) plus DPy (30 mM), and exposed to various light and dark regimes following an initial 17 h dark incubation period

Experiment	Treatment	Light regime (h)		Proto content (nmoles/100 mg protein)	Larval mortality (%) after	
		Light	Dark		17 h dark	65 h
A	Control	28	20	0.2 ¹	1	12
	ALA + DPy	0	48	62.0 ¹	28	31
		3	45	0.4 ²	21	60
		6	42	1.1 ²	22	73
		28	20	62.0 ¹	19	80
B	Control	28	20	0.2 ¹	0	22
	ALA + DPy	0	48	40.1 ¹	19	48
		3	45	1.2 ²	20	65
		6	42	0.6 ²	21	77
		28	20	40.1 ¹	22	95

SOURCE: Adapted from ref. 5.

¹ Proto content after the 17 h dark incubation period.

² Proto content after the 17 h dark incubation period and 3 or 6 hours of illumination.

Table IV. Comparison of the Effectiveness of ALA plus DPy Sprayed on Second Instar *Trichoplusia ni* in the Light or the Dark

Experiment	Light conditions	Treatment	Larval mortality after 3 days (%)
A	dark	control (solvent only)	21
	dark	20 mM ALA + 15 mM DPy	90
B	light	control (solvent only)	25
	light	20 mM ALA + 15 mM DPy	94
C	dark	control (solvent only)	14
	dark	40 mM ALA + 30 mM DPy	93
D	light	control (solvent only)	5
	light	40 mM ALA + 30 mM DPy	83

SOURCE: Adapted from ref. 5.

Porphyric Insecticidal Activity of 1,10-Phenanthroline

1,10-Phenanthroline, or ortho-phenanthroline (OPh), is also known to be a potent TDPH, inducing the formation of massive amounts of Proto and Mg-Proto in a variety of weed species (4). Thus, it was selected as an additional candidate for defining the nature of the porphyric insecticidal system. Initially, third instar *T. ni* larvae were sprayed with ALA (40mM) and OPh (30 mM) and analyzed for tetrapyrrole accumulation and larval mortality as previously described for DPy. OPh exhibited potent porphyric insecticidal properties, acting as both an inducer and enhancer of Proto formation and causing high levels of photodynamic death (Table V).

In addition to fluorescence emission originating in the Proto pool, another band of smaller amplitude was recorded in the hexane-extracted acetone fraction of the ALA plus OPh treated insects. Specifically the band exhibited an emission maximum at 590 nm at room temperature and at 687 nm at 77°K in ether, identifying it as Zn-Proto. Although less Zn-Proto than Proto accumulated in treated insects, both correlated positively with larval mortality (Table V).

Table V. Effect of ALA and OPh Sprays on the Accumulation of Proto and Zn-Proto, and the Extent of Mortality in Third Instar *Trichoplusia ni*

Experiment	Treatment	Proto content (nmoles/100 mg protein)	Zn-Proto content (nmoles/100 mg protein)	Larval mortality after 3 days (%)
A	Control (solvent only)	0.2	0	0
	40 mM ALA	3.2	0	16.8
	30 mM OPh	35.3	4.5	69.6
	40 mM ALA + 30 mM OPh	152.0	3.8	93.0
	B	Control (solvent only)	0.2	0
	40 mM ALA	2.1	0	5.3
	30 mM OPh	18.6	1.1	74.7
	40 mM ALA + 30 mM OPh	227.8	6.2	93.3

SOURCE: Adapted from ref. 6.

Insecticidal Activity of Ingested OPh and DPy

Ingestion of OPh and DPy by *T. ni* also resulted in high levels of insecticidal activity. In a series of experiments, third instar larvae were placed on untreated or porphyric insecticide treated diets and allowed to feed in darkness for 17 h. At the end of this incubation period, a portion of the larvae were analyzed for tetrapyrrole content while the remaining larvae were placed in the light for observation of photodynamic injury. Ingestion of either OPh or DPy (12 mM) induced and, in the presence of exogenous ALA (16 mM), enhanced the production of Proto and Zn-Proto (Table VI). Tetrapyrrole accumulation was highly correlated with larval mortality. As observed when treatments were applied as a spray, the highest levels of Proto accumulation and larval mortality were achieved in the modulator plus ALA treatments.

Table VI. Effect of Ingested ALA, DPy, and OPh on the Accumulation of Proto and Zn-Proto, and the Extent of Mortality in Third Instar *Trichoplusia ni*

<i>Experiment</i>	<i>Treatment</i>	<i>Proto content (nmoles/100 mg protein)</i>	<i>Zn-Proto content (nmoles/100 mg protein)</i>	<i>Larval mortality after 3 days (%)</i>
A	Control (solvent only)	0	0	14.5
	16 mM ALA	1.5	0	5.2
	12 mM OPh	88.1	1.3	40.4
	16 mM ALA + 12 mM OPh	224.6	1.5	94.4
B	Control (solvent only)	0	0	4.5
	16 mM ALA	2.6	0	4.7
	12 mM OPh	14.3	1.9	51.4
	16 mM ALA + 12 mM OPh	160.2	2.0	95.4
C	Control (solvent only)	0.4	0	18.2
	16 mM ALA	3.1	0	49.3
	12 mM DPY	20.3	8.8	11.4
	16 mM ALA + 12 mM DPY	55.2	11.4	100

SOURCE: Adapted from ref. 6.

OPh and DPy were effective at much lower doses when incorporated into diet rather than applied as a spray. A significant level of insecticidal activity was recorded when *T. ni* larvae ingested diet containing as little as 1 mM ALA and 0.05 mM OPh. Moreover, 100 % larval mortality occurred when diet baited with 2 mM ALA and 0.4 mM OPh was consumed (Table VII). Proto accumulation increased exponentially as the concentration of OPh in the baited diet was increased (6).

Further investigations with diet containing low doses of ALA and OPh indicated that both the accumulation and breakdown of Proto occurred fairly rapidly in *T. ni* (Rebeiz et al, unpublished data). Four hours of feeding prior to exposure to light was sufficient to achieve photodynamic injury of 90% or greater. On the flip side, Proto accumulation and death did not occur if larvae were transferred from treated to untreated diet during dark incubation and allowed to feed for at least 4 h prior to exposure to light.

Metal Cations as Inhibitors of Insecticidal Activity by OPh

The tetrapyrrole-inducing, herbicidal properties of bidentate metal chelators, such as DPy and OPh, are not expressed in the presence of metallic cations such as Fe^{++} and Zn^{++} . (4) This phenomenon suggested an additional method of evaluating the linkage between Proto accumulation and porphyric insecticidal activity. Third instar *T. ni* larvae were treated with diet containing OPh (0.5 mM), ALA (1.0 mM), and various concentrations of $FeCl_2$, $FeCl_3$, and $ZnCl_2$. All three cations inhibited the porphyric insecticidal properties of OPh (data not shown). The effect of three concentrations of the most potent inhibitor, Fe^{+++} , on Proto accumulation and photodynamic mortality is summarized in Table VIII.

Table VII. Effect of Ingested ALA (2mM) and Various Concentrations of OPh on the Accumulation of Proto and Zn-Proto, and the Extent of Mortality in Third Instar *Trichoplusia ni*

<i>Treatment</i>	<i>Proto content (nmoles/100 mg protein)</i>	<i>Zn-Proto content (nmoles/100 mg protein)</i>	<i>Larval mortality after 3 days (%)</i>
Control (solvent only)	0.6	0	16.0
2 mM ALA	3.6	0	54.0
2 mM ALA + 0.1 mM OPh	10.4	0	84.0
2 mM ALA + 0.4 mM OPh	46.4	2.7	100
2 mM ALA + 1.6 mM OPh	67.0	4.1	100

SOURCE: Adapted from ref. 6.

Table VIII. Effect of Various Concentrations of FeCl₃ on the Accumulation of Proto and the Extent of Mortality in Third Instar *Trichoplusia ni*

<i>Treatment</i>	<i>Proto content (nmoles/100 mg protein)</i>	<i>Larval mortality after 3 days (%)</i>
1 mM ALA	1.1	54.0
1 mM ALA + 0.5 mM OPh	46.7	74.0
1 mM ALA + 0.5 mM OPh + 0.5 mM FeCl ₃	11.2	14.7
1 mM ALA + 0.5 mM OPh + 1.0 mM FeCl ₃	2.1	6.7
1 mM ALA + 0.5 mM OPh + 2.0 mM FeCl ₃	0.8	1.3

SOURCE: Adapted from ref. 6.

Mode of Action of the Porphyrin Insecticidal System

The induction of Proto production by chemical treatment appears to involve modulation of the porphyrin-heme biosynthetic pathway which results in the accumulation of massive amounts of Proto and Zn-Proto in darkness. The molecular basis of the observed synergism between ALA and modulator is not understood, but we propose that enhancer-inducer modulators, such as DPy and OPh, act in a dual manner: a) by opening a closed regulatory step involved in the biosynthesis of ALA from endogenous precursors and b) by activating one or more steps of the porphyrin biosynthetic chain resulting in the enhanced conversion of exogenous and endogenous ALA to Proto and Zn-Proto.

This increased production of Proto appears to be the primary mode of action of the porphyrin insecticidal system. Specifically, upon exposure to light, the accumulated Proto most likely photosensitizes the formation of singlet oxygen which kills the treated insects by oxidation of their cellular membranes. A massive build-up of Proto is not mandatory for the occurrence of photodynamic injury. What is required is the steady-state formation of small amounts of Proto at rates large enough to initiate damaging chain reactions.

Porphyrin insecticide modulators may also act by causing the premature release of O₂⁻ and ⁻OH radicals from the active site of damaged cytochrome *c* oxidase. This non-photodynamic mode of kill is suggested by the occurrence of larval death in darkness and by the detection of Zn-Proto. Zn-Proto is not a natural metabolic intermediate of the porphyrin-heme pathway. Its occurrence in living cells and tissues usually denotes a poisoned porphyrin-heme metabolism (7). Most ferrocyclases (the enzymes that insert ferrous iron into Proto to form heme) can

insert zinc instead of iron into Proto to yield Zn-Proto, particularly under unfavorable conditions. Thus it is possible that the accumulation of Zn-Proto associated with DPy or OPh treatments may be caused by damage to the ferrochelatase system leading to the insertion of Zn instead of ferrous Fe into some of the Proto. Cytochrome *c* prosthetic groups that consist of Zn-Proto instead of heme in treated insects may no longer be able to prevent the premature release of oxygen superoxide and hydroxy free radicals. The intracellular release of these destructive free radicals in the biological membrane environment could then trigger peroxidation of the membrane lipoprotein, causing the same type of damage as singlet-oxygen mediated photodynamic damage.

Identification of Additional Porphyric Insecticide Modulators

Structure-activity studies of TDPH included the assembly of two databases of commercially available compounds with potential photodynamic herbicidal properties. The databases consisted of sets of six-membered and five-membered N-heterocyclic compounds. Extensive testing of 322 putative photodynamic herbicide modulators on a variety of plant species led to the identification of over 150 modulators with high levels of TDPH activity. Based on these results, about 200 compounds were evaluated for porphyric insecticidal properties.

Potential modulators were screened for activity against four insect species, *T. ni*, (cabbage looper), *Helicoverpa zea* (Boddie) (corn earworm), *Anthonomus grandis* Boheman (boll weevil), and *Blattella germanica* (L.) (german cockroach). Initial studies focused on determining the relative effects of these modulators when ingested by larvae of *T. ni*. Modulators and ALA were incorporated into liquid Waldbauer's medium to final concentrations of 4mM and 3mM, respectively. The experimental procedure consisted of placing 20 larvae and a 12 ml block of diet in a cardboard carton (9 cm h x 10 cm dia) sealed with a plastic lid. Treated larvae were held in darkness for 17 h and then placed in light for determination of photodynamic injury. Unbaited food was added daily to each container for the duration of the experiment. Treatment of *H. zea* entailed placing a 3 ml, untreated or treated, Waldbauer's diet cube and a single larva in each cell of a 20 cell plastic tray. Larvae were confined to their individual compartments by covering the tray with a glass plate. Preliminary tests indicated that higher concentrations of chemicals and longer exposure to them were required to achieve significant mortality of adults of *A. grandis* and *B. germanica*. To evaluate activity against *A. grandis*, modulators and ALA were incorporated into boll weevil diet (Bioserve, Inc) to final concentrations of 6 mM and 8 mM, respectively. *B. germanica* were fed Waldbauer's diet containing 24 mM of ALA and 16 mM of modulator. For both species, the experimental procedure consisted of placing 15 adults and a 12 ml block of diet in a cardboard carton (9 cm h x 10 cm dia) sealed with a plastic lid. Unbaited and baited food was replenished daily for the duration of the experiment. Dark incubation, subsequent illumination and evaluation of mortality of *H. zea* and *A. grandis* were as described for *T. ni*. *B. germanica*, however, were held in darkness at room temperature for a 40-h post-treatment and then placed under subdued light (20-40 ft. candles) for the duration of the experiment.

Initial screening of modulators belonging to eight different N-heterocyclic templates (chemical families) revealed a wide range of insecticidal activity against larvae of *T. ni*. This is readily illustrated by the variation in effectiveness of 12 phenanthrolines and 12 pyridyls (Table IX). Six phenanthrolines and three pyridyls proved very potent and resulted in larval death greater than 95%. Another five modulators exhibited high activity, causing greater than 70% mortality. The remaining 10 compounds were considerably less active.

Table IX. Insecticidal Effect of Various Substituted Phenanthrolines and Pyridyls on Third Instar *Trichoplusia ni* in the Presence of 4mM ALA and 3mM Modulator

<i>Modulator</i>	<i>Larval mortality (%) after</i>	
	<i>1 day</i>	<i>3 days</i>
None	0	0
1,10-Phenanthroline (OPh)	100	100
4-Methyl-OPh	98.9	98.9
5-Methyl-OPh	97.2	97.2
5,6-Dimethyl-OPh	97.2	97.2
4,7-Dimethyl-OPh	98.6	100
3,4,7,8-Tetramethyl-OPh	85.0	85.0
5-Chloro-OPh	94.5	95.7
5-Nitro-OPh	97.7	97.7
4,7-Dihydroxy-OPh	27.4	48.6
2,9-Dimethyl-4,7-diphenyl-OPh	4.5	38.7
2,9-Dimethyl-4,7-diphenyl-OPh-disulfonic acid	2.7	8.1
5,6-Dihydro-4,7-dimethyl-dibenzo-OPh	10.0	25.0
2,2'-Dipyridyl (DPy)	100	100
2,2'-Bypyridinium chlorochromate	96.7	98.3
2,2':6',2''-Terpyridine	65.3	69.9
4,4'-Dimethyl-DPy	60.9	71.1
4,4'-Diphenyl-DPy	3.3	6.7
2,2-Biquinoline	1.7	3.3
DPy disulfide	2.2	8.9
2,2'-Dithiobis (5-nitropyridine)	0	6.7
2,2'-Dithiobis (pyridine N-oxide)	69.3	73.3
6,6'-Dithionicotinic acid	0	0
Phenyl 2-pyridyl ketoxime	59.3	71.3
Di-2-pyridyl ketone oxime	98.8	98.8

Based on the entire series of screenings of potential modulators plus ALA against *T. ni*, 80 chemicals were also evaluated for activity against *H. zea*, *A. grandis* and *B. germanica*. These included all modulators that exhibited high activity against *T. ni*, as well as representative chemicals belonging to each template that were found to be moderately or poorly effective against this pest. Thirty-six of the 80 compounds caused greater than 70% mortality in at least one of the four insect species (Table X). Seven of the eight templates had at least one active compound. Only the substituted nicotinamides were completely inactive (data not shown).

Quantitative Structure-Activity Analysis of Porphyric Insecticide Modulators

Structure-activity analyses focused on the relationships between alterations in the electrostatic field of various chemicals, tetrapyrrole modulating activity and photodynamic death. The underlying hypothesis of this approach was structural complementarity between enzymatic receptor sites and tetrapyrrole modulators that may favor putative electrostatic binding of modulators to or close to the receptor sites of enzymes that catalyze various reactions of the porphyrin biosynthetic pathway. In particular, the detection of exclusive positive charge binding or repelling volumes in analogs within a chemical family that exhibit similar tetrapyrrole biosynthesis modulating activity may indicate that these analogs exert their effects by binding to the same enzymatic receptor site.

Chem-X software (Chemical Design Limited, Oxford, England) was used to build 3-dimensional chemical structures and to carry out quantitative structure-activity relationship (QSAR) analysis. The procedure involved optimization of chemical structures via Mopac (versions 5.0 or 6.0), using either the MNDO or AM1 hamiltonian, calculation of 17 different electronic and physical-organic properties (descriptors) for each structure, and analysis of correlations between the descriptors and insecticidal activity.

Calculation of electrostatic potential energy levels at various sites of a given molecule was also performed using Chem-X software. Chem-X calculates electrostatic potential energy levels by treating the charge on each atom in a molecule as a point charge positioned at the center of the atom. Subsequently, a positive unit charge equivalent to that of a proton is placed at each grid point and the electrostatic interaction between groups of atoms and the unit charge is calculated. This is followed by drawing isopotential contour lines. In our calculations, the number of grid points per molecule was set at 15. Values of 10 kcal/mole for positive potential energy levels and -10 kcal for negative potential energy levels were selected. Since the interaction of a positive charge with a positive region of the molecule generates positive energy levels, these energy levels were interpreted as repelling. Likewise, since the interaction of a positive charge with a negative region of the molecule generates negative energy levels, these energy levels were considered as binding or attracting energy levels. In this manner the attraction or repulsion at various loci of a particular molecule toward a positive charge was well defined by the negative and positive potential energy contour lines respectively, which in fact delineate positive charge binding or repelling electrostatic volumes surrounding various sections of a molecule.

Quantitative and positional differences among the electrostatic fields of various modulators within a chemical family were calculated by determining the exclusive positive charge binding and repelling volumes for each analog in comparison to a reference molecule. Phenanthrene, OPh, DPy, etc. were used as reference molecules. The calculation of exclusive volumes (i.e. non-overlapping volumes between two molecules) was achieved via a Chem-X software module that calculates exclusive volumes for pairs of molecules from the electrostatic volumes of each individual molecule.

Table X. Porphyrinic Insecticide Modulators with High Activity Against *Trichoplusia ni*, *Heliothis zea*, *Anthonomus grandis* and/or *Blatella germanica*.

Template	Modulator	Mortality (%)			
		Tn	Hz	Ag	Bg
1,10-Phenanthroline					
	1,10-Phenanthroline	100 ¹	100	90	100
	4-Methyl-1,10-Phenanthroline	99	95	76	87
	5-Methyl-1,10-Phenanthroline	97	55	64	30
	4,7-Dimethyl-1,10-Phenanthroline	100	90	85	96
	5,6-Dimethyl-1,10-Phenanthroline	97	50	51	93
	3,4,7,8-Tetramethyl-1,10-Phenanthroline	85	79	44	27
	5-Nitro-1,10-Phenanthroline	99	63	58	38
	5-Chloro-1,10-Phenanthroline	96	84	40	82
	4,7-Diphenyl-1,10-Phenanthroline	96	0	0	0
2,2'-Dipyridyl					
	2,2'-Dipyridyl	100	100	100	100
	4,4'-Dimethyl-2,2'-Dipyridyl	71	25	20	7
	Phenyl-2-Pyridyl ketoxime	71	5	7	0
	2,2'-Dithiobis (pyridine N-oxide)	73	0	67	67
	Benzyl viologen dichloride monohydrate	0	47	100	53
Quinoxaline					
	Neutral Red	81	20	11	7
8-Hydroxyquinoline					
	8-Hydroxy-7-(4-sulfo-1-naphylazo)-5-quinoline	74	35	2	0
	8-Hydroxy-5-sulfonic acid monohydrate	86	10	0	0
	8-Hydroxy-7-iodo-5-quinoline	78	10	0	0
2-Oxypyridine					
	2-Methoxy-5-nitropyridine	56	0	64	100
	Isocarbostyrl	84	0	60	80
Pyridinium					
	1,1-Diethyl-4,4-carbocyanine iodide	67	95	100	0
	1,1-Diethyl-2,4-cyanine iodide	36	11	53	93
	Cetylpyridinium chloride monohydrate iodide	49	0	78	40
	2-Chloro-1-methylpyridinium iodide	49	5	0	83
	2-(4-(Dimethylamino)-styryl)-1-ethylpyridinium	30	10	89	13
	2-(4-(Dimethylamino)-styryl)-1-methylpyridinium	11	0	73	80
	Poly (4-Vinylpyridinium) dichromate	85	5	4	3
	5-Phenyl-2-(4-pyridyl) oxazole	76	20	0	0
	Bis-N-methyl acridinium nitrate	75	0	56	27
Pyrrrole					
	3-Ethyl-2-methyl-4,5,6,7-tetrahydroindol-4-one	93	25	11	0
	tert-Butyl-4-acetyl-3,5-dimethyl-2-pyrrole-carboxylate	71	0	9	3
	1-Phenylpyrrrole	71	0	9	3

¹ Final concentrations of modulator and ALA in treated diets were 4 mM and 3 mM (*T. ni*, *H. zea*), 6 mM and 8 mM (*A. grandis*), or 16 mM and 24 mM (*B. germanica*).

To strengthen our analysis of structure activity relationships, more intensive studies were conducted with subsets of compounds within each template. In particular, their tetrapyrrole modulating properties were determined. *T. ni* was used in all of these experiments because in the screening process it was susceptible to the widest range of modulators (Table X). Chemicals were incorporated into diet cubes to final concentrations of 4mM ALA and 3mM modulator. Twenty-six fourth instars were placed in each container and allowed to feed in the dark for 17 h. Subsequently, six larvae were assayed for tetrapyrrole accumulation, while the remaining 20 larvae were exposed to light and monitored for photodynamic mortality for six days.

Structure-Activity Relationships of Substituted Phenanthrolines. The porphyric insecticidal activity of OPh and eight of its analogs is summarized in Table XI. Mortality of *T. ni* larvae was highly correlated with Proto accumulation in darkness. Specifically, the highly significant enhancement of conversion of exogenous ALA to Proto by OPh, 4,7-dimethyl-OPh, 3,4,7,8-tetramethyl-OPh, 5-nitro-OPh, and 5-Chloro-OPh was accompanied by greater than 95% photodynamic larval mortality. Two modulators, 4,7-dimethyl-OPh and 5-nitro-OPh, also induced the formation of Proto in the absence of exogenous ALA. However, concentrations of Proto accumulated under these conditions, as well as larval mortality following exposure to light, were significantly less than those recorded in the presence of exogenous ALA.

The presence of N atoms at positions 1 and 10 of the OPh macrocycle were essential for porphyric insecticidal activity. This was evidenced by the limited activity of phenanthrene (Table XI), in which positions 1 and 10 are occupied by C atoms (Figure 1). The major changes caused by this substitution were increases in the charges at positions 1 and 10 of the macrocycle, the magnitude of the dipole moment, and in positive charge binding volumes at the nucleophilic pole of the molecule (Tables XII & XIII).

Peripheral methyl group substitutions to the OPh macrocycle (Figure 1) did not significantly reduce biological activity (Table XI). Although these substitutions did cause some changes in positive charge binding and repelling volumes, overall maintenance of positive charge binding volumes at the nucleophilic pole of each of five analogs (Table XIII) appeared to allow for continued insecticidal activity.

Insecticidal activity was also maintained when H or CH₃ groups were replaced by Cl or NO₂ groups at position 5 of the macrocycle (Figure 1, Table XI). These modifications caused profound changes that resulted in a reorientation of the dipole moment by about 150° and a redistribution of positive charge binding volumes toward position 5 of the macrocycle (Tables XII & XIII). In our opinion maintenance of porphyric insecticidal activity was largely associated with the preservation of relatively high positive charge binding volumes at the southern pole (i.e. position N1-N10) of the substituted molecules.

Substituting hydroxy for methyl groups at positions 4 and 7 of the OPh macrocycle (Figure 1) had a pronounced deleterious effect on biological activity (Table XI). The major changes associated with the hydroxy substitutions most likely to account for reduced activity were changes in the configuration of electrostatic fields at the C4-C7 region of the macrocycle. Specifically, the appearance of small positive charge binding volumes at positions 4 and 7 flanking larger positive charge repelling volumes at positions C4-C5 and C6-C7 (Table XIII).

Replacement of methyl with phenyl groups at positions 4 and 7 also had a negative effect on insecticidal activity (Table XI). This was somewhat surprising in that positive charge binding volumes were maintained at the nucleophilic pole of the molecule (Table XIII). However, their effect may have been counteracted by the

Table XI. Effect of ALA (4 mM), Phenanthrene (3 mM) and Substituted Phenanthrolines (3 mM) on Proto Accumulation and Larval Mortality in Third Instar *Trichoplusia ni*

<i>Treatment</i>	<i>Proto content (nmoles/100 mg protein)</i>	<i>Larval mortality after 6 days (%)</i>
Control (solvent only)	1.5a ¹	0.0a ²
ALA	3.0a	15.0abcd
2,9-Dimethyl-4,7-diphenyl-OPh	1.2a	0.0a
Above + ALA	1.6a	0.0a
2,9-Dimethyl-4,7-diphenyl-OPh-disulfonic acid	0.8a	0.0a
Above + ALA	2.6a	10.0abc
Phenanthrene	1.0a	0.0a
Above + ALA	3.9a	23.3bcd
4,7-Diphenyl-OPh	1.3a	0.0a
Above + ALA	8.6a	36.7cd
3,4,7,8-Tetramethyl-OPh	5.1a	11.7abcd
Above + ALA	117.0c	95.0e
4,7-Dimethyl-OPh	15.9a	8.3ab
Above + ALA	131.5c	96.7e
5-Chloro-OPh	2.0a	10.0abc
Above + ALA	133.9c	96.7e
5-Nitro-OPh	50.4b	41.7d
Above + ALA	190.1d	98.3e
1,10-Phenanthroline (OPh)	8.5a	6.7a
Above + ALA	207.0d	100e
Correlation coefficient ³		0.95
Level of significance		0.1%

SOURCE: Adapted from ref. 8.

¹ Means followed by the same letter within a column are not significantly different at the 5% level of significance.

² Percentage larval mortality was arcsine transformed prior to statistical analysis.

³ Correlation between mortality and Proto content.

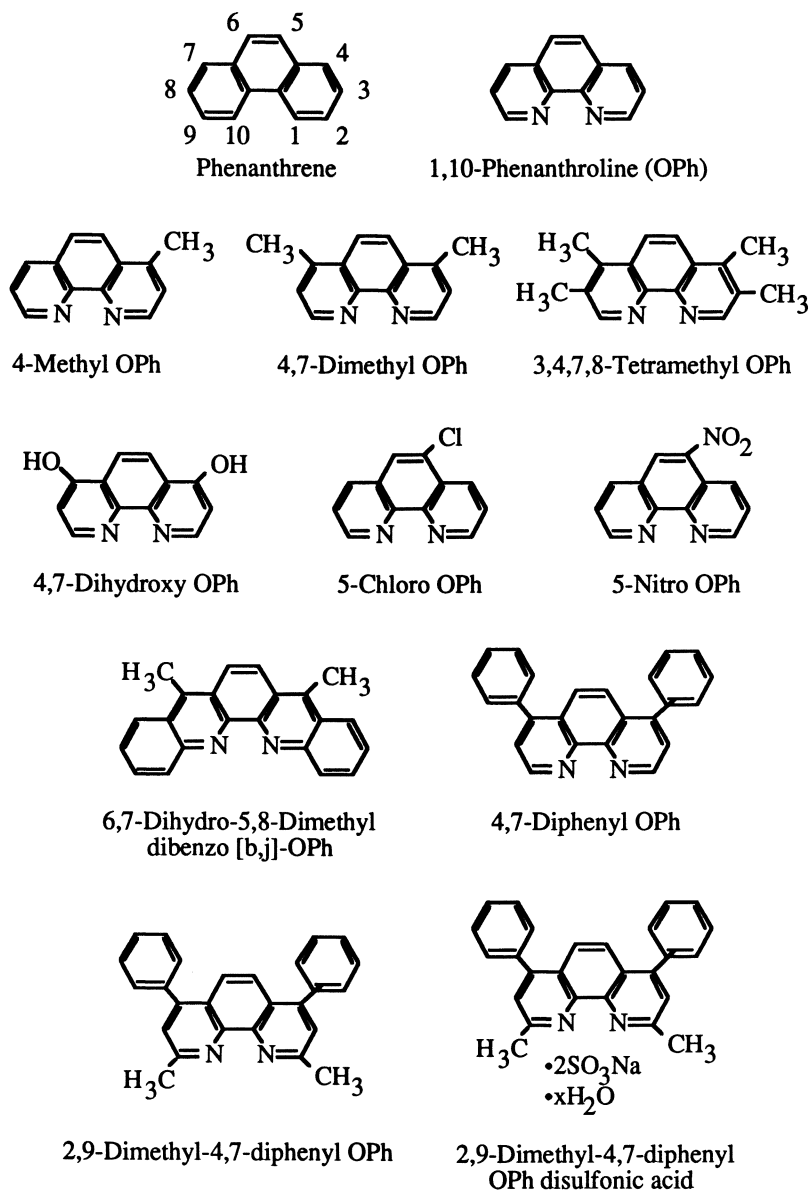


Figure 1. Chemical structures of Phenanthrene, 1,10-Phenanthroline, and various analogs of 1,10-Phenanthroline evaluated for insecticidal activity.

Table XII. Selected semi-empirical molecular and electronic properties^a of substituted phenanthrolines.

Modulator	VDWvol (Å ³)	DN ₁ N ₁₀ (Å°)	Chrgp1	Chrgp10	Dipole (D)	Sdunocmo (Kcal)	-Elstvol (Å ³)	+Elstvol (Å ³)
PHTN	142.5		-0.05	-0.05	0.04	0.45	102.5	11.2
OPh	139.4	2.78	-0.18	-0.18	2.83	0.79	146.0	22.5
4MOPh	153.3	2.76	-0.18	-0.18	2.84	0.93	149.2	22.5
5MOPh	153.3	2.76	-0.18	-0.18	2.79	0.86	150.2	22.5
56DMOPh	164.2	2.74	-0.18	-0.18	2.79	0.94	160.0	25.3
47DMOPh	168.8	2.74	-0.18	-0.18	2.87	1.09	157.2	25.3
3478TMOPh	202.9	2.73	-0.18	-0.18	2.82	1.25	181.1	28.1
47DOHOPh	153.0	2.73	-0.20	-0.20	3.66	1.38	144.6	53.3
47DPOPh	252.4	2.76	-0.18	-0.18	2.82	6.52	228.7	28.1
29DM47DPPh	286.5	2.75	-0.17	-0.17	2.94	5.69	255.5	26.3
56DH47DMDBOPh	257.8	2.66	-0.17	-0.17	2.32	4.88	227.4	33.7
5ClOPh	156.4	2.77	-0.18	-0.18	1.36	2.30	139.0	49.1
5NOPh	159.5	2.76	-0.18	-0.18	3.14	1.32	174.1	120.7

SOURCE: Adapted from ref. 8.

^a Listed properties were calculated using ChemX software. VDWvol = Van der Waals volume; DN₁N₁₀ = distance N₁N₁₀; Chrgp1, Chrgp10 = fractional charge at position 1 and 10, respectively, in units of electronic charge (a charge of -1 corresponds to the atom having gained an electron and being left with a residual charge of -1); Dipole = dipole moment in Debye; Sdunocmo = superdelocalisability (i.e. available electron density) over all unoccupied molecular orbitals in Kcal/mole⁻¹; -EpVol = overall volume of the negative molecular electrostatic field that attracts a unit positive charge with an energy of 10 Kcal/mole⁻¹; +EpVol = overall volume of the positive molecular electrostatic field that repulses a unit positive charge with an energy of 10 Kcal/mole⁻¹.

Table XIII. Distribution of Selected Positive Charge Binding and Repelling Electrostatic Exclusive Volumes of Various Phenanthrolines in Comparison to OPh^a.

<i>Modulator</i>	<i>Exclusive volumes (A²³)^b</i>											
	<i>C2- C9</i>	<i>C2- C3</i>	<i>C4</i>	<i>C4- C5</i>	<i>C5</i>	<i>C5- C6</i>	<i>C5- C9</i>	<i>C6- C7</i>	<i>C7</i>	<i>C7- C8</i>	<i>C8</i>	<i>C8- C9</i>
OPh	B36	R2	R5									R1
4MOPh			B10 R3									
5MOPh					B10 R3							
56DMOPh					R3	B16						
47DMOPh			R5					R5				
3478TMOPh			R3					R5			B5 R2	
47DOHOPh			B4	R8			R8	B4				
47DPOPh			B26 R8 B33				R3	B26 R8 B33	B26 R8 B33	-R2 -R4		
29DM47DPOPh					R2	-B7						B20 R10
56DH47DMDBOPh		B20 R10										
5CIOPh						B33 -R3	R4	R4	R4			
5NOPh	-B20	R12					R40					

SOURCE: Adapted from ref. 8.

^a Reference molecule for OPh was Phenanthrene.^b Exclusive volumes are on either side or orthogonal to the molecular plane at sites around the molecule indicated by atom numbers (i.e. C2, C3, etc.), or at sites indicated by a range of atoms (i.e. C2-C3, C4-C7, etc.). The atom numbering is the same as in Figure 1. B indicates the appearance of new positive charge binding volumes of a substituted molecule with respect to the reference molecule induced by a particular substitution; -B indicates a decrease in positive charge repelling volumes of a substituted molecule with respect to the reference molecule induced by a particular substitution; R indicates the appearance of new positive charge repelling volumes of a substituted molecule with respect to the reference molecule induced by a particular substitution; -R indicates a decrease in positive charge binding volumes of a substituted molecule with respect to the reference molecule induced by a particular substitution.

formation of well defined positive charge binding volumes at the 4 and 7 positions, the inhibitory effect of which was observed with 4,7-dihydroxy OPh. In addition, sizable increases in van der Waals volume and superdelocalisability over the unoccupied molecular orbitals (Table XII) may have inhibited porphyric insecticidal activity. Indeed substitutions of methyl groups to form 2,9-dimethyl-4,7-diphenyl OPh resulted in further increases in van der Waals volume and superdelocalisability over the unoccupied molecular orbitals, and consequently further reductions in insecticidal activity (Table XI). Similar effects were observed following benzyl substitution at the 2-3 and 8-9 positions, and reduction of the 5-6 bond to form 5,6-dihydro-4,7-dimethyl-dibenz OPh (Figure 1, Tables IX, XII, & XIII).

Structure-Activity Relationships of Substituted Pyridyls The porphyric insecticidal activity of DPy and eight of its analogs (Figure 2) is summarized in Table XIV. Photodynamic mortality of *T. ni* larvae again correlated highly with Proto accumulation in darkness. The highest levels of Proto accumulation occurred as a result of enhanced conversion of exogenous ALA to Proto. However, the two most active pyridyl modulators, DPy and 2,2':6'2"-terpyridine (Tpy), also induced the production of Proto.

DPy differs from OPh by the absence of the etheno-bridge, which is fused with rings A and B in OPh (Figure 2). This structural difference was accompanied by several physical-chemical alterations, including a smaller van der Waal volume, a larger negative 1,2,2',1' torsion angle, a smaller dipole moment, and smaller positive charge binding and repelling electrostatic volumes (Tables XV & XVI). These in turn were accompanied by changes in the distribution of positive charge binding and repelling electrostatic volumes. Because DPy was as potent a porphyric insecticidal modulator in the presence of ALA as OPh (Tables XI & XIV), physical differences between the two compounds did not appear to affect porphyric insecticidal activity.

Substitutions at the periphery of the DPy macrocycle (Figure 2), however, resulted in pronounced alterations in some physico-chemical properties and in porphyric insecticidal activity. As observed with OPh, the presence of N atoms at position 1 and 10 of the macrocycle appeared to be essential for activity. This was evidenced by a 30% reduction in activity of phenyl 2-pyridyl ketoxime with a N atom at position 1 and a carbon atom at position 10 as compared to dipyridyl ketoxime with 2 N atoms at position 1 and 10 (Figure 2, Tables IX & XIV). Insecticidal activity declined following 4,4'-dimethyl substitution and the associated appearance of small positive charge binding volumes at the C4 and C4'-C5' positions, flanked by positive charge repelling volumes at the C4,C4' positions (Tables XIV & XVI). As indicated previously, a similar electrostatic field profile for 4,7-dihydroxy-OPh also reduced insecticidal activity. The acquisition of a fourth phenyl or pyridyl ring which generated alternating positive charge binding and repelling electrostatic fields between rings C and D, as in 4,4'-Diphenyl-2,2'-DPy and 2,2"-Biquinoline, or a change in sign and magnitude of the 1,2,2',1' torsion angle as was observed with DPy disulfide, 2,2'-Dithiobis (5-nitropyridine) and Phenyl 2-pyridyl ketoxime also appeared to diminish activity (Tables XIV, XV, & XVI). The changes in electrostatic field profiles which accompanied changes in torsion angle direction and magnitude consisted in the appearance of positive charge repelling volumes at the C5'-C6; or C6' positions. Restoration of the torsion angle to negative values and disappearance of the positive charge repelling volumes at these positions, as in 2,2;Dithiobis (pyridine N-oxide) and di-2-pyridyl ketone oxime improved insecticidal effectiveness (Tables XIV, XV, & XVI).

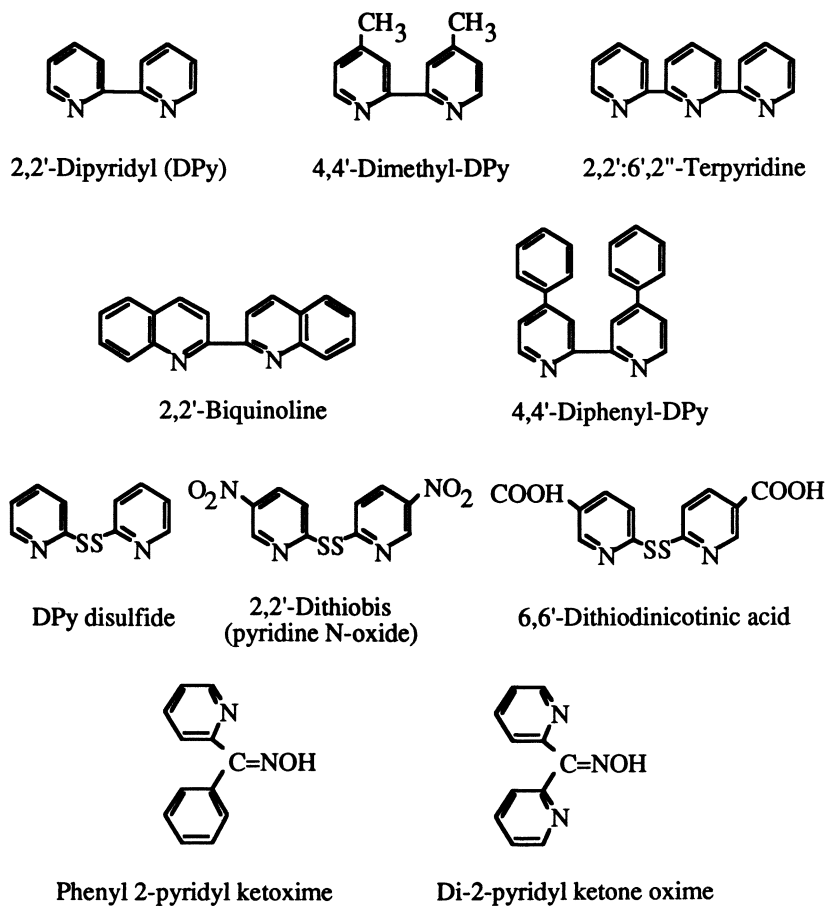


Figure 2. Chemical structures of 2,2'-Dipyridyl and various analogs of 2,2'-Dipyridyl evaluated for insecticidal activity.

Table XIV. Effect of ALA and Substituted Pyridyls on Proto Accumulation and Larval Mortality in Third Instar *Trichoplusia ni*

<i>Treatment</i>	<i>Proto content (nmoles/100 mg protein)</i>	<i>Larval mortality after 6 days (%)</i>
Control (solvent only)	0.9a ¹	0.0a ²
ALA	2.3a	1.7a
DPy disulfide	1.0a	0.0a
Above + ALA	1.6a	0.0a
2,2''-Biquinoline	0.9a	0.0a
Above + ALA	2.0a	0.0a
4,4'-Diphenyl-DPy	1.2a	1.7a
Above + ALA	2.3a	1.7a
2,2'-Dithiobis (5-nitropyridine)	0.7a	0.0a
Above + ALA	1.8a	5.0a
2,2'-Dithiobis (pyridine N-oxide)	0.7a	0.0a
Above + ALA	10.5a	56.7c
4,4'-Dimethyl-DPy	1.9a	0.0a
Above + ALA	18.1a	28.3b
Phenyl 2-pyridyl ketoxime	1.5a	1.7a
Above + ALA	21.9a	33.3b
2,2':6',2''-Terpyridine	6.2a	11.7a
Above + ALA	181.1b	98.2d
2,2'-Dipyridyl (DPy)	15.0a	48.3c
Above + ALA	176.3b	100d
Correlation coefficient ³		0.91
Level of significance		0.1%

¹ Means followed by the same letter within a column are not significantly different at the 5% level of significance.

² Percentage larval mortality was arcsine transformed prior to statistical analysis.

³ Correlation between mortality and Proto content.

Table XV. Selected semi-empirical molecular and electronic properties^a of substituted pyridyls.

<i>Modulator</i>	<i>VDWvol</i> (A^3)	<i>VDWen</i> (Kcal)	<i>Dp1p1'</i> (A°)	<i>Chrgp1p1'</i> (Deg)	<i>Tp1p1'</i> (Deg)	<i>Dipole</i> (D)	<i>Sdunocmo</i> (Kcal)	<i>-Elstvol</i> (A^{δ})	<i>+Elstvol</i> (A^{δ})
OPh	145.7	13.40	2.84	-0.10	-0.02	3.02	-0.18	234.5	73.5
DPy	122.1	12.78	3.02	-0.10	-57.08	2.84	-0.15	193.8	52.5
TPy	187.0	16.00	3.56	-0.13	-138.70	1.15	-0.23	267.8	66.6
44'DMDPy	152.9	-12.24	3.03	-0.11	-57.86	3.40	-0.19	233.1	45.7
BQ	206.6	11.30	3.03	-0.10	-59.63	2.45	-0.25	328.4	76.2
44'DDPpy	250.5	9.41	3.07	-0.11	-64.86	3.29	-0.31	359.4	85.5
DPYDS	157.4	10.17	4.74	-0.12	30.67	3.68	-0.22	204.4	72.2
22'DThPyNO	175.0	-25.53	5.31	0.36	-125.94	4.61	-0.22	260.8	125.9
22'DTh5NPY	194.6	13.94	6.25	-0.12	139.52	3.40	-0.25	280.2	280.2
Ph2PyKO	151.8	13.46	4.77	-0.12	-69.50	2.14	-0.20	213.8	54.2
Di2PyKtO	151.7	15.16	3.72	-0.11	155.13	2.87	-0.19	241.1	52.1

^a Listed properties were calculated using ChemX software. *VDWvol* = Van der Waals volume; *VDWen* = Van der energy; *N1N10*; *Chrgp1* = fractional charge at position 1 in units of electronic charge (a charge of -1 corresponds to the atom having gained an electron and being left with a residual charge of -1); *Tp1p1* = torsion angle for positions 1,2,1'2'; *Dipole* = dipole moment in Debye; *Sdunocmo* = superdelocalisability (i.e. available electron density) over all unoccupied molecular orbitals in Kcal/mole⁻¹; *-EpVol* = overall volume of the negative molecular electrostatic field that attracts a unit positive charge with an energy of 10 Kcal/mole⁻¹; *+EpVol* = overall volume of the positive molecular electrostatic field that repulses a unit positive charge with an energy of 10 Kcal/mole⁻¹.

Table XVI. Distribution of Selected Positive Charge Binding and Repelling Electrostatic Exclusive Volumes of Various Dipyriddyis in Comparison to DPy^a.

Modulator	<i>Exclusive volumes (Å³)^b</i>													
	N1- N1'	N1- C6	C3- C3'	C4- C4'	C5,5'- NO ₂	C5'- C6'	PR A	R B	PR B	R C	PR C	R D	PR D	
DPy	B15		B17	-R27										
TPy							R4	-B24		B45	R8			
44DMDPy				B3 R3										
44DPDPy										B23	R23	B23	R23	
Biq										B14	R17	B14	R17	
DPyDS						-R11		-B18 B28	R17					
22Dth5NPy								-B13						
	B16	R14			B81	R28								
22DthPyNO								-B15	-R7					
		B8						B40	R30					
Di2PyKeto								-B8						
								B21	R17					
Ph2PyKeto						R14		B22						

^a Reference molecule for DPy was OPh.

^b Exclusive volumes are on either side or orthogonal to the molecular plane at sites around the molecule indicated by atom numbers (i.e. C2, C3, etc.), or at sites indicated by a range of atoms (i.e. C2-C3, C4-C7, etc.). The atom numbering is the same as in figure 1. B indicates the appearance of new positive charge binding volumes of a substituted molecule with respect to the reference molecule induced by a particular substitution; -B indicates a decrease in positive charge repelling volumes of a substituted molecule with respect to the reference molecule induced by a particular substitution; R indicates the appearance of new positive charge repelling volumes of a substituted molecule with respect to the reference molecule induced by a particular substitution; -R indicates a decrease in positive charge binding volumes of a substituted molecule with respect to the reference molecule induced by a particular substitution.

Structure-Activity Relationships of Substituted Quinolines and OxyPyridines.

The structure activity relationships of four substituted 8-hydroxyquinolines (Table XVII) and two substituted oxypyridines (Table XVIII) were investigated. Porphyric insecticidal effects were positively correlated with Proto accumulation. Achieving significant activity required treatment with both modulator and exogenous ALA. The parent compound, 8-Hydroxyquinoline, and the NO₂⁻ substituted analog, 8-hydroxy-5-nitroquinoline (Figure 3), were inactive. However, substantial insecticidal effects were recorded when the nitro group was replaced by a sulfo group, forming 8-hydroxyquinoline-5-sulfonic acid. Further substitution with a 4-sulfo-1-naphthylazo group at position 7 to form 8-hydroxy-7-(4-sulfo-1-naphthylazo)-5-quinoline sulfonic acid, only resulted in a minor reduction in activity. For the compounds tested, the presence of a sulfonyl group at position 5 of the 8-hydroxyquinoline macrocycle (Figure 3) was required for expression of porphyric insecticidal activity. The main effect of sulfonyl substitution was a significant increase in the electrostatic positive charge binding volumes around the sulfonic acid group (Table XVIII).

Moving the exocyclic OH group to position 1 and the endocyclic N atom to position 2 to form the oxypyridine compound, isocarbostryl (Figure 3), also resulted in substantial insecticidal activity in comparison to 8-hydroxyquinoline (Tables XVII & XIX). QSAR analysis revealed an increase in the magnitude of the dipole moment from 2.33 to 3.53 D and an increase in electron density in the unoccupied molecular orbitals from 0.16 to 0.23 kcal/mole. In contrast, further substitution of a hydroxyl group at position 5 to form 1,5-isoquinolinediol (Figure 3) decreased the dipole moment but increased the electron density in the unoccupied molecular orbitals (Table XVIII). These changes were accompanied by a significant reduction in porphyric insecticidal activity (Table XIX).

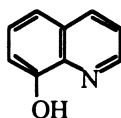
Table XVII. Effect of ALA and Substituted Quinolines on Proto Accumulation and Larval Mortality in Third Instar *Trichoplusia ni*

<i>Treatment</i>	<i>Proto content (nmol/100 mg protein)</i>	<i>Larval mortality after 6 days (%)</i>
Control (solvent only)	1.0b ¹	0.0a ²
ALA	1.7c	0.0a
8-Hydroxyquinoline	1.0b	0.0a
Above + ALA	1.9c	0.0a
8-Hydroxy-5-nitroquinoline	0.7a	0.0a
Above + ALA	3.0d	0.0a
8-Hydroxy-7-(4-sulfo-1-naphthylazo)-5-sulf acid	1.8c	1.7a
Above + ALA	41.8g	76.7b
8-Hydroxyquinoline-5-sulfonic acid	1.8c	0.0a
Above + ALA	32.1f	81.7b
Correlation coefficient ³		0.85
Level of significance		1%

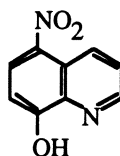
¹ Means followed by the same letter within a column are not significantly different at the 5% level of significance.

² Percentage larval mortality was arcsine transformed prior to statistical analysis.

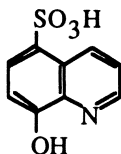
³ Correlation between mortality and Proto content.



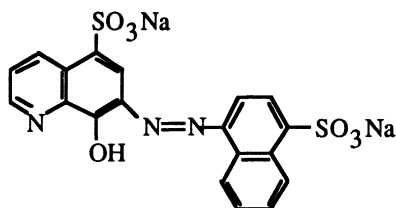
8-Hydroxyquinoline



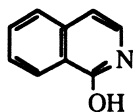
8-Hydroxy-5-nitroquinoline



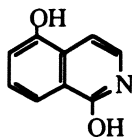
8-Hydroxyquinoline-5-sulfonic acid



8-Hydroxy-7-(4-sulfo-1-naphthylazo)-5-quinoline sulfonic acid



Isocarbostyryl



1,5-Isoquinolinediol

Figure 3. Chemical structures of various quinolines and oxypridines evaluated for insecticidal activity.

Table XVIII. Selected semi-empirical molecular and electronic properties^a of OPh related modulators.

<i>Modulator</i>	<i>VdwVol</i> (Å^3)	<i>ChrgP1</i>	<i>Dipole</i> (<i>D</i>)	<i>SdUnoc</i> (<i>EV</i>)	<i>-Elstvol</i> (Å^3)	<i>+Elstvol</i> (Å^3)
8OHQUIN	103.3	-0.24	2.33	0.16	89.7	23.2
8OH5NQUIN	120.9	-0.24	4.08	2.12	165.0	108.1
8OHQUIN5SA	140.9	-0.24	4.96	0.06	207.4	145.0
8OHSUNQUIN	466.9	-0.25	8.06	0.29	434.0	242.7
ICBS	113.4	-0.25	3.53	0.23	100.3	32.9
15IQD	119.7	-0.25	2.21	0.37	94.3	41.1
11D24CyI	275.3	-0.19	5.11	-2.04		233.2
11D44CBCyI	290.5	-0.25	2.88	1.65		145.3
13SPRPYOH	139.8	-0.19	17.03	0.48		13.9
EM4567THYDRO	147.7	-0.19	4.67	1.03	132.2	61.8
TBAC35M2PYBC	192.1	-0.17	4.93	2.03	175.7	92.7
4567THYDR	103.3	-0.20	1.82	0.52	61.8	16.4

^a Listed properties were calculated using ChemX software. VDWvol = Van der Waals volume; Chrgp₁ = fractional charge at position 1 in units of electronic charge (a charge of -1 corresponds to the atom having gained an electron and being left with a residual charge of -1); Dipole = dipole moment in Debye; Sdunocmo = superdelocalisability (i.e. available electron density) over all unoccupied molecular orbitals in Kcal/mole⁻¹; -EpVol = overall volume of the negative molecular electrostatic field that attracts a unit positive charge with an energy of 10 Kcal/mole⁻¹; +EpVol = overall volume of the positive molecular electrostatic field that repulses a unit positive charge with an energy of 10 Kcal/mole⁻¹.

Structure-Activity Relationships of Substituted Pyridiniums The structure activity relationships of four substituted pyridiniums was investigated. 1,1'-diethyl-2,4-cyanine iodide was a highly potent enhancer and inducer of Proto accumulation (Table XIX). As expected, treatment of *T. ni* with this modulator was accompanied by significant levels of photodynamic insecticidal activity. Treatment with 1,1'-diethyl-4,4-carbocyanine iodide resulted in even higher levels of mortality, but they did not appear to be entirely related to the degree of Proto production. Total loss of activity was observed in 1-(3-sulfopropyl) pyridinium hydroxide. QSAR analysis of this compound revealed a 3.3 fold increase in the value of its dipole moment in comparison to highly active, 1,1'-diethyl-2,4'-cyanine iodide (Table XVIII). The presence of a sulfonyl group at the N+ position also resulted in a substantial increase in positive charge binding volumes and a substantial decrease in positive charge repelling volumes relative to the two active pyridiniums. We suspect that the presence of an unbalanced positive charge at the N+ position was critical for insecticidal activity of pyridiniums. This was corroborated by the reduced activity of Bis-N-methylacridinium nitrate which has an NO₃⁻ counterion (Figure 4).

Structure-Activity Relationships of Substituted Pyrroles The structure activity relationships of three substituted pyrroles was investigated (Table XIX). Highly substituted pyrroles such as tert-butyl 4-acetyl-3,5-dimethyl-2-pyrrole-carboxylate

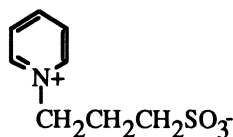
Table XIX. Effect of ALA and Substituted 2-Oxypyridines, Pyridiniums and Pyrroles on Proto Accumulation and Larval Mortality in Third Instar *Trichoplusia ni*

<i>Treatment</i>	<i>Proto content (nmol/100 mg protein)</i>	<i>Larval mortality after 6 days (%)</i>
Control (solvent only)	1.4abc ¹	1.7a ²
ALA	2.2bcd	3.3a
1,5-Isoquinolinediol	1.0a	1.7a
Above + ALA	3.7de	33.3b
Isocarbostyryl	1.2ab	1.7a
Above + ALA	16.3fg	86.7cd
1-(3-Sulfopropyl) pyridinium hydroxide	2.4cd	0.0a
Above + ALA	4.4de	0.0a
Bis-N-methylacridinium nitrate	5.6e	21.7b
Above + ALA	10.9f	65.0c
1,1'-Diethyl-2,4'-cyanine iodide	58.1h	75.0c
Above + ALA	87.0h	85.0cd
1,1'-Diethyl-4,4'-carbocyanine iodide	3.5a	96.7d
Above + ALA	21.9g	93.3d
4.5.6.7-Tetrahydroindole	1.3abc	1.7a
Above + ALA	2.6cd	1.7a
tert-Butyl 4-acetyl-3,5-dimethyl-2-pyrrole-carbox	1.3abc	0.0a
Above + ALA	2.7d	20.4b
3-Ethyl-2-methyl-4,5,6,7- tetrahydroindole-4-one	0.9a	0.0a
Above + ALA	10.0f	83.3cd
Correlation coefficient ³		0.76
Level of significance		0.1%

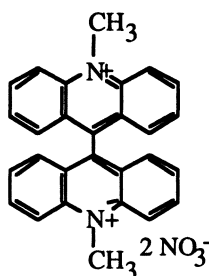
¹ Means followed by the same letter within a column are not significantly different at the 5% level of significance.

² Percentage larval mortality was arcsine transformed prior to statistical analysis.

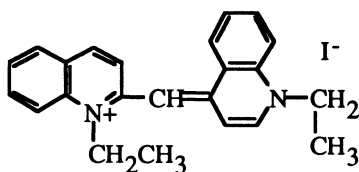
³ Correlation between mortality and Proto content.



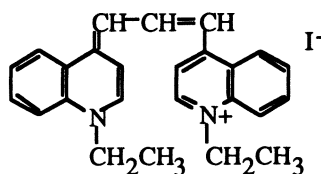
1-(3-Sulfopropyl)pyridinium hydroxide



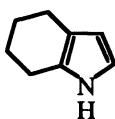
Bis-N-methylacridinium nitrate



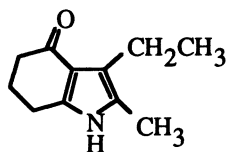
1,1'-Diethyl-2,4'-cyanine iodide



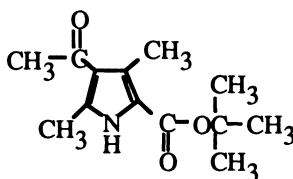
1,1'-Diethyl-4,4'-carbocyanine iodide



4,5,6,7-Tetrahydroindole



3-Ethyl-2-methyl-4,5,6,7-tetrahydroindole-4-one



tert-Butyl-4-acetyl-3,5-dimethyl-2-pyrrole-carboxylate

Figure 4. Chemical structures of various pyridinium ions and pyrroles evaluated for insecticidal activity.

exhibited minimal insecticidal activity. In contrast, tetrahydroindoles with an isolated keto group at position 4, such as 3-ethyl-2-methyl-4,5,6,7-tetrahydroindol-4-one, were active modulators. However, removal of the ketone group, as in 4,5,6,7-tetrahydroindole, resulted in a complete loss of activity. This was accompanied by substantial reductions in electron density in the unoccupied molecular orbitals and in volumes of the positive charge binding electrostatic field (Table XVIII).

Summary and Conclusions

A variety of synthetic compounds can effectively induce, and in the presence of ALA, enhance the accumulation of lethal amounts of photosensitizing Proto and Zn-Proto in insects. Insecticidally active compounds were identified from seven chemical families or templates. Because their mode of action entails the production of porphyrins, we have termed these compounds, porphyric insecticides. Quantitative structure-activity calculations indicated a relationship between insecticidal activity and some physico-chemical properties of the active modulator. The arrangement of positive charge binding and repelling volumes appeared to be particularly important. Future research on structure-activity relationships may enable us to identify compounds that are selectively toxic to insects or to particular groups of insects.

Acknowledgments

We thank Carol A. Rebeiz and Carl E. Bouton for their contributions to the research presented herein. This work was supported by funds from the Illinois Agricultural Experiment Station and by the John P. Trebellas photobiotechnology research endowment to C. A. Rebeiz.

Literature Cited

1. Rebeiz, C.A.; Montazer-Zouhoor, A.; Mayasich, J. M.; Tripathy, B. C.; Wu, S. M.; Rebeiz, C. C. In *Light Activated Pesticides*; Heitz, J. R.; Downum, K. R., Eds.; ACS Symposium Series 339; Washington, D. C., 1987; 295-328
2. Rebeiz, C.A.; Montazer-Zouhoor, A.; Mayasich, J. M.; Tripathy, B. C.; Wu, S. M.; Rebeiz, C. C. *Crit Rev. Plant Sci.* **1988**, *6*, 385-436.
3. Rebeiz, C.A.; Reddy, K. N.; Nandihalli, U. B.; Velu, J. *Photochem. Photobiol.* **1990**, *52*, 1099-1117.
4. Rebeiz, C.A.; Nandihalli, U. B.; Reddy, K. N. In *Herbicides*, Baker, N. R.; Percival, M., Eds.; Elsevier, Amsterdam, 1991; 173-208
5. Rebeiz, C. A.; Juvik, J. A.; Rebeiz, C. C.; *Pesticide Biochem. Physiol.* **1988**, *30*, 11-27.
6. Rebeiz, C. A.; Juvik, J. A.; Rebeiz, C. C.; Bouton, C. E.; Gut, L. J.; *Pesticide Biochem. Physiol.* **1990**, *36*, 201-207.
7. Lamola, A.A.; Yamane, T.; *Science.* **1974**, *186*, 936.
8. Gut, L. J.; Lee, Keywan; Juvik, J. A.; Rebeiz, C. C.; Bouton, C. E.; Rebeiz, C. A.; *Pesticide Sci. Physiol.* **1993**, *39*, 19-30.

RECEIVED February 16, 1994

Chapter 16

Porphyrins as Chemotherapeutic Agents

Biochemistry of Protoporphyrin IX Accumulation in Mammalian Cells

Natalie Rebeiz¹, Keith W. Kelley¹, and Constantin A. Rebeiz²

¹Department of Animal Sciences, University of Illinois,
Urbana, IL 61801

²Laboratory of Plant Pigment Biochemistry and Photobiology, 240A Plant
and Animal Biotechnology Laboratory, University of Illinois, 1201 West
Gregory Avenue, Urbana, IL 61801-4716

The induction of endogenous protoporphyrin IX (Proto) in neoplastic cells by the porphyrin precursor δ -aminolevulinic acid (ALA) and 1,10-phenanthroline (Oph) results in rapid cell photolysis. Exogenous porphyrins have previously been studied as potential chemotherapies, because of their ability to induce the formation of reactive oxygen intermediates, which cause cell death and tumor necrosis. This ability arises from the photophysical nature of porphyrin molecules. Exogenous porphyrins, however, cannot penetrate well into solid tumors and can also cause necrosis of healthy tissue. Since all eukaryotic cells have mitochondria, and thus have the potential to synthesize Proto for heme or cytochrome production, we investigated the possible use of ALA to induce the formation of endogenous Proto in mammalian cells. Addition of the porphyrin biosynthesis modulator Oph dramatically increased the amount of Proto accumulation and cell photolysis in ALA treated cells. Differential susceptibility was observed in three treated neoplastic cell lines, with little Proto accumulation occurring in normal cells.

Tetrapyrroles in Nature

Two tetrapyrroles, heme and chlorophyll, are essential for the maintenance and continuity of life. Chlorophyll catalyzes the conversion of solar energy, water and carbon dioxide to chemical energy in the process of photosynthesis. Plants convert this chemical energy into food and organic matter, while releasing oxygen into the atmosphere. Heme, the prosthetic group of hemoglobin and cytochromes, is involved either as an oxygen-carrier (hemoglobin) or in electron transport (cytochromes).

0097-6156/94/0559-0233\$08.00/0
© 1994 American Chemical Society

Structure and Function. Tetrapyrroles are macrocyclic structures comprised of four pyrrole rings, with alternating double bonds (Figure 1). The four pyrrole rings are linked by methene bridges, forming a tetrapyrrole ring. Side chain substitutions result in many different tetrapyrroles. Heme and chlorophyll are the two major tetrapyrroles of protoplasm, derived from the same precursor, protoporphyrin IX (Proto). The heme and chlorophyll biosynthetic pathways diverge after Proto formation. However, the functions of these compounds are quite similar. Heme is a catalyst for respiration, releasing energy stored in covalent bonds. Chlorophyll serves as a catalyst in the conversion of solar energy to chemical energy which is stored in covalent bonds. The Mg^{++} and Fe^{++} prosthetic groups have the redox properties needed for catalyzing the formation of charge separation within the tetrapyrrole molecule, thus rendering the molecule highly reactive. Porphyrin molecules also have photochemical properties that allow them to absorb light and fluoresce in the red region of the visible spectrum (1).

Protoporphyrin IX Biosynthetic Pathway. The first precursor in the synthesis of Proto is ALA. ALA is formed by condensation of succinyl coenzyme A and glycine. In animals and lower plants, such as algae and photosynthetic bacteria, this reaction is catalyzed by ALA synthetase [ALAS; succinyl-CoA: glycine c-succinyl transferase (decarboxylating EC 2.3.1.37)] (2). The mRNA for ALAS is encoded by one or more nuclear genes, and has been studied widely in the chicken. It is translated in the cytoplasm and the precursor form is post-translationally imported into the mitochondria, where it is proteolytically cleaved by its processing enzyme. In the mitochondria, the enzymatic activity is found in the intraorganellar compartment, i.e. the matrix (3). The enzyme ALAS is expressed in all animal tissues, but is found most abundantly in erythroid and liver cells because high levels of heme are needed by these cells for hemoglobin and cytochrome p-450 synthesis, respectively. Riddle et al. (4) studied the ALAS gene in chickens, and found that two genes encoded the ALAS isozymes. One form was expressed exclusively in erythroid cells (ALAS-E), whereas the hepatic form was expressed ubiquitously in all chicken tissues. They also found that neither the erythroid gene nor the enzyme were influenced by regulatory mechanisms operating on the hepatic form, such as negative feedback by heme.

Figure 2 depicts the biosynthesis of Proto from ALA. δ -Aminolevulinic acid dehydratase (ALA-D), the second enzyme in the pathway, catalyzes the condensation of two molecules of ALA to form porphobilinogen (PBG) via Schiff base formation, with the elimination of two water molecules. The ALA-D protein is 31 kd, with eight subunits, and is localized in the mitochondria. A lysine residue is involved in the catalytic site, and Zn is required as a cofactor (5). cDNA clones isolated from rat and human liver (6,7) show 86% homology. ALA-D is encoded by one open reading frame of 990 bases. Data are not currently available on ALA-D genomic structure. Formation of uroporphyrinogen (Urogen), the next precursor in the pathway, involves two enzymes. PBG deaminase, also called hydroxymethylbilane synthase (HMB synthase, EC 4.3.1.8), is involved in head to tail condensation of four PBG molecules. Uroporphyrinogen III

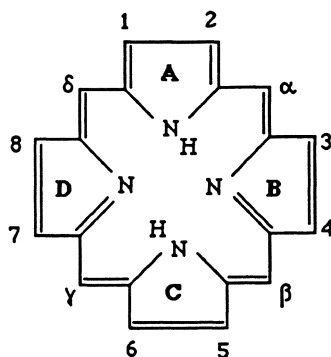


Figure 1. The structure of a tetrapyrrole molecule. The four pyrrole rings are labelled A-D. The methine bridges which connect the pyrrole rings are labelled α - δ . At the numbered positions, substitutions of different side chains leads to the formation of different porphyrins. Protoporphyrin IX: 1-methyl, 2-vinyl, 3-methyl, 4-vinyl, 5-methyl, 6-propionic, 7-propionic and 8-methyl.

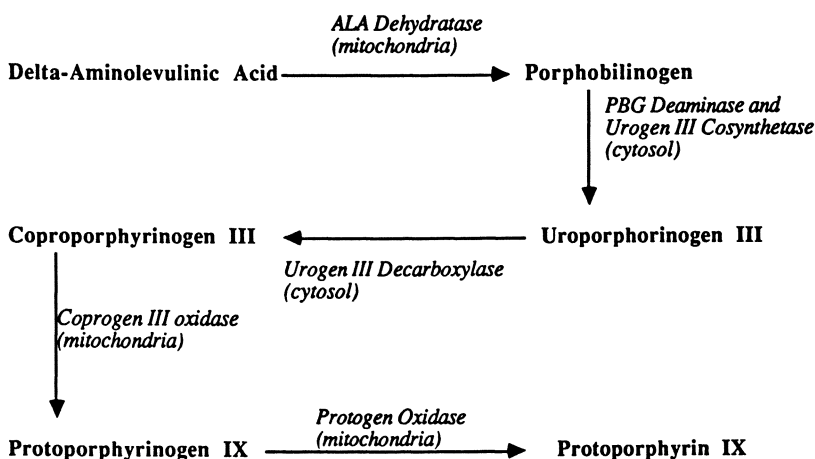


Figure 2. Biosynthesis of Protoporphyrin IX from ALA. In parentheses are the location of each enzyme within the cell, as proposed by Granick (1).

cosynthetase, the second enzyme, cyclizes the molecule to form uroporphyrinogen III (Urogen; 8). Whether these enzymes work independently or in a complex is unknown. PBG deaminase, a cytosolic enzyme, has been isolated from rat (9), mouse (10) and human (11) cells. There are both erythroid and non-erythroid forms of the enzyme. The erythroid form of the protein is 344 amino acids, and the non-erythroid form contains an additional 17 amino acids at the amino terminus (12). Studies of human cells indicated that the levels of PBG deaminase mRNA are modulated positively, both by the erythroid nature of the tissue and by cell proliferation (13). Uroporphyrinogen III cosynthetase (Uro-S, cyclizing enzyme, EC 4.2.1.75) is found in the cytosol. Without this enzyme, HMB forms Urogen I, a non-physiological isomer of Urogen III, non-enzymatically (14). Tsai et al., (15) cloned the human Uro-S gene. The protein is a monomer of 29.5 kd. The cDNA is 1.3 kb, and has one open reading frame which encodes a polypeptide of 265 amino acids. Little else is known about its gene structure or regulation in heme biosynthesis.

After Urogen III formation, the last cytosolic enzyme Urogen III decarboxylase (Uro-D), successively decarboxylates all four acetic acid side chains of Urogen III to yield coproporphyrinogen III (Coprogen III; 16). The catalytic site(s) is unknown but there are no cofactors involved with this decarboxylase. Uro-D is a single polypeptide of 367 amino acids, with a molecular weight of 40 kd (17), and is encoded by a gene of 10 exons spread over 3 kb of DNA. There are no Uro-D isozymes since Uro-D mRNA is identical in all human cell types examined (18).

Corprotoporphyrinogen III oxidase (EC 1.3.3.3) is located in the intermembrane space of mitochondria (19). This enzyme catalyzes the decarboxylation and oxidation of propionic acid side chains in rings A and B of Coprogen III to vinyl groups, yielding Protogen IX. The protein has been isolated from yeast, and from both bovine and murine liver (20). The proteins purified from all these sources are approximately 70 kd. There is some controversy as to whether the enzyme is a monomer or dimer. The isolation and characterization of cDNAs has not been reported, and molecular regulation of the gene in mammals has not yet been elucidated.

Protoporphyrinogen oxidase (Protogen oxidase; EC 1.3.3.4) catalyzes the penultimate step in heme biosynthesis. Protoporphyrinogen IX is oxidized to protoporphyrin IX by removal of six hydrogen molecules by Protogen oxidase (21). The enzyme is strongly bound to the inner mitochondrial membrane, with its active site facing the cytosol (22). Protogen oxidase has a molecular weight of 65 kd, and contains one subunit. As with most of the other enzymes involved in the synthesis of Proto, information about protogen oxidase regulation, gene structure or chromosomal location is not yet available.

Intracellular Localization of Heme Biosynthesis. The intracellular site of heme biosynthesis has been investigated by Granick (1). Using ox liver mitochondria, Granick proposed the following scheme: ALA is formed in the mitochondria and then translocates out of the mitochondria into the cytoplasm. In the cytoplasm, ALA is converted to Coprogen III. Coprogen III translocates back into the

mitochondrion where it is converted to Proto and heme. While this hypothesis has been popular for many years, it is beset with problems. Translocations into and out of the mitochondria are energetically wasteful. Secondly, since no evaluation of mitochondrial breakage during mitochondria isolation has been provided, it is difficult to evaluate contamination of the cytoplasm by mitochondrial stroma.

Photophysical and Photodynamic Properties of Porphyrins. Due to their structure, porphyrins have unique photophysical properties. Alternating double bonds around the four pyrrole rings results in a conjugated 18π electron system that give the macrocycle high stability (24). The double bond system is not at any fixed location. Thus, no bond is really single or double, but all bonds are hybrids of the two. From the view of molecular orbital theory, the stability is due to the delocalization of one π electron pair from each double bond over the whole conjugated system of molecular orbitals. When the conjugated atoms are in the same plane, the molecular orbitals overlap maximally. Since the porphyrin molecule is square planar (10 \AA wide), the net result is that the π electrons overlap and circulate all over the molecule, so that each resonance structure has equal energy and assumes maximum stability.

The photodynamic effect of porphyrins is due to their photoexcitable nature. The basic process can be summarized as follows (26). The ground state sensitizer (porphyrin) molecule is photoexcited to the first singlet state, S^1 . Next, intersystem crossing of an electron from the excited singlet state to the excited triplet state (S^3) occurs. Porphyrins are efficient generators of triplet excitation because they have a relatively small energy gap between the lowest singlet and triplet states and exhibit high intersystem crossing efficiencies (27). The excited triplet state has lower energy than the singlet state, but has a longer half-life. At this point, the excited triplet sensitizer may undergo one of two reactions. A type I reaction will occur when the excited triplet sensitizer reacts directly with a substrate molecule by hydrogen abstraction or electron transfer, to produce a reactive radical species, such as a lipid radical. These radicals can interact with oxygen to produce superoxide anion or hydroxy radical. A substrate molecule could be an amino acid residue of a protein, bases in nucleic acids, or lipids in membranes. A type II reaction leads to the formation of singlet oxygen, when the excited triplet sensitizer interacts with ground state triplet oxygen, to produce excited singlet oxygen. Singlet oxygen is extremely reactive, and will attack electron rich substrates to yield peroxides and other oxidized species.

The overall effect of these oxidized species is disturbances in metabolism, mutations or membrane defects. Cells can protect themselves from the detrimental effects of reactive oxygen intermediates with the help of scavengers such as myeloperoxidase, glutathione, superoxide dismutase, and catalase (26).

Use of Porphyrins in Chemotherapy

The photoactivation of photosensitizers to the triplet state and their reaction with oxygen to produce singlet oxygen and free radicals have made them ideal for studies of cytotoxic activity toward tumor cells and viruses. Sensitizers include

a variety of compounds, such as acridines, xanthenes, and porphyrins. Upon activation by light, these photosensitizers cause the oxidation of proteins, unsaturated fatty acids, cholesterol, and nucleic acids (28). As a consequence, a combination of catabolic effects leads to damage and inactivation of cells.

In 1978, Dougherty et al. (29) observed that upon injection of hematoporphyrin derivative (HpD), a chemically synthesized porphyrin molecule, this compound accumulated to higher concentrations in malignant tissue than in most normal tissues. This finding constituted the basis for the use of porphyrins, and specifically HpD, in photoradiation cancer therapy. This field of research is termed photodynamic therapy (PDT), and has concentrated primarily on hematoporphyrin (Hp) and its derivatives, such as dihydrohematoporphyrin ester (DHE) and the commercially available Photofrin I and II (which are patented derivatives of Hp), now used in clinical trials (30). Other porphyrins and related compounds from plant and animal sources have been considered as possible chemotherapeutic agents. Chlorins, psoralens, heme proteins and synthetic porphyrin derivatives have all received attention. It has been shown that these compounds act via different mechanisms because of inherent chemical properties that allow them to localize in different cell compartments (30).

Cellular Damage Produced by Porphyrins. Cell membrane damage by photosensitizing porphyrins is now acknowledged as the major photodynamic action in the light. Hp has been shown to cause deformation of cell membranes. Proto produces large holes in cell membranes, as shown by scanning electron microscopy (31). To study molecular damage caused by photosensitizers, experimental work has concentrated on erythrocytes. Proto was shown to crosslink protein components in erythrocyte membranes. Peroxidation of unsaturated membrane lipids occurred prior to protein denaturation (32).

The kinetics of porphyrin uptake are also important in determining the type of damage that may occur. The consensus is that short incubations (1 h or less) induce cell membrane damage, while longer incubations (> 2 h) induce nuclear damage (33). Kessel (33) used the mouse lymphocytic leukemic L1210 cell line to show that during a 10 min incubation, photosensitization increased with increased hydrophobicity of the sensitizer. Sensitizers were easily removed by washing with serum containing medium. Hydrophilic sensitizers gradually bound during longer incubations (24 h) to low molecular weight membrane components.

More recently, attention has centered on the mitochondria as an important site for porphyrin accumulation and damage. Dellinger et al. (34) studied the effect of Photofrin II, HpD, HVD (hydroxyethyldeuteroporphyrin), and Proto on isolated mitochondria. The results showed that mitochondrial membranes were less selective in their uptake of porphyrins, and accumulated more porphyrins than cytoplasmic membranes. At high concentrations, (about 9 nmol/mg of protein), porphyrins induced mitochondrial damage in the absence of light. This effect had been reported earlier with both Proto and deuteroporphyrin (35). Dellinger et al.'s results indicate that selective uptake of porphyrins is regulated at the plasma membrane level and this in turn determines the amount of photosensitizer that reaches the relatively unselective mitochondria.

The mechanism of cytotoxicity of sensitizers on mitochondrial membranes has also been addressed. Recent work suggests that the energy deficit caused by inhibition of mitochondrial respiration and uncoupling of oxidative phosphorylation by HpD might be responsible for tumor necrosis (36). The effects of HpD on energy metabolism occurred in both darkness and in the light. In darkness, HpD significantly affected cellular energy metabolism. Cytochrome c oxidase activity decreased and glucose utilization and lactate production, via glycolysis, increased (37). This may have been a response to inhibition of cellular respiration. Illumination of the treated cells caused inhibition of both glycolysis and respiration, which probably led to loss of cell viability.

Exogenous Porphyrins in Photodynamic Therapy. The use of HpD and other synthetic porphyrins in photodynamic therapy has drawbacks, such as impaired uptake in cells and tissues. In malignant tissues, HpD is not retained in the tumor cells, but rather in the vasculature (38). Vascular collapse is the first observed effect upon laser illumination of HpD treated malignant tissue. However, HpD accumulation in the vascular system may be associated with the high affinity of porphyrins for lipids, which may be present in higher concentrations in vascular endothelium. Serum albumin strongly binds porphyrins, and albumin may change porphyrin photophysical properties within tissues and cells (39).

Recent studies have demonstrated that photodynamic therapy with HpD can induce a variety of immunosuppressive states. Canti et al. (40) demonstrated decreased murine lymphocyte blastogenic responses to the mitogen PHA after treatment *in vitro* with HpD followed by illumination of the cells. The *in vitro* inhibition of cytotoxic T lymphocyte and natural killer (NK) cell activity by HpD and light treatment was shown by Franco et al. (41). Reports to the contrary can also be found in the literature. Marshall et al. (42) reported very little suppression of anti-tumor activity by cytotoxic lymphocytes, NK cells and phagocytes in mice after HpD injection intra-peritoneally and laser light treatment *in vivo*. However, Gomer et al. (43) showed a complete, but transitory, suppression of NK cell activity in mice treated with HpD and light. The question of whether porphyrins induce immunosuppression is still debated, with few results pointing to an unequivocal answer.

Another problem associated with photodynamic therapy is that normal tissues can accumulate porphyrins and are subsequently damaged (44). HpD is taken up by a variety of tissues, such as liver, spleen, muscle, skin, lung, and blood. Similarly, brain tissue appears to accumulate porphyrins, although some studies have shown that there is a threshold level below which no lesions are detected in the brain (45). Again there is controversy over this issue since some investigators have found significant damage to normal brain cells after injection with HpD and light treatment (46). When HpD is injected into mice, a large quantity is excreted into the urine and feces 48 h after injection (47). Even if the tumor alone is subjected to illumination, the surrounding tissue can be damaged, and the patient becomes sensitive to light for at least 24 h after treatment.

An ideal chemotherapy requires that a chemical be able to pervade a tumor, destroy the tumor without killing normal cells, and have little toxic side

effects. For the reasons stated above, exogenously applied porphyrins are not as well suited for chemotherapy as previously suggested. However, endogenously induced porphyrins appear to have some of the qualities needed as chemotherapeutic agents.

ALA-based herbicides and insecticides: Technology transfer for anti-tumor activity. Using exogenous ALA and chemicals that modulate the endogenous synthesis of chlorophyll, Rebeiz et al., (48) developed a large number of photodynamic herbicides. The herbicides were selective for plant species, age and plant organ. The basis of this selectivity was rooted in the heterogeneity of the chlorophyll biosynthetic pathway. Indeed, in 1983, Rebeiz et al. proposed a six-branched pathway for chlorophyll biosynthesis (49). Subsequent research on this pathway revealed that the chlorophyll pool and the pathway were chemically and biosynthetically heterogeneous. It has been proposed that this heterogeneity may also account for the structural and functional heterogeneity of photosynthetic membranes. Following development of photodynamic herbicides, the technology was successfully transferred to insecticides, (50).

With the knowledge that injected tetrapyrroles, such as hematoporphyrin derivative (HpD), act as strong photosensitizer in cancer treatment, Rebeiz developed the hypothesis that incubation with ALA, a precursor of protoporphyrin and heme, and chemical modulators which stimulate tetrapyrrole biosynthesis, would force green plants to accumulate tetrapyrroles (49). Following incubation with ALA and a modulator, it was conjectured that exposure of plants to light should result in destruction of the plant, as a consequence of singlet oxygen formation. Species specificity of the herbicide was related to the heterogeneity of the chlorophyll biosynthetic pathway (51). A similar photodynamic action was also shown to occur in insects (50).

Malik et al. (52) investigated the possibility of stimulating endogenous porphyrin production by supplementing the medium of transformed cells with exogenous ALA. The K562 cell line did not synthesize Proto during 4 days incubation with ALA in darkness. However, FELC (Friend erythroleukemia cells) and Esb (a highly metastatic cell line) were sensitive to ALA treatment and synthesized porphyrins in the dark during 4 days of incubation. Trypan blue exclusion and ^3H -thymidine incorporation were used to determine cell viability and proliferation, respectively. Chromatography was used to determine the type of porphyrin species that accumulated, and flow cytometry was used to determine porphyrin content by monitoring red fluorescence (longer than 630 nm) emitted from individual cells, which is proportional to porphyrin content. The cells that synthesized Proto became sensitive to light and exhibited 99% inactivation (cell death) at the optimal Proto concentration after 4 days of dark incubation.

Kennedy et al., (53) have used ALA to treat different types of skin cancers in clinical studies. In this protocol, ALA is mixed into a paste (10% glacial base; 35-100 mg ALA/lesion), and then applied topically to the skin. The skin was then photoirradiated with laser light. The results seem promising for skin cancer, but highly intense light (52 mW/hr/cm^2) and high doses of ALA also caused damage to normal tissue. This toxic effect, however, was shown to be reversible, and less

damaging to normal tissue than HpD phototherapy. Yang et al., (54) have recently shown that ALA treatment can ablate the rat endometrium after intrauterine administration, with little toxic effects to the myometrium. In the treated rats, ALA was converted to Proto selectively in the endometrium.

Work we have published (55) points to increased antitumor activity when a modulator is used in conjunction with ALA. Modulators are chemicals that affect tetrapyrrole biosynthesis. The modulators may mimic a substrate or affect the activity of porphyrin biosynthetic enzymes during heme synthesis. The modulator we utilized, 1,10-phenanthroline (Oph), is structurally similar to one-fourth of a porphyrin molecule. Oph is also a chelator, and thus may exert its effects by chelating iron, which would adversely affect the activity of the ferrochelatase enzyme. The antitumor properties of ALA and Oph phototherapy are described below (55).

ALA and 1,10-Phenanthroline Induction of Protoporphyrin IX Accumulation in Neoplastic Cells

We first determined the identity and fluorescent properties of the porphyrin moiety that was induced upon ALA and Oph treatment of a neoplastic cell line (MLA 144, gibbon monkey lymphoma) in darkness. The fluorescent properties of the induced porphyrin were identical to that of Proto, with a Soret excitation maxima at 404 nm and emission maxima at 632 nm at 298 K.

To further characterize the induced porphyrin, chemical derivatization was preformed. Authentic Proto DM and the induced porphyrin were subjected to Mg^{++} insertion. The resulting metallated porphyrins exhibited identical fluorescent properties at 77 K (emission maxima of 591 nm; Soret excitation maxima of 423 nm). Finally, a third parameter of identification was examined. Specifically, HPLC mobility of the induced porphyrin was compared to authentic Proto. This was performed on a Waters Bondapak reverse-phase C-18 bonded column, and eluted isocratically with methanol/acetic acid/water (83.2:2:1.5, v/v/v). Authentic Proto and the MLA 144 extracted pigment had retention times of 5.4-5.6 min. Taken together, these results demonstrated unequivocally that ALA and Oph treatment of MLA 144 cells induced Proto accumulation.

Quantification of Proto IX Accumulation and Specific Cell Lysis by Light Treatment. Spectrofluorometry, a very sensitive analytical technique, allowed us to detect and accurately quantify the amount of Proto accumulation in the ALA plus Oph treated MLA 144 cells (Table I, A). Cells treated with medium alone did not accumulate Proto after 3 hours in darkness. However, ALA plus Oph treated cells accumulated on average 46.2 nmoles/ 100 mg protein. At the same time, these cells were monitored for specific cell lysis after exposure to light (2.11 mW/cm^2) for 30 minutes. This was done by labelling the cells with $Na^{51}Cr$ prior to incubation with ALA plus Oph and subsequent light treatment. Untreated cells had low background lysis (10 %) in the absence or presence of light. However, ALA plus Oph treated cells were severely damaged, with 81% specific cell lysis. The next experiment (Table I, B), investigated the effect of Oph on increasing the

efficacy of ALA treatment. Synergism was observed in both Proto accumulation and specific cell lysis by the addition of Oph. Alone, Oph did not induce Proto accumulation, or increase photolysis significantly.

Table I. ALA and Oph-induced Proto Accumulation and Photolysis of MLA 144 cells

Exp.	ALA	Oph	N	Proto (nmoles/100 mg Protein)	% Specific cell lysis	
	(mM)	(mM)			-light	+light
A.	0	0	2	0*b	0 ¹ c	0*c
	1	0.75		46±18.0a	8±1.1b	81±2.0a
B.	0	0	2	0*c	0*c	0*c
	0	0.75		0c	12±8.8c	12±5.8c
	1	0		34.0±2.71b	1±1.1c	59±4.0b
	1	0.75		72.9±0.95a	13±8.2c	88±3.6a

SOURCE: Reprinted with permission from reference 55. Copyright 1992.

*Within each experiment and within each column, means followed by different letters are significantly different at the 5% level. Means are reported±SEM.

¹These values represent less than 15% non-specific background cell lysis. Tetrapyrrole and cell lysis were performed on the same day in experiment A, and on consecutive days in experiment B.

Comparison of the Effect of δ -Aminolevulinic Acid and 1,10-Phenanthroline on Specific Cell Lysis in Neoplastic Cell Lines. Our next question was whether other transformed, neoplastic cell lines were sensitive to ALA plus Oph treatment. Two cell lines, WEHI 164, a murine fibrosarcoma cell line, which is very sensitive to damage by tumor necrosis factor- α (TNF- α), and K562, a human leukemic cell line which is insensitive to TNF- α damage, were tested and compared to MLA 144 cells. Dose response curves for each cell line were first determined (unpublished data), and the optimal doses were chosen for the following experiment. At comparable doses of ALA and Oph, WEHI 164 cells were significantly more sensitive to photo-induced cell lysis than MLA 144 cells (Table II).

K562 cells were even more sensitive to ALA plus Oph treatment, requiring a ten-fold reduction in dosage for an equivalent level of specific cell lysis. These results demonstrate that different types of neoplastic cells have varying sensitivity to ALA plus Oph induced photolysis. Cells that are insensitive to natural, *in vivo* killing, such as that mediated by TNF- α , were nonetheless very sensitive to ALA and Oph treatment. Whether this enhanced sensitivity is due to ALA or the

modulator Oph is not yet known. However, this aspect of ALA plus Oph treatment is important for chemotherapeutic purposes. Certain tumors may be targeted that have high sensitivity to the treatment regime, while the surrounding normal tissue may remain unaffected. That leads us to the next question: How sensitive are normal cells to this treatment?

Table II. Photodestruction of Three Neoplastic Cell Lines Following ALA and Oph Treatment

Cell line	N	ALA (mM)	Oph (mM)	% Specific cell lysis	
				-light	+light
MLA 144	3	0.0	0.0	0 ¹ *a	0*a
		1.0	0.75	10±3.0b	71±8.4d
WEHI 164	3	0.0	0.0	0*a	0*a
		1.0	0.75	6±2.7b,c	93±6.2f
K562	3	0.0	0.0	0*a	0*a
		0.12	0.09	2±3.7a,c	86±1.6e

SOURCE: Reprinted with permission from reference 55. Copyright 1992.

*These values represent less than 18% non-specific background cell lysis.

¹Means followed by different letters are significantly different at the 5% level. Means are reported ±SEM.

Sensitivity of Normal and Concanavalin A Activated Splenocytes to δ -Aminolevulinic Acid and 1,10-phenanthroline Treatment. For Proto mediated chemotherapy to provide a rational therapeutic approach, it is important that normal cells be less sensitive to the effects of ALA plus Oph treatment than neoplastic cells. To this end, we based the next experiments on the hypothesis that normal cells would not accumulate Proto unless they were dividing as rapidly as transformed cells. The mitogenic lectin Concanavalin A (Con A) was used to enhance rapid cell division in a normal Balb/c splenocyte cell suspension. Con A treatment of 1.25 μ g/ml for 40 hours gave the highest proliferation rate, a 50-fold increase over control splenocytes, as shown by tritiated thymidine incorporation. Normal- or Con A-treated splenocytes were incubated with medium alone or ALA (1 mM) plus Oph (0.75 mM) for 3.5 h in darkness, and then assessed for Proto accumulation. Normal splenocytes accumulated an average of 2.8 nmoles/100 mg protein of Proto (n=2), which was significantly lower than the levels of Proto accumulation in MLA 144 cells (26.2 nmoles/100 mg protein) over the same time

period. This is probably not enough Proto accumulation to confer photosensitivity, but that has not been shown yet. However, upon stimulating the proliferation of splenocytes with Con A, Proto accumulation (23.6 nmoles/100 mg protein) was comparable to that observed in MLA 144 cells. These results led us to conclude that slowly dividing cells are likely to exhibit minimal damage to ALA plus Oph treatment, since cell destruction is determined by Proto accumulation.

Conclusions

Porphyrin molecules are powerful endogenous triggers of cell death in the light. The photophysical nature of porphyrins allow them to be photoexcited, thereby creating reactive oxygen intermediates. Normally, the biosynthesis of porphyrins for heme and cytochrome production in mammals is tightly regulated, with rapid conversion rates which prevent accumulation of toxic porphyrins. Once iron is inserted into heme, the toxic properties are lost, because of changes in the molecules photophysical properties. Cells also have protective mechanisms that quickly quench reactive oxygen species. However, by manipulating the porphyrin biosynthetic pathway, so that intermediates accumulate too rapidly for the cell to convert to a non-toxic form, one can selectively trigger a destructive response.

We have tested this hypothesis, based on work in plants, on mammalian tumor cell lines. The combination of ALA, a precursor to Proto, and Oph, a tetrapyrrole modulator, worked effectively in destroying transformed, neoplastic cells after light treatment. In this system, ALA provides an abundant source of precursor molecules, while Oph probably controls enzyme activity, keeping the enzymes in an active mode. The use of a tetrapyrrole precursor and porphyrin biosynthesis modulator leads to a synergistic production of Proto, thus making the cells even more sensitive to light. ALA and Oph are both small molecules that should easily penetrate into solid tumors. Though ALA is charged at physiological pH, it is probably transported on a carrier molecule, such as globin or albumin. As we have shown, neither ALA or Oph induce destruction of surrounding healthy tissue. We are currently investigating the capability of these compounds to cause tumor necrosis in an *in vivo* tumor model, with promising preliminary results. Our future studies will primarily focus on the mode of action of ALA and Oph phototherapy.

Literature Cited

1. Granick, S. In *Biochemistry of Chloroplasts*; Goodwin, T. W., Ed.; Academic Press, New York, N. Y., 1967, Vol. 2; pp 373-406.
2. Kikuchi, G.; Kumar, A.; Talmage, D.; Shemin, D. *J. Biol. Chem.* **1956**, *233*, 1214-19.
3. Kikuchi, G.; Mayashi, N. *Mol. Cell. Biochem.* **1981**, *37*, 27-41.
4. Riddle, R. D.; Yamamoto, M.; Engel, J.D. *Proc. Natl. Acad. Sci.* **1989**, *86*, 792-6.
5. Wetmur, J. G.; Bishop, D. F.; Ostasiewicz, L. *Gene* **1986**, *43*, 123-130.
6. Bishop, T. R.; Cohen, P. J.; Boyer, S. H. *Proc. Natl. Acad. Sci. USA* . **1986**, *83*, 5568-72.

7. Wetmur, J. G.; Bishop, D. F.; Ostasiewicz, L. *Proc. Natl. Acad. Sci. USA* **1986**, *83*, 7703-07.
8. Barnard, G. F.; Itoh, R.; Hohberger, L. M.; Shemin, D. *J. Biol. Chem* **1977**, *25*, 8965-74.
9. Grandchamp, B.; Romeo, P. H.; Dubart, A.; Nordmann, Y. *Proc. Natl. Acad. Sci. USA* **1984**, *81*, 5036-40.
10. Beaumont, C.; Porcher, C.; Picat, C.; Nordmann, Y.; Grandchamp, G. *J. Biol. Chem.* **1989**, *264*, 14829-34.
11. Raich, N.; Romeo, P. H.; Dubart, A. *Nucleic Acids Res.* **1986**, *14*, 5955-68.
12. Grandchamp, B.; Beaumont, C.; deVernuil, H.; Dubart, A.; Nordmann, Y. *J. Biol. Chem.* **1985**, *260*, 9630-5.
13. Grandchamp, B.; Beaumont, C.; de Vernuil, H.; Dubart, A.; Nordmann, Y. In *Porphyryns and Porphyrias*, Nordmann, Y., Ed.; John Libbey, Paris, France, 1984. pp35.
14. Frydman, R. B.; Levy, E. S.; Varasinas, A.; Frydman, B. *Biochemistry.* **1978**, *17*, 110-120.
15. Tsai, S-F.; Bishop, D. F.; Desnick, R. J. *Proc. Natl. Acad. Sci. USA.* **1988**, *85*, 7049-53.
16. Barnard, G. F.; Akhtar, M. *J. Chem. Soc. Perkin Trans.* **1979**, *I*, 2354-9.
17. Romeo, P. H.; Raich, N.; Dubart, A.; Beaupain, D.; Pryor, M.; Kushner, J.; Cohen-Solal, M.; Goossens, M. *J. Biol. Chem.* **1986**, *261*, 9825-31.
18. deVernuil, H.; Grandchamp, B.; Beaumont, C.; Picat, C.; Nordman, Y. *Science* . **1986**, *234*, 732-4.
19. Elder, G. H.; Evans, J. O. *Biochem. J.* **1978**, *172*, 345-7.
20. Bogard, M.; Camadro, J.; Nordmann, Y.; Labbe, P. *Eur. J. Biochem.* **1989**, *181*, 417-21.
21. Poulson, R.; *J. Biol. Chem.* **1976**, *251*, 3730-3.
22. Deybach, J. C.; daSilva, V.; Grandchamp, B.; Nordmann, Y. *Eur. J. Biochem.* **1985**, *149*, 431-5.
23. Smith, B. B.; Rebeiz, C. A. *Plant Physiol.* **1979**, *63*, 227-31.
24. Gouterman, M. *J. Chem. Phys.* **1959**, *30*, 1139-60.
25. Grossweiner, L. I.; Patel, A. S.; Grosswiener, J. B. *Photochem. Photobiol.* **1982**, *36*, 159-67.
26. Grossweiner, L. In *Porphyrin Localization and Treatment of Tumors*; Doiron, D.R., Gomer, C. J., Eds.; Alan R. Liss, Inc., New York, N. Y., 1984 pp. 391-96.
27. Caughy, W. S.; Eberspacher, M.; Fuchman, W. H.; McCoy, S.; Allen, J. D. *Ann. N. Y. Acad. Sci.* **1968**, *153*, 722-37.
28. Doleiden, F. H.; Fahrenholtz, S. R.; Lamol, A. A.; Trozzola, A. M. *Photochem. Photobiol.* **1984**, *20*, 519-21.
29. Dougherty, T. J.; Kaufman, J. E.; Goldfarb, A.; Weishaupt, K. R.; Boyle, D.; Mittleman, A. *Cancer Res.* **1978**, *38*, 2628-35.
30. Ito, T. *Photochem. Photobiol. Rev.* **1983**, *7*, 141-86.
31. Malik, Z.; Djaldetti, M. *Int. J. Cancer* **1980**, *26*, 495-500.
32. Girotti, A. W. *Biochem. Biophys. Res. Commun.* **1976**, *72*, 1367-74.
33. Kessel, D. *Cancer Res.* **1981**, *41*, 1318-23.

34. Dellinger, M.; Vever-Bizet, C.; Brault, D.; Moreno, G.; Salet, C. *Photochem. Photobiol.* **1990**, *51*, 185-9.
35. Koller, M. E.; Romsio, I. *Biochem. J.* **1980**, *188*, 329-35.
36. Hilf, R.; Murant, R. S.; Narayanan, U.; Gibson, S. L. *Cancer Res.* **1986**, *46*, 211-17.
37. Khanum, F.; Jain, V. *Photochem. Photobiol.* **1989**, *50*, 647-51.
38. Dougherty, T. J.; Henderson, B. W.; Bellnier, D. A.; Weishaupt, K. R.; Mixhalakeo, C.; Ziring, B.; Chang, C. *Ninth Ann. Soc. Photobiol.* (abstr.), **1981**, p. 124.
39. Reddi, E.; Ricchelli, F.; Jori, G. *Int. J. Pept. Protein Res.* **1981**, *18*, 402-8.
40. Canti, G.; Marelli, O.; Ricci, L.; Nicolini, A. *Photochem. Photobiol.* **1981**, *34*, 589-94.
41. Franco, P.; Nicdin, A.; Ricci, L.; Trave, F.; Canti, G. *Int. J. Immunopharmac.* **1983**, *5*, 533-40.
42. Marshall, J. F.; Chan, W. S.; Mart, I. R. *Photochem. Photobiol.* **1989**, *49*, 627-32.
43. Gomer, C. J.; Ferrario, A.; Murphree, A. *Photochem. Photobiol. Suppl.* **1986**, *43*, 635-7.
44. Dougherty, T. J. *Photochem. Photobiol.* **1987**, *45*, 879-89.
45. Kaye, A. M.; Morstyn, G.; Apunzo, M. L. *J. Neurosurg.* **1988**, *49*, 530-7.
46. Chopp, M.; Glasberg, M. R.; Riddle, J. M.; Hetzel, F. W.; Welch, K. M. A. *Photochem. Photobiol.* **1987**, *46*, 102-8.
47. Jeeves, W. P.; Wilson, B. C.; Firna, G.; Brown, K.; Dougherty, T. J. *Adv. Exp. Med. Biol.* **1986**, *193*, 51-67.
48. Rebeiz, C. A.; Montazer-Zouhoor, A.; Hopen, H. J.; Wu, S. M. *Enzyme Microb. Technol.* **1984**, *6*, 390-403.
49. Rebeiz, C. A.; Wu, S. M.; Kuhadja, M.; Daniell, M.; Perkins, E. *J. Mol. Cell. Biochem.* **1983**, *57*, 97-125.
50. Rebeiz, C. A.; Juvik, J. A.; Rebeiz, C. C. *Pestic. Biochem. Physiol.* **1980**, *30*, 11-27.
51. Belanger, F. C.; Rebeiz, C. A. *J. Biol. Chem.* **1982**, *257*, 1360-71.
52. Malik, Z.; Ehrenberg, B.; Faraggi, A. *J. Photochem. Photobiol. Bio.* **1989**, *4*, 195-205.
53. Kennedy, J. C.; Pottier, R. H.; Pross, D. C. *J. Photochem. Photobiol. B. Biol.* **1990**, *6*, 143-8.
54. Yang, J. Z.; Van Vugt, D. A.; Kennedy, J. C.; Reid, R. L. *Photochem. Photobiol.* **1993**, *57*, 803-7.
55. Rebeiz, N.; Rebeiz, C. C.; Arkins, S.; Kelley, K. W.; Rebeiz, C. A. *Photochem. Photobiol.* **1992**, *55*, 431-5.

RECEIVED April 4, 1994

Chapter 17

Effect of Protoporphyrinogen Oxidase Inhibitors on Mammalian Porphyrin Metabolism

J. Krijt, M. Vokurka, J. Sanitřák, and V. Janousek

Department of Pathological Physiology, First Medical Faculty, Charles University, CZ 128 53 Prague, Czech Republic

The herbicide fomesafen (100 ppm) significantly increased the porphyrin content of mouse liver and bile when fed to male ICR mice for 10 days. Liver porphyrin concentration increased from 0.7 to 1.6 and bile porphyrin concentration from 7.4 to 38.2 nmol/g wet wt. Feeding of 2500 ppm of fomesafen in the diet for 5 months increased the liver porphyrin content from 1.0 to 138.2 nmol/g, with uroporphyrin and heptacarboxylic porphyrin forming the major porphyrin fractions. Fomesafen, oxadiazon, and oxyfluorfen also caused *in vitro* porphyrin accumulation in experiments with mouse hepatocyte cultures and HepG2 cells. However, it is concluded that these herbicides probably pose no toxicological hazard when properly used.

Many xenobiotics are capable of disrupting the porphyrin biosynthetic pathway *in vivo*. A classic example is the fungicide hexachlorobenzene, which caused a massive outbreak of cutaneous porphyria in Turkey. Other polyhalogenated aromatic hydrocarbons like 2,3,7,8 tetrachloro-p-dioxin (TCDD), octachlorostyrene, and polychlorinated and polybrominated biphenyls have been documented to induce porphyria in experimental animals and, in some cases, in humans (1,2). All these polychlorinated aromatic hydrocarbons act through inhibition of uroporphyrinogen decarboxylase. Another porphyrogenic chemicals, the ferrochelatase-inhibiting drugs griseofulfin and DDC, cause a dramatic increase in hepatic protoporphyrin levels when fed to experimental animals (3). Thus, the porphyrin biosynthetic pathway clearly can become an inadvertent target of industrial chemicals or byproducts.

Recently, a new group of potentially porphyrogenic chemicals has been identified. Photobleaching herbicides like diphenyl ethers or oxadiazon have been demonstrated to inhibit the enzyme protoporphyrinogen oxidase (4,5,6). In addition, some other structurally unrelated herbicides are also capable of

0097-6156/94/0559-0247\$08.00/0
© 1994 American Chemical Society

protoporphyrinogen oxidase inhibition (7). Since these herbicides are in widespread use, their possible adverse effect on the heme biosynthetic pathway in mammals should be carefully considered.

Increased Porphyrin Concentration in Mouse Tissues Induced by Short Term Feeding of Photobleaching Herbicides.

Addition of 2500 ppm of fomesafen, oxyfluorfen, or oxadiazon to the diet increased the porphyrin content of liver, bile, and feces when fed to male mice of the ICR strain for 10 days (Table I). The pattern of liver, bile, and fecal porphyrin accumulation induced by these herbicides was determined by high performance liquid chromatography of the porphyrin methyl esters. In all cases, protoporphyrin and uroporphyrin constituted the major liver porphyrin fractions, while protoporphyrin and coproporphyrin predominated in the bile and feces. The same pattern of fecal porphyrin excretion is also found in the human disease variegate porphyria, which is caused by an inherited deficiency of protoporphyrinogen oxidase (3). Urine of oxadiazon-treated male Wistar rats (1000ppm, 6 days) contained elevated amounts of uroporphyrin, coproporphyrin and porphobilinogen. This excretion pattern again parallels the findings in variegate porphyria.

Table I. The Effect of Protoporphyrinogen Oxidase-inhibiting Herbicides on Porphyrin Accumulation in Male ICR Mice

<i>Treatment</i>	<i>Liver Porphyrin Content (nmol/g wet wt)</i>	<i>Bile Porphyrin Content (nmol/g wet wt)</i>	<i>Fecal Porphyrin Content (nmol/g dry wt)</i>
Control	1.2 ± 0.1	9.2 ± 5.1	28.9
Fomesafen	3.6 ± 0.1	134.5 ± 33.6	296.7
Oxyfluorfen	15.8 ± 3.4	340.3 ± 123.3	543.0
Oxadiazon	29.5 ± 2.1	481.2 ± 170.1	917.0

Mice were fed 2500 ppm of the herbicides in the diet for 10 days (n=3). Porphyrins were extracted and esterified by methanol/sulphuric acid (95:5 v/v), and quantified on a spectrofluorimeter (407/607 nm) using protoporphyrin dimethyl ester as standard. Fecal porphyrin content was determined in pooled samples.

The porphyrin accumulation induced by high dose, short term fomesafen treatment is reversible. Pretreatment of male ICR mice with 5000 ppm of fomesafen in the diet for 10 days resulted in increased porphyrin concentrations in liver, bile and feces (Table II). After further 5 days without fomesafen treatment, the fecal and bile porphyrin content returned to normal levels, and liver porphyrin content was only slightly elevated.

Table II. The Effect of a 5-day Recovery Period on Increased Porphyrin Levels Induced by Fomesafen Pretreatment

<i>Treatment</i>	<i>Porphyrin Concentration (nmol/g)</i>		
	<i>Liver</i>	<i>Bile</i>	<i>Feces</i>
Control diet, 10 days	1.2 ± 0.3	6.4 ± 4.3	34.5
Fomesafen, 5000 ppm, 10 days	6.0 ± 2.3	80.1 ± 15.3	527.3
Fomesafen 10 days, control diet 5 days	1.8 ± 0.3	9.6 ± 3.2	40.1

Fecal porphyrins were determined in pooled samples, n=3.

As indicated in Table I, a high dose of fomesafen produced only modest changes in liver porphyrin concentration. However, subsequent experiments demonstrated that lower doses of fomesafen are sufficient to induce a statistically significant increase in liver porphyrin content (Table III).

Table III. Liver and Bile Porphyrin Concentrations of Male ICR Mice Fed 100 ppm of Fomesafen in the Diet for 10 Days

<i>Treatment</i>	<i>Relative liver weight (%)</i>	<i>Liver porphyrin content (nmol/g)</i>	<i>Bile porphyrin content (nmol/g)</i>
Control diet	5.0 ± 0.1	0.7 ± 0.1	7.4 ± 4.6
Fomesafen 100 ppm	7.2 ± 0.4 ^a	1.6 ± 0.2 ^a	38.7 ± 8.9 ^a

^aStatistically different from control values, p<0.05 (n=3).

Elevated Levels of Uroporphyrin and Heptacarboxylic Porphyrin Induced by Long Term, High Dose Treatment with Diphenyl Ether Herbicides.

When diets containing high concentrations (2500 or 5000 ppm) of fomesafen were fed to ICR mice for a sufficiently long period, the pattern of liver porphyrin accumulation gradually changed. In some animals, highly carboxylated porphyrins, i.e. uroporphyrin and heptacarboxylic porphyrin, formed the major liver porphyrin fraction after 3 to 5 months of treatment (Table IV). The total liver porphyrin content of these animals was dramatically increased but showed marked individual variation. Interestingly, the same pattern of porphyrin

accumulation, as well as the wide scatter of individual values, is typically observed after long term treatment with polyhalogenated aromatic hydrocarbons like hexachlorobenzene, polychlorinated biphenyls, or TCDD (1,3). This unexpected accumulation of highly carboxylated porphyrins after long term treatment with a protoporphyrinogen oxidase inhibitor was further confirmed in one experiment with the commercial herbicide formulation Blazer, containing acifluorfen-sodium. Addition of Blazer (corresponding to 2500 ppm of acifluorfen) to the diet resulted in a similar pattern of liver porphyrin accumulation in male ICR mice after three months of treatment. Uroporphyrin I was found to predominate over uroporphyrin III in both fomesafen and Blazer-treated groups.

Table IV. The Effect of Fomesafen and Iron Treatment on Liver and Kidney Porphyrin Concentrations of Male ICR Mice

<i>Treatment</i>	<i>Liver Porphyrin Content (nmol/g)</i>	<i>Kidney Porphyrin Content (nmol/g)</i>	<i>Bile Porphyrin Content (nmol/g)</i>
Control	1.0 ± 0.5	0.7 ± 0.1	9.3 ± 5.3
Fomesafen	138.2 ± 152.3	3.5 ± 2.1	186.6 ± 103.8
Fomesafen-iron	190.1 ± 55.8	12.0 ± 3.0	473.2 ± 144.9

Mice were fed 0.25% of fomesafen in the diet for 5 months, iron pretreated groups received 600mg/kg of iron by subcutaneous injection (n=4).

It has been demonstrated many times that the experimental porphyrias induced by polyhalogenated aromatic hydrocarbons, as well as the human disease porphyria cutanea tarda, can be modulated by manipulating the body iron stores. Iron pretreatment accelerates the development of hexachlorobenzene-induced uroporphyrin, while phlebotomy is a widely used therapeutic approach to porphyria cutanea tarda (3). As can be seen in Table IV, iron pretreatment further significantly increased the elevated porphyrin levels induced by fomesafen. Thus, the mechanism of uroporphyrin induction by fomesafen and polychlorinated aromatic hydrocarbons appears to be to some extent similar.

Modulation of Hepatic Microsomal Cytochrome P450 Activities by Diphenyl Ether Herbicides.

Microsomal cytochromes of the P450 family are the major hepatic hemoproteins. Their levels and activities can be altered by drug pretreatment and they play a key role in most experimental porphyrias, as well as in detoxification and/or activation of many xenobiotics. Typically, all porphyrogenic aromatic hydrocarbons induce cytochromes of the P450IA family in susceptible mouse strains (8).

As can be seen in Table V, the P450IA-related ethoxyresorufin O-deethylase (EROD) activity was not induced by fomesafen or oxyfluorfen treatment in

C57Bl/6J mice, although this mouse strain is highly susceptible to P450IA induction by porphyrigenic aromatic hydrocarbons. Oxyfluorfen caused a moderate increase in hepatic pentoxyresorufin O-dealkylase (PROD) activity, which is typically induced by the model drug phenobarbital.

Table V. Changes in Cytochrome P450 Content and Activities after Long Term Treatment with Diphenyl Ether Herbicides

<i>Treatment</i>	<i>Total Microsomal P450 (nmol/mg)</i>	<i>EROD (pmol/mg/min)</i>	<i>PROD (pmol/mg/min)</i>
Control	0.60 ± 0.09	75 ± 13	18 ± 2
Oxyfluorfen	0.41 ± 0.02	73 ± 13	61 ± 10
Fomesafen	0.64 ± 0.05	75 ± 9	30 ± 2

Male C57Bl/6J mice were fed 2500 ppm of the herbicides in the diet for 3 months. Results are expressed per mg of microsomal protein.

The inability of diphenyl ethers to induce hepatic EROD activity indicates that the development of PCT-type porphyria after fomesafen treatment is not caused by dibenzodioxin or dibenzofuran contamination of the herbicide preparations.

The Effect of Protoporphyrinogen Oxidase-inhibiting Herbicides on Porphyrin Accumulation in Human Hepatoma-derived HepG2 Cells.

Diphenyl ethers and oxadiazon have been reported to increase the porphyrin content of rat hepatocytes in culture (9,10). Figure 1 shows the effect of three photobleaching herbicides on the cellular porphyrin content of human hepatoma-derived HepG2 cells. It is evident that all three herbicides increased the cellular porphyrin content over a wide concentration range. Although oxyfluorfen and oxadiazon were more potent than fomesafen in the in vivo experiments, the extent of in vitro porphyrin accumulation is roughly similar for all three herbicides. This probably reflects in vivo differences in absorption and metabolism of these compounds, or different interactions with hepatic cytochromes P450.

Toxicological Aspects of the Protoporphyrinogen Oxidase-inhibiting Herbicides in Experimental Animals and Man.

The presented results clearly indicate that the protoporphyrinogen oxidase-inhibiting herbicides can influence the porphyrin and heme metabolism in mammals. Although very high doses (2500 or 5000 ppm) were used in most experiments, it is evident that fomesafen has a significant effect on porphyrin accumulation at much lower daily doses of circa 20 mg/kg. In addition, significantly increased liver porphyrin concentrations were reported after feeding of 50 ppm of oxadiazon to male ICR mice for 14 days (11).

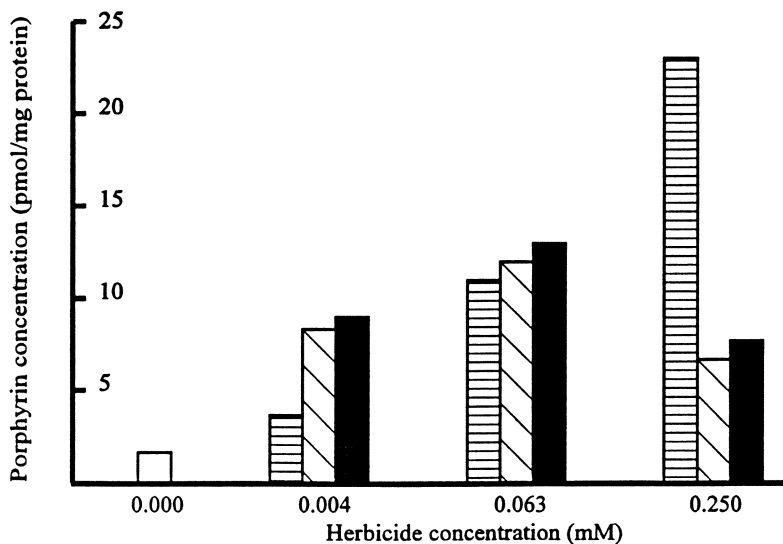


Figure 1. The effect of fomesafen (horizontally hatched bars), oxyfluorfen (diagonally hatched bars), and oxadiazon (closed bars) on the porphyrin content of HepG2 cells in culture.

Cells were incubated with the herbicides for 24 hours, porphyrins were determined in washed cells after extraction by methanol/sulphuric acid.

Previously published results show that the protoporphyrinogen oxidase-inhibiting herbicides can induce porphyrin accumulation in a variety of cells, including plant cells, rat hepatocytes, and human-derived HepG2 hepatoma cells. Consequently, these herbicides could theoretically interfere with the porphyrin biosynthetic pathway in man as well. However, rather high doses are needed to produce relatively slight changes in porphyrin concentrations in vivo. Also, the accumulation of liver porphyrins induced by fomesafen treatment is clearly reversible (Table III). Therefore, it is perhaps reasonable to speculate that, in view of these results, the risk of a serious disturbance of heme metabolism caused by exposure to protoporphyrinogen oxidase-inhibiting herbicides is small.

An inherited enzymatic defect of the heme biosynthetic pathway is found in human porphyrias. Protoporphyrinogen oxidase deficiency is characteristic of variegate porphyria. Although acute attacks of variegate porphyria can be life-threatening, a proportion of subjects with impaired activity of protoporphyrinogen oxidase can remain asymptomatic throughout life (12). This fact further supports the assumption that a slight, transient decrease in protoporphyrinogen oxidase activity - if it occurred - would have no serious consequences.

Prolonged treatment with high doses of fomesafen or acifluorfen resulted in an unexpected accumulation of highly carboxylated porphyrins in the liver of ICR mice. Accumulation of uroporphyrin has also been reported in in vitro experiments with acifluorfen-methyl (9). The observed pattern of porphyrin accumulation and excretion in vivo is a typical diagnostic feature of human porphyria cutanea tarda. The same porphyrin pattern is also encountered in acquired porphyrias induced by polychlorinated aromatic hydrocarbons, both in experimental animals and man. Although this type of porphyria only developed when extremely high doses of fomesafen or acifluorfen were administered for long periods, it is theoretically possible that these diphenyl ethers could potentiate the toxic effect of the known environmental pollutants like hexachlorobenzene, polychlorinated biphenyls, or TCDD. In this respect, it is also interesting to note that nearly all porphyrogenic aromatic hydrocarbons are carcinogenic, and that acifluorfen has also been classified as a probable human carcinogen (13).

Notwithstanding the fact that the porphyrogenic action of diphenyl ethers and polychlorinated aromatic hydrocarbons is to some extent similar, their interaction seems to have little possible toxicological consequence for man. As pointed out, only extremely high doses of the diphenyl ethers induce a porphyria cutanea tarda-like porphyria in rodents (fomesafen is about two orders of magnitude less potent than hexachlorobenzene when the total porphyrogenic doses are compared). The porphyrogenic polychlorinated aromatic hydrocarbons are persistent environmental pollutants and their levels are carefully monitored, which further reduces the risk of interaction. Also, the available data on diphenyl ethers point to a relatively rapid excretion (14), as compared to the polyhalogenated aromatic hydrocarbons. Thus, it can be again concluded that the diphenyl ethers would probably pose a small toxicological hazard to man when properly used. However, since the heme moiety, of which protoporphyrinogen is a precursor, has a wide variety of specific functions, further experiments are needed to definitely confirm this assumption.

Acknowledgments

This work was supported by Charles University Grant No.268. A significant part of the experiments was generously funded and supported by the Rotary Club Baarn-Soest, the Netherlands.

Literature cited

1. Strik, J.J.T.W.A.; Debets, F.M.H.; Koss, G. In *Halogenated biphenyls, terphenyls, naphthalenes, dibenzodioxins and related products*; Kimbrough, R.D., Ed.; Elsevier/North-Holland Biomedical Press, Amsterdam, 1980, pp 191-239.
2. Jirásek, L.; Kalenský, J.; Kubec, K.; Pazderová, J.; Lukás, E. *Hautartz* **1976**, *27*, 328-333.
3. Kappas, A.; Sassa, S.; Anderson, K. In *The metabolic basis of inherited disease*; Stanbury, R.D.; Wijngaarden, J.B.; Frederickson, D.S.; Goldstein, J.L.; Brown, M.S., Eds.; McGraw-Hill, New York, NY, 1983, pp 1301-1384.
4. Matringe, M.; Camadro, J.M.; Labbe, P.; Scalla, R. *Biochem. J.* **1989**, *260*, 231-235.
5. Matringe, M.; Camadro, J.M.; Labbe, P.; Scalla, R. *FEBS Lett.* **1989**, *245*, 35-38.
6. Witkowski, D.A.; Halling, B.P. *Plant Physiol.* **1989**, *90*, 1239-1242
7. Duke, S.O.; Lydon, J.; Becerril J.M.; Sherman T.D.; Lehen L.P.; Matsumoto, H. *Weed Sci.* **1991**, *39*, 465-473
8. De Matteis, F. In *Hepatotoxicology*; Meeks, R.G.; Harrison, S.D.; Bull, R.J., Eds.; CRC Press, Boca Raton, 1991, pp 437-478
9. Jacobs, J.M.; Sinclair, P.R.; Gorman, N.; Jacobs, N.J.; Sinclair, J.F.; Bement, W.J.; Walton, H. *Biochem. Toxicol.* **1992**, *7*, 87-95.
10. Krijt, J.; van Holsteijn, I.; Hassing, I.; Vokurka, M.; Blaauboer, B.J. *Arch. Toxicol.* **1993**, *67*, 255-261.
11. Krijt, J.; Pleskot, R.; Sanitrak, J.; Janousek, V. *Pestic. Biochem. Physiol.* **1992**, *42*, 180-187.
12. Moore M.R.; McColl, K.E.L.; Rimington, C.; Goldberg, A. *Disorders of porphyrin metabolism*, Plenum Medical Book Company, New York, NY, 1987, pp 91-94.
13. Quest, J.A.; Phang, W.; Hamernik, K.L.; van Gemert, M.; Fisher, B.; Levy, R.; Farber, T.M.; Burnam, W.L.; Engler, R. *Regulat. Toxicol. Pharmacol.* **1989**, *10*, 149-159.
14. Adler, I.L.; Jones, B.M.; Wargo, J.P. *J. Agric. Food. Chem.* **1977**, *25*, 1339-1341.

RECEIVED March 8, 1994

Chapter 18

Photodynamic Therapy with Porphyrin Derivatives

Leonard I. Grossweiner

Department of Physics, Illinois Institute of Technology,
Chicago, IL 60616-3793
Wenske Laser Center, Ravenswood Hospital Medical Center,
Chicago, IL 60640

Photodynamic therapy (PDT) is an experimental treatment for malignant tumors utilizing the combined action of visible light and a tumor-localizing photosensitizing agent. PDT drugs derived from the porphyrin mixture hematoporphyrin derivative are being employed for clinical trials. This paper reviews the current status of PDT, emphasizing clinical results, the mechanism of action, and recent developments.

Approximately 5000 patients have been treated with PDT on an experimental basis since 1978. The voluminous PDT literature includes the results of clinical trials, photosensitization studies on biochemical and biological systems, light dosimetry modeling, PDT devices, and combination therapies. This paper reviews the current status of clinical and preclinical PDT research.

History of Photodynamic Therapy

Photodynamic treatment of tumors was first attempted in 1903 by Tappenier and Jesionek (1). An unsuccessful effort was made to treat skin cancer by topical application of eosin dye followed by exposure of the lesions to direct sunlight. The early failure probably resulted from an insufficient localized dye concentration and an inadequate sunlight dose. These limitations were surmounted with the discovery of new PDT drugs and the availability of strong artificial light sources. The first practical PDT drug was synthesized by Lipson in 1961 (2). The porphyrin mixture hematoporphyrin derivative (HPD) was obtained by treating commercial hematoporphyrin with a mixture of glacial acetic and sulfuric acids, followed by neutralization and extensive washing of the resultant brown powder. A dilute solution of HPD localizes in neoplastic tissues after intravenous injection. Tissue uptake of HPD is identified by a characteristic red fluorescence. HPD fluorescence has been used for

0097-6156/94/0559-0255\$08.00/0
© 1994 American Chemical Society

tumor diagnosis and visualization since the 1960s. In 1975, Kelley and Snell used HPD for PDT on one patient with bladder cancer (3). Interest accelerated in 1978 when the group of Dougherty at Roswell Park Cancer Institute reported preliminary PDT results for 25 patients with recurrent skin cancers (4). The procedure was first referred to as "photoradiation therapy" and more recently as "photodynamic therapy". Photofrin porphyrin sodium (QLT Phototherapeutics, Vancouver, BC) is the HPD drug currently approved for Phase II and Phase III clinical trials in the U.S.

Overview of a PDT Procedure

Photofrin (PF) is administered by intravenous injection 24-48 hours prior to the light treatment. Cutaneous photosensitization develops within a few hours and the patient must avoid direct sunlight for a variable period which averages about 6 weeks. The fluorescence of the localized drug varies for different tumor sites from barely perceptible to bright. PDT light is provided by an argon-ion pumped tunable dye laser at 630 nm or another source of strong red light. Superficial tumors are irradiated via an external optical fiber, usually terminated with a "microlens" to provide a more uniform irradiance. Deep lesions can be treated by inserting the unclad tip of an optical fiber in the tumor mass. Endoscopic techniques are employed for PDT of interstitial tumors, e.g., a cylindrical diffuser in the esophagus and a spherical diffuser in the urinary bladder. PDT treatment times range from several minutes to more than an hour, depending on the tumor coloration and size, drug dose, laser power, and mode of light delivery. Blanching of tumor tissue and diffuse hemorrhage may be evident during or immediately after the light treatment. Tissue necrosis and eschar formation progress over a 2-3 week period, followed by a healing after about 6-8 weeks. The necrosed areas become almost natural appearing in time, probably because PDT does not damage collagen.

Survey of PDT Clinical Trials

PDT has been employed for patients who have failed or refused conventional therapies. The objective for many patients was palliation of advanced disease. Phase I and Phase II clinical trials are in progress for the evaluation of PF and several "second generation" PDT photosensitizers. Randomized Phase III studies are being coordinated by Lederle Laboratories of American Cyanamid Company (Pearl River, NY). The PDT response of a tumor site is evaluated by histological diagnosis at 3 months after treatment as: "complete response" (CR), partial response (PR), "no response" (NR), and "progressive disease" (PD). The duration of long-term follow-up has been highly variable, ranging from a few months to many years.

Skin Cancer. More than 700,000 case of skin cancer are reported annually in the U.S., mostly basal cell carcinoma (BCC) and squamous cell carcinoma (SCC) on skin areas exposed to sunlight. Excisional surgery, curettage and electrodesiccation, cryosurgery, and radiation therapy are effective conventional therapies. PDT is useful for patients who are not candidates for surgery and cancer sites which are difficult to access. PDT of small, multiple lesions is a

potential PDT application, including recurrent breast cancer on the chest wall after mastectomy, Bowen's disease, and basal cell nevus syndrome. A 1987 review indicates CR rates of 70-80% for BCC, 20% for SCC, and 60-70% for metastatic breast cancer (5). Typical light dose levels varied from 20-40 J/cm² with PF administered at 2 mg/kg of body weight. The good results for BCC are supported by a 1990 report in which a CR was achieved for 133 of 157 sites (37 patients) with a minimum follow-up of 12 months (6). PF was administered at 1 mg/kg, which necessitated a light dose of 200 J/cm². This "non-reciprocity" between drug dose and light dose is attributed to PF photobleaching (7).

Bladder Cancer. Superficial bladder cancer has been diagnosed in 50,000 patients per year in the U.S resulting in 10,000 annual cancer deaths. Over 90% of these are noninvasive transitional cell carcinoma. The disease can occur as carcinoma-in-situ (CIS) or small papillary tumors. Surgical excision is the standard therapy for superficial papillary tumors. CIS is resistant to chemotherapy and immunotherapy with a recurrence rate of 40-70%. PDT offers an alternative to cystectomy, which is the standard treatment for refractory bladder CIS. A review of PDT results from 1983-1991 indicates that 216 patients were treated for all stages of bladder cancer with a 47% CR rate (8). Uniform light exposure of the fluid-distended bladder wall is required. An optical fiber with a spherical diffuser may be centered by sounding and ultrasound techniques. Whole bladder light doses ranged from 10-70 J/cm² at 2 mg/kg PF. An ongoing Phase III study specifies a whole bladder light dose of 15 J/cm². In addition to skin photosensitivity, many patients experienced irritative bladder symptoms for a few days to several weeks.

Endobronchial Lung Cancer. Lung cancer is the leading cause of cancer death in the U. S. Non-small cell lung cancer occurs in approximately 120,000 patients in the U.S. annually, frequently accompanied by endobronchial obstruction. Partial removal of tumor by laser is a standard treatment. PDT results were reported from 1985-1990 for 260 patients with various lung malignancies, including small cell and large cell cancers, adenocarcinomas, and SCC ranging from stage 1 to advanced disease (8). The overall response rate was 22% CR, 48% PR, and 30% NR plus PD. Surface light doses ranged from 20-500 J/cm². Debridement of necrotic tumor via bronchoscopy after PDT was required. An additional 154 patients were treated with PDT for palliation or improved operability. Clinical improvement was reported for 132 patients including 17 CR. The advantages of PDT over conventional laser surgery include decreased likelihood of bronchial perforation, selective tumor cell destruction, facility of treating superficial wall lesions, minimal bleeding, and absence of an irritative laser plume.

Head and Neck Cancer. More than 40,000 cases of head and neck cancers are diagnosed in the U.S. each year. Radiation therapy and surgery are the standard treatments for SCC of the lip, oral cavity, pharynx, and larynx. Many PDT patients had already received the maximum ionizing radiation. Results were reported for 164 patients with primary, recurrent, and metastatic head and neck cancers from

1984-1990 with an overall CR rate of 28% (9). Small, early stage tumors showed the best response. The CR rate was 73% in a study on 41 patients treated for epidermoid carcinoma of the glottis for periods up to 5 years for 8 patients (9). Analytical light dosimetry modeling was used as a guide to treatment planning in a Phase II study on head and neck SCC (10). The tumor dimensions were diagnosed by magnetic resonance imaging scans. Tumors less than 7 mm in depth were treated by surface delivery at 125 J/cm²; deeper lesions were treated first by surface delivery followed by fiber insertions spaced 7-8 mm apart at 75 J/cm. A CR was achieved for 20 of 26 patients of which 16 patients remained free of tumor for up to 51 months.

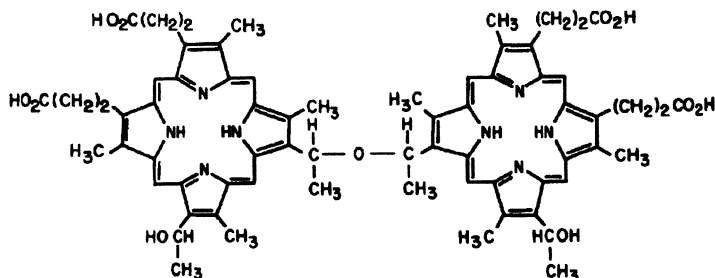
Gynecological Malignancies. Approximately 50,000 women per year are diagnosed for cancer of the cervix. Vulvar and vaginal cancer account for 5% of female malignancies. Conventional and laser surgery are the standard treatments for CIS and superficial malignancies. The PDT literature for gynecological cancers includes lesions of all stages in the cervix, perineum, cervix, vulva, vagina, perianal, and endometrium (8). The results for 73 women indicate an overall CR rate of 48%. A recent Phase II study for 17 patients was limited to CIS of the vulva, vagina, perineum, and perianal (11). Most patients were treated for multiple lesions with an overall CR rate of 71%. Ten patients remained free of recurrences for 2 to 7 years. Venereal warts associated with vulvar CIS recurred soon after PDT. The results to date do not demonstrate that PDT has any clear advantages over conventional modalities for treatment of CIS. The limited results for invasive gynecological cancers are not encouraging.

Other Malignancies. Approximately 10,000 cases of esophageal cancer are diagnosed annually in the U.S. Palliation of malignant dysphagia has been achieved by radiation therapy, Nd:YAG laser ablation, and intraluminal placement of a tubular prosthesis. Regardless of the therapy, fewer than 4% of patients achieve five-year survival. PDT results reported for 71 patients with superficial lesions led to 62% CR with some long-term remissions (8). Removal of obstructing tumor with PDT can prolong and increase the quality of life for patients who are not candidates for surgery. Relief of malignant dysphagia was reported for 95% of 55 treated patients. A study on PDT of early gastric cancer was carried out in Japan where screening is normally practiced (12). A CR rate of 82% was achieved for 32 patients with cancers described as ulcerative and circumscribed. PDT of brain tumors has been used as an adjunct to surgery. In a recent study on 50 patients with malignant supratentorial tumors, the median survival was 17.1 months for 12 patients evaluated as CR, with 1 and 2 year survivals of 62% and 38%, respectively (13).

How Does HPD Plus Light Eradicate Tumors?

The current theories of PDT action mechanism have been developed by extrapolating information derived from *in vitro* photosensitization studies and animal tumor models. Comparative results for HPD drugs and "second generation" PDT sensitizers provide some clues about the role of molecular structure.

Composition of HPD Drugs. HPD contains monomeric porphyrins, including hematoporphyrin, protoporphyrin, and hydroxyethylvinyl-deuteroporphyrin, and a higher molecular constituent that is responsible for essentially all of the antineoplastic activity. The chemical structure of the active constituent was tentatively identified as "dihematoporphyrin ether" (DHE) (14). This material comprises approximately 35% of HPD and 85% of PF. Subsequent work



DHE: Bis-1-[8-(1-hydroxyethyl)deuteroporphyrin-3-yl]ethyl ether

has shown DHE has a variable structure, depending on the method of preparation and history (15). Ether and ester linkages have been identified in covalent dimers and small oligomers. The structural analysis is further complicated by positional and stereo isomers. The active material will be referred to as "DHE", although the compound depicted above is only one of many possible structures. PF absorption is typical of metal-free porphyrins, with a strong Soret band near 370 nm and four progressively weaker bands near 510, 540, 575, and 630 nm. The fluorescence emission bands are located near 630 and 680 nm. The band maxima and intensities are highly dependent on the medium owing to aggregation. Photophysical properties of HPD-derived drugs are reported in the literature. The relevance of this data for the PDT action mechanism *in vivo* is questionable owing to the variable pharmacokinetics and metabolic reactions of the constituents.

Pharmacokinetics and Biodistribution. The porphyrins in PF are photosensitizing compounds with different degrees of hydrophobicity. Monomeric porphyrins are eliminated from tissue more rapidly than DHE. It is not known why certain porphyrins tend to localize in tumors. Suggested contributing factors include hydrophobicity, aggregate formation, selective binding to cellular components, molecular charge, low tumor pH, poor lymphatic drainage, vascular permeability, and hypervascularity. PDT drugs are transported by plasma proteins. The pattern of drug distribution in tissues shows a rough correlation with the presence of receptors for low density lipoprotein (LDL). Hydrophilic PDT drugs are more strongly bound to albumin and less to LDL (16). A recent report for seven human patients showed that the plasma half-life of PF is highly variable with a mean of 19 days (17). The highest tissue concentrations of PF in mice are found in tissues high in reticuloendothelial components: liver, adrenal gland, urinary bladder > pancreas, kidney, spleen >

stomach, bone, lung, heart > skin > muscle > brain (19). PF accumulates preferentially in stroma compared to tumor parenchyma, and especially in endothelial cells. Tissue binding sites include free and fixed macrophages of connective tissue, fibrous tissue matrix, mast cells, and Kupffer cells of the liver. At the subcellular level, PF localizes first in the plasma membrane, followed by redistribution to other lipophilic sites, including the mitochondrial, endoplasmic reticulum, and nuclear membranes.

Effects of Light. Indirect evidence indicates that tumor eradication is initiated by a Type II photosensitization pathway, in which singlet molecular oxygen is generated by energy transfer from the DHE triplet state. A singlet oxygen molecule can diffuse about 0.1 μm during its short lifetime in tissue, which confines the primary reactions close to the sites of DHE localization. The acute effects of PDT on cells and tissues are summarized in a recent review (18). Photosensitization of cell cultures by PF requires about 5% oxygen for the maximum effect. Direct evidence for the oxygen requirement in animals was shown by clamping (19). Vascular damage is evident in the initial stages of PDT. Hypoxia develops within minutes after the start of irradiation. The contribution of direct tumor cell kill has been estimated as 20-30% for PF in animal models. The early cellular responses to PDT include leakage of lactate dehydrogenase and release of eicosanoids (prostaglandins, thromboxanes) and histamine. These fast acting vasoactive agents are implicated in the vascular damage component. This action is accompanied by the induction of heat stress proteins (20).

"Second Generation" PDT Drugs

Hundreds of new PDT drugs have been proposed and the list continues to grow. A useful PDT sensitizer must be non-toxic, tumor-localizing, and tumor-photosensitizing. Emphasis has been given to drugs with less skin photosensitization than PF and stronger red or near-infrared absorptions. Chemical structure is the key determinant of the pharmacokinetics and tissue distribution. In general, a higher fraction of a hydrophilic agent localizes in cancer cells compared to PF. The properties of some "second generation" PDT drugs are summarized in Table I, with the abbreviations used in the current literature for the class of compounds or a specific derivative. Chlorins are characterized by a strong enhancement of the far-red absorption band compared to metal-free porphyrins. Mono-L-aspartyl chlorin e6 (NPe6, MACE) was one of the first PDT sensitizers proposed as an alternative to PF (21). Tissue uptake and clearance of NPe6 are much faster than PF. This property enables PDT shortly after administration of the drug, but complicates treatment planning for lengthy procedures. The increased double-bond conjugation in phthalocyanines (Pc) compared to porphyrins leads to stronger and red-shifted absorptions. The Pc structure accepts many types of metal ions. Diamagnetic ions (aluminum, zinc, gallium) are better photosensitizers than paramagnetic ions (cobalt, copper, iron, nickel, chromium) which quench the triplet state. Unsubstituted Pc are insoluble in water, but they can be rendered soluble by sulfonation. Tetrasulfonated AlSPc has a low tendency to aggregate in water and a high singlet oxygen yield (22). Related compounds are

Table I. Some Proposed "Second Generation" PDT Photosensitizers

<i>Photosensitizer</i>	<i>Hydrophobicity</i>	λ_{max}^a	<i>Ref.</i>
Mono-L-aspartyl chlorin e6 (NPe6, MACE)	water soluble	660 (9)	21
Sulfonated aluminum phthalocyanine (AlSPc)	water soluble	670 (40)	22
Benzoporphyrin derivative monoacid ring A (BPD-MA)	hydrophobic	690 (5)	23
Octaethylpurpurin (NT2)	hydrophobic	700 (15)	24
Pheophorbides (HEDP)	hydrophobic	660 (20)	25
5-Aminolevulinic acid (ALA)	hydrophilic	640 (2) ^b	26
Cationic dyes (CPS)	hydrophilic	^c	27

^a The approximate location of the longest wavelength absorption band is indicated with the absorption intensity relative to PF at 630 nm in parenthesis.

^b Topical ALA is converted to protoporphyrin IX within tumors.

^c Many different types of CPS have been suggested for PDT with absorptions from 600-900 nm.

sulfonated zinc phthalocyanine (ZnSPc) and chloro-aluminum sulfonated phthalocyanine (ClAlSPc). Benzoporphyrin derivatives (BPD) are benzo-derivatives of protoporphyrin IX (23). BPD are insoluble in water and must be administered in a vehicle such as liposomes or an oil emulsion. The potentially useful features are fast uptake, selectivity for neoplastic tissues and significant clearance after about 24 hours. Purpurins are benzochlorins with additional conjugation through substitution. Octaethylpurpurin (NT2) and tin etiopurpurin dichloride (SnET2.2Cl) are proposed PDT sensitizers (24). The metal atom induces a blue-shift to about 650 nm. Animal studies are indicative of high photodynamic efficacy and low skin photosensitization. Pheophorbides are metal-free derivatives of chlorophyll without the aliphatic phytol side chain. Animal tumor model studies indicate that 2(1-O-alkyl) ethyl-desvinyl-methyl pheophorbide-a (HEDP) is an effective PDT sensitizer with a low skin reaction after 3 days (25).

5-Aminolevulinic acid (ALA) is the common metabolic precursor of porphyrins in microorganisms, plants, and animals. The use of ALA as a PDT photosensitizer exploits the enhanced rate of protoporphyrin IX (PP) formation in tumors compared to normal tissues (26). This innovative approach minimizes the protracted skin photosensitization induced by intravenous porphyrins. Most PDT drugs have anionic structures. Cationic photosensitizing dyes (CPS) have been proposed

for PDT under anoxic conditions and in combination with hyperthermia (27). CPS are selectively localized in mitochondria of tumor cells. Representative classes of CPS include cyanines, triarylmethanes, oxazines, and chalcogenapyryliums. Very high light doses are required for tumor necrosis compared to porphyrins. The anionic cyanine dye merocyanine 540 (MC 540) is being tested as an photosensitizing antiviral agent (28). In the presence of serum components, MC 540 binds preferentially to electrically excitable cells, leukemia cells, and certain classes of immature normal blood cells. Exposure to white light leads to rupture of the plasma membrane and cell death.

PDT as an Adjuvant Therapy and Modified Procedures

Intraoperative PDT may be effective for procedures in which surgical excision cannot remove the entire tumor. The combination of localized hyperthermia (HT) and PDT has received attention. Animal tumor results indicate that a sub-curative PDT dose can initiate tumor necrosis when combined with simultaneous HT (29). HT may be provided by a microwave generator or a Nd:YAG laser coupled into the PDT laser (30). The response of normal tissues exposed to PDT light sets a practical limit on PDT light dose. The PDT efficacy may be improved by selectively increasing tumor response and protecting normal tissues. Experimental techniques directed to this objective include protection of normal tissue with radioprotective agents, increasing the localized drug concentration by coupling to monoclonal antibodies, and increasing tumor oxygenation by fractionating the light dose. The combination of porphyrin photosensitization with ultrasound is an interesting concept that has been found to increase lethality in cell cultures (31). A possible mechanism involves the generation of cavitation energy at the interface between the cell surface and the medium. Administration of glucose to mice prior to PDT potentiated the tumor response (32). The effect of hyperglycemia was attributed to lowering of intratumoral pH.

PDT Photophysics and Phototechnology

A high fraction of all tumors treated with PDT have shown at least a partial response. However, the statistics for long-term tumor eradication are widely variable. Many factors can lead to a partial response including local heterogeneities in the light dose, drug concentration, and the intrinsic tumor photosensitivity. The treatment parameters are controlled in clinical trials to allow for statistical evaluation of the results. Individualized treatment planning for each tumor site will be required when PDT is fully approved. Light dosimetry modeling based on tissue optics has been employed for this purpose (33-35). The "threshold hypothesis" assumes that tumor eradication requires a minimum absorbed energy density by the localized photosensitizer. The modeling objective is to relate the incident fluence to the effective intratumoral light dose for given treatment conditions. According to the photon diffusion approximation, the absorbed energy density equals the product of the local fluence rate and the photosensitizer absorption coefficient integrated over time. This quantity must exceed the absorbed energy threshold in tissue regions most distant from light

entry. Monte Carlo simulation provides an independent test of the calculations (36). Recent advances in tissue optic theory motivated by PDT have been extended to other biomedical applications, including modeling of localized hyperthermia, laser ablation of tissues, and non-invasive methods of optical diagnosis and imaging.

PDT phototechnology is a collateral research area. Noninvasive measurements of localized drug dose based on fluorescence and diffuse reflection should improve the reliability of modeling calculations. Much effort has been directed to the development of improved PDT lasers. Argon-ion pumped dye lasers are bulky, require frequent adjustments, and do not provide adequate power output in the far-red and near-infrared regions for "second generation" photosensitizers. Other dye pumping lasers employed for PDT include the pulsed Nd:YAG laser doubled to 532 nm with a potassium titanyl phosphate (KTP) crystal, the copper vapor laser (511 nm, 578 nm), and the XeCl excimer laser (308 nm). PDT has been carried out with the gold vapor laser (628 nm), the titanium-sapphire laser pumped by an argon-ion or doubled Nd:YAG laser (670-1100 nm), and the Alexandrite laser (720-790 nm). Semiconductor diode lasers are very compact, emit stable CW or pulsed light, have very long lifetimes, and may be temperature tuned. However, the applications have been limited by low power output, less than 1 W in the 660-690 nm region, and low irradiance that limits efficient coupling into an optical fiber.

The Future of PDT?

PDT remains an experimental therapy after almost two decades of clinical trials. Encouraging short-term responses are reported for some malignancies. The lack of evidence for superior long-term efficacy compared to conventional treatments has contributed to the slow acceptance of PDT. Cutaneous photosensitization has been cited as a negative factor. However, only a small fraction of noncompliant PDT patients have experienced adverse reactions that required medical attention. Many clinicians are unfamiliar with phototherapy procedures and instrumentation. Active clinical groups generally include a physicist for this expertise. PDT has been the subject of a major preclinical research effort. A recent review cites 900 publications through 1989 (37). This number may have since doubled. Much of this work is reported in journals that are not usually read by clinicians. Unnecessary redundancy in reporting appears to be a characteristic of this field. The present impasse may be broken when PDT is fully approved for at least one condition. Recently, Canada's Health Protection Branch cleared Photofrin for PDT of bladder cancer (39). This step should accelerate the acquisition of clinical data and provide the information required for a more definitive evaluation of the therapy.

Acknowledgments

The author is pleased to acknowledge the helpful comments of Rocco V. Lobraico, M.D. of Ravenswood Hospital Medical Center and James B. Grossweiner, M.D. During the preparation of this paper the author received partial support from the National Institutes of Health on Grant No. GM 20117 to Illinois Institute of Technology.

Literature Cited

1. Tappenier, H. V.; Jesionek, A. *Muchen. Med. Wehnschr.* **1903**, *1*, 2042-2044.
2. Lipson, R. L.; Baldes, E. J.; Olsen, A. M. *J. Natl. Cancer. Inst.* **1961**, *26*, 1-11.
3. Kelley, J. J.; Snell, M. E. *J. Urol.* **1976**, *115*, 150-151.
4. Dougherty, T. J.; Kaufman, J. E.; Goldfarb, A.; Weishaupt, K. R.; Boyle, D.; Mittleman, A. *Cancer Res.* **1978**, *38*, 2628-2635.
5. Dougherty, T. J. *Photochem. Photobiol.* **1987**, *45*, 879-889.
6. Wilson, B. W.; Mang, T. E.; Cooper, M. C.; Stoll, H. *Facial Plastic Surg.* **1990**, *6*, 185-189.
7. Potter, W. R.; Mang, T. S.; Dougherty, T. J. *Photochem. Photobiol.* **1987**, *46*, 97-101.
8. Marcus, S. L. *Proc. IEEE* **1992**, *80*, 869-889.
9. de Corbiere, S.; Ouayoun, M.; Sequert, C.; Freche, Ch.; Carbolle, F. In *Photodynamic Therapy and Biomedical Lasers*, Spinelli, P.; Dal Fante, M.; Marchesini, R., Eds., Excerptia Medica, Amsterdam, 1992, pp 656-661.
10. Wenig, B. L.; Kurtzman, D. M.; Grossweiner, L. I.; Mafee, M. G.; Harris, D. M.; Lobraico, R. V.; Prycz, R. A.; Appelbaum, E. L. *Arch. Otolaryngol. Head Neck Surg.* **1990**, *116*, 1267-1270.
11. Lobraico, R. V.; Grossweiner, L. I. *J. Gynecol. Surg.* **1993**, *9*, 29-34.
12. Nakamura, T.; Ejiri, M.; Fujisawa, T.; Akiyama, H.; Ejiri, K.; Ishida, M.; Fulimori, T.; Maeda, S.; Saeki, S.; and Baba, S. J. *Clin. Surg.* **1990**, 63-67.
13. Muller, P. J.; Wilson, B. C. *Can. J. Neurol. Sci.* **1990**, *17*, 193-198.
14. Dougherty, T. J.; Potter, W. R.; Weishaupt, K. R. In *Porphyrin Localization and Treatment of Tumors*, Doiron D., R.; Gomer, C. J. Eds., Alan R. Liss, New York, NY, 1984, pp 301-314.
15. Byrne, C. J.; Marshallsay, S. Y.; Sek, S. Y.; Ward, A. D In *Photodynamic Therapy of Neoplastic Disease*, Kessel, D., Ed., CRC Press, Boca Raton, FL, 1990, Vol. II, pp 131-144.
16. Kessel, D. *Oncology Res.* **1992**, *4*, 219-225.
17. Brown, S. B.; Vernon, D. I.; Holroyd, J. A.; Marcus, S.; Trust, R.; Hawkins, W.; Shah, A.; Tonelli, A. In *Photodynamic Therapy and Biomedical Lasers*, Spinelli, P.; Dal Fante, M.; Marchesini, R., Eds., Excerptia Medica, Amsterdam, 1992, 475-479.
18. Henderson, B. W.; Dougherty, T. J. *Photochem. Photobiol.* **1992**, *55*, 145-157.
19. Gomer, C. J.; Razum, N. J. *Photochem. Photobiol.* **1984**, *40*, 435-439.
20. Gomer, C. J.; Ferrario, A.; Rucker, N. In *Photodynamic Therapy of Neoplastic Disease*, Vol. I, Kessel, D., Ed., CRC Press, Boca Raton, FL, 1990, Vol. I, pp 189-195.
21. Nelson, J. S.; Roberts, W. G.; Liaw, L.-H.; Berns, M. W. In *Photodynamic Therapy of Neoplastic Disease*, Kessel, D., Ed., CRC Press, Boca Raton, FL, 1990, Vol. I, pp 147-167.
22. van Lier, J. E. In *Photodynamic Therapy of Neoplastic Disease*, Kessel, D., Ed., CRC Press, Boca Raton, FL, 1990, Vol. I, pp 279-290.
23. Sternberg, E.; Dolphin, D. In *Photodynamic Therapy and Biomedical Lasers*, Spinelli P.; Dal Fante, M.; Marchesini, R., Eds., Excerptia Medica, Amsterdam, 1992, pp 470-474.

24. Morgan, A. R.; Selman, S. H. In *Photodynamic Therapy of Neoplastic Disease*, Kessel, D., Ed., CRC Press, Boca Raton, FL, 1990, Vol. I, pp 247-262.
25. Ho, Y.-K.; Pandey, R. K.; Sumlin, A. B.; Missert, J. R.; Bellnier, D. A.; Dougherty, T. J. In *Photodynamic Therapy: Mechanisms II*, Dougherty, T. J., Ed., SPIE-Int. Soc. Opt. Eng., Bellingham, WA, 1990, Vol. 1203, pp 293-300.
26. Kennedy, J. C.; Pottier, R. H. J. *Photochem. Photobiol. B Biol.* **1992**, *14*, 275-292.
27. Oseroff, A. R.; Ara, G. A.; Wadwa, K. S.; Dahl, T. In *Photodynamic Therapy of Neoplastic Disease*, Kessel, D., Ed., CRC Press, Boca Raton, FLA, 1990, Vol. I, pp 291-306.
28. Sieber, F. In *Future Directions and Applications in Photodynamic Therapy*, Gomer, C. J., Ed., SPIE-Int. Soc. Opt. Eng., Bellingham, WA, 1990, Vol. IS 6, pp 209-218.
29. Waldow, S. M.; Dougherty, T. J. *Radiat. Res.* **1984**, *97*, 380-385.
30. Mang, T. S. *Lasers Surg. Med.* **1990**, *10*, 173-178.
31. Kessel, D.; Jeffers, R.; Cain, C. In *Optical Methods for Tumor Treatment and Detection: Mechanisms and Techniques in Photodynamic Therapy*, Dougherty, T. J., Ed., SPIE-Int. Soc. Opt. Eng., Bellingham, WA, 1992, Vol. 1645, pp 82-89.
32. Nelson, J. S.; Kimel, S.; Brown, L.; Berns, M. W. *Lasers Surg. Med.* **1992**, *12*, 153-158.
33. Grossweiner, L. I. *Lasers Surg. Med.* **1991** *11*, 165-173.
34. Svaasand, L. O.; Gomer, C. J.; Morinelli, E. In *Future Directions and Applications in Photodynamic Therapy*, Gomer, C. J., Ed., SPIE-Int. Soc. Opt. Eng., Bellingham, WA, 1990, Vol. IS 6, pp 233-248.
35. Star, W. M.; Wilson, W. C.; Patterson, S. In *Photodynamic Therapy*, Henderson, B. W.; Dougherty, T. J., Eds., Marcel Dekker, New York, NY, 1992, pp 335-368.
36. Prahl, S. A.; Keijzer, M.; Jacques, S. I.; Welch, A. J. In *Dosimetry of Laser Radiation in Medicine and Biology*, Müller, G. J.; Sliney D. H., Eds, SPIE-Int. Soc. Opt. Eng., Bellingham, WA, 1989, Vol. IS 5, pp 102-111.
37. *Photodynamic Therapy of Neoplastic Disease*, Kessel, D., Ed., CRC Press, Boca Raton, FLA, 1990, Vol. I-II.
38. *Medical Laser Report* **1993** *7*, 1-2.

RECEIVED April 5, 1994

Chapter 19

Effects of Diphenyl Ether Herbicides on the Heme Pathway in Cultured Liver Cells

P. R. Sinclair¹⁻³, N. Gorman^{1,2}, H. S. Walton^{1,2}, J. F. Sinclair¹⁻³,
Judith M. Jacobs⁴, and Nicholas J. Jacobs⁴

¹Veterans Administration Medical Center, White River
Junction, VT 05009

Departments of ²Biochemistry, ³Pharmacology/Toxicology, and

⁴Microbiology, Dartmouth Medical School, Hanover, NH 03775-3842

The toxicity of diphenyl ether herbicides (DPEs) in plants has been attributed to inhibition of protoporphyrinogen (PGEN) oxidase, an enzyme in the heme biosynthetic pathway. This inhibition results in accumulation of phototoxic protoporphyrin (PROTO). To assess the potential toxicity of diphenyl ether herbicides for mammals we investigated whether these chemicals also inhibit PGEN oxidase in primary cultures of chicken and rat hepatocytes. These cultures, when treated with acifluorfen were shown to accumulate PGEN. Rat hepatocyte cultures accumulated PROTO when treated with AF or AFM. However, chicken hepatocyte cultures treated with acifluorfen accumulated uroporphyrin (URO). URO accumulation is prevented by inhibitors of cytochrome P450 and by ascorbate. These results indicate that diphenyl ethers affect two different steps of the heme synthetic pathway.

The heme biosynthetic pathway is composed of seven enzymatic steps (Figure 1). Some of these reactions can be specifically inhibited by exogenous chemicals in animals and humans *in vivo* (for reviews see 1, 2). Lead inhibits ALA (5-aminolevulinic) dehydrase. Polyhalogenated aromatic compounds (PHAs) such as hexachlorobenzene and planar halogenated biphenyls, cause decreases in uroporphyrinogen decarboxylase (UROD) activity, associated with URO accumulation and skin photosensitivity. Chelators, substituted collidines, and lead inhibit ferrochelatase resulting in PROTO accumulation. These inhibitions may produce a number of pathological effects due to accumulated intermediates (for review see 3). Such effects range from neurological damage thought to be due to accumulation of ALA and porphobilinogen, to skin lesions due to accumulation of the photosensitive porphyrins in the skin (3). There may also be tissue damage at the site of porphyrin accumulation. In Porphyria Cutanea Tarda (PCT), massive hepatic URO accumulation is associated with increased incidence of hepatoma (1-3).

Chemicals that cause blocks at different steps of the heme biosynthetic pathway, can also cause induction of the rate-limiting enzyme of the pathway, ALA synthase (ALA-S). This latter effect can greatly increase accumulation of toxic intermediates of the pathway. The inductive effect on ALA-S is due to inhibition of heme synthesis

0097-6156/94/0559-0266\$08.00/0
© 1994 American Chemical Society

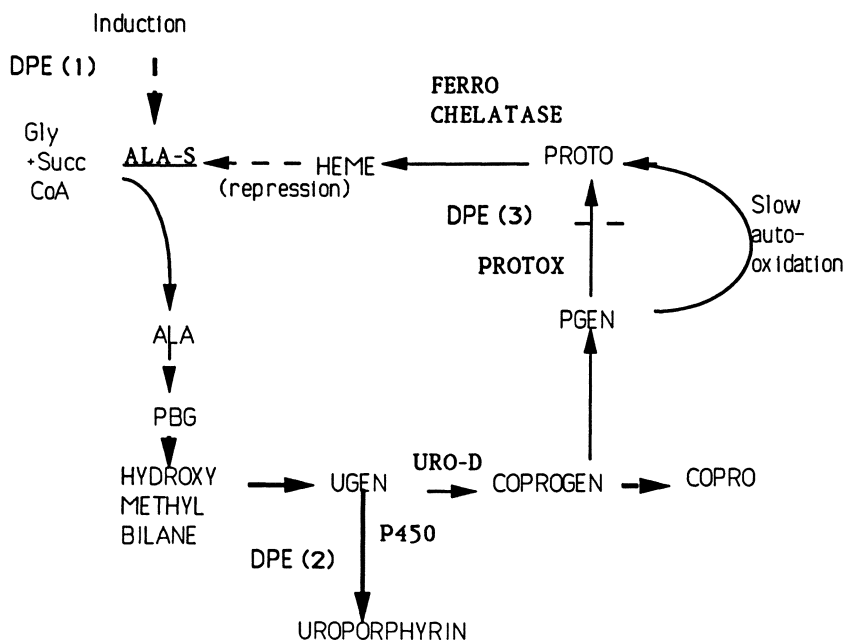


Figure 1. Scheme of sites of action of DPEs on the heme synthetic pathway.

Enzymes : ALA-S, ALA synthase; URO-D, UGEN decarboxylase; PROTOX, PGEN oxidase.

1. Induction of ALA-S at DNA level.

2. URO accumulation due to oxidation of UGEN by DPE-induced cytochrome P450.

3. Inhibition of PROTOX.

resulting in loss of negative regulation of ALA-S by heme, the end product of the pathway (see Figure 1).

Recently, it was shown that the herbicidal effects of several DPEs in plants are due to inhibition of protoporphyrinogen oxidase (PROTOX), causing accumulation of phototoxic PROTO. DPEs and other phototoxic herbicides (such as oxadiazon) have also been found to competitively inhibit mammalian PROTOX *in vitro* (4) suggesting that the enzyme is similar in plants and animals. In contrast, the bacterial enzyme is not inhibited by DPEs (5). These findings raise the question of whether exposure of animals, including humans, to DPEs could result in inhibition of PROTOX *in vivo* and accumulation of PGEN and PROTO, leading to potential pathological effects. Here we have summarized our recent investigations on the effects of DPEs on porphyrin accumulation in the liver, using cultured hepatocytes from avian and mammalian sources as model systems. We found two major effects: i) that DPEs cause accumulation of PGEN in the hepatocyte cultures and ii) an unexpected effect, that DPEs cause a cytochrome P450-mediated accumulation of URO.

The hepatocyte cultures have been widely used to determine the toxicological effects of exogenous chemicals on the liver (1,6,7). The cultured hepatocytes retain highly differentiated properties, including the inducibility of ALA-S and hepatic cytochrome P450s by exogenous chemicals and drugs. The cytochrome P450s are membrane-bound oxidases that activate many hepatotoxins and carcinogens (8). Thus, these hepatocyte cultures can be used i) to test the ability of DPEs to block hepatic heme synthesis with accumulation of porphyrins as well as induction of ALA-S, and ii) to investigate the possible involvement of cytochrome P450s in the response.

Methods

In these experiments, hepatocytes are isolated from 16-day-old chick embryos and cultured in a chemically defined medium (6). Cultures are treated as described in figure and table legends and porphyrins extracted from cells plus medium with acid-organic solvent mixtures such as perchloric acid-methanol (1M PCA/methanol (1/1,v/v), aceton-conc. HCl (97.5/2.5,v/v) or ethyl acetate/acetic acid (3/1,v/v)). The composition of the porphyrins is usually determined by spectrofluorimetry, using a matrix that allows determination of porphyrins as URO, coproporphyrin (COPRO) or PROTO (6). These determinations are verified by reversed phase HPLC of the extracted porphyrins (9). Rat hepatocytes from adult male Fischer 344 rats are cultured in a chemically defined medium in dishes coated with a matrix isolated from a mouse tumor (7).

Porphyrin Accumulation in Cultured Chick Hepatocytes Treated with DPEs

Although DPEs cause PGEN accumulation in the avian culture, which will be described later, we have found that the major effect on the heme pathway of DPEs, particularly those derivatives with hydrophobic substitutions in the benzene rings, is to cause massive URO accumulation.

Effects of DPEs on URO Accumulation in Avian Hepatocytes. In most of the experiments, we have used as representative DPEs, acifluorfen (AF) or AF methyl (AFM). In the latter, the free carboxyl group of AF is present as the methyl ester. In our initial study (9), we found no accumulation of URO caused by addition of either AF or AFM alone to these cultures at concentrations up to 80 μ M. Table I shows that URO accumulation occurs when AFM is combined with an esterase inhibitor, bis-*p*-nitrophenylphosphate (BNPP). As shown by HPLC (9), BNPP prevented conversion of AFM to AF by hydrolysis of the carboxymethyl group. Under this condition, the cultures accumulated large amounts of URO. We attribute the ability of AFM plus

BNPP to cause URO accumulation to be due to a dual effect of AFM plus BNPP: i) induction of cytochrome P450, an effect which can be replaced by other cytochrome P-450 inducers (see below) and ii) an effect of either AF or AFM to stimulate the P450-catalyzed oxidation of UGEN to URO by a mechanism similar to that caused by PHAs (see below).

Table I. Effect of DPEs on URO accumulation in the presence of an esterase inhibitor in chick embryo hepatocytes in culture.

<i>Compound</i>	<i>Concentration</i> (μM)	<i>URO</i> ^a (nmol/dish)	<i>COPRO</i> (nmol/dish)	<i>PROTO</i> (nmol/dish)
EXPT 1				
AFM plus BNPP ^b	13	1.95	0.39	0.12
Lactofen	11	0.06	0.09	0.08
Lactofen plus BNPP	11	0.78	0.57	0.15
Lactofen	55	0.11	0.14	0.13
Lactofen plus BNPP	55	1.14	0.35	0.05
EXPT 2				
AFM plus BNPP	13	1.53	0.10	0.00
Nitrofen	14	0.78	0.06	0.00
Nitrofen plus BNPP	14	0.83	0.05	0.00
EXPT 3				
Oxadiazon	14	0.55	0.11	0.01
Oxadiazon plus BNPP	14	0.60	0.10	0.10

Cultures were treated for 18 h and cells plus medium was extracted with PCA-methanol. Porphyrins were determined spectrofluorimetrically. Values for untreated dishes were less than 0.02 nmole /dish for URO, COPRO and PROTO.

^aValues are means for 2 dishes and ranges were within 10%.

^bBNPP was present at 30 μM .

Table I also shows that other phototoxic DPEs caused URO accumulation in the avian liver culture. These DPEs are lactofen (similar to AFM except for a larger ester group which on hydrolysis also yields AF) and nitrofen (which has no substituent at that position), as well as the phototoxic herbicide, oxadiazon (which is not a DPE, but rather an oxadiazole ring with a substituted phenyl group and no ester group). Lactofen, like AFM, was ineffective in causing URO accumulation in the absence of BNPP, consistent with the need to retain the ester group intact for production of URO, whereas nitrofen and oxadiazon were effective in producing URO irrespective of the presence of BNPP. Table I also shows that the higher concentration of lactofen was partially effective in the absence of BNPP, probably due to incomplete ester hydrolysis. These results suggest that it is the increase in hydrophilicity from the conversion of the ester groups of AFM and lactofen to free carboxylic acids, which destroys the ability of the resultant DPEs to cause URO accumulation.

Figures 2A and 3 also present data relevant to this question. AF alone at higher concentrations also caused some accumulation of URO (Figure 2A). However

achieving URO accumulations similar to those produced by AFM plus BNPP, required the addition of 2-propyl-2-isopropylacetamide (PIA) (Figure 2A). The role of PIA in this combination is attributed to the known effects of PIA to cause induction of both ALA-S and cytochrome P4502H, as indicated by increases in their mRNAs (10). Figure 3 shows the dose response of AF on URO and PRTO accumulations in cells also treated with PIA. URO was increased by AF up to a concentration of 0.22 mM AF. Figure 2A also shows that the accumulation of URO caused by PIA plus AF was suppressed by ascorbate.

Mechanism of the URO Accumulation in Avian Hepatocytes Caused by Chemicals other than DPEs: Role of Cytochrome P450

Accumulation of URO caused by DPEs in avian hepatocytes is not unique to this class of chemicals; many other chemicals cause this effect. Here we present a summary of the current concepts of the mechanism of URO accumulation and discuss how the results described above for DPEs are consistent with this mechanism.

Polyhalogenated Aromatic Compounds (PHAs) and URO Accumulation.

Hexachlorobenzene was the first PHA reported to cause URO accumulation in mammals, following consumption of treated seed wheat by humans in Turkey in the late 1950s (11). This phenomenon could also be produced with PHAs in rodents and cultured avian hepatocytes. This URO accumulation was attributed, in part, to induction of a microsomal oxidizing enzyme system containing the cytochrome P450 (P450) hemoproteins. The role of the P450s was initially thought to be the conversion of PHAs to inhibitors of the heme synthetic pathway enzyme, UROD, resulting in accumulation of the substrate UGEN, which then spontaneously oxidizes to URO. This idea became untenable when non-metabolizable PHAs were also found to cause experimental uroporphyrin (see review, 12). Work from this laboratory showed that P450 inhibitors prevented URO accumulation in avian cultures treated with PHAs (6,13) suggesting a role for the P450. One hypothesis to account for this result was that the P450 induced by PHAs produced reactive oxygen intermediates, which would then oxidize UGEN to URO (13,14). An alternative hypothesis was that P450 directly oxidized UGEN, and this hypothesis found experimental support. UGEN oxidation was catalyzed by hepatic microsomes from avians and rodents treated with 3-methylcholanthrene to induce P450 1A (14-16). Only one of the two highly homologous rodent P450s that were induced by the PHAs (P4501A2), is involved in the reaction (16). This form is found only in the liver, explaining why URO originates in the liver, from which it leaks into the blood and hence is carried to the skin and other sites. UGEN oxidation activity can be reconstituted with purified mouse P450 1A2, P450 flavin reductase, and phospholipid (17). UROGEN oxidation can also be reconstituted with purified avian P450 1A (Sinclair, P., Gorman, N., Lambrecht, R., Sinclair, J., and Rifkind, A., unpublished studies). Most recently, ascorbic acid has been shown to be a competitive inhibitor of microsomal UGEN oxidation and, when added to the avian culture, prevents URO accumulation (18). Since this inhibition occurs at ascorbate concentrations within the range found in human plasma, we have suggested that ascorbate effectively prevents URO accumulation caused by PHAs and other chemicals in humans (18). We hypothesize that precipitation of the human uroporphyrin known as Porphyria Cutanea Tarda (PCT) by agents such as ethanol, might be due to decreases in hepatic ascorbate concentrations.

Inactivation of UROD. In animals treated with chemicals that cause URO accumulation, the activity of the enzyme, UROD, becomes markedly decreased at the time that URO accumulates (19). However, UROD protein is still detectable (20). This suggests that the enzyme is inactivated, although the mechanism of the inactivation is

not known. Several workers have reported that a heat-stable inhibitor of UROD can be extracted from the liver of these animals (for review see 12). There is evidence suggesting that this inhibitor may be derived from UGEN, perhaps during the P4501A-catalyzed oxidation (21). We also found that when 9000g liver supernatants, containing both cytosolic UROD and induced microsomal P4501A, are incubated with UGEN and NADPH, there is complete inhibition of UGEN decarboxylation (22). We attributed this inhibition of UGEN decarboxylation to a short-lived UROD inhibitor formed during the UGEN oxidation, but the relationship between the stable and labile UROD inhibitors remains to be established.

URO Accumulation in Avian Hepatocytes Caused by Non-PHA Compounds. In the avian culture system, but not as yet in intact animals, there are a number of compounds other than PHAs which cause URO accumulation. These compounds which include phenobarbital, glutethimide, carbamezapine, nifedipine, and aliphatic alcohols, such as ethanol and isopentanol, are inducers of members of the 2H subfamily of P450 rather than 1A subfamily induced by PHAs (13,23,24). In the avian cultures, inhibitors of P450 2H activity (piperonyl butoxide and SKF-525A) block URO accumulation caused by these compounds (13). Although piperonyl butoxide is a non-specific inhibitor of activities catalyzed by P450 isozymes, SKF-525A is more specific and does not inhibit P450s of the 1A subfamily. As with PHA-induced URO accumulation, ascorbate is also effective in preventing URO accumulation caused by these compounds in the avian culture (unpublished studies, Sinclair, P., Walton, H., Gorman, N., Sinclair, J.).

Mechanism of URO Accumulation Caused by DPEs in Avian Cells

Role of Cytochrome P450s. The observations described above (Table I and Figure 2A) indicate that the mechanism of URO accumulation caused by DPEs in avian hepatocytes has some similarities to the URO accumulation caused by both PHAs and non-PHA compounds. However, there are some features that are unique to the URO accumulation caused by DPEs. Previously we reported that AFM plus BNPP caused increases in P450s of the 1A subfamily (9). P450 2H was also induced by AFM plus BNPP in the avian cultures (9). In addition, we found that URO accumulation caused by AFM was inhibited by piperonyl butoxide (a non-specific P450 inhibitor), by ellipticine (a specific inhibitor of P450 1A), and by SKF-525A (an inhibitor of P450 2H) (Sinclair, P., Walton, H., Gorman, N., Sinclair J., unpublished results). These data suggest, that for AFM, more than one form of P450 may be involved in URO accumulation.

Figure 2A shows that URO accumulation stimulated by AF required co-treatment with PIA for maximal effect. We attribute this to the requirement for induction of P450 2H by PIA. With AFM, the role of the hydrophobic -COOCH₃ group would be to induce P450 2H as shown by the increase in P450 2H caused by AFM plus BNPP (9). The exact mechanism by which AF or AFM cause URO accumulation is not known, but we postulate it is a P450-catalyzed oxidation of UGEN by analogy with the mechanism demonstrated for URO accumulation caused by PHAs (6,13). More work is required to elucidate the complete mechanism of the P450-mediated URO accumulation caused by DPEs.

Further evidence consistent with a role for cytochrome P-450 in DPE-mediated URO accumulation is the finding that URO accumulation caused by PIA plus AF was inhibited by ascorbate (Figure 2). We have shown that ascorbate competitively inhibits P450 1A-catalyzed UGEN oxidation (18). A similar inhibition may occur with P450 2H. There was also a decrease of URO accumulation in the presence of PIA plus AF when the ferric iron chelator, desferrioxamine (DES), was added to the cultures (compare Figures 2A and 2B). PIA plus DES causes a large accumulation of PROTO

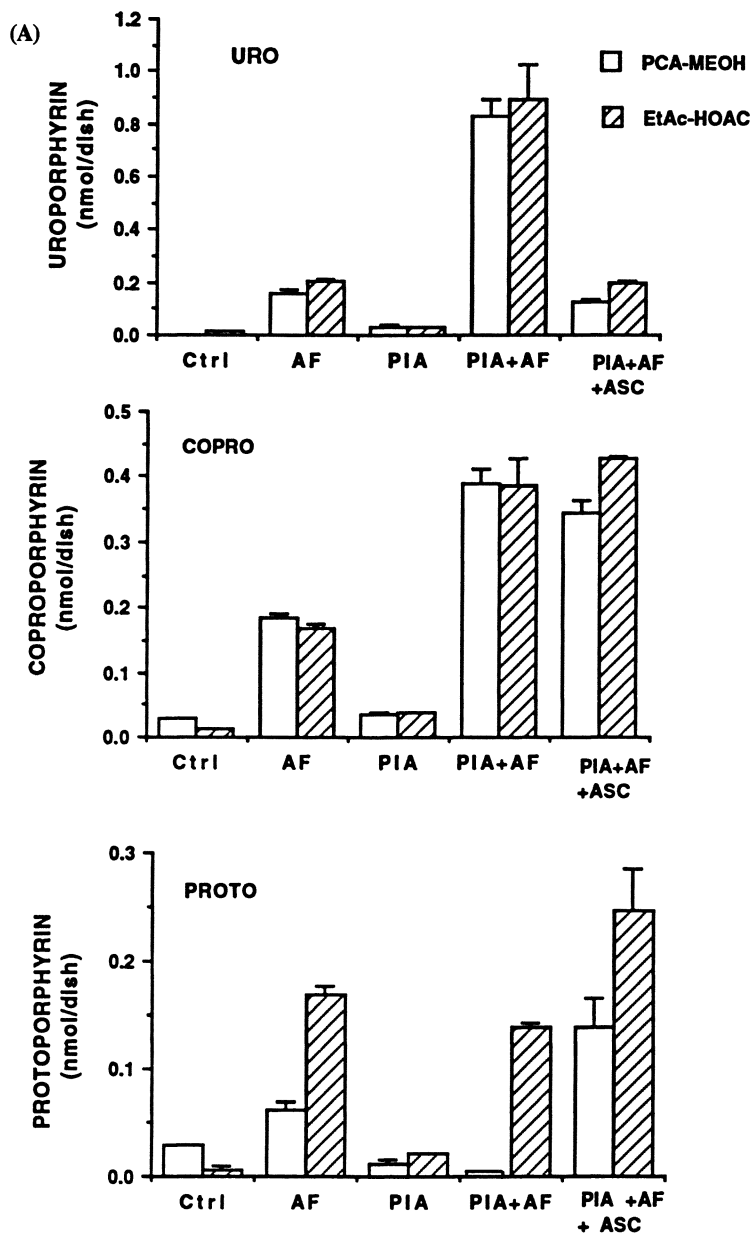


Figure 2. Accumulation of porphyrins caused by treatments with AF, PIA, DES, and ascorbate in chick embryo hepatocytes. A: Effects of AF, PIA and ascorbate. B: Effects of AF, PIA and DES. Cells in 3.5 cm dishes containing 1 ml medium were treated with the chemicals for 18 h. Porphyrins were extracted with PCA-methanol (MeOH) or ethyl acetate-acetic acid followed by exposure to light (EtAc/AcAc). Concentrations of chemicals were (μM): AF, (220); 2-propyl-2-isopropylacetamide (PIA), (420); ascorbate (Asc) (1000); DES, (120). Values are means and range for 2 dishes.

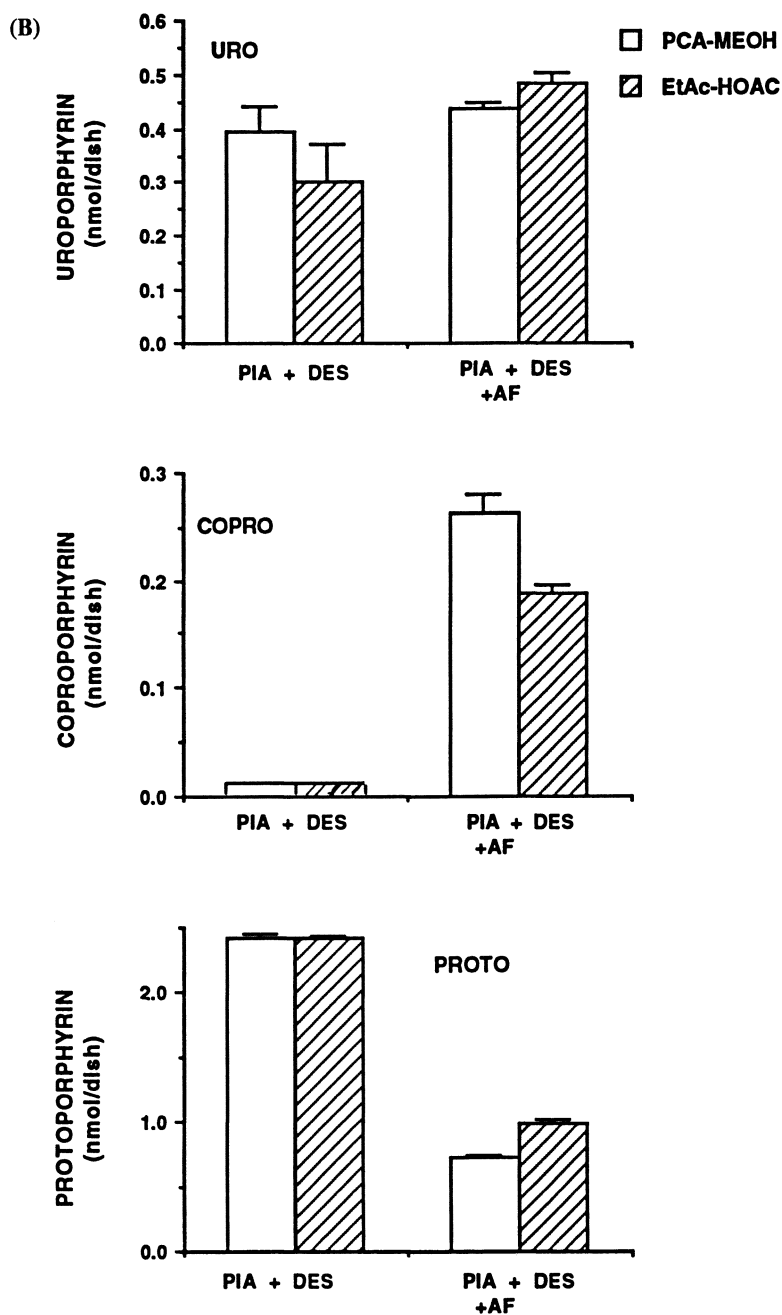


Figure 2. Continued.

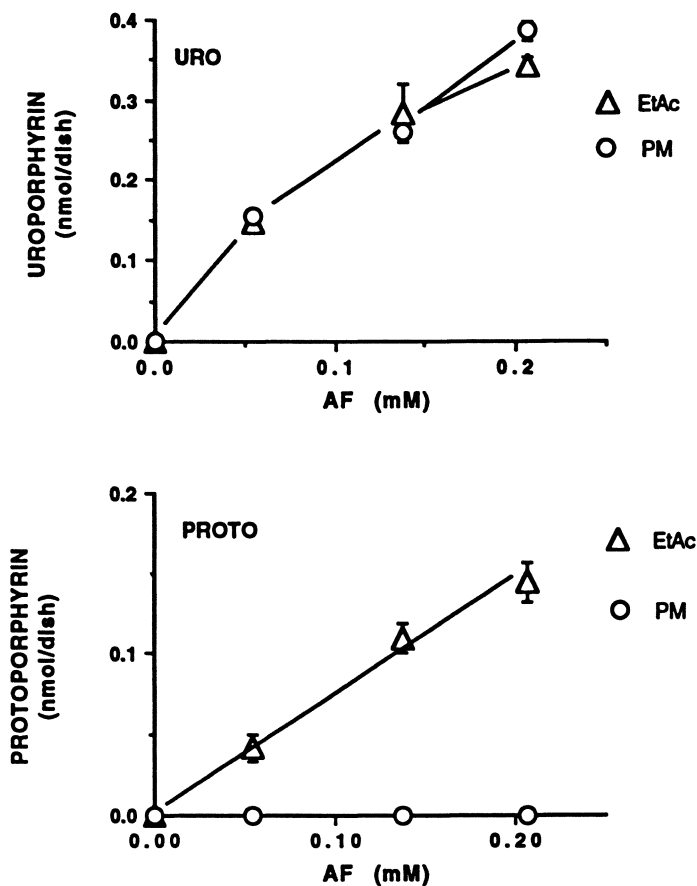


Figure 3. Comparison of extraction methods for URO and PGEN in chick embryo hepatocyte cultures treated with AF. Cells were treated and extracted as in Figure 2. PIA was present at 0.042 mM in all dishes. EtAc (ethyl acetate-acetic acid); PM (PCA-methanol). Values are means and ranges for 2 dishes.

because DES inhibits the iron insertion enzyme, ferrochelatase. DES has been shown previously to decrease URO accumulation by decreasing the induced level of P450s as a result of inhibited heme synthesis (6).

URO accumulation in rat hepatocyte cultures and intact animals.

Contrary to their effects on avian hepatocytes, AF and AFM did not cause URO accumulation in rat hepatocyte cultures (9). However, Krijt et al have recently reported (25, this volume) that liver from mice treated with DPEs or oxadiazon in the diet, accumulated URO as the major hepatic porphyrin. This suggests that the rat hepatocyte cultures lack the appropriate P450 required for URO accumulation. We and others have shown that these cultures lack P450 1A2 (26) whereas mouse hepatocyte cultures which are inducible for P450 1A2 in response to PHAs, accumulate URO (27). We have presented evidence for a role of P450 1A2 to produce URO accumulation in rodents (16). The lack of URO accumulation caused by DPEs in rat hepatocytes is consistent with a lack of inducible P450 1A2 in these cultures.

Accumulation of Protoporphyrinogen (PGEN) in Cultured Hepatocytes treated with DPEs

In our initial investigations (9), avian and rat hepatocytes were treated with AF and AFM with and without the esterase inhibitor, BNPP, to see if they accumulated PROTO. Such an accumulation was expected since these compounds had been shown to inhibit mouse and chick embryo PROTOX activity in isolated mitochondrial preparations (9). PROTOX inhibition would be expected to inhibit heme synthesis and to result in induction of ALA-S due to relief of normal feedback regulation (Figure 1). If PGEN accumulated in the hepatocytes, it would be expected to oxidize to PROTO during the extraction. However, in the avian hepatocyte cultures treated with AF or AFM plus BNPP, we could not detect an increase in PROTO (9). In the rat hepatocyte cultures, a small increase in PROTO was found, but only after treatment with AFM plus BNPP or with high concentrations of AF (9). These findings with rat hepatocytes were recently confirmed in rat hepatocyte cultures by Krijt et al using other DPEs (25, this volume). For the avian cultures, the inability to detect PROTO accumulation was attributed to the major block of the heme pathway at the earlier UROD step (9), thus limiting conversion of UGEN to PGEN and therefore minimal accumulation of PGEN due to PROTOX inhibition.

Alternative extraction methods for greater recovery of PGEN. Recent work by Jacobs and Jacobs (5, this volume) who have investigated DPE inhibition of PGEN oxidation by barley plastids, showed that the recovery of accumulated PGEN as PROTO is poor following extraction with perchloric acid (PCA)-methanol, the solvent used in our culture experiments (9, this volume). Sano and Granick (28), in their classical enzymatic studies of PGEN formation by rat liver mitochondrial coproporphyrinogen oxidase, extracted PGEN with a milder acid mixture (ethyl acetate-acetic acid) followed by photo-oxidation to PROTO (28). Figure 2A shows that treatment of avian hepatocytes with AF alone caused some PROTO accumulation, as determined by extraction with PCA-methanol. This accumulation was increased 2.5-fold by extraction with ethyl acetate-acetic acid. Therefore the method of extraction is important for optimal recovery of PROTO. In the presence of PIA, the lack of PROTO recovery by PCA-methanol was probably due to increased conversion of PROTO to heme in PIA-treated cells, as described previously (29). With ethyl acetate-acetic acid extraction of these cells, PROTO was again recovered. The recovery increased with increasing AF (Figure 3). There was no further PROTO recovered using this extraction procedure from cells treated with PIA plus AF than from cells treated with AF alone, suggesting that the effect of AF to inhibit PROTOX, unlike its effect to cause URO accumulation, was not dependent on the additional induction of P450 by PIA.

The presence of ascorbate increased recovery of PROTO with both extraction protocols (Figure 2A). This may have been due to the large decrease in URO accumulation in the presence of ascorbate thus allowing more flux of ALA equivalents down the heme pathway.

Extent of Recovery of PGEN as PROTO from Avian Cultures. Some quantitation of the capacity of the cultures to accumulate PGEN is shown in an experiment where cultures were treated with PIA plus DES, with and without AF (Figure 2B), in which the conversion of ALA to heme is stopped at PROTO. There was a further increase in PROTO due to the increased activity of ALA-S. AF has no effect on the induction of ALAS activity by PIA plus DES (Sinclair, P., Walton, H., Gorman, N., Jacobs, J. Jacobs, N. and Sinclair J., unpublished studies). Therefore, when AF was added to PIA plus DES, an amount of PROTO equivalent to the PROTO accumulated with PIA plus DES was expected. However, in the presence of AF, the amount of PROTO actually extracted by PCA-methanol was only 30 % of that expected (Figure 2B). This observation suggests the accumulation of PGEN which was then destroyed by the extraction procedure. Use of ethyl acetate-acetic acid extraction rather than PCA-methanol resulted in only a small increase in PROTO recovery. This suggests that neither ethyl acetate-acetic acid nor PCA-methanol were able to recover all the PGEN formed. However, in preliminary experiments, we have used another approach to this problem. Cell sonicates were treated with *E.coli* membranes, that contain an AF-resistant PROTOX activity (5), to oxidize accumulated PGEN. Under these conditions, an amount of PROTO was recovered that was equivalent to that expected, suggesting that PGEN had accumulated and was stable in these cultures.

Coproporphyrin (COPRO) Accumulation in Avian Hepatocytes caused by DPEs. Figure 2A shows that AF caused an increase in the accumulation of COPRO with a further increase in the presence of PIA. We attribute the COPRO accumulation to inhibition of the enzyme preceding PROTOX in the pathway, coproporphyrinogen oxidase, due to product inhibition by PGEN. These data suggest that COPROgen is more stable than PGEN in the PCA-methanol extraction procedure. We previously noted (9), that treatment with either AF or AFM increased the accumulation of COPRO with the degree of increase in COPRO being greater than the increase in PROTO. This was probably due to the loss of most of the accumulated PGEN during the extraction with PCA-methanol.

PGEN Accumulation in Rat Hepatocyte Cultures. Our previous investigations showed that rat hepatocyte cultures treated with AF and AFM accumulated PROTO and COPRO when extracted with acetone-conc. HCl (9). AFM, when combined with BNPP, was more potent than AF in causing HCO accumulation. However the amount of PROTO accumulation was relatively small. The recent discovery, discussed above, that PGEN accumulating in such cells is destroyed by the strong acid solvents used in the extraction, indicates that accumulation of PGEN, due to PROTOX inhibition in those cultures, was probably much greater than reported previously (9,25). Recent work using the *E. coli* membranes to oxidize accumulated PGEN indicates that this is the case (Sinclair, P., Walton, H., Gorman, N., Jacobs, J. Jacobs, N. and Sinclair J., unpublished studies).

Conclusions on PROTOX Inhibition by DPEs in Hepatocyte Cultures. Our previous publication (9), plus the results presented here, show that PROTOX in intact hepatocytes is inhibited by both AF and AFM with subsequent accumulation of PGEN and COPRO. PGEN appears to be unstable in strong acid solvents and, unlike

coproporphyrinogen and UGEN, requires special attention in order to recover the PGEN as PROTO. This finding suggests that measurements of PGEN content in the liver of mice treated with DPEs (25), may have also considerably underestimated the PGEN content, due to PGEN destruction by the extraction solvent used (methanol-sulfuric acid). In these mice, most of the increase in PROTO after DPE treatment was found in the feces, possibly due to bacterial oxidation of excreted PGEN in the bile and GI tract.

This underestimation of PGEN may also apply to analyses of liver samples from patients with Variegate Porphyria in which there is a genetic defect in PROTOX and a decrease in liver PROTOX activity of 50 % (3). It was recently reported that transformed lymphocytes from such patients when incubated with excess ALA, accumulate about 30% more PROTO than lymphocytes from control patients (30). It seems possible that the lymphocytes from the VP patients actually accumulated large amounts of PGEN which was lost in the extraction with methanol-sulfuric acid. Clearly further work is needed to determine the extent of PGEN accumulation in liver of animals treated with DPEs, in patients with Variegate Porphyria, and in cells derived from such patients.

Concluding remarks.

In cultured hepatocytes from avian and mammalian sources, not only did DPEs cause blockage of the heme pathway at the PROTOX step resulting in accumulations of PROTO, PGEN, and COPRO, but they also caused blockage at the UROD step, resulting in accumulations of large amounts of URO (see Figure 1). The block at the UROD step probably requires the induction by DPEs of form(s) of cytochrome P450 that catalyze oxidation of UGEN; the exact form involved remains to be identified. Induction of the P450 may be limited by two properties of the DPEs: i) the hydrophobicity of the compound (AFM is more effective than AF, but in mammalian cells with high esterase activity, AFM may be rapidly converted to AF) and ii) the extent of the block of heme synthesis at the PROTOX step which itself is apparently also affected by the lipophilicity of the compounds as shown by others (31), and in our study by comparison of the effects of AF and AFM.

The block at the PROTOX step was detected by accumulation of PGEN, detected as PROTO. The detection of PGEN required an appropriate extraction solvent or specific oxidizing enzyme, since use of conventional strong acid solvents resulted in poor recovery of PROTO, probably due to destruction of PGEN. Since the DPEs inhibit two separate steps of the heme pathway, they represent a new class of chemicals acting on this pathway.

The fact that the chemically unrelated oxadiazon had effects similar to those of the DPEs, suggests that there may be other classes of chemicals that cause blocks of the pathway at both sites. However, the effective photo-bleaching herbicides seem to have similar sizes and shapes as observed previously (32). Since oxadiazon lacks a readily hydrolysable group, it has a higher potential to cause URO accumulation than do the readily hydrolysed DPEs, AFM and lactofen (Table I). This difference in metabolism may also affect the overall metabolism and excretion of the compounds from the body. Structure-function relationships of DPEs and other compounds to affect heme synthesis at the two steps of the heme pathway in hepatocytes remain to be established. Since all these compounds also have the potential to increase ALA-S, there is the added potential for large hepatic accumulations of URO and PGEN (PROTO).

As indicated by the current state of knowledge, there is a well established toxicity and pathology associated with excess URO accumulation (the disease, Porphyria Cutanea Tarda). PGEN and COPRO accumulation are also associated with the human disease, Variegate Porphyria (VP), which is characterised by a genetic deficiency of

PROTOX (3). The effects of DPEs would represent a chemically induced form of this disease and individuals with this inherited deficiency would be expected to be especially susceptible to PROTOX inhibition by DPE exposure. Furthermore, there is the potential for PGEN to become covalently bound to macromolecules in the cells and cause further toxicity as has been reported for UGEN (33).

In terms of DPE toxicity to humans, our studies suggest that URO accumulation may mask an inhibition of PROTOX. Whether there is primarily a block at the UROD or PROTOX steps caused by DPE exposure, may depend on several factors that may include the form of cytochrome P450 induced and the relative esterase activities of the cells. Overall, we conclude there is a significant potential of DPEs for toxicity to mammalian liver through the action on the heme pathway even though the acute toxicity seems to be low (34).

Acknowledgements.

We thank Dr S. Duke, USDA, Stoneville, MS, for AFM; Rhone-Poulenc Research Triangle Park, NC, for AF and oxadiazon; EPA Pesticide Repository for lactofen and nitrofen. This work was supported by funds from the US Department of Veterans Affairs, National Institute of Health (CA25012), US Department of Agriculture (9237303-7660) and the US National Science Foundation (IBN-9205174).

Literature Cited.

1. Marks, G.S. *Crit. Rev. Toxicol.* **1985**, *15*, 151-79.
2. *Biosynthesis of heme and chlorophylls*; Dailey, H.A.; Ed.; McGraw-Hill: New York, NY, 1990.
3. Bonkovsky, H. L. In *Hepatology*; 2nd Ed.; Zakim, D.; Boyer, T.; Eds.; W.B. Saunders: Philadelphia, PA, 1990, pp 378-424.
4. Matringe, M.; Camadro, J.-M.; Labbe, P.; Scalla, R. *Biochem. J.* **1989**, *260*, 231-5.
5. Jacobs, J. M.; Jacobs, N.J. *Plant Physiol.* **1993**, *101*, 1181-7.
6. Sinclair, P.R.; Bement, W.J.; Bonkovsky, H.L.; Sinclair, J.F. *Biochem. J.* **1984**, *222*, 737-748.
7. Sinclair, P.R.; Bement, J.; Haugen, S.A.; Sinclair, J.F.; Guzelian, P.S.: *Cancer Res.* **1990**, *50*, 5219-5224.
8. *Cytochrome P450*. Schenkman, J.B.; Greim, H.; Eds.; Springer-Verlag: Berlin, 1993.
9. Jacobs, J.M.; Sinclair, P.R.; Gorman, N.; Jacobs, N.J.; Sinclair, J.F.; Bement, W.J.; Walton, H. *J.Biochem. Toxicol.* **1992**, *7*, 87-95.
10. Hamilton, J.W.; Bement, W.J.; Sinclair, P.R.; Sinclair, J.F.; Wetterhahn, K.E. *Biochem. J.* **1988**, *255*, 267-275.
11. Elder, G.H. In *Heme and Hemoproteins*; De Matteis, F.; Aldridge, W., Eds.; Springer-Verlag: Berlin, 1978 pp. 157-200.
12. Smith, A.G.; De Matteis, F. *Xenobiotica* **1990**, *20*, 865-877; De Matteis, F. in *Hepatotoxicology*; Marks, R.G.; Harrison, S.D.; Bull, R.J. Eds., CRC Press: Boca Raton, FL, 1991. pp 437-479.
13. Sinclair, P.R.; Bement, W.J.; Bonkovsky, H.L.; Lambrecht, R.W.; Frezza, J.E.; Sinclair, J.F.; Urquhart, A.J.; Elder, G.H. *Biochem. J.* **1986**, *237*, 63-71.
14. De Matteis, F.; Harvey, C.; Reed, C.; Hempenious, R. *Biochem. J.* **1988**, *250*, 13-21.
15. Sinclair, P.; Lambrecht, R.; Sinclair, J. *Biochem. Biophys. Res. Commun.* **1987**, *146*, 1324-1329.
16. Jacobs, J.M.; Sinclair, P.R.; Bement, W.J.; Lambrecht, R.W.; Sinclair, J.F.; Goldstein, J.A. *Biochem. J.* **1989**, *258*, 247-253.

17. Lambrecht, R.W.; Sinclair, P.R.; Gorman, N.; Sinclair, J.F. *Arch Biochem. Biophys.* **1992**, *294*, 504-510.
18. Sinclair, P.; Gorman, N.; Walton, H.S.; Bement, H.S.; Jacobs, J.M.; Sinclair, J.F. *Arch. Biochem. Biophys.* **1993**, *304*, 464-470
19. Elder, G.H.; Evans, J.O.; Matlin, S.A. *Clin. Sci. Mol. Med.* **1976**, *51*, 71-80; Smith, A.G.; Francis, J.E.; Kay, S.J.E.; Greig, J.B.; Stewart, F.P. *Biochem. J.* **1986**, *238*, 871-878.
20. Elder, G.; Sheppard, D. *Biochem. Biophys. Res. Commun.* **1982**, *109*, 113-120.
21. Urquhart, A.J.; Elder, G.H.; Roberts, A.G.; Lambrecht, R.W.; Sinclair, P.R.; Bement, W.J.; Gorman, N.; Sinclair, J.A. *Biochem J.* **1988**, *253*, 357-362.
22. Lambrecht, R.W.; Jacobs, J.M.; Sinclair, P.R.; Sinclair, J.F. *Biochem. J.* **1990**, *269*, 437-441.
23. Sinclair, J.F.; Zaitlin, L. M.; Smith, E.L.; Howell, S.K.; Bonkowsky, H.L.; Sinclair, P.R. *Biochem. J.* **1986**, *234*, 405-411.
24. Bonkowsky, H.L. *Hepatology.* **1989**, *10*, 354-364
25. Krijt, J.; Holsteijn, I.V.; Hassing, I.; Vokurka, M.; Blaauboer, B.J. *Arch. Toxicol.* **1993**, *67*, 255-261.
26. Sinclair, J.F.; Schaeffer, B.K.; Wood, S.G.; Lambrecht, L.K.; Gorman, N., Bement, J.B.; Smith, E.L.; Sinclair, P.R.; Waldren, C.A. *Cancer Res.* **1992**, *52*, 3615-3621.
27. Sinclair, P.R.; Bement, W. J.; Lambrecht, R.W.; Gorman, N.; Sinclair, J.F. *Arch. Biochem. Biophys.*; **1990**, *281*, 225-232.
28. Sano, S.; Granick, S. *J. Biol. Chem.* **1961**, *234*, 1173-1180.
29. Shedlofsky, S.I.; Sinclair, P.R.; Bonkovsky, H.L.; Healey, J.F.; Swim, A.T.; Robinson, J.M. *Biochem. J.* **1987**, *248*, 229-236.
30. Meissner, P.; Adams, P.; Kirsch, R. *J. Clin. Inv.* **1993**, *91*, 1436-1444.
31. Nandihalli, U.B.; Duke, M.V.; Duke, S.O. *Pesti. Biochem. Physiol.* **1993**, *43*, 193-211
32. Akagi, T.; Sakashita, N. *Z. Naturforsch.* **1993**, *48c*, 345-349.
33. Vincent, S.H.; Smith, A.G.; Muller-Eberhard, U. *Cancer Lett.* **1989**, *45*, 109-114.
34. Adler, I.L.; Jones, B.M.; Wargo, J.P. *J. Agric. Food Chem.* **1977**, *25*, 1339-1341

RECEIVED April 13, 1994

Chapter 20

Protoporphyrinogen Oxidase Inhibitors for Tumor Therapy

B. P. Halling¹, D. A. Yuhas¹, V. F. Fingar², and J. W. Winkelmann³

¹Research and Development, Agricultural Chemical Group, FMC Corporation, Princeton, NJ 08543

²Department of Surgical Oncology, University of Louisville, Louisville, KY 40292

³Department of Pathology and Clinical Laboratories, Brigham and Women's Hospital and Harvard Medical School, Boston, MA 02115

The use of potent enzymatic inhibitors of tetrapyrrole biosynthesis might offer an alternative approach to photodynamic tumor therapy. This utilization was discovered in the course of testing herbicides that affect chlorophyll synthesis. This report provides an overview of *in vitro* and *in vivo* experiments conducted in mammalian derived cells in culture and in animals. The implications of these findings are considered in the context of current thinking about porphyrin biosynthesis, as well as photodynamic therapy.

The conspicuous brilliant red fluorescence of endogenous porphyrins that accumulated in tumors was the initial observation that spawned increasingly vigorous attempts to exploit the presumed affinity of porphyrins for neoplastic cells for practical medical purpose. Most studies, and virtually the entire field of photodynamic therapy (PDT) have attempted to establish high concentrations of exogenous photosensitizers in tumor. Such parentally administered compounds include naturally occurring, derived, or synthetic porphyrins, phthalocyanines, and other porphyrin-like compounds. The potential applications that have been examined have included direct visualization of tumors during surgery, external detection of tumors by scintillation scanning of radioactively labeled porphyrins, neutron activation therapy with boron containing porphyrin derivatives, visualization of porphyrin fluorescence of tumors during endoscopy, and treatment of tumor in animals and man by irradiation with light in the visible spectrum from conventional and laser sources (1, 2, 3, 4). In clinical treatments of tumors by PDT, photosensitizers are administered directly to patients, then specific destruction of the neoplastic cells is initiated by irradiation of the tumor with light of an appropriate wavelength for photodynamic activation (5, 6; for reviews see 3, 4, 7, 8). Superior outcomes for PDT have been sought by developing numerous chemical modifications of the porphyrins or related compounds so that they would achieve higher concentration in tumors compared to other tissues and organs after parenteral administration. Other chemical modifications of the photosensitizers have attempted to improve PDT by exploiting fluorescence activation at wavelengths which penetrate tissues to greater depths.

A number of commercial and experimental herbicides cause rapid bleaching and desiccation in treated foliage through lipid peroxidation reactions induced by the build-

0097-6156/94/0559-0280\$08.00/0
© 1994 American Chemical Society

up of endogenous photodynamic tetrapyrroles (9, 10, 11, 12, 13). Recently, the intracellular accumulation of protoporphyrin IX (proto IX) associated with these compounds was shown to be due to inhibition of protoporphyrinogen oxidase (Protox, EC 1.3.3.4), the enzyme just antecedent to the chelatases of the chlorophyll (magnesium chelatases) and heme ferrochelatase, (FC) biosynthetic pathways (14, 15, 16). Protox carries out the penultimate step in heme and Mg proto IX synthesis by removal of six hydrogen atoms from the protoporphyrinogen (protogen) nucleus to form proto IX (17, 18). We have observed increases in the levels of proto IX, which occurs after inhibition of Protox in plants (10, 13). It is the product of the inhibited reaction which actually increases because the Protox substrate, protogen, which accumulates through inhibition of Protox, is converted to proto IX by a DPE resistant protoporphyrinogen oxidizing activity in the plasmalemma, at least in plant cells (19, 20). Protogen can also autooxidize spontaneously and nonenzymatically, *in vitro*, under aerobic conditions at an appreciable rate (17, 21).

The proto IX formed in this manner is unavailable to the magnesium and ferrochelatases, possibly due to substrate channeling between Protox and FC reducing the accessibility of proto IX originating from outside of the membrane-bound enzyme complex to chelation (22). If reentry of proto IX into the pathway does occur, its rate of return is significantly less than the rate of accumulation so that the concentration of the photosensitizer increases. Cytotoxicity is then induced through irreversible membrane damage as a consequence of light-induced lipid peroxidation.

We reasoned that if phytotoxic Protox inhibitors had sufficient affinity for human Protox, they might provide a significant, new approach to photodynamic therapy, in which the intercellular accumulation of photosensitizers in tumor cells would derive from biosynthetic inhibition causing a build-up of endogenous porphyrins rather than through diffusion of exogenous photodynamic agents. Matringe *et al.* (15) had already shown that Protox isolated from mammalian sources was susceptible to some phytotoxic Protox inhibitors and so there was a rationale for expecting activity against the human enzyme.

We report here, for the first time, a new approach to achieving high levels of endogenous porphyrin in animal tissue, including transplanted tumors. It consists of parentally administering compounds that are not photosensitizers themselves, as in all previous approaches to PDT, but pharmaceutical-like compounds that act as Protox inhibitors. We have established that in certain animal-tumor systems, readily tolerated doses lead to substantial increases in the endogenous proto IX content of the tumors with favorable concentration ratios compared to non-tumor tissues. Photodynamic killing of such tumors was achieved.

Materials and Methods

Tissue Culture. HeLa cells (American Type Culture Collection) were incubated for five to six days in one liter flasks at 37°C. The cells were then washed in phosphate buffered saline (PBS) and removed from culture flasks by the addition of 0.25% trypsin. The cells were transferred to fresh Minimum Essential Medium supplemented with 25 mM Hepes, 10% w/v deactivated calf serum, 2 mM glutamine, 11,000 units of penicillin and 11,000 µg streptomycin. Aliquots of 5.0 mL of the resuspended cells were placed in 50 mL tissue culture flasks and treated with DMSO or acetone stock solutions of the inhibitors, controls received 0.2% v/v DMSO or acetone. The suspensions were incubated for three or four days until the controls formed a confluent cell layer across the bottom of the flasks.

Cell Extractions. The cells from each flask were resuspended with trypsin as before into a total volume of 0.8 ml. The cells were then disrupted by two freeze-thaw cycles, or by ultrasonification, subsequent microscopic examination of the suspensions revealed no intact cells after either method. Each replicate was extracted with 10 mL of basic acetone (90% acetone:10% 0.1 N NH₄OH), then centrifuged to remove debris and protein. The supernatant was adjusted to pH 6.8 with 0.5 mL of NaCl and 2M

KH_2PO_4 following the addition of 5 mL of water. The 50:50 aqueous acetone extract was then loaded onto Baker C8 preparatory columns. The columns were dried, then washed with 2 mL of water on a vacuum manifold. Tetrapyrroles were then eluted from the columns with two 1.5 mL volumes of 90% MeOH:10% H_2O and quantified by spectrofluorimetry as described previously (16).

Transmissible Animal-Tumors. Tumor-bearing DBA/2 Ha mice were purchased from Thomas Dougherty of Roswell Park Memorial Institute, Buffalo NY. The mice had been injected with SMT-F subcutaneous tumors in the right shoulder (Day 0) one day prior to their arrival at the Princeton R&D facility. The mice were randomized into cages, individually housed, and fed untreated Purina Rodent Chow. On Days 2 through 10 of tumor development the mice were given diet treated with 2000 ppm of the appropriate test chemicals (Figure 1). Diet incorporation was effected by dissolving compounds into 100 to 200 μl of acetone, which was then stirred into a Rodent Chow 5001 mash. Treatments were replicated by dosing two animals for each treatment. Mice were sacrificed on Day 10 of tumor development and subjected to gross necropsy; kidneys, intestines, adrenals, liver and tumors were removed and transferred to saline solution.

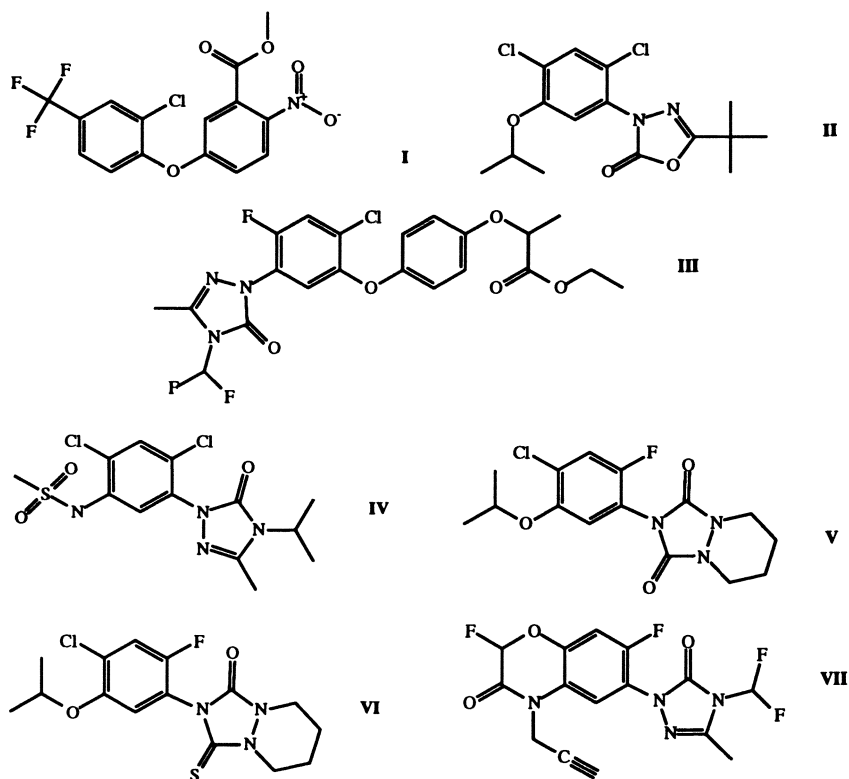


Figure 1. Structures of the protoporphyrinogen oxidase inhibitors surveyed in this study. Compound I is acifluorfen-methyl, II is oxadiazon, compounds III - VII are experimental FMC compounds.

Organ Extractions. The organs were refrigerated at 4°C overnight, then blotted dry, and the fresh weight of each tissue sample was recorded. The tissues were then homogenized in 5 ml, or 10 mL in the case of intestines and liver, of basic acetone. The homogenates were then centrifuged at 1500 g and the supernatants were analyzed on a SPEX Fluorolog spectrofluorometer at wavelengths of; 400 nm excitation, 630 nm emission, for quantification of proto IX (13, 16). Porphyrin accumulation was calculated according to a standard curve developed for authentic proto IX (Porphyrin Products Logan, UT) in the basic acetone used to extract organs.

Results and Discussion

Fluorimetric scans made of HeLa cells treated with a phytotoxic Protox inhibitor (Compound III) showed dramatic stimulation of a peak characteristic of proto IX (Figure 2). The spectra were identical to extracts made of cells treated with the rate-limiting substrate of the tetrapyrrole pathway, aminolevulinic acid (data not shown). As a precursor of the tetrapyrroles, ALA stimulates the porphyrin biosynthetic pathway providing a standard treatment for inducing elevated porphyrin levels which could be compared to the effects of the experimental compounds.

Compound III and ALA inhibited cell growth while stimulating porphyrin levels. Growth inhibition was manifested by small patches of cells at the bottom of the plate wells, compared to the confluent sheets formed in controls. The ALA treatments were especially inhibitory, with essentially no growth following the initial seeding of cells.

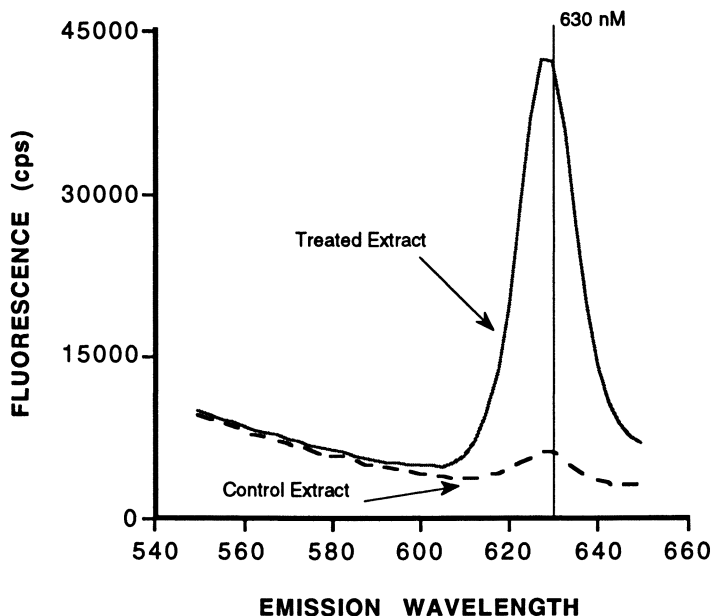


Figure 2. Fluorimetric emission scan of extracts from HeLa cells treated with 100 μ M Compound III (upper solid curve) compared to spectra of control extracts (lower dashed curve). Excitation wavelength of 400 nm. Cells were disrupted in their treatment media by ultrasonification. The suspension was extracted with basic acetone.

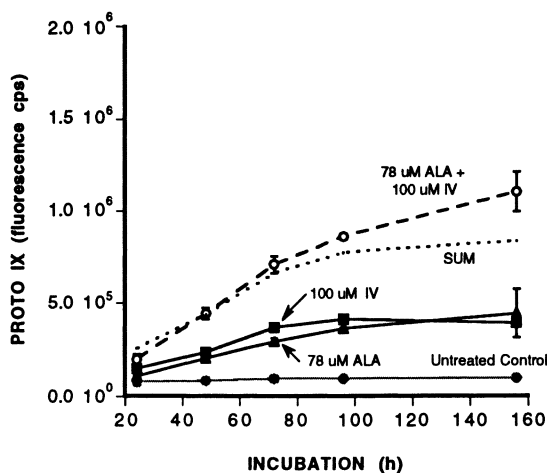
The degree to which cell growth and tetrapyrrole accumulation were affected simultaneously depended both on inhibitor structure and dose (Table I). Compound III, at 100 μM , partially inhibited cell growth while stimulating porphyrin levels 14-fold; at 10 μM , cell growth was unaffected but tetrapyrrole levels still showed a significant increase indicating that proportionate growth inhibition was not an invariable consequence of porphyrin stimulation. Two commercial herbicides, Compounds I and II, completely blocked growth at 100 μM as evidenced by a failure of cell numbers to increase over original seeding densities; yet, simultaneously, they caused a significant elevation in porphyrin levels relative to controls on a per cell basis. The possibility that Protox inhibitors used in conjunction with ALA might have a synergistic effect on proto IX accumulation was investigated in tissue culture experiments. An examination of the timecourse of proto IX accumulation in HeLa cells shows higher levels of porphyrin in cells treated simultaneously with ALA and Compound IV, than would be expected from the simple combined additive effects of the two agents (Figure 3). This synergy may be due to the Protox inhibitor effectively preventing the accumulation of heme, a feedback regulator of tetrapyrrole biosynthesis. In the presence of ALA alone, heme concentrations would increase rapidly, depressing further porphyrin build-up; with the addition of the Protox inhibitor, porphyrin synthesis would be further deregulated. Under these conditions of simultaneous stimulation and deregulation of the pathway, final accumulation levels are probably a reflection of the limitations of metabolic reserves. The tissue culture system was then utilized as a screen to identify additional inhibitors as candidates for *in vivo* testing in animals. Four additional Protox inhibitors varying in lipophilicity and heterocyclic chemistry were chosen (Figure 4).

Table I. Accumulation of porphyrins in HeLa cells treated with experimental compounds. HeLa cells, at an initial seeding density of 3×10^5 cells/ml, were incubated with test compounds for four days.

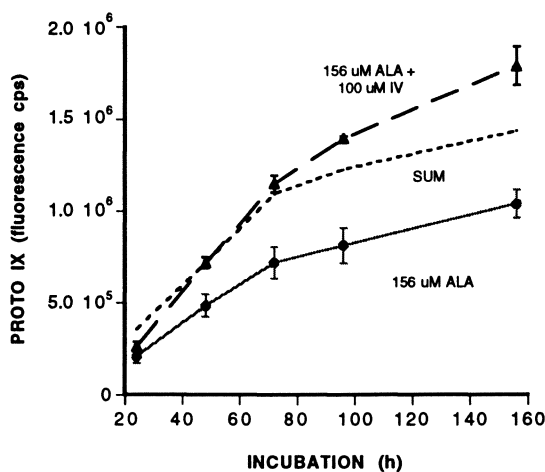
Compound	μM	Cell Density ¹ 10 ⁵ /ml	pmols porphyrin ²	
			Total	Specific ³
I	100	2.8	7.9	5.2
II	100	2.5	3.8	2.7
III	100	4.1	9.8	4.4
	10	6.4	2.0	0.6
	1	6.8	0.7	0.2
Control		6.0	0.7	0.2
LSD _{0.05} ⁴		1.6	1.7	

- 1 Cell density at time of harvest determined by hemacytometer counts of trypsinized cells
- 2 Values are the means of two replicates
- 3 Specific concentration expressed as pmols porphyrin/million cells
- 4 Least Significant Difference at the 95% confidence level

One of the compounds identified in the screen, a sulfonamide (Compound IV) had already been examined for toxicity and metabolism in feeding trials in rats. Following 18 days of *ad libitum* daily feeding of diet formulated with 5000 ppm of Compound IV, a female rat was observed to be walking on the tips of her feet due to



(A)



(B)

Figure 3. The interaction of ALA and a Protox inhibitor in cultured HeLa cells. Cells were grown as 1 mL volumes in 24-well culture plates in the presence of ALA, Compound IV, or a combination of the two treatments. Replicate treatments were harvested at daily intervals over the course of 6 days and analyzed spectrofluorimetrically for proto IX in the total media. The first plot (A) shows the stimulation caused by 100 μM Compound IV or 78 μM ALA alone relative to untreated controls as well as the combination of the two drugs. The second plot (B) shows the effect of 156 μM ALA alone and in combination with 100 μM Compound IV. The dashed lines labeled "SUM" (no data points) are derived from the addition of the signals for the ALA and Compound IV treatments when given alone and therefore represent the predicted signal for a simple additive effect. Where the signal for the combined treatments exceeds the predicted additive effect, synergy is indicated. Error bars represent the standard deviation for two replicates.

lesions on the footpads. The feet and snout showed pink fluorescence under UV illumination characteristic of porphyrins. The papers lining the cage were also highly fluorescent indicating that porphyrins had been passed in the urine. Following necropsy, examination of the organs under UV illumination revealed bright red fluorescence in many of them, denoting high levels of porphyrins. These results suggested that incorporation into the diet provided a route of administration. Other routes were also examined in preliminary experiments. Intravenous (IV) and intraperitoneal (IP) injections of the solvents typically used to solubilize the test compounds were toxic to DBA mice. However, by administering relatively small concentrations daily over an extended treatment period, it proved possible to introduce significant doses of Compound IV into DBA mice by injection. Test compounds were first solubilized in a minimal volume of DMSO which was then formulated as a 1% w/v solution in mineral oil and administered as IP injections once daily at a rate of 5 mL formulation/kg body weight. IV formulations were made as 2% w/v solutions in DMSO and administered at a rate of 2.5 ml/kg body weight. Oral treatments were prepared by dissolving compounds in minimal acetone, then formulating to 1% w/v in corn oil. For a period of eight days these formulations were given at a rate of 50 mg compound/kg body weight either orally (gavage) or by IP injection. IV treatments were discontinued after five days by which time the veins of the test animal had collapsed. These methods were compared to diet incorporated treatments at 2000 ppm administered over the same eight day period.

At the end of the treatment period, the animals were sacrificed and organs were homogenized in Tween detergent buffer. Animals treated by IP injections showed elevated porphyrin levels in the stomach, trachea, intestines and bladder. IV injections raised the levels in the trachea and intestines. The highest proto IX levels, indicated by spectrofluorimetric analysis of the detergent homogenates, were found in the organs of mice that had received Compound IV incorporated in their diet, with the highest levels observed in the trachea, intestines and kidneys. Front face fluorescence analysis of total crude detergent homogenates of tissues, similar to the procedure used for the cultured cell screen (Figure 4), were utilized in preliminary experiments. But high levels of proteins in the detergent homogenates of animal tissues produced such levels of fluorescence quenching that quantification of porphyrins was unreliable. Therefore, organic extractions made with basic acetone were used in subsequent experiments.

Unlike the injection methods which had shown deleterious effects on the mice, the diet incorporation treatments did not impose a risk of loss of test animals during the treatment period. Since the diet incorporated treatments had induced the greatest increases in porphyrin levels and this method had shown the least effect on animal viability, all subsequent experimentation involving tumor bearing mice proceeded with all of the selected test chemicals administered through diet incorporation.

In tumor bearing mice, Compounds I, II, III, IV and VII caused significant accumulation of porphyrins in the cultured tumors (Table II). Most of the tumor active compounds were in the higher ranges of the sampled ClogP values (more lipophilic) with the dramatic exception of Compound IV, which was nearly eight-fold more active than Compound II, the next most effective material. The activity of Compound IV in tumors would not have been predicted from the *in vitro* efficacy; compound IV induced only a fourth as much apparent proto IX accumulation in HeLa cells as did treatments with Compound VII.

Differences in structure among the inhibitors affected the distribution of porphyrin increases among the tissues (Table II). The kidney and intestines were the organs that showed the greatest increases in porphyrin in treatments with Compounds I, II and III, whereas the liver and adrenal gland were the most affected in treatments with Compound VI. The tumor showed the highest percentage increase, relative to controls, in response to Compound IV. These results suggest that differences in drug physico-chemical properties can influence the distribution of porphyrin accumulation so that it

may be possible to optimize the structures still further for even greater specificity against the tumor.

As a sulfonamide, Compound IV was the only inhibitor in the set with an ionizable moiety which may have significantly influenced transport and distribution in the animals (4). Studies by Paquette (23) on the uptake of aluminum phthalocyanines indicated that cytotoxicity correlated with cell penetration. Those results led to the conjecture that optimal uptake was facilitated by the amphiphilic nature of sulfonated

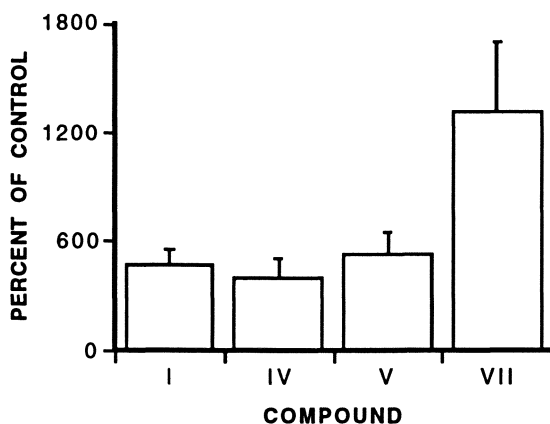


Figure 4. Cell based screening assay for tetrapyrrole accumulation. HeLa cells were grown in the presence of 100 μM of each of the inhibitors for four days. Values represent porphyrin concentrations in the total extracts taken from each treatment replicate and are not adjusted for cell number. Values are the means of two replicates, the error bars indicate the standard deviation of the means.

Table II. Distribution of porphyrin in tissue fractions of DBA/2 Ha mice treated with various Protox inhibitors

Compound	Porphyrin Concentration $\mu\text{g}/\text{gram}$ fresh weight tissue				
	Adrenal	Intestine	Kidneys	Liver	Tumor
I	23	51	22	12	14
II	4	51	117	14	18
III	60	54	99	39	11
IV	126	91	148	25	131
VI	12	19	8	8	8
VII	18	4	6	7	2
CONTROL	14	2	5	5	2
LSD _{0.05} ¹	120	16	8	11	23
F value ²	1.28	45.78	514.05	13.84	46.76

¹ Least Significant Difference at the 95% confidence level

² F value from the simple oneway ANOVA

molecules with the lipophilic portion, allowing penetration into the membrane while the sulfonate substituents then interacted with membrane transport proteins. This factor was considered in the general treatment of stereospecificity of hydrophobic and hydrophilic photodynamically active porphyrins (24). The water solubility of Compound IV is significantly influenced by pH, within the range of physiological pH, becoming more hydrophobic as the pH decreases. Some tumors have been observed to be more acidic than normal cells (25, 26). Thus, Compound IV might be rendered more lipophilic in tumor cells than in normal cells and so be sequestered in the neoplastic membranes.

The high levels of fluorescence found in the intestines with most of the treatments may be a consequence of administration through the diet; the rapidly dividing epithelial cells of the small intestine are probably especially susceptible to biosynthetic inhibition. High porphyrin levels in the kidneys would also seem to be an inherent consequence of tetrapyrrole accumulation generally, as porphyrins leaking out of affected tissues and into the blood and lymph are concentrated in the kidneys prior to excretion. Thus, high levels of porphyrins in the kidneys is not necessarily indicative of an actual increase in production in that tissue. It is not possible from these experiments to determine whether Compound IV actually concentrated in the tumors or whether the high rates of metabolism and growth in the oncogenic cells rendered them more susceptible to Protox inhibition. Such determinations would require experiments with the radiolabelled compound.

The measured differences in accumulation patterns correlated with visual observations of the tissues under UV lights (367 nm) following necropsy. Compound IV treated animals showed fluorescence in the face, bladder, preputial glands, stomach and kidneys; while Compounds II and III caused visible accumulation in the intestines, stomach, and ribs. In Compound I treatments, only the intestines appeared visibly fluorescent.

Implications of the mechanism of action. Hematoporphyrin derivatives which are natural extracts containing a mixture of porphyrins, have been used most often as photosensitizers for PDT. A disadvantage of treatment with these agents is long term cutaneous photosensitivity resulting from the accumulation of the exogenous porphyrins within skin and other tissues, especially the liver and spleen. Patients must refrain from exposure to direct sunlight for as long as four to six weeks (2, 27). Porphyrins such as O,O'-diacetylhematoporphyrin and other porphyrins with bulky substituents in the 2,4-positions have been shown to be effective competitive inhibitors of FC (28, 29). Thus, the accumulation of natural product mixtures of porphyrins in the liver might reduce cytochrome levels leading to the reports of liver toxicity resulting from hematoporphyrin treatments (1). The inherent drawbacks of the present natural product phototherapy treatments have stimulated the search for alternative, synthetic agents.

Proto IX is one of the most effective photosensitizers yet examined; however, it was not an important candidate for photodynamic therapy since it did not accumulate within tumors after parenteral administration (6). Protox inhibitors lead to high proto IX levels by the entirely different mechanism of inducing intercellular build-up through blockage of the endogenous pathway. Kessel (6) and Milanese *et al* (30) have reported that effective photodynamic therapy can be realized when porphyrins concentrate to a critical level of about 5 - 10 $\mu\text{g/g}$ tumor fresh weight. The tumors in this set of mouse experiments were not irradiated; however, the proto IX concentrations observed in tumors treated with compound IV were at least ten-fold greater than the critical level cited above (Table II). High accumulations of a photosensitizer as effective as proto IX may make possible the direct photodestruction of tumor cells, unlike Photofrin (Quadrologic Corp, Vancouver, Canada) and certain other exogenous porphyrins which

cause tumor necrosis by initiating the collapse of the microvasculature supplying blood to the neoplasm (4, 31, 32, 33).

Experiments involving treatment of chondrosarcoma tumors in Sprague-Dawley rats and SMT-F tumors in DBA mice with Compound IV, (manuscript in preparation) have suggested a mechanism of photodynamic tumor destruction different from exogenous photodynamic agents. The observation that killing of the tumor was achieved without vascular stasis in the treatment area is consistent with Protoc inhibitors mediating the direct destruction of oncogenic cells rather than working indirectly through hypoxia and nutrient starvation.

Divaris and Kennedy (34) have shown that the rate of clearance of intracellularly accumulated endogenous proto IX is very much greater than that of hematoporphyrin derivative in human patients. Proto IX accumulations in the skin of mice and humans, resulting from treatments with ALA, caused cutaneous photosensitization for less than 24 hours. Differential tissue responses were noted in the sebaceous glands and hair follicles, which developed pronounced proto IX fluorescence. The basal layer of the epidermis showed a weaker response, and the dermis essentially none. Selectivity towards neoplasms was also demonstrated when topical applications of ALA made to human skin malignancies induced proto IX fluorescence that was limited to the lesions. Subsequent experiments involving irradiation of ALA treated basal cell and squamous cell carcinomas of epidermal origin achieved effective treatment in human clinical trials (35). These ALA trials demonstrate that endogenously accumulated proto IX can be rapidly cleared from normal tissues and that the intracellular build-up of proto IX in malignancies provides the basis for efficacious photodynamic therapy of selected human skin cancers.

Working with pure enzyme inhibitors provides opportunities for accessing biochemical selectivity mechanisms that are not offered by photosensitizing porphyrins alone or mixtures of natural products. Physiological characteristics of tumor cells which well designed Protoc inhibitors might be especially able to exploit include indications that tetrapyrrole synthesis in neoplastic cells differs from normal cellular biosynthesis. Schoenfeld (36) has reported that metabolism of heme is impaired in lymphocytes from patients with malignant lymphoproliferative disorders (MLPD). Levels of ALA dehydratase and ferrochelatase activities were significantly decreased while ALA synthase levels were normal in MLPD patients with the result that heme levels decreased. Dailey (29) also found aberrations in porphyrin synthesis in Morris hepatoma 7288C cells which showed FC activity at only 2% of normal hepatic activities. Inhibition of the already low heme metabolism levels would further derepress the rate limiting step, ALA synthase, suggesting that at least some tumor cells might already be poised for the accumulation of porphyrin intermediates. Clearance of cytosolic proto IX occurs by transport into mitochondria where Fe chelation can make it available to heme oxygenase for breakdown. Reduced levels of FC activity in tumor cells would then be expected to render them less capable of clearing accumulated proto IX than normal cells. Depressed FC activity might also lead to reductions in P-450 and b5 proteins as has been reported by Stout (37) in hepatomas. A reduced monooxygenase system might mean that some tumors would have a reduced capability for the metabolism of xenobiotics such as the Protoc inhibitors. We have observed that the physicochemical parameters of Protoc inhibitors can be varied greatly without reducing enzymatic activity, increasing the range of modifications which might be attempted for optimizing pharmacokinetic properties.

Literature Cited

1. Dougherty TJ, KR Weishaupt, DG Boyle 1985. In *Principles and Practices of Oncology* (ed 2) eds. VJ DeVita, S Hellman, SA Rosenberg, Lippincott, Philadelphia.

2. Dougherty TJ 1986. In *Methods in Porphyrin Photosensitization* ed. D Kessel, Plenum Press, New York, pp 313-328.
3. Henderson BW, TJ Dougherty, PB Malone 1984. In *Porphyrin Localization and Treatment of Tumors* eds. DR Doirn, and CJ Gomer, Liss, New York, pp 601-612.
4. Winkelmann JW, S Kimel 1990. In *Photodynamic Therapy of Neoplastic Diseases* ed D Kessel, CRC Press Inc, Boca Raton Fl pp 29-42.
5. Berenbaum MC, R Bonnett, PA Scourides 1982. *Brit J of Cancer* 45: 571-581.
6. Kessel D 1982. *Cancer Res* 42: 1703-1706.
7. Dougherty TJ 1984. *CRC Crit Rev Oncol Hematol* 2: 83-116. 312-319.
8. Manyak MJ, A Russo, PD Smith, E Glatstein 1988. *J Clin Oncol* 6: 380-391.
9. Becerril JM, SO Duke 1988. *Plant Physiol* 90: 1175-1181.
10. Lydon J, SO Duke 1988. *Pestic Biochem and Physiol* 31: 74-83.
11. Matringe M, R Scalla 1987. Proc Brit Crop Protec Conf - Weeds: 981-988.
12. Matringe M, R Scalla 1988. *Pestic Biochem and Physiol* 32: 164 - 172.
13. Witkowski DA, BP Halling 1988 *Plant Physiol* 87: 632-637.
14. Matringe M, J-M Camadro, P Labbe, R Scalla 1989. *Biochem J* 260: 231-235.
15. Matringe M, J-M Camadro, P Labbe, R Scalla 1989. *FEBS Letters* 245: 35-38.
16. Witkowski DA, BP Halling 1989. *Plant Physiol* 90: 1239-1242.
17. Jacobs JM, Jacobs NJ, DeMaggio AE 1982. *Arch Biochem Biophys* 218: 233-239.
18. Jacobs JM, and Jacobs, NJ 1984. *Arch Biochem Biophys* 229: 312-319.
19. Jacobs JM, NJ Jacobs, TD Sherman, SO Duke 1991. *Plant Physiol* 97: 197-203.
20. Lee HJ, MV Duke, SO Duke 1993. *Plant Physiol* 102: 881-889.
21. Brenner DA, and Bloomer JR 1980. *Clinica Chimica Acta* 10: 259-266.
22. Ferreira GC, Andrew TL, Karr SW, and Dailey HA 1988. *J Biol Chem* 263: 3835-3839.
23. Paquette B, H Ali, R Langlois, JE van Lier 1988. *Photochem and Photobiol* 47: 215-220.
24. Winkelmann JW, D Arad, S Kimel 1993 *J. Photochem. Photobiol.* 18: 181-189.
25. Brault D, C Vever-Bizet, M Dellinger 1986. *Biochimie* 68: 913-921.
26. Brault D, C Vever-Bizet, T Le Doan 1986. *Biochim Biophys Acta* 238-250.
27. Roberts WG, KM Smith, JL McCullough, MW Berns 1989. *Photochem and Photobiol.* 49: 431-438.
28. Dailey HA, JE Fleming 1983. *J Biol Chem* 258: 11453-11459.
29. Dailey HA, A Smith 1984. *Biochem J* 223: 441-445.
30. Milanesi C, R Biolo, E Redi, G Jori 1987. *Photochem Photobiol.* 46: 675-681.
31. Henderson BW, SM Waldow, TS Mang, RW Potter, PB Malone, TJ Dougherty 1985. *Cancer Res* 45: 572.
32. Selman SH, M Kreimer-Birnbaum, JE Klaunig, PJ Goldblatt, RW Keck, SL Britton 1984. *Cancer Res* 44: 1924.
33. Selman SH, AJ Milligan, M Kreimer-Birnbaum, RW Keck, PJ Goldblatt, SL Britton 1985. *J Urol* 133: 330.
34. Divaris DXG, JC Kennedy, RH Pottier 1990. *Amer J Pathology* 136: 891-897.
35. Kennedy JC, DC Pross, RH Pottier 1990. Abstract XVI/7 in Proc of the 3rd Biennial Meeting of the IPA, Buffalo NY pg 20.
36. Scoenfeld N, O Epstein, M Lahav, R Mamet, M Shaklai, A Atsmon 1988. *Cancer Letters* 43: 43-48.
37. Stout DL, FF Becker 1986. *Cancer Res* 46: 2756-2759.

RECEIVED March 8, 1994

Chapter 21

Using δ -Aminolevulinic Acid in Cancer Therapy

James C. Kennedy^{1,3} and Roy H. Pottier^{2,3}

Departments of ¹Oncology and ²Urology, Queen's University, Kingston, Ontario K7L 3N6, Canada

³Department of Chemistry and Chemical Engineering, Royal Military College of Canada, Kingston, Ontario K7K 5L0, Canada

The administration of an appropriate dose of 5-aminolevulinic acid (ALA) to patients with certain types of cancer leads to the preferential accumulation of fluorescing and/or photosensitizing concentrations of protoporphyrin IX (Proto IX) within the malignant cells. Subsequent exposure of such cancers to photoactivating light may cause selective destruction of the malignant tissue by photodynamic action, with sparing of adjacent normal tissues.

Photodynamic therapy is an experimental form of treatment for certain types of cancer (1-5). Originally termed photoradiation therapy, it involves the administration of a tissue photosensitizer (usually a modified porphyrin, chlorin, or phthalocyanine) that shows a clinically significant tendency to accumulate preferentially in the malignant tissue. Subsequent exposure of the treatment site to an appropriate dose of photoactivating light may cause selective phototoxic destruction of the abnormal tissue. If the dose of light is chosen correctly, the adjacent normal tissues will experience only minor damage. Although normal tissues often contain significantly lower concentrations of photosensitizer than do malignant tissues, differences in cellular mechanisms of protection and/or repair may make some contribution to the difference in tissue response.

The primary cause of cell death is thought to be damage to essential membrane structures by singlet oxygen, possibly with minor contributions from other activated species (6-8). Such a mechanism distinguishes photodynamic therapy from PUVA therapy (psoralen UV-A therapy), another form of photochemotherapy in which UV-A radiation is used to induce photochemical rather than photodynamic reactions. The formation of covalent bonds between a psoralen (usually 8-methoxy or 5-methoxy psoralen) and DNA prevents the target cells from dividing in a normal manner. Since UV-A is strongly absorbed by many tissue components, it penetrates tissue so poorly that PUVA therapy normally is limited to very superficial lesions such as psoriasis or the diffuse form of mycosis fungoides

0097-6156/94/0559-0291\$08.00/0
© 1994 American Chemical Society

(9-10). However, the red light normally used for photodynamic therapy is absorbed less readily, so that under suitable conditions it may be possible to give a lethal dose of photoactivating light to tissues up to 10 mm thick. Since PUVA therapy kills cells by cross-linking DNA, the induction of mutations with occasional malignant transformation is a major hazard associated with its use (11). Although singlet oxygen also can cause damage to DNA (12), photodynamic therapy does not induce many mutations in mammalian cells, presumably because most of the cells whose DNA is damaged by singlet oxygen are dying already from concomitant damage to essential membrane structures.

Although porphyrin-based photodynamic therapy for cancer and porphyrin-based pesticides share some basic biochemical and photobiological mechanisms, it is important to realize that the goal of photodynamic therapy is to cure patients, not to kill them. Pesticides normally are used to kill healthy individuals of the target species, with selective killing on the basis of species specificity often being an important consideration. The identity of the specific tissue or tissues whose destruction results in death of the individual certainly is of interest, but one tissue is as good as another if the damage causes death. In contrast, the primary requirement in photodynamic therapy is for the photosensitizer to show sufficient tissue specificity to permit phototoxic destruction of a specific target tissue without causing serious damage to the patient.

Characteristics of an Ideal Tissue Photosensitizer

Ideally, one would like to cause total destruction of the malignant tissue within a given treatment field without causing any damage to adjacent non-malignant tissues within the same field. A perfect photosensitizer would be completely specific for the malignant tissue. However, all photosensitizers tested to date accumulate to some degree in normal tissues, and thus cause clinical problems of varying degrees of importance.

Problem of Light Dosimetry. Since the specificity of photosensitizers for malignant tissues is not perfect, photodynamic therapy unavoidably causes a certain amount of phototoxic damage to normal tissues also. The problem is particularly acute if the photosensitizer is not readily photobleached during treatment, since photosensitizers that are stable to light will continue to transfer the energy of photons to molecules of oxygen for as long as exposure to the photoactivating light continues. Under such conditions, phototoxic damage is determined by both the concentration of the photosensitizer in the tissue and the total dose of light (intensity \times duration of exposure). Consequently, even those tissues that contain relatively low concentrations of photosensitizer will experience increasing phototoxic damage as the total dose of photoactivating light is increased. In clinical practice, the combination of a photosensitizer that is relatively stable to light and an overdose of photoactivating light can cause complete necrosis of normal tissues within the treatment field. Unfortunately, sometimes the geometrical relationships between normal and malignant tissues are such that it is not possible to give all of the malignant tissue a lethal dose of light without giving at least part of the normal tissue a lethal overdose. This may be the case if the light must pass through a

significant thickness of normal tissue in order to reach the target tissue. For example, carcinoma of the breast commonly metastasizes to form deposits of malignant tissue either within the skin or immediately beneath the skin. The thickness of such plaques or nodules ranges from less than 1 mm to several cm. An external beam of photoactivating light must pass through both the overlying normal tissues of the skin and the upper layers of the malignant tissue before reaching the base of the plaque or nodule. Since the intensity of light will decrease rapidly because of scatter and absorption as it passes through these tissues, it will be necessary to give the overlying normal tissues of the skin an overdose of light in order to ensure that the base of the malignant plaque or nodule receives a lethal dose. Also, if the surface of the treatment field is complex (a mixture of concave and convex curves in multiple planes), it is extremely difficult to illuminate all parts of the surface with equal intensity (13).

However, light dosimetry calculations are greatly simplified if the photosensitizer is readily photobleached during treatment. The intensity of the phototoxic response in each tissue then is determined primarily by the concentration of the photosensitizer in that tissue. If the normal tissues within the treatment field contain a relatively low concentration of a photosensitizer that rapidly photobleaches during treatment, then even very large increases in the dose of light beyond the usual therapeutic range do not cause any additional phototoxic damage. Under such circumstances, it is quite safe to give what would otherwise be exceedingly foolhardy doses of light in an attempt to ensure that the deepest or most shadowed parts of the malignant tissue are given a lethal dose.

Problem of Persistence of Photosensitizer in Normal Skin. Clinically significant concentrations of certain photosensitizers may persist for several weeks to several months in normal tissues. Such persistence of photosensitizer in the skin seriously inconveniences most patients, since they must be careful to avoid exposure to either direct sunlight or sunlight that has passed through window glass for as long as they remain photosensitized. Failure to comply with this requirement has resulted in serious second degree burns. Residual photosensitizer in the skin may cause problems for the physician also, if the tumor being treated is too large to be destroyed by a single treatment. If multiple treatments are given, it is necessary to wait between treatments long enough to allow substantial clearance of residual photosensitizer from the normal tissues. Failure to do so leads to progressive accumulation of photosensitizer in certain normal tissues (such as the skin) until there no longer is a useful concentration differential between the normal and malignant tissues. Treatment under such conditions has caused full thickness necrosis of the skin. However, if the tumor enlarges very rapidly between treatments, a delay long enough to ensure clearance of residual photosensitizer may permit the tumor to escape from therapeutic control.

Endogenous Porphyrins as Tissue Photosensitizers

Until recently, every photosensitizer used for photodynamic therapy in either experimental animals or patients was synthesized and/or purified outside of the body. These exogenous photosensitizers usually are administered to the subject by

injection, and therefore normally reach the target tissue via the blood. They then accumulate preferentially within the target tissue at sites that vary with the different types of photosensitizer, by mechanisms that still are not completely clear (14). The exogenous photosensitizers that have been evaluated experimentally are chemically quite diverse, the only absolute requirements being (a) that they are effective tissue photosensitizers, (b) that they show a useful degree of specificity for the target tissue, and (c) that they are not excessively toxic or otherwise harmful in the absence of light.

In contrast, the endogenous photosensitizers are synthesized within the body itself. They include uroporphyrins I and III, coproporphyrins I and III, and protoporphyrin IX. The uroporphyrins and coproporphyrins appear to be biologically useless byproducts that are produced primarily under pathological conditions, while Proto IX is the immediate precursor of heme (15). Although it has long been accepted that every nucleated cell in the body requires heme-containing enzymes for energy metabolism and therefore must have at least a minimal capacity to synthesize Proto IX, until recently there was little recognition that tissues other than liver and the hemopoietic system could synthesize quite substantial amounts of Proto IX under appropriate conditions.

Endogenous Porphyrins and the Porphyrrias. The porphyrias are a group of metabolic diseases that are caused by abnormalities at various steps in the biosynthetic pathway for heme. Seven of the porphyrias are characterized by an abnormal accumulation of one or more of the naturally occurring porphyrins, and five of these seven (congenital erythropoietic porphyria, porphyria cutanea tarda, hereditary coproporphyria, variegate porphyria, and erythropoietic protoporphyria) can cause some degree of cutaneous photosensitivity (15).

Since we had been using hematoporphyrin derivative (a complex mixture of porphyrin monomers, dimers, polymers, and aggregates) to induce preferential photosensitization of various types of cancer in human patients (16), it seemed appropriate to study the mechanisms by which porphyrins can cause skin photosensitization in the various natural and chemically-induced porphyrias. Numerous studies had demonstrated that interference with specific enzymes or manipulation of the concentration of specific substrates at various steps in the biosynthetic pathway for heme could lead to the accumulation of one or more of the naturally-occurring porphyrins (17-22). We wondered therefore whether it might be possible to induce a transient photosensitizing porphyria in malignant tissue but not in adjacent normal tissues, so that the malignant tissue could be destroyed by photodynamic action without causing clinically significant damage to the normal tissues.

At that time it was accepted as dogma that the metabolic abnormalities responsible for the various porphyrias affected primarily the liver and/or the hemopoietic system. Porphyrins that accumulated in other tissues were thought to have been synthesized in liver, spleen, or marrow, and then transported via the blood to other tissues. Accordingly, we injected a series of naturally-occurring porphyrins into mice in the hope of observing useful tissue specificity. The results were quite disappointing. Exogenous uroporphyrins and coproporphyrins are good photosensitizers, but they failed to show any particular tissue specificity, possibly

because they are too soluble to remain localized. However, since Proto IX is only slightly soluble in pure water at physiologic pH, there was hope that it might do better. Unfortunately, when solubilized with DMSO, serum, bile salts, or detergent and then injected into mice, Proto IX showed no particular tissue specificity.

It seemed possible that the naturally-occurring porphyrins that had been injected into the body might be processed or transported differently than chemically identical porphyrins that are synthesized in the liver. Porphyria researchers had reported that certain hepatotoxic compounds could induce various types of hepatic porphyria in rats and mice by inhibiting specific steps in the biosynthetic pathway for heme. We tested some of these compounds in mice, in the hope that at least some of the excess porphyrins that were formed in the liver might enter the circulation and then accumulate preferentially in specific tissues. This hope was not realized. We discarded this approach (the compounds were too hepatotoxic in any case to be of much value clinically), and began to study the effect on porphyrin synthesis of manipulating the concentration of specific substrates in the heme biosynthetic pathway.

ALA-induced Protoporphyrin IX. ALA is the first committed precursor in the biosynthetic pathway for heme (15). It is soluble in water, readily available, and relatively inexpensive. Moreover, there were reports that the oral administration of ALA to volunteers during a study of porphyrin metabolism had caused transient skin photosensitization (21-22). Accordingly, we began to study the effect of administering ALA on porphyrin accumulation in various benign and malignant tissues of mice and rats.

The systemic administration of ALA induced Proto IX fluorescence in certain tissues but not in others. Malignant tissues usually developed much stronger fluorescence than did the adjacent normal tissues. We found that (contrary to dogma) the porphyrins in at least some of the fluorescing tissues were being synthesized *in situ* rather than in the liver or hemopoietic organs (23). These observations formed the basis for our subsequent studies in experimental animals, cancer patients, and human volunteers (24-31).

ALA-induced Protoporphyrin IX Photodynamic Therapy

ALA can induce Proto IX fluorescence and/or photosensitization when administered orally, by injection, by infusion into accessible body cavities, by topical application, or *in vitro* (24-64). When given systemically (orally, or by intravenous, subcutaneous, or intraperitoneal injection), ALA induces the accumulation of Proto IX in certain types of cells and tissues, but not in others. When administered locally (by topical application to skin or mucous membranes, by intradermal injection, or by infusion into the bladder or uterus), ALA induces a localized accumulation of Proto IX in susceptible tissues, although a small amount of the ALA may enter the lymphatics and the general circulation. Intralesional injections produce an intermediate degree of localization. Given by any route, ALA-induced Proto IX fluorescence and/or photosensitization shows definite tissue specificity.

Since ALA-induced Proto IX is photobleached very readily when exposed to

photoactivating light, its phototoxic effect is determined primarily by the concentration of Proto IX in the tissues within the treatment field rather than by the total dose of light. It becomes very difficult to give an overdose of light, and the calculations for light dosimetry are greatly simplified.

ALA-induced Proto IX has another advantage over many exogenous photosensitizers in that it is essentially cleared from most tissues within 48 hours. Consequently, it is possible to repeat photodynamic therapy every other day for an indefinite period if the malignant tissue is very large or growing rapidly.

Tissue Specificity of ALA-induced Proto IX. ALA can induce significant Proto IX fluorescence and photosensitization in most of the tissues that cover body surfaces or line body cavities, and also in the exocrine glands whose ducts secrete onto such surfaces. The carcinomas that may be derived from such tissues usually develop more intense fluorescence and photosensitization than do the non-malignant tissues from which they arose. In contrast, although most connective tissues show very little response to exogenous ALA, at least some sarcomas (which may be derived from connective tissue) show strong ALA-induced fluorescence and clinically significant photosensitization.

ALA-inducible cells are present in the epidermis, the conjunctiva, one layer of the retina, the mucosa of the respiratory system, the mucosa of the digestive system, the lining of the bladder and urethra, the lining of the uterus, and the lining of the abdominal cavity (including the external covering of the abdominal organs). Major exocrine glands that are ALA-inducible include the mammary glands, the salivary glands, the liver (which is too highly pigmented to show strong fluorescence even when it contains large amounts of Proto IX), and the pancreas. Various types of smaller exocrine glands accumulate Proto IX also. The gonads (ovaries and testes), which may be regarded as exocrine glands that secrete living cells onto surfaces that communicate with the exterior of the body, are inducible also. Tissues that develop little or no ALA-induced Proto IX fluorescence include muscle (all types), the dermis (excluding the pilosebaceous units and the exocrine glands derived from the epidermis), the blood vessels, and the cells of the bone marrow, spleen, and lymph nodes.

The thymus is of unusual interest. Although thymocytes develop intense Proto IX fluorescence and become highly photosensitized when exposed to exogenous ALA, the thymus neither lines a surface nor secretes onto a surface. The stroma of the thymus is thought to originate embryologically from tissues originally located on the surface of the embryo. However, the thymocytes as such arise from mesodermally-derived multipotent stem cells of the hemopoietic system which do not seem to be ALA-inducible. Committed stem cells divide and differentiate in the thymus to become the highly inducible thymocytes. Later, when the thymocytes enter the circulation and the lymphoid organs as mature T-cells, they lose most of their ability to accumulate clinically significant concentrations of Proto IX. However, malignant T-cells in the circulation (T-cell leukemias) or in tissue (T-cell lymphomas) can be as highly inducible as the thymocytes that were their precursors.

Malignant tissues often show much stronger ALA-induced fluorescence than do the tissues from which they were derived. Such fluorescence can be used to

locate occult cancers or to determine the boundaries of a malignant process. However, the development of localized ALA-induced fluorescence is not diagnostic of malignancy, since certain non-malignant lesions such as psoriasis, actinic keratosis, and porokeratosis may develop equally strong fluorescence when exposed to exogenous ALA.

Malignant tissues that are known to develop a clinically useful degree of Proto IX fluorescence and/or photosensitization when exposed to exogenous ALA include basal cell carcinomas, most squamous cell carcinomas of the skin, squamous cell and small cell carcinomas of the lung, carcinoma of the breast, carcinoma of the bowel, adenocarcinoma of the sebaceous gland, squamous cell carcinoma of the parotid gland, hepatocellular carcinoma, rhabdomyosarcoma, mycosis fungoides, T-cell leukemia, and erythroleukemia.

Mechanisms Responsible for Tissue Specificity. Two aspects of tissue specificity must be considered: differences in ALA-induced Proto IX accumulation between normal tissues of different histological types, and differences between malignant tissues and the normal tissues from which they arose.

The rate of synthesis of heme in tissues such as the liver is regulated by a feedback control system in which heme that has not yet been linked with specific proteins to form the various heme-containing enzymes, hemoglobin, myoglobin, etc., interferes with the synthesis of ALA (65). Free heme will be present if the rate of synthesis of heme is greater than the rate at which it is being used up. Since ALA is the first committed precursor in the heme biosynthetic pathway, inhibition of the synthesis of ALA causes a decrease in the rate of synthesis of heme and consequently a decrease in the concentration of free heme. This in turn reduces the inhibition of ALA synthesis, which is reflected by an increase in the rate of synthesis of heme.

This feedback control system can be bypassed by supplying the tissues with a large excess of exogenous ALA. Under such conditions, the rate of formation of heme is determined primarily by the maximum rate at which the biosynthetic pathway downstream from ALA can produce heme from what is effectively an unlimited supply of ALA. The maximum rate for this process is limited by the rate of the slowest step downstream from ALA.

If the slowest step in this pathway is the conversion of Proto IX into heme, then Proto IX will accumulate within the mitochondria. If the slowest step is the conversion of protoporphyrinogen into Proto IX, protoporphyrinogen will accumulate within the mitochondria, and then diffuse into the cytosol where it may be converted into Proto IX. If the slowest step is downstream from uroporphyrinogen or coproporphyrinogen, then uroporphyrins or coproporphyrins may be produced. However, we have not yet identified localized uroporphyrins or coproporphyrins in experimental animals or patients given ALA, possibly because these particular porphyrins are too soluble to remain localized within their tissues of origin and are quickly excreted.

All nucleated cells must have at least some capacity to synthesize heme (and therefore Proto IX), since all nucleated cells use heme-containing enzymes for energy metabolism. However, not all cells regulate heme biosynthesis by the feedback control system described above, which has been studied chiefly in the

liver. Cells of the hemopoietic system synthesize large amounts of heme, but the mechanism by which this synthesis is regulated is still quite obscure. Hemopoietic cells of the marrow, spleen, lymph nodes, and peripheral blood develop very little Proto IX fluorescence when exposed to ALA. It therefore is of considerable interest that ALA causes malignant erythroid cells (erythroleukemia) and malignant T-cells (mycosis fungoides; T-cell leukemia) to become strongly fluorescent and highly photosensitized.

For most other tissues there is very little hard data to explain the very different responses to exogenous ALA observed in cells of different histological types. It is probable that the regulation of heme metabolism in the types of cells (benign or malignant) that accumulate large amounts of Proto IX when exposed to exogenous ALA is by a mechanism similar to that in the liver, and that the rate-limiting step in such cells is either the conversion of protoporphyrinogen into protoporphyrin, or protoporphyrin into heme. Differences between cell types may be caused by differences in the maximum capacity of the heme biosynthetic pathway to produce either protoporphyrinogen or Proto IX, or by differences in its capacity downstream from Proto IX to convert Proto IX into heme. The mechanism responsible for the increased accumulation of ALA-induced Proto IX that usually is associated with malignant transformation may be merely an increase in the capacity of what normally is the rate-limiting step that lies upstream from protoporphyrinogen. Alternatively, the mechanism may involve the formation of a partial block downstream from Proto IX, perhaps as the result of defective ferrochelatase and/or a relative lack of iron for chelation. A partial block between protoporphyrinogen and protoporphyrin would produce somewhat the same effect, since it would allow protoporphyrinogen to diffuse out of the mitochondria to sites where it could be converted into Proto IX without subsequently being lost through conversion into heme. However, at present the literature contains only fragmentary data to support any of these hypotheses.

Deliberate Modification of Tissue Specificity. Tissue specificity is the beginning, the end, and most of the middle of the story of photodynamic therapy. Ideally, one would like to accumulate high concentrations of photosensitizer in malignant tissues while accumulating none whatever in adjacent normal tissues (14,66,67). Consequently, the discovery of an acceptably non-toxic technique that would produce a significant increase in the accumulation of ALA-induced Proto IX in malignant tissues would be very welcome, but only if it did not result in a proportional (or greater than proportional) increase in the Proto IX concentration in normal tissues. As discussed above, many different types of tissue develop a substantial increase in capacity to accumulate ALA-induced Proto IX when they undergo malignant transformation. The biochemical reason for this difference in response to ALA is not yet clear, but we want at all costs to maintain that difference. Any biochemical manipulation that makes normal cells behave like malignant cells with respect to ALA-induced Proto IX accumulation will be highly undesirable for clinical applications.

It certainly would be possible to use an iron chelator to decrease the rate at which Proto IX is lost by conversion into heme, or to administer a compound that selectively interferes with the conversion of protoporphyrinogen into Proto IX, thus

shunting the formation of Proto IX away from the mitochondria to sites where it is not readily converted into heme. In some cases this might lead to a substantial increase in photosensitization of the malignant tissue. However, there would be no net gain if the differential between the normal and the malignant tissues was thereby reduced.

Fluorescence vs Photosensitivity

In simple solute/solvent systems and at relatively low concentrations, both the intensity of Proto IX fluorescence and its potential for photodynamic action can be directly related to the concentration of the Proto IX. However, such a relationship does not necessarily hold *in vivo*.

Tissue Pigments. Tissues vary in composition. Melanin, necrotic material, and old blood are efficient absorbers of the UV-A or far blue wavelengths that normally are used to excite Proto IX fluorescence. However, such materials are somewhat less efficient absorbers of red wavelengths. Tissues that contain large quantities of dark pigments may not emit enough fluorescence to be detected visually, but still show a significant level of photosensitization. For example, squamous cell carcinoma-in-situ of the skin often is brown in colour and shows very little ALA-induced fluorescence when exposed to 410 nm light. However, such cancers usually can be destroyed if exposed to 635 nm light.

Singlet oxygen traps. Tissues may vary in their content of compounds that react readily with singlet oxygen. Anti-oxidants such as beta-carotene and alpha-tocopherol react very readily with singlet oxygen, and if present at high concentration may protect cells against lethal phototoxic damage. Ascorbic acid and sulfhydryl-containing compounds such as glutathione may be protective also. Consequently, certain tissues (such as one particular squamous cell carcinoma that we attempted to destroy) may show intense Proto IX fluorescence but sustain only minor phototoxic damage when exposed to light.

Nonhomogeneous Intracellular Distribution of Proto IX. ALA-induced Proto IX presumably is formed within the mitochondria if the rate-limiting step in the biosynthetic pathway for heme is between Proto IX and heme, but it may be formed in the cytosol or on the cell membranes if the bottleneck is between protoporphyrinogen and Proto IX. All other environmental factors being equal, the intensity of fluorescence per cell will reflect the total amount of Proto IX within each cell. However, at the subcellular level, cells that are equally fluorescent may have their Proto IX distributed very differently, with consequent large differences in local Proto IX concentrations. Proto IX that remains within the mitochondria or Proto IX that has become bound to cell membranes will be much more concentrated than the same amount of Proto IX that is dispersed throughout the cytosol. Presumably concentrated Proto IX is more phototoxic than the same amount of Proto IX when diluted. Also, since some sites within the cell are more important than others, the precise intracellular distribution of the ALA-induced Proto IX may have a substantial effect upon the phototoxic potential of Proto IX.

Unfortunately, at present very little information is available about the intracellular localization of ALA-induced Proto IX in different types of normal and malignant cells. Such studies should be made a high priority.

Clinical Studies. Although clinical studies of ALA-induced Proto IX photodynamic therapy for a wide variety of malignant and non-malignant lesions are in progress at major centres throughout the world, to date the published reports of such studies have been concerned primarily with malignant and pre-malignant lesions of the skin. Our own studies of superficial basal cell carcinoma (23,24,25) indicate that the technique is quite effective even though optimal treatment parameters have not yet been identified. The data for the first four years indicate that the complete response rate following a single treatment of a previously untreated superficial basal cell carcinoma is approximately $188/190 = 99\%$ for males, but only $50/58 = 86\%$ for females. There is no apparent effect of age for either sex. The cause of this very significant sex-related difference is under investigation.

Acknowledgments. This research has been supported in part by the Ontario Cancer Treatment and Research Foundation, the National Cancer Institute (Canada), the Medical Research Council (Canada), the Department of National Defence (Canada), and DUSA Pharmaceuticals.

Literature Cited

1. Pass, H. I. *J. Natl. Cancer Inst.* **1993**, *85*, 443-456.
2. Lui, H.; Anderson, R. R. *Dermatol. Clin.* **1993**, *11*, 1-13.
3. Edell, E. S.; Cortese, D. A. *Chest* **1992**, *102*, 1319-1322.
4. Noske, D. P.; Wolbers, J. G.; Sterenborg, N. J. *Clin. Neurol. Neurosurg.* **1991**, *93*, 293-307.
5. Windahl, T.; Lofgren, L. A. *Br. J. Urol.* **1993**, *71*, 187-191.
6. Weishaupt, K. R.; Gomer, C. J.; Dougherty, T. J. *Cancer Res.* **1976**, *36*, 2326-2329.
7. Henderson, B. W.; Miller, A. C. *Radiat. Res.* **1986**, *108*, 196-205.
8. Athar, M.; Elmets, C. A.; Bickers, D. R.; Mukhtar, H. *J. Clin. Invest.* **1989**, *83*, 1137-1143.
9. Lindelof, B.; Sigurgeirsson, B. *Acta Dermato-Venereologica* **1991**, *169* Supplementum, 3-6.
10. Piccinno, R.; Caccialanza, M.; Mainardi, L. *Giornale Italiano Di Dermatologia E Venereologia* **1989**, *124*, 369-373.
11. Stern, R. S. *Blood Cells* **1992**, *18*, 91-97.
12. Kvam, E.; Moan, J. *Photochem. Photobiol.* **1990**, *52*, 769-773.
13. Kennedy, J. C., Oswald, K. In *Porphyryns in Tumor Phototherapy*; Andreoni, A.; Cubeddu, R., Eds.; Plenum: New York, NY, 1984; pp 365-374.
14. Jori, G.; Reddi, E. In *Photodynamic Therapy of Neoplastic Diseases*; Kessel, D., Ed.; CRC: Boca Raton, FL, 1990; Vol. 2; pp 117-130.
15. Anderson, K. E. In *Hematology*; Williams, W. J.; Beutler, E.; Erslev, A. J.; Lichtman, M. A., Eds.; McGraw-Hill: New York, NY, 1990; pp 722-742.

16. Kennedy, J. In *Porphyrin Photosensitization*; Kessel, D.; Dougherty, T. J., Eds; Plenum: New York, NY, 1983, 53-62.
17. Granick, S. *J. Biol. Chem.* **1966**, *241*, 1359-1375.
18. De Matteis, F. S. *A. J. Lab. Clin. Med. - Special Issue* **1971**, *17*, 126-133.
19. Marks, G. S.; Krupa, F. M.; Taub, H.; Bluttel, R. A. *Ann. N. Y. Acad. Sci.* **1975**, *244*, 472-479.
20. Healey, J. F.; Bonkowsky, H. L.; Sinclair, P. R.; Sinclair, J. F. *Biochem. J.* **1981**, *198*, 595-604.
21. Berlin, N. I.; Neuberger, A.; Scott, J. J. *Bioch. J.* **1956**, *64*, 80-89.
22. Berlin, N. I.; Neuberger, A.; Scott, J. J. *Bioch. J.* **1956**, *64*, 90-100.
23. Sima, A. A. F.; Kennedy, J. C.; Blakeslee, D.; Robertson, D. M. *Can. J. Neurological Sci.* **1981**, *8*, 105-114.
24. Riopelle, R. J.; Kennedy, J. C. *J. Physiol. Pharmacol.* **1982**, *60*, 707-714.
25. Pottier, R. H.; Chow, Y. F. A.; LaPlante, J. P.; Truscott, T. G.; Kennedy, J. C.; Beiner, L. A. *Photochem. Photobiol.* **1986**, *44*, 679-687.
26. Divaris, D. X. G.; Kennedy, J. C.; Pottier, R. H. *Am. J. Pathol.* **1990**, *136*, 891-897.
27. Kennedy, J. C.; Pottier, R. H.; Pross, D. C. *J. Photochem. Photobiol. B: Biology* **1990**, *6*, 143-148.
28. Kennedy, J. C.; Pross, D. *Can. Derm. Assoc. J.* **1991**, *5*, 45-46.
29. Kennedy, J. C.; Pottier, R. H. *J. Photochem. Photobiol. B: Biology* **1992**, *14*, 275-292.
30. Yang, J. Z.; Van Vugt, D. A.; Kennedy, J. C.; Reid, R. L. *Am. J. Obstet. Gynecol.* **1993**, *168*, 995-1001.
31. Yang, J. Z.; Van Vugt, D. A.; Kennedy, J. C.; Reid, R. L. *Photochem. Photobiol.* **1993**, *57*, 803-807.
32. Malik, Z.; Lugaci, H. *Br. J. Cancer* **1987**, *56*, 589-595.
33. Malik, Z.; Ehrenberg, B.; Faraggi, A. *J. Photochem. Photobiol. B: Biol.* **1989**, *4*, 195-205.
34. Loh, C. S.; Bedwell, J.; MacRobert, A. J.; Krasner, N.; Phillips, D.; Bown, S. G. *Br. J. Cancer* **1992**, *66*:452-462.
35. Peng Q.; Moan, J.; Warloe, T.; Nesland, J. M.; Rimington, C. *Int. J. Cancer* **1992**, *52*, 433-443.
36. Bedwell, J.; MacRobert, A. J.; Phillips, D.; Bown, S. G. *Br. J. Cancer* **1992**, *65*, 818-824.
37. Van Hillegersberg, R.; Van Den Berg, J. W.; Kort, W. J.; Terpstra, O. T.; Wilson, J. H. *Gastroenterology* **1992**, *103*, 647-651.
38. Goff, B. A.; Bachor, R.; Kollias, N.; Hasan, T. *J. Photochem. Photobiol. B: Biology* **1992**, *15*, 239-251.
39. Fukuda, H.; Paredes, S.; Battle, A. M. *Comp. Biochem. Physiol. [B]* **1992**, *102*, 433-436.
40. Hanania, J.; Malik, Z. *Cancer Lett.* **1992**, *65*, 127-131.
41. Charlesworth, P.; Truscott, T. G. *J. Photochem. Photobiol. B: Biol.* **1993**, *18*, 99-100.
42. Grant, W. E.; Hopper, C.; MacRobert, A.J.; Speight, P. M.; Bown, S. G. *Lancet* **1993**, *342*, 147.
43. Ortel, B.; Tanew, A.; Honigsmann, H. *J. Photochem. Photobiol B* **1993**, *17*, 273-278.
44. Wolf, P.; Rieger, E.; Kerl, H. *J. Am. Acad. Dermatol.* **1993**, *28*, 17-21.

45. Iinuma, S.; Bachor, R.; Hasan, T. *Proc. Am. Assoc. Cancer Res.* **1993**, *34*, A2157.
46. Shanler, S. D.; Mang, T.; Wacxwa, K. W.; Whitaker, J. E.; Wilson, B. D., Oseroff, A. R. *Proc. Am. Assoc. Cancer Res.* **1993**, *34*, A2161.
47. Licznernski, B.; Shanler, S. D.; Paszkiewicz, G.; Whitaker, J. E.; Wan, W.; Oseroff, A. R. *Proc. Am. Assoc. Cancer Res.* **1993**, *34*, A2164.
48. Kennedy, J. C. *Photochem. Photobiol.* **1993**, *57*, 76S.
49. Bown, S. B.; Holroyd, J. A.; Vernon, D. I. *Photochem. Photobiol.* **1993**, *57*, 76S.
50. Konig, K.; Ruck, A.; Schneckenburger, H. *Photochem. Photobiol.* **1993**, *57*, 76S.
51. Shulman, G.; Golub, A. *Photochem. Photobiol.* **1993**, *57*, 77S.
52. van der Veen, N.; van Leengoed, E.; Star, W. M. *Photochem. Photobiol.* **1993**, *57*, 77S.
53. Campbell, D. L.; Kennedy, J. C.; Pottier, R. H.; Forkert, P. G. *Photochem. Photobiol.* **1993**, *57*, 77S.
54. Andersson-Engels, S.; Berg, R.; Svanberg, K.; Svanberg, S.; Wang, I. *Photochem. Photobiol.* **1993**, *57*, 78S.
55. Chan, L.; Wilton, D.; Newman, E. L.; Johnson, B. E. *Photochem. Photobiol.* **1993**, *57*, 78S.
56. Malik, Z.; Babushkina, T.; Shafran, M.; Nordenberg, Y.; Mamet, R.; Sheinfeld, N. *Photochem. Photobiol.* **1993**, *57*, 78S.
57. Sac, A.; Nadeau, P.; Kennedy, J. C.; Pottier, R. H. *Photochem. Photobiol.* **1993**, *57*, 79S.
58. Kennedy J. C.; Laplante, J. P.; Nadeau, P.; Pimiente, V.; Pottier, R. *Photochem. Photobiol.* **1993**, *57*, 79S.
59. Kennedy, J. C. *Photochem. Photobiol.* **1993**, *57*, 108S.
60. Yang, J. Z.; Van Dijk-Smith, J. P.; Van Vugt, D. A.; Kennedy, J. C.; Reid, R. L. *Fertility and Sterility* (Annual Meeting Program Supplement) **1993**, *60*, S137.
61. Reid, R. L.; Kennedy, J. C.; Van Vugt, D. A.; Yang, J. Z.; Fletcher, A.; Foster, W. 40th Annual Meeting of the Society for Gynecologic Investigation, **1993**, 97.
62. Konig, K.; Schneckenburger, H.; Ruck, A.; Steiner, R. *J. Photochem. Photobiol. B: Biology* **1993**, *18*, 237-290.
63. Loh, C. S.; MacRobert, A. J.; Bedwell, J.; Regula, J.; Krasner, N.; Bown, S. G. *Br. J. Cancer* **1993**, *68*, 41-51.
64. Rebeiz, N.; Rebeiz, C. C.; Arkins, S.; Kelley, K. W.; Rebeiz, C. A. *Photochem. Photobiol.* **1992**, *55*, 431-435.
65. Sassa, S. In *Hematology*; Williams, W. J.; Beutler, E.; Erslev, A. J.; Lichtman, M. A., Eds.; McGraw-Hill: New York, NY, 1990; pp 322-329.
66. MacRobert, A. J.; Bown, S. G.; Phillips, D. In *Photosensitizing Compounds: Their Chemistry, Biology and Clinical Use*; Bock, G.; Harnett, S., Eds.; Ciba Foundation Symposium 146; Wiley: Chichester, 1989, pp 4-16.
67. Bonnett, R.; Berenbaum, M. In *Photosensitizing Compounds: Their Chemistry, Biology and Clinical Use*; Bock, G.; Harnett, S., Eds.; Ciba Foundation Symposium 146; Wiley: Chichester, 1989, pp 40-59.

RECEIVED March 8, 1994

Author Index

- Amindari, S., 48
Anderson, R. J., 18
Böger, Peter, 147
Boynton, John E., 91
Brouillet, Nicole, 81
Camadro, Jean-Michel, 81
Clark, Robert D., 34
Duke, Mary V., 191
Duke, Stephen O., 1,133,191
Fingar, V. F., 280
Gillham, Nicholas W., 91
Gorman, N., 266
Grossweiner, Leonard I., 255
Gullner, G., 177
Gut, Larry J., 206
Halling, B. P., 280
Harris, Elizabeth H., 91
Hess, F. D., 18
Ishizuka, K., 120
Iwata, Shuji, 147
Jacobs, Judith M., 105,266
Jacobs, Nicholas J., 105,266
Janousek, V., 247
Juvik, John A., 206
Kelley, Keith W., 233
Kennedy, James C., 291
Komives, T., 177
Krijt, J., 247
Labbe, Pierre, 81
Lee, Hee Jae, 191
Lee, J. J., 120
Matringe, Michel, 81
Matsumoto, H., 120
Moubarak, M. B., 48
Nakayama, Naoko, 147
Nandihalli, Ujjana B., 48,133,191
Norris, A. E., 18
Oshio, Hiromichi, 91
Pottier, Roy H., 291
Rebeiz, Constantin A., 1,48,161,206,233
Rebeiz, Natalie, 233
Reddy, Krishna N., 48,161
Sanitrák, J., 247
Sato, Ryo, 91
Shibata, Hideyuki, 91
Sinclair, J. F., 266
Sinclair, P. R., 266
Sumida, Motoo, 147
Tanaka, Takaharu, 147
Thomé, Françoise, 81
Tripathy, Baishnab Charan, 65
Velu, J. A., 48
Vokurka, M., 247
Wakabayashi, Ko, 147
Walton, H. S., 266
Winkelmann, J. W., 280
Yamamoto, Masako, 91
Yuhas, D. A., 280

Affiliation Index

- Agricultural Research Service,
1,133,161,191
Brigham and Women's Hospital, 280
Charles University, 247
Dartmouth Medical School, 105,266
Duke University, 91
FMC Corporation, 280
Harvard Medical School, 280
Hazleton Laboratories, 133,191
Hungarian Academy of Science, 177
Illinois Institute of Technology, 255
Jawaharlal Nehru University, 65
Monsanto Company, 34
Queen's University, 291

- Ravenswood Hospital Medical Center, 255
 Royal Military College of Canada, 291
 Sandoz Agro, Inc., 18
 Sumitomo Chemical Company Ltd., 91
 Suntory Ltd., 147
 Tamagawa University, 147
 U.S. Department of Agriculture, 1,133,161,191
 Universität Konstanz, 147
 Université Joseph Fourier, 81
 Université Paris 7, 81
 University of Illinois, 1,48,161,206,233
 University of Louisville, 280
 University of Tsukuba, 120
 Veterans Administration Medical Center, 266

Subject Index

A

Accumulated protoporphyrinogen, role in protoporphyrinogen inhibition, 120

Acifluorfen

structure, 81,82f

use for protoporphyrinogen

oxidase characterization, 81,83

Acifluorfen-methyl

immature cell effect of *Marchantia polymorpha*, 149–150,151f

protoporphyrin IX accumulation effect, 133–134,193,195f

Active oxygen species generated by

photodynamic herbicide, detoxification, 187–188

δ -Aminolevulinic acid

behavior as herbicide, 49–50

cancer therapy, 292–300

description, 2,4,49

field applications, 50

fluorescence vs. photosensitivity, 299–300

function, 161–162,206

ideal tissue photosensitizer

characteristics, 292–293

induction of protoporphyrin IX

accumulation in neoplastic cells, 241–244

insecticidal potency via ingestion, 8–9

occurrence in plant tissue, 4

properties, 261,295

δ -Aminolevulinic acid—*Continued*
 protoporphyrin IX photodynamic therapy, 295–299

synthesis, 65

use as herbicide, 4–5

δ -Aminolevulinic acid herbicides and insecticides, technology transfer for antitumor activity, 240–241

δ -Aminolevulinic acid induced

photodynamic damage to cucumber plants mediated by singlet oxygen electrolyte leakage, 68,70f,79

exogenous photosystem II electron donor effect, 74t,79

experimental procedure, 66–67

fluorescence variation, 74–75,79

isolated chloroplast damage, 72–73

light effect, 67

low light intensity damage, 72t,79

photosystem II protection by active oxygen species scavengers, 75,76f,79

pigment content, 67–68,69f,79

superoxide radical production, 77t,79

tetrapyrrole involvement, 75,77–79

thylakoid membrane linked function

effect, 68,71f,79

δ -Aminolevulinic acid induced protoporphyrin IX photodynamic therapy

advantages, 295–296

clinical studies, 300

fluorescence vs. photosensitivity, 299–300

tissue specificity, 296–299

- Ravenswood Hospital Medical Center, 255
 Royal Military College of Canada, 291
 Sandoz Agro, Inc., 18
 Sumitomo Chemical Company Ltd., 91
 Suntory Ltd., 147
 Tamagawa University, 147
 U.S. Department of Agriculture, 1,133,161,191
 Universität Konstanz, 147
 Université Joseph Fourier, 81
 Université Paris 7, 81
 University of Illinois, 1,48,161,206,233
 University of Louisville, 280
 University of Tsukuba, 120
 Veterans Administration Medical Center, 266

Subject Index

A

- Accumulated protoporphyrinogen, role in protoporphyrinogen inhibition, 120
 Acifluorfen
 structure, 81,82f
 use for protoporphyrinogen oxidase characterization, 81,83
 Acifluorfen-methyl
 immature cell effect of *Marchantia polymorpha*, 149–150,151f
 protoporphyrin IX accumulation effect, 133–134,193,195f
 Active oxygen species generated by photodynamic herbicide, detoxification, 187–188
 δ -Aminolevulinic acid
 behavior as herbicide, 49–50
 cancer therapy, 292–300
 description, 2,4,49
 field applications, 50
 fluorescence vs. photosensitivity, 299–300
 function, 161–162,206
 ideal tissue photosensitizer characteristics, 292–293
 induction of protoporphyrin IX accumulation in neoplastic cells, 241–244
 insecticidal potency via ingestion, 8–9
 occurrence in plant tissue, 4
 properties, 261,295
 δ -Aminolevulinic acid—*Continued*
 protoporphyrin IX photodynamic therapy, 295–299
 synthesis, 65
 use as herbicide, 4–5
 δ -Aminolevulinic acid herbicides and insecticides, technology transfer for antitumor activity, 240–241
 δ -Aminolevulinic acid induced photodynamic damage to cucumber plants mediated by singlet oxygen electrolyte leakage, 68,70f,79
 exogenous photosystem II electron donor effect, 74t,79
 experimental procedure, 66–67
 fluorescence variation, 74–75,79
 isolated chloroplast damage, 72–73
 light effect, 67
 low light intensity damage, 72t,79
 photosystem II protection by active oxygen species scavengers, 75,76f,79
 pigment content, 67–68,69f,79
 superoxide radical production, 77t,79
 tetrapyrrole involvement, 75,77–79
 thylakoid membrane linked function effect, 68,71f,79
 δ -Aminolevulinic acid induced protoporphyrin IX photodynamic therapy
 advantages, 295–296
 clinical studies, 300
 fluorescence vs. photosensitivity, 299–300
 tissue specificity, 296–299

δ -Aminolevulinic acid synthase, induction, 266–267

Anilide protoporphyrinogen oxidase inhibitor derivatives, synthesis, 41–43

Antioxidant, defense mechanisms, 187–188

Antioxidative system, oxyfluorfen vs. plant species, 127–129

Aromatic compounds, polyhalogenated inhibition of uroporphyrinogen decarboxylase, 266

uroporphyrin accumulation effect in avian hepatocytes, 270–271

Aromatic hydrocarbons, polychlorinated, disruption of porphyrin biosynthetic pathway, 247

C³-Arylpyrazoles, synthesis, 39–41

N-Arylpyrazoles, synthesis, 44

Avian hepatocytes, uroporphyrin accumulation, 270–271, 273f, 275

B

Benzoporphyrin derivatives, 261

Biochemical characterization

Chlamydomonas reinhardtii mutant resistant to protoporphyrinogen inhibitors, 98

protoporphyrin IX accumulation, 233–246

protoporphyrinogen oxidase experimental procedure, 83–84

molecular properties, 86–87, 88t

photoaffinity labeling of membranes by acifluorfen, 86–87, 88f, 89

relative abundance, 84–87

specific activity, 84–87

Biosynthesis of porphyrins, pest management tool, 1–13

Biphenyls, polychlorinated and polybrominated, disruption of porphyrin biosynthetic pathway, 247

Bipyridyliums, biochemical site of action, 18–19

C

C-bridged protoporphyrinogen oxidase inhibitors, 39–41

Cancer therapy, use of δ -aminolevulinic acid, 291–300

See also Tumor therapy (Carbonylphenyl)uracils, synthesis, 41–42

Cationic photosensitizing dyes, 261–262

Cellular damage, production by porphyrins, 238–239

Chemotherapy, use of porphyrins, 237–241

Chirality, role in activity of protoporphyrinogen oxidase inhibitors, 143f

Chlamydomonas reinhardtii mutant resistant to protoporphyrinogen inhibitors, 91–102

advantages for mechanism of action studies, 92–93

biochemical characterization, 98

cloning by transformation, 100–103

cloning strategies, 98–100

genetic characterization, 95–97

herbicide structure, 92, 94f

isolation, 93

physiological characterization, 93, 94f, 97f

Chlomethoxyfen

ethane evolution of crop and weed seedlings, 121, 122f

growth response of crop and weed seedlings, 121, 122f

mechanism of differential activity, 130

metabolism vs. plant species, 123

protoporphyrin IX accumulation vs. plant species, 123, 125–127

uptake vs. plant species, 123, 124f

Chlorins, properties, 260–261

- Chlorophyll
 biosynthetic pathway, 2,3*f*,106,107*f*
 function, 233–244
- Chloroplasts, photodynamic effects of
 metabolic tetrapyrroles, 49
- Crop seedlings, growth response to
 oxyfluorfen and chlomethoxyfen,
 121,122*f*
- Cucumber plants, δ -aminolevulinic acid
 induced photodynamic damage, 65–79
- Cucumis sativus* L., δ -aminolevulinic acid
 induced photodynamic damage
 mediated by singlet oxygen, 65–79
- Cultured chick hepatocytes, porphyrin
 accumulation after diphenyl ether
 herbicide treatment, 268–270,272–274*f*
- Cultured hepatocytes, accumulation of
 protoporphyrinogen treated with
 diphenyl ether herbicides, 275–277
- Cyclic tetrapyrroles
 production in pests, 2
See also Porphyrins
- Cytochrome P450
 hepatic microsomal, modulation of
 activities by diphenyl
 ether herbicides, 250–251
 role in uroporphyrin
 accumulation, 270–271,273*f*,275
- Cytosolic fraction of plant,
 protoporphyrinogen destruction,
 112–113
- D**
- Detoxification of photodynamic
 herbicides in plants
 catalytic conjugation of endogenous
 thiols, 184–185
 metabolism, 182–183
 transformation products, 183–184
- Diaryl ethers
 diphenyl ethers, 19–23*t*
 heterocyclic phenyl ethers, 22,24–25
 structure, 19
- (2,4-Dichlorophenyl)-1-pyrrolidine-
 carboxylate, *See* Phenopylate
 herbicides
- Diphenyl ether(s)
 examples, 19–22,23*t*
 synthesis, 35–37
- Diphenyl ether herbicide(s)
 biochemical site of action, 18–19
 crop response variation, 121–131
 factors affecting protoporphyrin
 accumulation, 105–117
 heme pathway effect in cultured liver
 cells, 268–277
 induction of elevated levels of
 uroporphyrin and heptacarboxylic
 porphyrin, 249–250
 mechanism of action, 120–121
 modulation of hepatic microsomal
 cytochrome P450 activities, 250–251
 plant and yeast protoporphyrinogen
 oxidase as target, 81–88
 protoporphyrin oxidase inhibition,
 81,105
 porphyrin accumulation in cultured
 chick hepatocytes, 268–270,
 272–274*f*
 protoporphyrinogen accumulation in
 cultured hepatocytes, 275–277
 reasons for study, 268
 quantitative structure–activity
 relationships, 137–138
 toxic action, 105
 uroporphyrin accumulation in avian
 hepatocytes, 271,273*f*,275
- 2,2'-Dipyridyl
 ingestion and insecticidal activity,
 210–211
 porphyrin insecticidal activity, 207–208
 structure, 56
 structure–activity relationships, 58
 tetrapyrrole-dependent modulators,
 56–58
 use as modulator, 162
- Dipyridyl-related modulators, porphyrin
 pathway effect, 171,174*t*

Divinyl monocarboxylic route, schematic representation, 52,53f

E

Endogenous porphyrins, use as tissue photosensitizers, 293–295

Enzymes beyond protoporphyrinogen oxidase in porphyrin pathway, 201

Ethane evolution, crop and weed seedlings, oxyfluorfen and chlomethoxyfen, 121,122f

Exogenous photosystem II electron-donor effect, δ -aminolevulinic acid induced photodynamic damage to cucumber plants mediated by singlet oxygen, 74t,79

Exogenous porphyrins, use in photodynamic therapy, 239–240

F

590FP

accumulation in herbicide-treated immature liverwort cells, 150,152f
physiological effect in herbicide-treated immature liverwort cells, 150,153–156

Five-membered N-heterocyclic modulators that mimic a tetrapyrrole quadrant, 62–63

Fungicides, porphyric, *See* Porphyric fungicides

G

Genetic characterization, *Chlamydomonas reinhardtii* mutant resistant to protoporphyrinogen inhibitors, 95–97

Green plants, greening groups, 7–8, 52,54f

Grow response of crop and weed seedlings, oxyfluorfen and chlomethoxyfen, 121,122f

H

Hematoporphyrin derivative
biodistribution, 259–260
composition, 259
history of use for photodynamic therapy, 255–256
light effects, 260
mechanism of action, 258–260
pharmacokinetics, 259–260

Heme

function, 233–234
pathway, effects of diphenyl ether herbicides, 266–279
protoporphyrinogen oxidase inhibitor effect on levels, 194f

Heme biosynthesis

interorganellar localization of terminal enzymes, 114–115
intracellular localization, 236–237
pathway
enzymatic steps, 106,107f,266,267f
inhibition, 266
schematic representation, 2,3f

Hepatic microsomal cytochrome P450, modulation of activities by diphenyl ether herbicides, 250–251

HepG2 cells, human hepatoma derived, protoporphyrinogen oxidase inhibiting herbicide effect on porphyrin accumulation, 251,252f

Heptacarboxylic porphyrin, induction of elevated levels by diphenyl ether herbicides, 249–250

Herbicide(s)

diphenyl ether, effects on heme pathway in cultured liver cells, 266–279

light-dependent bleaching in sensitive plants, 120

- Herbicide(s)—*Continued*
 peroxidizing, inducing porphyrin synthesis in liverwort cells, 147–158
 photodynamic, mechanisms of plant tolerance, 177–190
 porphyrin-generating photodynamic, *See* Porphyrin-generating photodynamic herbicides
 weed control, 65
 Herbicide-resistant weeds, advantages for herbicide mechanism of action studies, 91
 Herbicide site, optimal, protoporphyrinogen oxidase, 191–204
 Heterocyclic carboxamides, examples, 31
 Heterocyclic phenyl ethers, examples, 22,24–25
 Hexachlorobenzene, disruption of porphyrin biosynthetic pathway, 247
 Human hepatoma-derived HepG2 cells, protoporphyrinogen oxidase inhibiting herbicide effect on porphyrin accumulation, 251,252*f*
- I
- Ingestion and porphyric insecticidal activity, 210–211,212*t*
 Insecticides, porphyric, *See* Porphyric insecticides
 Intact plastids, protoporphyrinogen export, 111–112
 Isolated chloroplast damage, δ -aminolevulinic acid induced photodynamic damage to cucumber plants mediated by singlet oxygen, 72–73
- L
- Light and protoporphyrinogen, 110
 Light–dark regimens and porphyric insecticides, 208–209
 Light dosimetry problem, tissue photosensitizer for photodynamic cancer therapy, 292–293
 Liverwort cells, porphyrin synthesis induced by peroxidizing herbicides, 147–160
 Low light intensity damage, δ -aminolevulinic acid induced photodynamic damage to cucumber plants mediated by singlet oxygen, 72*t*,79
- M
- Magnesium tetrapyrroles, use as photosensitizers, 65
 Mammalian cells, biochemistry of protoporphyrin IX accumulation, 233–244
 Mammalian porphyrin metabolism and protoporphyrinogen oxidase inhibitor, 247–253
 Management of pests, porphyrin biosynthesis as tool, 1–13
Marchantia polymorpha L. cells, *See* Liverwort cells
 Metabolic tetrapyrroles, photodynamic effects on chloroplasts, 49
 Metabolism of oxyfluorfen and chlomethoxyfen, 123
 Metal cations, inhibitors of insecticidal activity by 1,10-phenanthroline, 211,212*t*
 Mitochondrial protoporphyrinogen oxidase, properties, 197*t*,199
 Modulators
 function, 206
 porphyric insecticides
 identification, 213–215,216*t*
 quantitative structure–activity analysis, 215,217–232

Modulators—Continued

- porphyrin pathway beyond
 - protoporphyrinogen oxidase
 - classifications, 167
 - dipyridyl analogues, 171,174t
 - experimental procedure, 162–168
 - light effect, 169
 - mode of action, 171
 - pyridinium analogues, 171–173t
 - pyrrole analogues, 169–171
 - target sites, 171,175
- porphyrin synthesis in plants
 - categories, 7
 - discovery, 6–7
 - efficacy under greenhouse vs. field
 - conditions, 8
 - insecticidal potency via ingestion, 8–10
 - structure, 7

Monovinyl monocarboxylic route,
schematic representation, 52,53f

Mutant of *Chlamydomonas reinhardtii*
resistant to protoporphyrinogen
oxidase inhibitors, 91–102

N

Nicotinic acid and substituted analogues,
59–61

O

O-bridged protoporphyrinogen oxidase
inhibitors, synthesis, 35–39

Octachlorostyrene, disruption of
porphyrin biosynthetic pathway, 247

Organic chemicals, synthetic, that act
through porphyrin pathway, 18–31

Oxadiazon
structure, 25
synthesis, 44

Oxyfluorfen
antioxidative system vs. plant species,
127–129

Oxyfluorfen—Continued

- ethane evolution of crop and weed
 - seedlings, 121,122f
 - factors determining tolerance of
 - plant species, 130–131
 - growth response of crop and weed
 - seedlings, 121,122f
 - mechanism of differential activity, 130
 - metabolism vs. plant species, 123
 - protoporphyrin IX accumulation vs.
 - plant species, 123,125–127
 - protoporphyrinogen oxidase inhibition
 - vs. plant species, 127t
 - uptake vs. plant species, 123,124f
- Oxygen, singlet, mediated photodynamic**
damage to cucumber plants induced by
 δ -aminolevulinic acid, 65–78
- Oxypyridines, substituted,**
structure–activity relationships,
227–229,230t

P**Peroxidizing herbicides**

- induction of porphyrin synthesis in
 - liverwort cells, 149–160
- mechanism of action, 147–148
- protoporphyrin IX accumulation,
192–196

Persistence problem in normal skin, tissue
photosensitizer for photodynamic
cancer therapy, 293–295

Pest(s), production of cyclic
tetrapyrroles, 2

Pest management, porphyrin biosynthesis
as tool, 1–13

1,10-Phenanthroline

- induction of protoporphyrin IX
 - accumulation in neoplastic cells,
241–244
- ingestion and insecticidal activity,
210–211,212t
- metal cations as inhibitors, 211,212t
- porphyric insecticidal activity, 210

- 1,10-Phenanthroline—*Continued*
 structure–function relationships, 56
 substituted, structure–activity relationships, 217–222
 tetrapyrrole-dependent modulators, 52,54–56
- Penopylate herbicides, quantitative structure–activity relationships, 138–139
- Phenyl carbamates, synthesis, 39
- Phenyl heterocycles
 C-phenyl heterocycles, 26
 N-phenyl heterocycles, 26–30
 O-phenyl carbamates, 31
 structure, 25
- Phenylhydrazine protoporphyrinogen oxidase inhibitor derivatives, 43–46
- N-Phenylimides, synthesis, 42–43
- Phenyltetrahydrophthalimide herbicides, quantitative structure–activity relationships, 139–141
- Pheophorbides, properties, 261
- Photobleaching herbicides
 disruption of porphyrin biosynthetic pathway, 247–248
 modulation of hepatic microsomal cytochrome P450 activities, 250–251
 porphyrin accumulation in human heptoma-derived HepG2 cells, 251,252f
 porphyrin concentration, 248–250
 site of action, 133
 toxicology in experimental animals and humans, 251,253
- Photodynamic compounds, 1–2
- Photodynamic damage to cucumber plants
 δ -aminolevulinic acid induced, 65–79
- Photodynamic herbicides
 description, 65
 examples, 177
 factors affecting selective action evaluation, 177–178
 phytotoxicity, 177,179f
 plant tolerance mechanisms, 178–188
See also Porphyrin herbicides
- Photodynamic therapy
 adjuvant therapy, 262
 applications, 280
 description, 291
 future, 263
 gynecological malignancy, 258
 history, 255–256
 mechanism of action, 258–260
 photophysics, 262–263
 phototechnology, 263
 porphyrin derivatives, 255–265
 procedures, 256,262
 requirement, 292
 second-generation drugs, 260–261
 skin cancer clinical trials, 256–257
 use as exogenous porphyrins, 239–240
 use as protoporphyrinogen oxidase inhibitors, 280–289
- Photofrin, use in photodynamic therapy, 256
- Photoradiation therapy, *See* Photodynamic therapy
- Photosystem II protection by active oxygen species scavengers,
 δ -aminolevulinic acid induced photodynamic damage to cucumber plants, 75,76f,79
- Phthalocyanins, properties, 260–261
- Physiological characterization,
Chlamydomonas reinhardtii mutant resistant to protoporphyrinogen inhibitors, 93,94f,97f
- Phytotoxicity of photodynamic herbicides
 description, 177,179f
 resistance, 181
 selectivity vs. weed species, 178,180f,181
 tissue sensitivity, 181
- Picolinic acid and substituted analogues,
 tetrapyrrole-dependent modulators, 61–62
- Plant(s)
 factors in determining tolerance to oxyfluorfen, 130–131

Plant(s)—*Continued*

- mechanism of differential tolerance, 123–129
- treated with diphenyl ether herbicides, factors affecting protoporphyrin accumulation, 105–119
- Plant protoporphyrinogen oxidase, 81
- Plant tolerance to photodynamic herbicides, 177–190
 - antioxidant defense mechanisms, 187–188
 - catalytic conjugation of endogenous thiols, 184–185
 - future research, 188
 - herbicide resistance, 181
 - herbicide selectivity, 178,180f,181
 - metabolism, 182–183
 - protoporphyrin IX concentration in plant cell, 186–187
 - target site selectivity, 185–186
 - tissue sensitivity, 181
 - transformation products, 183–184
 - translocation, 182
 - uptake, 181–182
- Plasma membrane bound protogen IX oxidizer, activities, 199r
- Plastids, protoporphyrinogen oxidase properties, 197–199
- Polychlorinated and polybrominated biphenyls, disruption of porphyrin biosynthetic pathway, 247
- Polychlorinated aromatic hydrocarbons, disruption of porphyrin biosynthetic pathway, 247
- Polyhalogenated aromatic compounds
 - inhibition of uroporphyrinogen decarboxylase, 266
 - uroporphyrin accumulation in avian hepatocytes, 270–271
- Porphyrias, treatment using endogenous porphyrins, 294–295
- Porphyric fungicides, 10
- Porphyric herbicides
 - δ -aminolevulinic acid, 2,4–5
 - modulators of porphyrin synthesis, 6–8

Porphyric herbicides—*Continued*

- protoporphyrin accumulation, 161
- protoporphyrinogen oxidase inhibitors, 5–6
- Porphyric insecticides, 206–232
 - database of commercially available compounds, 9–10
 - development, 206
 - 2,2'-dipyridyl, 207–208,210–211
 - discovery, 8,207
 - light–dark regimen effect, 208–209
 - metal cations as inhibitors, 211,212r
 - mode of action, 212–213
 - modulator identification, 213–215,216r
 - 1,10-phenanthroline, 210–211,212r
 - potency via ingestion, 8–9
 - quantitative structure–activity analysis of modulators, 215,217–232
- Porphyric pesticides
 - future prospects, 12–13
 - resistance and tolerance mechanisms, 10–11
 - toxicology, 12
 - use in photodynamic therapy, 11
- Porphyrin(s)
 - accumulation in cultured chick hepatocytes treated with diphenyl ether herbicides, 268–270,272–274f
 - applications, 2
 - biosynthesis as tool in pest management, 1–15
 - cellular damage production, 238–239
 - chemotherapeutic agents in mammalian cells, 233–246
 - concentration related to photobleaching herbicide, 248–250
 - derivatives, photodynamic therapy, 255–263
 - endogenous, use as tissue photosensitizers, 293–295
 - exogenous, use in photodynamic therapy, 239–240
 - function, 161
 - intermediates, protoporphyrin conversion, 113,114r

Porphyrin(s)—Continued

- metabolism, mammalian, and protoporphyrinogen oxidase inhibitor, 247–253
- photodynamic therapy, 255–265
- photophysical and photodynamic properties, 237
- protoporphyrinogen oxidase inhibiting herbicide effect on accumulation in human hepatoma-derived HepG2 cells, 251,252f
- use in chemotherapy, 237–241
- use in photodynamic therapy, 11
- Porphyrin-generating photodynamic herbicides**
 - δ -aminolevulinic acid, 2,4–5
 - categories, 2,4–8
 - modulators of porphyrin synthesis, 6–8
 - protoporphyrinogen oxidase inhibitors, 5–6
- Porphyrin pathway**
 - enzymes beyond oxidase, 201
 - modulators beyond oxidase, 161–175
 - optimal herbicide cite, 191–204
 - organic chemicals, 18–31
 - scheme, 191–192
- Porphyrin synthesis in liverwort cells**
 - induced by peroxidizing herbicides, 147–158
 - acifluorfen-methyl effects on immature cells, 149–150,151f
 - experimental procedure, 148–149
 - 590FP accumulation, 150,152f
 - 590FP physiological effect, 150, 153–156
 - protoporphyrin IX accumulation in mature cells, 156–160
- Porphyrinogenesis**, applications, 2
- Porphyrinogenic compounds**, use in photodynamic therapy, 11
- Porphyrinogenic photodynamic herbicide phenomenology**, developments, 48–49
- Protochlorophyllide** and protoporphyrinogen oxidase inhibitor, 192–194

Protoporphyrin IX

- accumulation caused by peroxidizing herbicides, 192–196
- accumulation in plants treated with diphenyl ether herbicides, 105–118
- biochemistry of accumulation, 233–246
- biosynthetic pathway, 234,235f,236
- concentration in plant cells, 186–187
- in mature liverwort cells, effect of peroxidizing herbicides, 156–160
- in oxyfluorfen-treated plants, 123, 125–127
- induction of accumulation in neoplastic cells, 241–244
- nonhomogeneous intracellular distribution, 299–300
- structure, 81,82f
- Protoporphyrinogen**
 - accumulation in cultured hepatocytes, 275–277
 - destruction in cytosolic fraction, 112–113
 - synthetic rate, 113–114
 - molecular similarities with protoporphyrinogen oxidase inhibitors, 134–136
 - structure, 81,82f
- Protoporphyrinogen export**, intact plastids, 111–112
- Protoporphyrinogen oxidase**
 - biochemical characterization procedure, 83–89
 - competitive inhibition, 134
 - forms in plants, 197t
 - function, 106,281
 - inhibition vs. plant species, 127t
 - mitochondrial form, 197t,199
 - modulators of porphyrin pathway beyond enzyme, 161–175
 - need for understanding mechanism of action, 91–92
 - optimal herbicide site in porphyrin pathway, 191–204

- Protoporphyrinogen oxidase—*Continued*
- plant, characterization, 81–88
 - plastid properties, 197–199
 - protoporphyrinogen catalysis, 81
 - resistant mutant, 91–102
 - substrate, product, and inhibitor properties, 200
 - yeast, characterization, 81–90
- Protoporphyrinogen oxidase inhibitors
- categories, 35
 - competitive inhibition of enzyme, 134
 - crop response variation, 120–131
 - description, 5
 - diaryl ethers, 19–25
 - effect on mammalian porphyrin metabolism, 247–254
 - future prospects, 12–13
 - heterocyclic carboxamides, 31
 - insecticidal potency via ingestion, 8–9
 - mammalian porphyrin metabolism, 247–253
 - mechanism, 200–201
 - mode of action, 5
 - molecular similarities with
 - protoporphyrinogen, 134–136
 - phenyl heterocycles, 25–31
 - porphyrin accumulation, effect in
 - human hepatoma-derived HepG2 cells, 251,252*f*
 - properties, 200
 - protoporphyrinogen accumulation during herbicide inhibition, 106
 - quantitative structure–activity relationships, 136
 - reasons for success as herbicides, 191–192
 - resistance mechanisms, 10–11
 - structure–activity relationships, 133–146
 - synthesis, 34–46
 - tolerance mechanisms, 10–11
 - toxicology in experimental animals and humans, 12,251,253
 - tumor therapy, 280–290
- Protoporphyrinogen oxidase inhibitors—*Continued*
- tumor therapy—*Continued*
 - fluorometric emission scans of cell extracts, 283
 - mechanism of action, 288–289
 - porphyrin accumulation vs. inhibitor structure and dose, 284–288
 - use as herbicide, 5–6
 - use as photodynamic therapy, 11
 - variation in crop response, 120–130
- Protoporphyrinogen oxidation
- demonstration, 106,108–109
 - reductant effect, 109–110
- Protox, *See* Protoporphyrinogen oxidase
- Psoralen UV-A therapy, 291–292
- Purpurins, properties, 261
- Pyrazole nitrophenyl ethers, 37–38
- Pyridinium(s), substituted, structure–activity relationships, 229,230*t*,231*f*
- Pyridinium-related modulators, porphyrin pathway, 171,172–173*t*
- Pyridinium(s) that mimic a quadrant or half a tetrapyrrole, 62
- Pyridonecarboxanilides, synthesis, 41
- Pyridyls, substituted, structure–activity relationships, 222–226
- Pyrrole(s)
- substituted, structure–activity relationships, 229–230,232
 - tetrapyrrole-dependent modulators, 62
- Pyrrole-related modulators, porphyrin pathway, 169–171
- Q
- Quantitative structure–activity analysis, modulators of porphyric insecticides, 215,217–232
- Quantitative structure–activity relationships of protoporphyrinogen oxidase inhibiting herbicides
- chirality, 143*f*
 - different chemical classes, 141–143

- Quantitative structure–activity relationships of protoporphyrinogen oxidase inhibiting herbicides—
Continued
diphenyl ether analogues, 137–138
future research, 144
phenopylate analogues, 138–139
phenyltetrahydrophthalimide analogues, 139–141
previous studies, 136–137
- Quinolines, substituted,
structure–activity relationships, 227–229,230*t*
- R**
- Rat hepatocyte cultures, uroporphyrin accumulation, 275
- Reductants, protoporphyrinogen oxidation, 109–110
- Resistance mechanisms, 10–11
- rs-3* gene
cloning by transformation, 100–103
cloning strategies, 98–100
- S**
- S–23142, structure, 92,94*f*
- Singlet oxygen mediated photodynamic damage to cucumber plants induced by δ -aminolevulinic acid, 65–78
- Six-membered N-heterocyclic modulators that mimic a tetrapyrrole quadrant
nicotinic acid and substituted analogues, 59–61
picolinic acid and substituted analogues, 61–62
- Six-membered N-heterocyclic modulators that mimic half a tetrapyrrole
dipyridyls, 56–58
phenanthrolines, 52,54–56
- Structure–activity relationships
oxypyridines, 227–229,230*t*
- Structure–activity relationships—
Continued
phenanthrolines, 217–222
protoporphyrinogen oxidase inhibiting herbicides, 133–144
pyridiniums, 229,230*t*,231*f*
pyridyls, 222–226
pyrroles, 229–230,232
quinolines, 227–229,230*t*
- Substituted oxypyridines,
structure–activity relationships, 227–229,230*t*
- Substituted phenanthrolines,
structure–activity relationships, 217–222
- Substituted pyridiniums,
structure–activity relationships, 229,230*t*,231*f*
- Substituted pyridyls, structure–activity relationships, 222–226
- Substituted pyrroles, structure–activity relationships, 229–230,232
- Substituted quinolines, structure–activity relationships, 227–229,230*t*
- Superoxide radical production,
 δ -aminolevulinic acid induced photodynamic damage to cucumber plants mediated by singlet oxygen, 77*t*,79
- Synthesis of protoporphyrinogen oxidase inhibitors, 34–45
anilide derivatives, 41–43
C-bridged inhibitors, 39–41
O-bridged inhibitors, 35–39
phenylhydrazine derivatives, 43–46
- Synthetic organic chemicals that act through porphyrin pathway, 18–31
- T**
- Target site sensitivity, photodynamic herbicides, 185–186
- 2,3,7,8-Tetrachloro-*p*-dioxin,
disruption of porphyrin biosynthetic pathway, 247

- Tetrapyrrole(s)
 biosynthesis modulators, 48–62
 function, 233–234
 metabolic, photodynamic effects on chloroplasts, 49
 structure, 234,235f
- Tetrapyrrole-dependent photodynamic herbicide(s)
 mode of action, 206
See also Porphyrin insecticides
- Tetrapyrrole-dependent photodynamic herbicide modulators
 classifications, 52
 discovery, 50–52
 five-membered N-heterocyclic modulators that mimic a tetrapyrrole quadrant, 62–63
 future prospects, 63
 pyridiniums that mimic a quadrant or half a tetrapyrrole, 62
 six-membered N-heterocyclic modulators that mimic a tetrapyrrole quadrant, 59–62
 six-membered N-heterocyclic modulators that mimic half a tetrapyrrole, 52,54–58
- Tetrapyrrole involvement,
 δ -aminolevulinic acid induced photodynamic damage to cucumber plants mediated by singlet oxygen, 75,77,78f,79
- Tetrazolones, synthesis, 45
- Thylakoid membrane linked function,
 δ -aminolevulinic acid induced photodynamic damage to cucumber plants, 68,71f,79
- Tissue(s), singlet oxygen traps, 299
- Tissue photosensitizer for photodynamic cancer therapy
 characteristics, 292–293
 light dosimetry problem, 292–293
 persistence problem in normal skin, 293–295
 use of endogenous porphyrins, 293
- Tissue specificity of δ -aminolevulinic acid induced protoporphyrin IX
 evidence, 296–297
 mechanisms, 297–298
 modification, 298–299
- Tolerance
 mechanisms, 10–11
 plants to photodynamic herbicides, *See* Plant tolerance to photodynamic herbicides
- Toxicology
 experimental animals and humans, protoporphyrinogen oxidase inhibiting herbicides, 251,253
 porphyrin pesticides and protoporphyrinogen oxidase inhibitors, 12
- Transformation, cloning of *rs-3* gene, 100–103
- Translocation of photodynamic herbicides, mechanism, 182
- Triazinediones, synthesis, 44
- Triazolidinones, synthesis, 45–46
- Tumor therapy, protoporphyrinogen oxidase inhibitors, 280–289
See also Cancer therapy
- U
- Uptake
 oxyfluorfen and chlormethoxyfen, 123,124f
 photodynamic herbicides, 181–182
- Uroporphyrin
 accumulation in avian hepatocytes, 270–271,273f,275
 induction of elevated levels by diphenyl ether herbicides, 249–250
- W
- Weed control, importance, 65

Weed seedlings

ethane evolution using oxyfluorfen
and chlomethoxyfen, 121,122*f*
growth response to oxyfluorfen and
chlomethoxyfen, 121,122*f*

X

Xenobiotics, disruption of porphyrin
biosynthetic pathway, 247

Y

Yeast protoporphyrinogen oxidase, 81

Production: Meg Marshall
Indexing: Deborah H. Steiner
Acquisition: Anne Wilson
Cover design: Peggy Corrigan

Printed and bound by Maple Press, York, PA